EDITORIAL

The Editors of the *Journal of Polymer Science* have been aware of the fact that the growth of the field has led to greater specialization of the research effort and of the investigators involved in it.

There has been, in recent years, an increasing differentiation between the chemical and the physical approach toward the solution of problems and interpretation of data. It has always been the general philosophy of this *Journal* to foster the interdependence of these two approaches and to act as a medium for publication of all groups engaged in polymer research. Just the same, we feel that it would be appropriate to give greater emphasis to the field of polymer physics by a stronger representation on the Editorial Board.

We are, therefore, happy to announce that Richard S. Stein, Director of the Polymer Research Institute of the University of Massachusetts, Amherst, has joined our editorial group as of January 1964. His special function will be the editorial handling of all papers in the field of polymer physics.

We have furthermore added Dr. H. D. Keith, Bell Telephone Laboratories, and Dr. Karl Wolf, BASF, Ludwigshafen, to the Advisory Board.

JOURNAL OF POLYMER SCIENCE: PART A VOL. 2, PP. 1539–1548 (1964)

Photosensitized Polymerization of Acrylic Monomers. III. Kinetics of Polymerization of Acrylamide in the Absence of Oxygen

S. TOPPET, G. DELZENNE,* and G. SMETS, *Laboratoire de Chimie Macromoléculaire, University of Louvain, Belgium*

Synopsis

Acrylamide polymerizes at 25°C. in aqueous solution by photosensitization with eosin, in absence of any reducing agent and of oxygen; a strong photoreduction of the dyestuff proceeds simultaneously. The photopolymerization has been followed gravimetrically, while the rate of photoreduction was followed colorimetrically. The rate of photoreduction is proportional to the absorbed light intensity. The rate constants are proportional to the monomer concentration when this concentration is lower than 0.42 mole/l.; above this value they are independent from it. The rate of photopolymerization is proportional to the square root of the eosin concentration when this concentration is $\leq 10^{-6}$ mole/l.; above this value, the rate becomes independent of the eosin concentration. With respect to the monomer the order of reaction varies from 1.5 to 1.85 when the eosin concentration is 0.4×10^{-6} and 6×10^{-6} moles/l., respectively. With respect to the light intensity, the order of reaction is 0.35 when the monomer and eosin concentrations are, respectively, 2.8 moles/l. and 0.4×10^{-6} moles/l. The kinetics of photoreduction are interpreted on the basis of a reaction between the excited triplet state of the dye and the monomer, and a kinetic scheme is presented. The kinetics of photopolymerization are explained by a termination process between a growing chain and a primary radical, besides the usual termination process between two growing chains.

INTRODUCTION

The photopolymerization of vinyl compounds, sensitized by dye reducing agents systems, was described by Oster et al.[1–4] These systems are characterized by their high efficiency in the presence of oxygen and are therefore described as suitable elements for photoreproduction techniques. The initiation of these photopolymerizations was attributed to free radicals formed during the photoreduction and the reoxidation of the semiquinone radicals and the leuco dyes.[5] From the kinetic study of the photopolymerization of acrylic monomers in aqueous and semiorganic solutions, a photoinitiation could also be presumed in the complete absence of oxygen and reducing agent.[6]

It is precisely the aim of this paper to present the kinetics of the eosin-sensitized photopolymerization of acrylamide in aqueous solution in the

* Present address: Gevaert Photoproducten N. V., Mortsel-Antwerp, Belgium.

absence of oxygen and reducing agent, as well as the kinetics of photoreduction of the sensitizing dye occurring at the same time.

EXPERIMENTAL

Pure acrylamide was used after recrystallization from methylene chloride. Tetrabromofluorescein (eosin) was a biological Michrome reagent (E. Gurr, Ltd., London); acetamide was an analytical grade reagent (Merck). Water was purified from any dissolved gas by repeated distillations in high vacuum.

Photopolymerization Technique

Solution containing eosin was evaporated under high vacuum in order to isolate an adequate amount of dyestuff. The monomer was added, a given volume of water distilled in the reaction cell, and the dissolved oxygen finally removed from the solution by repeated outgassing under high vacuum.

The reaction cell was a cylindrical glass vessel of 2 cm. diameter and a total volume of about 30 ml. The solution was irradiated at 25°C. with a 150-w. Osram BA 155 lamp, stabilized by an automatic Sola voltage stabilizer; the incident light intensity is equal to 2.7×10^{-7} Einsteins/cm.^{2} min., as measured with the actinometric procedure of Parker and Hatchard.[7,8] The irradiation system was fixed on an optical bench, while the light intensity was varied by intercalating wire gauzes of different mesh sizes between the lamp and the reaction cell. The rate of polymerization was determined gravimetrically after several purifications of the polymer by dissolving in water and precipitating in acetone.

Photoreduction Technique

The photoreduction of esoin was followed colorimetrically with an Eppendorf photometer working with a cadmium vapor light source. The extinction coefficient of the eosin solution was determined at 509 mμ (λ_{max} eosin = 518 mμ) and its concentration calculated from a calibration curve at the same wavelength.

RESULTS

A. Photoreduction of Eosin

The irradiation of an evacuated aqueous solution of eosin produces only a very slight photoreduction even after prolonged exposure. However the addition of acrylamide to the solution enhances the photoreduction rate of eosin whereas the presence of acetamide is without effect on the rate. The rate of photoreduction R_{red} of the sensitizer can be expressed as follows:

$$R_{red} = -dc/dt = KI_{abs} \qquad (1)$$

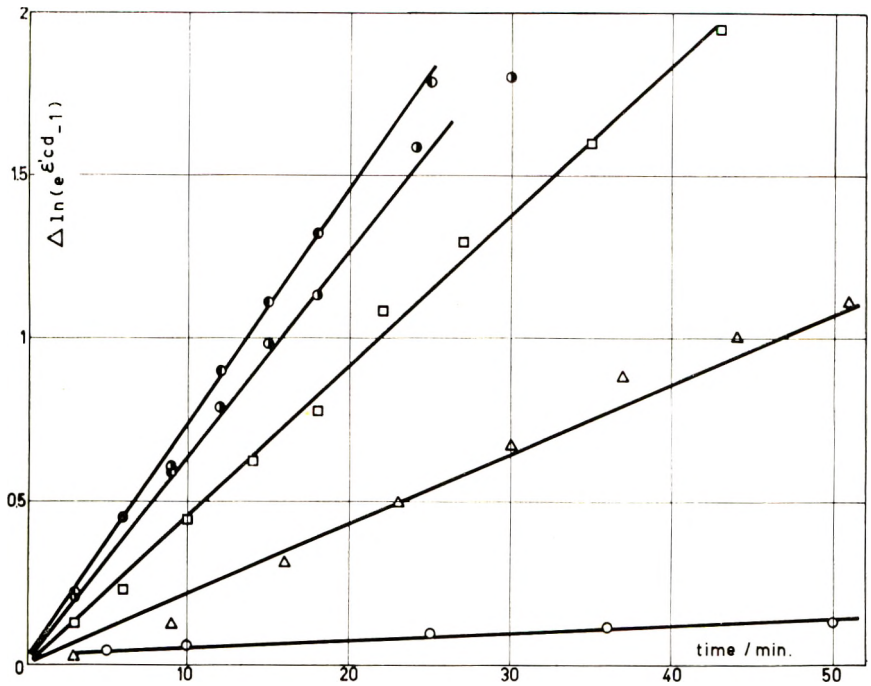

Fig. 1. Rate of photoreduction of eosin at different acrylamide concentrations: (○) 0 mole/l.; (△) 0.14 mole/l.; (□) 0.28 mole/l.; (◑) 0.42 mole/l.; (◐) 0.7 mole/l.

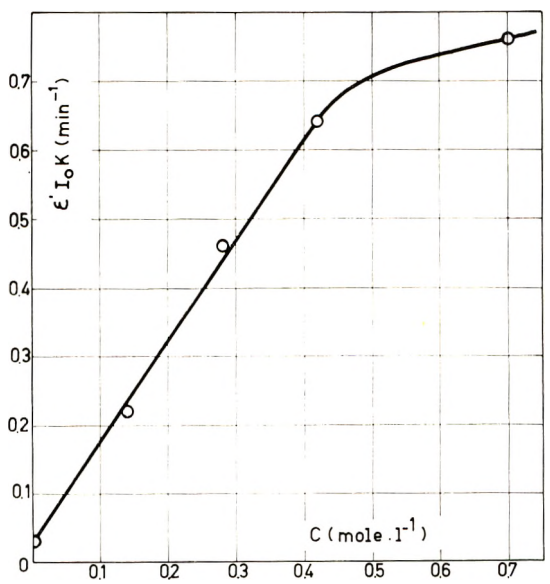

Fig. 2. Influence of the monomer concentration on the rate of photoreduction of eosin.

TABLE I

Influence of the Acrylamide Concentration on the Photoreduction Rate of Eosin in Aqueous Solution

Monomer, mole/l.	Time, min.	Eosin, moles/l. $\times 10^6$	$\Delta \ln (e^{\epsilon' cd} - 1)$	$\epsilon' I_0 K$, min.$^{-1}$
0	0	8.15	0	0.003
	5	7.9	0.043	
	10	7.88	0.057	
	25	7.65	0.099	
	36	7.5	0.112	
	51	7.43	0.126	
0.14	0	8.38	0	0.022
	3	8.25	0.021	
	9	7.65	0.124	
	16	6.75	0.31	
	23	5.9	0.495	
	30	5.15	0.67	
	37	4.35	0.882	
	44	3.97	1	
	51	3.56	1.13	
	65	2.85	1.39	
0.28	0	7.07	0	0.046
	3	6.47	0.122	
	6	5.97	0.225	
	10	5.1	0.442	
	14	4.4	0.626	
	18	3.88	0.777	
	22	3	1.086	
	27	2.5	1.294	
	35	1.91	1.596	
	43	1.38	1.946	
0.42	0	7	0	0.064
	3	6.03	0.208	
	6	5	0.453	
	9	4.5	0.612	
	12	3.82	0.789	
	15	3.24	0.987	
	18	2.85	1.135	
	24	1.91	1.585	
	30	1.56	1.802	
	40	0.97	2.217	
0.7	0	6.4	0	0.071
	3	5.44	0.219	
	6	4.55	0.441	
	9	4.05	0.591	
	12	3.12	0.901	
	15	2.59	1.113	
	18	2.15	1.32	
	25	1.41	1.788	
	35	0.795	2.388	

where c is the eosin concentration in moles/l. and I_{abs} is the absorbed light intensity/cm.^{3} sec. Taking the relationship between the light intensity absorbed per volume unit (I_{abs}), the incident light intensity (I_0) and the transmitted light intensity (I_{tr}) into account, eq. (1) can be transformed into eq. (2):

$$R_{red} = K\ (I_0 - I_{tr})/d = (K/d)\ I_0\ (1 - e^{-\epsilon' cd}) \qquad (2)$$

where ϵ' indicates the apparent molar extinction coefficient and d the thickness of the cell.

By integrating eq. 2 between c_0, the initial eosin concentration and c, the concentration at time t, one obtains:

$$\ln\ (e^{\epsilon' c_0 d} - 1) - \ln\ (e^{\epsilon' cd} - 1) = \epsilon' K I_0 t \qquad (3)$$

The linear relationships obtained from plots of $\Delta \ln\ (e^{\epsilon' cd} - 1)$ as a function of irradiation time indicates the proportionality of the photoreduction rate to the concentration of excited dye molecules, i.e., to the absorbed light intensity.

The slopes are proportional to the rate constants and, for pure photoreduction processes, can be assimilated to quantum yields. Equation (3) was used to plot the results (Table I) of the photoreduction of eosin solutions in the presence of various acrylamide concentrations. From the slopes of Figure 1 the values of $\epsilon' I_0 K$ were calculated for the different monomer concentrations; they are proportional to the monomer concentration up to 0.42 mole/l., as shown in Figure 2.

B. Photopolymerization of Acrylamide

The very important photoreduction of eosin in deoxygenated aqueous solutions of acrylamide is accompanied by the polymerization of this monomer. Its rate of polymerization was followed gravimetrically and the influence of the concentration of monomer and of the sensitizing dye as well as the influence of the light intensity have been examined.

Influence of the Sensitizer Concentration. The influence of the eosin concentration on the rate of photopolymerization of acrylamide in aqueous solution was determined at constant light intensity and constant monomer

TABLE II
Influence of the Eosin Concentration on the Rate of Photopolymerization of Acrylamide[a]

Eosin, moles/l. $\times 10^6$	Light absorption, %	Rate, moles/l. min. $\times 10^2$
0.2	5.5	0.9
0.4	10.5	1.13
0.8	20	1.63
4	66.8	1.8
8	89	1.8
12	96.3	1.8

[a] Temperature, 25°C.; I_0, 2.7×10^{-7} Einsteins/cm.^{2}/min.; acrylamide, 2.82 moles/l.

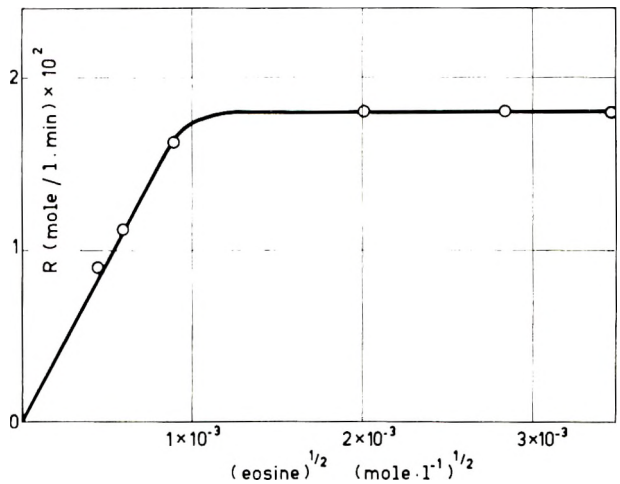

Fig. 3. Rate of photopolymerization of acrylamide at different eosin concentrations.

concentration. At concentrations lower than 10^{-6} moles/l. the rate is practically proportional to the square root of the eosin concentrations; above this concentration, however, the rate dependence decreases and becomes rapidly independent of it. The results are summarized in Table II and Figure 3.

Influence of the Monomer Concentration. The influence of the monomer concentration was determined in both eosin concentration ranges, where the rate was dependent or not on the sensitizer concentration, i.e., [eosin] $< 10^{-6}$ mole/l. and $> 10^{-6}$ moles/l., respectively.

For an eosin concentration 0.4×10^{-4} moles/l. the rate was proportional to the 1.5 power of the monomer concentration, while at sensitizer concentration of 6×10^{-6} moles/l., the rate dependence increases and is proportional to the 1.85 power of the monomer concentration. The results are summarized in Table III.

TABLE III
Influence of the Monomer Concentration on the Rate of Photopolymerization[a]

Eosin, moles/l. × 10^6	Monomer, moles/l.	Rate, moles/l. min. × 10^2
0.4	2.25	0.85
	2.82	1.13
	3.1	1.27
	4.23	2.22
6	2.11	0.497
	2.82	0.86
	3.52	1.2
	4.22	1.82
	4.93	2.14

[a] Temperature, 25°C.; I_0, 2.7×10^{-7} Einsteins/cm.² min.

Influence of the Incident Light Intensity. The influence of the incident light intensity on the rate of photopolymerization was determined for acrylamide and eosin concentrations of 2.82 moles/l. and 0.4×10^{-6} moles/l., respectively. The results are summarized in Table IV. The intensity exponent of the rate expression is equal to ± 0.35. Above 10^{-6} moles/l. (at an eosin concentration of 4×10^{-6} moles/l.) preliminary measurements indicated an even lower value of this intensity exponent.

TABLE IV
Influence of the Light Intensity on the Rate of Photopolymerization of Acrylamide[a]

I_0, Einsteins/cm.^{2} min. $\times 10^7$	Rate moles/l. min. $\times 10^2$
0.84	0.65
3.13	1.02
3.6	1.1
6.55	1.35

[a] Temperature, 25°C.; eosin, 0.4×10^{-6} moles/l; acrylamide, 2.82 moles/l.

DISCUSSION

A. Photoreduction of Eosin

The photoreduction rate of eosin in aqueous acrylamide solution can be expressed by the empirical eq. (4):

$$R = K I_{abs} = \frac{k\,[M]}{\alpha + \beta[M]} I_{abs} \tag{4}$$

The influence of the sensitizer concentration on the photoreduction must be attributed to the reaction of photoexcited eosin molecules, while the influence of the acrylamide on the rate of photoreduction can be interpreted on the basis of a scheme analogous to that proposed by Uchida, Kato, and Koizumi.[9,10]

These authors explained the marked accelerating effect of *n*-hexene and cyclohexene on the rate of photoreduction of eosin in alcoholic solution assuming the formation of a transient complex between the triplet state of the excited dye and the solvent (alcohol) and an improved reductive decomposition of this complex under the influence of these promotors.

The formation of a transient complex between excited dye and solvent molecules was admitted on the basis of flash photolysis measurements. An analogous reaction mechanism is therefore proposed for the photoreduction of eosin in aqueous solution in the presence of acrylamide (M). In this scheme D, D_s, and D_t represent the eosin in the ground state, in the excited singlet state, and the excited triplet state, respectively, while DH· is a semiquinone radical. Although not demonstrated kinetically, the existence of a transient complex (D_t... HOH) between D_t and a water molecule may be admitted [reaction (d)]. The very slow rate of photoreduction in aqueous solution agrees with a much less favorable energetical situation than in alcoholic medium; consequently reaction

(f) becomes negligible in our experiments. Reaction (g) accounts for the promoting effect of acrylamide on the photoreduction; it is evident that a saturated amide, as acetamide, is unable to carry out such a reaction.

$$D \xrightarrow{h\nu} D_s \tag{a}$$

$$D_s \rightarrow D + h\nu' \quad \text{(fluorescence)} \tag{b}$$

$$D_s \rightarrow D_t \tag{c}$$

$$D_t + HOH \rightarrow (D_t \ldots HOH) \quad \text{(transient activated complex)} \tag{d}$$

$$(D_t \ldots HOH) \rightarrow D + HOH \tag{e}$$

$$(D_t \ldots HOH) \rightarrow DH\cdot + OH\cdot \text{ (negligible)} \tag{f}$$

$$(D_t \ldots HOH) + M \rightarrow DH\cdot + HO\text{-}M\cdot \tag{g}$$

$$D_t \rightarrow D + h\nu'' \text{ (delayed fluorescence and phosphorescence} \tag{h}$$

The rate of photoreduction of eosin is equal to:

$$R_{red} = -dC/dt = k_g [D_t \ldots HOH] [M] \tag{5}$$

Assuming steady-state conditions for the intermediate species, this equation becomes:

$$R_{red} = \frac{k' I_{abs}}{\alpha + \beta [M]} k_g [M] \tag{6}$$

where $k' = k'_d k_c$; $k'_d = k_d [HOH]$; $\alpha = (k'_d + k_h)(k_b + k_c)k_c$; and $\beta = k_g (k'_d + k_h)(k_b + k_c)$.

This equation agrees with the experimental expression (4).

B. Photopolymerization of Acrylamide

The photopolymerization of acrylamide in evacuated aqueous solution is initiated by the free radicals formed in the scheme discussed above. The kinetics of photopolymerization show discrepancies, however, with respect to the classical rate expression as well for the influence of the monomer concentration (order between 1.5 and 1.85), the sensitizer concentration (from 0.5 progressively to zero) and the influence of the light intensity (0.35 and lower).

These results can be interpreted by assuming chain termination reaction between primary radicals and growing chains. Indeed, if this chain termination prevails, the rate of polymerization becomes proportional to the square of the monomer concentration and independent of the rate of initiation.[11] This interpretation is strengthened on considering the nature of the primary semiquinone radicals which are formed in these experiments and which are undoubtedly stabilized by resonance.

A similar behavior was recently described by Misra, Haffeez, and Sharma[12] in the bulk polymerization of styrene at 50°C. in the presence

of phenyl azo triphenylmethyl radicals as initiator. This particular effect of semiquinone radicals will be evidently more important at high eosin concentrations. Moreover the increased viscosity of the reaction medium due to the very high molecular weight of the polyacrylamide causes a decrease of the recombination (or disproportionation) reaction of two macroradicals. This termination reaction becomes progressively diffusion-controlled[13,14] and will be more affected than the reaction in which only one macroradical is involved. Consequently this viscosity effect enhances also a chain termination process involving primary radicals.

The authors are indebted to the IRSIA (Institut pour la Recherche Scientifique dans l'Industrie et l'Agriculture) and to Gevaert Photoproducten N. V. (Antwerp) for supporting this research, and to the IRSIA for a fellowship to one of them (S. T.).

References

1. Oster, G., *Nature*, **173**, 300 (1954).
2. Oster, G. K., G. Oster, and G. Prati, *J. Am. Chem. Soc.*, **79**, 595 (1957).
3. Oster, G., and Y. Mizutani, *J. Polymer Sci.*, **22**, 173 (1956).
4. Oster, G., and M. Taniyama, *Bull. Chem. Soc. Japan*, **30**, 856 (1957).
5. Delzenne, G., S. Toppet, and G. Smets, *J. Polymer Sci.*, **55**, 767 (1961).
6. Delzenne, G., S. Toppet, W. Dewinter, and G. Smets: *J. Polymer Sci.*, **A2**, 1069 (1964).
7. Parker, C. A., *Proc. Roy. Soc. (London)*, **A220**, 104 (1953).
8. Parker, C. A., and C. G. Hatchard: *Proc. Roy. Soc. (London)*, **A235**, 518 (1956).
9. Uchida, K., S. Kato, and M. Koizumi, *Bull. Chem. Soc. Japan*, **33**, 169 (1960).
10. Kato, S., T. Watanabe, S. Nagaki, M. Koizumi: *Bull. Chem. Soc. Japan*, **33**, 262 (1960).
11. Chapiro, A., P. Cordier, K. Hayashi, I. Mita, and J. Sebban, *J. Chim. Phys.*, **56**, 447 (1959).
12. Misra, G. R., A. Haffeez, and K. Sharma, *Makromol. Chem.*, **51**, 123 (1962).
13. Allen, P., and C. Patrick, *Makromol. Chem.*, **47**, 154 (1961).
14. Benson, S., and A. North, *J. Am. Chem. Soc.*, **81**, 1332 (1959).

Résumé

L'acrylamide polymérise à 25°C en solution aqueuse par photosensibilisation au moyen d'éosine, en absence de tout réducteur et d'oxygène; cette polymérisation s'accompagne d'une photoréduction simultanée du colorant. La photopolymérisation a été suivie par la méthode gravimétrique, tandis que la vitesse de photoréduction a été suivie colorimétriquement. La vitesse de photoréduction est proportionnelle à l'intensité lumineuse absorbée; aux concentrations en monomère inférieures à 0.42 mole/l les constantes de vitesse sont proportionnelles à la concentration en monomère; au delà, elles en sont indépendantes. La vitesse de photopolymérisation de l'acrylamide est proportionnelle à la racine carrée de la concentration en éosine lorsque la concentration en éosine est inférieure ou égale à 10^{-6} mole/l; au delà, la vitesse devient indépendante de la concentration en colorant. L'ordre par rapport au monomère varie de 1.5 à 1.85 lorsque la concentration en éosine s'élève à 0.4×10^{-6} et 6×10^{-6} moles/l; par rapport à l'intensité lumineuse, l'ordre s'élève à 0.35 à une concentration en monomère égale 2.8 moles/l et une concentration en éosine de 0.4×10^{-6} moles/l. La cinétique de photoréduction est interprêtée par la réaction de l'état activé triplet avec le monomère, et un schéma cinétique est présenté. La cinétique de photopolymérisation s'explique sur la base d'une réaction de terminaison entre les chaînes en croissance et un radical primaire, outre la terminaison habituelle entre les deux chaînes en croissance.

Zusammenfassung

Acrylamid polymerisiert bei Photosensibilisierung mit Eosin bei 25°C in wässriger Lösung in Abwesenheit von Reduktionsmitteln und Sauerstoff; gleichzeitig tritt eine starke Photoreduktion des Farbstoffes auf. Die Photopolymerisation wurde gravimetrisch, die Geschwindigkeit der Photoreduktion kolorimetrisch gemessen. Die Geschwindigkeit der Photoreduktion ist der absorbierten Lichtintensität und die Geschwindigkeitskonstante bei Monomerkonzentrationen unterhalb 0,42 Mol/Lit dieser Konzentration proportional; oberhalb dieses Wertes ist sie davon unabhängig. Die Geschwindigkeit der Photopolymerisation ist bei Eosinkonzentrationen unterhalb 10^{-6} Mol/Lit der Wurzel aus der Eosinkonzentration proportional; oberhalb dieses Wertes wird die Geschwindigkeit von der Eosinkonzentration unabhängig. In bezug auf des Monomere ändert sich die Reaktionsordnung beim Übergang der Eosinkonzentration von $0{,}4 \times 10^{-6}$ auf 6×10^{-6} Mol/Lit von 1,5 zu 1,85. In bezug auf die Lichtintensität ist die Reaktionsordnung bei einer Monomer- und Eosinkonzentration von 2,8 Mol/Lit bzw. $0{,}4 \times 10^{-6}$ Mol/Lit gleich 0,35. Ein kinetisches Schema für die Photoreduktion wird aufgestellt, dem die Annahme einer Reaktion zwischen dem angeregten Triplettzustand der Farbstoffes und dem Monomeren zu Grunde liegt. Für die Kinetik der Photopolymerisation wird neben der üblichen Abbruchsreaktion zwischen zwei wachsenden Ketten noch ein Kettenabbruch zwischen einer wachsenden Kette und einem Primärradikal angenommen.

Received February 18, 1963

JOURNAL OF POLYMER SCIENCE: PART A VOL. 2, PP. 1549–1566 (1964)

1,5-Hexadiene Polymers. I. Structure and Properties of Poly-1,5-Hexadiene*

HENRY S. MAKOWSKI, BENJAMIN K. C. SHIM,† and ZIGMOND W. WILCHINSKY, *Chemicals Research Division, Esso Research and Engineering Company, Linden, New Jersey*

Synopsis

1,5-Hexadiene has been polymerized with a number of modified alkyl metal coordination catalysts to crystalline polymers having an unusual combination of properties. These polymers are crystalline, have high tensile strengths, high melting points, high densities, and yet are very flexible. Poly-1,5-hexadiene has a chain identity period of 4.80 A., and is best defined as consisting primarily of 1-methylene-3-cyclopentyl units in which the substituents are *cis* and the cyclopentane ring is in an envelope conformation. Since not all the monomer units incorporated into the chain are cyclized, the polymer more closely resembles an interpolymer than a homopolymer.

INTRODUCTION

A mechanism for the polymerization of certain 1,5- and 1,6-dienes to soluble, saturated polymers was first proposed in 1957 by Butler.[1] This mechanism, cyclopolymerization or intra-intermolecular polymerization to polymers having recurring cyclic units, has since been fully substantiated with a variety of monomer and catalyst systems.[2,3] In 1958 Marvel and Stille reported the preparation of hydrocarbon soluble polymers from the polymerization of 1,5-hexadiene with the triisobutylaluminum–titanium tetrachloride catalyst system.[4] The benzene-soluble portions of poly-1,5-hexadienes prepared with variations of this catalyst system were found to contain only 5–8% residual unsaturation. On this information the most probable principal recurring unit in these polymers was proposed as the 1-methylene-3-cyclopentyl group.

This paper presents a study of the structure and properties of crystalline poly-1,5-hexadiene prepared with triethylaluminum–titanium chloride catalyst combinations. The principal recurring unit and chain conformation of this polymer are defined consistent with the polymer's chain identity period and physical properties. These considerations present more detailed information on the structure of polymers produced via the intra-

* Presented before the Division of Polymer Chemistry, 137th National Meeting, American Chemical Society, Cleveland, Ohio, April 1960.

† Present address: Central Research, Lord Manufacturing Company, Erie, Pa.

intermolecular polymerization mechanism and add more evidence for the correctness of this mechanism.

EXPERIMENTAL

Starting Materials

n-Heptane (Phillips Petroleum Company) was percolated through Alcoa F-5 alumina at 1–2 v./v./hr. under nitrogen and was stored over sodium ribbon prior to use. Chlorobenzene (Matheson, Coleman & Bell) was percolated through Alcoa F-5 alumina under nitrogen at 1–2 v./v./hr.

1,5-Hexadiene (Aldrich Chemical Company) was purified immediately prior to use by refluxing with a sodium dispersion and distilling through a 15-plate Oldershaw distillation column under nitrogen. The product boiling at 60.5–63.0°C. was collected and used.

Triethylaluminum (specifications of >22.5% aluminum)[5] was used without further purification and was handled as a 0.88*M* solution in dry *n*-heptane. A preformed $TiCl_3 \cdot 0.22\ AlCl_3$ catalyst component was prepared[6] by reacting 9 parts of titanium tetrachloride (Baker Chemical Company), 1 part of titanium powder (Metal Hydrides, Inc.), and 2 parts of Alcoa #140 atomized aluminum metal at 250°C. for 6 hr. The reaction product was washed with dry *n*-heptane, dried *in vacuo*, and ball-milled in a stainless steel jar for 5 days. A preformed $TiCl_2 \cdot 0.5\ AlCl_3$ catalyst component was prepared[6] by reacting titanium tetrachloride with aluminum powder at 220°C. for 5 hr., and the resultant product was ball-milled for 6 days. The ball-milled product was heated for 6 hr. at 220°C. and then additionally flint pebble-milled for 4 days.

Catalyst Preparations

All catalysts were prepared immediately prior to use. The preformed catalysts and triethylaluminum were mixed in a dropping funnel in an amount of diluent sufficient to allow a clean catalyst transfer to the polymerization vessel. Split-pretreated catalysts were prepared in *n*-heptane as follows. A titanium tetrachloride solution was heated to 70°C. and triethylaluminum was added in sufficient amount to make the Al/Ti molar ratio = 0.5 and the catalyst concentration = 21.8 g./l. The catalyst slurry was maintained at 70°C. for 1 hr. The catalyst slurry was added to the reactor containing the diluent and sufficient triethylaluminum to make the overall Al/Ti molar ratio = 2.0. A normal pretreat catalyst was prepared by mixing triethylaluminum and titanium tetrachloride in *n*-heptane at room temperature at a catalyst concentration of 3.65 g./l. and an Al/Ti molar ratio of 2.0. The catalyst so prepared was then immediately added to the diluent in the polymerization vessel.

Polymerizations

Polymerizations were conducted in glass resin reaction flasks which were thoroughly dried and swept with scrubbed, dry nitrogen. The diluent was

TABLE I. Preparation and Properties of Poly-1,5-Hexadiene

	Run 1	Run 2	Run 3	Run 4	Run 5	Run 6	Run 7	Run 8	Run 9
Catalyst	$Al(C_2H_5)_3/TiCl_3 \cdot 0.22AlCl_3$				$Al(C_2H_5)_3/TiCl_2 \cdot 0.5AlCl_3$	$Al(C_2H_5)_3/TiCl_4$			
Al alkyl/Ti Ratio	1.39[a]	1.39[a]	1.26[a]	1.26[a]	2.0[a]	2.0[b]	2.0[c]	2.0[c]	2.0[c]
Total, g.	1.25	2.51	1.68	1.68	4.50	0.73	0.73	1.84	1.84
Catalyst concn., g./l.	2.91	0.84	1.68	1.68	4.50	3.65	3.65	1.23	0.92
Diluent	Chlorobenzene		*n*-Heptane		*n*-Heptane		*n*-Heptane		
Volume, ml.	430	3000	1000	1000	1000	200	200	1500	2000
1,5-Hexadiene feed, g.	65	261	100	100	100	34.6	34.6	250	346
Polymerization temp., °C.	63–>100	48–66	53–64	53–64	58–62	48–87	50–70	60–62	40–72
Polymerization time, min.	55	125	40	40	60	120	120	240	130
Solid Polymer, g.	35.0	210.0	42.0	39.4	54.0	11.1	18.9	107.0	67.0
Catalyst efficiency, g./g.	28.0	83.7	25.0	23.5	12.0	15.2	25.9	58.2	36.4
1,5-Hexadiene conversion, %	53.8	80.5	42.0	39.4	54.0	32.1	54.6	42.8	19.4
Polymer Properties									
Inherent viscosity, dl./g.	2.00	2.33	1.22	1.13	1.32	1.43	1.18	1.52	1.67
S.P./M.P., °C.	121/128	122/134	114/128	119/130	123/139	111/118	109/119	137/146	131/138
Density, g./cc.	1.009	1.006	1.008	1.006	—	1.010	1.003	1.009	1.122
Tensile strength, psi	1390	2430	1580	1930	805	720	3400	4360	5420
Elongation, %	520	270	365	290	285	14	240	310	270
Apparent modulus of elasticity, psi $\times 10^{-5}$									
At 25°C.	—	0.05	—	—	—	0.12	0.15	—	—
At 0°C.	0.43	0.64	0.72	0.72	0.69	0.85	1.65	0.93	0.86
At −25°C.	0.78	1.02	1.07	1.10	1.12	1.32	2.32	1.70	1.25
At −50°C.	1.47	1.54	1.86	1.70	2.24	1.99	3.43	2.40	2.00
n-Heptane-soluble, %	—	—	11.7	10.2	—	—	—	8.0	—
Benzene-Soluble, %	—	—	—	23.8	—	—	—	6.7	—
Benzene-insoluble, %	—	—	—	66.0	—	—	—	85.3	—

[a] Preformed catalysts. [b] Normal pretreat catalysts. [c] Split pretreat catalysts.

added to the reaction flask and brought to temperature. The catalyst was added followed immediately by the 1,5-hexadiene. Polymerization was terminated by the addition of 30–100 ml. of isopropyl alcohol. The resulting polymer slurry was added to 1.5 volumes of acetone or an acetone–isopropyl alcohol solution. The product was filtered and washed 2–5 times with acetone or an acetone–isopropyl alcohol solution. The filtered and washed product was dried *in vacuo* at 55°C. Nine polymerizations were made, and full details of polymerization conditions and polymer yields are given in Table I.

Physical Properties

Softening and melting points were determined with a Nalge melting point apparatus. Inherent viscosities were determined in tetralin solution at 125°C. Densities, tensile properties, and apparent moduli of elasticity were determined according to ASTM procedures D792-50, D412-51T, and D1043-51, respectively.[7] The physical properties of the polymers obtained are listed in detail in Table I.

X-Ray Diffraction

X-ray diffractometer traces and diffraction photographs with a flat plate camera were obtained by using nickel-filtered Cu Kα radiation. The camera was calibrated using the values of Bragg spacings reported by the National Bureau of Standards for reagent grade $Pb(NO_3)_2$ powder.[8] The diffractometer trace of poly-1,5-hexadiene (Fig. 1) revealed a crystalline pattern with only one peak which was very intense and sharp, *d*-spacing of 4.87 A., superimposed over an amorphous background in the region

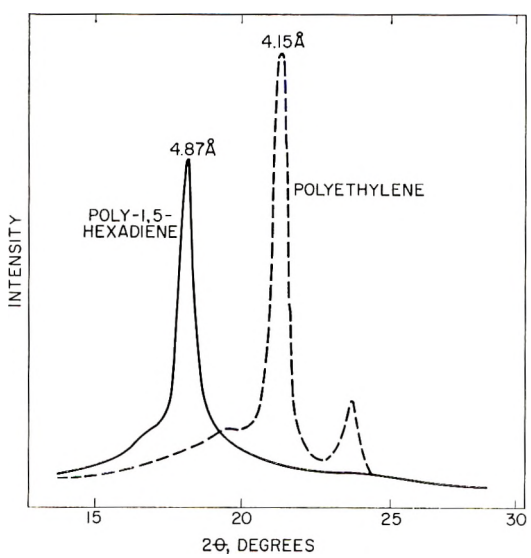

Fig. 1. X-ray diffraction patterns of poly-1,5-hexadiene and polyethylene.

2θ = 5–30°. Diffraction photographs of cold-drawn, oriented strips of poly-1,5-hexadiene showed a fiber-type pattern with a spacing of 4.80 A. along the fiber axis.

Infrared Spectra

Spectra of total poly-1,5-hexadiene polymers were obtained on thin films. The major absorption bands in the 7.0–13.0μ region were: 7.5 (strong, broad), 8.0 (medium), 8.3 (medium), 9.5 (weak, broad), 10.05 (weak), 10.4 (medium, broad), 11.05 (medium), 11.7 (medium, broad), and 12.7 (weak). The bands at 10.05 and 11.05μ were assigned to residual vinyl unsaturation.

Solvent Extraction of Polymers

n-Heptane-soluble fractions were obtained on the polymers from runs 3, 4, and 8 by Sohxlet extraction for 48 hr. Benzene-soluble fractions were obtained on the polymers from runs 4 and 8 by Sohxlet extraction of the *n*-heptane residues for 48 hr. Full details on the size and on the properties of these fractions are given in Tables I and II.

Calculations

For the 1,4-cyclohexane system the following assumptions were made: the cyclohexane ring is in the chair form; all C–C–C bond angles are 109° 28′; all C–C distances are 1.54 A.[9]

For the 1,2-cyclobutane system the following assumptions were made: the cyclobutane ring is planar (i.e., all internal angles = 90°); the ring C–C distances = 1.56 A.; all external C–C bond distances = 1.54 Å; all external C–C–C bond angles = 109° 28′; the $H–C_{ring}–C_{external}$ bond angles = 109° 28′ and the planes of these groups are perpendicular to the plane of the cyclobutane ring and bisect the ring angles.[10,11]

For the 1,3-cyclopentane system calculations were made according to Pitzer and Donath.[12] All C–C bond distances were assumed to be 1.54 A.

RESULTS AND DISCUSSION

Poly-1,5-hexadienes were prepared with a number of modified metal alkyl coordination catalysts in either *n*-heptane or chlorobenzene diluent (Table I). The best physical properties of poly-1,5-hexadiene were obtained with a split pretreated $Al(C_2H_5)_3/TiCl_4$ catalyst at an Al/Ti ratio of 2.0. This catalyst system gave higher melting points, better tensile properties, and lower *n*-heptane and benzene solubles than both preformed $Al(C_2H_5)_3/TiCl_3 \cdot 0.22\ AlCl_3$ and $Al(C_2H_5)_3/TiCl_2 \cdot 0.5\ AlCl_3$ catalyst systems; however, the latter two systems gave higher monomer conversions and catalyst efficiencies.

Although the yields of polymers and their respective properties varied with the catalyst modification and the mode of preparation, every poly-

TABLE II
Extraction of Poly-1,5-Hexadiene

	Inherent viscosity, dl./g.	Ultimate tensile strength, psi	Ultimate elongation, %	Apparent modulus of elasticity, psi × 10^{-5} 0°C.	−25°C.	−50°C.	Density, g./cc.	S.P./M.P., °C.	% of Original
Original polymer (Run 4)	1.13	1930	290	0.72	1.10	1.70	1.006	119/130	100.0
n-Heptane-soluble	0.20	—	—	—	—	—	—	68/90	10.2
Benzene-soluble	1.76	—	—	—	—	—	—	65/85	23.8
Benzene-insoluble	[a]	[b]	[b]	[b]	[b]	[b]	1.005	—	66.0
Original polymer (Run 8)	1.52	4360	310	0.93	1.70	2.40	1.009	137/146	100.0
n-Heptane Soluble	0.31	—	—	—	—	—	—	91/111	8.0
Benzene-soluble	2.06	—	—	—	—	—	—	123/136	6.7
Benzene-insoluble	[a]	[b]	[b]	[b]	[b]	[b]	1.009	—	85.3
Original polymer (Run 3)	1.22	1580	365	0.72	1.07	1.86	1.008	114/128	100.0
n-Heptane-soluble	0.61	—	—	—	—	—	—	108/113	11.7
n-Heptane-insoluble	1.18	1810	270	0.64	0.98	1.69	1.008	128/139	88.3

[a] Incompletely soluble in tetralin at a concentration of 0.5 g./l.
[b] Unable to mold perfect pad for testing. Apparently polymer was crosslinked.

1,5-hexadiene prepared was crystalline, had a density exceeding 1.0 g./cc., a melting point in excess of 100°C., and was very flexible. The high density of poly-1,5-hexadiene is a particularly interesting physical property and is offered as a proof that the polymers formed do contain carbocyclic rings. No aliphatic poly-α-olefin has a density as high as poly-1,5-hexadiene, and poly-1-hexene, the poly-α-olefin analog to poly-1,5-hexadiene, is a low density, amorphous product.[13]

Poly-1,5-hexadiene has about the same strength amd melting point as high density polyethylene, i.e., Ziegler type or Phillips type, and its density is higher than polyethylene (Table III). Yet it is an unexpectedly flexible product as indicated by its apparent modulus of elasticity. It is about as flexible as low density polyethylene. This combination of properties can best be explained through structures resulting from an intra-intermolecular polymerization mechanism. Poly-1,5-hexadiene more closely resembles an interpolymer than a homopolymer, as shown by its structure:

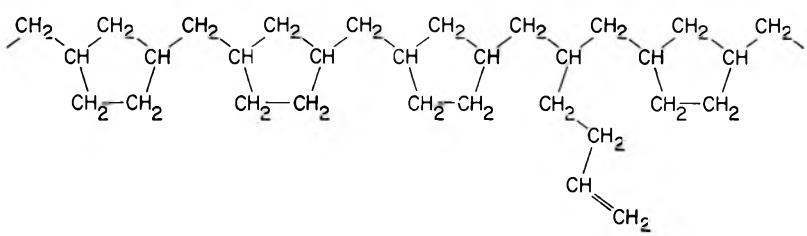

Marvel and Stille have already shown that not all of the monomer units in poly-1,5-hexadiene are incorporated through both bonds; some are incorporated through one bond only.[4] The noncyclized units tend to disrupt the regularity of the chain composed of cyclized monomer units resulting in a polymer which is less crystalline, lower melting, less dense, and considerably more flexible. The carbocyclic ring in the polymer chain makes the chain more rigid and also contributes a degree of symmetry which aids in the packing of the molecules in the unit cell. The net effect is a greater weight per volume ratio than could be achieved with poly-α-olefins, and, therefore, the density is higher.

A rather peculiar phenomenon was observed upon the extraction of 1,5-hexadiene polymers with *n*-heptane or benzene. The polymers after extraction had densities identical to those of the original polymers even though as much as 34% of the polymer had been extracted (Table II). Normally it is expected that the density of the residue will increase upon removal of less dense amorphous fractions. It must be concluded in this case that the extracted polymers differ from the residues only in molecular weight and not in composition.

As mentioned previously poly-1,5-hexadiene is a crystalline polymer. Figure 1 illustrates the x-ray diffraction pattern for poly-1,5-hexadiene and compares it with that of polyethylene. The general nature of the x-ray diffraction pattern of poly-1,5-hexadiene is seen to be very similar to that

of polyethylene. The d-spacing for the most intense crystalline peak is 4.87 A. for poly-1,5-hexadiene, whereas that for polyethylene is 4.15 A. An x-ray diffraction photograph of a highly oriented poly-1,5-hexadiene fiber showed equatorial reflections from the (hk0) planes. Of these the reflection corresponding to d = 4.87 A. was very intense; several very weak reflections were also observed. Nonequatorial reflections were present at two levels but only along the meridian indicating a symmetry corresponding to orthorhombic or higher. From an analysis of the photographs a repeat distance of 4.80 ± 0.05 A. was determined on the basis that the observed layer line reflections were from the (001) and (002) planes.

It is concluded from the low value of the chain identity period that poly-1,5-hexadiene has a linear, zigzag rather than a helical chain conformation. The chain identity period for a helical poly-1,5-hexadiene would be expected to be at least as large as that of isotactic polypropylene, 6.5 A.[14]

By using this value of the chain identity period, it is possible to deduce the structure of poly-1,5-hexadiene via calculations on all of the theoretically possible structures. The "possible" recurring units for poly-1,5-hexadiene occurring via the intramolecular-intermolecular polymerization mechanism are considered in structures I and II:

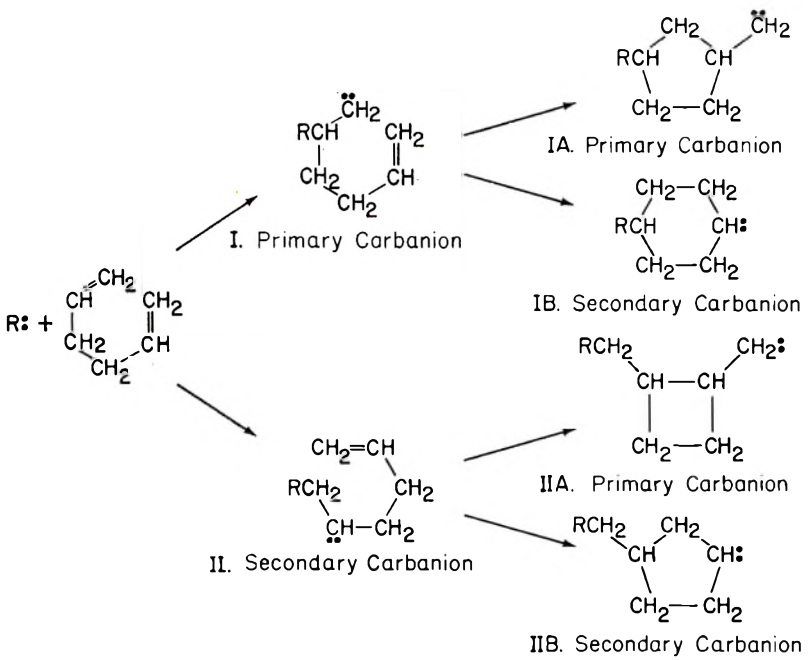

It is not necessary to distinguish the polymer chain end as an anion, a cation, or a free radical when considering these possible structures since the same considerations apply regardless of choice. However, considerable evidence does exist that polymerization via metal alkyl coordination catalysts is anionic in nature.[15] If it is so assumed, it is readily seen that

TABLE III
Comparison of Properties of Polyethylene and Poly-1,5-Hexadiene

	Polyethylene		
	High density[a]	Low density[b]	Poly-1,5-hexadiene[c]
Tensile strength, psi	4330	2630	5420
Elongation, %	230	130	270
S.P./m.p., °C.	125/132	122/124	131/138
Density, g./cc.	0.949	—	1.122
Apparent modulus of elasticity, psi × 10^{-5}			
At 25°C.	0.80	0.41	—
At 0°C.	1.63	0.75	0.86
At −50°C.	3.00	2.24	2.00

[a] Ziegler type (Ethyl).
[b] Alkathene high density (ICI).
[c] From Run 9.

cyclopentane rings are formed if two consecutive primary or two consecutive secondary anions are formed. The primary anions, of course, would be the more likely. On the other hand the formation of cyclobutane rings or cyclohexane rings requires the alternate formation of primary and secondary anions, which *per se* is very unlikely, at least in a regular fashion. However, calculations have been made on the cyclobutane and cyclohexane ring systems to determine whether they could be ruled out on the basis of

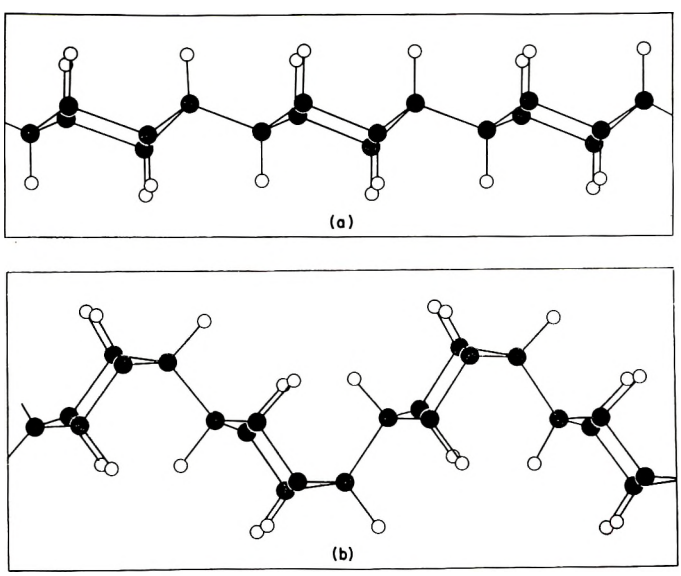

Fig. 2. Chain conformations of the 1,4-cyclohexane systems: (*a*) 1*e*, 4*e*-cyclohexane, repeating monomer distance = 4.36 A.; (*b*) 1*e*, 4*a*-cyclohexane, repeating monomer distance = 3.55 A., identity period = 7.10 A.

TABLE IV

System	Ring configuration	Chain conformation	Repeating monomer distance, A.	Most probable chain identity period, A.
1,4-Cyclohexane	*e*, *e* (Chair)	Linear, zigzag	4.36	4.36
	e, *a* (Chair)	Linear, zigzag	3.55	7.10
	a, *a* (Chair)	Linear, zigzag	3.55	3.55
1,2-Cyclobutane	*cis*[a]	Linear, zigzag	4.36	8.72
	cis[b]	Linear, zigzag	4.36	8.72
	cis[c]	Linear, zigzag	3.21	5.64
	trans[d]	Linear, zigzag	4.98	9.96
	trans[e]	Linear, zigzag	3.99	7.37
1,3-Cyclopentane	*cis*-Planar	Helix (?)	4.19	>6.5[f]
	cis-Half chair	Helix (?)	4.19	>6.5[f]
	trans-Envelope	Helix (?)	4.88	>6.5[f]
	trans-Planar	Linear, zigzag	4.88	9.76
	trans-Half chair	Linear, zigzag	~5.0	~10.0
	cis-Envelope	Linear, zigzag	4.93	4.93

[a] Where both cyclobutane carbons in the polymer backbone and the extranuclear carbons are planar *trans* and alternate cyclobutane rings are on opposite sides of the polymer chain.

[b] Same as in *a* except that alternate cyclobutane rings are on the same side of the polymer chain.

[c] Where one backbone and one nonbackbone cyclobutane carbons and the extranuclear carbons are planar *trans* and alternate cyclobutane rings are on opposite sides of the chain.

[d] Where both backbone cyclobutane carbons and the extranuclear carbons are planar *trans* and alternate cyclobutane rings are on opposite sides of the chain.

[e] Where one backbone and one nonbackbone cyclobutane carbons and the extranuclear carbons are planar *trans* and alternate cyclobutane rings are on opposite sides of the chain.

[f] Chain identity period of isotactic polypropylene.

the experimentally determined chain identity period, 4.80 A. A summary of these calculations is given in Table IV.

In considering the cyclohexane system the rings (chair form) must be interconnected in the 1,4-positions. When these positions are *e*,*e* (Fig. 2*a*) the "repeating monomer distance," herein defined as the distance from the beginning of one monomer unit to the beginning of the adjacent monomer unit, is 4.36 A., and this distance is also the most probable chain identity period. When the 1,4-positions are *e*,*a* (Fig. 2*b*) the repeating monomer distance is only 3.55 A., and the most probable chain identity period would

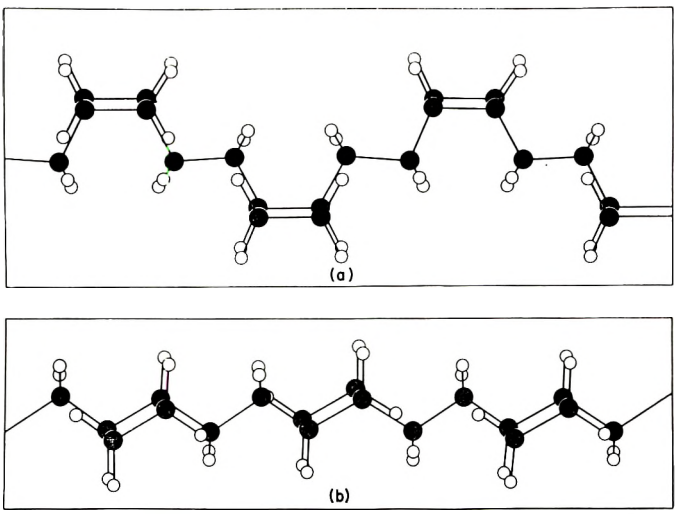

Fig. 3. Chain conformations of the 1,2-cyclobutane systems: (*a*) 1,2-*cis*-cyclobutane, repeating monomer distance = 4.36 A., identity period = 8.72 A.; (*b*) 1,2-*trans*-cyclobutane, repeating monomer distance = 4.98 A., identity period = 9.96 A.

be twice that, 7.1 A. When the 1,4-positions are *a,a* both the repeating monomer distance and the chain identity period are 3.55 A. On the basis of these calculated values and on the assumption that the poly-1,5-hexadiene chain must be linear, zigzag rather than helical, the cyclohexane system is ruled out as being the major repeating structural unit.

The cyclobutane system can also be ruled out on the basis of similar calculations. In the 1,2-cyclobutane system 36 chain conformations are theoretically possible as a result of *cis–trans* isomers, conformation about the C_{ring}–$C_{external}$ bond, conformation about the $C_{external}$–$C_{external}$ bond, and the positioning of alternate cyclobutane rings on the same or on opposite sides of the polymer chain. Of these possibilities only five will produce linear, zigzag polymer chain conformations (Table IV). The most probable chain conformation of the 1,2-*cis*-cyclobutane system (Fig. 3*a*) has a repeating monomer distance of 4.36 A. and a most probable chain identity period of 8.72 A. The most probable 1,2-*trans*-cyclobutane system (Fig. 3*b*) has a repeating monomer distance of 4.98 A. and a chain identity period of 9.96 A. Incidentally, only planar cyclobutane rings have been considered here. Spectroscopic studies show the unsubstituted cyclobutane ring to be planar.[10] It is possible that the substituted rings may be folded,[11,16] but even in that event the cyclobutane ring system can be ruled out as the chief recurring unit in the polymer chain.

In the remaining system, the cyclopentane system, it can be considered possible not only for the substituents to be either *cis* or *trans* but also for the ring to be planar or puckered into either a half-chair conformation or an envelope conformation. (The names envelope and half-chair are descriptive names originally suggested by Brutcher[17] and corresponding

to the C_s and C_2 symmetry forms, respectively, of cyclopentane). Considerations on a planar cyclopentane ring system are included here only to show that it can be excluded on the basis of these calculations and to serve as a comparison in subsequent considerations. Certainly, plentiful evidence is available for the existence of pseudorotation in cyclopentane and for the barriers to this pseudorotation in substituted cyclopentanes which exist in the most stable ring-puckered conformations.[12,18,19]

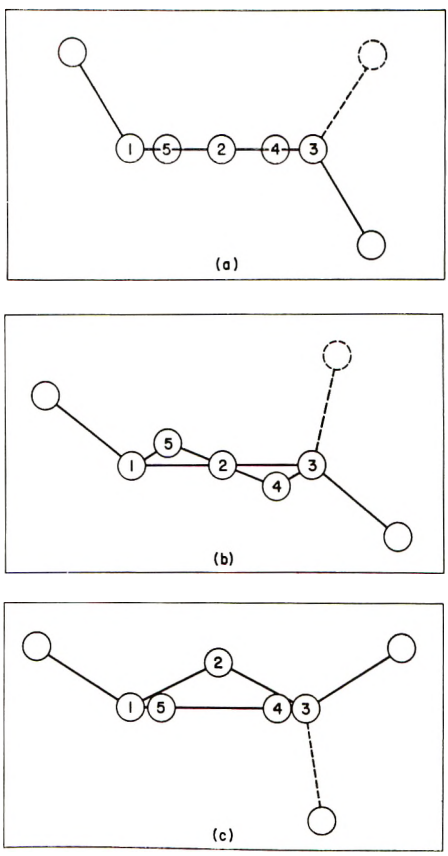

Fig. 4. The cyclopentane system: (*a*) planar conformation; (*b*) half-chair conformation, (*c*) envelope conformation.

The planar 1,3-cyclopentane ring system is illustrated in Figure 4*a*. If the substituents in this system are placed *cis*, then the repeating monomer distance is 4.19 A., and the polymer chain resulting from this recurring unit would most probably be of a helical nature. On the other hand, if the substituents are placed *trans* a linear, zigzag polymer can be obtained with a repeating monomer distance of 4.88 A. which closely corresponds to the experimentally determined chain identity period. However, as is illustrated in Figure 5*a*, the chain identity period of this linear, zigzag poly-

mer is twice the repeating monomer distance, i.e., 9.76 A. Obviously this rules out the planar cyclopentane system.

In considering the possible conformations for a half-chair or for an envelope 1,3-cyclopentane system, it should be remembered that the system must satisfy two requirements: It must have a repeating monomer distance of about 4.80 A., and it must have a chain identity period of about 4.80 A., i.e., in this instance, the polymer chain must be linear, zigzag. It

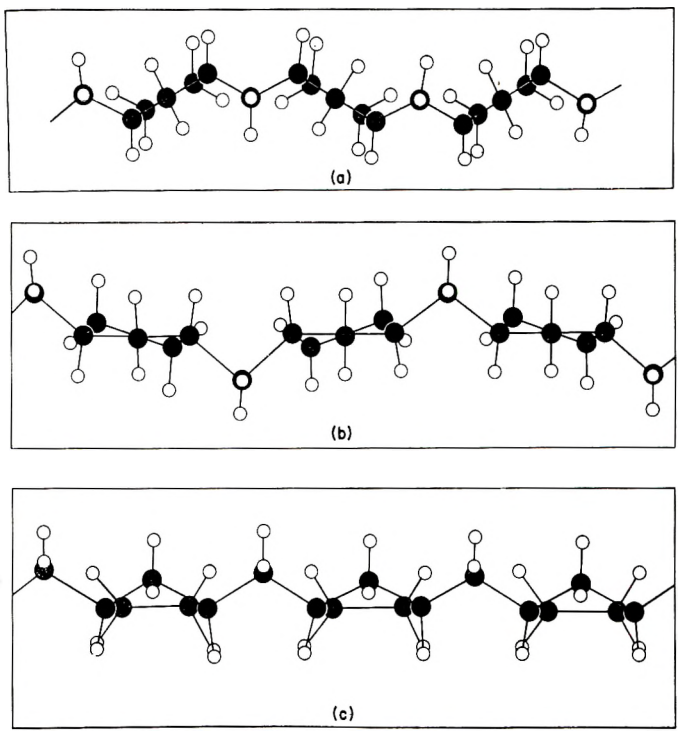

Fig. 5. Chain conformations of the 1,3-cyclopentane systems: (*a*) 1,3-*trans*-cyclopentane, planar ring conformation, repeating monomer distance = 4.88 A., identity period = 9.76 A.: (*b*) 1,3-*trans*-cyclopentane, half-chair ring conformation, repeating monomer distance ~5.0 A., identity period ~10.0 A.; (*c*) 1,3-*cis*-cyclopentane, envelope ring conformation, repeating monomer distance = 4.93 A., identity period = 4.93 A.

follows that it will be necessary for puckering to identically affect the displacement of the methylene groups, i.e., that the displacement be symmetrical.

One of the possible half-chair forms for the 1,3-cyclopentane ring system is illustrated in Figure 4*b*. Here C_5 is above the ring and C_4 at an equal distance below the ring. When the substituents are placed in the *cis* configuration it makes no difference which of these carbon atoms is above and below the plane. The repeating monomer distance for the *cis* system remains constant for symmetrical and reasonably small puckering. The

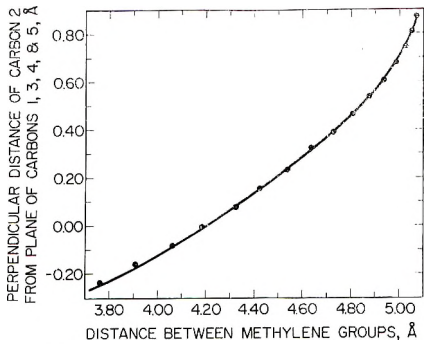

Fig. 6. The 1,3-*cis*-cyclopentane system, envelope ring conformation. Pucker vs. repeating monomer distance.

value of this repeating monomer distance is the same as that obtained in the *cis* planar cyclopentane system, i.e., 4.19 A. Another fact ruling out this system is that the polymer chain resulting from this recurring unit would most probably be helical. In the *trans* half-chair system, when C_5 is above and C_4 below the plane, the distance between the methylene groups increases thereby increasing the repeating monomer distance over that obtained in the *trans* planar cyclopentane system. Its most stable conformation would result in a repeating monomer distance of at least 5.0 A. A linear, zigzag chain can be obtained with this system (Fig. 5*b*); however, the chain identity period is twice that of the repeating monomer distance, at least 10.0 A. When the puckering in the *trans* system is reversed, i.e., when C_5 is below and C_4 is above the plane of the ring, the distance between the methylene groups decreases over that obtained in *trans* planar cyclopentane, 4.88 A. Again a linear, zigzag chain can be obtained with this system, but the chain identity period is twice that of the repeating monomer distance, i.e., somewhat less than 9.64 A. Consequently all three possibilities with a C_4, C_5 half-chair cyclopentane conformation are ruled out.

In the cyclopentane envelope system, puckering on any ring carbon except C_2 will result in an unsymmetrical displacement of the methylene substituents and, in most cases, the improper repeating monomer distance. When C_2 is puckered and the substituents are placed *trans* (Fig. 4*c*) the distance between the methylene groups remains relatively constant with pucker, i.e., about the same as that obtained in the *trans* planar cyclopentane system. Although this value of about 4.88 A. corresponds closely to the experimentally determined value of the chain identity period, the polymer chain resulting from such a recurring unit would most probably be helical, at least it would not be linear, zigzag.

When the substituents in the 1,3-cyclopentane system are placed *cis* (Fig. 4*c*), pucker of C_2 into an envelope form exerts a marked effect on the distance between the methylene groups. In addition the displacement of the methylene groups is perfectly symmetrical. The change in distance

between the methylene groups with the change in perpendicular distance of C_2 from the plane of C_1, C_3, C_4, and C_5 is plotted in Figure 6. The calculations of the conformation of cyclopentane and the relative positions of substituents thereon were made according to the procedure of Pitzer and Donath.[12] As the plot shows, at zero pucker, i.e., when the ring is planar, the distance between methylene groups is 4.19 A. When C_2 is out of the plane of the other four ring carbons at a distance of 0.46 A., the distance between the methylene substituents is 4.80 A. However, a linear, zigzag polymer chain cannot be well constructed. In order for this model to give a linear, zigzag structure the C_{ring}–$C_{methylene}$–C_{ring} bond angle would have to be about 100°. This bond angle would be expected to be at least tetrahedral, if not somewhat larger, based on the fact that the zigzag angle in polyethylene is 112°.[20] In order for this bond angle to be tetrahedral, a displacement of C_2 above the plane of the other four of 0.61 A. is required. With this extent of pucker the distance between the methylene substituents is 4.93 A. With this model as the repeating unit a linear, zigzag chain conformation is obtained as illustrated in Figure 5*c*. It is interesting to note that the equilibrium displacement of C_2 in the 1,3-*cis*-cyclopentane model is below 0.75 A., the point at which the C_2, C_3 and C_2, C_1 axial bonds are *trans* and coplanar. The fit of the calculated value from the Pitzer mathematical model[12] with that of the experimental value is considered to be good. Relatively minor and energetically inexpensive changes in internal bond angles would be sufficient to arrive at a value closely coincident with that obtained experimentally. It is therefore, concluded that the major repeating unit in poly-1,5-hexadiene is the *cis*-1-methylene-3-cyclopentyl group wherein the cyclopentane ring is in an envelope form. The system where poly-1,5-hexadiene is depicted as being composed primarily of these units and a minor amount of uncyclized monomer fits all the known facts. This system accounts for polymer physical properties, such as density and flexibility, and for the experimentally determined chain identity period.

Substantiating evidence for the correctness of the structure of poly-1,5-hexadiene as outlined here is available from the work of Truett, et al. on polynorbornene.[21] It was found that norbornene could be polymerized with a $LiAlR_4/TiCl_4$ catalyst system to a crystalline polymer. It was postulated on the basis of chemical and infrared evidence that norbornene polymerized via a ring opening reaction with the retention of unsaturation to give polymer chains composed of cyclopentane rings linked in a *cis*-1,3-fashion with *trans*-CH=CH groups.

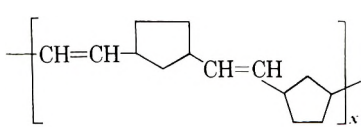

Thus polynorbornene is similar to poly-1,5-hexadiene in that both polymers contain the 1,3-*cis*-cyclopentane system as part of the major repeating

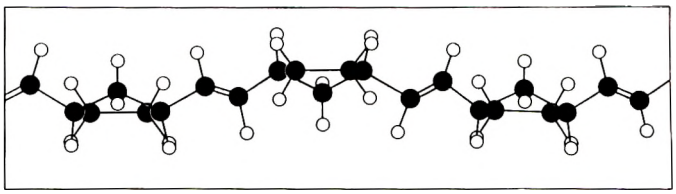

Fig. 7. Most probable chain conformation of polynorbornene. Identity period = 11.8 A.

unit. This grouping should have identical dimensions in both polymers. Polynorbornene was found to have a chain identity period of 11.8 A. which the authors say corresponds to two monomer units. Using the chain identity period of poly-1,5-hexadiene (4.80 A.) as the distance between methylene groups in the 1,3-*cis*-cyclopentane portion of the polynorbornene chain, a chain identity period of 11.75 A. was calculated for polynorbornene which, of course, corresponds exactly to the experimentally determined chain identity period.

In performing this calculation it was assumed that C_2 and C_3 of one cyclopentane ring, the CH=CH group, and C_1 and C_2 of the adjacent cyclopentane ring are all in the same plane. In this conformation the maximum distance along the chain axis is achieved. Other conformations about the

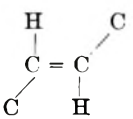

single bonds will produce linear, zigzag structures but with chain identity periods always less than 11.75 A. The conformation with the six carbon atoms coplanar would be the expected one. For example, *trans*-1,4-polypentadiene has a chain identity period of 4.8 A. which corresponds to a linear, zigzag, planar structure[22] virtually identical to that assumed for these polynorbornene segments. It should be pointed out, however, that the polynorbornene backbone is not perfectly planar. Only the six-carbon segments are coplanar, and these coplanar segments intersect at an angle of about 155° with each other. The polynorbornene chain is illustrated in Figure 7.

As pointed out by Huggins,[23] poly-1,5-hexadiene may possess a ribbon-like structure which he theorizes for planar, zigzag structures, such as polyethylene, in order to explain several apparently anomalous phenomena. Indeed, if this ribbon phenomenon is due to the steric repulsion of 1,3-hydrogen atoms as Huggins suggests, then the ribbon effect should be even more pronounced in poly-1,5-hexadiene where (assuming Pitzer's model of cyclopentane is correct) the distance between the centers of the hydrogen atoms on adjacent cyclopentane rings is considerably shorter (ca. 1.8–2.1

A.) than the 2.54 A. distance in polyethylene. This can be visually depicted in Figure 5*c*.

With the large number and wide variety of presently available coordination catalysts, it might be possible to prepare a poly-1,5-hexadiene wherein the methylene substituents are *trans* rather than *cis*. In this event it is predicted that the cyclopentane ring conformation from considerations on the *cis* polymer chain would be a C_4, C_5 half-chair conformation and the resultant chain conformation would be linear, zigzag with a chain identity period of approximately 10 A.

The authors wish to thank Mr. H. W. Dougherty for his experimental assistance and Dr. E. Tornqvist for some of the catalyst preparations.

References

1. Butler, G. B., and R. J. Angelo, *J. Am. Chem Soc.*, **79**, 3128 (1957).
2. Marvel, C. S., *J. Polymer Sci.*, **48**, 101 (1960).
3. Butler, G. B., *J. Polymer Sci.*, **48**, 279 (1960).
4. Marvel, C. S., and J. K. Stille, *J. Am. Chem. Soc.*, **80**, 1740 (1958).
5. Ethyl Corporation, "Technical Information on Aluminum Alkyls and Alkyl Aluminum Halides," February 1959.
6. Tornqvist, E., and A. W. Langer, Jr., U. S. Pat. 3,032,510 (May 1, 1962); A. W. Langer, Jr., and E. Tornqvist, U. S. Pat. 3,032,511 (May 1, 1962); E. Tornqvist, A. W. Langer, Jr., and C. W. Seelbach, French Pat. 1,173,537 (October 27, 1958).
7. *ASTM Standards on Plastics*, American Society for Testing Materials, Philadelphia, Pa., September 1958.
8. *Natl. Bur. Std. Circ. 539*, **5**, 37 (October 21, 1955).
9. Andrews, E. R., and R. G. Eades, *Proc. Roy. Soc. (London)*, **A216**, 398 (1953).
10. Wilson, T. P., *J. Chem. Phys.*, **11**, 369 (1943).
11. Lemaire, H. P., and R. L. Livingston, *J. Am. Chem. Soc.*, **74**, 5732 (1952).
12. Pitzer, K. S., and W. E. Donath, *J. Am. Chem. Soc.*, **81**, 3213 (1959).
13. Reding, F. P., *J. Polymer Sci.*, **21**, 547 (1956).
14. Natta, G., P. Corradini, and M. Cesari, *Atti. Accad. Nazl. Lincei, Rend. Classe Fiz. Sci. Mat. Nat.*, **21**, 365 (1956).
15. Gaylord, N. G., and H. F. Mark, *Linear and Stereoregular Addition Polymers: Polymerization with Controlled Propagation*, Interscience, New York, 1959.
16. Owen, T. B., and J. L. Hoard, *Acta Cryst.*, **4**, 172 (1951).
17. Brutcher, F. V., Jr., T. Roberts, S. J. Barr, and N. Pearson, *J. Am. Chem. Soc.*, **81**, 4915 (1959).
18. Kilpatrick, J. E., K. S. Pitzer, and R. Spitzer, *J. Am. Chem. Soc.*, **69**, 2483 (1947).
19. McCullough, J. P., R. E. Pennington, J. C. Smith, I. A. Hossenlopp, and G. Waddington, *J. Am. Chem. Soc.*, **81**, 5880 (1959).
20. Bunn, C. W., *Trans. Faraday Soc.*, **35**, 482 (1939).
21. Truett, W. L., D. R. Johnson, I. M. Robinson, and B. A. Montague, *J. Am. Chem. Soc.*, **82**, 2337 (1960).
22. Natta, G., L. Porri, P. Corradini, and D. Morero, *Chim. Ind. (Milan)*, **40**, 362 (1958).
23. Huggins, M. L., *J. Polymer Sci.*, **50**, 65 (1961).

Résumé

On polymérise le 1,5-hexadiène avec des catalyseurs alcoyl-métallique de coordination en polymères cristallins ayant des propriétés combinées intéressantes. Ces polymères sont cristallins, ont une haute force de tension, un point de fusion élevé, une haute

densité et sont très flexibles. Le poly-1,5-hexadiène présente une périodicité identique de 4.80 A. et se définit le mieux comme étant constitué d'unités 1-méthylène-3-cyclopentyle dans lesquels les substituants sont en *cis* et le noyau cyclopentane sous forme d'une enveloppe. Etant donné que toutes les unités monomériques dans la chaîne ne sont pas cyclisées le polymère ressemble plus à un interpolymère qu'à un homopolymère.

Zusammenfassung

1,5-Hexadien wurde mit einer Anzahl modifizierter MetallalkylKoordinationskatalysatoren zu kristallinen Polymeren mit einer ungewöhnlichen Kombination von Eigenschaften polymerisiert. Diese Polymeren sind kristallin, besitzen hohe Zugfestigkeit, hohen Schmelzpunkt und hohe Dichte und sind dennoch sehr flexibel. Poly-1,5-Hexadien hat eine Identitätsperiode von 4,80 A. und besteht hauptsächlich aus 1-Methylen-3-cyclopentyl-Einheiten, in denen die Substituenten in *cis*-Stellung stehen und der Cyclopentanring eine Envelop-Konformation einnimmt. Da nicht alle in die Kette eingebauten Monomereinheiten cyclisiert sind, ähnelt das Polymere mehr einem Interals einem Homopolymeren.

Received February 18, 1963
Revised March 11, 1963

JOURNAL OF POLYMER SCIENCE: PART A VOL. 2, PP. 1567–1585 (1964)

Coloration in Acrylonitrile Polymers

TOSHIHIRO TAKATA and IWAO HIROI, *Research Institute, Toho Rayon Co. Ltd., Tokushima, Japan*, and MASAKAZU TANIYAMA, *Toho Beslon Co. Ltd., Tokyo, Japan*

Synopsis

The heat coloration and alkali coloration of PAN was investigated with model compounds by measuring infrared absorption spectra and ultraviolet absorption spectra. Some of the information obtained from this work supported the opinion of Grassie et al., who proposed the formation of partly hydrogenated naphthyridine-type structure to explain the alkali coloration of PAN. The intramolecular ring closure mechanism of the initiation to propagate to the partly hydrogenated naphthyridine-type structure of heat-treated PAN proposed by Grassie et al., which, however, may involve the dehydrogenated structure somewhere, was supported, too. On the other hand, the formation of intermolecular azomethine-type crosslinking structure proposed by Schurz et al. was not supported by any results of the experiments with model compounds.

Since Houtz[1] proposed the formation of substituted pyridines, naphthyridines, and higher condensed systems to explain the heat coloration of polyacrylonitrile (PAN), many papers have been published to discuss those phenomena. Among them, Schurz and his co-workers[2] emphasized that the naphthyridine-type ring structure is purely hypothetical, never having been proved experimentally, and they proposed the formation of azomethine-type intermolecular crosslinking structure, while Grassie and his co-workers[3] proposed the formation of an intramolecular ring structure, which initiates the formation of partly hydrogenated naphthyridine-type structure.

In the base coloration of PAN, Schurz et al.[4] proposed the formation of intermolecular crosslinking structure like secondary amide bridge, while Grassie et al.[5] proposed the formation of the partly hydrogenated naphthyridine-type structure, which is initiated by nucleophylic reagents (OH^-, NH_2^-, etc.).

Overberger et al.,[6] too, presumed that the coloration of polymethacrylonitrile in the ionic polymerization with lithium amide in ammonia is due to the formation of the type of partly hydrogenated naphthyridine structure initiated by the NH_2 anion suggested by Grassie.

The present authors had synthesized model compounds[7,8] of PAN and its related compounds[9,11,12] to use for the investigation on the coloration of PAN described above. Thus were obtained somewhat obvious results, which answer the problems discussed by Schurz et al. versus Grassie et al.

RESULTS AND DISCUSSION

Changes of Structure by Alkali Treatment

2,4-Dicyano-*n*-pentane (I)[7] and 2,4,6-tricyano-*n*-heptane (II)[7], as the model compounds of PAN, had been treated with sodium amide[10] to form α,α'-dimethylglutaroimidine (IV), m.p. 209–210°C. (decomp.), from I, and octahydro-2,7-diimino-3,6-dimethyl-1,8-naphthyridine (VI), m.p. 222–224°C. (decomp.), from II,[11] as follows:

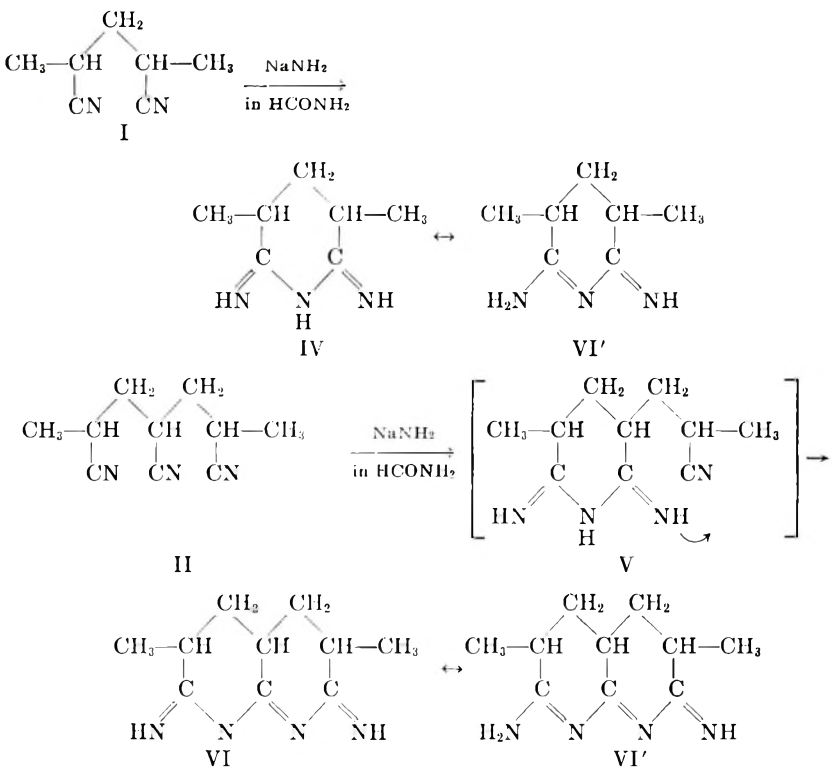

Since in this reaction compound V, regarded as an intermediate, was not actually isolated,[11,12] the reaction V → VI was presumably fast. These results support the speculation of Overberger et al., moreover, IV and VI are the model compounds of Grassie-type partly hydrogenated naphthyridine-like structure.

The solubility of VI in dimethylformamide (DMF) is very poor, therefore the formation of the ring structure in PAN molecule obviously relates to the insolubilization of colored PAN, and it is not proper to conclude that the insolubility of colored PAN is due to the formation of a crosslinked structure only.[2]

Then from IV and VI, respectively, 3,5-dimethylpyridine (VII),[12] b.p. 168–171°C., and 3,6-dimethyl-1,8-naphthyridine (VIII),[12] m.p. 191–192°C. were derived.

The infrared absorption spectra of the compounds described above were measured to permit comparison with the spectra of alkali-treated PAN, as shown in Figure 1.

As shown in Figure 1, though the fully aromatic naphthyridine (VIII) and pyridine (VII) have strong absorption bands at 10–15μ (1000–650

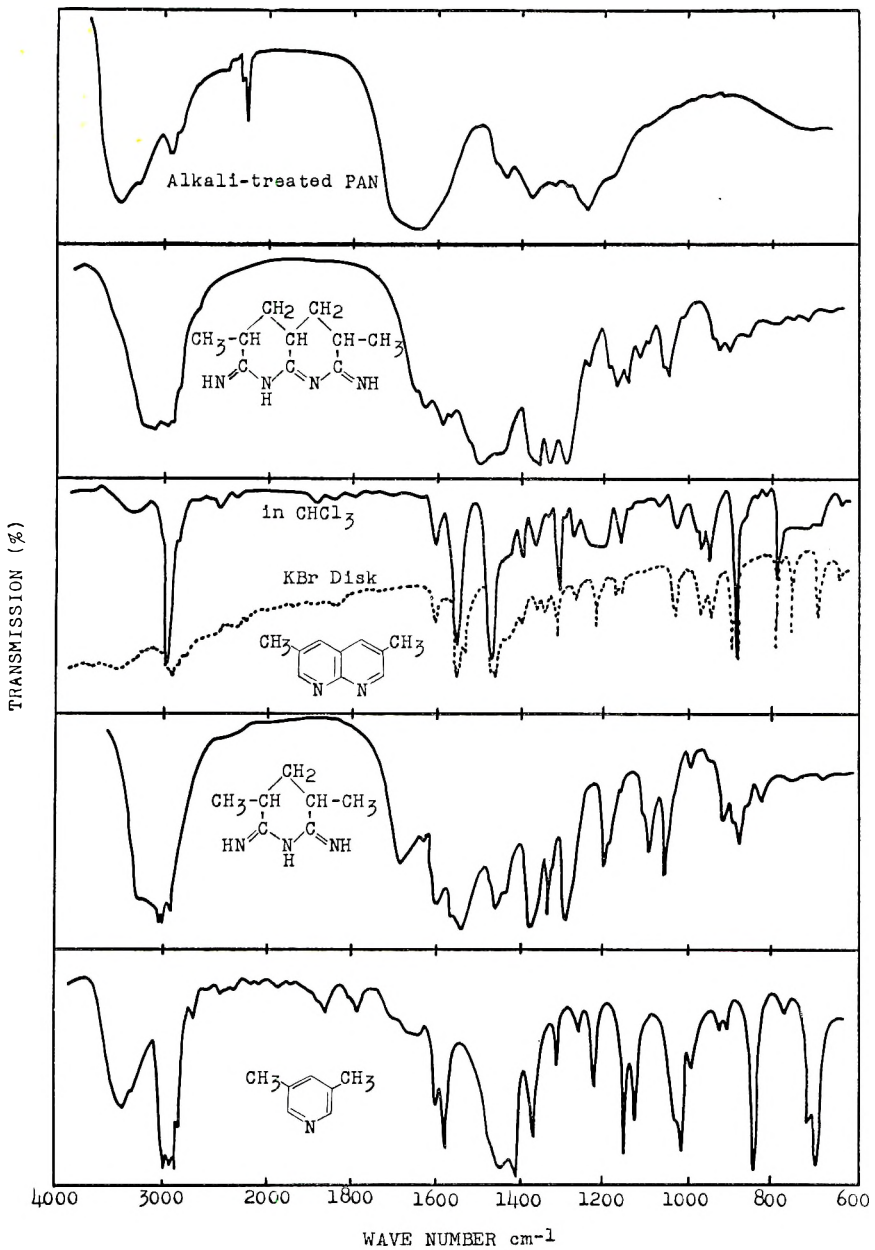

Fig. 1. Infrared absorption spectra of model compounds and alkali-treated PAN.

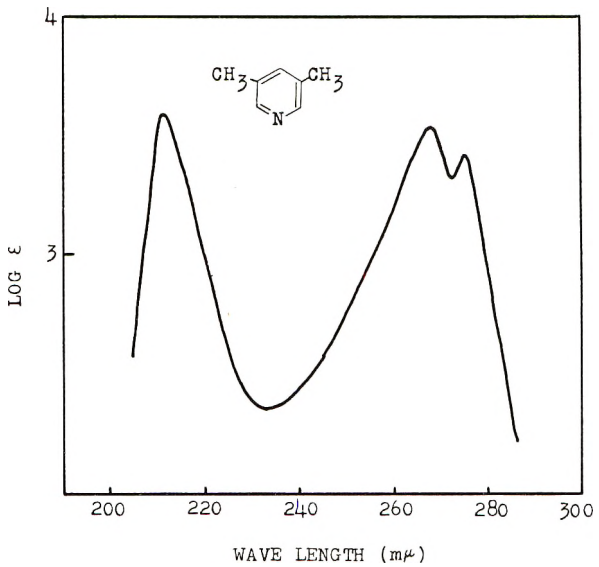

Fig. 2. Ultraviolet absorption spectrum of 3,5-dimethylpyridine (VII) in ethanol.

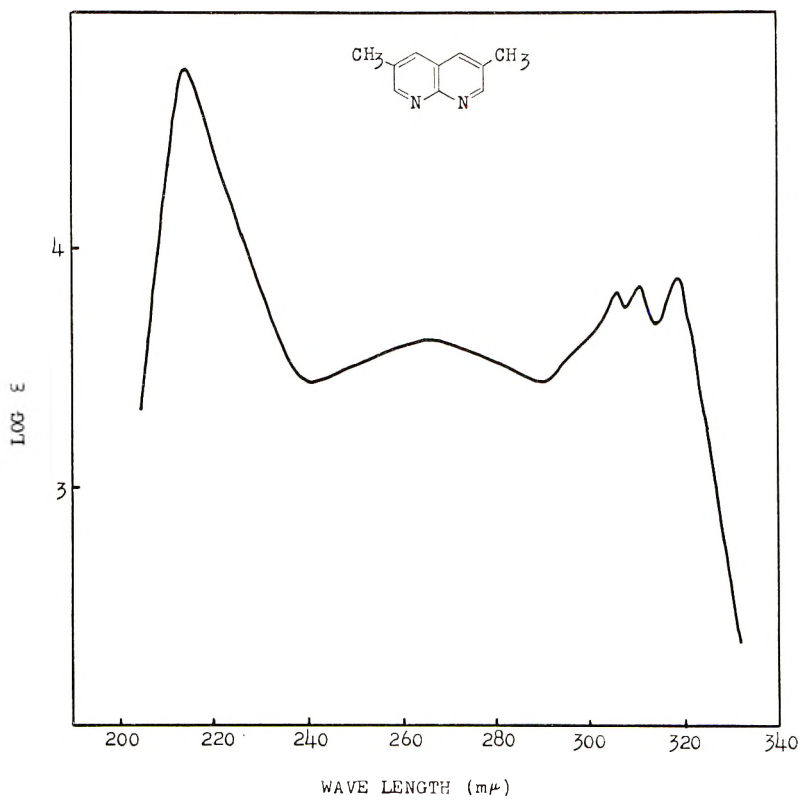

Fig. 3. Ultraviolet absorption spectrum of 3,6-dimethyl-1,8-naphthyridine (VIII) in ethanol.

TABLE I. Ultraviolet Absorption Maxima (λ_{max}) and Molecular Extinction Coefficient (ϵ_{max}) of Model Compounds

Formula	Solvent	λ_{max}, mμ	log ϵ_{max}	Note
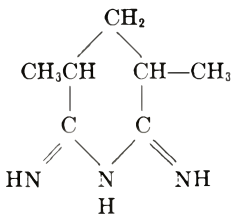	C_2H_5OH	254.5	4.33	
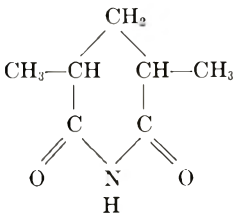	C_2H_5OH	209	3.89	Literature[14]
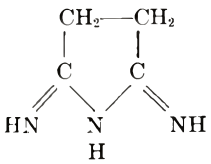	CH_3OH	237	4.30	Literature[10]
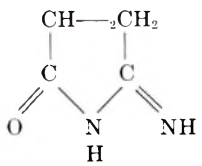	H_2O	227	4.31	Literature[11]
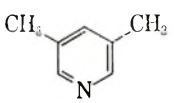	C_2H_5OH	212 268 275	3.59 3.53 3.41	See Fig. 2
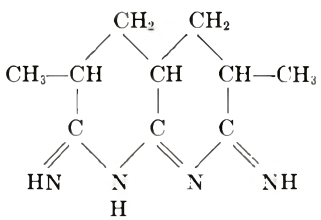	C_2H_5OH	300	3.39	
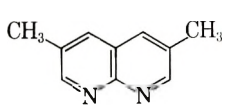	C_2H_5OH	211.5 265.5 306 311.5 319	4.76 3.62 3.82 3.85 3.88	See Fig. 3
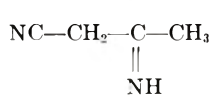	Hexane	259 (3860 mm.$^{-1}$)	4.28	Literature[19]
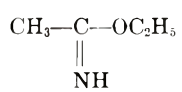	CH_3OH	253 (3940 mm.$^{-1}$)	1.10	Literature[19]

$cm.^{-1}$) as Schurz pointed out,[2] the model compounds IV and VI have not such strong bands in this region. This fact supports the opinion of Grassie et al.[13]

The ultraviolet absorption maxima of these compounds and related compounds are shown in Table I.

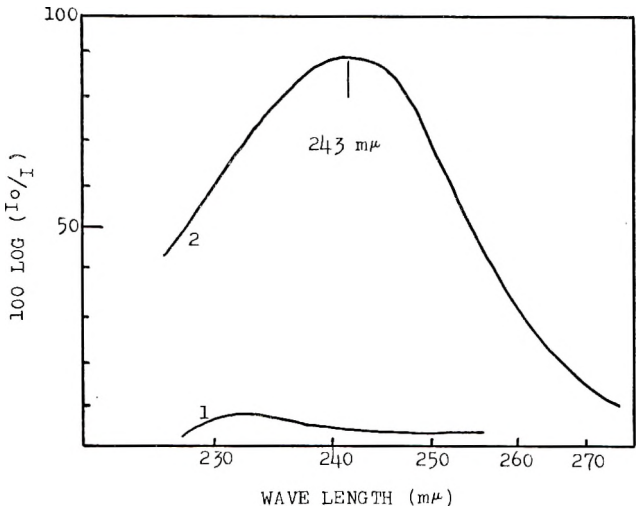

Fig. 4. Ultraviolet absorption spectra of 2,4-dicyano-*n*-pentane (I) measured at the concentration of 1370 mg./l. in ethanol mixed with $^1/_{10}$ volume (to 1 volume of ethanol) of 1.340*N* KOH–ethanol: (*1*) 6 min. after dissolving; (*2*) 37 hr. after dissolving.

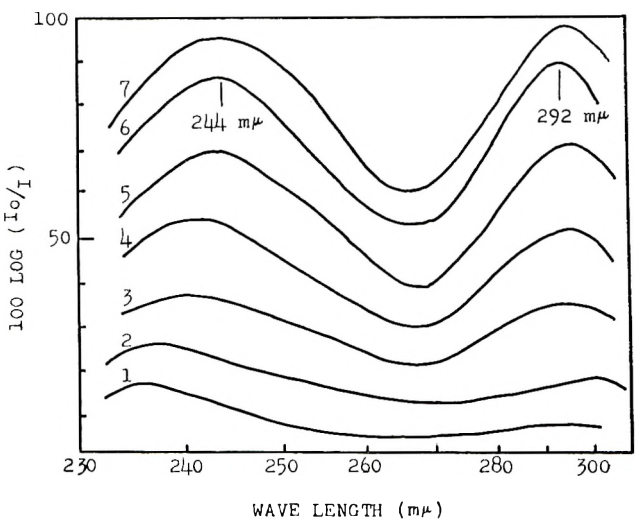

Fig. 5. Ultraviolet absorption spectra of 2,4,6-tri-cyano-*n*-heptane (II) measured at the concentration of 1070 mg./l. in ethanol mixed with $^1/_{10}$ volume (to 1 volume ethanol) of 1.340*N* KOH–ethanol: (*1*) 4.2 min. after dissolving; (*2*) 21.8 min. after dissolving; (*3*) 45.0 min. after dissolving; (*4*) 62.2 min. after dissolving; (*5*) 82.8 min. after dissolving; (*6*) 103.5 min. after dissolving; (*7*) 113.0 min. after dissolving.

The ultraviolet absorption spectra of VII and VIII agree with Bayzer and Skoda's results[20,21] dealing with substituted pyridines and substituted naphthyridines.

Next, 2,4-dicyano-*n*-pentane(I), 2,4,6-tricyano-*n*-heptane(II), and 2,4,6,-8-tetracyano-*n*-nonane(III) were treated with potassium hydroxide in ethanol, and the changes of their ultraviolet absorption spectra were observed as shown in Figures 4–6.

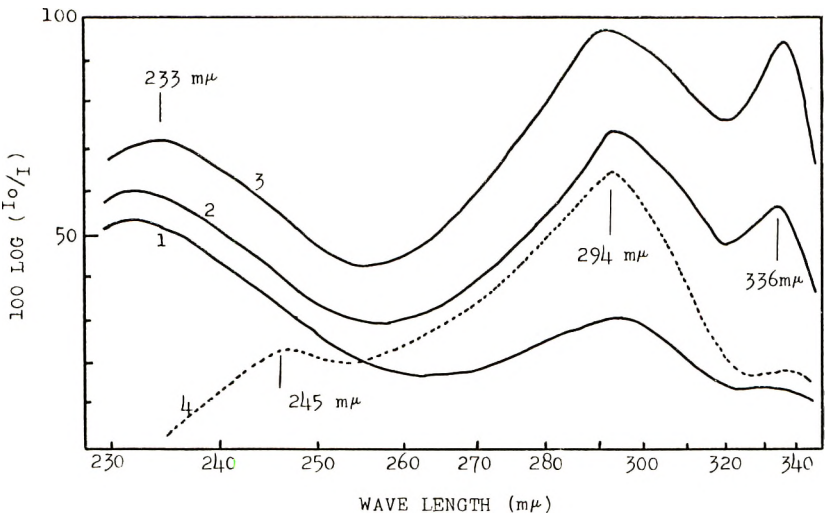

Fig. 6. Ultraviolet absorption spectra of 2,4,6,8-tetracyano-*n*-nonane (III) measured at the concentration of 500 mg./l. (curves *1–3*) and 95.4 mg./l. (curve *4*) in ethanol mixed with $^1/_{10}$ volume (to 1 volume ethanol) of 1.340*N* KOH–ethanol: (*1*) 2.5 min. after dissolving; (*2*) 12.5 min. after dissolving; (*3*) 22.5 min. after dissolving; (*4*) 43 hr. after dissolving.

It has been shown[14] that under such conditions as described here the absorption band at 233–245 mμ is due to the structures of the type

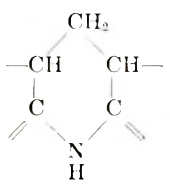

and that at 286–300 mμ is due to structures of the type:

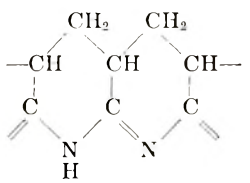

Then the absorption band at 336 mμ, shown in the case of III (Fig. 6), is presumably due to the structures

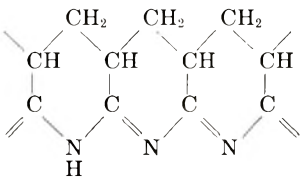

According to Bayzer and Schurz,[4] the alkali-treated PAN film had an absorption band increasing at 30,000 cm.$^{-1}$ (333 mμ). This band is perhaps due to the same structure having absorption maxima at 336 mμ as mentioned above (Fig. 6).

Though they presumed the formation of intermolecular secondary amide bridge having absorption bands at 3401 cm.$^{-1}$ (2.94 μ), 1667 cm.$^{-1}$ (6.0 μ) and 1570 cm.$^{-1}$ (6.37 μ) when PAN was treated with aqueous alkaline solution,[15] this was not observed[14] when the model compounds such as I, II, III and containing amide groups were treated with potassium hydroxide, but there was formation of a ring structure as described above. Acrylonitrile copolymer having a primary amide group has absorption bands[23] near 3400 cm.$^{-1}$ and 1670 cm.$^{-1}$, and compound IV has a strong band at 1540–1570 cm.$^{-1}$ (Fig. 1). Therefore from those absorption bands the formation of secondary amide crosslink can not be concluded.

When model compounds[7,9] were treated in DMF with potassium hydroxide, the formation of such a ring structure proceeded more rapidly[11] than in ethanol.

The ring formation in alkaline medium was accelerated by an amide group[14] attached to the main molecular chain instead of one of the nitrile groups. This effect of the amide group is comparable to the fact that the PAN which was treated alkali and hydrochloric acid successively, was recolored with alkali more rapidly than the original PAN,[4] because the former should have amide groups.

Thus the hypothesis of Grassie et al. on the alkali coloration of PAN is supported by the results of experiments with model compounds.

Changes of Structure by Heat Treatment

The formation of azomethine-type intermolecular crosslink[2] as follows has been proposed by Schurz et al.:

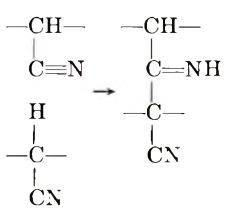

while Grassie et al.[3] proposed the formation of an intramolecular ring, from which the hydrogenated naphthyridine-type structure is propagated as follows:

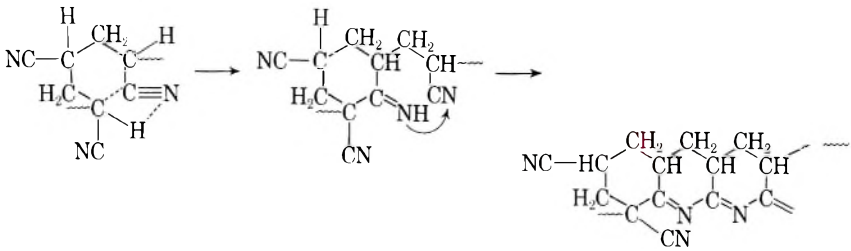

Schurz et al.[2] have been pointed out that the heat-treated PAN has no strong absorption band at 10–15μ (1000^{-1}–650 cm.$^{-1}$) and has an absorption maximum at 37,000 cm.$^{-1}$ (270 mμ), whereas substituted naphthyridines have strong absorption bands at 10–15μ and absorption maxima at 330–300 mμ (30,000–33,000 cm.$^{-1}$) and 233–217 mμ (43,000–46,000 cm.$^{-1}$).

On the other hand, Grassie et al.[3,13] have emphasized that the heat coloration almost coincided with the alkali coloration in the formation of the hydrogenated naphthyridine-type structure except for the initiation step described above, so it is natural that the differences of absorption spectra were observed between fully aromatic structure and heat-treated PAN.

On the problem of absorption spectra the findings shown in Figure 1 and Table I support Grassie's opinion. However, since the hydrogenated naphthyridine-type structure may be propagated from Schurz's intermolecular azomethine crosslink,[5] the heat treatments of model compounds I, II, and III were carried out, and the resulting samples were submitted to the measurement of infrared and ultraviolet absorption spectra to discuss the change of structure.

In this case the model compounds separated into the stereoisomers[8] as mentioned in Table II were used.

TABLE II
Model Compounds of Polyacrylonitrile

Formula	No.	M.p., °C.	Optical activity
$CH_3CHCH_2CHCH_3$ (CN, CN)	Ia	Liquid at room temp.	
	Ib	55	
$CH_3CHCH_2CHCH_2CHCH_3$ (CN, CN, CN)	IIa	45–46	Active
	IIb	80–81	Inactive
$CH_3CHCH_2CHCH_2CHCH_2CHCH_3$ (CN, CN, CN, CN)	IIIa	130–132	Active
	IIIb	158	Inactive

The infrared absorption spectra of heat-treated model compounds and of heat-treated PAN are shown in Figures 7–13.

The absorption maxima in ultraviolet absorption spectra of heat-treated model compounds are given in Table III.

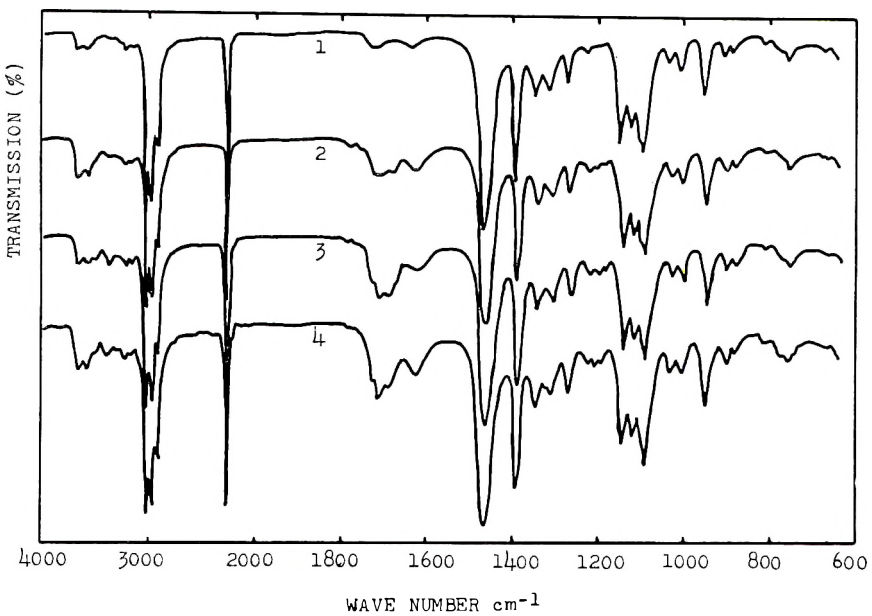

Fig. 7. Infrared absorption spectra of 2,4-dicyano-*n*-pentane (Ia): (*1*) original; (*2*) treated at 200°C. for 9 hr.; (*3*) treated at 250°C. for 9 hr.; (*4*) treated at 300°C. for 6 hr.

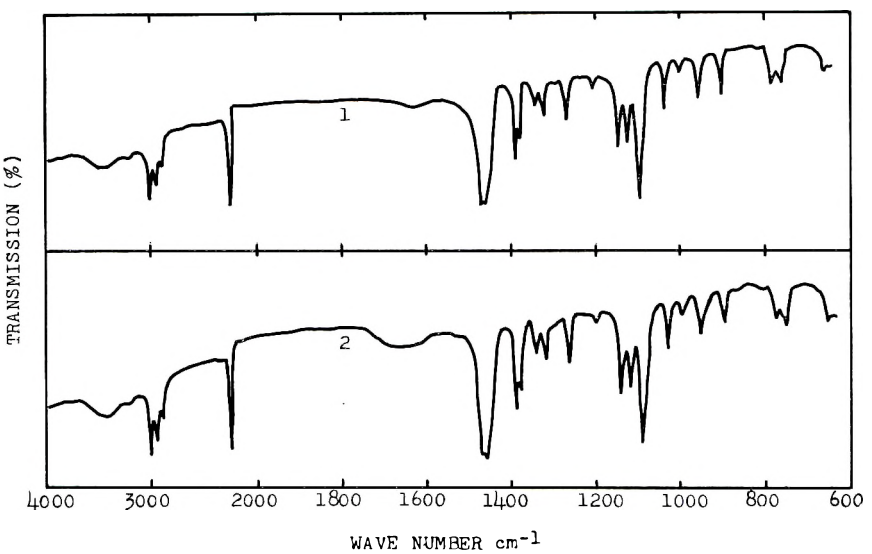

Fig. 8. Infrared absorption spectra of 2,4-dicyano-*n*-pentane (Ib): (*1*) original; (*2*) treated at 300°C. for 6 hr.

TABLE III
Ultraviolet Absorption Maxima (λ_{max}) and Molecular Extinction Coefficient (ϵ_{max}) of Heat-Treated Model Compounds in Ethanol

	200°C.			250°C.			300°C.		
Compound	Time, hr.	λ_{max}, mμ	log ϵ	Time, hr.	λ_{max}, mμ	log ϵ	Time, hr.	λ_{max}, mμ	log ϵ
Ia	0	209	1.38						
	9	210	1.73	9	209.5	1.64	6	209.5	1.18
Ib	0	—	—						
	9	—	—	9	211	1.20	6	210.5	1.95
IIa	0	—	—						
	9	210.5	1.41	9	210	1.23	6	210	1.23
IIb	0	—	—						
	9	210	1.11	9	209	1.36	6	209.5	1.53
IIIa	0	209	2.34						
					209	4.11		210	3.75
	9	209	2.23	9	235	4.08	6	234	3.84
					322	3.83		320	3.23
IIIb	0	—	—						
	9	—	—	9	210.5	2.74	6	233	4.11
					232	2.77			

These observations indicate that if an azomethine-type intermolecular crosslinking structure of the type proposed by Schurz et al. could be formed, its formation should occur in the heat-treatment of compounds I and II. However in the ultraviolet absorption spectra of heat treated I and II no absorption band of azomethine structure (at 3860 mm.$^{-1}$ mentioned in Table I) reported by Schurz et al.[19] was observed (Table III).

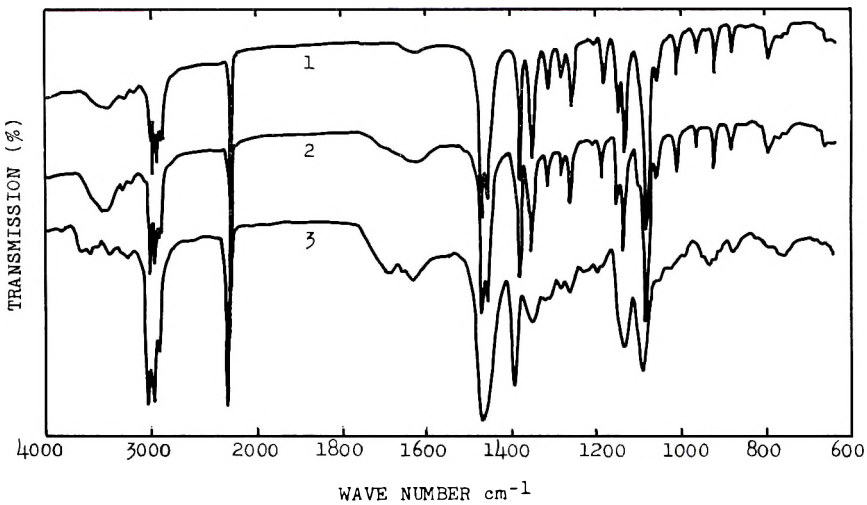

Fig. 9. Infrared absorption spectra of 2,4,6-tricyano-*n*-heptane (IIa): (*1*) original; (*2*) treated at 250°C. for 9 hr.; (*3*) treated at 300°C. for 6 hr.

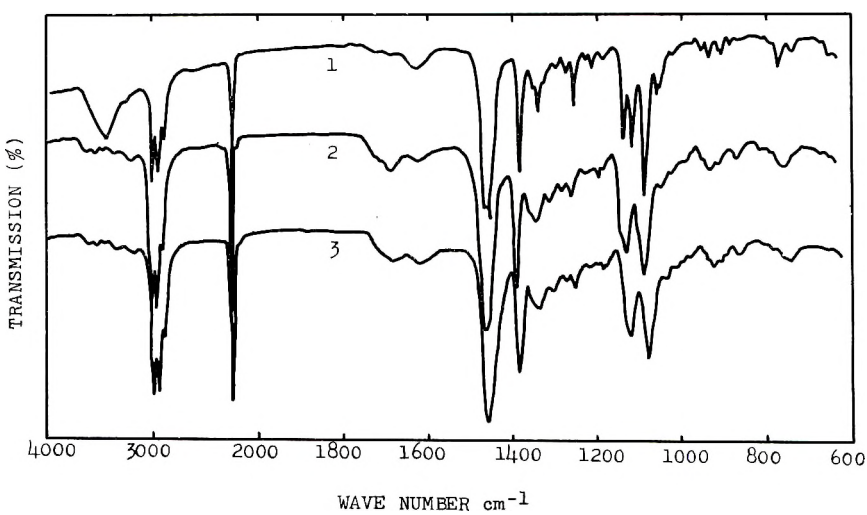

Fig. 10. Infrared absorption spectra of 2,4,6-tricyano-*n*-heptane (IIb): (*1*) original; (*2*) treated at 250°C. for 9 hr.; (*3*) treated at 300°C. for 6 hr.

If the following reaction could occur as soon as the azomethine structure was formed,

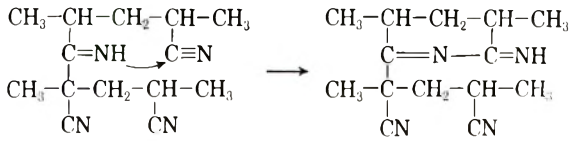

this product should have a stronger absorption band in the ultraviolet and infrared region than that observed here.

Schurz et al. observed absorption maxima at 26,500 cm.$^{-1}$ (377 mμ) and 37,500 cm.$^{-1}$ (267 mμ) in the DMF extracts of heat-treated PAN.[16] These bands are probably due to the by-products of the heat treatment. The main products should remain in the insoluble part.

Moreover Schurz et al. reported that the hydrochloric acid extracts of colored insoluble PAN heat-treated in the presence of ammonia had an absorption maximum at 4800 mm.$^{-1}$ (208 mμ) which agreed with that of hydrochloric acid extract of PAN heat-treated in the absence of ammonia.[17] It is probably due to the formation of a glutaroimide ring having an absorption maximum near 210 mμ, because the glutaroimide ring is formed from the structure

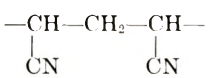

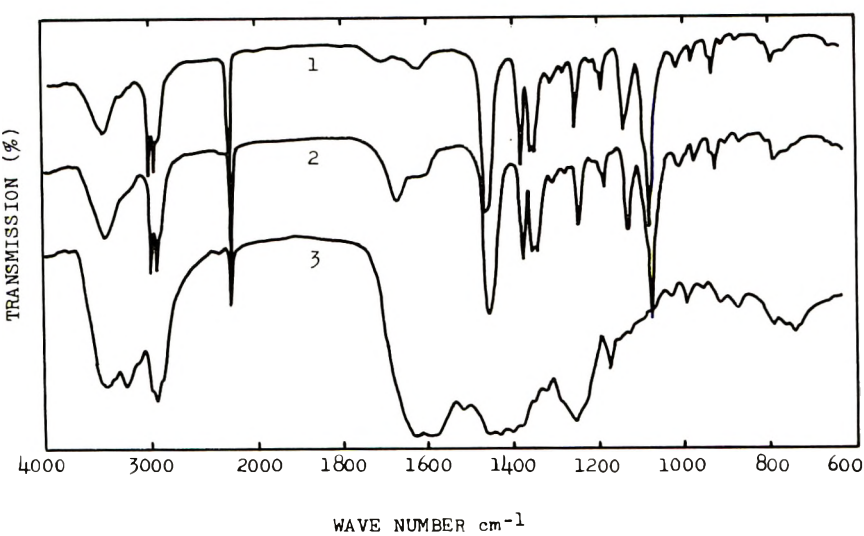

Fig. 11. Infrared absorption spectra of 2,4,6,8-tetracyano-*n*-nonane (IIIa): (*1*) original; (*2*) treated at 200°C. for 9 hr.; (*3*) treated at 250°C. for 9 hr.

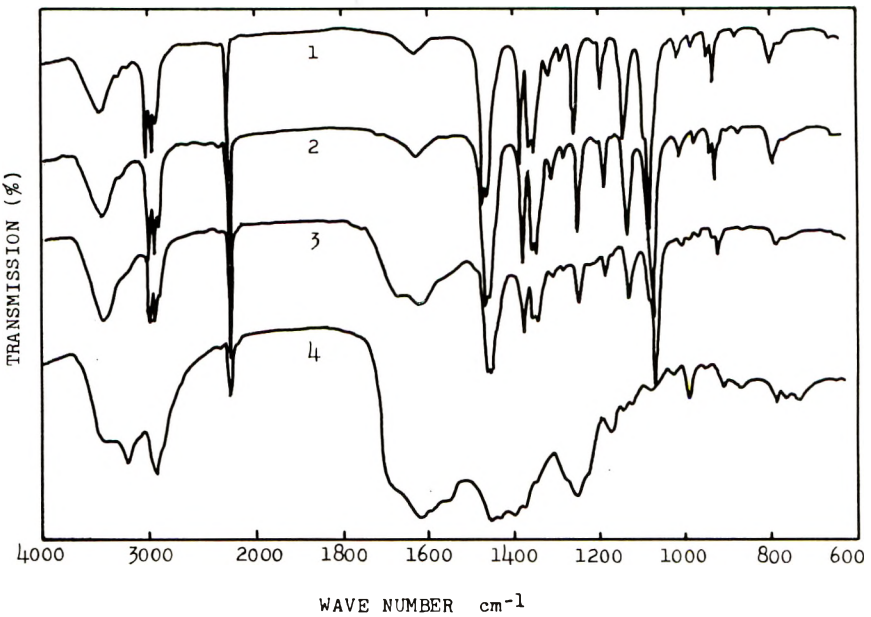

Fig. 12. Infrared absorption spectra of 2,4,6,8-tetracyano-*n*-nonane (III*b*): (*1*) original; (*2*) treated at 200°C. for 9 hr.; (*3*) treated at 250°C. for 9 hr.; (*4*) treated at 300°C. for 6 hr.

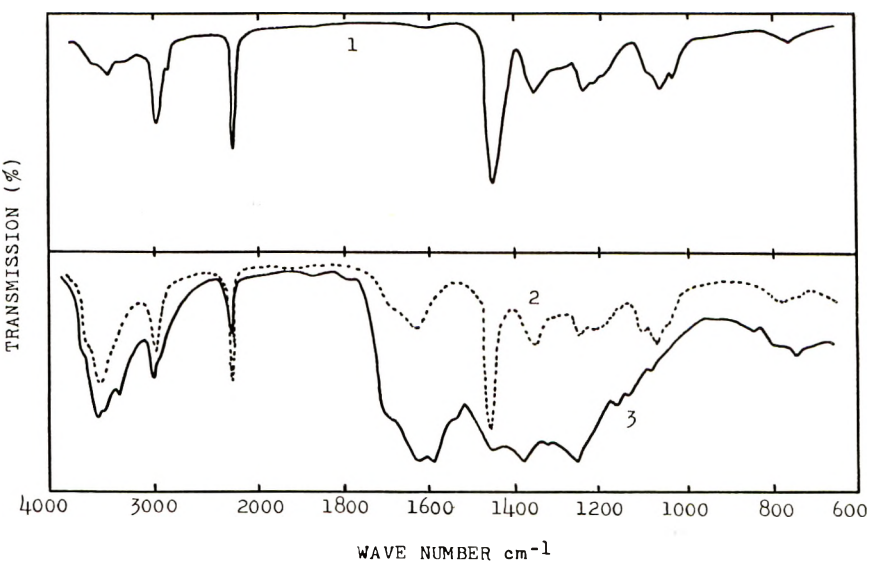

Fig. 13. Infrared absorption spectra of polyacrylonitrile (PAN): (*1*) original; (*2*) treated at 200°C. for 0.5 hr.; (*3*) treated at 200°C. for 9 hr.

by treatment with hydrochloric acid,[11] and the structure

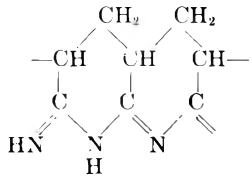

presumably yields the glutaroimide ring in the treatment with hydrochloric acid as follows:

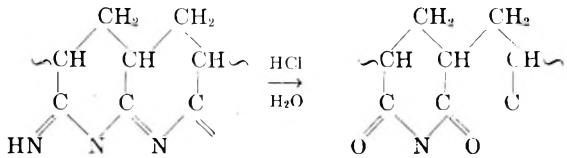

If the initiation step proposed by Grassie et al.[3] is applied to the model compounds, the scheme may proceed as follows:

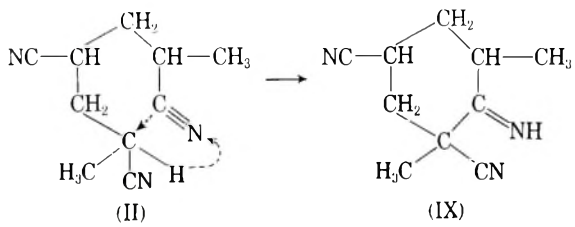

(II) (IX)

1-Imino-2,6-dimethyl-4,6-dicyanocyclohexane

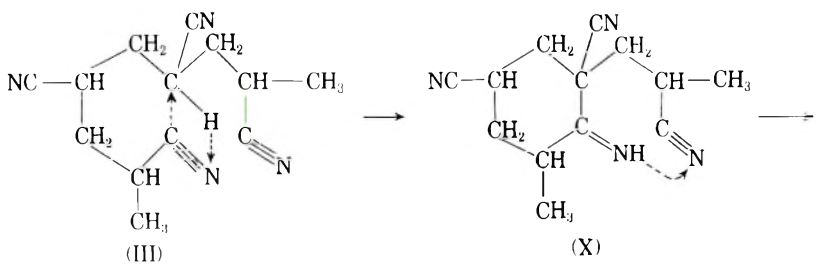

(III) (X)

1-Imino-2,4-dicyano-6-methyl-2-(2-cyano-*n*-propyl)cyclohexane

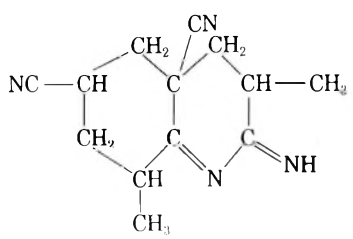

(XI)

2-Imino-3,9-dimethyl-5,7-dicyano-2,3,4,5,6,7,8,9-octahydroquinoline

Though none of the compounds IX, X, and XI has yet been isolated, the infrared and the ultraviolet spectra described above show that the reaction II → IX has not proceeded to any great extent but the reaction III → XI has proceeded.

However if IX was formed, the infrared spectrum at 1500–1800 cm.$^{-1}$ would not change remarkably, since cyclohexanone oxime[18] has no absorption band in this region except at 1665 cm.$^{-1}$.

The results shown in Figures 11 and 12 and Table III show the probability of the reaction III → X → XI at >250°C. Moreover the difference of configuration[8] has a greater influence upon the reactivity in the heat treatment, where IIIb was more stable than IIIa. In Grassie's initiation step mentioned above the configuration would influence the reaction velocity of ring formation, which agrees with those results.

In summary, these are the facts which support the hypothesis of Grassie et al.[3] in the heat treatment of model compounds.

Further, in the heat treatment of the model compounds having amide, carboxyl, and ester group[9] the ring formation had been accelerated by nucleophilic groups[22,23] in the molecules, as mentioned by Grassie et al.[5] Among them, though it had been observed that the methyl carboxylates were stable to heat,[24] the structure

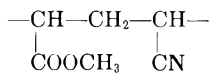

was converted by heat treatment into the glutaroimide ring, with elimination of ethylene.[23] This suggests the possibility of the mechanism shown below owing to the nitrile group at the β-position to methyl ester group.

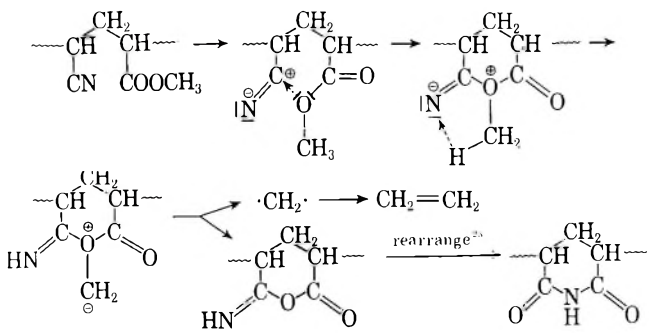

On the other hand, there are several other opinions. For example, dehydrogenation occurs in the heat treatment of PAN at 100–120°C. in air before the reaction involving the nitrile function,[26] and the triazine structure is formed in the heat treatment of PAN,[27] and the fully aromatic naphthyridine-type structure is formed by the dehydrogenation of the hydrogenated naphthyridine-type structure.[28] In the present paper these phenomena were not considered, but in the synthesis of hydrogenated 1,8-

naphthyridine, the analogous dehydrogenation occurred to form aromatic rings under some conditions.[12,22]

Saum's study on the nitrile dipole pair bond[31] suggests the difficulty of formation of the intermolecular azomethine-type crosslinking structure.

Finally, with respect to the difference between accessibilities of heat-treated and alkali-treated PAN to hydrochloric acid[2] it may be considered that the partly hydrogenated naphthyridine-type structure proposed by Grassie et al. should be easily hydrolyzed[29] with hydrochloric acid, but the heat-treated PAN should have dehydrogenated structures (aromatic structure)[12,22,26,28,30] somewhere, which exhibits different stabilities to hydrochloric acid.

Though in this paper the effects of abnormal structure, which may be present in polymer, were not considered, it should be important especially in the study on heat treatment of PAN to consider the presence of abnormal structure.

EXPERIMENTAL

Measurements of Infrared Absorption Spectra

Infrared spectral measurements were carried out with a Hitachi EPI Type-2 spectrophotometer and NaCl prism on KBr disk or liquid film according to the state of the sample, whether solid or liquid.

Measurements of Ultraviolet Absorption Spectra

Ultraviolet spectroscopy was carried out with a Hitachi EPS Type-2 spectrophotometer and quartz cell (1 cm. thickness).

Heat Treatment of Sample

About 300 mg. of sample was heated at 200, 250, or 300°C. in a sealed glass tube of 8 mm. diameter and 70 mm. length.

The authors express gratitude to the Toho Rayon Co. Ltd. for allowing them to publish this paper, and are grateful to Mr. Y. Nishiyama and Mr. K. Kubo, who helped them with the infrared spectra work, and to the Department of Applied Chemistry of Tokushima University, who allowed them to use the ultraviolet absorption spectrophotometer.

References

1. Houtz, R. C., *Textile Res. J.*, **20**, 786 (1950).
2. Schurz, J., *J. Polymer Sci.*, **28**, 438 (1958).
3. Grassie, N., and J. N. Hay, *J. Polymer Sci.*, **56**, 189 (1962).
4. Bayzer, H., and J. Schurz, *Z. Physik. Chem. (Frankfurt)*, **13**, 30 (1957).
5. Grassie, N., and I. C. McNeill, *J. Polymer Sci.*, **39**, 211 (1959).
6. Overberger, C. G., E. M. Pearce, and N. Mayes, *J. Polymer Sci.*, **34**, 109 (1959).
7. Takata, T., and M. Taniyama, *Kobunshi Kagaku*, **16**, 693 (1959).
8. Takata, T., H. Ishii, Y. Nishiyama, and M. Taniyama, *Kobunshi Kagaku*, **18**, 235 (1961).

9. Takata, T., and M. Taniyama, *Kobunshi Kagaku*, **18**, 240 (1961).
10. Elvidge, J. A., and R. P. Linstead, *J. Chem. Soc.*, **1954**, 445.
11. Takata, T., *Kobunshi Kagaku*, **19**, 641 (1962).
12. Takata, T., *Bull. Chem. Soc. Japan*, **35**, 1438 (1962).
13. Grassie, N., J. N. Hay, and I. C. McNeill; *J. Polymer Sci.*, **31**, 205 (1958).
14. Takata, T., *Kobunshi Kagaku*, **19**, 653 (1962).
15. Bayzer, H., and J. Schurz, *Z. Physik. Chem. (Frankfurt)*, **13**, 223 (1957).
16. Skoda, W., J. Schurz, and H. Bayzer, *Z. Physik. Chem. (Leipzig)*, **210**, 35 (1959).
17. Schurz, J., A. Ullich, and H. Zah, *Monatsh. Chem.*, **91**, 741 (1960).
18. Bredereek, H., A. Wagner, D. Hummel, and H. Kreiselmeier, *Chem. Ber.*, **89**, 1532 (1956).
19. Schurz, J., E. Treiber, and H. Toplak, *Z. Elektrochem.*, **60**, 67 (1956).
20. Bayzer, H., *Monatsh. Chem.*, 88, 72 (1957).
21. Skoda, W., and H. Bayzer, *Monatsh. Chem.*, **89**, 5 (1958).
22. Takata, T., *Kobunshi Kagaku*, **19**, 682 (1962).
23. Takata, T., *Kobunshi Kagaku*, **19**, 690 (1962).
24. Araki, J., *Nippon Kagaku Zasshi*, **79**, 496 (1958); C. D. Hurd and F. H. Blunck, *J. Am. Chem. Soc.*, **60**, 2421 (1938); W. J. Bailey and C. King, *J. Am. Chem. Soc.*, **77**, 75 (1955).
25. Allendorf, O., *Chem. Ber.*, **24**, 2346 (1891).
26. Conley, R. T., and J. F. Bieron, *Am. Chem. Soc. Div. Paint, Plastics, Printing Ink Chem., Preprints*, **20**, No. 1, 325 (1960).
27. Fukui, K., and T. Yamabe, *J. Polymer Sci.*, **45**, 305 (1960); Slrepikheev and Derevitskaya, *Osnovyi Khimii Vysokomolekulyarnkh Soedinenii*, Moscow, 1961, pp. 230–262.
28. Topchiev, A. V., M. A. Gayderikh, B. E. Davydov, V. A. Kargin, B. A. Krentsel, I. M. Kustanovich, and L. S. Polak; *Chem. Ind. (London)*, **1960**, 184.
29. Overberger, C. G., H. Yuki, and N. Urakawa, *J. Polymer Sci.*, **45**, 127 (1960).
30. Burlant, W. J., and J. L. Parsons, *J. Polymer Sci.*, **22**, 249 (1956).
31. Saum, A. M., *J. Polymer Sci.*, **42**, 57 (1960).

Résumé

La coloration du PAN due à la chaleur ou au milieu alcalin a été étudiée à l'aide de composés modèles, en mesurant les spectres d'absorption infrarouge et des spectres d'absorption ultra-violette. Certaines informations obtenues dans ce travail confirment l'opinion de Grassie et collaborateurs qui proposent, pour expliquer la coloration du PAN en milieu alcalin, la formation d'un composé de structure du type de la naphthyridine partiellement hydrogénée. On a également confirmé la mécanisme d'initiation avec cyclisation intramoléculaire, qui donne lieu, lors du chauffage du PAN, à la formation d'une structure du type de la naphthyridine partiellement hydrogénée comme l'ont proposé Grassie et ses collaborateurs; ce mécanisme peut cependant comprendre à un moment donné une structure déhydrogenée. Lex expériences effectuées avec des composés modèles n'ont, par contre, jamais confirmé, dans leurs résultats, la formation d'une structure intermoléculaire pontée du type azométhine, proposée par Schurz et collaborateurs.

Zusammenfassung

Die Hitze- und Alkaliverfärbung von PAN wurde anhand von Modell-verbindungen durch Messung der IR- und UV-Absorptionsspektren untersucht. Gewisse bei dieser Untersuchung erhaltene Ergebnisse stützen die Ansicht von Grassie u. Mitarb., die zur Erklärung der Alkali-verfärbung von PAN die Bildung partiell hydrierter naphthyridinartiger Strukturen vorschlagen. Ebenso wurde der von Grassie u. Mitarb. vorgeschlagene Mechanismus eines intramolekularen Ringschlusses gestützt, der die Bildung

von partiell hydrierten naphthyridinartigen Strukturen von hitzebehandeltem PAN einleitet, an dem aber an irgendeiner Stelle auch die dehydrierte Sgruktur beteiligt sein kann. Andererseits lieferte keines der an den Modellverbindungengewonnenen experimentellen Ergebnisse eine Stütze für die von Schurz u. Mitarb. vorgeschlagene Bildung einer Struktur mit intermolekularer Vernetzung vom Azomethintyp.

Received February 28, 1963

JOURNAL OF POLYMER SCIENCE: PART A VOL. 2, PP. 1587–1594 (1964)

Rubber Elasticity in Highly Crosslinked Polyesters

DOV KATZ* and ARTHUR V. TOBOLSKY, *Frick Chemical Laboratory, Princeton, University, New Jersey*

Synopsis

Three unsaturated polyesters were crosslinked with different amounts of styrene, and for the resulting polymers the 10-sec. shear modulus was measured as a function of temperature. It was observed that the polymers have well defined glassy, transition, and rubbery regions. The equation for the shear modulus from the theory of rubber elasticity was applied for the plateau regions of the polymers.

This work is a continuation of our studies in the field of viscoelastic behavior of highly crosslinked systems with the same aim of finding the correlation between the structure and properties of the system.[1–3]

The present investigation was carried out on three unsaturated polyesters crosslinked by polymerization with different amounts of styrene. Each one of the polymers thus obtained has a 10-sec. shear modulus–temperature curve with well defined glassy, transition, and rubbery plateau regions. We tried to apply the concepts of the theory of rubber elasticity for the plateau regions.

The three unsaturated polyesters, kindly supplied by the American Cyanamid Company, were prepared from the monomers in the ratios shown and had the number-average molecular weight shown in Table I.

TABLE I

Sample	Supplier's designation	Composition (mole)			Molecular weight
		Propylene glycol	Maleic anhydride	Phthalic anhydride	
P_I	S-4857-58	1	1	—	1800
P_{II}	B-133-23	2	1	1	1550
P_{III}	B-409-28	3	2	1	1400

The number of unsaturated residues per polyester molecule is 12, 4, and 6 for polyesters, P_I, P_{II}, and P_{III}, respectively. The average molecular weights between the double bonds in polyesters P_I, P_{II}, and P_{III} are approximately 156, 362, and 259, respectively.

It is well known that varying amounts of isomerization of the double

* On leave from the Scientific Department, Israel Ministry of Defence.

bonds occurs during the esterification process, depending on conditions.[4] We were informed by the supplier of these resins that although the alkyds we used were prepared from maleic anhydride, the double bonds found in the resulting unsaturated polyesters are substantially all of the fumarate type.[5] We shall accordingly for simplicity use the term fumarate units to refer to all the segments of polyester which originated from the maleic anhydride, and this may include minor amounts of maleate units.

The crosslinking reaction occurs by a vinyl-type copolymerization between styrene and the double bonds of the polyester. The unsaturated bonds of the polyester do not react among themselves, and the polyester molecules can be crosslinked only through bridges of one or more styrene molecules. A complication occurs in certain cases when nontransparent polymers, probably heterogeneous mixtures of the crosslinked polyester and the styrene homopolymer, are obtained as the products of the reaction. The structure of the homogeneous polymers depends on the amount of styrene used, and three possibilities can be considered.

(*1*) The molar amount of styrene is equal to the molar amount of unsaturated bonds in the polyester. In this case ideally all polyester double bonds will be interconnected by single styrene units because of the alternating tendency of styrene and fumarate double bonds. This assumption is considered justified from chemical evidence.[5] In this case the network chain consists of the portion of the polyester between fumarate units.

(*2*) The molar amount of styrene is smaller than the molar amount of unsaturated groups in the polyester. The reacted double bonds are bridged by single styrene units. In this case the network chains are longer than the average distance between neighboring fumarate units in the polyester molecule.

(*3*) The molar amount of styrene is larger than the molar amount of unsaturated bonds in the polyester. We assume that in this case the styrene residues joining the maleic residues will be randomly distributed in length and the average number of styrene units in the polystyryl bridges is equal to the molar ratio of styrene to maleic anhydride residues. Here the polystyryl bridges may also act as network chains if they are sufficiently long. In the appendix we consider the effect of the "free ends" of the polyester emanating from the first and the last double bond in the polyester chains.

Experimental

The monomer mixtures were prepared by weighing and mixing of adequate amounts of polyester uninhibited styrene, 0.006% cobalt added in the form of a 6% solution of Co naphthenate (Nuodex Products Company) and 0.5% Lupersol DDM, a 60% solution of methyl ethyl ketone peroxide in dimethyl phthalate (Wallace and Tiernan, Inc.). The percentages of the catalyst and promoter were calculated on the total amount of monomers. The mixture was cast into aluminum foil molds, polymerized at room temperature in an atmosphere of CO_2 for 24 hr., and post-

TABLE II

Sample No.	P_I, wt.-%	Density d, g./cm.^{3}	Mole ratio s/m	m, moles/cm.^{3}	G, dynes/cm.^{2a}	Φe
1	70	1.241	0.64	0.00557	4.35×00^8	3.13
2[b]	65	1.232	0.81	0.00513	5.83×10^8	
3[b]	60	1.229	1.00	0.00473	6.30×10^8	
4[b]	50	1.206	1.50	0.00387	6.50×10^8	

[a] Measured at $T = 470°K.$

[b] Opaque sample.

cured for 2 hr. at 105°C. The samples were used for determination of the relation of the 10-sec. Gehman modulus versus temperature and their specific density was measured by displacement. The molar ratios of styrene to maleic anhydride are listed in Tables II–IV.

In the experiments with polyester P_I, as the molar ratio of styrene to the polyester increased the polymers showed increasing opacity. Only sample one was completely clear. The opacity in the other samples was probably due to the existence of heterogeneous mixtures of the crosslinked polymers with polystyrene homopolymer.

The polymers of P_{III} behaved similarly. Samples 1 and 2 were completely clear, the others showed increasing opacity.

TABLE III

Sample No.	P_{II}, wt.-%	Density d, g./cm.^{3}	Mole ratio s/m	m, moles/cm.^{3}	G, dynes/cm.^{2a}	Φez	Φe
1	70	1.227	1.49	0.002373	9.82×10^7	1.22	1.22
2	65	1.225	1.87	0.002200	1.10×10^8	1.46	1.46
3	60	1.214	2.32	0.002012	1.35×10^8	2.06	2.06
4	50	1.193	3.48	0.001648	1.14×10^8	2.03	2.03
5	40	1.145	5.22	0.001265	8.32×10^7	1.93	
6	30	1.139	8.12	0.000944	6.45×10^7	2.00	
7	20	1.129	13.92	0.000624	3.18×10^7	1.50	

[a] Measured at $T = 410°K.$

TABLE IV

Sample No.	P_{III}, wt.-%	Density d, g./cm.^{3}	Mole ratio s/m	m, moles/cm.^{3}	G, dynes/cm.^{2a}	Φez	Φe
1	70	1.241	1.07	0.003354	2.50×10^8	1.99	1.99
2	60	1.217	1.66	0.002819	2.94×10^8	2.79	2.79
3[b]	50	1.170	2.49	0.002259	3.00×10^8		
4[b]	40	1.167	3.74	0.001802	2.06×10^8		

[a] Measured at $T = 450°K.$

[b] Opaque samples.

All of the samples from polyester II were completely clear. Shear moduli were measured by a modified form of the Gehman instrument.[6]

Discussion of Results

The 10-sec. shear moduli plotted in the form of log G versus temperature are shown in Figures 1–3. Some calculated numerical results discussed later are given in Tables II–IV.

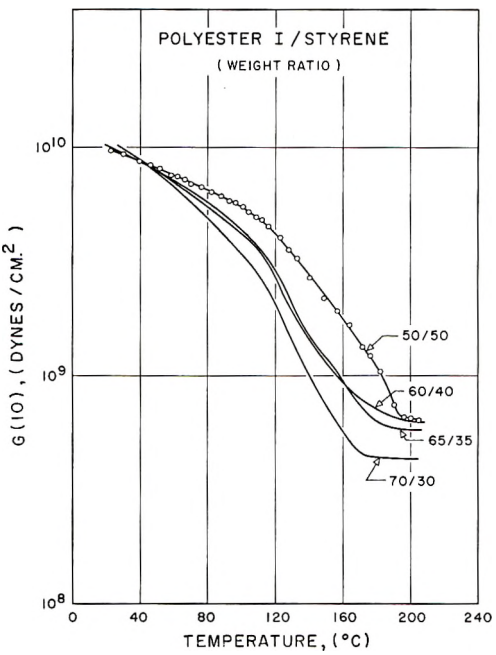

Fig. 1. Modulus-temperature curves for the system polyeste I/styrene.

The graphs show that all of the polymers exhibit a glassy region, transition region, and rubbery plateau region of viscoelastic behavior.

It is our particular concern to test the applicability of the theory of rubber elasticity to these highly crosslinked systems in the region of the rubbery plateau. We applied the equation

$$G = \Phi nRT \tag{1}$$

In eq. (1) n is the concentration of network chains per cubic centimeter, R is the gas constant, T is the absolute temperature, and Φ is the "front factor" discussed in earlier publications.[7] For an ideal rubber, Φ should be unity at all temperatures. For a nonideal rubber Φ may differ from unity; also Φ may or may not depend on temperature. For each sample a suitable temperature T in the rubbery plateau region was chosen at which to apply eq. (1). These temperatures are indicated in the tables.

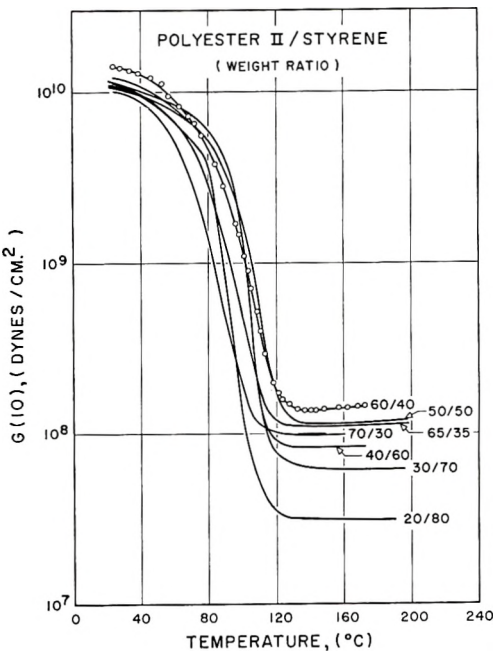

Fig. 2. Modulus–temperature curves for the system polyester II/styrene.

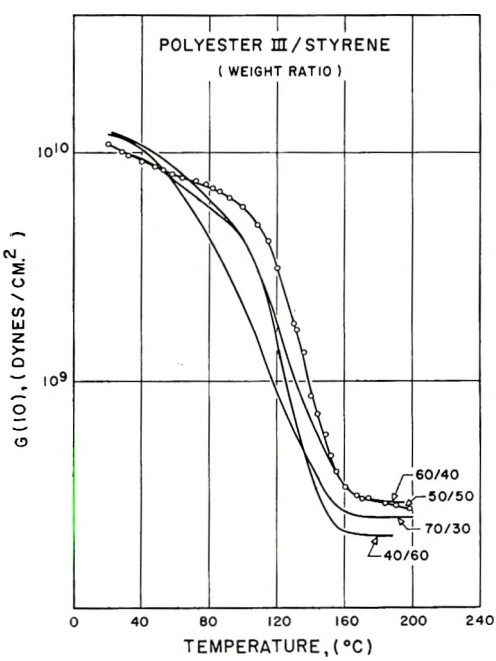

Fig. 3. Modulus–temperature curves for the system polyester III/styrene.

The major problem is to relate the concentration of network chains to the known concentration of fumarate residues or of styrene residues.

We consider the moles of network chains n per cubic centimeter of crosslinked polymer as related to the number of moles m per cubic centimeter of fumarate units or to the number of moles s of styrene per cubic centimeter.

In the case that s is smaller or equal to m, then

$$n = es \qquad s \leqq m \qquad (2)$$

In the case that s is larger than m, we have

$$me < n < 2me \qquad s > m \qquad (3)$$

We therefore can rewrite eq. (1) as follows:

$$G = \Phi esRT \qquad s \leqq m \qquad (4)$$

$$G = \Phi ezmRT \qquad s > m \qquad (5)$$

In eq. (5), z varies between 1 and 2, depending on whether the polystyryl bridges are sufficiently long to count as network chains.

In eqs. (2)–(5) the quantity e is introduced in the sense of a crosslink efficient, or, more exactly, as a measure of the deviation of the actual structure from our idealized model. For example, when $s < m$ it is possible that in spite of the alternating tendency in this type of vinyl polymerization that some of the bridges connecting fumarate residues contain more than one styrene residue. In this case e would be less than unity. When $s > m$ it is possible that some of the fumarate units are nevertheless not reacted. In this case e would again be less than unity. If our model of the structure is an exact one, e should be unity.

A chemical estimation of e is in principle possible by hydrolytic cleavage of the crosslinked network. No data pertinent to the samples we used are as yet available. We believe that e is close to unity because of the chemical probability of our model and because of the results we described below.

Equations (4) and (5) were applied to the data presented in Tables II–IV. Where eq. (4) applies, Φe can be obtained directly from the equation and from the data presented in the tables. The calculated values of Φe are tabulated for these cases, i.e., for s/m smaller than or equal to one.

Where eq. (5) applies, Φez can be obtained directly from the equation and from the data presented in the tables. The calculated values of Φez are tabulated for these cases, i.e., for s/m larger than unity.

For s/m between 1 and 3.5 we assume that the shortness of the polystyryl bridges between the fumarate units is such that they cannot count as network chains. We have in these cases assumed that z is equal to unity and tabulated both Φez and Φe.

For all cases presented in the tables both Φe and $\Phi \epsilon z$ lie between 1.2 and 3.1. We believe that this indicates that both Φ and e are of the order of magnitude of unity.

We consider it very interesting that the portions of the polyester chains between fumarate double bonds are sufficiently long to act as rubbery network chains, and that the deviation from ideal rubber elasticity (with a front factor of unity) is so relatively small.

In fact, if for an unknown sample of this type the equation for ideal elasticity were assumed, i.e.,

$$G = nRT \tag{6}$$

the concentration of network chains could be calculated within a factor of two or three.

In the case of ethyl acrylate crosslinked with ethylene glycol dimethacrylate we have shown that up to 12 mole-% of dimethacrylate, corresponding to very short polyethyl acrylate chains, the shear modulus obeys eq. (1) with a front factor of unity.[2]

In previous studies[7] we have shown that the front factor of rubber networks depends on the structure of the repeating unit of the polymer chain. For crosslinked polymethyl methacrylate the front factor is 1.5; for crosslinked polystyrene 1.7; for crosslinked polyacrylates or polymethacrylates with long alkyl side chains the front factors are considerably less than unity.[7] We have also shown in as yet unpublished work that the front factors for these various systems remain relatively constant up to 12 mole-% of dimethacrylate crosslinks.

The results obtained on the crosslinked polyesters can perhaps be examined somewhat more critically in the light of these results.

For polyester II the molecular weight between fumarate units is 362. The quantity Φe is 1.6 $\pm$ 0.4. Perhaps in this case the deviation of the front factor from unity is characteristic of the particular chain structure.

For polyesters I and III the molecular weights between fumarate units are 156 and 259, respectively, and the values of Φe are 3.1 and 2.4 $\pm$ 0.4, respectively. Perhaps in these cases the deviations of the front factors from unity are in part characteristic of the particular chain structure, but also partly due to the tightness of the crosslinking.

Appendix

For simplicity the discussion of the number of network chains per fumarate unit was presented for a hypothetical case where the polyester molecule has a very large number of fumarate groups. Practically, the number of fumarate residues in a polyester molecule is not very large; in the cases considered in this paper between four and twelve. The number z of network chains per opened fumarate bond in the resin will depend to some extent on the average number a of fumarate bonds in the molecule of the

polyester. For cases where s is smaller or equal to m, the total amount of moles of network chains per cubic centimeter is:

$$n = \left(s - \frac{s}{a}\right) e$$

where a is the number of fumarate groups in the polyester molecule. For s larger than m,

$$\left(m - \frac{m}{a}\right) e < n \left(2m - \frac{m}{a}\right) e$$

Another important point is that in order to obtain a structural network after copolymerization with styrene, the polyester molecule must have at least two reacted fumarate bonds.

The support of the Office of Naval Research is gratefully acknowledged, and the authors express their thanks to the American Cyanamid Company for sending their samples of polyesters.

References

1. Tobolsky, A. V., D. Katz, R. Thach, and R. Schaffhauser, *J. Polymer Sci.*, **62**, S176 (1962).
2. Katz, D., and A. V. Tobolsky, *J. Polymer Sci.*, **A2**, 1595 (1964).
3. Katz, D., and A. V. Tobolsky, *Polymer*, in press.
4. Lawrence, J. R., *Polyester Resins*, Reinhold, New York, 1960, p. 20.
5. Updegraff, I. H., American Cyanamid Co., private communication of January 9, 1963.
6. Designation ASTM D 1053-58, *ASTM Standards on Rubber Products*, Am. Soc. Testing Materials, Philadelphia, A58, p. 550 (1958).
7. Tobolsky, A. V., D. Carlson, and N. Indicator, *J. Polymer Sci.*, **54**, 175 (1961).

Résumé

Trois polyesters insaturés ont été pontés avec différentes quantités de styrène et on a mesuré le module de cisaillement de ces polymères formés en fonction de la température. On a trouvé que les polymères ont des régions vitreuses, de même que des régions de transitions et caoutchouteuses bien définies. L'équation du module de cisaillement à partir de la théorie de l'élasticité fut appliquée pour les régions plateau des polymères.

Zusammenfassung

Drei ungesättigte Polyester wurden mit verschiedenen Mengen von Styrol vernetzt und an den erhaltenen Polymeren der 10-Sekunden-Schermodul in Abhängigkeit von der Temperatur gemessen. Die Polymeren haben gut definierte Glas-, Übergangs- und Kautschukbereiche. Die aus der Theorie der Kautschukelastizität folgende Gleichung für den Schermodul wurde auf die Plateau-Bereiche der Polymeren angewandt.

Received March 4, 1963

JOURNAL OF POLYMER SCIENCE: PART A VOL. 2, PP. 1595–1605 (1964)

Rubber Elasticity in Highly Crosslinked Polyethyl Acrylate

DOV KATZ* and ARTHUR V. TOBOLSKY, *Frick Chemical Laboratory, Princeton University, Princeton, New Jersey*

Synopsis

Copolymers of ethyl acrylate with three different dimethacrylates were prepared over the complete range of copolymer composition. Modulus temperature curves of these polymers were constructed and contrasted with the modulus temperature curves of phenol–formaldehyde type polymers. The ethyl acrylate–dimethacrylate polymers appeared to have rubbery plateau regions at high temperatures, even for very high mole percentages of dimethacrylate. This was especially true if the dimethacrylate molecule had a long flexible chain within it, as in tetraethylene glycol dimethacrylate. On the other hand the phenol–formaldehyde type polymers and polyethylene glycol dimethacrylate did not appear to have rubbery plateau regions. Up to 12 mole-% of dimethacrylate the shear moduli of the ethyl acrylate copolymers in the rubbery plateau region were independent of the structure of the dimethacrylate at equivalent crosslink concentrations. Furthermore these polymers appear to obey the laws of ideal rubber elasticity with a front factor of unity.

Introduction

The purpose of this study was threefold: (1) to provide an overall view of the viscoelastic properties of crosslinked amorphous polymers over a very extensive range of crosslink densities, (2) to evaluate the effect of the "length" of the crosslink on the elastic behavior, and (3) to evaluate the applicability of the theory of rubber elasticity over a wide range of crosslink densities.

Experimental

Copolymer samples in the form of flat sheets were prepared from ethyl acrylate and the three following divinyl compounds: ethylene glycol dimethacrylate (EGDM), triethylene glycol dimethacrylate (TrEGDM) and tetraethylene glycol dimethacrylate (TEGDM). Samples were prepared over the entire range of copolymer compositions by a method already described.[1] Molded sheets of phenol–formaldehyde, urea–formaldehyde, and melamine–formaldehyde polymers, supplied by the Allied Chemical Company, were also studied.

Densities of all the polymers were measured by displacement at 25°C.

* On leave from the Scientific Department, Israel Ministry of Defence.

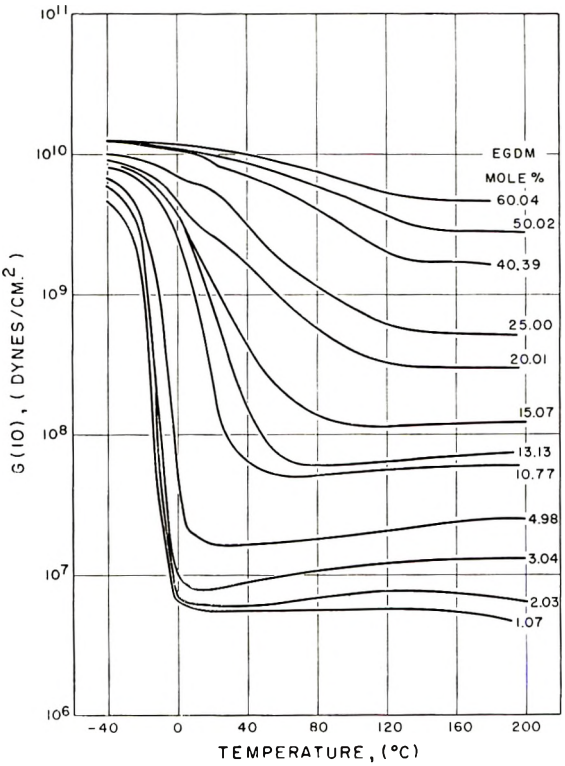

Fig. 1. Plots of 10-sec. shear modulus G vs. temperature for ethyl acrylate–ethylene glycol dimethacrylate copolymers.

The shear modulus measured after 10 sec. was determined as a function of temperature for all of the polymers by using a modified Gehman apparatus.[2] For some of the samples with very high torsion moduli, the Clash-Berg torsion apparatus[3] was also used. The agreement of the two methods was quite good.

The composition of the copolymers that were prepared, their densities and certain calculated quantities to be discussed later are shown in Tables I–III. Shear modulus versus temperature curves are shown in Figures 1 and 2.

Efficiency of Crosslinking

The problem of the crosslinking efficiencies of dimethacrylates with methyl methacrylate was discussed by others,[4–6] and in this paper we utilized the method of Loshaek and Fox[4] to study the efficiency of crosslinking of ethyl acrylate by the three dimethacrylates. The agreement between our results and the previous results on methyl methacrylate[4] was very good. The calculations for efficiency are based on the molar contraction of the monomers during polymerization as revealed by the change of density. The following data for molar contraction were used: for each

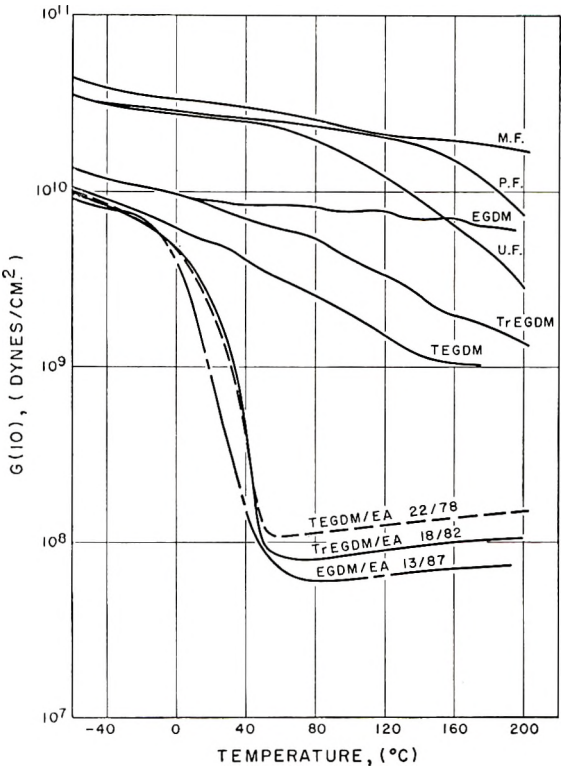

Fig. 2. Plots of 10-sec. shear modulus G vs. temperature for polymers of melamine-formaldehyde, phenol-formaldehyde, urea-formaldehyde, ethylene glycol dimethacrylate, triethylene glycol dimethacrylate, tetraethylene glycol dimethacrylate, and some copolymers of ethyl acrylate with the three dimethacrylates.

vinyl group in the dimethacrylate 22.5 cm.^{3}; for ethyl acrylate 20.75 cm.^{3}

In Tables I–III we list the mole percentage of the crosslinking agent, and from this value and the polymer density we compute and tabulate c, the moles per cubic centimeter of dimethacrylate incorporated in the polymer. Some of these incorporated dimethacrylate molecules have reacted through only one double bond; the other double bond remaining unreacted. These are ineffective as crosslinks and hence the concept of crosslink efficiency. For less than 5 mole-% of dimethacrylate the calculation of efficiency requires an accuracy in the density measurements that was beyond our experimental means. Loshaek and Fox suggested that the crosslinking efficiency should approach 100% as the crosslink concentration approaches zero. However, we had no reliable way of extrapolating the experimental results from 5 mole-% to zero dimethacrylate.

From the moles of dimethacrylate per cubic centimeter and the efficiency ϵ, the true crosslink density c' (in moles per cubic centimeter) is obtained by:

$$c' = \epsilon c \tag{1}$$

Regions of Viscoelastic Behavior

In Figure 1 are shown the modulus–temperature curves for ethyl acrylate copolymerized with EGDM. Preliminary data on the modulus temperature curves of ethyl acrylate–TEGDM copolymers appeared in an earlier communication.[7]

As for other linear amorphous-polymers, the modulus–temperature curve for the homopolymer of ethyl acrylate shows five regions of viscoelastic behavior: a glassy region, a transition region, a rubbery plateau, a rubbery flow region, and a liquid flow region.[8] Introduction of small amounts of crosslinking agent suppresses the last two regions, and we then have a glassy region, a transition region, and a rubbery plateau region.

Increasing the amount of the dimethacrylate increases the temperature of onset of the transition region and also broadens the temperature range of the transition region, as can be seen in a qualitative way in Figure 1.

Increasing the amount of dimethacrylate also increases the magnitude of the rubbery plateau modulus, as is clear from Figure 1.

An unresolved question is: how high can we go in crosslink density and still have a rubbery plateau region? This can be answered at present only in a qualitative way by an examination of the shape of the modulus temperature curve.

For comparative purposes we have shown in Figure 2, the modulus temperature curves of phenol–formaldehyde polymer, urea–formaldehyde polymer, and melamine–formaldehyde polymer.

These very highly crosslinked polymers exhibit modulus–temperature curves which appear to be "glassy" at all temperatures until their decomposition temperatures. It is, of course, possible to prepare samples of these thermosetting resins which are much less highly crosslinked than the samples used in this study, e.g., by incomplete cure.

In the same figure are plotted the modulus–temperature curves of the homopolymers of EGDM, TrEGDM, and TEGDM. The TEGDM homopolymer appears to have a glassy region, a transition region, and a rubbery plateau region. The existence of the rubbery plateau region here is probably due to the long length of chain within this dimethacrylate molecule.

The homopolymer of EGDM, on the other hand, did not give a modulus–temperature curve that definitely proved or disproved the existence of a rubbery plateau. Unfortunately the samples of this polymer are very brittle and the curve was constructed from numerous samples. We do not believe that a rubbery plateau exists here because of the short molecular chain within this dimethacrylate.

The sense in which we use the word "rubbery" in the above discussion is only very qualitatively defined from the appearance of a modulus–temperature curve.

We have much more confidence in the existence of rubbery plateaus for the copolymers of ethyl acrylate with about 25 mole-% of EGDM, Tr-

EGDM, and TEGDM. Some modulus–temperature curves of these polymers are also shown in Figure 2.

For mole percentages of dimethacrylate below 12 mole-%, the copolymers have true rubbery plateau regions which indeed are in full accord with the theory of rubbery elasticity as discussed below.

Equation for Rubber Elasticity

The equation of state for rubber elasticity gives the following formula for shear modulus G:

$$G = \Phi nRT \tag{2}$$

In eq. (2), n is the concentration of network chains per cubic centimeter, R is the gas constant, and T is the absolute temperature. The quantity Φ is the front factor, which is unity at all temperatures for ideal rubbers. For nonideal rubbers the front factor may differ from unity and may or may not be temperature-dependent.[1]

The concentration of network chains must be related to the concentration of crosslinks and hence to the copolymer composition. We utilize the following equation:

$$n = c'z = \epsilon cz \tag{3}$$

The z value of a network is defined by eq. (3). For a tetrafunctional "point" crosslink z is two. We believe that the length of chain within EGDM is sufficiently short so that it can be considered as a point crosslink up to 12 mole-%, and z is equal to two in this case.

For the case of TrEGDM and TEGDM the *a priori* evaluation of z is difficult. It might appear that for very small dimethacrylate concentrations $z = 2$ (here the length of chain within the dimethacrylate is negligible with respect to the length of polyethyl acrylate chains between dimethacrylate molecules). At intermediate concentrations c', z may perhaps be three (here the length of chain within the dimethacrylate is comparable with the length of chain between dimethacrylate molecules). At very high mole percentages of dimethacrylate, z may approach unity (here the length of polyethyl acrylate chain between dimethacrylate molecules is negligible compared with the length of the molecular chain within the dimethacrylate). However, we must emphasize that the present theory of rubber elasticity is based on point crosslinks. We have no reliable theoretical guide for the treatment of flexible chains within a crosslinking molecule.

However, as shown below there is an experimental solution to the problem of z values for concentrations of dimethacrylate less than 1×10^{-3} moles/cm.[3] (roughly corresponding to 12–15 moles-% of dimethacrylate).

Experimental Results on Equation for Rubber Elasticity

By combining eqs. (2) and (3) we obtain

$$G = \Phi zc\epsilon RT \tag{4}$$

TABLE I
Ethyl Acrylate (EtAc)–Ethylene Glycol Dimethacrylate (EGDM)

No.	EGDM, mole-%	c_{EGDM}, mole/cm.^{3}	Density, g./cm.^{3}	G, dynes/cm.^{2}	Crosslink efficiency ϵ	c'_{EGDM}, mole/cm.^{3}	$z\Phi\epsilon$	$z\Phi$	$\Phi\epsilon$	Φ
1	1.07	0.000120	1.1331	5.65×10^6			1.33		0.67	
2	2.03	0.000226	1.1355	7.60×10^8			0.95		0.48	
3	3.04	0.000336	1.1374	1.25×10^7			1.05		0.53	
4	4.98	0.000464	1.1453	2.34×10^7	0.68	0.000316		2.09		1.05
5	10.77	0.001061	1.1601	5.72×10^7	0.76	0.000806		2.01		1.01
6	13.13	0.001352	1.1679	6.90×10^7	0.73	0.000987		1.97		0.99
7	15.07	0.001539	1.1722	1.13×10^8	0.71	0.001093		2.92		
8	20.01	0.001979	1.1828	2.96×10^8	0.71	0.001405		5.94		
9	25.00	0.002395	1.1929	5.43×10^8	0.70	0.001677		9.14		
10	40.39	0.003517	1.2155	1.70×10^8	0.62	0.002181		21.99		
11	50.02	0.004107	1.2237	2.87×10^9	0.57	0.002341		34.62		
12	60.04	0.004648	1.2296	4.70×10^9	0.51	0.002370		55.95		

TABLE II
Ethyl Acrylate (EtAc)–Triethylene Glycol Dimethacrylate (TrEGDM)

No.	TrEGDM, mole-%	c_{TrEGDM} mole/cm.^{3}	Density, g./cm.^{3}	G, dynes/cm.^{2}	Crosslink efficiency ϵ	c'_{TrEGDM}, mole/cm.^{3}	$z\Phi\epsilon$	$z\Phi$	$\Phi\epsilon$	Φ
1	1.01	0.000113	1.1310	5.40×10^6			2.35		0.68	
2	3.04	0.000327	1.1377	1.31×10^7			1.13		0.57	
3	6.98	0.000711	1.1504	3.30×10^7	0.67	0.000476		1.95		0.98
4	13.12	0.001224	1.1662	6.10×10^7	0.73	0.000894		1.92		0.96
5	18.05	0.001593	1.1790	9.77×10^7	0.77	0.001227		2.25		1.13
6	24.96	0.002031	1.1912	1.76×10^8	0.76	0.001544		3.22		
7	59.79	0.003468	1.2252	6.11×10^8	0.66	0.002289		7.53		
8	74.85	0.003859	1.2333	1.07×10^9	0.64	0.002470		12.23		

TABLE III
Ethyl Acrylate (EtAc)–Tetraethylene Glycol Dimethacrylate (TEGDM)

No.	TEGDM, mole-%	c_{TEGDM}, mole/cm.^{3}	Density, g./cm.^{3}	G, dynes/cm.^{2}	Crosslink efficiency ϵ	c'_{TEGDM}, mole/cm.^{3}	$z\Phi\epsilon$	$z\Phi$	$\Phi\epsilon$	Φ
1[a]		0.000037[a]							1.09[a]	
2	1.41	0.000154	1.1309	6.88×10^6			1.26		0.63	
3	3.42	0.000362	1.1406	1.37×10^7			1.07		0.54	
4	5.46	0.000557	1.1472	2.16×10^7	0.71	0.000395		1.54		0.77
5	7.10	0.000702	1.1505	3.90×10^7	0.70	0.000491		2.24		1.12
6	10.17	0.000956	1.1593	5.74×10^7	0.72	0.000688		2.35		1.18
7	13.39	0.001191	1.1680	6.60×10^7	0.74	0.000881		2.12		1.06
8	15.10	0.001253	1.1691	7.80×10^7	0.75	0.000940		2.34		1.17
9	18.13	0.001507	1.1781	8.99×10^7	0.81	0.001221		2.08		1.04
10	22.29	0.001747	1.1856	1.35×10^8	0.85	0.001485		2.57		
11	30.41	0.002140	1.1961	1.96×10^8	0.81	0.001733		3.19		
12	35.18	0.002339	1.2026	2.29×10^8	0.80	0.001871		3.45		
13	41.57	0.002564	1.2066	2.65×10^8	0.78	0.002000		3.74		
14	67.60	0.003244	1.2252	6.30×10^8	0.76	0.002465		7.22		

[a] Data of Tobolsky et al.[1]

The experimental results on shear modulus versus temperature for the different copolymer compositions were interpreted according to eq. (4). The temperature at which this equation was applied was 426°K., since this was well within the rubbery plateau region for all the ethyl acrylate copolymers.

In eq. (4) the quantities, G, c, ϵ, R, and T are experimental quantities or constants. Hence we were able to compute Φz for all samples which contained more than 5 mole-% of crosslinking agent. In cases with a lower

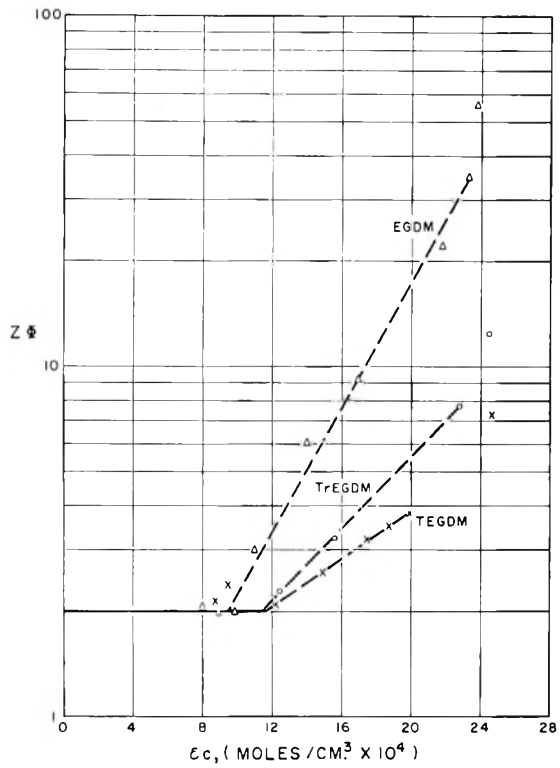

Fig. 3. Plots of $z\Phi$ vs. ϵc for copolymers of ethyl acrylate with ethylene glycol dimethacrylate, triethylene glycol dimethacrylate, and tetraethylene glycol dimethacrylate.

amount of dimethacrylate than 5 mole-% we calculated the $\Phi z\epsilon$ values and listed them in a separate column, leaving open the question of the crosslinking efficiency.

We utilized eq. (4) for calculational purposes for all crosslink densities, even the very high ones. This does not mean that we believe eq. (4) is truly applicable for very high crosslink densities. However, until a convincing theory for the elastic properties of the very highly crosslinked networks is available, it is interesting to tabulate the Φz values obtained by eq. (4) for all crosslink densities.

For c' values of dimethacrylate between 3×10^{-4} and 1×10^{-3} moles/cm.^{3} a very clear and simple though perhaps somewhat surprising result emerges, as can be seen in detail in Tables I–III. The values Φz for all three dimethacrylates are equal to 2.0 ± 0.25. Inasmuch as the z value for EGDM copolymers is two, it appears that below about 13% dimethacrylate or c' below 1×10^{-3} moles/cm.^{3} the copolymers of ethyl acrylate with TrEGDM and TEGDM act as if their z values are also two. By taking $z = 2$ in this range we were able to list Φ_ϵ and Φ in the tables. As can be seen, the front factor Φ is very close to unity. This agrees with earlier data[1] from this laboratory for very low crosslink densities, if one assumes that the efficiency of crosslinking is unity at a value of $c = 4 \times 10^{-5}$ moles/cm.^{3}

Between the range of $c = 4 \times 10^{-5}$ and 4×10^{-4} moles/cm.^{3}, there is some reason to surmise from the tabulated values of Φ_ϵ that the front factor values fall slightly below unity, if we assume that the efficiencies do not fall below the experimental value measured at 5 mole-% of dimethacrylate.

At any rate, the front factor of these crosslinked ethyl acrylate copolymers are very nearly unity up to quite high crosslink densities. Furthermore, it was shown in an earlier publication[1] that the front factor for crosslinked ethyl acrylate is independent of temperature.

For the ethyl acrylate–EGDM copolymers the rubber network behaves ideally up to $c' = 1 \times 10^{-3}$ moles/cm.^{3} This corresponds to a molecular weight between the idealized point crosslinks of $M_c = 508$, using the formula $M_c = d/2c'$, where d is density. This means that this rubber network behaves ideally with only ten single bonds between network junctures.

High Crosslink Densities

In Figure 3 we show a plot of Φz versus c' for ethyl acrylate copolymerized with all three dimethacrylates, up to 75 mole-% of the divinyl compound. We show results only for c' larger than 8×10^{-4} moles/cm.^{3}, which corresponds to dimethacrylate contents higher than 10 mole-%. At these high crosslink densities the difference between EGDM, TrEGDM, and TEGDM crosslinks shows up very markedly. For the EGDM copolymers the applicability of eq. (4) probably ceases slightly beyond $c' = 10^{-3}$. For the TrEGDM and TEGDM copolymers, one might possibly extend the range over which eq. (4) applies to a value of $c' = 2 \times 10^{-3}$ moles/cm.^{3}, corresponding to 40 mole-% of TEGDM. An *a priori* evaluation of z and Φ, however, is very difficult.

It should be pointed out that the number of single bonds between the vinyl group is 7 for EGDM, and this appears insufficient to act as a rubbery network chain in ethyl acrylate–EGDM copolymers. The number of single bonds between vinyl groups in TrEGDM and TEGDM are 13 and 16, respectively, and these intramolecular chains possibly act as rubbery network chains under certain conditions in the copolymers studied here,

namely between $c' = 1 \times 10^{-4}$ and 2×10^{-4}. However, our experimental results indicate that these long intramolecular chains do not contribute much to the elastic behavior of the network for dimethacrylate contents below 13 mole-%.

The partial support of the Office of Naval Research is gratefully acknowledged.

References

1. Tobolsky, A. V., D. Carlson, and N. Indictor, *J. Polymer Sci.*, **54**, 175 (1961).
2. Designation D 1053–58, *ASTM Standards*, Am. Soc. Testing Materials, Philadelphia, 1958.
3. Designation D 1043–51, *ASTM Standards*, Am. Soc. Testing Materials, Philadelphia, 1951.
4. Loshaek, S., and T. G Fox, *J. Am. Chem. Soc.*, **75**, 3544 (1953).
5. Shultz, A. R., *J. Am. Chem. Soc.*, **80**, 1854 (1958).
6. Hwa, J. C. H., *J. Polymer Sci.*, **58**, 715 (1962).
7. Tobolsky, A. V., D. Katz, R. Thach, and R. Schaffhauser, *J. Polymer Sci.*, **62**, S176 (1962).
8. Tobolsky, A. V., *Properties and Structure of Polymers*, Wiley, New York, 1960.

Résumé

On a préparé des copolymères d'acrylate d'éthyle avec trois diméthacrylates différents dans tout le domaine de la composition de copolymère. On a tracé les courbes module/température de ces polymères et on les a comparées avec les courbes module/température des polymères du type phénol-formaldéhyde. Les polymères acrylate d'éthyle-diméthacrylate semblent avoir des régions caoutchouteuses à des températures relativement élevées, même pour des pourcentages molaires très elévés en diméthacrylate. Ceci est surtout vrai quand les molécules du diméthycrylate contiennent une longue chaîne flexible dans le copolymère, comme dans le cas du diméthacrylate de tétraéthylène glycol. D'autre part les polymères du type phénol formaldéhyde et diméthacrylate de polyéthylène glycol ne semblent pas avoir des régions caoutchouteuses. Les modules de cisaillement des copolymères d'acrylate d'éthyle dans la région caoutchouteuse sont indépendants de la structure du diméthacrylate à des concentrations de pontage atteignant jusqu'à 12% molaire de diméthacrylate. En plus, ces polymères semblent suivre les lois d'élasticité idéale des caoutchouc avec un facteur qui est égal à l'unité.

Zusammenfassung

Copolymere aus Äthylacrylat und drei verschiedenen Dimethacrylaten wurden im gesamten Bereich der Copolymerzusammensetzung hergestellt. Die Modul-Temperatur-Kurven dieser Polymeren wurden ermittelt und denen von Polymeren des Phenol-Formaldehyd-Typs gegenübergestellt. Die Äthylacrylat-Dimethacrylat-Polymeren haben anscheinend auch bei sehr hohem Dimethacrylatgehalt bei hohen Temperaturen Kautschukplateau-Bereiche. Dies ist besonders dann der Fall, wenn das Dimethacrylatmolekül eine lange flexible Kette enthält, wie im Tetraäthylenglykol-dimethacrylat. Andererseits haben Polymere des Phenol-Formaldehyd-Typs und Polyäthylenglykol-dimethacrylat offenbar keine Kautschukplateau-Bereiche. Bis hinauf zu 12 Molprozent Dimethacrylat waren die Schermoduln der Äthylacrylat-Copolymeren im Kautschukplateau-Bereich bei äquivalenten Vernetzungskonzentrationen von der Struktur des Dimethacrylates unabhängig. Überdies gehorchen diese Polymeren offenbar den Gesetzen der idealen Kautschukelastizität mit einem Frontfaktor eins.

Received March 4, 1963

JOURNAL OF POLYMER SCIENCE: PART A VOL. 2, PP. 1607–1631 (1964)

Stereoregulated Polydideuteroethylene. II. Infrared Spectra and Normal Vibration Analysis

MITSUO TASUMI and TAKEHIKO SHIMANOUCHI, *Department of Chemistry, Faculty of Science, The University of Tokyo, Bunkyo-ku, Tokyo, Japan*, and HIROSHI TANAKA and SAKUJI IKEDA, *Research Laboratory of Resources Utilization, Tokyo Institute of Technology, Meguro-ku, Tokyo, Japan*

Synopsis

Poly-(*trans*-CHD=CHD) and poly-(*cis*-CHD=CHD) have been obtained with [$Al(Et)_3$ + $TiCl_4$] and with [$Al(i\text{-}Bu)_3$ + $TiCl_4$]. Poly-(*trans*-CHD=CHD) and poly-(*cis*-CHD=CHD) obtained with [$Al(Et)_3$ + $TiCl_4$] give mutually different infrared spectra. The characteristic absorption bands of the former are found at 1335, 1288, and 594, and 586 cm.$^{-1}$, and those of the latter at 1306, 597, and 590 cm.$^{-1}$. In order to interpret these spectra, the normal vibration frequencies of the model structures, namely, erythro-diisotactic and threo-diisotactic structures, have been calculated. From the comparison of the observed and calculated frequencies, it has been concluded that poly-(*trans*-CHD=CHD) obtained with [$Al(Et)_3$ + $TiCl_4$] consists mainly of the threo-diisotactic and disyndiotactic portions and poly-(*cis*-CHD=CHD) obtained with the same catalyst consists mainly of the erythro-diisotactic and disyndiotactic portions. The relation between the type of double bond opening and the structure of the resultant polymer has been discussed, and it has been concluded that the *cis*-opening of the double bond occurs in the polymerization reaction with [$Al(Et)_3$ + $TiCl_4$]. The spectra of poly-(*trans*-CHD=CHD) and poly-(*cis*-CHD=CHD) obtained with [$Al(i\text{-}Bu)_3$ + $TiCl_4$] are not so different from each other, but they are different from the spectra of the polymers obtained with [$Al(Et)_3$ + $TiCl_4$]. The polymers obtained with [$Al(i\text{-}Bu)_3$ + $TiCl_4$] show characteristic bands at 2919, 2850, 2176, 2095, 1453, 660, 623, 600, 593, 581, 566, and 545 cm.$^{-1}$. These bands give evidence of the presence of isolated CH_2 and CD_2 groups. This fact indicates that the hydrogen–deuterium exchange reaction in monomers as well as the polymerization is promoted by [$Al(i\text{-}Bu)_3$ + $TiCl_4$].

INTRODUCTION

Previously Ikeda et al. polymerized *trans*-1,2-dideuteroethylene and *cis*-1,2-dideuteroethylene separately with a Ziegler catalyst and found small differences between the infrared spectra of the resultant polymers.[1] It is expected that some information on the molecular structures of these polymers may be obtained from the analysis of these spectral differences. As was mentioned briefly in the previous paper,[1] we may approach an understanding of the mechanism of polymerization with this catalyst through the structural analysis of these polymers. In such hopes we have begun this study.

EXPERIMENTAL

I. Samples

Films prepared from the samples shown in Table I were used for the measurements of the infrared spectra. The procedures of the preparation of these polymer samples were described in the previous paper.[1] The films were prepared from xylene solutions by evaporating the solvent over a hot plate at 120°C.

TABLE I
Polymer Samples Used for the Infrared Measurements

Sample	Monomer	Catalyst	Polymerization temperature, °C.
A	*trans*-CHD=CHD	$Al(Et)_3 + TiCl_4$	0
B	*cis*-CHD=CHD	$Al(Et)_3 + TiCl_4$	0
C	*trans*-CHD=CHD	$Al(i\text{-}Bu)_3 + TiCl_4$	0
D	*cis*-CHD=CHD	$Al(i\text{-}Bu)_3 + TiCl_4$	0
E	*trans*-CHD=CHD	$Al(Et)_3 + TiCl_4$	+70
F	*trans*-CHD=CHD	$Al(Et)_3 + TiCl_4$	−70
G	*trans*-CHD=CHD + *cis*-CHD=CHD (50%–50%)	$Al(Et)_3 + TiCl_4$	0
H-1	$CD_2=CD_2$	$Al(Et)_3 + TiCl_4$	0
H-2[a]	$CD_2=CD_2$	$Al(Et)_3 + TiCl_4$	0
I	$CH_2=CH_2$	$Al(Et)_3 + TiCl_4$	0

[a] This sample contains a considerable amount of H atoms as impurity.

II. Measurements of Infrared Spectra

Infrared spectra in the region of 4000–650 cm.$^{-1}$ were recorded by a Hitachi EPI-2 double-beam spectrometer equipped with a NaCl prism (Fig. 1) and a Perkin-Elmer 112G single-beam grating spectrometer equipped with a KBr fore-prism (Figs. 2–9). A Koken DS 401G double-beam grating spectrometer[2] equipped with a CsBr fore-prism was used for the measurements in the region below 700 cm.$^{-1}$ (Figs. 10–14). For the polarized infrared measurements commercial AgCl polarizers and the polarizer described by Yamaguchi et al.[3] were used. Melted state spectra were obtained for the samples sandwiched and heated between two KCl or KRS-5 plates.

III. Results and Preliminary Interpretation

1. General Aspects. Figure 1 shows the low-resolution spectra of the samples A, B, C, and D. The polymerization was repeated a few times for each sample and all the spectra shown in this figure were confirmed by the several repeated measurements.

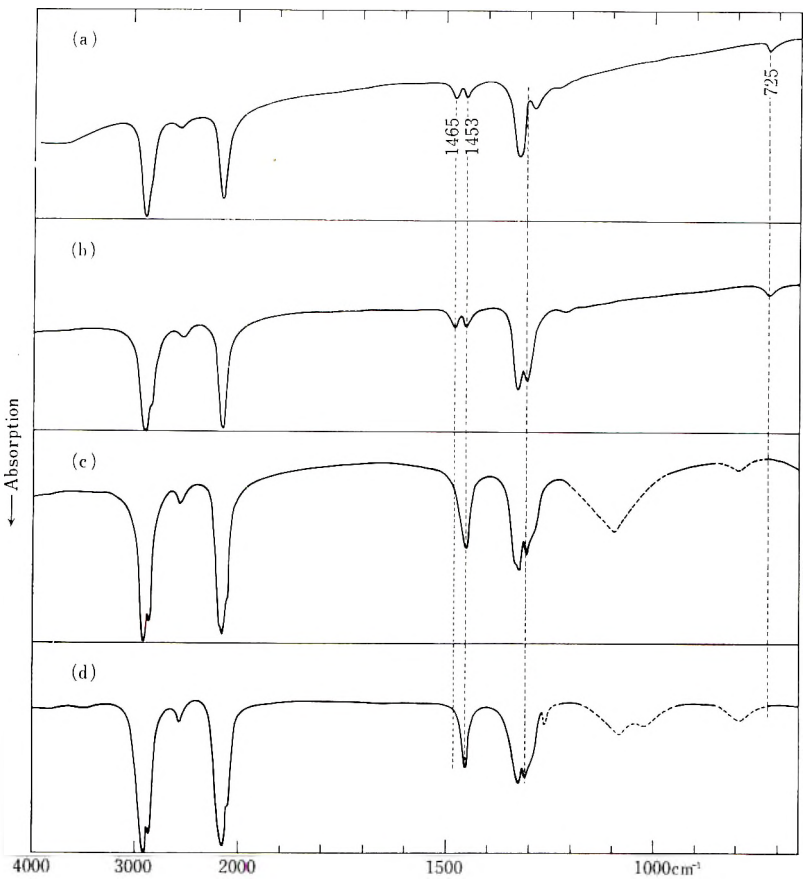

Fig. 1. Infrared spectra of poly-(*trans*-CHD=CHD) and poly-(*cis*-CHD=CHD): (*a*) sample A; (*b*) sample B; (*c*) sample C; (*d*) sample D. Broken lines indicate absorptions arising from impurity.

Samples A and B show definite differences in the region of 1350–1200 cm.$^{-1}$. It is noted that the absorptions in this region are affected not only by the monomer species, but also by the catalyst. Samples C and D show very small differences in this region, and both of them are similar to B rather than A. Differences between the samples obtained with [$Al(Et)_3$ + $TiCl_4$] and those obtained with [$Al(i\text{-}Bu)_3$ + $TiCl_4$] are seen at about 1460 and 720 cm.$^{-1}$ also. In these two regions the former samples show two characteristic bands which are not observed for the latter ones. These bands may be assigned to the CH_2 bending and the CH_2 rocking vibrations of normal polyethylene produced from the ethyl group of $Al(Et)_3$.[4] The 1453 cm.$^{-1}$ band which always appears for each sample may be assigned to the bending vibration of the CH_2 group placed between two CHD groups.

2. CH and CD Stretching Vibration Regions. The spectra of the CH and the CD stretching vibration regions are shown in Figures 2 and 3. In these regions poly-(*trans*-CHD=CHD) and poly-(*cis*-CHD=CHD)

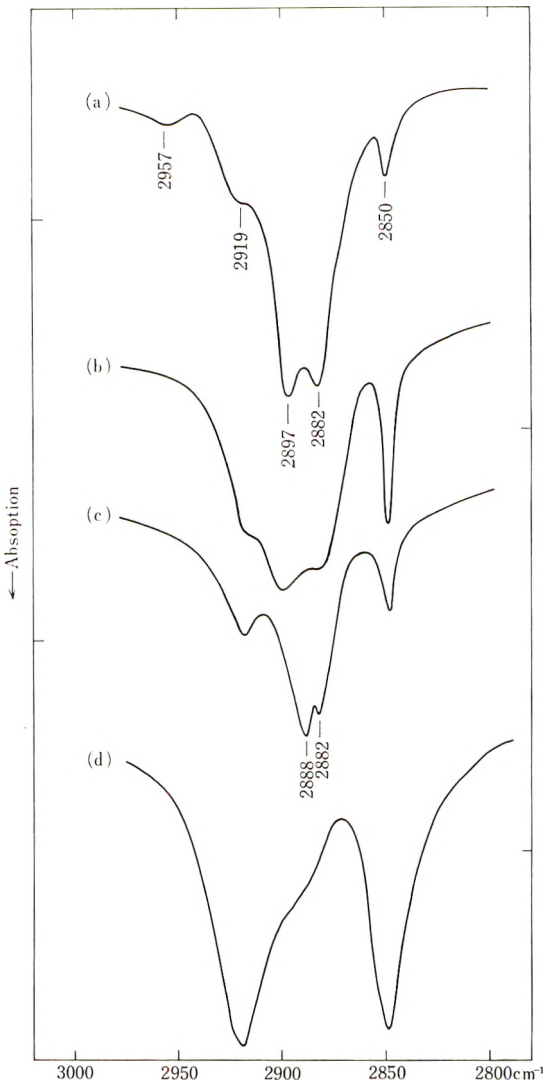

Fig. 2. Infrared spectra of poly-(*trans*-CHD=CHD), poly-(*cis*-CHD=CHD), poly-(CD_2=CD_2), and poly-(CH_2=CH_2) in the CH stretching vibration region: (*a*) sample A; (*b*) sample C; (*c*) sample H-1; (*d*) sample I.

obtained with a common catalyst give almost the same spectra. In Figure 2 only the spectra of poly-(*trans*-CHD=CHD) are shown. Some differences are seen between the samples obtained with [$Al(Et)_3$ + $TiCl_4$] and those obtained with [$Al(i\text{-}Bu)_3$ + $TiCl_4$], especially in the CD stretching vibration region (Fig. 3). The latter samples have two bands at ca. 2176 and 2095 cm.$^{-1}$ which are not observed for the former ones. These are close to the 2192 and 2088 cm.$^{-1}$ bands of perdeuterated polyethylene (Fig. 3*e*). The 2919 and 2850 cm.$^{-1}$ bands of sample A (Fig. 2*a*) may be as-

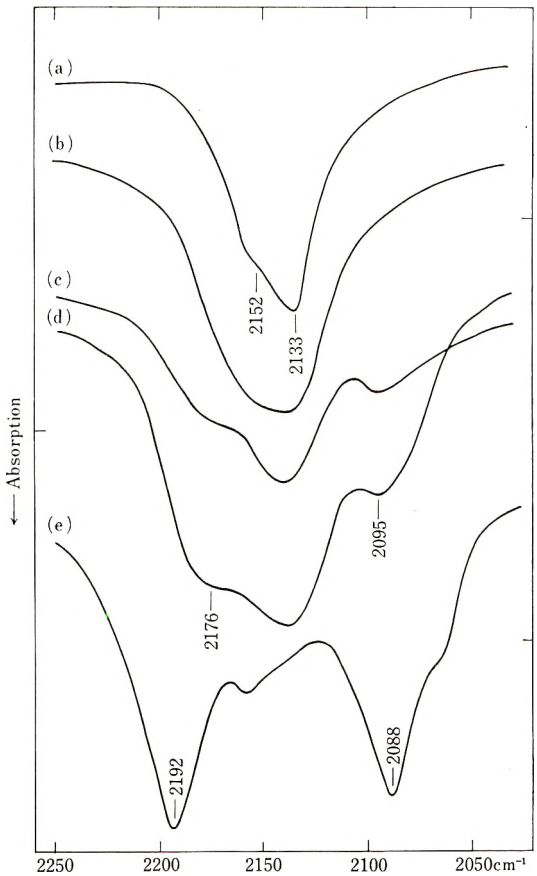

Fig. 3. Infrared spectra of poly-(*trans*-CHD=CHD), poly-(*cis*-CHD=CHD), and poly-(CD_2=CD_2) in the CD stretching vibration region: (*a*) sample A; (*b*) sample B, (*c*) sample C; (*d*) sample D; and (*e*) sample H-1.

sociated with normal polyethylene produced from the ethyl group of Al-$(Et)_3$ by referring to the spectrum of poly-(CH_2=CH_2) shown in Figure 2*d*. The samples obtained with [Al(*i*-Bu)$_3$ + $TiCl_4$] show absorptions at about the same frequencies (Fig. 2*b*). The assignment of these bands will be considered later. The 2888 and 2882 cm.$^{-1}$ bands of sample H (Fig. 2*c*) may be assigned to the CH stretching vibrations arising from the remaining CH groups in the perdeuterated polymer.

3. CHD Bending Vibration Region. The absorption bands associated with the CHD bending vibrations are expected to appear at about 1300 cm.$^{-1}$. The spectra in this region are shown in Figure 4. As described in the previous section, definite differences are observed between samples A and B. Samples C and D are slightly different from each other. The polymerization temperature has little effect on the spectra (Figs. 4*e* and *f*). Sample G (a copolymer of *trans*-monomer and *cis*-monomer) gives a spectrum intermediate between those of the A and B samples.

All the bands (of samples A and B) in this region show dichroism perpendicular to the direction of stretching of the film (Fig. 5). This is in agreement with the assignment of these bands to the CHD bending modes.

The crystalline normal polyethylene shows two bands at 1473 and 1463 cm.$^{-1}$, while in the melted state they are replaced by a single band at

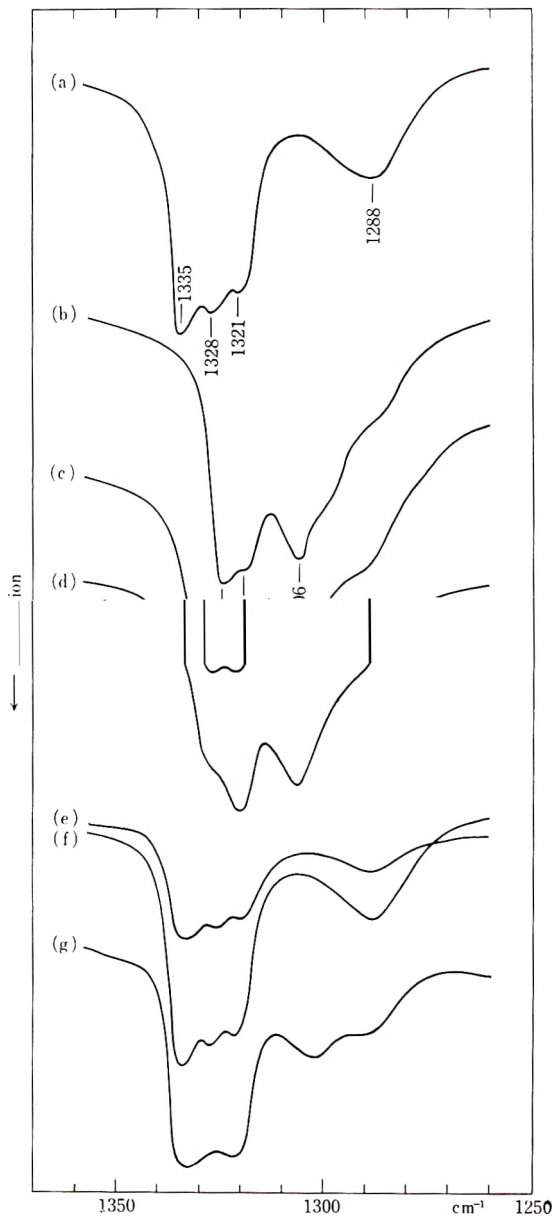

Fig. 4. Infrared spectra of poly-(*trans*-CHD=CHD) and poly-(*cis*-CHD=CHD) in the CHD bending vibration region: (*a*) sample A; (*b*) sample B; (*c*) sample C; (*d*) sample D; (*e*) sample E; (*f*) sample F; (*g*) sample G.

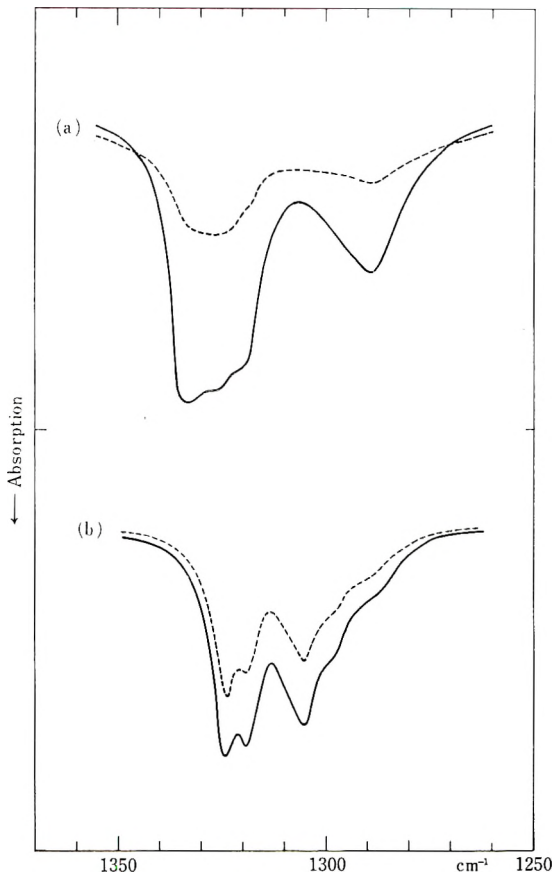

Fig. 5. Polarized infrared spectra of poly-(*trans*-CHD=CHD) and poly-(*cis*-CHD=CHD) in the CHD bending vibration region: (*a*) sample A; (*b*) sample B; (——) radiation with electric vector perpendicular to the stretching direction; (----) radiation with electric vector parallel to the stretching direction.

1463 cm.$^{-1}$. The doublet in the crystalline phase was interpreted as a result of the interaction between neighboring chains in the crystal.[5] This interpretation was confirmed by the work on the solid solutions of $C_{64}H_{130}$ in $C_{100}D_{202}$.[5] It is expected, therefore, that the bands in the region of 1340–1320 cm.$^{-1}$ might be associated with such a crystal field splitting. Experiments were carried out in order to test this expectation, and the rather complicated results shown in Figures 6–9 were obtained. In the spectrum of sample A a broad band at 1325 cm.$^{-1}$ is found in the melted state, and on cooling the sample the intensity of the 1335 cm.$^{-1}$ band increases slightly (Fig. 6). The solid solution which is composed of 30% poly-(*trans*-CHD=CHD) (sample A) and 70% poly-(CH_2=CH_2) shows a single band at 1331 cm.$^{-1}$ instead of the two bands at 1335 and 1328 cm.$^{-1}$ of the original sample A (Fig. 9). These results indicate that, as was expected, the 1335 and 1328 cm.$^{-1}$ bands of sample A are related to the

crystal field. Yet, the reason why the 1328 cm.$^{-1}$ band is weaker than the 1335 cm.$^{-1}$ band remains unanswered. Sample B has two bands at 1325 and 1320 cm.$^{-1}$. This doublet is also replaced by a broad singlet in the melted state spectrum (Fig. 7). Sample G gives spectrum intermediate between those of samples A and B in the melted state also (Fig. 8).

For all these three samples the change of the intensity ratio of the lower frequency bands (the 1288 cm.$^{-1}$ band of sample A and the 1306 cm.$^{-1}$ band

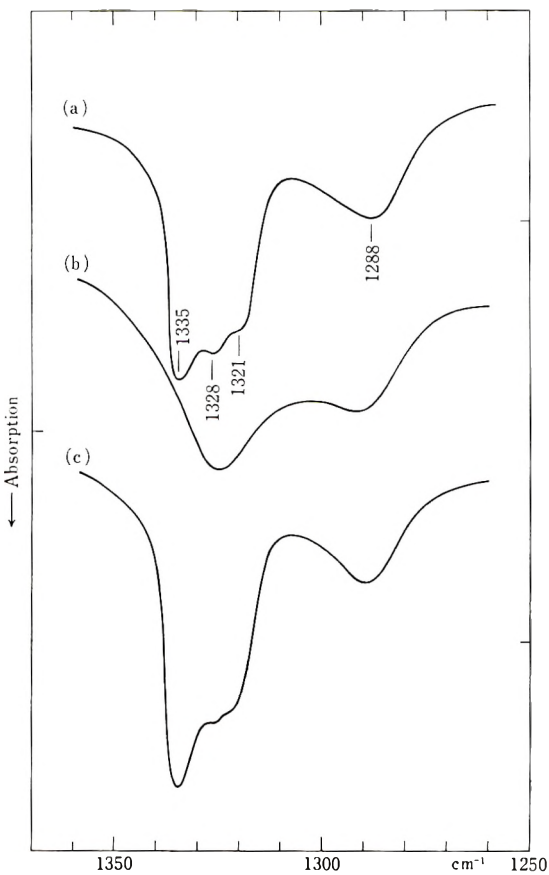

Fig. 6. Infrared spectra of poly-(*trans*-CHD=CHD) (sample A) in the CHD bending vibration region: (*a*) Solid before melting; (*b*) melted state; (*c*) solid obtained on cooling the melt.

of sample B) to the higher frequency ones (at ca. 1320 cm.$^{-1}$ in the melted state) is observed in going from the solid to the melted state (Figs. 6–8). The intensities of the lower frequency bands increase relatively in the melted state. There is no good explanation for this. However, the intensities of these two groups of bands may depend differently upon the temperature, since they are to be assigned to the different vibrational modes as will be described later.

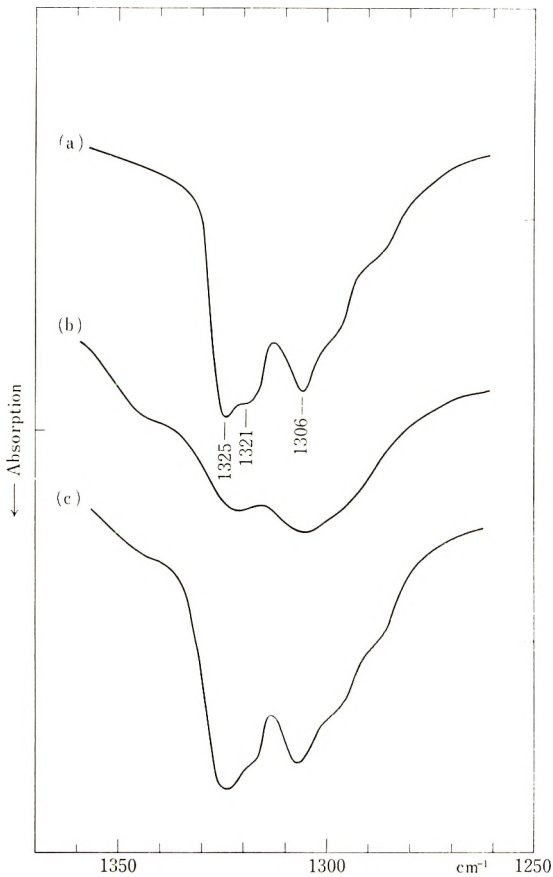

Fig. 7. Infrared spectra of poly-(*cis*-CHD=CHD) (sample B) in the CHD bending vibration region: (*a*) solid before melting; (*b*) melted state; (*c*) solid obtained on cooling the melt.

4. CDH Rocking Vibration Region. The infrared-active CH_2 rocking vibration of $-(CH_2)_n-$ and the corresponding CD_2 vibration of $-(CD_2)_n-$ appear, respectively, at about 725 and 520 cm.$^{-1}$. Therefore, the CDH rocking mode of $-(CHD)_n-$ will appear between these two frequencies. In fact, a doublet is found at ca. 590 cm.$^{-1}$ in the spectrum of either sample A or B (Fig. 10). The mean frequency of the doublet of sample B (594 cm.$^{-1}$) is a little higher than that of sample A (590 cm.$^{-1}$). The doublet of each sample is perpendicularly polarized in accord with the assignment (Fig. 11). In order to examine the origin of the doublet, measurements were made for the melted state and solid solutions. The doublet is replaced by a singlet in the melted state and reappears on cooling (Figs. 12 and 13). As a result of this heat treatment, the intensity of the higher frequency component is enhanced in comparison with that of the lower frequency one. The doublet disappears completely in the spectrum of the solid solution composed of 30% sample A and 70% normal polyethylene 70% (Fig. 14*b*), whereas it

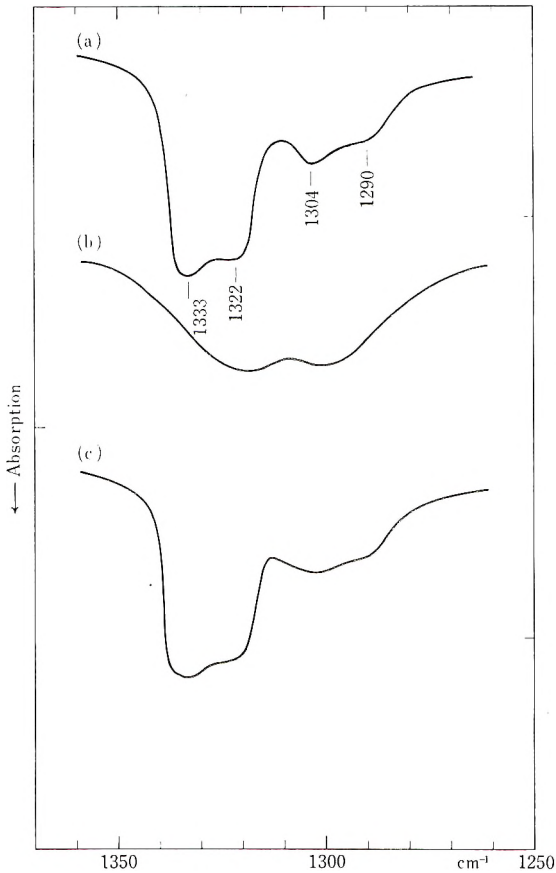

Fig. 8. Infrared spectra of copolymer of *trans*-CHD=CHD and *cis*-CHD=CHD (sample G) in the CHD bending vibration region: (*a*) solid before melting; (*b*) melted state; (*c*) solid obtained on cooling the melt.

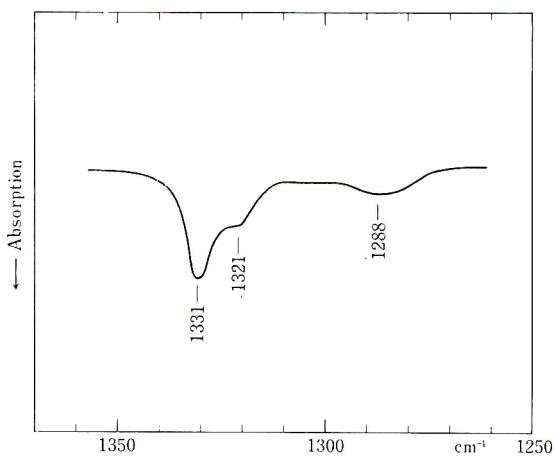

Fig. 9. Infrared spectrum of the solid solution of 30% poly-(*trans*-CHD=CHD) (sample A) in 70% poly-(CH_2=CH_2) in the CHD bending vibration region.

still remains in the solid solution of the reversed composition (Fig. 14*c*). It is clear from these results that the doublet is associated with the crystal field, as in the case of the doublet at 731 and 720 cm.$^{-1}$ in the spectrum of normal polyethylene.

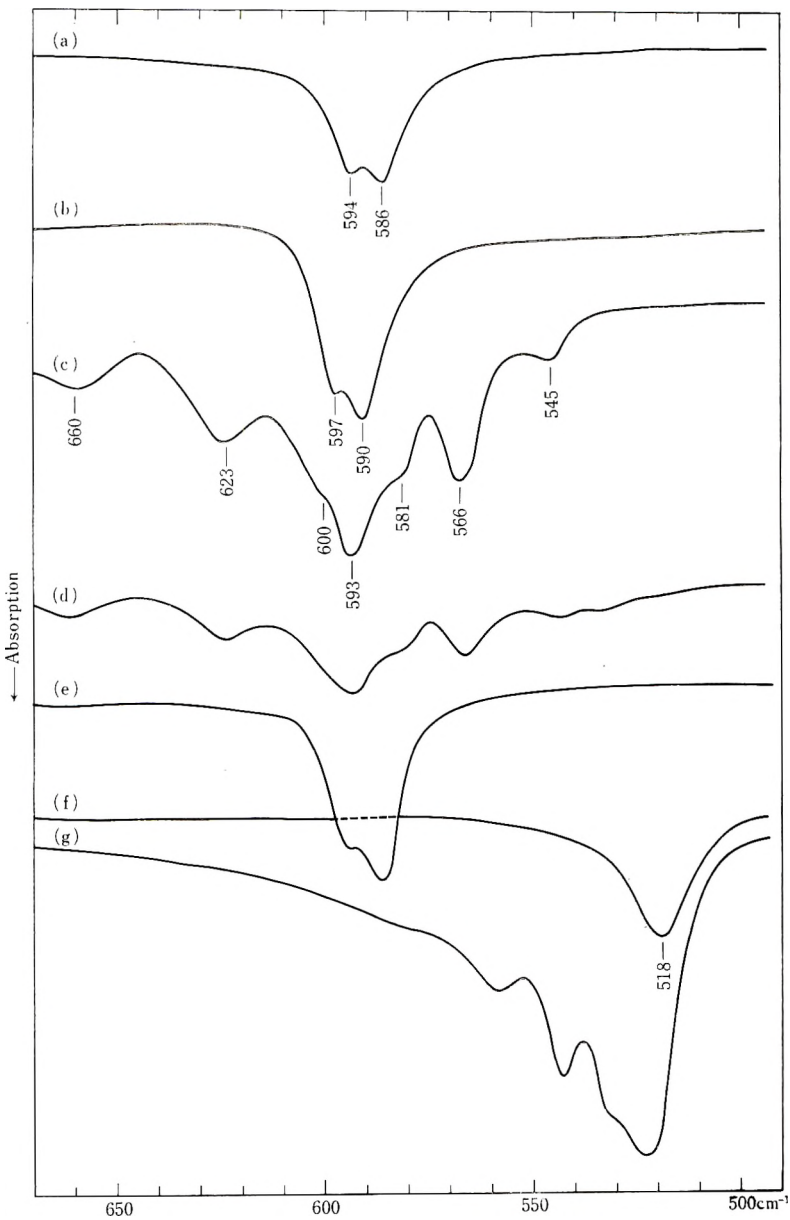

Fig. 10. Infrared spectra of poly-(*trans*-CHD=CHD), poly-(*cis*-CHD=CHD), and poly-(CD_2=CD_2) in the CDH rocking vibration region: (*a*) sample A; (*b*) sample B; (*c*) sample C; (*d*) sample D; (*e*) sample G; (*f*) sample H-1; (*g*) sample H-2.

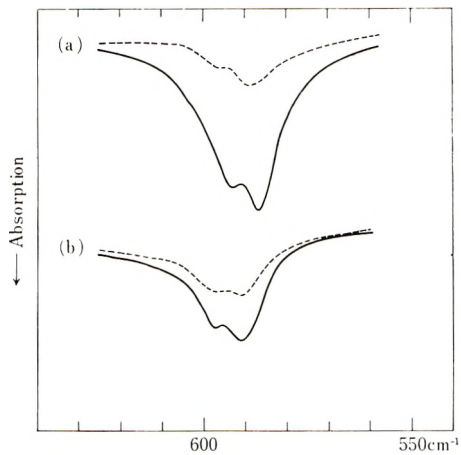

Fig. 11. Polarized infrared spectra of poly-(*trans*-CHD=CHD) and poly-(*cis*-CHD=CHD) in the CDH rocking vibration region: (*a*) sample A; (*b*) sample B; (——) radiation with electric vector perpendicular to the stretching direction; (----) radiation with electric vector parallel to the stretching direction.

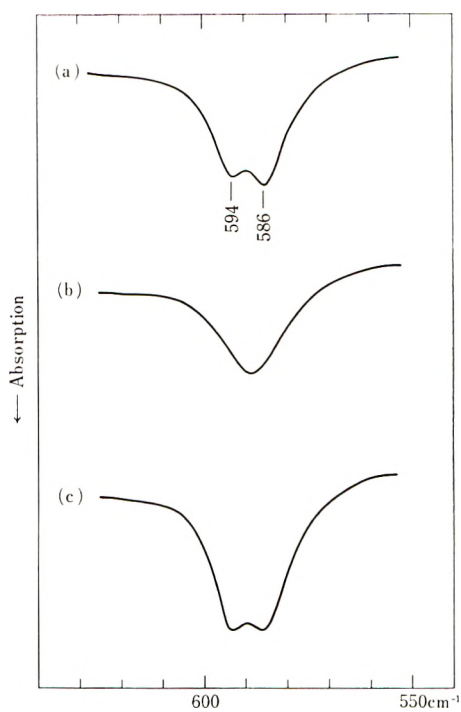

Fig. 12. Infrared spectra of poly-(*trans*-CHD=CHD) (sample A) in the CDH rocking vibration region: (*a*) solid before melting; (*b*) melted state; (*c*) solid obtained on cooling the melt.

Samples C and D show many absorption bands in this region (Fig. 10). They appear roughly symmetrical in both sides of the strongest band at ca. 590 cm.$^{-1}$. The assignments of these bands will be discussed later.

5. Summary. Poly-(*trans*-CHD=CHD) and poly-(*cis*-CHD=CHD) obtained with [$Al(Et)_3$ + $TiCl_4$] give mutually different infrared spectra.

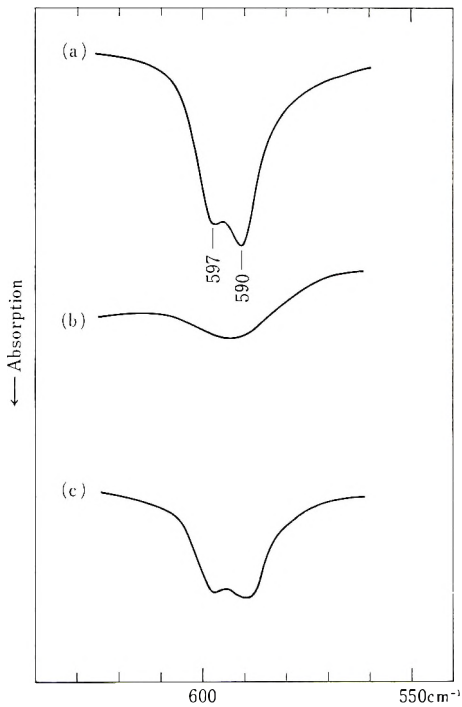

Fig. 13. Infrared spectra of poly-(*cis*-CHD=CHD) (sample B) in the CDH rocking vibration region: (*a*) solid before melting; (*b*) melted state; (*c*) solid obtained on cooling the melt.

The characteristic absorption bands of the former are found at 1335, 1288, and 590 cm.$^{-1}$ (mean frequency of the doublet) and those of the latter at 1306 and 594 cm.$^{-1}$ (mean frequency of the doublet). The spectra of poly-(*trans*-CHD=CHD) and poly-(*cis*-CHD=CHD) obtained with [$Al(i\text{-}Bu)_3$ + $TiCl_4$] are not so different from each other, but they are different from the spectra of the polymers obtained with [$Al(Et)_3$ + $TiCl_4$].

CALCULATION OF NORMAL VIBRATIONS OF MODEL STRUCTURES

I. Models

The differences between the infrared spectra of poly-(*trans*-CHD=CHD) and poly-(*cis*-CHD=CHD) must be associated with some structural dif-

ferences between these polymers. Accordingly, the analysis of the infrared spectra will provide some information on the molecular structures of these polymers. However, it is not practical to derive the molecular structures of such polymers unambiguously from the frequency analysis. On the other hand, it is comparatively easy to calculate the normal vibration frequencies of a given model structure. If the normal vibration frequencies of various

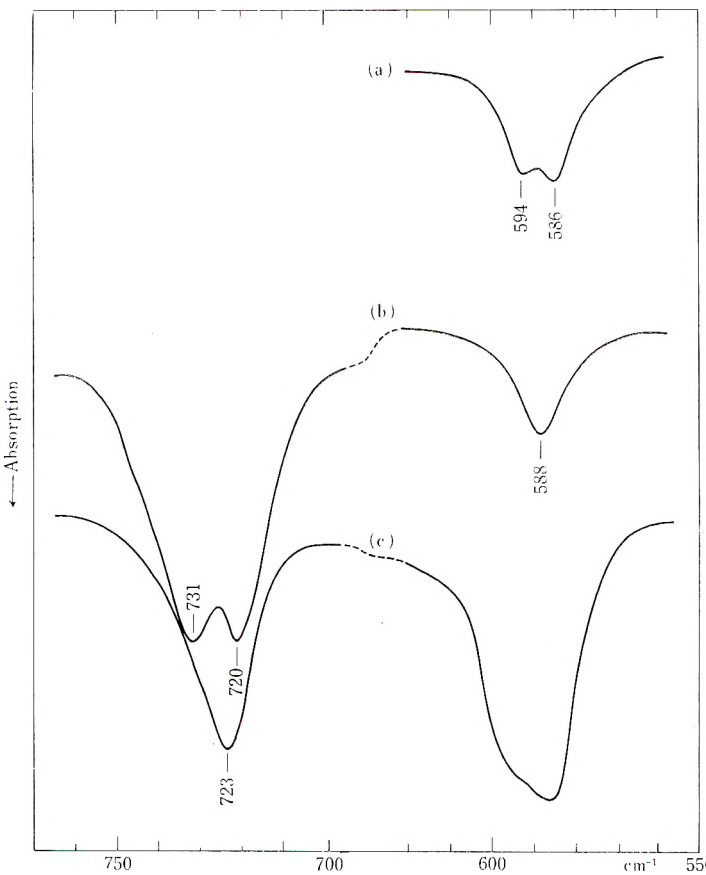

Fig. 14. Infrared spectra of the solid solutions of poly-(*trans*-CHD=CHD) in poly-(CH_2=CH_2) in the CDH rocking vibration region: (*a*) sample A; (*b*) 30% sample A and 70% sample I; (*c*) 70% sample A and 30% sample I.

model structures are calculated and the frequency-structure correlation is established, the observed spectra may be interpreted on the basis of this correlation. In such hopes we have calculated the normal vibrations for the two model structures of infinite length, namely, erythro-diisotactic structure (e-DI) and threo-diisotactic structure (t-DI) shown in Figure 15. For these models all the bond angles around the carbon atom are assumed to be tetrahedral, and the lengths of the C—C and C—H bonds are assumed to be 1.54 and 1.09 A., respectively.

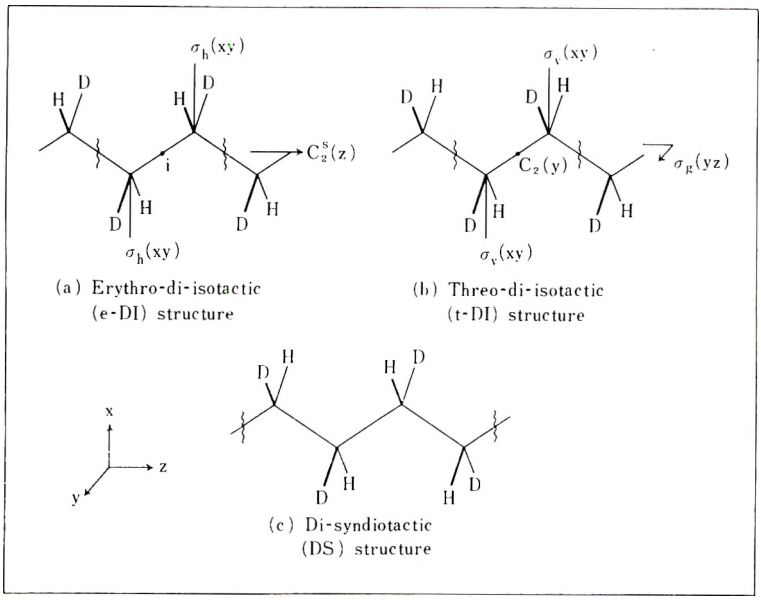

(a) Erythro-di-isotactic (e-DI) structure

(b) Threo-di-isotactic (t-DI) structure

(c) Di-syndiotactic (DS) structure

Fig. 15. Unit cells and symmetry elements of model structures.

II. Calculation of Normal Vibrations

An infinite chain has an infinite number of normal vibrations. Among them the modes in which all the corresponding atoms in all the unit cells move in phase are infrared- or Raman-active. In Table II the symmetry species, characters, number of such normal modes (n_i), and selection rules are given for the two model structures. The frequencies of such normal modes may be calculated conveniently according to the method worked out by Shimanouchi and Mizushima[6] and applied to normal and perdeuterated polyethylenes[6,7] and some vinyl polymers.[8] (The normal vibrations of the syndiotactic and isotactic polyvinyl alcohols have been calculated.[9]) When we want to carry out this calculation and draw a certain conclusion from the comparison of the observed and the calculated frequencies, we must use a set of reliable force constants. The problem of the intramolecular force field of normal paraffins including polyethylene has been studied,[10,11] and now a set of modified Urey-Bradley force constants is available. (The Urey-Bradley force constants consist of the repulsive force constants between non-bonded atoms as well as the bond-stretching and the angle-bending force constants. The details have been described by Shimanouchi.[7] Recently some modifications of this force field were proposed.[10,12,13] A review on the application of this force field to the calculation of the normal vibrations of many molecules has been written.[14]) The present calculation was carried out on the basis of the force constants given by Tasumi et al.[11] as obtained with the PC-2 computer of the Computing Center of the University of Tokyo. The results are shown in Table III. In Table IV the observed frequencies of normal and perdeuter-

TABLE II
Symmetry Species, Number of Normal Modes, and Selection Rules for the Two Model Structures

Erythro-diisotactic structure								Threo-diisotactic structure							
C_{2h}	E	C_2^z	σ_h	i	R	IR	n_i	C_{2v}	E	C_2	σ_v	σ_v'	R	IR	n_i
A_g	1	1	1	1	a	f	5	A_1	1	1	1	1	a	M_y	5
A_u	1	1	−1	−1	f	M_z	2	A_2	1	1	−1	−1	a	f	3
B_g	1	−1	−1	1	a	f	3	B_1	1	−1	1	−1	a	M_x	4
B_u	1	−1	1	−1	f	M_x,M_y	4	B_2	1	−1	−1	1	a	M_z	2

TABLE III
Calculated Frequencies for Model Structures

e-DI structure			t-DI structure		
Species	Calculated frequency, cm.$^{-1}$	Assignment	Species	Calculated frequency, cm.$^{-1}$	Assignment
A_g	2874	CH stretch.	A_1	2891	CH stretch.
	2100	CD stretch.		2109	CD stretch.
	1312	CHD bend.		1295	CHD bend.
	1150	Skeletal		1112	Skeletal
	1000	CDH rock.		588	CDH rock.
A_u	1127	CHD wag.	A_2	1328	Skeletal
	802	CDH twist.		1040	CHD wag.
B_g	1369	CHD wag.		783	CDH twist.
	1123, 867	CDH twist. and skeletal	B_1	2898	CH stretch.
				2132	CD stretch.
B_u	2914	CH stretch.		1323	CHD bend.
	2142	CD stretch.		1041	CDH rock.
	1304	CHD bend.	B_2	1238	CHD wag.
	595	CDH rock.		900	CDH twist.

TABLE IV
Observed and Calculated Frequencies of Normal and Perdeuterated Polyethylenes[a]

	Normal polyethylene		Perdeuterated polyethylene	
Species	Observed frequency, cm.$^{-1}$	Calculated frequency, cm.$^{-1}$	Observed frequency, cm.$^{-1}$	Calculated frequency, cm.$^{-1}$
A_g	2848	2852	—	2058
	1440	1445	—	1192
	1131	1143		961
B_{1g}	1415	1406	—	1230
	1061	1036	—	836
B_{2g}	1295	1295	—	916
B_{3g}	2883	2896	—	2141
	1168	1168	—	1007
A_u	1050	1050	—	743
B_{1u}	2919	2925	2192	2160
	731, 720	725	518	524
B_{2u}	2851	2903	2088	2119
	1473, 1463	1469	1092, 1087	1077
B_{3u}	1176	1175	—	889

[a] For the assignments of the observed values of normal polyethylene, see Tasumi et al.[10]

ated polyethylenes are compared with the frequencies calculated on the basis of this set of force constants. The calculation on the basis of the set of force constants given by Tasumi et al.[10] was also made, and it gave almost the same results as the present one. The use of a set of more refined force constants may alter the calculated frequencies a little from the present ones. However, it is unlikely that the order of frequencies, for example, B_1(t-DI) > B_u(e-DI) > A_1(t-DI) for the CHD bending vibration is changed by the refinement of force constants. Such frequency order is utilized in the discussion of the next section.

DISCUSSION

I. Polymers Obtained with [$Al(Et_3)$ + $TiCl_4$]

In the first place, let us discuss the origin of the small spectral differences between poly-(*trans*-CHD=CHD) and poly-(*cis*-CHD=CHD) in the CHD bending and the CDH rocking vibration regions. In Table V the observed frequencies are compared with the calculated frequencies for the model structures. The approximate vibration patterns for these calculated frequencies are illustrated in Figure 16. The following correspondence between the observed and the calculated frequencies can be seen from Table V: 1335 and 1328(*trans*)–1323(t-DI), 1288(*trans*)–1295(t-DI), 594 and 586(*trans*)–588(t-DI), 1306(*cis*)–1304(e-DI), and 597 and 590(*cis*)–595-(e-DI). In short, the frequencies of poly-(*trans*-CHD=CHD) and poly-(*cis*-CHD=CHD) are close to those of the t-DI and e-DI structures, respectively. This correspondence suggests that the actual structure of poly-(*trans*-CHD=CHD) is closer to t-DI than e-DI, and the situation is reversed for poly-(*cis*-CHD=CHD). In the present discussion, however, the band at 1321 cm.$^{-1}$ of poly-(*trans*-CHD=CHD) and the bands at 1325 and 1321 cm.$^{-1}$ of poly-(*cis*-CHD=CHD) are set aside. Before we

TABLE V
Observed and Calculated Frequencies in CHD Bending Vibration and CDH Rocking Vibration Regions

Observed frequency, cm.$^{-1}$		Calculated frequency, cm.$^{-1}$	
trans[a]	*cis*[b]	e-DI	t-DI
1335			
1328	1325		
1321	1321		1323(B_1)
		1312(A_g)	
	1306	1304(B_u)	
1288			1295(A_1)
	597		
594	590	595(B_u)	588(A_1)
586			

[a] Sample A.
[b] Sample B.

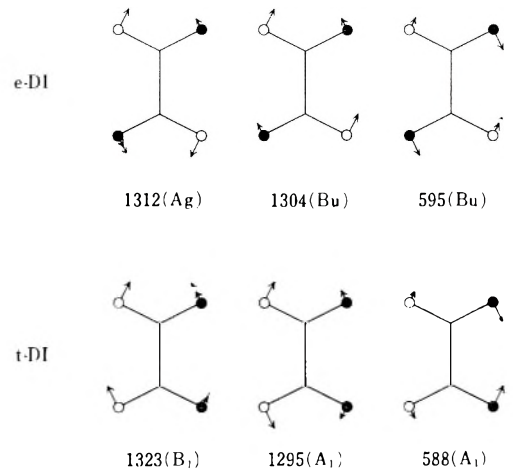

Fig. 16. Approximate vibrational patterns for the CHD bending and the CDH rocking vibrations: (O) H; (●) D.

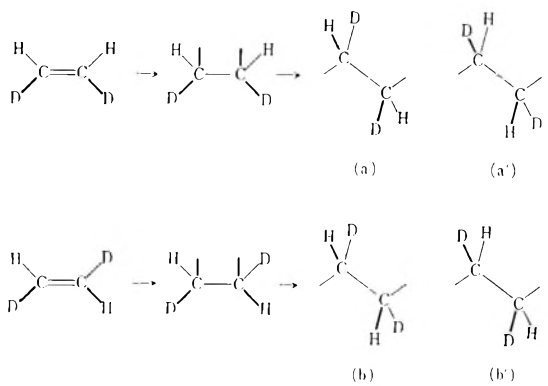

Fig. 17. *cis*-Opening of the double bond.

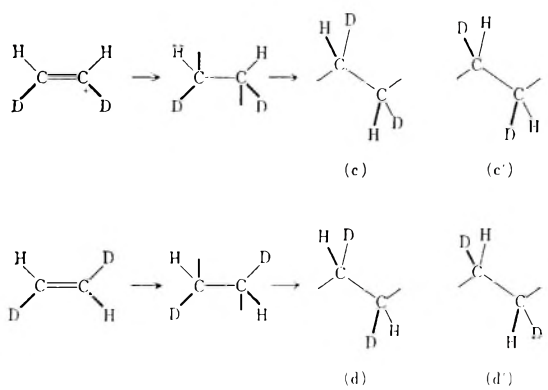

Fig. 18. *trans*-Opening of the double bond.

consider the assignments of these bands, we wish to discuss the relation between the type of the double bond opening in the polymerization reaction and the structure of the resultant polymer.

In the case of the cis-opening of the double bond which is illustrated in Figure 17, the structural unit (a) or (a′) is expected for poly-(*cis*-CHD=CHD) and the unit (b) or (b′) is expected for poly-(*trans*-CHD=CHD). The chain —aaaa— or —a′a′a′a′— corresponds to the e-DI structure and —bbbb— or —b′b′b′b′— corresponds to the t-DI structure. The chains —aa′aa′— and —bb′bb′— reduce to an identical structure, namely, the disyndiotactic structure (see Fig. 15*c*). Naturally, polymers of completely regular structures are not to be expected. Poly-(*cis*-CHD=CHD) will be a mixture of e-DI and DS portions and poly-(*trans*-CHD=CHD) will be a mixture of t-DI and DS portions.

In the case of the *trans*-opening which is illustrated in Figure 18, the structural unit (c) or (c′) is expected for poly-(*cis*-CHD=CHD) and the unit (d) or (d′) is expected for poly-(*trans*-CHD=CHD). The units (c) and (c′) are identical with (b) and (b′), respectively, and the units (d) and (d′) are identical with (a) and (a′), respectively. Hence, in this case poly-(*cis*-CHD=CHD) will be a mixture of t-DI and DS portions and poly-(*trans*-CHD=CHD) will be a mixture of e-DI and DS portions.

As described above, if only one of the two types of double bond opening takes place in the polymerization reaction with [$Al(Et)_3$ + $TiCl_4$], a certain local regularity is expected for the produced polymer. On the contrary, if both of these two types of double bond opening take place, there will be no regularity at all concerning the relative positions of the H and D atoms in the produced polymer. Accordingly, no difference can be expected between poly-(*trans*-CHD=CHD) and poly-(*cis*-CHD=CHD).

Combining the expectation described above with the suggestion obtained from the comparison of the observed and the calculated frequencies, we may conclude as follows. (*1*) Poly-(*trans*-CHD=CHD) consists mainly of t-DI and DS portions, and poly-(*cis*-CHD=CHD) consists mainly of e-DI and DS portions. (*2*) The *cis*-opening of the double bond occurs in the polymerization reaction with [$Al(Et)_3$ + $TiCl_4$].

The band at 1321 cm.$^{-1}$ of poly-(trans-CHD=CHD) and the bands at 1325 and 1321 cm.$^{-1}$ of poly-(cis-CHD=CHD), which were set aside in the preceding discussion, may reasonably be assigned to the CHD bending vibrations of the DS portions.

II. Polymers Obtained with [$Al(i\text{-}Bu)_3$ + $TiCl_4$]

The spectra of poly-(*trans*-CHD=CHD) and poly-(*cis*-CHD=CHD) obtained with [$Al(i\text{-}Bu)_3$ + $TiCl_4$] are not much different from each other. This suggests that [$Al(i\text{-}Bu)_3$ + $TiCl_4$] works differently from [$Al(Et)_3$ + $TiCl_4$].

The most apparent difference between the spectra of the polymers obtained with [$Al(Et)_3$ + $TiCl_4$] and those of the polymers obtained with [$Al(i\text{-}Bu)_3$ + $TiCl_4$] is seen in the CDH rocking region (Fig. 10). Several

bands are observed in this region for the polymers obtained with [Al(*i*-Bu)$_3$ + TiCl$_4$]. The tentative assignments of these bands may be given as follows. The strongest band at 593 cm.$^{-1}$ and the shoulder bands at ca. 600 and ca. 581 cm.$^{-1}$ arise from the CDH rocking vibrations of —(CHD)$_n$—, where $n \geqq 3$. The band at 623 cm.$^{-1}$ may be associated with the portion —CHD—CHD—CH$_2$— or —CHD—CH$_2$—CHD—. Similarly, the other bands may be associated with the various portions in the polymer chain: the 660 cm.$^{-1}$ band is with —CHD—CH$_2$—CH$_2$— or —CH$_2$—CHD—CH$_2$—, the 566 cm.$^{-1}$ band is with —CHD—CHD—CD$_2$— or —CHD—CD$_2$—CHD, and the 545 cm.$^{-1}$ band is with —CD$_2$—CHD—CD$_2$— or —CD$_2$—CD$_2$—CHD—. Such point of view is supported by the fact that, as shown in Figure 10*g*, perdeuterated polyethylene containing a considerable amount of the H atoms as impurity shows a few bands in the region of 560–530 cm.$^{-1}$, which may be associated with —CD$_2$—CHD—CD$_2$—, —CHD—CD$_2$—CD$_2$—, —CHD—CD$_2$—CHD, and so on. However, this point of view is based on the assumption that the hydrogen–deuterium exchange reaction such as CHD=CHD → CHD=CH$_2$ or → CHD=CD$_2$ takes place simultaneously with the polymerization. This assumption appears somewhat strange, but there are other experimental results which may be well explained on it. (*1*) In the CD stretching vibration region, bands characteristic of the polymers obtained with [Al(*i*-Bu)$_3$ + TiCl$_4$] appear at 2095 and 2176 cm.$^{-1}$. These are close to the bands at 2088 and 2192 cm.$^{-1}$ of perdeuterated polyethylene and may be assigned, respectively, to the symmetric and antisymmetric stretching vibrations of the isolated CD$_2$ group. (*2*) In the CH stretching vibration region also, the spectra of the polymers obtained with [Al(*i*-Bu)$_3$ + TiCl$_4$] are somewhat different from those of the polymers obtained with [Al(Et)$_3$ + TiCl$_4$] (Fig. 2). The bands at 2850 and ca. 2919 cm.$^{-1}$ are much stronger in the spectra of the polymers obtained with [Al(*i*-Bu)$_3$ + TiCl$_4$]. The corresponding bands of the polymers obtained with [Al(Et)$_3$ + TiCl$_4$] have been assigned to the CH$_2$ symmetric and antisymmetric stretching vibrations of normal polyethylene produced from the ethyl group of Al(Et)$_3$. However, the bands of the polymers obtained with [Al(*i*-Bu)$_3$ + TiCl$_4$] cannot be attributed to normal polyethylene, because these polymers absorb neither at 1463 nor 720 cm.$^{-1}$ and it is clear from this fact that these polymer samples do not contain normal polyethylene. Hence, these bands must be assigned to the symmetric and antisymmetric stretching vibrations of the isolated CH$_2$ group. (*3*) The intensity of the 1453 cm.$^{-1}$ band, which has been assigned to the bending vibration of the isolated CH$_2$ group placed between CHD groups, is much stronger in the spectra of the polymers obtained with [Al(*i*-Bu)$_3$ + TiCl$_4$] than in the spectra of those obtained with [Al(Et)$_3$ + TiCl$_4$]. This indicates the existence of a considerable amount of the isolated CH$_2$ groups in the polymers obtained with [Al(*i*-Bu)$_3$ + TiCl$_4$]. (The CH$_2$ group which is sandwiched between CHD and CD$_2$ or between CHD and CH$_2$ will absorb at the frequencies close to 1453 cm.$^{-1}$.) (*4*) The band which is assignable to the CD$_2$ bending

vibration seems to exist at 1085 cm.$^{-1}$ in the spectra of the polymers obtained with [Al(*i*-Bu)$_3$ + TiCl$_4$], although it is obscured by the overlap of a broad band arising from impurity.

We may regard the findings described above as enough evidence to prove the validity of our following conclusions. Not only the polymerization but also the hydrogen–deuterium exchange reaction in monomers is promoted by the catalyst [Al(*i*-Bu)$_3$ + TiCl$_4$]. On account of this no significant difference can be found between poly-(*trans*-CHD=CHD) and poly-(*cis*-CHD=CHD) obtained with this catalyst.

III. Band Assignments

The band assignments which have been obtained in the present discussion are summarized in Tables VI and VII. All the observed bands showed perpendicular dichroism. Our trial to find parallel bands did not succeed.

TABLE VI
Assignments of the Infrared Bands of Poly-(*trans*-CHD=CHD) and Poly-(*cis*-CHD=CHD) obtained with [Al(Et)$_3$ + TiCl$_4$]

Observed frequency, cm.$^{-1}$		
trans[a]	*cis*[b]	Assignment
2957(vw)	2957(vw)	$\nu_{as}(CH_3)$
2923(vw)	2923(vw)	$\nu_a(CH_2)$ of $-(CH_2)_n-$
2897(vs)	2900(vs)	ν(CH)
2882(vs)	2880(vs)	ν(CH)
2850(w)	2850(w)	$\nu_s(CH_2)$ of $-(CH_2)_n-$
2590(w)	2590(w)	
2152(sh)	2155(sh)	ν(CD)
2133(s)	2137(s)	ν(CD)
1463(w)	1463(w)	$b(CH_2)$ of $-(CH_2)_n-$
1453(w)	1453(w)	$b(CH_2)$ of isolated CH_2
1335(m), 1328(m)		b(CHD) of t-DI portion
	1325(m), 1321(m)	b(CHD) of DS portion
1321(m)		
	1306(m)	b(CHD) of e-DI portion
1288(w)		b(CHD) of t-DI portion
1230(vw)		
725(vw)	725(vw)	$r(CH_2)$ of $-(CH_2)_n-$
	597(w), 590(w)	r(CDH) of e-DI portion
594(w), 586(w)		r(CDH) of t-DI portion

[a] Sample A.
[b] Sample B.

IV. Conclusion

It has already been recognized that the normal vibration calculation is useful in the interpretation of vibrational spectra[14,15] and also in the

TABLE VII
Assignments of the Infrared Bands of Poly-(*trans*-CHD=CHD) and Poly-(*cis*-CHD=CHD) obtained with [Al(*i*-Bu)$_3$ + TiCl$_4$]

Observed frequency, cm.$^{-1}$	Assignment
2919(sh)	$\nu_a(CH_2)$ of isolated CH_2
2899(vs)	$\nu(CH)$
2880(vs)	$\nu(CH)$
2850(s)	$\nu_s(CH_2)$ of isolated CH_2
2176(m)	$\nu_a(CD_2)$ of isolated CD_2
2140(s)	$\nu(CD)$
2095(m)	$\nu_s(CD_2)$ of isolated CD_2
1327(m) 1321(m)	$b(CHD)$ of DS or t-DI portion
1306(m)	$b(CHD)$ of c-DI portion
1290(sh)	$b(CHD)$ of t-DI portion
660(vw)	Rocking-type vibration of —CHD—CH_2—CH_2— or —CH_2—CHD—CH_2—
623(w)	Rocking-type vibration of —CHD—CHD—CH_2— or —CHD—CH_2—CHD—
600(sh) 593(m) 581(sh)	Rocking-type vibration of —$(CHD)_n$—, where $n \geqq 3$
566(w)	Rocking-type vibration of —CHD—CHD—CD_2— or —CHD—CD_2—CHD—
545(vw)	Rocking-type vibration of —CD_2—CHD—CD_2— or —CHD—CD_2—CD_2—

determination of molecular conformations.[15,16] In the present work the normal vibration calculation was applied to the study of the "configuration" of the polymer chain —$(CHD)_n$—, and the usefulness of this method was shown. The configuration of this polymer is directly related to the type of double bond opening in the polymerization reaction, and we may say that the normal vibration calculation has provided a new method for the study of the reaction mechanism.

Recently the knowledge on the force constants of many molecules is increasing. If the transferability of force constants among molecules with similar structures is assumed, the normal vibration frequencies of various molecules may be calculated. We believe that such calculation will give information to the study of various chemical problems.

References

1. Ikeda, S., A. Yamamoto, and H. Tanaka, *J. Polymer Sci.*, **A1**, 2925 (1961).
2. Kyogoku, Y., T. Shimanouchi, and T. Miyazaki, *Spectrochim. Acta*, **19**, 451 (1963).
3. Yamaguchi, A., I. Ichishima, and S. Mizushima, *Spectrochim. Acta*, **12**, 294 (1958).
4. Kern, R. J., and H. J. Hurst, *J. Polymer Sci.*, **34**, 272 (1960).

5. Krimm, S., C. Y. Liang, and G. B. B. M. Sutherland, *J. Chem. Phys.*, **25**, 549 (1956).
6. Shimanouchi, T., and S. Mizushima, *J. Chem. Phys.*, **17**, 1102 (1949).
7. Shimanouchi, T., *J. Chem. Phys.*, **17**, 245, 734, 848 (1949).
8. Shimanouchi, T., and M. Tasumi, *Bull. Chem. Soc. Japan*, **34**, 359 (1961).
9. Tasumi, M., to be published.
10. Tasumi, M., T. Shimanouchi, and T. Miyazawa, *J. Mol. Spectroscopy*, **9**, 261 (1962).
11. Tasumi, M., T. Shimanouchi, and T. Miyazawa, *J. Mol. Spectroscopy*, in press.
12. Overend, J., and J. R. Scherer, *J. Chem. Phys.*, **33**, 1681 (1960).
13. Suzuki, I., and T. Shimanouchi, *J. Mol. Spectroscopy*, **8**, 222 (1962).
14. Shimanouchi, T., presented at Symposium on Molecular Structure and Spectroscopy (Tokyo), 1962, *Preprints* C216.
15. Mizushima, S., *Structure of Molecules and Internal Rotation*, Academic Press, New York, 1954.
16. Miyazawa, T., *J. Chem. Phys.*, **35**, 693 (1961).

Résumé

On a obtenu la poly-(*trans*-CHD=CHD) et le poly-(*cis*-CHD=CHD) au moyen de [$Al(Et)_2$ + $TiCl_4$] et au moyen de [$Al(i\text{-}Bu)_3$ + $TiCl_4$]. Le poly-(*trans*-CHD=CHD) et le poly-(*cis*-CHD=CHD) obtenus au moyen de [$Al(Et)_3$ + $TiCl_4$] donnent des spectres infra-rouges différents entre eux. Les bandes d'absorption caractéristiques du premier sont 1335, 1288, 594 et 586 $cm.^{-1}$ et ceux du dernier 1306, 597 et 590 $cm.^{-1}$. On a calculé en vue d'interprêter ces spectres, les fréquences normales de vibration des structures modèles, notamment les structures erytho-diisotactiques et thrèo-diisotactiques. A partir de la comparaison des fréquences observées et calculées, on conclut que le poly-(*trans*-CHD=CHD) obtenu au moyen de [$Al(Et)_3$ + $TiCl_4$] consiste principalement de portions thréo-diisotactiques et disyndiotactiques et le poly-(*cis*-CHD=CHD) obtenu avec le même catalyseur consiste principalement de portions érythro-diisotactique et disyndiotactique. On discute la relation entre le type de double liaison ouverte et la structure du polymère résultant, et on conclut que l'ouverture de la double liaison *cis* se passe dans la réaction de polymérisation avec [$Al(Et)_3$ + $TiCl_4$]. Les spectres du poly-(*trans*-CHD=CHD) et du poly-(*cis*-CHD=CHD) obtenus au moyen de [$Al(i\text{-}Bu)_3$ + $TiCl_4$] ne sont pas différents l'un de l'autre, mais ils sont différents des spectres des polymères obtenus au moyen de [Al(ET)$_3$ + $TiCl_4$]. Les polymères obtenus au moyen de [$Al(i\text{-}Bu)_3$ + $TiCl_4$] montrent des bandes caractéristiques à 2919, 2850, 2176, 2095, 1453, 660, 623, 600, 593, 581, 566, et 545 $cm.^{-1}$. Ces bande sprouvent la présence de groupes isolés CH_2 et CD_2. Ces faits indiquent que la réaction d'échange hydrogène–deutérium dans les monomères aussi bien qu'au cours de la polymérisation est activée par [$Al(i\text{-}Bu)_3$ + $TiCl_4$].

Zusammenfassung

Poly-(*trans*-CHD=CHD) und Poly-(*cis*-CHD=CHD) wurden mit [$Al(Et)_3$ + $TiCl_4$] und [$Al(i\text{-}Bu)_3$ + $TiCl_4$] erhalten. Mit [$Al(Et)_3$ + $TiCl_4$] dargestelltes Poly-(*trans*-CHD=CHD) und Poly-(*cis*-CHD=CHD) weisen verschiedenartige Infrarotspektren auf. Die charakteristichen Absorptionsbanden des ersteren liegen bei 1335, 1288, 594, und 586 $cm.^{-1}$, die des letzteren bei 1306, 597, und 590 $cm.^{-1}$. Zur Zuordnung dieser Spektren wurden die Normalschwingungsfrequenzen der Modellstrukturen, nämlich der erythro-diisotaktischen und der threo-diisotaktischen Struktur, berechnet. Der Vergleich der beobachteten und der berechneten Frequenzen zeigte, dass das mit [$Al(Et)_3$ + $TiCl_4$] erhaltene Poly-(*trans*-CHD=CHD) hauptsächlich aus threo-diisotaktischen und disyndiotaktischen Anteilen und das mit dem gleichen Katalysator erhaltene Poly-(*cis*-CHD=CHD) hauptsächlich aus erythro-diisotaktischen und di-

syndiotaktischen Anteilen besteht. Die Beziehung zwischen dem Doppelbindungsöffnungstyp und der Struktur des resultierenden Polymeren wurde diskutiert und der Schluss gezogen, dass die *cis*-Öffnung der Doppelbindung bei der Polymerisation mit [$Al(Et)_3$ + $TiCl_4$] auftritt. Mit [$Al(i\text{-}Bu)_3$ + $TiCl_4$] dargestelltes Poly-(*trans*-CHD=CHD) und Poly-(*cis*-CHD=CHD) zeigen keine so grossen Unterschiede in ihren Spektren, sie unterschieden sich aber von den Spektren der mit [$Al(Et)_3$ + $TiCl_4$] erhaltenen Polymeren. Die mit [$Al(i\text{-}Bu)_3$ + $TiCl_4$] erhaltenen Polymeren besitzen charakteristische Banden bei 2919, 2850, 2176, 2095, 1453, 660, 623, 600, 593, 581, 566, und 545 $cm.^{-1}$. Diese Banden beweisen die Gegenwart isolierter CH_2— und CD_2-Gruppen. Diese Tatsache läss erkennen, dass [$Al(i\text{-}Bu)_3$ + $TiCl_4$] neben der Polymerisation auch die Wasserstoff–Deuterium-Austauschreaktion katalysiert.

Received March 8, 1963

JOURNAL OF POLYMER SCIENCE: PART A VOL. 2, PP. 1633–1640 (1964)

Fractionation of Chemically Heterogeneous Latex Particles by Centrifugation

J. B. YANNAS,* *W. R. Grace and Company, Cambridge, Massachusetts*

Synopsis

A simple centrifugation method for the clean separation of chemically heterogeneous latex particles is described in some detail. It exploits density differences among particles that could be due to differences in composition, degree of crosslinking, crystallinity or other structural features. Particles differing in density by as little as 0.005 g./ml. have been cleanly separated. The fractionation of particles differing in density by less than the above should be feasible with this method which is applicable to concentrated as well as dilute latices.

Introduction

A tacit assumption underlying characterization work on latex systems is that a latex comprises a population of spherical polymer particles dispersed in an aqueous phase which are identical in all respects except size. No attempt has been made to investigate heterogeneity among particles that could result from differences in chemical composition, gel content, crystallinity and other structural features.

A simple and relatively rapid method for the separation of latex particles into fractions differing in density has been developed and is described here in some detail. This method is applicable to concentrated as well as dilute latices and makes use of a simple preparative centrifuge with no special provision for temperature control or convective control. In spite of the lack of sophistication in the apparatus used, latex particles differing in density by as little as 0.005 g./ml. have been cleanly separated. The resolution obtainable with this method makes it therefore suitable for investigations of structural and composition heterogeneity among particles of latex as long as this heterogeneity gives rise to small density differences among these particles. Heterogeneity due to differences in chemical composition has already been unmistakably detected in certain copolymer latices in this laboratory and the results of this investigation will be reported at a later time. The present paper will deal with the description of the separation procedure itself.

Briefly, the method calls for the addition of a suitable low molecular

* Present address: Frick Chemical Laboratory, Princeton University, Princeton, New Jersey.

weight solute to the latex (here assumed to contain only two distinct particle species) so that the density of the aqueous phase is controlled to the desired level. If the density of the aqueous phase matches exactly that of one of the species, the latter is held buoyant while the other species either floats or sediments in the centrifugal field. If the density of the aqueous phase is adjusted to an intermediate level, particles of one species float whereas particles of the other sediment, leaving a layer of practically clear serum in the middle of the tube. In principle, the method is similar to that used by Harvey for the fragmentation of sea urchin eggs,[1] by Behrens for the separation of cell constituents,[2] and by Lindgren et al. for the isolation of human blood lipoproteins.[3]

Experimental Method

The centrifuge used was a Servall SS-3 model equipped with an SM-24 rotor.

The separation method can be followed in detail by reference to the schematic diagram in Figure 1, where ρ_w represents the density of distilled water at the temperature of the investigation. Line I is the density–concentration relation of a latex all of whose particles are assumed to have a uniform density ρ_I.* The particles in this latex will be held buoyant when their density is equal to the aqueous phase density. This will occur at a certain latex dilution level corresponding to a polymer weight concentration which here is called the buoyancy concentration. At the buoyancy concentration, the densities of particles, aqueous phase and, therefore, that of the whole latex itself are all equal to ρ_I. In line I, the black dot indicates the point of buoyancy for the particles in this latex; it corresponds to a polymer concentration of 20.0%. Similarly, line II is the density–concentration relation for another latex all of whose particles have a uniform density ρ_{II}. Particles II will be held buoyant when this latex has the density ρ_{II}. In Figure 1, the black dot in line II is the point of buoyancy corresponding to a polymer concentration of 15.0%.

A physical blend of these two latices (for example, in the ratio 50/50 by weight of particles) gives the density–concentration relation represented by line III (Fig. 1). The horizontal lines in the diagram are drawn at the density levels of particles I and II and intersect line III at points A and B, respectively. Vertical lines projected from points A and B to the abscissa define concentration levels of latex III whose density is exactly equal to the density of particles I and II. In the diagram, these concentration levels are 12.5 and 37.5%, respectively.

If now the concentration of latex III (containing the two particle species) is adjusted to 12.5% and the latex is centrifuged, particles I will be held buoyant while the heavier particles II will sediment. Correspondingly, at

* This relation has been found to be quite linear for all latices examined so far. It can be obtained by measuring the density of the latex at several levels of dilution with distilled water.

a concentration of 37.5%, the density of latex III will be equal to the density of particles II which, upon centrifugation, will be immobilized while the lighter particles I will float and collect at the top of the tube. In the concentration range 12.5–37.5%, particles I will float while particles II will sediment, leaving a particle-free serum layer in the middle of the tube. Outside the concentration range 12.5–37.5%, both particles I and II will either sediment or float together, failing to accumulate in distinct fractions.

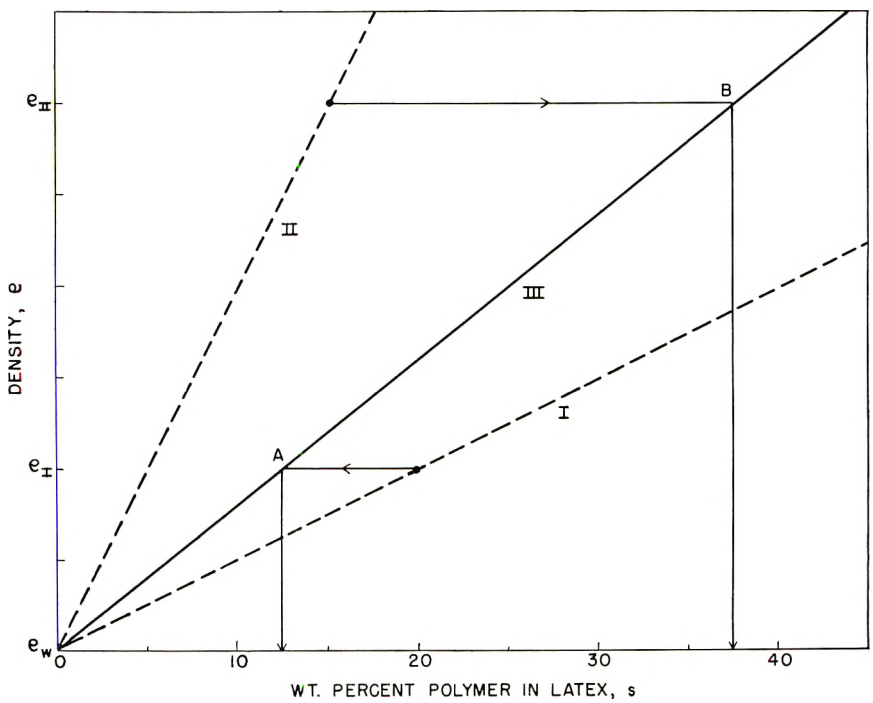

Fig. 1. Density–concentration relations for two latices (lines I and II) and a 50/50 (by weight) blend of particles (line III). The dots on lines I and II indicate the buoyancy concentration for the corresponding latices.

Given a certain unknown latex on which information with respect to particle heterogeneity is desired, one has to proceed without the benefit of the auxiliary lines I and II in Figure 1. Instead one can obtain experimentally only the density–concentration relation for the unknown which, in the case of this hypothetical latex, is shown as the solid line in Figure 2. The vertical, broken line in Figure 2 represents the highest concentration level at which the latex remains colloidally stable. For this hypothetical case, instability occurs above 60 wt.-% polymer at which concentration the unknown latex has a density of ρ_{max}. On the assumption that the particle components in this latex are two, three possible cases can be seen to arise.

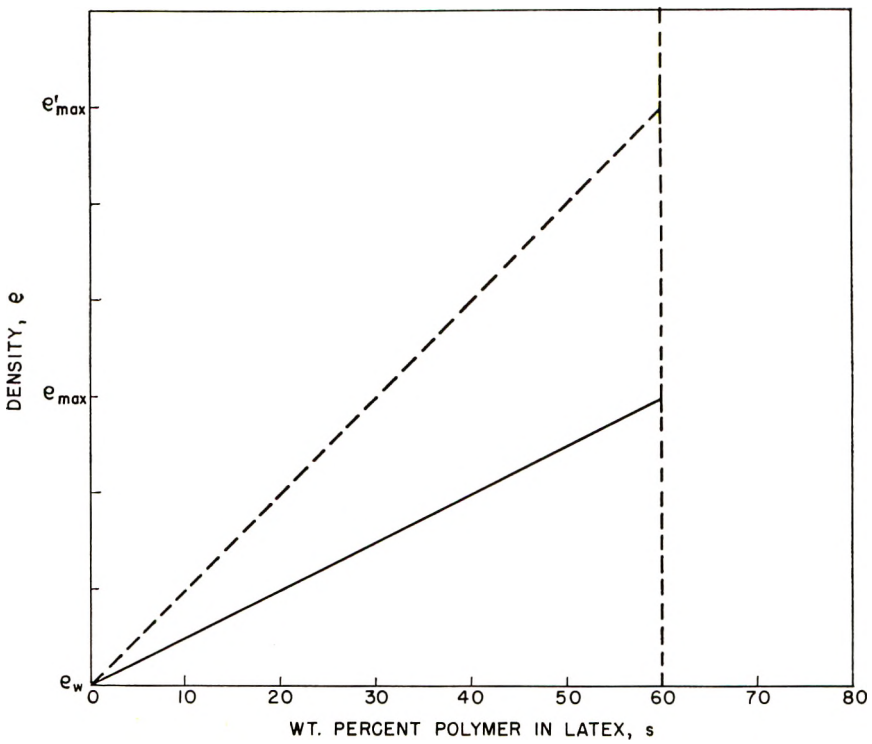

Fig. 2. Density–concentration relation for a latex (——) and for the same latex to which a heavy low molecular weight solute has been added (– –).

Case 1. The density of at least one of the two particle components lies inside the range ρ_w to ρ_{max}. In this case, the latex is simply diluted with water to several concentration levels and centrifuged whereupon a yield of particle fractions is obtained according to the scheme of Figure 1 and the accompanying explanation.

Case 2. The densities of both components are higher than ρ_{max}. This distinction can be made when protracted centrifugation of the unknown latex at its highest concentration causes sedimentation of all particles. In such a case, a heavy solute is added to the aqueous phase of the latex to increase the slope of the density-concentration line (see dotted line in Fig. 2). The value of ρ_{max} is thus increased to ρ'_{max}* until the latter becomes just higher than the density of the lighter component as evidenced by a trial centrifugation. The procedure of case 1 is now applicable.

Case 3. The densities of both components are lower than ρ_w. This can be inferred to be the case when centrifugation of the unknown latex in highly diluted form causes flotation of all particles. In a situation of

* For simplicity of graphical presentation, the stability of the latex is taken as independent of the nature and amount of solute added; thus ρ'_{max} corresponds to a polymer concentration of 60% (Fig. 2) as was the case prior to the addition of solute.

this kind, a solute lighter than water is added to the latex until the density of the aqueous phase becomes lighter than the heavier component. Once this is achieved, the procedure of case 1 becomes again applicable.

It must be emphasized at this point that the adjustment of the latex aqueous phase which becomes mandatory in cases 2 and 3 involves a certain amount of trial. This is necessary because the choice of low molecular weight solute is limited not only by its density and solubility but also by its effect on latex stability. Many latices are very sensitive even to low concentrations of metallic ions; use of most salts to increase the aqueous phase density of such latices (required in case 2) is, therefore, precluded. Most latices, however, can be specially stabilized for this purpose with nonionic emulsifiers. Where such stabilization by nonionic emulsifiers is not possible or desirable, materials such as glucose (density 1.54 g./ml.) or bromoacetic acid (density 1.93 g./ml.) can be used to increase the density of the aqueous phase without affecting latex stability.

The choice of aqueous phase solute in case 3 is very limited, since the number of compounds (usually liquids) which are lighter than water and which do not affect latex stability are very few. For example, several soluble derivatives of ethylamine destabilize many latices even at very low concentrations. Soluble alcohols also coagulate latices but usually at higher concentrations; here, again, the sensitivity of the latex to alcohol can be usually improved considerably by addition of nonionic emulsifiers of the polymerized ethylene oxide type.

Results

As an illustration of the purity of fractions obtainable by this method, the results of a few actual separations will be reported in some detail. All latices investigated were butadiene–styrene copolymers prepared at various comonomer compositions. Particle size for these essentially monodisperse latices ranged from 1900 to 2100 A. Latices of known composition were mixed in known proportion to give blends which were then subjected to the procedure described below.

In one case (blend 1 in Table I) two butadiene–styrene latices (designated components I and II in Table I) were prepared with butadiene content of 36.6 and 33.2 wt.-% in the polymer particles so that the density difference between particles in these latices amounted to 0.005 g./ml. From previous experience with these latices it was clear that the proposed separation would fall under case 2 (see previous section), so that adjustment of the latex density upwards would be necessary. For this reason, a small amount of sodium pyrophosphate decahydrate (density 1.82 g./ml.) was added during the polymerization. This solute did not affect latex stability at the low concentration at which it was used; in fact, it performs as a useful buffer in many emulsion polymerizations which are initiated by persulfate, as the ones considered here were.

Blend 1 was prepared by mixing these latices in equal proportions (by weight of particles) and stirring carefully. The resulting blend was diluted

TABLE I
Characteristics of Particles Separated by Centrifugation

Blend	Component I		Component II		Density difference, g./ml.
	Butadiene, wt.-%	Particle density at 25°C., g./ml.	Butadiene, wt.-%	Particle density at 25°C., g./ml.	
1	36.6	1.005	33.2	1.010	0.005
2	47.1	0.986	33.2	1.010	0.024
3	70.3	0.943	8.1	1.048	0.105

at several levels with water and centrifuged for 3 hr. at 15,500 rpm corresponding to ca. 30,000 g in the centrifuge used. This procedure gave a ready indication of the concentration levels at which particles I and II, respectively, were buoyant. Accordingly, fresh samples of the blend were centrifuged at polymer concentrations corresponding to the following three levels of density: 1.005 g./ml. (equal to the density of particles I), 1.008 g./ml. (intermediate between the density of the two species) and 1.010 g./ml. (equal to the density of particles III).

In the first instance (buoyancy-sedimentation), a neatly packed sediment was collected. In the second (flotation-sedimentation), both top and bottom fractions of particles in highly concentrated form were collected. In the third instance (buoyancy-flotation), a concentrated fraction of particles was removed from the top.

TABLE II
Purity of Fractions Obtained by Centrifugation

Procedure	Density relation	Fraction obtained	Purity of fraction, %
Buoyancy-sedimentation	$\rho_{II} > \rho_I = \rho_{III}$	Bottom	86–86
Flotation-sedimentation	$\rho_{II} > \rho_{III} > \rho_I$	Bottom	>97
		Top	>97
Buoyancy-flotation	$\rho_{II} = \rho_{III} > \rho_I$	Top	70–75

The above three procedures were used to separate heterogeneous particles from two more blends of latices which were prepared and centrifuged in exactly the same manner. One of the two additional latex blends prepared (blend 2 in Table I) contained particles analyzing 33.2 and 47.1 wt.-% butadiene. The other blend (blend 3 in Table 1) contained particles with 8.1 and 70.3% butadiene.

At the completion of centrifugation, all fractions removed from the tubes were carefully analyzed for (a) polymer content by ASTM method D1417-61 and with proper corrections for the presence of nonpolymeric solids and (b) butadiene content by an infrared absorption method standardized against copolymers of known composition. Results of several runs at the same density level for each blend were obtained and the purity

of fractions collected and analyzed was expressed as the weight per cent of the major component in it.

In all, therefore, three latex blends were prepared and each was centrifuged several times following the three procedures that could yield distinct fractions. The results are collectively presented in Table II where ρ_{III} is the density level of the blended latex at which the latter was centrifuged and ρ_I and ρ_{II} are the densities of the component particles in each case.

The results in Table II show that the flotation-sedimentation procedure is clearly superior. Unsatisfactory results were obtained with the buoyancy-flotation procedure, while the buoyancy-sedimentation procedure gave results of intermediate quality.

Discussion

The high degree of purity of fractions obtained by the flotation-sedimentation procedure can be attributed to the migration of the two species in opposed directions inside the tube. It can also be concluded that there was negligible entrainment of one particle species by the other as the two transferred past each other. This was found to be true even in cases where the total weight fraction of particles in the latex was as high as 40% (corresponding to a volume fraction of 40%). At weight fractions higher than ca. 45%, however, the purity of the fractions was somewhat lower.

The relatively lower quality of separation obtained by the buoyancy-sedimentation procedure (see Table II) is certainly due to the fact that only one species transfers along the tube. The other species is held buoyant thus contaminating the bottom wherein the migrating species collects. On the other hand, the migration of the heavier species toward the bottom of the tube leads to the creation of a positive concentration gradient along the same direction. This concentration gradient corresponds to a positive density gradient along the same direction. Apparently, the latter gradient must have been steep enough to protect the system from stirring caused by mechanical and thermal convection. Thus the purity obtained with this procedure was reasonably high at 82–86%. The reverse situation holds true in the case of buoyancy-flotation. Here, the negative density gradient formed by the floating species leads to hydrodynamic instability at the top of the tube which causes mixing of the two species.[4] This probably accounts for the unsatisfactory purity of the fractions obtained with this procedure (70–75%).

Under the particular centrifugation conditions used, the purity of separation was found to be independent of the density differential between the heterogeneous particle species. The particle size of the components as well as its distribution (although not studied as variables) should also not affect the quality of separation as long as centrifugation is conducted at an appropriately high rotor speed and for an adequate period of time.

It appears at present that the resolution of the method is limited mainly

by the sensitivity of the physicochemical methods used in characterization of the fractions. Fractionation of latex particles differing in density by less than 0.005 g./ml. should probably, therefore, be feasible. The method is currently used to study the effect of emulsion copolymerization variables on the chemical heterogeneity of the resulting latex particles. It could possibly be extended toward the study of particles differing in degree of crosslinking or fraction of crystallinity.

The skillful assistance of Mr. A. D. Clarke in obtaining the experimental data is acknowledged. Dr. A. S. Wexler and Miss Jane Hosking analyzed the copolymers and the fractions for butadiene content.

References

1. Harvey, E. B., *Biol. Bull.*, **62,** 155 (1932).
2. Behrens, M., *Hoppe-Seylers Z. Physiol. Chem.*, **253,** 185 (1938).
3. Lindgren, F. T., A. V. Nichols, F. T. Upham, and R. D. Wills, *J. Phys. Chem.*, **66,** 2007 (1962).
4. Pickels, E. G., *J. Gen. Physiol.*, **26,** 341 (1943).

Résumé

On décrit de façon quelque peu détaillée une méthode simple de centrifugation pour la séparation nette de particules de latex chimiquement hétérogène. Elle exploite des différences de densité entre les particules qui pourraient être dues à des différences de composition, degré de pontage, cristallinité ou autres facteurs structurels. On a séparé avec netteté des particules dont la densité ne diffère pas de plus de 0.005 g./ml. Il serait possible avec cette méthode, qui est applicable aussi bien à des latex concentrés que dilués, de fractionner des particules dont la densité diffère encore moins fort.

Zusammenfassung

Eine einfache Zentrifugiermethode zur sauberen Trennung chemisch heterogener Latexteilchen wird ausführlich beschrieben. Sie macht sich Dichteunterschiede zwischen den Teilchen zunutze, die auf Verschiedenheiten in Zusammensetzung, Vernetzungsgrad, Kristallinität oder anderen strukturellen Eigenschaften beruhen. Teilchen mit so kleinen Dichteunterschieden wie 0,005 g./ml. wurden sauber getrennt. Teilchen mit noch geringeren Dichteunterschieden sollten mit dieser Methode, die sowohl auf konzentrierte als auch auf verdünnte Latices anwendbar ist, fraktioniert werden können.

Received March 6, 1963

JOURNAL OF POLYMER SCIENCE: PART A VOL. 2, PP. 1641–1645 (1964)

α-Trifluoromethyl Vinyl Acetate

HOWARD C. HAAS and NORMAN W. SCHULER, *Chemical Research Laboratories, Polaroid Corporation, Cambridge, Massachusetts*

Synopsis

α-Trifluoromethyl vinyl acetate has been synthesized. Although the homopolymer has not been obtained, this new monomer readily copolymerizes with a variety of vinyl monomers including styrene. Alcoholysis of vinyl acetate/α-trifluoromethyl vinyl acetate copolymers leads to trifluoromethyl-substituted polyvinyl alcohols having new and unusual properties. These polyvinyl alcohol derivatives, containing about 30 wt.-% of fluorine, are completely insoluble in water but dissolve in the lower alcohols. Because of the increased acidity of fluorosubstituted alcohols, they are also soluble in dilute aqueous alkalies to yield polyalkoxide-type solutions.

Continuing our research on polyvinyl alcohol (PVA) and related hydroxyl containing polymers,[1–6] we have now prepared and studied a new monomer, α-trifluoromethyl vinyl acetate. It was thought that replacement of the allylic hydrogens of isopropenyl acetate[7–9] by fluorine would reduce degradative chain transfer during polymerization, modify copolymerization behavior, and perhaps lead to some interesting materials. Copolymerization of this new monomer with vinyl acetate and alcoholysis of the resulting copolymer has yielded CF_3-substituted PVA having rather unique properties.

Monomer Preparation

After numerous attempts to prepare 3,3,3-trifluoro-2-acetoxypropene, this material was finally synthesized in good yield by the following sequence of reactions:

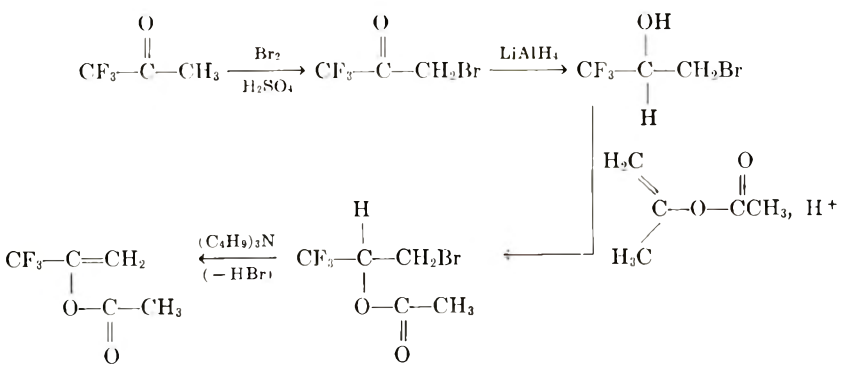

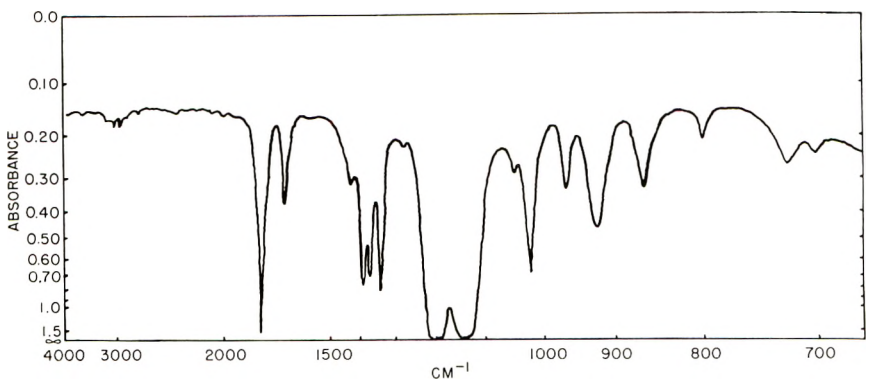

Fig. 1. Infrared spectrum of α-trifluoromethyl vinyl acetate.

The infrared spectrum of the pure monomer is presented in Figure 1. Direct acylation of the enol form of trifluoroacetone with isopropenyl acetate, vinyl acetate, acetic anhydride, or acetyl chloride, with the use of a variety of acidic and basic catalysts and conditions, failed to yield product except perhaps in trace quantities as did the attempted addition of acetic acid to 3,3,3-trifluoropropyne. On the other hand, we were able to prepare 3,3,3-trifluoro-2-trifluoroacetoxypropene by reacting trifluoroacetone with trifluoroacetic anhydride in a steel bomb at 100°C. with a potassium acetate catalyst.

Polymerization

We have not been successful in preparing the homopolymer of α-trifluoromethyl vinyl acetate, although an exhaustive study of all available polymerization techniques has not been made. Heating the monomer with 0.4% azobisisobutyronitrile at temperatures ranging from 70 to 120°C. and also prolonged irradiation with a General Electric AH-4 ultraviolet source failed to polymerize the monomer. Examination of these reactions showed that dimerization did not occur, and except for a slight coloration, the monomer remained unchanged. Several emulsion recipes using a persulfate initiator at 50°C. were similarly unsuccessful and the monomer was recovered unhydrolyzed. Butyllithium, sodium in liquid ammonia, sodium methoxide, boron trifluoride, and its etherate did not initiate polymerization. Difficulty in preparing the homopolymer is not too surprising, considering the results obtained with 3,3,3-trifluoropropene.[10-12]

α-Trifluoromethyl vinyl acetate copolymerizes with a variety of vinyl monomers when polymerization is initiated with ultraviolet radiation or free radical-producing catalysts. Although we have not measured copolymerization reactivity ratios or Alfrey-Price Q and e values for this monomer, we can make some qualitative statements regarding its reactivity. From a series of high conversion copolymerizations at 60°C. employing equal weights of the two monomers, it was learned from the infrared spectra

of the resulting polymers that α-trifluoromethyl vinyl acetate copolymarizes readily with vinyl acetate and vinyl trifluoroacetate. With maleic anhydride (in benzene) no copolymer is obtained, while methyl methacrylate yields essentially methyl methacrylate homopolymer and vinylidene chloride allows a small quantity of the fluoro monomer to enter the radical chain. A copolymer is obtained with styrene. These results verify the expected behavior, that this new monomer should have a low reactivity, Q, and a fairly positive e value. It is the latter which enhances the tendency to alternate with styrene to produce a copolymer. This ability to copolymarize with monomers of the styrene and vinylpyridine type now permits the introduction of vinyl alcohol type residues into these structures.

Trifluoromethyl-Substituted PVA

The infrared spectrum of a copolymer of α-trifluoromethyl vinyl acetate and vinyl acetate is duplicated in Figure 2. This copolymer was produced by an ultraviolet-initiated high conversion bulk copolymerization of a

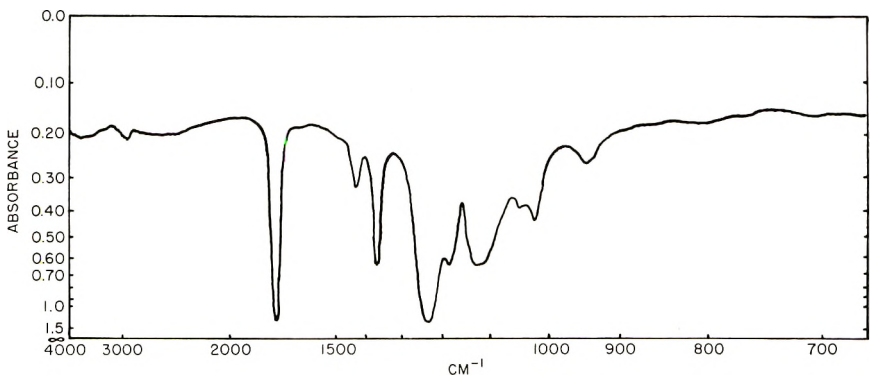

Fig. 2. Infrared spectrum of a copolymer of vinyl acetate and α-trifluoromethyl vinyl acetate.

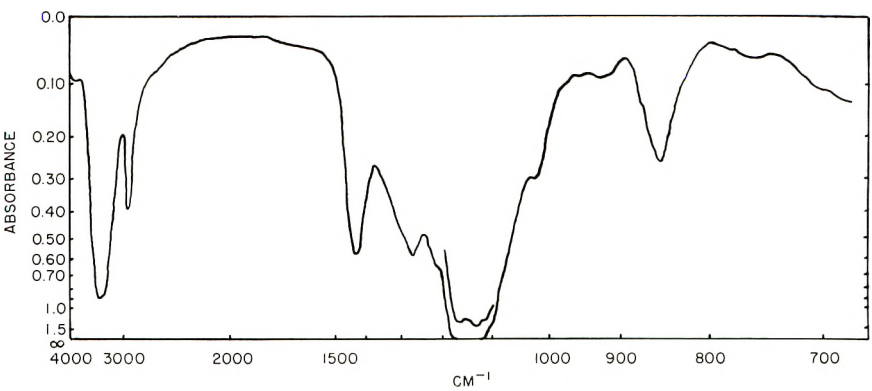

Fig. 3. Infrared spectrum of a trifluoromethyl-substituted polyvinyl alcohol.

monomer mixture having a mole fraction of 0.35 in fluoro monomer. Absorptions arising from carbon–fluorine stretching vibrations are readily discernible in the 1100–1200 cm.$^{-1}$ range. The copolymer, like polyvinyl acetate, is soluble in benzene, acetone, and ethyl acetate but unlike polyvinyl acetate, swells but does not dissolve in the lower alcohols.

The above copolymer was converted to PVA containing —[$CH_2C(CF_3)OH$]— residues in the chain both by refluxing with methanol containing hydrogen chloride and by treatment with methanol containing a catalytic amount of sodium methoxide. Both methods produce products having identical infrared spectra but the alkoxide catalyzed alcoholysis is much faster. The purified, dried, polyalcohol had a fluorine analysis of 29.05% which corresponds to something less than an ABAB copolymer (36.5% F). However, it must be remembered that the product was not initial copolymer.

The trifluoromethyl-substituted polyvinyl alcohols have rather surprising properties. They dissolve in methanol, are completely insoluble in water, and are somewhat swelled by acetone. Further, because of the acidity of fluorinated alcohols (trifluoroethanol has a $K_a = 4 \times 10^{-12}$), trifluoromethyl PVA dissolves in dilute aqueous alkalies to yield polyelectrolyte-type solutions. Films may be cast from methanol or from ammoniacal water–alcohol solutions. The films are clear, reasonably tough, and more slippery to the touch than normal PVA films. Like PVA, the films may be oriented by stretching.

Ultraviolet absorption spectra of methanol solutions of trifluoromethyl PVA show that the bands[6] generally found at 220, 280, and 330 mμ are present. The infrared spectrum of CF_3-modified PVA is reproduced in Figure 3. Strong absorptions again appear in the 1100–1200 cm.$^{-1}$ region.

Experimental

3-Bromo-1,1,1-trifluoro-2-propanol was prepared following the method of McBee and Burton.[13] This was converted to 3-bromo-2-acetoxy-1,1,1-trifluoropropane as follows. A 162-g. portion (0.84 mole) of 3-bromo-1,1,1-trifluoro-2-propanol was refluxed with 220 g. (2.2 mole) of isopropenyl acetate and 1 g. of *p*-toluenesulfonic acid. Acetone (47 g.) was removed through a 2-ft. packed column. The reaction mixture was treated with excess sodium bicarbonate to neutralize the acid, filtered and fractionated. After a forerun, the ester was collected at 85°C. at 130 mm.; the yield was 113 g. (58%), $n_D^{25} = 1.3877$, $d_{25}^{25} = 1.554$.

3,3,3-Trifluoro-2-acetoxy propene was obtained by dehydrobromination of 3-bromo-2-acetoxy-1,1,1-trifluoropropane. A 52-g. portion (0.22 mole) of 3-bromo-2-acetoxy-1,1,1-trifluoropropane was heated with 130 ml. of freshly distilled tributylamine at an oil bath temperature of 175–190°C., and monomer was collected at 75–90°C.; the yield was 22 g., corresponding to 64%. The product was carefully fractionated thru a spinning band column; b.p. 86.5°C.; $d_{25}^{25} = 1.2119$; $n_D^{25} = 1.3380$. The molecular refractivity, M_R, from the Lorentz-Lorentz equation is 26.50 compared to a

value 26.78 obtained by summing increments and using a value of 1.2 for fluorine.

Anal. Calc.: C, 39.0%; H, 3.7%; F, 37.0%. Found: C, 39.3%; H, 3.8%; F, 35.7%.

The authors wish to thank Professor Derek Barton, and Drs. Lloyd Taylor and Martin Idelson for helpful suggestions regarding the monomer synthesis.

References

1. Cohen, S. G., H. C. Haas, and H. Slotnick, *J. Polymer Sci.*, **11**, 193 (1953).
2. Haas, H. C., E. S. Emerson, and N. W. Schuler, *J. Polymer Sci.*, **22**, 291 (1956).
3. Haas, H. C., *J. Polymer Sci.*, **26**, 391 (1957).
4. Haas, H. C., and N. W. Schuler, *J. Polymer Sci.*, **31**, 237 (1958).
5. Haas, H. C., and A. S. Makas, *J. Polymer Sci.*, **46**, 524 (1960).
6. Haas, H. C., H. Husek, and L. D. Taylor, *J. Polymer Sci.*, **A1**, 1215 (1963).
7. Gwynn, B. H., and E. F. Degering, *J. Am. Chem. Soc.*, **64**, 2216 (1942).
8. Hagemeyer, H. J. *Ind. Eng. Chem.*, **41**, 765 (1949).
9. Gaylord, N. G., and F. R. Eirich, *J. Polymer Sci.*, **5**, 743 (1950).
10. Goldschmidt, A., *J. Am. Chem. Soc.*, **73**, 2940 (1951).
11. Overberger, C. G., and E. B. Davidson, *J. Polymer Sci.*, **62**, 23 (1962).
12. Denison, G., and A. Goldschmidt U. S. Pat. 2,549,580 (April 17, 1951).
13. McBee, E. T., and T. M. Burton, *J. Am. Chem. Soc.*, **74**, 3022 (1952).

Résumé

On a synthétisé le α-trifluorométhylacétate de vinyle (TMF). Bien que l'homopolymère n'ait pas été obtenu, ce nouveau monomère copolymérise facilement avec de nombreux monomères vinyliques, y compris le styrène. L'alcoolyse des copolymères TFM/acétate de vinyle fournit des alcools polyvinyliques porteurs de groupes CF_3 et présentant des propriétés nouvelles inhabituelles. Les dérivés d'alcool polyvinylique, contenant environ 30% de fluor, sont complètement insolubles dans l'eau, mais se dissolvent dans les alcools inférieurs. Par suite de l'acidité accrue des alcools par substitution fluorée, ces substances sont aussi solubles dans les solutions aqueuses alcalines en formant des solutions contenant des ions polyalcoolates.

Zusammenfassung

α-Trifluormethylvinylacetat wurde dargestellt. Das Homopolymere konnte zwar nicht erhalten werden, doch copolymerisiert dieses neue Monomere leicht mit einer Anzahl von Vinylverbindungen einschliesslich Styrol. Die Alkoholyse der Vinylacetat-α-Trifluormethylvinylacetat-Copolymeren führt zu trifluormethylsubstituierten Polyvinylalkoholen mit neuen und ungewöhnlichen Eigenschaften. Diese Polyvinylalkoholderivate mit einem Fluorgehalt von etwa 30 Gewichtsprozent sind in Wasser vollkommen unlöslich, lösen sich aber in den niedrigen Alkoholen. Wegen der erhöhten Acidität fluorsubstituierter Alkohole lösen sie sich auch in verdünnten wäßrigen Alkalien unter Bildung von Polyalkoxyd-Lösungen.

Received January 24, 1963

JOURNAL OF POLYMER SCIENCE: PART A VOL. 2, PP. 1647–1653 (1964)

Nitrogen Adsorption Isotherms on Polyolefins

JOE W. HIGHTOWER and P. H. EMMETT, *Department of Chemistry, The Johns Hopkins University, Baltimore, Maryland*

Synopsis

Nitrogen adsorption isotherms were determined for a number of polyolefinic compounds. B.E.T. calculations showed that most of the samples possess surface areas averaging about 0.5 m.²/g., although a few very high molecular weight polyolefins precipitated during polymerization have areas of about 8 m.²/g. On most of the polyolefins, the C values from the B.E.T. equation are unusually small, indicating a relatively low heat of nitrogen adsorption. Adsorption isotherms were determined with krypton on two of the high polymers and were found to yield areas in satisfactory agreement with those obtained from the nitrogen adsorption experiments.

INTRODUCTION

For many years the B.E.T. method[1] of estimating surface areas by the use of low temperature gas adsorption measurements has been employed for a wide variety of materials. However, up to the present time, relatively few organic substances have been measured by this procedure. The present measurements are submitted with a view to showing that the adsorption of nitrogen or krypton at −195°C. can be used effectively for measuring the surface areas of polyolefins.

EXPERIMENTAL

Apparatus

The conventional B.E.T. apparatus having a mercury manometer to measure the pressure was used to determine the nitrogen isotherms at −195°C.; for krypton isotherms a similar apparatus having a calibrated thermistor for measuring pressure was used.

Materials

The polyethylene and ethylene–butylene copolymers were made by the Phillips Process (chromic oxide on silica–alumina as a catalyst). The polypropylene samples were prepared over a titanium trichloride–aluminum alkyl catalyst. All samples were furnished by the W. R. Grace Co.

Prepurified nitrogen was passed over reduced copper turnings at 350°C. and through an activated charcoal trap at −195°C. Prepurified helium

TABLE I

Sample No. (WRG Code)	Description	Melt index[a]	Viscosity number[b]	Sample size, g.	V_m, cm.^{3} (STP)	Surface area, m.^{2}/g.	C value	$n = V_a/V_m$ (at various P/P_0) 0.1	0.2	0.3	0.4	0.5	0.6	0.7	0.8	0.9
—	Original Polyethylene	—	—	4.3192	0.383	0.388	47.7	0.93	1.20	1.36	1.50	1.62	1.76	2.08	2.63	3.49
994-4-1	GREX linear polyethylene Type 60-002E, precipitated from hydrocarbon solution	0.2	2.9	3.4204	0.341	0.436	11.0	0.61	0.91	1.14	1.35	1.55	1.76	1.99	2.29	3.52
994-4-2	GREX linear polyethylene Type 60-007E, precipitated from hydrocarbon solution	0.8	1.9	2.7904	0.211	0.330	43.0	0.85	1.20	1.38	1.49	1.58	1.67	1.90	2.37	3.35
					0.182[c]	0.345[c]	30.5[c]	0.88	1.12	1.32	1.50	1.67	1.81			
994-4-3	Sample 994-4-2 ground to pass 20 mesh screen	0.8	1.9	3.3690	0.305	0.396	18.0	0.70	0.99	1.16	1.25	1.34	1.49	1.71	2.17	3.22
					0.263[c]	0.412[c]	36.2[c]	0.88	1.16	1.33	1.52	1.70	1.87			
994-4-4	GREX ethylene-butylene copolymer Type 50-004C, precipitated from hydrocarbon solution	0.4	2.4	3.3152	0.315	0.430	107.0	0.92	1.23	1.45	1.66	1.85	2.04	2.25	2.66	4.07

994-4-5	GREX linear polyethylene Type 60-050E, precipitated from hydrocarbon solution	3.8	1.5	4.5869	0.612	0.584	26.0	0.85	1.11	1.37	1.60	1.81	2.06	**2.32**	**2.73**	**3.60**
994-4-6	Experimental linear polyethylene of very high molecular weight, precipitated during polymerization	0.0	5.5[d]	5.1313	10.44	8.91	40.5	0.91	1.14	1.35	1.56	1.76	2.04	2.41	3.21	**5.65**
994-4-7	"	0.0	4.0[d]	4.7128	6.04	5.62	31.1	0.82	1.09	1.32	1.51	1.72	1.96	2.31	2.88	4.10
994-4-8	"	0.0	16.8[d]	3.7882	7.38	8.54	39.7	0.87	1.12	1.35	1.56	1.76	2.02	2.40	3.10	4.84
994-4-13	Experimental isotactic polypropylene precipitated during polymerization	—	20.5	4.2678	0.547	0.561	26.4	0.78	1.06	1.32	1.54	1.71	1.94	2.26	2.77	3.73
869-13	Ethylene–butylene copolymer	9.0	1.4, 1.5	4.1521	0.278	0.293	124.0	1.04	1.19	1.33	1.51	1.69	1.91	2.16	2.44	3.23
TiO_2	Bone char research project Reference sample no. 2 Bottle no. 7, Oct. 1, 1952	—	—	2.4795	5.475	9.67	153.0	1.04	1.23	1.40	1.57	1.73	1.94	2.07	2.63	3.46

[a] According to ASTM D1238-57T.

[b] 0.1% concentration in decahydronaphthalene at 135°C.

[c] Krypton data. 19.5 A.^{2} was used as the cross-sectional area of the krypton atom. P_0 for krypton was taken as the extrapolated vapor pressure of liquid krypton, 2.8 mm. at −195.8°C.

[d] 0.02% concentration instead of 0.1%.

was passed through an activated charcoal trap at −195°C. Krypton (99.99%) was used as purchased from Airco.

RESULTS

The experimental results are summarized in Table I. Typical adsorption isotherms are given in Figure 1. The corresponding B.E.T. plots are shown in Figure 2.

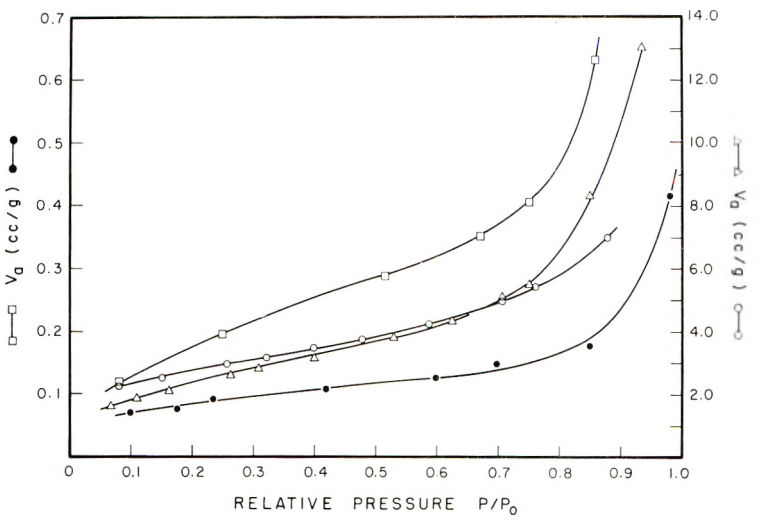

Fig. 1. Representative isotherms: (△) 994-4-6; (□) 994-4-13; (◆) 869-13; (○) TiO_2.

As can be seen from Table I, only two of the samples were measured by krypton, and since the area values obtained on these two samples were in reasonable agreement with the areas obtained by nitrogen, no further krypton measurements on the samples were carried out.

DISCUSSION

The results presented in Table I are, for the most part, self-explanatory. Most of the polyolefins have areas in the range 0.3–0.6 m.²/g. Only the three samples of linear polyethylene having very high molecular weight precipitated during polymerization had surface areas in the range 5–9 m.²/g. Presumably, the high surface areas are associated with the fact that this particular polymer was precipitated during polymerization.

The C values obtained from the B.E.T. plots are, for the most part, in the range 11–48 for the various nitrogen adsorption isotherms. Since the C values are related to the heats of adsorption,[1] the results suggest that nitrogen is not as strongly adsorbed on the polymeric materials as it is on the miscellaneous inorganic substances on which B.E.T. isotherms have been determined.

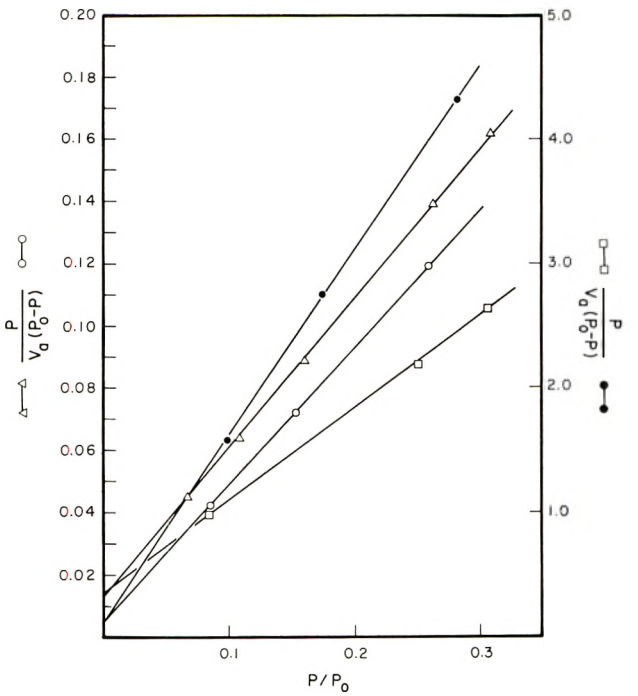

Fig. 2. B.E.T. plots for isotherms in Fig. 1: (△) 994-4-6; (□) 994-4-13; (●) 869-13; (⊙) TiO_2.

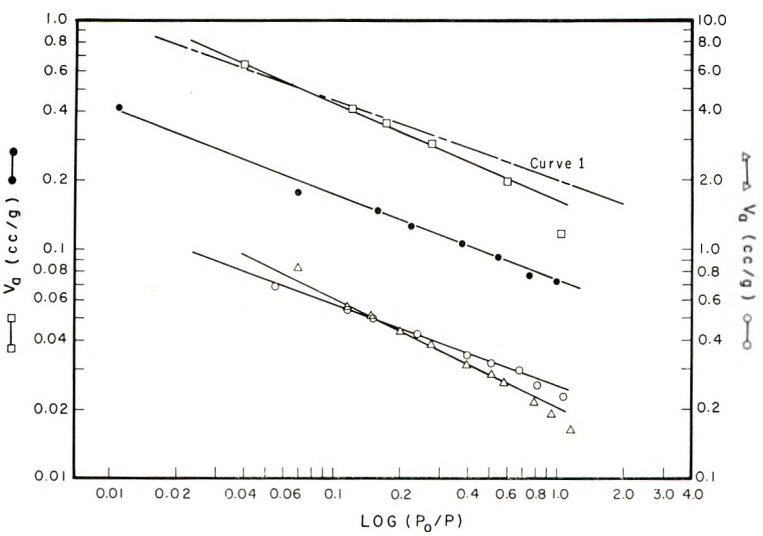

Fig. 3. Pierce plots for isotherms in Fig. 1. Curve 1 shows the slope given in Pierce's papers.[2,3] Symbols are as in Figs. 1 and 2. Curve 1 is from a plot made by Pierce.[2,3]

Attention should be called to one peculiar exception with respect to the heat of adsorption. The two isotherms determined on ethylene–butylene copolymers showed low surface areas but relatively high C values (107 and 124 for the two samples). Presumably, for some reason that is not clear, the nitrogen adsorption on the copolymers involves a somewhat higher heat of adsorption than on the polyethylene and polypropylene samples.

There have been some suggestions that krypton sometimes exhibits type 3 adsorption isotherms and, therefore, is not suitable for surface area measurements. It is reassuring that on the present polyolefins the krypton curves were normal, have good B.E.T. plots and yielded surface area values that are in reasonable agreement with those obtained from nitrogen isotherms.

In recent publications, Pierce[2,3] has pointed out that a plot of the logarithm of the volume of nitrogen adsorbed at −195°C. by a solid versus log log P_0/P yields a straight line from very low to very high relative pressures. In Figure 3 is shown a plot that he has presented as typical of nitrogen adsorption on solids. In this same figure are shown plots of our data for TiO_2 and also for the high polymers for which isotherms were shown in Figure 1. It will be noted that the plot for the ethylene–butylene copolymers yields a slope parallel to the plot for TiO_2 and for the standard plot furnished by Pierce. On the other hand, the plots for those materials having low C values yield curves of very different slopes from the ones suggested by Pierce. This is a necessary consequence of the fact that the slopes of the actual isotherms for systems with relatively low heats of adsorption will be considerably greater than the slopes of isotherms with higher heats of adsorption. Accordingly, plots of the type recommended by Pierce will be helpful not only in disclosing unusual packing in the first layer or in indicating capillary condensation as he suggested, but will also be useful in giving an estimate of the C value for the B.E.T. plots, or in other words, for the relative values of the heats of adsorption of the adsorbate on the solids being studied.

References

1. Brunauer, S., P. H. Emmett, and E. Teller, *J. Am. Chem. Soc.*, **60**, 309 (1938).
2. Pierce, C., *J. Phys. Chem.*, **64**, 1184 (1960).
3. Pierce, C., and B. Ewing, *J. Am. Chem. Soc.*, **84**, 4070 (1962).

Résumé

On détermine les isothermes d'adsorption de l'azote pour un nombre de composés polyoléfiniques. Les calculs de BET montre que les échantillons poosèdent une surface moyenne d'emiron 0.5 m.²/g., alors que quelques polyoléfines de très haut poids moléculaire, précipitées au cours de la polymérisation, ont une surface d'environ 8 m.²/g. Pour la plupart des polyoléfines, les valeurs de C provenant de l'équation B.E.T. sont inhabituellement petites et indiquent une relativement faible chaleur d'adsorption de l'azote. On détermine les isothermes avec du krypton sur deux des hauts polymères et on trouve des surfaces en accord satisfaisant avec celles obtenues au départ des expèriences d'adsorption d'azote.

Zusammenfassung

Für eine Anzahl von Polyolefinverbindungen wurden Stickstoff-Adsorptionsisothermen bestimmt. Wie B.E.T.-Berechnungen zeigen, besitzen die meisten Proben Oberflächen von durchschnittlich etwa 0,5 m.²/g., ausgenommen ein paar sehr hochmolekulare Polyolefine, die schon während der Polymerisation ausgefällt wurden und Oberflächen von etwa 8 m.²/g. haben. Bei den meisten Polyolefinen wiesen ungewöhnlich kleine *C*-Werte in der B.E.T.-Gleichung auf eine relativ niedrige Stickstoff-Adsorptionswärme hin. Die Ermittlung der Adsorptionsisothermen von zweien der Hochpolymeren mit Krypton ergab Oberflächenwerte, die mit den für Stickstoff erhaltenen Werten befriedigend übereinstimmen.

Received March 6, 1963

JOURNAL OF POLYMER SCIENCE: PAA TR VOL. 2, PP. 1655–1668 (1964)

Effect of Temperature on Molecular Weight Measurements in Polyethylene

H. P. SCHREIBER and M. H. WALDMAN, *Canadian Industries Limited, Central Research Laboratory, McMasterville, Quebec, Canada*

Synopsis

Light-scattering evaluations of molecular weight and gyration radii have been carried out over a range of temperatures for linear and branched polyethylenes in α-chloronaphthalene solutions. In a number of cases the molecular size parameters have been found to depend on the solution temperature. When observed, the temperature dependence can change molecular weight values by as much as 50%. The temperature dependence tends to be more pronounced at higher molecular weights, in linear than in branched polyethylenes, and is particularly noticeable at solution temperatures below that of the normal crystalline melting temperature of the polymer. It is suggested that the temperature dependence of molecular weight parameters may be due to a gradual dissociation in solution of polymer aggregates arising from persisting interchain entanglements. A relationship was established between intrinsic viscosity and molecular weight for selected fractionated polyethylenes by using molecular weight data obtained under conditions unfavorable to the persistence of polymer aggregates. A number of published viscosity–molecular weight functions for polyethylenes was compared with the calibrated relationship. Some of the published equations gave results in good agreement with the present function, but a number of others resulted in gross overestimates of molecular weight. Polymer aggregation problems may have been encountered in the derivation of some of these viscosity–molecular weight functions. The comparison indicates the danger of indiscriminate choice of viscosity–molecular weight functions for use in rapid estimates of polymer molecular weight.

INTRODUCTION

Light-scattering techniques are now widely used for determinations of weight-average molecular weights ($\bar{M}_w$) in polyethylenes and other polydisperse polymers which can only be dissolved at high temperatures. Application of the technique to these polymers is complicated by experimental difficulties, notably the sensitivity of Zimm plots to polymer polydispersity,[1] the related problem of dissymmetry correction[2–4] and solution clarification.[3,5] An additional serious problem has been raised recently by Trementozzi,[6] who showed that the molecular weight of some low and high pressure polyethylenes depended on the solvent used in the light-scattering determinations. The suggestion was made[6] that polymer association could take place in α-chloronaphthalene (α-CN) but not in tetralin, a thermodynamically superior solvent for polyethylene. This assumption was supported by the apparent dependence of $\bar{M}_w$ for one high

pressure (branched) polyethylene on the temperature of α-CN solutions used in the light-scattering experiments. Some recent results of Tung[7] can also be interpreted as supporting the polymer association hypothesis, although the author did not draw this conclusion himself. Finally, an examination in this laboratory[8] of the temperature dependence of intrinsic solution viscosities $[\eta]$ for high and low pressure polyethylenes in α-CN and tetralin also gave results which are consistent with an assumed polymer association in α-CN solutions. On the other hand, Billmeyer and coworkers,[9] using α-CN, tetralin, and decalin solutions of polyethylenes, could not corroborate Trementozzi's reported molecular weight dependence on solvent medium for either high or low pressure polyethylenes, and criticized the assumption of polymer association as being devoid of an obvious physical basis. These workers did not investigate possible temperature variations of $\bar{M}_w$, all light-scattering measurements being done at constant temperature in a given solvent.[9] A study of the effect of temperature on light-scattering results in α-CN and tetralin solutions of polyethylenes, in the range 80–125°C., was reported by Nicolas,[10] who found no evidence for polymer association. However, the refractive index increment, dn/dc, for α-CN solutions used by Nicolas was some 35% greater than other reported values for this solvent,[2,6,11] so that the results of this work cannot be regarded as unequivocal evidence either for or against the association hypothesis.

Clearly, the question of polyethylene association in the α-CN solutions commonly used in light scattering is as yet unresolved. Consequently some uncertainty also exists regarding the absolute meaning of molecular weight values and allied parameters, such as gyration radii, derived from light-scattering data. In view of the importance of these parameters, an attempt was made to determine whether or not polyethylene associates in α-CN by carrying out light-scattering measurements for linear and branched polyethylenes over broad ranges of temperature. This experimental approach was based on the reasonable assumption that as temperature rises any existing polymer aggregates will tend to dissociate thereby reducing the apparent weight-average molecular weight. The purpose of this paper is to present and discuss the results of this study. The consistency of various published relationships between intrinsic viscosity and $\bar{M}_w$ of low pressure (linear) polyethylenes is also examined in the light of the results of this work.

EXPERIMENTAL

1. Materials

Both low and high pressure polyethylenes were used in this work. The high pressure (branched) resins were chosen to cover an apparent molecular weight range from about 10^5 to greater than 10^6. The linear polyethylenes were of the Phillips type. A number of these were frac-

tionated by the coacervation technique of Blackmore and Alexander[12] to provide fractions which, while not particularly sharp, were substantially narrower in molecular weight distribution than the parent polymers.

2. Intrinsic Viscosities

Intrinsic viscosities were measured in redistilled α-CN and tetralin solutions at 125 and 120°C. respectively and in reagent grade decalin solutions at 135°C. by use of previously described techniques.[8]

3. Light Scattering

Light-scattering measurements were performed in a Brice-Phoenix apparatus modified to permit high temperature operation. In all cases α-CN solutions were used, the temperature varying from 90 to 150°C., though the entire range was not covered for every sample investigated. Vertically polarized light, with $\lambda = 5460$ A., was used.

4. Refractive Index Increment

Highly consistent values of dn/dc for polyethylene in α-CN have been reported by Billmeyer,[2] Chiang,[11] Henry,[13] and Tung.[14] We have adopted the procedure followed by Billmeyer[9] of averaging the literature values and taking the correct dn/dc values as -0.190 at 135°C. -0.192 at 125°C., and -0.199 at 90°C. In this way a self-consistent set of increments was obtained for the temperatures involved in our experiments. The dn/dc values, as well as values of the light-scattering constant H, are given in Table I.

TABLE I
Light-Scattering Parameter Values

Temp., °C.	$-dn/dc$, cm.³/g.	$H \times 10^6$, mole cm.²/g.
90	0.199	6.30
100	0.197	6.09
110	0.195	6.00
120	0.193	5.81
130	0.191	5.70
140	0.189	5.50
150	0.187	5.42

5. Solution Clarification

It has been shown, notably by Muus and Billmeyer,[3] that large, "insoluble" particles in polyethylene solutions (e.g., dust particles, etc.) can produce marked curvature in Zimm plots and lead to erroneous molecular weight estimates. Thus, solution clarification aimed at removal of such foreign particles is a necessary prerequisite to light-scattering measurements. On the other hand, Moore and Peck[15] have demonstrated the presence, in branched polyethylenes especially, of large polymer molecules

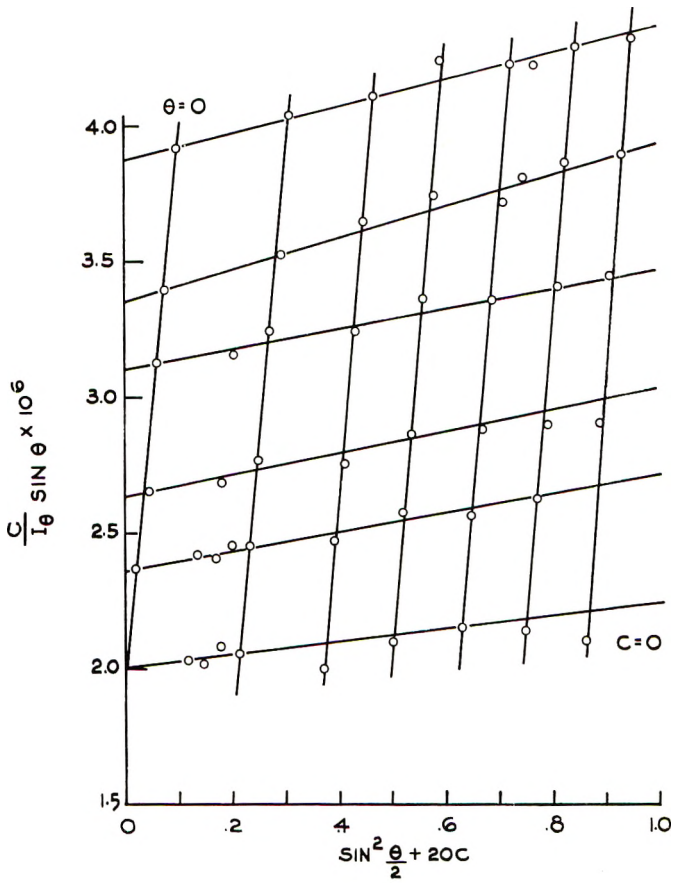

Fig. 1. Zimm plot for linear polyethylene LPPE-3F, T = 140°C.

which could conceivably classify as "insoluble" particles in terms of Muus and Billmeyer.[3] The removal of such particles is certainly not desirable if it is proposed to characterize the polymer sample as originally constituted, since even a small number of such supermolecules can have substantial influence or rheological and physical properties of the polymer.

In this work, previously prepared solutions of polyethylene in α-CN at 140°C. were placed in a heated filter holder, fitted with a Millipore filter disk (Millipore Filter Corp., Watertown, Mass.) having a mean pore size of 0.65 μ. The filter had been previously conditioned by repeated washing with hot solvent. None of the solutions exceeded 0.5% by weight solute concentration. The solutions were filtered under mild nitrogen pressure directly into light-scattering cells which had been previously washed, solvent-conditioned, and dried. This procedure was adopted because it seemed adequate for removing foreign particles without significantly affecting the composition of the polymer as received. The criterion for the latter assertion was a comparison of apparent Newtonian melt viscosity

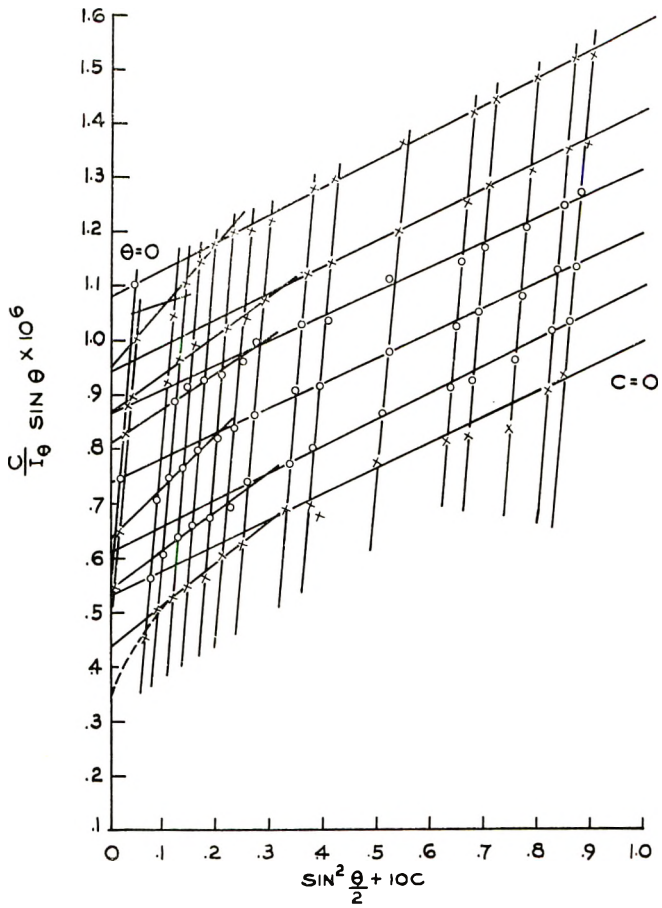

Fig. 2. Zimm plot for branched polyethylene HPPE-4, showing curvature in low-angle, high dilution segment, T = 120°C.

η_0*, and the shear stress τ_1 for onset of non-Newtonian melt flow for polymer as received and after precipitation from solutions subjected to various filtration procedures. It has been shown that η_0* is sensitive to weight-average molecular weight and long branch incidence,[16] while τ_1 is particularly dependent on the molecular weight of the high end of the distribution.[17] The described filtration procedure was found to have little significant influence on these characteristics. On the other hand, use of finer filter disks, or solutions in which the polyethylene concentration appreciably exceeded 0.5% by weight resulted in significant changes both in η_0* and τ_1. Coarser filter disks were not desirable because of the danger of failure to remove dust and other foreign materials.[3]

The standard solution preparation procedure did not result in linear Zimm plots in all cases, however. Typical plots are shown in Figure 1 for a fractionated linear polyethylene and in Figure 2 for a whole branched

polyethylene. Here c is the concentration (in grams per milliliter), I_θ is the scattering intensity ratio with respect to the initial intensity at 0° viewing angle, and θ is the viewing angle. From these plots $\bar{M}_w$ is calculated from the relationship

$$1/\bar{M}_w = Hi \tag{1}$$

where i is the intercept at infinite dilution of the zero angle scattering line, and values of H are given in Table I. The curvature in the zero concentration extrapolation in Figure 2 may be interpreted as evidence for broad molecular weight distribution[15,18] in this sample. In a few cases curvature in the low angle, zero concentration segment of the Zimm plot made accurate extrapolation of the $\bar{M}_w$ value impossible. In these cases the molecular weight was obtained by extrapolating the linear segment of the zero concentration line at higher viewing angles to the zero angle intercept, as shown in Figure 2. Molecular weight values so obtained are designated $\bar{M}_w'$. These values do not fully weigh the contribution of very high molecular weight constituents of the distribution in the given polymer, but they are preferable in this context because of the increased precision with which they may be defined.

RESULTS AND DISCUSSION

1. Temperature Dependence in $\bar{M}_w$ Determinations

Five low pressure (LPPE) and four high pressure (HPPE) polyethylenes were used in this part of the experimental program. Pertinent $\bar{M}_w$ or $\bar{M}_w'$ values for these resins averaged from two or more determinations are given in Table II, which also includes a tabulation of the z-average mean square radius of gyration, $(r^2)_z^{1/2}$, for all samples except LPPE-1. The $(r^2)_z^{1/2}$ parameter is calculated in each case from the initial slope of the infinite dilution curve in the light-scattering plot.[1,19] In the case of LPPE-1, the Zimm plot curvature was too great to permit meaningful evaluation of the limiting slope. The $\bar{M}_w$ precision is about $\pm 10\%$.

It is evident from Table II that in some cases (e.g., samples HPPE-1 and LPPE-3F) there is no detectable evidence of a temperature variation in $\bar{M}_w$, while in others (e.g., samples HPPE-4 and LPPE-4F), the molecular weight does appear to vary with the solution temperature. Decreasing $\bar{M}_w$ or $\bar{M}_w'$ at rising solution temperatures could of course be regarded consistent with a dissociation of molecular "aggregates" as solvent–solute interaction increases. In cases where such a dissociation may occur, it would be reasonable also to expect a decrease in $(r^2)_z^{1/2}$. Because of slight data scatter in all cases and some curvature in the high dilution, low viewing angle segments of the Zimm plots for two of the polymers (see Table II), the $(r^2)_z^{1/2}$ values cannot be considered reproducible to better than 5%. Thus, the samples showing no temperature dependence in the molecular weight parameter also can be considered as showing no significant change

TABLE II
Temperature Dependence of Molecular Dimensions of Polyethylenes

Sample	$\bar{M}_w$ or $\bar{M}_w' \times 10^5$							$(r^2)_z^{1/2}$, A.						
	90°C.	100°C.	110°C.	120°C.	130°C.	140°C.	150°C.	90°C.	100°C.	110°C.	120°C.	130°C.	140°C.	150°C.
HPPE-1	1.11	1.22	1.05	1.12	1.06	1.11	—	486	486	465	—	544	446	—
HPPE-2[a]	—	—	16.0	15.7	14.5	13.4	13.7			5400	4600	4500	4300	4300
HPPE-3	8.34	8.64	7.80	7.28	6.80	6.66	6.72	940	850	810	710	690	690	690
HPPE-4[a]	4.12	3.19	2.88	2.93	2.92	2.93	3.01	810	796	755	731	732	—	704
LPPE-1[a]	—	—	2.60	1.92	1.70	1.44	—	—	—	—	—	—	—	—
LPPE-2	—	—	1.30	1.28	1.16	1.07	—			—	530	500	450	—
LPPE-3F[b]	—	1.09	—	0.94	1.02	0.96	1.00	—	490	—	450	465	410	432
LPPE-4F[b]	—	5.1	—	4.5	—	3.9	3.7	—	1075	—	922	—	690	720
LPPE-5F[b]	—	—	2.53	—	2.39	—	2.18			380	—	360	—	310

[a] In these cases curvature in Zimm plots led to calculation of $\bar{M}_w'$ (cf. Fig. 2 and text).
[b] Fractionated high density polyethylene.

in $(r^2)_z^{1/2}$, whereas in such cases as HPPE-4, LPPE-4F, etc., where a significant inverse temperature variation in molecular weight is noted, there is also a corresponding inverse temperature variation in the gyration radius. It is readily shown that such an inverse dependence of $(r^2)_z^{1/2}$ on solution temperature is, in these cases, not explicable in terms of the theoretically expected temperature dependence of the gyration radius. Flory[20] and Ciferri[21] have developed a relationship between the temperature dependence of the mean square radius of gyration of the unperturbed polymer molecule and the temperature dependence of the intrinsic viscosity of polymer solutions. From their development it is apparent that the sign of the temperature variation of these parameters will be equivalent—a result in keeping with their experimental findings which, in the case of Flory,[20] involve solutions of polyethylene in *n*-alkanes. The theoretical result may be applied to the *z*-average gyration radius as a good approximation, and since the slope of the intrinsic viscosity versus solution temperature plot for both high and low pressure polyethylenes in α-CN is positive,[8] a direct dependence of $(r^2)_z^{1/2}$ and T would be expected. The results in Table II therefore suggest a more radical effect of rising temperature on the dimension of solute particles, such as might be expected if partial dissociation of aggregates were taking place.

Inspection of Table II further suggests that the temperature dependence of molecular dimension parameters is negligible above about 120°C. for the high pressure polyethylenes; because of apparatus limitations which made work above 150°C. impossible it is more difficult to find a similar trend in the low pressure resins, but the inference to be drawn from the results for the fractions suggests a decreased temperature sensitivity above about 140°C. It is not possible from the present results to define unequivocally an "exuilibrium" molecular weight for the experimental samples, but the conclusion can nevertheless be drawn that light-scattering experiments should proceed above 120°C. for high pressure and at no lower than 140°C. in low pressure polyethylenes, if α-CN is the solvent medium.

The apparent temperature dependence of $\bar{M}_w$ and $\bar{M}_w'$ in these cases can be further analyzed along the lines of Figure 3. Here the quantity $(\bar{M}_w)_r$ is defined as a "reference" molecular weight for each sample and represents the experimental $\bar{M}_w$ value at the highest temperature in which the sample was involved (either 140 or 150°C.). Figure 3 is therefore a plot of proportional molecular weight change versus experimental temperature. The plot suggests the following regarding the temperature dependence of $\bar{M}_w$: (*a*) whole, low pressure (linear) polyethylenes appear to be more subject to temperalure sensitivity than high pressure resins at comparable $(\bar{M}_w)_r$ (compare HPPE-1 and LPPE-2); (*b*) the temperature dependence in the low pressure polymers is clearly more pronounced at higher $(\bar{M}_w)_r$; a similar but less well defined situation seems to obtain for high pressure resins; (*c*) the molecular weights of fractionated low pressure samples are less affected by solution temperature than those for whole polymers (compare LPPE-5F to LPPE-1 and LPPE-3F to LPPE-2).

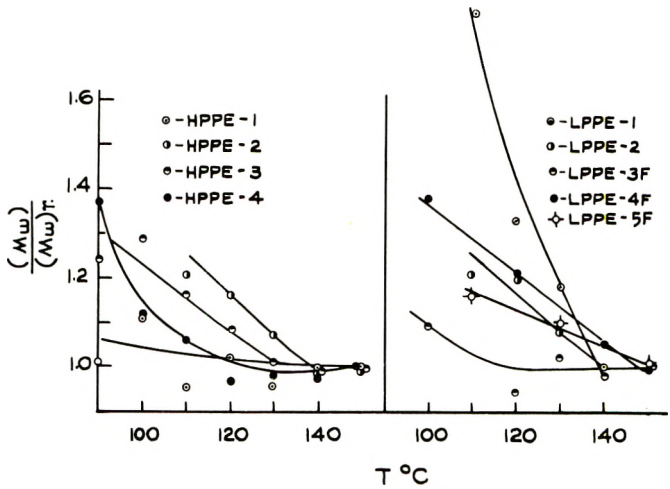

Fig. 3. Comparison of temperature dependence of $\bar{M}_w$ for high and low pressure polyethylenes.

The above may be used to formulate a physical basis for the existence of polyethylene "aggregates"[6] in α-CN solutions. It is widely believed that a distinguishing characteristic of non-Newtonian fluids such as polyethylene is the ability of polymer chains to participate in chain entanglements,[22] thereby creating an extensive viscoelastic network. The degree to which a given polymer chain is involved in this network (i.e. the complexity of the network) is logically dependent on the detailed molecular structure. Thus, at given $\bar{M}_w$ the more compact branched polymer is less capable of participating in entanglements than a linear molecule,[23] with important results on the bulk viscosity of the polymer.[16] Further, the involvement of a molecule in interchain entanglements may be expected to rise with molecular weight and also with a broadening of the molecular weight distribution at constant number-average molecular weight, by virtue of the presence of longer than average polymer chains. These concepts lead to expectations which are fully consistent with Figure 3 if it is assumed, in keeping with an earlier suggestion,[8] that the polyethylene aggregates in α-CN solutions arise from an inability of this solvent at the temperature in question to fully eliminate chain entanglements in the polymer sample. The degree of polymer-solvent interaction will of course increase with temperature, leading to gradual disentanglement and consequently to changes in molecular dimension parameters. This suggestion at once accounts for Trementozzi's finding[6] of a lower aggregation tendency for polyethylene in tetralin—a thermodynamically superior solvent—and furnishes the physical basis for polymer aggregates which Billmeyer[9] found lacking in Trementozzi's original postulate. Moreover, it tends to shed light on the previously noted apparent decrease in temperature sensitivity of the molecular size parameters above about 120°C. for low density and above 140°C. for high

density polyethylenes. These temperatures are, respectively, slightly above the expected crystalline melting points of these polymers. The persistence of chain entanglements in polymer solutions may therefore be favored at temperatures below the normal crystalline melting point of the polymer, where solvent–solute interactions may be offset by polymer cohesive forces arising from some crystalline memory effect.

If the suggested existence of polymer aggregates in solution due to incomplete dispersion of pre-existing entanglements in the bulk polymer is correct, then a similar temperature dependence of light-scattering parameters could conceivably exist in systems involving polymers other than polyethylene, which are characterized by viscoelastic properties due to interchain entanglements.

2. Comparison of $[\eta]$–$\bar{M}_w$ Relationships for Polyethylene*

A number of relationships linking $[\eta]$ and $\bar{M}_w$ have been reported in the literature for linear polyethylenes. Chiang[11] has already noted discrepancies among some of these, accounting for the results of different workers in terms of variations in solution clarification, dissymmetry correction and polymer fractionation procedures. Since substantial differences also exist in the temperature used for light-scattering determinations and in the solvents used for the evaluations of $[\eta]$ in the reported functions, it seems possible that existing discrepancies among these relationships could be due, at least in part, to varying degrees of persisting polymer entanglements. In this section a number of $[\eta]$–$\bar{M}_w$ functions is therefore examined with respect to a reference relationship established for series of fractionated linear polyethylenes under conditions tending to minimize the severity of polymer aggregation. While the comparison is made from the viewpoint of possible aggregation effects, no formal cause and effect hypothesis is being attempted since differences in sample polydispersity and experimental procedures among the various experimental systems undoubtedly contribute to observed differences.

Six polyethylene fractions of somewhat varying polydispersity, prepared by the coacervation technique,[12] were used in this portion of the experimental program. A reference $[\eta]$–$\bar{M}_w$ function was established for these materials by using light-scattering data from α-CN solutions at 140°C. and intrinsic viscosities of tetralin solutions at 120°C. The Zimm plots in each of these cases were linear, permitting evaluation of true $\bar{M}_w$ values. The data, in part reported previously,[17] are given in Table III; the reference $[\eta]$–$\bar{M}_w$ function they define is

$$\log [\eta]_{t,120} = -3.281 + 0.71 \log (\bar{M}_w)_r \qquad (2)$$

where the subscripts t,120 refer to tetralin solutions at 120°C.

* **Note Added In Proof:** The reader is referred to a paper on this topic by M. O. De La Cuesta and F. W. Billmeyer, Jr. which was published in *J. Polymer Sci.*, **A1**, 1721 (1963) while this paper was in press.

TABLE III
Molecular Weights and Intrinsic Viscosities of Six Fractionated Linear Polyethylenes

Sample	$(\bar{M}_w)_r \times 10^{-5}$	$[\eta]_{t,120}$, dl./g.	$[\eta]_{\alpha CN,125}$, dl./g.	$[\eta]_{d,135}$, dl./g.
1	0.96	1.92	1.63	2.31
2	3.90	5.11	4.21	6.08
3	2.75	3.80	3.14	4.53
4	1.55	2.41	1.96	2.86
5	1.35	2.33	1.88	2.74
6	0.73	1.63	1.31	1.93

In subsequent comparisons, the following published $[\eta]$–$\bar{M}_w$ relationships were employed.

Duch and Kuchler:[4]

$$\log [\eta]_{t,120} = -3.627 + 0.78 \log \bar{M}_w \quad (3)$$

Tung[14] (light scattering, α-CN at 125°C.):

$$\log [\eta]_{t,130} = -3.337 + 0.725 \log \bar{M}_w \quad (4)$$

Henry[13] (light scattering, α-CN at 135°C.):

$$\log [\eta]_{d,135} = -3.337 + 0.73 \log \bar{M}_w \quad (5)$$

Chiang[11] (light scattering, α-CN at 135°C.):

$$\log [\eta]_{d,135} = -3.208 + 0.70 \log \bar{M}_w \quad (6)$$

Francis, Cooke, and Elliott[24] (light scattering, α-CN at 135°C.):

$$\log [\eta]_{d,135} = -3.169 + 0.67 \log \bar{M}_w \quad (7)$$

Atkins et al.[25] (light scattering, α-CN at 125°C.):

$$\log [\eta]_{\alpha CN,125} = -3.367 + 0.67 \log \bar{M}_w \quad (8)$$

The subscripts, d, above, refer to decalin solutions. Molecular weights for the six selected samples were calculated from each of eqs. (3)–(8) by using the appropriate intrinsic viscosity data given in Table III. Intrinsic viscosities in tetralin at 130°C. [eq. (4)] were calculated from the $[\eta]$–T relationship for linear polyethylenes published earlier.[8] Values of $[\eta]_{\alpha CN,125}$ were obtained experimentally; the ratio $[\eta]_{t,120}/[\eta]_{\alpha CN,125} = 1.24 \pm 0.03$ was in very good agreement with that used by Atkins.[25] The ratio $[\eta]_{d,135}/[\eta]_{\alpha CN,125}$ was found to be 1.46 ± 0.03 and $[\eta]_{d,135}/[\eta]_{t,130} = 1.16 \pm 0.02$, in excellent agreement with Billmeyer's values[2] for these ratios. The calculated $\bar{M}_w$ values, along with the appropriate $(\bar{M}_w)_r$ value in Table III, were used to obtain the ratios of calculated to reference molecular weights. These ratios are given in Table IV.

The various $[\eta]$–$\bar{M}_w$ relationships give data which fall into two broad categories. If allowance is made for experimental inaccuracies, permitting a scatter of about ± 0.15 in $\bar{M}_w/(\bar{M}_w)_r$ values, then eqs. (3) and (4) may be taken as consistent with the reference function [eq. (2)], with the results

TABLE IV
Ratio of $\bar{M}_w$ Calculated from Various $[\eta]$–$\bar{M}_w$ Functions to Experimental Reference $(\bar{M}_w)_r$ Value[a]

Sample	$\frac{(\bar{M}_w)_2}{(\bar{M}_w)_r}$	$\frac{(\bar{M}_w)_3}{(\bar{M}_w)_r}$	$\frac{(\bar{M}_w)_4}{(\bar{M}_w)_r}$	$\frac{(\bar{M}_w)_5}{(\bar{M}_w)_r}$	$\frac{(\bar{M}_w)_6}{(\bar{M}_w)_r}$	$\frac{(\bar{M}_w)_7}{(\bar{M}_w)_r}$	$\frac{(\bar{M}_w)_8}{(\bar{M}_w)_r}$
1	1	1.05	1.00	1.19	1.28	1.91	1.92
2	1	0.95	1.00	1.16	1.31	2.09	2.32
3	1	0.93	0.91	1.07	1.20	1.87	2.11
4	1	0.90	0.87	1.01	1.11	1.66	1.86
5	1	0.98	0.95	1.10	1.19	1.80	2.00
6	1	1.14	1.07	1.26	1.33	1.97	2.18

[a] Subscript identifies equation from which particular $\bar{M}_w$ is calculated.

from eq. (5) only slightly out of line with this group. There is insufficient variation among the ratios computed from any of these functions to suggest that the state of aggregation of the polymers in the various solutions differed significantly from that operative in the present study. The discrepancy between the relationships of Henry[13] and Tung[14] [eqs. (5) and (4)] has already been discussed by these authors and the confirmation of its existence here is not construed as evidence for residual entanglement aggregates in Henry's solutions. Molecular weight ratios computed from eqs. (6)–(8) clearly show these equations to form a second category giving molecular weight values very much higher than those obtained from the former group of functions. It is doubtful whether differences of this magnitude could be accounted for in terms of polydispersity differences* among the samples used in this work and those involved in defining eqs. (6)–(8). In these cases therefore, it may be suggested that the presence of residual entanglement aggregates influences the $[\eta]$–$\bar{M}_w$ functions with consequent overestimates in $\bar{M}_w$ calculations, relative to the reference function (2) or the group of functions given by eqs. (3)–(5).

CONCLUSION

The presented results suggest that polyethylene aggregates arising from a persistence of chain entanglements in dilute solutions of the polymer in thermodynamically weak solvents such as α-CN, may lead to estimates of $\bar{M}_w$ which are erroneously high. The possibility of error due to aggregation increases with the molecular weight of the polymer, and seems especially prevalent at solution temperatures below the normal crystalline melt temperature of the polymer. The aggregation effect therefore may compromise, in certain instances, the absolute validity of weight-average molecular weights estimated from Zimm plot extrapolations. Similarly, the

* As noted, the fractionated samples used in this work were not particularly sharp in molecular weight distribution. Thus overcalculations of $\bar{M}_w$ from eqs. (6)–(8) would imply that these equations were based on the use of polymer samples with very much broader weight distributions than the present ones. This seems unlikely in view of the reported fractionation procedures[11,24,25] in these cases.

effect may account for gross differences among a number of reported relationships between $[\eta]$ and $\bar{M}_w$ of polyethylenes. This work shows that regardless of the exact cause of discrepancy among the various examined $[\eta]$–$\bar{M}_w$ functions, these are not indiscriminately interchangeable for calculations of polymer molecular weights from intrinsic viscosity data. Rather, when this expedient is resorted to, it is advisable to restrict use to a function which has been derived from experiments performed under conditions tending to reduce the potential effects of solute aggregates.

We are indebted to Dr. H. W. Holden for preparing fractionated polyethylene samples, and to Drs. A. Rudin and E. B. Bagley for valuable discussions.

References

1. Zimm, B. H., *J. Chem. Phys.*, **16**, 1093 (1948).
2. Billmeyer, F. W., Jr., *J. Am. Chem. Soc.*, **75**, 6118 (1953).
3. Muus, L. T., and F. W. Billmeyer, Jr., *J. Am. Chem. Soc.*, **79**, 5079 (1957).
4. Duch, E., and L. Küchler, *Z. Elektrochem.*, **60**, 218 (1956).
5. Kobayashi, T., A. Chitale, and H. P. Frank, *J. Polymer Sci.*, **24**, 156 (1957).
6. Trementozzi, Q. A., *J. Polymer Sci.*, **36**, 113 (1959).
7. Tung, L. H., *J. Polymer Sci.*, **46**, 409 (1960).
8. Schreiber, H. P., *Can. J. Chem.*, **39**, 1557 (1961).
9. Kokle, V., F. W. Billmeyer, Jr., L. T. Muus, and E. J. Newitt, *J. Polymer Sci.*, **62**, 251 (1962).
10. Nicolas, L., *Compt. Rend.*, **244**, 80 (1957).
11. Chiang, R., *J. Polymer Sci.*, **36**, 91 (1959).
12. Blackmore, W. R., and W. Alexander, *Can. J. Chem.*, **39**, 1888 (1961).
13. Henry, P. M., *J. Polymer Sci.*, **36**, 3 (1959).
14. Tung, L. H., *J. Polymer Sci.*, **36**, 287 (1959).
15. Moore, L. D., Jr., and V. G. Peck, *J. Polymer Sci.*, **36**, 141 (1959).
16. Schreiber, H. P., and E. B. Bagley, *J. Polymer Sci.*, **58**, 29 (1962).
17. Schreiber, H. P., *Polymer*, in press.
18. Benoit, H., A. M. Holtzer, and P. Doty, *J. Phys. Chem.*, **58**, 635 (1954).
19. Zimm, B. H., and W. H. Stockmayer, *J. Chem. Phys.*, **17**, 1301 (1949).
20. Flory, P. J., A. Ciferri, and R. Chiang, *J. Am. Chem. Soc.*, **83**, 1023 (1961).
21. Ciferri, A., *Trans. Faraday Soc.*, **57**, 853 (1961).
22. Bueche, F., *J. Chem. Phys.*, **20**, 1959 (1952).
23. Fox, T. G, and S. Loshaek, *J. Appl. Phys.*, **26**, 1080 (1955).
24. Francis, P. S., R. C. Cooke, Jr., and J. H. Elliott, *J. Polymer Sci.*, **31**, 453 (1958).
25. Atkins, J. T., L. T. Muus, C. W. Smith, and E. T. Pieski, *J. Am. Chem. Soc.*, **79**, 5089 (1957).

Résumé

On a évalué, au moyen de mesures de diffusion lumineuse effectuées à diverses températures, les poids moléculaire et les rayons de gyration de polyéthylènes linéaires es ramifiés en solution dans l'α-chloronaphtalène. Dans un certain nombre de cas, let dimensions moléculaires dépendent de la température de la solution. La dépendance en fonction de la température peut modifier les valeurs du poids moléculaire jusqu'à 50%; elle tend à être beaucoup plus prononcée pour les poids moléculaires plus élevés, pour les polyéthylènes linéaires que pour les ramifiés et est particulièrement marquée pour les températures situées endessous de la température de fusion cristalline normale du polymère. On pense que la dépendance du poids moléculaire en fonction de la température peut être due à une dissociation progressive en solution des aggrégats polymériques

provenant de l'encombrement entre les chaênes. On a pu établir une relation entre la viscosité intrinsèque et le poids moléculaire pour des polyéthylènes fractionnés en utilisant les poids moléculaires obtenus dans des conditions non-favorabes à la persistance des agrégats polymériques. Les diverses relations entre la viscosité et le poids moléculaire, déjà publiées pour les polyéthylènes, ont été comparées avec la relation calibrée. Certaines équations publiées donnent des résultats en parfait accord avec le fonction présente, mais d'autres présentent une très grande surestimation du poids moléculaire. Les problèmes soulevés par l'aggrégation polymérique peuvent être abordés en tenant compte de ces fonctions entre la viscosité et le poids moléculaire. La comparaison montre le danger qu'il y a à choisir d'une façon aveugle les fonctions reliant la viscosité au poids moléculaire lorsqu'on utilise ces fonctions en vue d'une estimation rapide du poids moléculaire des polymères.

Zusammenfassung

Molekulargewichte und Gyrationsradien linearen und verzweigter Polyäthylene wurden durch Lichtstreuungsmessungen an α-Chlornaphthalinlösungen bei mehreren Temperaturen bestimmt. In einer Reihe von Fällen waren die Molekülgrössenparameter von der Lösungstemperatur abhängig. Die beobachtete Temperaturabhängigkeit kann die Molekulargewichtswerte um bis zu 50% verändern. Die Temperaturabhängigkeit ist bei höheren Molekulargewichten mehr ausgeprägt, bei linearen stärker als bei verzweigten Polyäthylenen, und ist besonders bei Lösungstemperaturen unterhalb der normalen Kristallschmelztemperatur des Polymeren merklich. Es wird angenommen, dass die Temperaturabhängigkeit der Molekulargewichtsparameter auf eine graduelle Dissoziation von Kettenverschlingungs-Polymeraggregaten in Lösung zurückzuführen ist. Aus Molekulargewichtsdaten, die unter ungünstigen Bedingungen für die Beständigkeit von Polymeraggregaten gewonnen worden waren, wurde eine Viskositätszahl-Molekulargewichtsbeziehung aufgestellt. Eine Reihe publizierter Viskositäts-Molekulargewichtsbeziehungen für Polyäthylen wurde mit der hier erhaltenen verglichen. Einige der publizierten Gleichungen lieferten dabei eine gute Übereinstimmung, andere dagegen ergaben viel zu hohe Molekulargewichte. Das Problem der Polymeraggregation schient bei der Ableitung einiger dieser ViskositätsMolekulargewichtsbeziehungen eine Rolle gespielt zu haben. Der Vergleich lasst die Gefahr einer kritiklosen Auswahl von Viskositäts Molekulargewichtsbeziehungen zur raschen Bestimmung des Molekulargewichts von Polymeren erkennen.

Received March 7, 1963

JOURNAL OF POLYMER SCIENCE: PART A VOL. 2, PP. 1669–1685 (1964)

Les Polymeres à l'Interface Eau-Air

J. JAFFE et J.-M. LOUTZ,* *Laboratoire de Chimie générale II, Faculté des Sciences, Université libre de Bruxelles, Belgique*

Synopsis

Even at high superficial dilution ($\pi < 40$ mdyne/cm.$^{-1}$) it is impossible to determine the molecular weight of a flexible polymer. Using statistical equations containing an adjustable parameter it can be accounted for the compression isotherms. This parameter corresponds not to an experimental relation, and is without any physical significance. The polymeric layers can be described by Singer's equation, if one attributes to the term x the significance of an experimental parameter.

I. INTRODUCTION

La constatation, due à Guastalla[1] que la pression superficielle d'un film de hauts polymères obéit, aux grandes dilutions, à une loi analogue à celle de l'état gazeux non parfait, a suscité un grand nombre de travaux.

Cette technique permet, dans certains cas, de déterminer la masse moléculaire de la molécule étalée.[2] Elle peut également fournir des renseignements concernant les dimensions et la forme de cette molécule.[3] Les résultats obtenus sont ici en bon accord avec ceux fournis par les techniques courantes.

Dans d'autres cas cependant, on constate que la masse moléculaire trouvée par osmométrie superficielle ne correspond nullement à celle fournie par les méthodes classiques. Ce désaccord se marque principalement dans le domaine des hauts polymères de synthèse où l'on obtient des masses moléculaires superficielles inférieures aux masses réelles.[4]

Cela doit sans doute être attribué au fait que la distance moyenne entre molécules étalées est nettement inférieure à celle des molécules dissoutes et que l'extrapolation à deux dimensions est par conséquent plus difficile.

Pour les molécules compactes, cet effet de concentration se fera moins sentir du fait que les interactions entre molécules n'engagent que les groupements périphériques. Par contre, si la chaine polymérique est suffisamment souple et déployée en surface, il y aura imbrication mutuelle des molécules qui seront sujettes à un mouvement microbrownien.[5–7]

Des substances telles que l'acétate de cellulose ou les protéines fournissent des valeurs concordantes de la masse moléculaire parce que l'existence de liaisons secondaires (ponts d'hydrogène, par exemple) entre fragments de chaînes conduit à un édifice moléculaire fort raccrapoté.

* Present address: Laboratorie de recherches-U.C.B., Drogenbos, Belgium.

Pour des molécules flexibles, nous avons préféré baser la détermination de la masse moléculaire sur la mesure de la viscosité superficielle de couches extrêmement diluées. Cette méthode plus générale nécessite cependant un étalonnage préliminaire.[8]

Comme l'équation de Guastalla ne rendait pas compte de tous les résultats, certains auteurs ont proposé de la remplacer par d'autres établies à partir des théories de Flory-Huggins.

On assimile la surface à un quasi-réseau dont les macromolécules peuvent occuper statistiquement un certain nombre de sites.

Ces théories introduisent un paramètre de flexibilité qui permet de traduire les résultats expérimentaux dans un assez large domaine de pressions superficielles.[9]

Parmi les théories les plus usitées, citons celle de Singer et celle de Frisch-Simha.

Essentiellement, Singer considère que la macromolécule linéaire est complètement étalée sur la surface assimilée à un réseau bidimensionnel.[10] Le processus suivi par Singer pour calculer la variation d'entropie résultant du dépôt des molécules en surface est analogue à celui de Huggins décrivant le comportement des solutions de hauts polymères.[11]

Quant à Frisch et Simha, ils considèrent que V des X segments que comporte une chaîne se trouvent, en moyenne, dans le plan de l'interface. Ces segments adsorbés sont isolés sur la surface et reliés les uns aux autres par des ponts $(X-V)$ se déployant dans la solution.[12]

Chacune de ces relations néglige les contributions énergétiques d'origine enthalpique.

Dans le présent travail, nous avons réalisé des mesures de pressions superficielles aux plus faibles concentrations actuellement accessibles à l'expérience correspondant à $\pi < 40$ mdyne/cm; les résultats obtenus sont traités par chacune des trois théories que nous venons d'énumérer et nous essayons d'en tirer des conclusions quant à leur utilisation pour décrire les films étalés.

Nous appellerons M_{3D} les masses moléculaires réelles déterminées par les méthodes classiques, M_{2D} les masses moléculaires obtenues par extrapolation à concentration nulle des isothermes de compression.

II. APPAREILS

1. Basses Pressions

Nous avons employé le micromanomètre à fil tendu de Guastalla.[13] Celui-ci nous permet d'évaluer des pressions comprises entre 0 et 5×10^{-2} dyne/cm. Les modifications que nous avons apportées ont été signalées dans un travail antérieur.[2]

Depuis, nous avons ajouté un dispositif qui a pour but l'amortissement des vibrations de l'appareil. Ce dispositif comprend essentiellement une table massive en béton reposant sur des ressorts en acier. Ces derniers

prennent assise sur deux colonnes en briques faisant corps avec les poutres maîtresses du bâtiment. En plus, le centre de gravité de l'ensemble a été abaissé par la suspension, à la table, d'une masse inerte importante.

L'amortissement obtenu a rendu nos mesures plus faciles et plus précises.

L'ensemble de la technique expérimentale est identique à ce qui a été décrit antérieurement.[2,3]

2. Pressions Moyennes

Nous avons utilisé le manomètre à suspension pendulaire décrit par Guastalla.[13] Notre appareil nous permet d'évaluer des pressions comprises entre 0 et 5 dyne/cm. Dans ces conditions, il est aisé d'atteindre une précision de 10^{-2} dyne/cm. De manière à éviter une contamination de la surface de mesure par des poussières, l'appareil est enfermé dans une caisse en Plexiglas.

3. Hautes Pressions

Celles-ci jusqu'à 25 dyne/cm. sont évaluées à l'aide d'un tensiomètre Dognon-Abribat fourni commercialement.[14] La précision relative à la balance peut être évaluée à $\pm 6 \times 10^{-2}$ dyne/cm. La seule modification que nous y avons apportée consiste en le remplacement de la cuve livrée avec l'appareil par un cristallisoir de plus grande surface (227 cm^2). Cette modification nous permet d'obtenir avec une meilleure précision des concentrations superficielles élevées.

III. SUBSTANCES

Nous avons utilisé (*1*) l'acétate de cellulose (AcC), (*2*) l'acétate de polyvinyle (PVA), (*3*) l'acide polyacrylique (PAA).

Les fractions d'acétate de cellulose sont obtenues au départ d'une solution à 2,5% de polymère brut, dans l'acétone.

Le fractionnement s'effectue par évaporation. Nous avons obtenu sept fractions. Chaque fraction est redissoute puis reprécipitée, en solution concentrée, par de l'alcool éthylique. La masse moléculaire M_{2D} déterminée par la méthode des couches superficielles fournit, à condition de prendre un bon solvant d'étalement ($CHCl_3$ à 15% d'éthanol) un résultat comparable à celui de la viscosimétrie classique.[4,15] (La masse moléculaire M_{3D} de AcC est obtenue par viscosimétrie dans l'acétone au moyen de $[\eta] = 1{,}54 \times 10^{-4} M^{0{,}82}$.)[16]

TABLEAU I

Fraction	Masse moléculaire	Masse monomère	Degré polymérisation
II	97.000	281	346
VI	21.000	256	82

L'indice d'acétyle est déterminé à partir de l'hydrolyse basique du polymère dissous dans la pyridine. Le Tableau I caractérise les deux fractions utilisées.

La méthode d'obtention de différentes fractions de PVA a été décrite antérieurement.[8]

Les masses moléculaires M_{3D} ont été déterminées par viscosimétrie dans l'acétone au moyen d'un viscosimètre du type Ostwald (Tableau II) au moyen de:[17]

$$[\eta] = 2{,}09 \times 10^{-4} M^{0{,}68}$$

TABLEAU II

Fraction	Masse moléculaire	Masse monomère	Degré polymérisation
II	98.000	86	1139
V	14.000	86	163

Les caractéristiques se rapportant à l'acide polyacrylique ont également été données précédemment.[8]

Nous avons utilisé un échantillon de M viscosimétrique = 38.000.

IV. RESULTATS EXPERIMENTAUX ET DISCUSSIONS

1. Theorie de Guastalla

On a que

$$\pi(S - b) = (m/M)RT$$

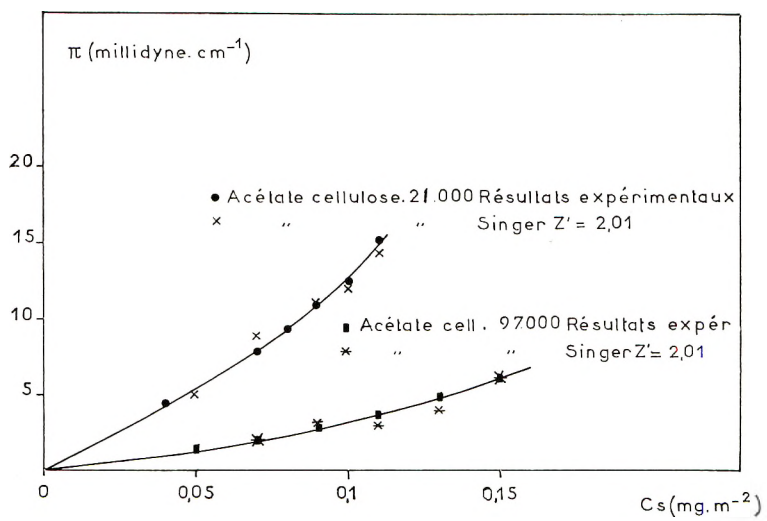

Fig. 1. Courbe $\pi = f(C_s)$ pour l'acetate de cellulose.

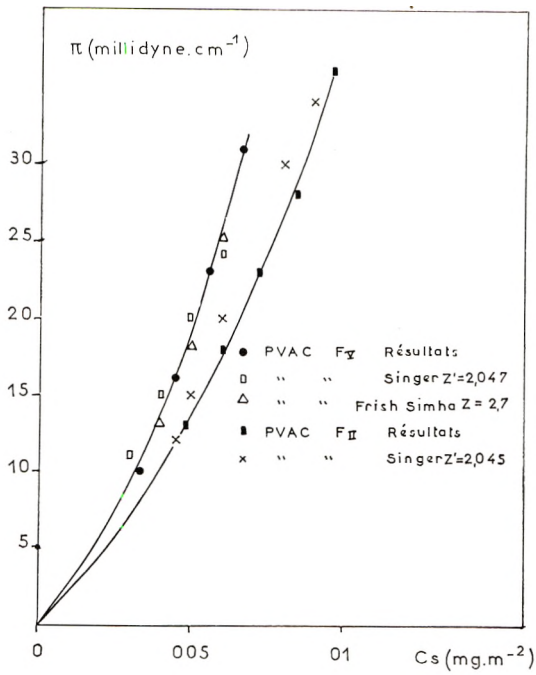

Fig. 2. Courbe $\pi = f(C_s)$ pour l'acetate de polyvinyle.

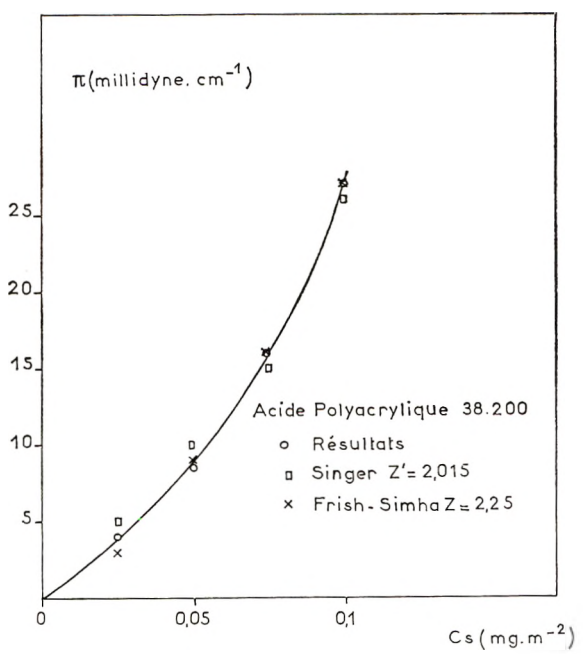

Fig. 3. Courbe $\pi = f(C_c)$ pour l'acide polyacrylique.

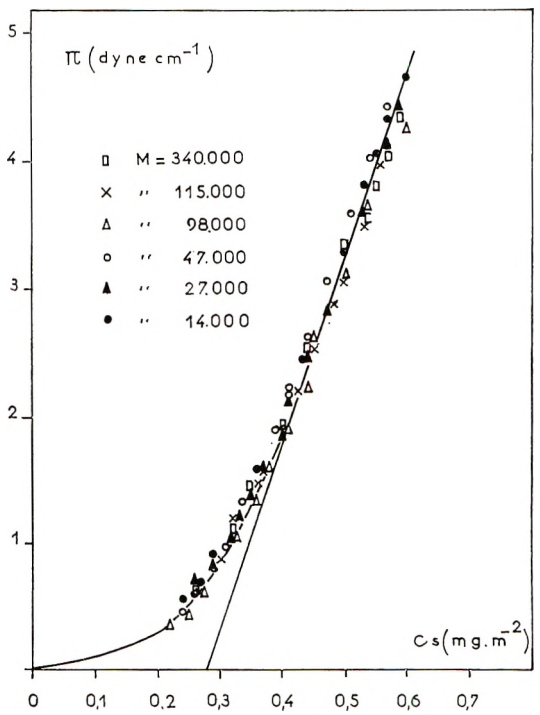

Fig. 4. Acetate de polyvinyle. Pression superficielle en fonction de la concentration.

ou π = pression superficielle, b = cosurface, S = surface sur laquelle se trouvent étalés m grammes de substance, M = masse moléculaire superficielle de la substance étalée.

Les isothermes de compression relatives à nos substances sont présentées dans les Figures 1, 2, et 3. Le support est une solution HCl $N/100$. La température est fixée à 20°C ± 1°C.

En utilisant cette équation, on trouve que: pour AcC, les masses moléculaires 2D et 3D coïncident dans la limite des erreurs acceptables commises sur leur détermination (environ 10%). Dans le cas de PVA, et principalement pour la grande masse moléculaire, il y a discordance entre les résultats fournis par les pressions superficielles et ceux que l'on obtient par les méthodes tridimensionnelles (Tableau III).

TABLEAU III

Fraction	M_{3D}	M_{2D}	$f = M_{2D}/M_{3D}$
II	98.000	11.600	0.12
V	14.000	10.400	0.74

Pour les fractions 3 et 4, on confirme que M_{2D} reste comprise entre 10.400 et 11.600. En dépit de la sensibilité de notre appareil, l'écart entre M_{2D} et M_{3D} indique que le champ de nos investigations est encore trop éloigné

du domaine des grandes dilutions pour nous permettre d'obtenir à extrapolation $C \rightarrow 0$ la masse moléculaire correcte (Fig. 4).

PAA présente un comportement superficiel en tout point analogue à celui de PVA. Les mesures de basses pressions superficielles ne permettent pas de trouver directement la masse moléculaire. Les mesures de viscosité indiquent cependant que la molécule présente une rigidité intermédiaire entre celle de AcC et PAA:[8,18] $M_{3D} = 38.200$; $M_{2D} = 19.500$; $f = 0.51$.

2. Theories de Singer et de Frisch-Simha

Chacune des équations développées par Singer ou Frisch-Simha comporte un paramètre que l'on peut ajuster pour faire coïncider la courbe expérimentale et l'isotherme théorique. Dans ce cas, suivant la valeur de ce paramètre, l'une ou l'autre de ces théories permet de vérifier l'expérience.

Rappelons que dans le cas de la théorie de Singer la pression superficielle est donnée par l'expression

$$\pi = \frac{kT}{A_0} \frac{x-1}{2x} Z' \ln\left(1 - \frac{2}{Z'}\frac{A_0}{A}\right) - \ln\left(1 - \frac{A_0}{A}\right) \qquad (1)$$

ou A_0 représente l'aire occupée par un segment de la chaîne dans le film condensé, x = degré de polymérisation, A = l'aire disponible par monomère sous la pression π; Z' est lié à Z l'indice de coordination du réseau. Cette équation considère que toute la molécule se trouve dans le plan de l'interface.

Davies[19] a proposé de relier arbitrairement Z' à la flexibilité de la chaîne. Si la molécule constitutive du film est complètement rigide, chaque unité aura deux premiers voisins.

Ceci s'exprime quantitativement en terme de coordination Z' qui dans ce cas sera égal à 2. Si autour de chaque segment il y a plus que deux positions possibles, ce nombre sera supérieur à 2. Ceci traduira qu'un certain fléchissement de la chaîne est admis, la valeur maximum Z' étant 4.

Quant à la théorie de Frisch et Simha, elle conduit à l'expression suivante de la pression:

$$\pi = \frac{kT}{A_0}\left\{\frac{Z}{2}\frac{V-1}{V[1-(1/X)]}\ln\left[1 - \frac{2}{X}\left(1 - \frac{1}{X}\right) f\frac{A_0}{A}\right] - \ln\left(1 - f\frac{A_0}{A}\right)\right\} \qquad (2)$$

Dans ce cas, on considère qu'il y a des segments dans le support et la relation $V = fX$ relie le nombre total de segments X au nombre de segments V se trouvant dans le plan de l'interface.

Cette équation n'est en général pas utilisée parce que l'accessibilité expérimentale de V est mal définie.

Etant donné que les deux équations statistiques contiennent une variable Z, il faut si l'on veut s'assurer de la validité de l'une ou l'autre de ces formu-

lations trouver une relation expérimentale supplémentaire liant les différentes grandeurs X, f, et Z.

Huggins[20] a montré que l'équation de Singer pouvait être mise sous la forme:

$$\pi = (kT/A_0)C(1 + B_1C + B_2C^2 + \ldots) \tag{3}$$

A_0 = étant la surface occupée dans le film compact par une molécule de polymère, $C = A_0/A$ représentant la fraction de la surface qui est réellement occupée, A = la surface disponible, à la pression π, par molécule.

Dans ce cas,

$$B_1 \text{ (Singer)} = \frac{x}{2}\left(1 - \frac{2}{Z'}\right)$$

$$B_2 \text{ (Singer)} = \frac{x}{3}\left(1 - \frac{4}{Z'^2}\right) \tag{3'}$$

Quant à l'équation de Frisch-Simha mise sous la même forme, elle conduit à:

$$B_1 \text{ (Frisch-Simha)} = \frac{xf^2}{2}\left(1 - \frac{2}{Z}\right)$$

$$B_2 \text{ (Frisch-Simha)} = \frac{xf^3}{3}\left(1 - \frac{4}{Z^2}\right)$$

f représente la fraction des segments de la chaîne qui se trouve effectivement dans la monocouche.

Pour une molécule ne présentant pas de fragments dissous dans le support $f = 1$ et $Z' = Z$, les deux expressions de B_1 et de B_2 sont identiques.

A partir de A_0 et de la densité superficielle d, on peut obtenir M:

$$M = A_0dN \tag{4}$$

ou N = nombre d'Avogadro.

La densite superficielle est également nécessaire pour calculer la fraction superficielle C.

$$C = m/dS \tag{5}$$

où m est la masse de substance étalée sur la surface S.

A partir des équations (3), (4), et (5), on établit l'équation:

$$\frac{SM}{m} - \frac{RT}{\pi} = A_0B_1N + N^2(A_0^2B_2 - A_0^2B_1^2)\frac{\pi}{RT} + \ldots$$

En portant $SM/m - RT/\pi$ en fonction de π/RT pour de faibles valeurs de π, on obtient une droite dont la pente et l'ordonnée à l'origine permettent de définir le rapport B_2/B_1^2.

En effet:

$$\frac{B_2}{B_1^2} = 1 + \frac{\text{pente}}{(\text{intersection})^2}$$

De cette manière, nous pouvons comparer une valeur expérimentale du rapport B_2/B_1^2 indépendante de toute hypothèse de structure superficielle à une valeur calculée à partir des équations (3') qui tiennent compte des paramètres Z, X, et f du quasi-réseau bidimensionnel.

Nous allons appliquer cette méthode à nos polymères.

Acétate de Cellulose. Ainsi que nous l'avons rappelé, ce polymère fournit, par application de l'équation de Guastalla une masse moléculaire superficielle comparable à la masse moléculaire viscosimétrique. L'écart peut en partie être attribué à la polydispersité des échantillons; l'osmométrie superficielle donnant une masse moléculaire en nombre. Les auteurs qui ont étudié des couches d'étalement de ce polymère sont d'accord pour reconnaître que, si certaines conditions sont respectées (faibles concentrations superficielles, bon solvant d'étalement),[2,15,21] les molécules sont disposées à plat dans le plan de l'interface et les zones expérimentales sont suffisamment proches de l'état gazeux pour permettre une détermination de M.

Les isothermes de compression doivent dans ce cas être calculées à l'aide de l'équation de Singer.

Le seul facteur qui doit être préalablement déterminé est A_0, l'aire réellement occupée par un monomère dans la couche.

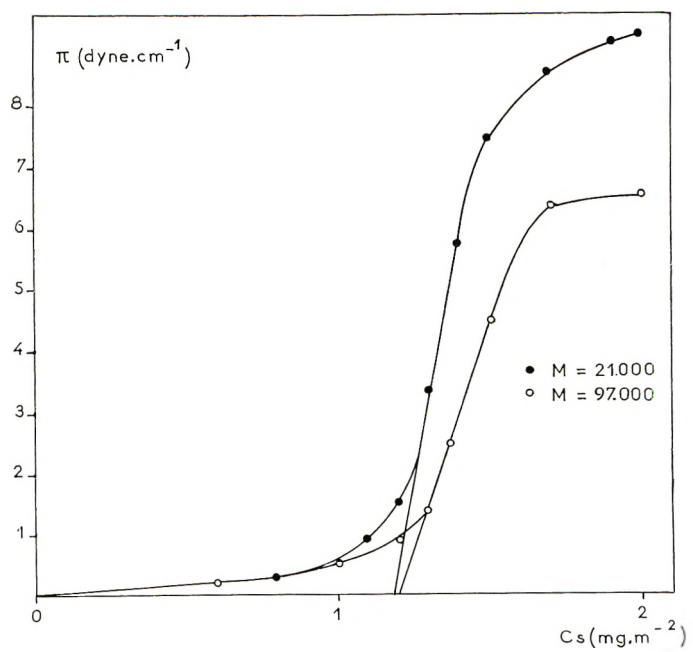

Fig. 5. Acetate de cellulose. Détermination de A_0.

On considère en général que la partie linéaire de la courbe des hautes pressions fournit cette grandeur.

Pour obtenir la zone du film continu jusqu'au collapse, nous avons employé un tensiomètre de Dognon-Abribat.

Les courbes ainsi obtenues sont représentées dans la Figure 5 et le Tableau IV.

TABLEAU IV

M	C_s pour $\pi = 0$, mg/m²	A_0/monomère, Å²
21.000	1.18	36
97.000	1.20	39

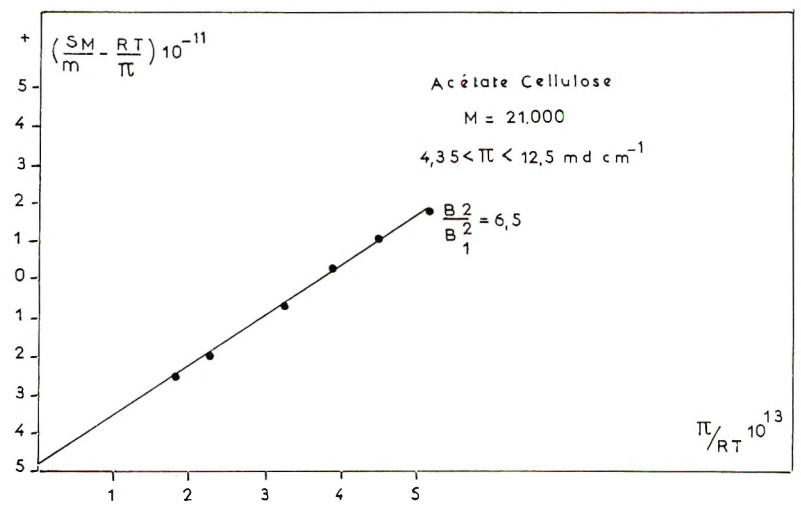

Fig. 6. Détermination experimentale de B_2/B_1^2.

A partir de cette donnée et de la valeur de X, il ne reste plus qu'à trouver par interpolation la valeur de Z' qui permet de représenter le mieux possible la courbe expérimentale.

Dans le cas de l'acétate de cellulose, une valeur de $Z' = 2{,}01$ représente correctement l'isotherme de compression (Fig. 1).

A partir de cette valeur nous pouvons calculer théoriquement à l'aide de (3′) le rapport B_2/B_1^2 Singer.

$$\frac{B_2}{B_1^2} = \frac{4}{3}\,\frac{1}{x}\,\frac{[1 - (4/Z'^2)]}{[1 - (2/Z')]^2} = \frac{532}{x}$$

D'autre part, la méthode graphique, que nous avons indiquée précédemment, fournit la valeur expérimentale de ce même rapport (cf. Fig. 6 et 7). Les résultats sont rassemblés dans le Tableau V.

TABLEAU V

M	B_2/B_1^2 calculé	B_2/B_1^2 mesuré
21.000	6,48	6,5
97.000	1,53	1,5

La correspondance entre les valeurs mesurées et calculées, pour chacune des deux fractions, justifie l'utilisation de l'équation de Singer appliquée à l'entité physico-chimique.

Acetate de Polyvinyle. PVA étant un polymère linéaire flexible, susceptible à priori de dérouler certains de ses segments dans le support, se rapproche du modèle imaginé par Frisch et Simha pour l'établissement de leur relation.

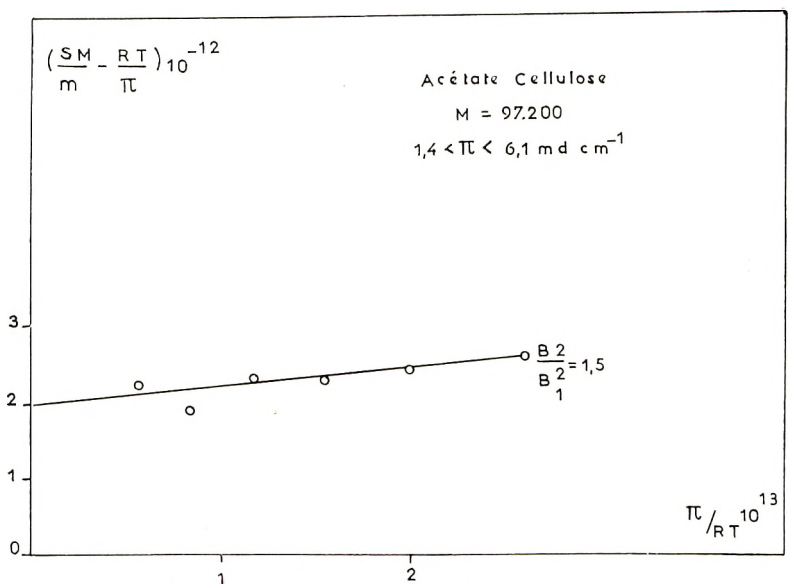

Fig. 7. Détermination experimentale de B_2/B_1^2.

Dans ce cas, en utilisant les grandeurs reprises dans le TableauVI, nous pouvons chercher à déterminer la valeur du paramètre Z.

Pour évaluer A_0, nous avons construit un modèle de Stuart en posant tous les carboxyles sur l'interface. La distance entre deux $C = 0$ voisins est de l'ordre de 5,5 Å, ce qui entraîne une valeur, de l'aire par monomère

TABLEAU VI

Fraction	M	X	V	f	A_0, Å^2
II	98.000	1139	135	0,12	24
V	14.000	163	121	0,74	24

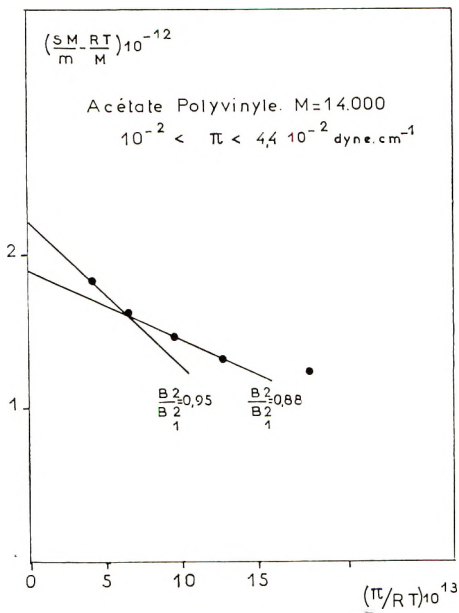

Fig. 8. Détermination du rapport B_2/B_1^2 en prenant M = 14,000.

de 24 Å^2 environ. Cette aire concorde avec celle renseignée dans la littérature.[5]

La Figure 2 montre qu'une valeur de Z = 2,7 permet de parfaitement rendre compte de l'isotherme relative à la fraction V.

Quant à la courbe $\pi = f(C_s)$ obtenue à l'aide de la fraction II, aucune valeur de Z inférieure à 4 ne permet de la représenter.

Par exemple, pour C_s = 0,05 mg/m^{-2}, l'équation de Frisch-Simha devient:

$$\pi = 19.421\ Z \log [1 - (0,0201/Z)] + 0,170$$

Si l'on prend pour Z la valeur de 4, habituellement considérée comme limite supérieure de ce paramètre[19] on trouve une valeur de π proche de 0.

D'autre part, si pour la fraction V on compare la valeur théorique de B_2/B_1^2 Frisch-Simha calculée avec Z = 2,7, f = 0,74, et X = 163 avec le même rapport expérimental (Fig. 8), on trouve une discordance très nette (Tableau VII).

Au lieu de traiter les résultats obtenus avec le PVA au moyen de la théorie de Frisch-Simha, nous avons essayé de nous rendre compte dans quelle mesure celle de Singer pouvait leur être appliquée.

TABLEAU VII

Fraction	B_2/B_1^2 (F.-S.) calculé	B_2/B_1^2 mesuré
V	0,075	0,915

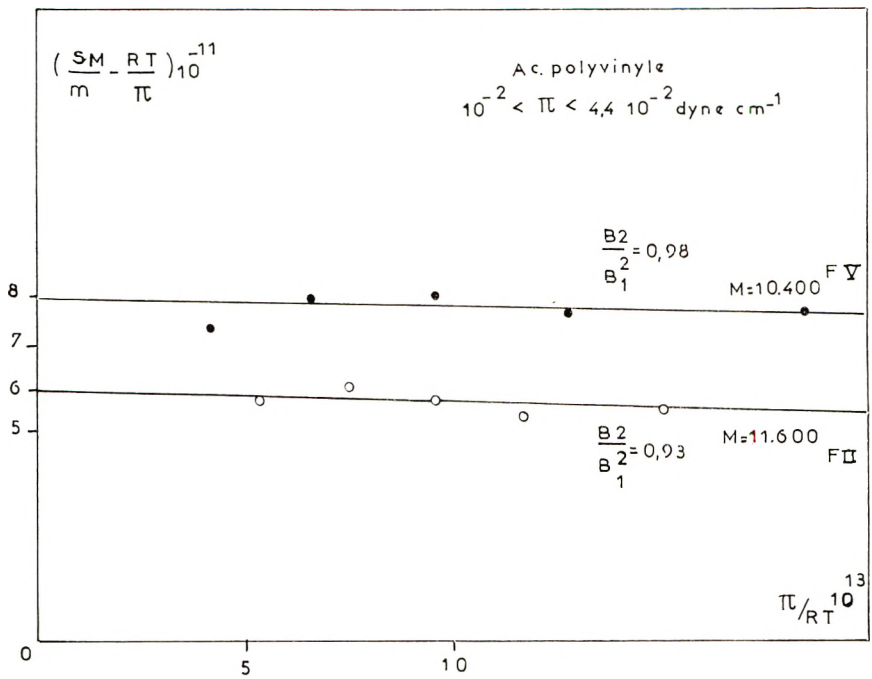

Fig. 9. Détermination experimentale de B_2/B_1^2.

Si on représente l'isotherme de compression de PVA par l'équation de Singer, on trouve une bonne concordance avec l'expérience pour $Z' = 2,48$.[22] Dans ce cas, on calcule pour la fraction II un rapport $B_2/B_1^2 = 0,01$ et pour V un rapport égal à 0,075. L'ordre de grandeur totalement différent de celui mesuré (0,915) indique que, pour les molécules flexibles, le seul paramètre Z' ne peut aucunement caractériser la couche.

Dans ce cas, à côté de l'hypothèse qui considère que toute la molécule se trouve dans le plan de l'interface et que par conséquent $f = 1$, nous envisageons que dans ce plan les molécules sont caractérisées par un second paramètre qui sera la grandeur expérimentale M_{2D}.

Les résultats ainsi obtenus sont rassemblés dans le Tableau VIII, et Figure 9.

Nous remarquons que l'application de l'équation de Singer moyennant les hypothèses faites conduit à une bonne concordance des valeurs observées et calculées.

TABLEAU VIII

Fraction	M_{2D}	Z'	B_2/B_1^2 (Singer) calculé	B_2/B_1^2 mesuré
II	11.600	2,045	0,90	0,93
V	10.400	2,047	0,96	0,98

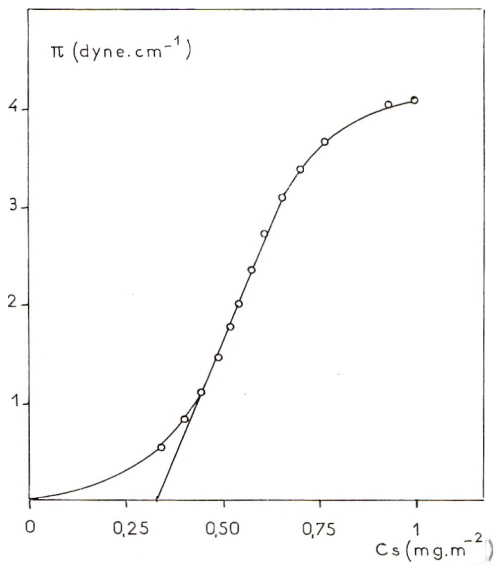

Fig. 10. Acide polyacrylique. Dtéermination de A_0.

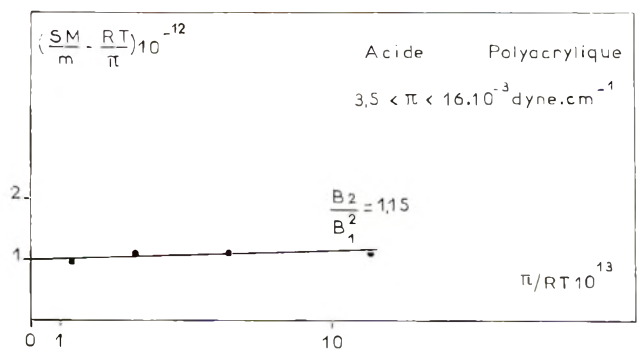

Fig. 11. Détermination experimentale de B_2/B_1^2.

Acide Polyacrylique. La même methode que celle suivie pour PVA peut être adoptée pour PAA. On peut cependant supposer que sur un support à pH = 2, la molécule est plus pelotonnée. Les groupes —COOH non ionisés contribuent à la cohésion de l'édifice par suite de leurs liaisons hydrogènes présentes en très grand nombre.

Les films de PAA collapsant assez rapidement par compression, la valeur de A_0 est déterminée à aide de l'appareil des moyennes pressions (Fig. 10).

Les différentes grandeurs statistiques relatives à une fraction de ce polymère sont consignées dans les Tableaux IX et X et Figure 11.

Dans ce cas également, nous constatons une meilleure coïncidence de l'expérience et de la théorie, si l'on considère l'existence sur la surface de particules caractérisées par la grandeur M_{2D}.

TABLEAU IX

M_{3D}	A_0, Å^2	f	x	Z (F.-S.)	B_2/B_1^2 (F.-S.) calculé	B_2/B_1^2 mesuré
38.000	37	0,51	530	2,25	0,82	1,15

TABLEAU X

M_{2D}	x	Z' (Singer)	B_2/B_1^2 (Singer) calculé
19.500	271	2,015	1,15

V. CONCLUSIONS

Nos mesures nous ont permis de montrer que, même dans une région de faibles concentrations ($A_0/A < 0,1$) rarement utilisée, l'application de l'équation de Guastalla à des couches de hauts polymères flexibles ne permet pas d'obtenir la valeur de la masse moléculaire réelle.

La validité de la méthode ne peut cependant être mise en doute puisqu'elle fournit des renseignements corrects dès que la macromolécule garde en surface une cohésion suffisante.

Cet insuccès provient de ce que pour des molécules telles que PVA et PAA même dans ce domaine de concentrations les molécules sont encore à ce point imbriquées que les grandeurs déterminées, par extrapolation à C_s nulle, sont sans relation avec les dimensions exactes de la particule.[4]

Les équations de Frisch-Simha et de Singer qui négligent la contribution enthalpique dans l'évaluation de l'énergiede formation du film ne pourront dans ce cas fournir qu'une représentation approchée des résultats expérimentaux.

Comme, d'autre part, ces équations renferment un paramètre leur permettant de décrire les isothermes de compression expérimentales, on ne peut tirer aucune conclusion quant à la validité des modèles physiques qu'elles représentent.

Le caractère semi-empirique de ces paramètres apparaît dans le désaccord existant entre les valeurs de l'indice de coordination obtenu à partir de Z'[23] et celui trouvé par l'application de la théorie de Frisch-Simha (Tableau XI).

TABLEAU XI

Substance	Z'	Z calculé à partir de Z'	Z (F.-S.)
PVA (II)	2,045	2,028	indéterminable
PVA (V)	2,047	2,030	2,7
PAA	2,015	2,000	2,25

Tout au plus peut-on utiliser Z' pour fournir en unité arbitraire une mesure de la flexibilité de la molécule.[10]

On constate effectivement dans ce cas, en accord avec d'autres expériences[24] que l'acétate de cellulose apparaît comme plus rigide que PAA, lui-même moins flexible que PVA.

Nous constatons également pour AcC une valeur de Z' plus faible que celle renseignée dans la littérature.[22]

Ceci provient du fait que l'équation de Singer est dérivée à partir d'une hypothèse de random-mixing des segments à la surface. Dans le domaine beaucoup plus dilué que nous utilisons, la distribution des sites devient plus discontinue. Il y a formation d'îlots où la densité est en moyenne plus élevée que sur le reste de la surface, ce qui entraîne des écarts à cette hypothèse. On note d'ailleurs le même effet dans le cas des solutions classiques de hauts polymères pour lesquelles, aux grandes dilutions, le nombre de coordination est plus petit.[23]

Suivant une méthode indiquée par Huggins, nous avons caractérisé chacun de nos polymères par une constante indépendante de tout modèle superficiel. Nos calculs montrent que cette grandeur (B_2/B_1^2) est retrouvée en considérant les paramètres relatifs à la description de la molécule considérée comme étalée dans le plan de l'interface.

Pour AcC l'accord théorique et expérimental est très bon en utilisant une valeur de Z' déterminée par l'équation de Singer décrivant l'isotherme et une valeur de la masse moléculaire correcte.

Pour PVA et PAA, l'équation de Frisch-Simha, qui devrait a priori fournir les meilleurs résultats, ne conduit pas à une bonne concordance. Ceci provient vraisemblablement du fait que le terme V ne peut être défini comme nous l'avons fait par M_{3D}/M_{2D}.

Pour les molécules flexibles, il semble que leur caractérisation par un terme Z' calculé grâce à une équation de Singer relève de l'arbitraire. Il faut en plus de cette valeur introduire un second paramètre M_{2D}, lequel, sans relations quelconques avec la masse moléculaire, est également lié à la rigidité de la chaîne polymérique.

Il y a lieu de rappeler que nos mesures sont effectuées à très basses pressions et à l'interface eau/air. On a tout lieu de croire que pour des pressions plus élevées, voisines de celle du collapse, ou qu'à des interfaces huile/eau, la théorie de Frisch-Simha permettra une meilleure représentation des résultats. Dans ces conditions, des parties de la chaîne polymérique doivent se déployer en dehors du plan de l'interface, soit par extrusion mécanique, soit par meilleure solvatation des parties hydrocarbonées. De toute manière, une image mathématique des couches d'étalement qui tiendrait compte du fait que des segments moléculaires peuvent se trouver dans l'air aussi bien que dans la phase aqueuse serait susceptible de représenter au mieux la réalité physique. La solution statistique d'un tel problème n'est pas simple. En effet, on ne sait pas quel modèle choisir pour calculer la ΔS résultant du passage des segments dans l'air, étant donné que l'image réticulaire d'un tel milieu, à laquelle on devrait avoir recours, n'aurait pas beaucoup de sens.

Nous adressons nos sincères remerciements à Mademoiselle L. de Brouckère pour l'intérêt qu'elle a constamment porté à ce travail, ainsi que pour les conseils qu'elle nous a prodigués.

References

1. Guastalla, J., *Compt. Rend.*, **208**, 1078 (1939).
2. Jaffe, J., *J. Chim. Phys.*, **51**, 243 (1954).
3. Jaffe, J., et R. de Coene, *J. Polymer. Sci.*, **23**, 665 (1957).
4. Hotta, M., *Bull. Chem. Soc. Japan*, **27**, 80 (1954).
5. Benson, G. C., et R. L. McIntosh, *J. Colloid Sci.*, **3**, 323 (1948).
6. Schick, N. J., *J. Polymer Sci.*, **25**, 465 (1957).
7. Crisp, D. J., *J. Colloid Sci.*, **1**, 49 (1946).
8. Jaffe, J., et J. M. Loutz, *J. Polymer Sci.*, **29**, 381 (1958).
9. Davies, J. T., et J. Llopis, *Proc. Roy. Soc.* (*London*), **A227**, 537 (1955).
10. Singer, S. J., *J. Chem. Phys.*, **16**, 872 (1948).
11. Huggins, M. L., *Ann. N. Y. Acad. Sci.*, **43**, 1 (1942).
12. Frisch, H. L., et R. Simha, *J. Chem. Phys.*, **27**, 702 (1957).
13. Guastalla, J., *Mem. Serv. Chim. Etat* (*Paris*), **30**, 345 (1947).
14. Dognon, A., et M. Abribat, *Bull. Soc. Chim. Biol.*, **23**, 62 (1941).
15. Ruyssen, R., et S. Frank, *Ind. Chim. Belge*, **16**, 389 (1951).
16. Mark, H., *Molécules géantes*, Ed. Sciences et Lettres, Liège.
17. Faltakhov, K. Z., E. S. Pisarenko, et L. N. Verkhotina, *Kolloid. Zh.*, **18**, 101 (1956).
18. Dieu, H. A., *Bull. Soc. Chim. Belge*, **65**, 1035 (1956).
19. Davies, J. T., *Biochim. Biophys. Acta*, **11**, 165 (1953).
20. Huggins, M. L., Symposium über Makromoleküle in Wiesbaden, Section IIB2 (1959).
21. Clement, P., et L. Pouradier, *J. Chim. Phys.*, **46**, 621 (1949).
22. Crisp, D. J., *Surface Phenomena in Chemistry and Biology*, Pergamon Press, London, 1958, p. 23.
23. Flory, P. J., *J. Chem. Phys.*, **13**, 453 (1945).
24. Dieu, H. A., Thèse d'Agrégation, Université de Liège, 1957.

Résumé

Même dans un domaine de grande dilution superficielle ($M < 40$ mdyne/cm), il n'est pas possible de déterminer la masse moléculaire d'un polymère flexible. L'utilisation d'équations statistiques introduisant un paramètre ajustrable permet de rendre compte des isothermes de compression. Ce paramètre ne satisfait cependant pas une relation expérimentale et il apparaît qu'on ne peut lui accorder aucune signification physique rigoureuse. Les couches de polymères étudiés peuvent être décrites au moyen de l'équation de Singer si on accorde au terme x la signification d'un paramètre expérimental.

Zusammenfassung

Selbst im Bereiche sehr grosser Oberflächenverdünnung ($N < 40$ mdyne/cm^{-1}) ist es nicht möglich das Molekulargewicht eines flexiblen Polymeren zu bestimmen. Die Benützung von statistischen Gleichungen mit einem adjustierbaren Parameter erlaubt eine Darstellung der Kompressions-isothermen. Dieser Parameter gehorcht allerdings der experimentell gewonnenen Beziehung nicht und er scheint keine strenge physikalische Bedeutung zu besitzen. Die untersuchten Polymerschichten können mit der Gleichung von Singer beschrieben werden, wenn man den Term x als experimentellen Parameter auffasst.

Received April 30, 1962
Revised March 12, 1963

JOURNAL OF POLYMER SCIENCE: PART A VOL. 2, PP. 1687–1698 (1964)

The Distinction between Terminal and Penultimate Copolymerization Models

M. BERGER and IRVING KUNTZ, *Esso Research and Engineering Company, Linden, New Jersey*

Synopsis

An examination of the usual terminal and penultimate mechanisms of copolymerization shows that, for a great many comonomer pairs, copolymer composition data are not sufficient to choose one model over the other. The reactivity ratios based on one copolymerization model can be derived from the reactivity ratios of the other model. Predicted copolymer composition, based on both models, will agree with the observed experimental data within the precision of the usual methods used for copolymer analysis. Hypothetical cases and examples from the literature all show this behavior. The literature comonomer systems were α-methylstyrene–acrylonitrile, and styrene with maleic anhydride, citraconic anhydride, and acrylonitrile. Polymer structure, however, predicted by the two mechanisms do differ appreciably in detail. In particular, predictions of the sequential arrangements of the monomers in the copolymers produced are different for the terminal and penultimate mechanisms. It would seem that the development of experimental procedures for determining the sequential arrangement of the comonomers will be necessary before one can easily and definitely distinguish between terminal and penultimate copolymerization models for a particular system.

Introduction

This publication compares reported experimental observations of copolymer compositions with predicted values based on terminal and penultimate copolymerization models.[1] In the systems we have examined, copolymer composition results cannot be used to distinguish between terminal and penultimate models; where penultimate mechanisms had been favored, we found that terminal model predictions could also explain copolymer composition within the expected precision of the experimental procedure. This publication expresses no preference for one model over the other. Indeed, it indicates that while similarities in copolymer composition can be explained by both models, large differences in comonomer sequence lengths are predicted by the two models. In any particular comonomer system, based on our analysis, there seems to be two methods for distinguishing decisively between the two mechanisms. The first is to develop extremely precise methods of determining comonomer feed ratios and copolymer compositions. The second is to develop analytical procedures for determining comonomer sequence lengths. We would suggest the latter approach receive more attention in polymer research.

Discussion

The usual terminal copolymerization model characterizes the comonomer system in terms of the reactivity ratios which describe the ratios of specific rate constants for the addition of monomer units to the growing macromolecular chain end.[1] Only the terminal monomer residue is considered. The reactivity ratios can be obtained from monomer-feed data and copolymer compositions using the familiar copolymer composition equation, eq. (1).

$$\frac{m_1}{m_2} = \frac{M_1}{M_2}\left[\frac{(r_1)M_1 + M_2}{(r_2)M_2 + M_1}\right] \tag{1}$$

Here, m_1/m_2 refers to the ratio of monomer residues in the copolymer and M_1 and M_2 to the concentration of the two monomers.[1]

Merz, Alfrey, and Goldfinger introduced the concept that the next to last monomer residue, as well as the terminal unit, might influence the addition of the next monomer molecule.[2] This approach was later expanded on by others.[3–5] Recently, certain stereospecific polymerization systems have been characterized by means of this penultimate model.[6] Table I compares the two copolymerization models and shows the notation we will use. (The notation suggested for penultimate systems by F. P. Price[7] has much to commend it, but we will not use it in this paper.)

For the copolymerization of two monomers, the penultimate theory requires eight specific rate constants and hence is considerably more complex than the terminal model. The relationship, eq. (2), corresponding to eq. (1) for the penultimate case is more involved, so that it is impossible to obtain the reactivity ratios from the usual copolymer composition-mono-

TABLE I
Copolymerization Models

Growing chain	Monomer	Rate constant	New structure	Reactivity ratios
Terminal				
-1	1	k_{11}	-11	$(r_1) = k_{11}/k_{12}$
-2	1	k_{21}	-21	
-1	2	k_{12}	-12	
-2	2	k_{22}	-22	$(r_2) = k_{22}/k_{21}$
Penultimate				
-1-1	1	k_{111}	-1-1-1	
-2-1	1	k_{211}	-2-1-1	$r_1 = k_{111}/k_{112}$
-2-2	1	k_{221}	-2-2-1	
-1-2	1	k_{121}	-1-2-1	$r_1' = k_{211}/k_{212}$
-1-1	2	k_{112}	-1-1-2	
-2-1	2	k_{212}	-2-1-2	$r_2 = k_{222}/k_{221}$
-2-2	2	k_{222}	-2-2-2	
-1-2	2	k_{122}	-1-2-2	$r_2' = k_{122}/k_{121}$

mer feed data. Very often simplifying assumptions, i.e., setting certain reactivity ratios equal to zero, or estimates of the reactivity ratios by other procedures have been made in applying the penultimate approach.

$$\frac{m_1}{m_2} = \frac{1 + r_1' \left[\frac{M_1}{M_2} \frac{M_2 + r_1 M_1}{M_2 + r_1' M_1} \right]}{1 + r_2' \left[\frac{M_2}{M_1} \frac{M_1 + r_2 M_2}{M_1 + r_2' M_2} \right]} \tag{2}$$

In a particular experiment, at a certain molar comonomer feed ratio, $M_1/M_2 = X$, the exact equivalence between the reactivity ratios of the terminal and penultimate models shown in eqs. (3) and (4) can be drawn. (The Appendix shows other relationships of the two models. Reactivity ratios from the terminal mechanism are shown in parentheses.)

$$(r_1) = r_1' \left(\frac{r_1 X + 1}{r_1' X + 1} \right) \tag{3}$$

$$(r_2) = r_2' \left(\frac{X + r_2}{X + r_2'} \right) \tag{4}$$

Since copolymerization experiments are always carried out over a range of monomer feed ratios, it is obvious that the values for (r_1) and (r_2) will vary over the range of X. There will be no constant values for (r_1) and (r_2) on the one hand, and r_1, r_1', r_2, and r_2' on the other, which will both lead to exactly the same predicted copolymer composition.

The important question is whether there are values for (r_1) and (r_2), averaged over the experimental range of monomer feed ratios, which will lead to copolymer compositions which are experimentally indistinguishable from the predictions of the penultimate model.

From eq. (3), we can define the average value of $(\bar{r}_1)$ shown in eq. (5) over the interval from the lower feed ratio

$$(\bar{r}_1) = \frac{r_1' \int_{X_1}^{X_2} \frac{r_1 X + 1}{r_1' X + 1}}{\int_{X_1}^{X_2} dX} \tag{5}$$

X_1, to the higher molar monomer feed ratio X_2. In order to use eq. (4) to define the average value $(\bar{r}_2)$, we must average over $1/X$ since X is defined as M_1/M_2; eq. (6) shows the relationship.

$$(\bar{r}_2) = \frac{r_2' \int_{X_1}^{X_2} \frac{X + r_2}{X + r_2'} d(1/X)}{\int_{X_1}^{X_2} d(1/X)} \tag{6}$$

Integrating eqs. (5) and (6) over the interval ΔX ($= X_2 - X_1$) gives eqs. (7) and (8), respectively.

$$(\bar{r}_1) = \frac{r_1\left[\Delta X + (1 - r_1/r_1') \ln \dfrac{1 + r_1'X_2}{1 + r_1'X_1}\right]}{\Delta X} \tag{7}$$

$$(\bar{r}_2) = r_2 \frac{\left[(1/X_1 - 1/X_2) + (r_2/r_2' - 1) \ln \dfrac{X_2(X_1 + r_2')}{X_1(X_2 + r_2')}\right]}{1/X_1 - 1/X_2} \tag{8}$$

Results

The logical step at this point is to develop a mathematical relationship which would express the difference between the predicted copolymer compositions as a function of the reactivity ratios and the monomer feed ratios.

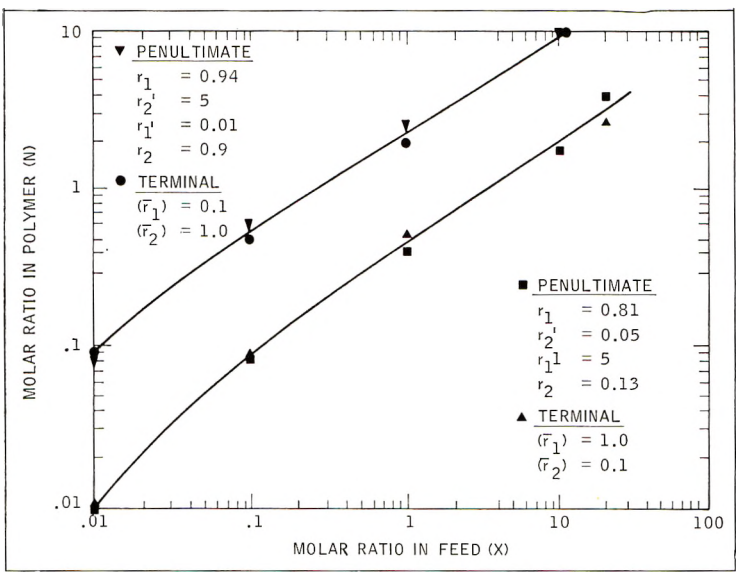

Fig. 1. Composition vs. feed for two hypothetical copolymerizations.

One could then determine if these differences are always within the estimates of experimental error. This procedure appears to be mathematically complex. A less general approach is to consider specific systems. That is, to use the reactivity ratios of one model to calculate the reactivity ratios of the other and then to use these values to calculate copolymer compositions at the same monomer feed ratios. An estimate of the validity of eqs. (7) and (8) is then how well these predicted compositions agree. We have used this latter approach.

Two of these cases are shown in Figure 1. Here we have considered two hypothetical polymerizations: (*a*) a copolymerization where the reactivity

ratio ($\bar{r}_1$) is 0.1 and ($\bar{r}_2$) is 1.0, and (*b*) one where the reactivity ratio ($\bar{r}_1$) is 1.0 and ($\bar{r}_2$) is 0.1. Then, using eqs. (7) and (8), we have calculated a set of values for r_1, r_1', r_2, and r_2' to closely match the copolymer composition-monomer feed curves defined by (*a*) and (*b*). Figure 1 shows that the penultimate ratios give approximately the same ratio of monomer residues in the polymer, N, at all monomer feed ratios, X, over the range 0.01 to 20. This range of monomer feed ratios is wider than those used experimentally in much copolymerization research. Figure 1 indicates the difficulty of

TABLE II
Comparison of Copolymer Compositions

Comonomer system (M_1–M_2)	Molar feed ratio M_1/M_2	Copolymer composition M_1/M_2 Residues			Reference
		Experimental	Terminal	Penultimate	
Styrene–maleic anhydride[a]	12	1.37	1.27	1.51	3
	25	1.87	1.57	1.85	
	50	2.25	2.15	2.41	
	100	3.25	3.27	3.30	
	150	4.00	4.30	4.20	
Styrene–citraconic anhydride[b]	0.05	0.79	0.78	0.77	3
	0.33	0.935	1.01	1.04	
	1.0	1.13	1.14	1.22	
	3.0	1.76	1.41	1.52	
	19	2.77	3.60	2.93	
Styrene–acrylonitrile[c]	1.25	1.4	1.43	1.47	5
	2.5	2.0	1.86	1.93	
	4.0	2.6	2.37	2.42	
	15.	5.5	6.10	5.80	
α-Methylstyrene–acrylonitrile[d]	1.2	1.0	1.03	1.02	4
	1.8	1.2	1.145	1.15	
	3.5	1.3	1.28	1.28	
	10	1.7	1.81	1.72	

[a] Reported: r_1, 0.017; r_1', 0.063; r_2, 0; r_2', 0. We find ($\bar{r}_1$), 0.0227, (r_2), 0.

[b] Reported: r_1, 0.07; r_1', 0.25; r_2, 0.15; r_2', 0.015. We find ($\bar{r}_1$), 0.136; ($\bar{r}_2$), 0.015.

[c] Reported: r_1, 0.30; r_1', 0.45; r_2, 0.03; r_2', 0.45. We find ($\bar{r}_1$), 0.338, (r_2), 0.03.

[d] Reported: r_1, 0.055; r_1', 0.093; r_2, 0.06; r_2', 0.06. We find ($\bar{r}_1$), 0.0805; ($\bar{r}_2$), 0.06.

differentiating the copolymerization mechanism using copolymer composition and monomer feed data. Note that these general results are not restricted to any specific initiation mechanism.

Table II further examines this difficulty of mechanism selection by examining actual experimental results from the literature. In these cases, penultimate mechanisms were favored by the original authors. We have used eqs. (7) and (8) to calculate the terminal model ($\bar{r}_1$) and ($\bar{r}_2$), and from these the predicted copolymer compositions at the different monomer feed ratios. The evidence from these comparisons is clearly that when experi-

mental error is considered, copolymer compositions do not permit a definite choice between the terminal or penultimate mechanisms.

Conclusions

Since these results indicate that the experimentally observed composition of the copolymer cannot differentiate between the two models, it is appropriate to determine if any parameter of copolymer structure can be used for this purpose. It appears that the distribution of monomer units in the macromolecule does make this distinction possible. Using the equations of Miller and Nielsen[6] given in the Appendix, we have calculated

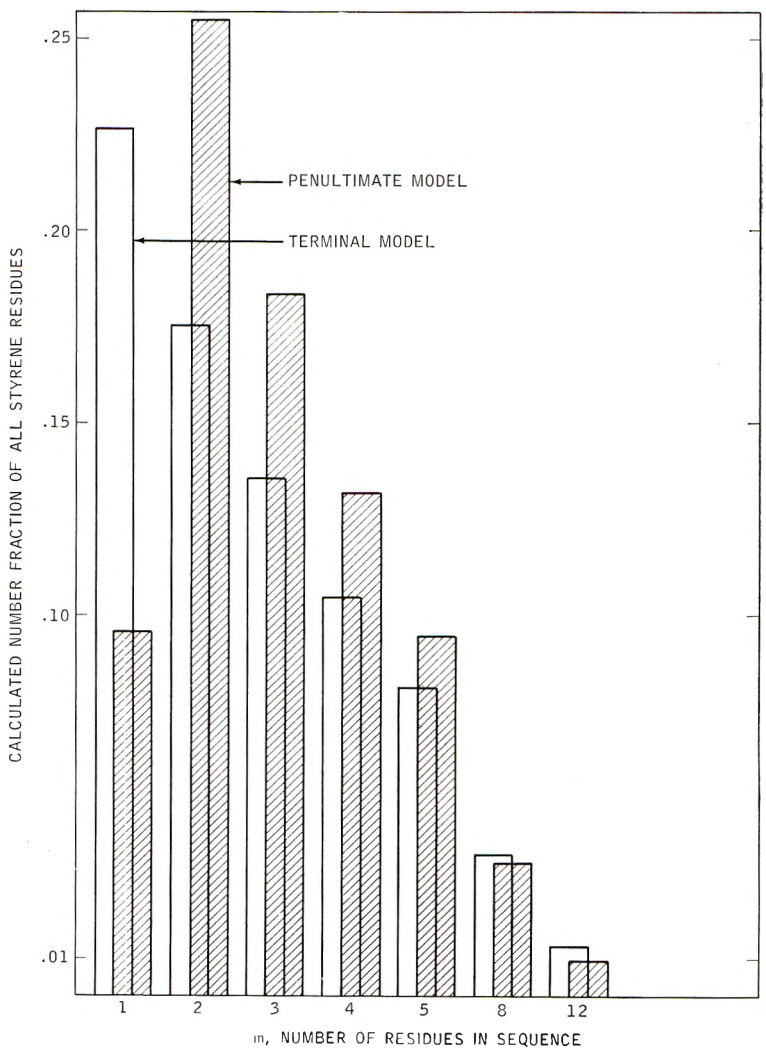

Fig. 2. Number distribution of styrene residues: styrene–maleic anhydride copolymer. Calculated from terminal and penultimate models. $X = 150$; $N = 4$.

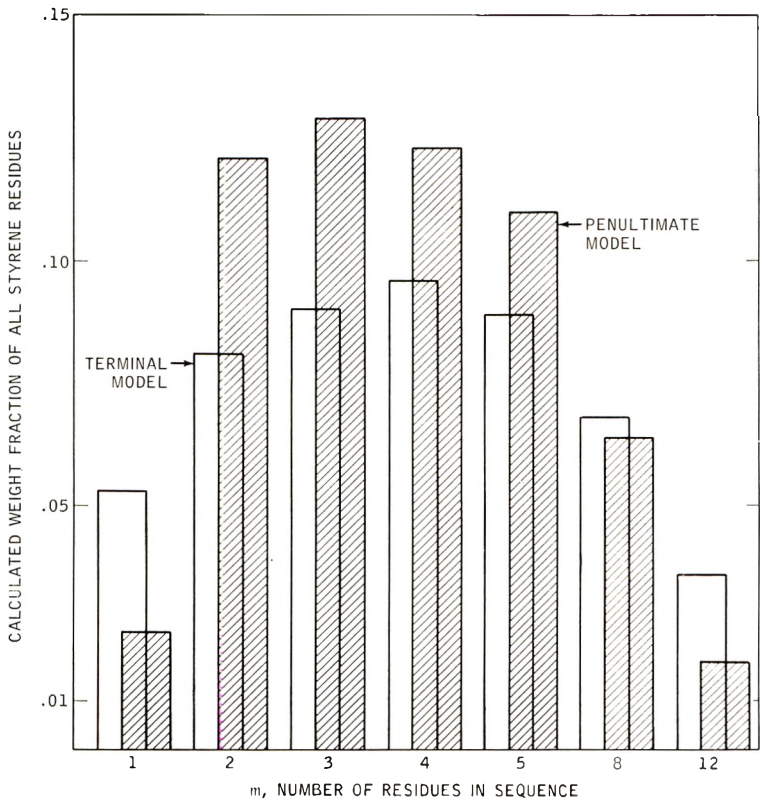

Fig. 3. Weight distribution of styrene residues: styrene–maleic anhydride copolymer. Calculated from terminal and penultimate models. $X = 150$; $N = 4$.

the number and weight distribution of styrene units in the styrene-maleic anhydride copolymer prepared at a feed ratio X of 150 and in the styrene–citraconic anhydride copolymer prepared at a feed ratio X of 3. The results are shown in Figures 2–5. These copolymers have quite different relative compositions; for the first, the found ratio of styrene residues to the comonomer was 4/1, for the second 1.76/1. While the differences in copolymer compositions predicted by the different models for these two cases is only 2.5 and 4.5%, respectively (Table II), the differences in comonomer sequence length predictions is quite large. It would appear that such distribution data should permit a selection between the terminal and penultimate mechanism.

It is important to recognize that we believe the penultimate model to be a valuable concept among the theories of polymerization mechanisms. Its power in understanding the factors influencing stereoregularity in polymers has recently been demonstrated.[6] What we suggest is that until data are available on the distribution of monomer units in copolymers, the final selection of terminal or penultimate copolymerization models for most comonomer systems cannot be made.

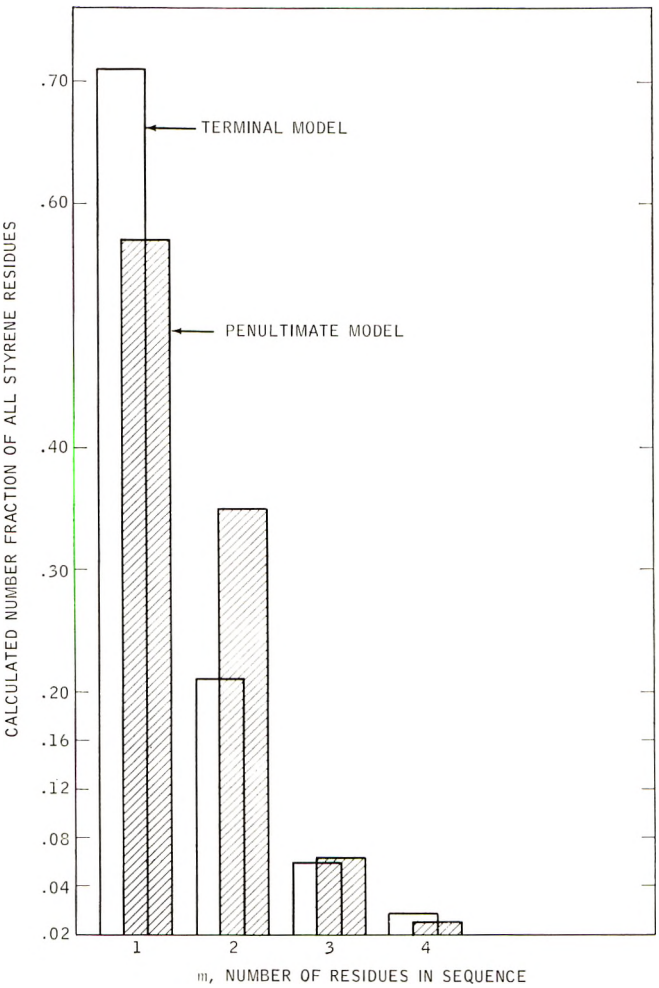

Fig. 4. Number distribution of styrene residues: styrene–citraconic anhydride copolymers. Calculated from terminal and penultimate models. $X = 3$; $N = 1.76$.

APPENDIX

These relationships are taken from Miller and Nielsen,[6] expressed in the notation used in this paper. They are also generally described by Price.[7]

We define $X = M_1/M_2$, molar ratio of monomer 1 to monomer 2 in feed; $N = N_1/N_2$, molar ratio of residue from monomer 1 to residue from monomer 2 in copolymer.

Probabilities

Penultimate Model. Probabilities for the penultimate model are as follows.

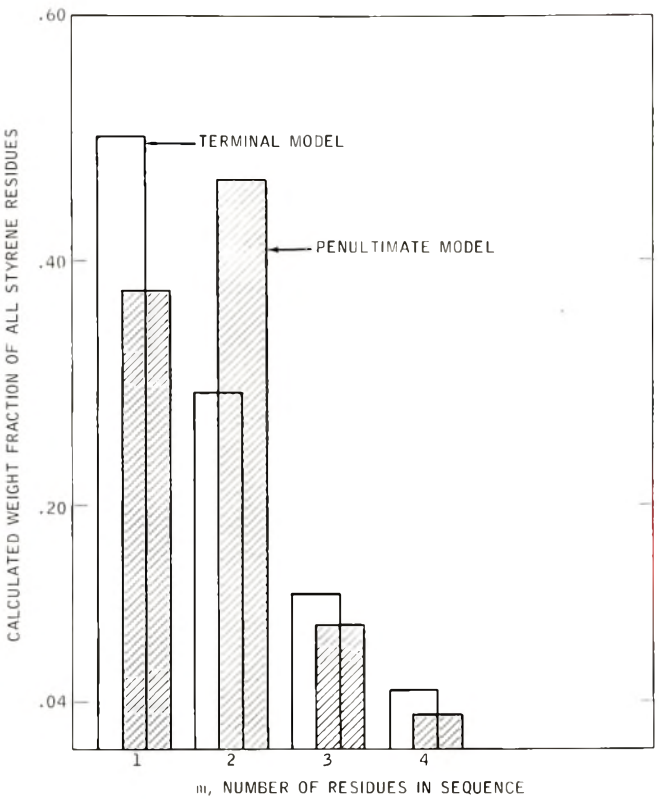

Fig. 5. Weight distribution of styrene residues: styrene–citraconic anhydride copolymer. Calculated from terminal and penultimate models. $X = 3$; $N = 1.76$.

That a chain ending in 11 will add a 1 monomer:

$$P_{111} = \frac{r_1 X}{r_1 X + 1}$$

That a chain ending in 11 will add 2 monomer:

$$P_{112} = \frac{1}{r_1 X + 1}$$

That a chain ending in 21 will add 1 monomer:

$$P_{211} = \frac{r_1' X}{1 + r_1' X}$$

That a chain ending in 21 will add 2 monomer:

$$P_{212} = \frac{1}{1 + r_1' X}$$

That a chain ending in 22 will add 2 monomer:

$$P_{222} = \frac{r_2}{X + r_2}$$

That a chain ending in 22 will add 1 monomer:

$$P_{221} = \frac{X}{X + r_2}$$

That a chain ending in 12 will add 2 monomer:

$$P_{122} = \frac{r_2'}{X + r_2'}$$

That a chain ending in 12 will add 1 monomer:

$$P_{121} = \frac{X}{X + r_2'}$$

Terminal Model. Probabilities for the terminal model are as follows. That a chain ending in 1 will add a 1 monomer:

$$P_{11} = \frac{(r_1)X}{1 + (r_1)X}$$

That a chain ending in 1 will add a 2 monomer:

$$P_{12} = \frac{1}{1 + (r_1)X}$$

That a chain ending in 2 will add a 2 monomer:

$$P_{22} = \frac{(r_2)}{X + (r_2)}$$

That a chain ending in 2 will add a 1 monomer:

$$P_{21} = \frac{X}{X + (r_2)}$$

Sequence Length of Monomer Residues in Copolymer. This is the probability that a sequence of 1 monomer residues contains m units.

Number Fraction—Penultimate Model. This is:

$$W_n(m) = P_{211}P_{112}P_{111}^{m-2} \qquad m > 1$$

and

$$W_n(1) = P_{212} \qquad m = 1$$

Weight Fraction—Penultimate Model. This is:

$$W_w(m) = \frac{mP^2_{112}P_{211}P_{111}^{m-2}}{P_{112} + P_{211}} \qquad m > 1$$

and

$$W_w(1) = \frac{P_{112}P_{212}}{P_{112} + P_{211}} \qquad m = 1$$

Number Fraction—Terminal Model. This is:

$$W_n'(m) = P_{11}^{m-1}P_{12}$$

Weight Fraction—Terminal Model. This is:

$$W_w' = mP_{12}^2P_{11}^{m-1}$$

References

1. For a general reference see T. Alfrey, Jr., J. J. Bohrer, and H. Mark, *Copolymerization*, Interscience, New York, 1952, Chap. 2.
2. Merz, E., T. Alfrey, and G. Goldfinger, *J. Polymer Sci.*, **1**, 75 (1946).
3. Barb, W. G., *J. Polymer Sci.*, **11**, 117 (1953).
4. Ham, G. E., *J. Polymer Sci.*, **14**, 87 (1954).
5. Chapin, E. C., G. E. Ham, and C. L. Mills, *J. Polymer Sci.*, **4**, 597 (1949).
6. Miller, R. L., *J. Polymer Sci.*, **57**, 975 (1952); R. L. Miller and L. E. Nielsen, *ibid.*, **46**, 303 (1960); R. A. Bovey and G. V. D. Tiers, *ibid.*, **44**, 173 (1960); R. A. Bovey, *ibid.*, **46**, 59 (1960).
7. Price, F. P., *J. Chem. Phys.*, **36**, 209 (1962).

Résumé

Une étude des mécanismes usuels de copolymérisation, le mécanisme terminal et le mécanisme pénultième, démontre que, pour beaucoup de paires de comonomères, les données de la composition des copolymères ne permettent pas de choisir un des deux mécanismes. On peut calculer les rapports des réactivités basés sur un mécanisme de copolymérisation à partir des rapports des réactivités de l'autre mécanisme. La composition des copolymères, prévue selon les deux mécanismes sera en accord avec les données expérimentales, dans les limites de précision des méthodes employées couramment pour l'analyse des copolymères. Cela est prouvé par des cas hypothétiques et des exemples de la littérature. Les systèmes de comonomères, trouvées dans la littérature sont l'alpha-méthylstyrène-acrylonitrile, styrène-anhydride maléique, et anhydride citraconique-acrylonitrile. Par contre, la structure des polymères, prévue par les deux mécanismes, diffère nettement dans les détails. En particulier, les prévisions des séquences de monomères dans le copolymère diffèrent pour le mécanisme terminal et le mécanisme pénultième. Il nous semble qu'il sera nécessaire de développer des méthodes expérimentales pour la détermination des séquences de comonomères, avant que l'on puisse aisément et définitivement distinguer les deux mécanismes, terminal et pénultième, pour un système donné.

Zusammenfassung

Eine Überprüfung der bekannten Copolymerisationsmechanismen mit Einfluss der Endgruppe und der vorletzten Gruppe zeigt, dass für eine grosse Zahl von Comonomerpaaren die Copolymer-Zusammensetzungsdaten zur Bevorzugung eines der beiden Modelle nicht ausreichen. Die auf dem einen Copolymerisationsmodell beruhenden Reaktivitätsverhältnisse können aus den Reaktivitätsverhältnissen des anderen Modells abgeleitet werden. Die nach beiden Modellen zu erwartende Copolymerzusammensetzung stimmt innerhalb der Genauigkeit der üblichen Methoden der Copolymeranalyse mit den Versuchsdaten überein. Angenommene Fälle und Literaturbeispiele zeigen

alle dieses Verhalten. Die aus der Literatur entnommenen Systeme waren α-Methylstyrol-Acrylnitril und Styrol mit Maleinsäureanhydrid, Citraconsäureanhydrid und Acrylnitril. Die nach den beiden Mechanismen zu erwartende Polymerstruktur unterscheidet sich aber in den Einzelheiten beträchtlich. Besonders unterscheiden sich die nach dem Endgruppen- und dem Vorletzten-Gruppen-Mechanismus zu erwartenden Monomersequenzanordnungen. Es scheint, dass die Entwicklung von Versuchsmethoden zur Bestimmung der Comonomersequenzanordnung notwendig ist, bevor leicht und endgültig zwischen dem Mechanismus mit Endgruppenwirkung und demjenigen mit Einfluss der vorletzten Gruppe in einem bestimmten Fall unterschieden werden kann.

Received July 11, 1962
Revised March 14, 1963

JOURNAL OF POLYMER SCIENCE: PART A VOL. 2, PP. 1699–1711 (1964)

Radiolysis of Polyisobutene. Part I. Yields of Fractures, Double Bonds, and Gas

D. T. TURNER,* *Camille Dreyfus Laboratory, Research Triangle Institute, Durham, North Carolina*

Synopsis

Purified polyisobutene with approximately a random molecular weight distribution and a number-average molecular weight of 3.5×10^5 was irradiated *in vacuo* at about 25°C. with 4 M.e.v. electrons. The degradation of the polymer was studied by osmometry and viscometry and the G (fracture) value determined as 4.1. The G value for total unsaturation was determined as 5.3 by a chemical method suitable for olefins branched in the vicinity of the double bond. Little or no internal unsaturation was detected by ozonolysis of the irradiated polymer. Hydrogen and methane were formed with G values of 1.3–1.6 and 0.8–0.5, respectively. At doses greater than about 10 Mrad all the above G values decreased. The G value for isobutene formation (≤ 0.1) remained approximately constant up to a dose of at least 150 Mrad. On lowering the temperature of irradiation to −196°C. the yield of fractures was markedly decreased while the yield of hydrogen plus methane was scarcely affected. This is interpreted as evidence that the degradation reaction is due predominantly to the direct fracture of carbon–carbon bonds rather than to any reaction associated with gas formation. The observed ratio of double bonds to fractures is shown to be consistent with this interpretation.

The radiolysis of polyisobutene has been studied previously in some detail by Alexander, Black, and Charlesby.[1] These authors determined yields of fractures and double bonds and qualitatively investigated the formation of gas which they found to comprise mostly hydrogen and methane. They proposed a mechanism of polymer degradation according to which a carbon–carbon bond is directly fractured on irradiation with the formation of one double bond. Actually they reported experimentally that 1.87 double bonds were formed per fracture but attributed the excess unsaturation to an unspecified side reaction involving the formation of hydrogen and methane. Another mechanism was proposed at about the same time by Wall[2] according to which both hydrogen formation and polymer degradation resulted from the primary fracture of carbon–hydrogen bonds. Subsequent to the tentative conclusion of Alexander et al. that about one molecule of methane was evolved per random fracture of the polymer molecule, Chapiro[3] and Shultz[4] proposed different mechanisms in which polymer degradation was associated with the formation of methane.

* Post-Doctoral Fellow on leave from The Natural Rubber Producers' Research Association, Welwyn Garden City, Herts, England.

The present work was undertaken as an attempt to distinguish between the rival suggestions that polymer degradation is due to the direct fracture of the main chain of carbon atoms or by some reaction associated with gas formation. The interpretation of the experimental data should be simpler than of that previously reported insofar as the polymer was purified, characterized, and irradiated *in vacuo*. Determinations are provided of yields of gas as well as of fractures and double bonds.

EXPERIMENTAL

A sample of high molecular weight polyisobutene was obtained from Polymer Consultants Ltd. A lower molecular weight polymer which was used only in ozonolysis experiments was prepared from isobutene.[5] Both polymers were purified by three precipitations from petroleum ether (b.p 40–60°C.) with methanol. The higher molecular weight polymer was additionally thinly sheeted on a mill and extracted with acetone at ca. 60°C. for 24 hr. under nitrogen. The polymers were rigorously degassed and stored *in vacuo* for several weeks before use.

All solvents were of analytical reagent grade.

Preparation of Samples

Polymer was weighed into breakseal tubes of glass (diameter 0.8 cm., wall thickness 0.1 cm.) or silica (diameter 0.6 cm., wall thickness 0.1 cm.). The polymer was thoroughly degassed and the tubes sealed at $<10^{-4}$ mm. Hg pressure.

Irradiation of Samples

The irradiation (supervised by Mr. J. McCann) was carried out at Wantage Radiation Laboratory. The tubes were exposed to the electron beam from a 4 m.e.v. linear accelerator. The pulses of electrons from the accelerator were 2.5 μsec. wide and were emitted at a rate of 600 pulses/sec.

The temperature of irradiation was controlled by spraying the tubes with water. Temperatures near −196 and −80°C. were approached by irradiating silica tubes in close fitting thin walled tubes of polyethylene through which flowed liquid nitrogen or acetone precooled with solid carbon dioxide.

Dosimetry measurements were made with a water calorimeter and checked at low doses (<5 Mrad) by estimation of the yield of hydrogen from cyclohexane [$G(H_2) = 5.3$].[6] Doses of 10 Mrad or less were administered at a mean dose rate of 1 Mrad/min. and higher doses at rates ranging from 1 to 5 Mrad/min., as convenient.

Tubes were opened three or more days after irradiation.

G values were calculated from eq. (1) in which n is the number of moles of product per gram of polymer and R the dose in Mrad.

$$G \text{ (specified product)} = 9.6\, nR^{-1} \times 10^5 \qquad (1)$$

Polymer Characterization

The flow times of solutions of the polymer were measured in Ubbelohde viscometers at 25°C. The kinetic energy correction of flow was less than 1% and was neglected. A linear extrapolation of three viscosity numbers to zero concentration gave the limiting viscosity number in milliliters per gram.

Number-average molecular weights were determined with benzene solutions of the polymer at 25°C. in Zimm-Meyerson osmometers with Ultracellafilter "feinst" grade membranes. (The characterization of polymer was supervised by Miss M. A. Place.)

Total Unsaturation

To aliquots from a solution of polymer in carbon tetrachloride were added varying amounts of iodine monochloride in the same solvent. The iodometric titer of each solution was determined after 1 hr. in the dark.[7,8]

Ozonolysis of Polymer

In ozonolysis of polymer,[9] polymer (2.5 g.) was dissolved in a mixture of carbon tetrachloride (100 ml.), methanol (15 ml.), and di-*n*-butyl monosulfide (1 ml.). The solution was stirred at −20°C. while ozone was passed in. Aliquots (10 ml.) were withdrawn periodically and $[\eta]$ determined after further dilution with carbon tetrachloride.

Gas Analysis

Preliminary examinations of the gas volatile at room temperature were made by gas–solid chromatography (Dr. R. W. Hummel, Wantage Research Laboratories).

The gaseous products, volatile at various temperatures, were compressed into a known volume with a Töpler pump and the pressure measured with a silicone oil manometer.[10] The yield of gas was calculated from the pressure and temperature.

The gas volatile at −196°C. was rigorously removed from the polymer and the proportions of hydrogen and methane estimated by thermal conductivity measurements[11,12] and reference to pure hydrogen and methane and to known mixtures.

RESULTS AND DISCUSSION

Yield of Fractures

The number of moles of fractures per gram of polyisobutene F was calculated from eq. (2), in which M_0 and M_n are, respectively, the number-average molecular weights before and after irradiation.

$$F = M_n^{-1} - M_0^{-1} \tag{2}$$

After very low doses number-average molecular weights were determined directly by osmometry and gave a $G(F)$ value of 4.1 (Table I). After higher doses the molecular weight of the polymer was too low for reliable osmometry measurements.

TABLE I
$G(F)$ Values Determined by Osmometry

Dose, Mrad	Molecular weight $\times 10^{-5}$	$G(F)$
0	3.52	—
0.65	1.78	4.1
1.5	1.08	4.1

The degradation of the polymer was followed down to much lower molecular weights by solution viscosity measurements. Viscosity-average molecular weights M_v were calculated from relationships (3) and (4) based on data reported by Fox and Flory[13] for narrow fractions of polyisobutene. Number-average molecular weights were calculated from eq. (5) on the assumption that the polymers have a random molecular weight distribution.[1,14]

$$[\eta]_{25°C.} = 2.9 \times 10^{-4} M^{0.68} \quad \text{(carbon tetrachloride)} \tag{3}$$

$$[\eta]_{25°C.} = 2.15 \times 10^{-4} M^{0.67} \quad \text{(toluene)} \tag{4}$$

$$M_v/M_n = 1.85 \tag{5}$$

In fact, polyisobutenes sometimes do approximate to a random molecular weight distribution and direct justification for the use of eq. (5) for the polymer used in this work is provided by the closeness of experimentally determined ratios of M_v/M_n to 1.85 (Table II). The fact that viscosity measurements give an almost identical $G(F)$ value to osmometry measurements is probably fortuitous but suggests that such measurements may be used to provide approximate estimates of fractures up to about 10 Mrad (Table III). At higher doses, however, the $G(F)$ value decreases, and estimates are not necessarily quantitatively correct as the molecular weight distribution of the polymer might eventually change on irradiation.

The $G(F)$ value as determined by osmometry would be the resultant of chain fracture and any crosslinking. However, as other work[5] indicates

TABLE II
Relationships between M_v and M_n for Initial Polymer[a]

Solvent	$M_v \times 10^{-5}$	M_v/M_n
Toluene	6.22	1.76
Carbon tetrachloride	6.82	1.94

[a] Osmotic molecular weight $M_n = 3.52 \times 10^5$.

TABLE III
Effect of Dose on Yields of Fractures and Gas[a]

Dose, Mrad	$G(F)$	G(gas)
5	4.0	2.1
7	4.1	2.1
10	4.0	2.0
30	3.5	1.9$_5$
40	2.9	1.8

[a] Fractures determined from $[\eta]$ in toluene.

that virtually no crosslinking occurs in polyisobutene at low doses, the value of 4.1 may be taken as applying to simple fracture alone.

Other $G(F)$ values of 5.0,[1] 1.5,[15,16] and 1.5–2.8[16] have been reported previously for polyisobutene. These were all calculated from solution viscosity measurements of polymers irradiated at about 20°C. On this basis similarly diverse results have also been obtained in these laboratories with different samples of polyisobutene and it would appear that the method is not generally reliable in cases where the molecular weight distribution is not known.

Yields of fractures calculated from viscosity measurements over a much more extended dose range are shown in Figure 1. The rate of fracture apparently decreases with increasing dose until it eventually attains a limiting value which approximately applies up to the highest value investigated of 150 Mrad. These results, although they are based on similar measurements and calculations, do not agree with the general conclusion of

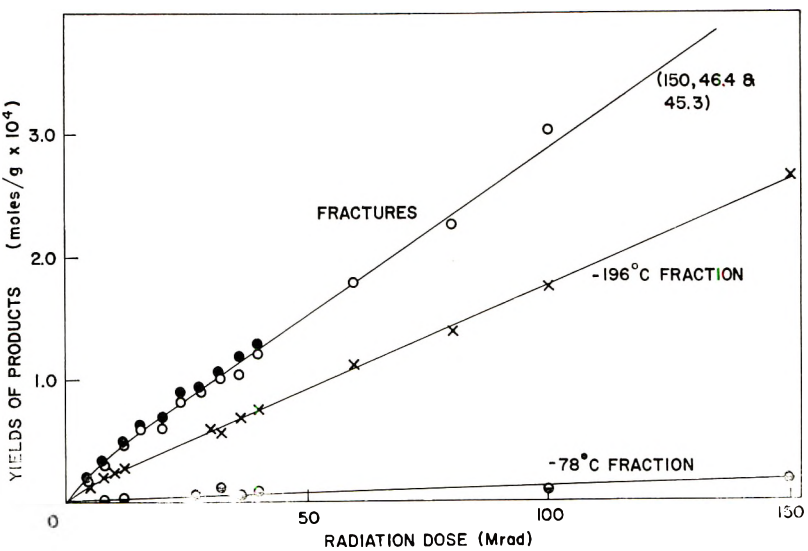

Fig. 1. Effect of dose on yields of products: (●) calculated from viscosities in toluene; (○) calculated from viscosities in carbon tetrachloride.

Alexander et al. that the yield of fractures is simply proportional to the dose R. Examination of the plots of log M_v^{-1} against log R presented by these workers reveals that although their conclusion may be justified by data reported for Co^{60} and pile radiation it is not supported by their more limited results with 4 M.e.v. electrons which instead follow a trend similar to the present results.

Yield of Double Bonds

The method used to determine unsaturation was developed by Lee, Kolthoff, and Johnson[7,8] for olefins branched in the vicinity of the double bond and has been used successfully with 2,4,4-trimethylpent-1-ene which contains the predominant unsaturated group found in irradiated polyisobutene. As the method has, furthermore, been developed for high molecular weight copolymers of isobutene with a small amount of diolefin, it is admirably suited to the present purpose. The typical results for an irradiated polyisobutene in Figure 2 indicate how the concentration of double bonds is defined by the intersection of two branches which has been shown to correspond to theoretical values in olefins of known structure. In this one experiment the irradiated polymer was heated *in vacuo* for 72 hrs. at 50°C. before examination to ensure that all the unsaturation detected was combined in the polymer. As the very small volatile fraction had a negligible iodometric titer this precaution was unnecessary in samples given smaller doses (<100 Mrad).

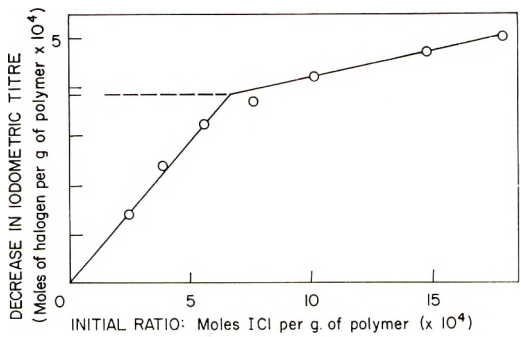

Fig. 2. Determination of unsaturation from decrease in iodometric titer. Dose: 100 Mrad.

The G values for double bond formation after various doses shown in Table IV are very different from the value of 9.4 reported by Alexander et al. Probably a more appropriate form of comparison is of the ratio of the yield of double bonds to fractures which was obtained using the same stock solution of the polymer in carbon tetrachloride. Table IV shows that up to about 10 Mrad the ratio is about 1.35, but that at higher doses it decreases (1.1 at 150 Mrad). The value of 1.87 reported by Alexander et al. is believed to be too high because their method of de-

TABLE IV
Effect of Dose on Yields of Double Bonds

Dose, Mrad	G (C=C)[a]	C=C/F
4	5.4	1.35
6	5.3	1.37
8	5.3	1.33
10	5.2	1.36
60	4.1	1.28
100	3.6	1.2
150	3.0	1.1

[a] Allowance made for initial unsaturation of polymer (0.08×10^{-4} mole/g.).

termining unsaturation usually gives overestimates when applied to olefin branched in the vicinity of the double bond.

Rehner[17] has shown that when copolymers of isobutene and small proportions of diolefin are ozonized the internal double bonds are cleaved and may therefore be estimated by the decrease in molecular weight of the polymer. This procedure was adopted to detect any internal unsaturation in irradiated polyisobutene and ethanol was included as a polar additive to expedite cleavage. Moreover, as Rehner had found that polyisobutene is itself degraded by ozone, although at a slower rate than the copolymer, di-*n*-butyl monosulfide was included as a buffer. This additive was chosen because in studies of graft polymers it has been found not to interfere with the ozonolysis of polyisoprene yet to prevent degradation of polymethyl methacrylate.[9]

Figure 3 shows how di-*n*-butyl monosulfide protected an unirradiated polyisobutene from ozonolytic degradation up to the time calculated for its consumption by ozone. As the irradiated polymer was not rapidly degraded on introduction of ozone it is concluded that G (internal unsaturation) is probably very small and certainly less than 0.3.

Yields of Gas

The total gas volatile at ca. 25°C. produced at doses ranging from 100 to 200 Mrad was examined by gas–solid chromatography and found to comprise mostly hydrogen and methane in the ratio of about 2 to 1 with much smaller amounts of isobutene and even smaller amounts of ethane. These results agree qualitatively with the mass spectrometer data of Alexander et al. except that these latter workers found no evidence at all for the formation of ethane.

A G value of 0.74 for the total gas from polyisobutene after a dose of about 100 Mrad has been reported by Karpov.[15] This is much lower than the value of 1.8 calculated for the same dose from Figure 1. Karpov's G values for gas formation from other polymers are also usually lower than those generally reported.

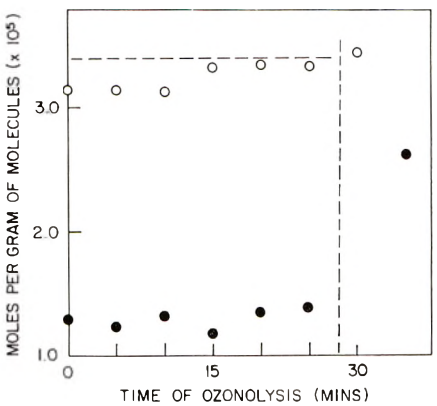

Fig. 3. Ozonolysis of polyisobutene in presence of di-*n*-butyl monosulfide: (●) Unirradiated low molecular weight polymer; (○) irradiated polymer (8 Mrad). Vertical broken line indicates the protection time calculated before the consumption of di-*n*-butyl monosulfide. Horizontal broken line indicates increase in number of molecules corresponding to G (internal unsaturation) = 0.3.

The fraction of gas from the irradiated polymer which is volatile at −196°C. evidently comprises hydrogen and methane. The rate of formation of this fraction decreases up to a dose of about 40 Mrad and then remains approximately constant up to about 150 Mrad (Fig. 1). The decline in rate is shown more precisely by the G values in Table III, which decrease from an initial value of 2.1 to 1.8 at 40 Mrad. A decline in the rate of formation of hydrogen with increasing dose has been reported previously in the radiolysis of various saturated hydrocarbons and has been attributed to the scavenging of hydrogen atoms by double bonds.[18] Comparison of the decreasing G values for gas and double bonds with increasing dose in Tables III and IV suggests a similar scavenging of radical gas precursors in the present system. However, it is unusual that the decline apparently does not persist beyond doses of about 40 Mrad.

The proportion of hydrogen in the −196°C. fraction formed by a dose of 40 Mrad was determined by thermal conductivity measurements as 72%. As the method was not suitable for very small quantities of gas it could not be used satisfactorily after smaller doses. Therefore, the initial composition of the gas is in doubt according to the composition of the 14% of gas which is presumed to be scavenged by double bonds. Accepting limits imposed by the possibility that all the scavenged gas may be either hydrogen or methane the composition of the initial gas is compared in Table V with yields reported for the radiolysis of other hydrocarbons.[19] Evidently, the general effect of a methyl group is to decrease the overall yield of gas and increase the yield of methane.

After removal of the gas volatile at −196°C. the polymer was maintained at −78°C. and a further rather sluggish fraction pumped off. This evidently comprised mostly isobutene (b.p. −7°C.) as only negligible amounts of gas could subsequently be pumped off from the polymer at

TABLE V
Gaseous Yields on Radiolysis of Hydrocarbons

Hydrocarbon	*G* values		
	H_2	CH_4	$H_2 + CH_4$
n-Hexane[a]	5.0	0.2	5.2
2,2,4-Trimethylpentane[a]	3.0	0.7	3.7
2,2-Dimethylbutane[a]	2.0	1.2	3.2
Polyisobutene	1.6–1.3	0.5–0.8	2.1

[a] Data of Dewhurst.[19]

room temperature. The amount of gas formed was proportional to the dose [G (-78°C. fraction) $\sim$ 0.1] up to at least 150 Mrad (Fig. 1). By contrast, Alexander et al. reported that the ratio of isobutene to hydrogen and to methane rose rapidly with increasing radiation dose. However, their results covered a higher dose range of about 50–500 Mrad and were obtained at a temperature of 70°C. in an atomic pile.

Alexander et al. interpreted their data on isobutene formation as consistent with a mechanism of double random fracture of the main chain of carbon atoms of the polymer, a reaction which would depend on the square of the radiation dose. By contrast, the present results must be explained by invoking a reaction which stems from a single absorption of energy. A possibility is the formation of a polymer radical which then eliminates isobutene [eq. (6)].[20]

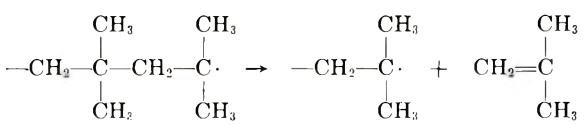

(6)

The energy for this reaction might be carried over by the polymer radical during its formation or alternatively a spontaneous depolymerization chain reaction could occur if the polymer is above its "ceiling" temperature.[21]

Influence of Temperature on Yields of Fractures and Gas

Tubes were removed from the heating or cooling liquid immediately after irradiation. Those which had been irradiated in liquid nitrogen emitted a blue glow which made immediate inspection of the contents difficult, but later it could be seen that the polymer had acquired an intense violet-black coloration which disappeared within about 2 min.

The yield of fractures determined from viscosity measurements in toluene is given in Figure 4 in the form of moles per gram per megarad to allow a comparison with results calculated from data of Alexander et al. The two sets of results agree that there is apparently a linear relationship between the rate of fracture and temperature of irradiation in the range 77–290°K. This unusual temperature dependence has also been noted in the radiation damage of certain biological systems but remains unexplained. Above

300°K. the results of Alexander et al. indicate a marked increase in the rate of fracture which was not observed in the present experiments up to 360°K. A rapid increase in the rate of fracture might be expected at high temperatures because of the known formation of free radicals on irradiation and hence the possibility of a degradative chain reaction but its onset might be sensitive to the difference in reaction conditions in the two sets of experiments.

Although the temperature of irradiation has such a drastic influence on the yield of fractures it has little influence of the yield of gas volatile at −196°C. Similarly, it has been reported that lowering the temperature of irradiation reduces the yield of crosslinks in polyethylene[22] and, possibly, in a polyisoprene,[23] while the yield of gas is virtually unaffected although for the former polymer there is additionally a conflicting report that the yield of gas also decreases.[24]

Polymer Degradation

The observation that on lowering the temperature of irradiation the solution viscosity is markedly reduced while the yield of gas is scarcely affected indicates that the predominant mode of polymer degradation is by direct fracture of the main chain of carbon atoms [eq. (7)].

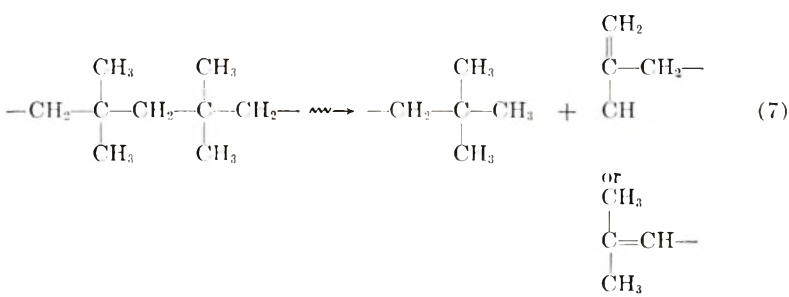

(7)

This reaction would account for double bonds up to a G value equal to the yield of fractures, 4.1, and therefore the higher value observed, 5.3, together with the indications that double bonds are located at the ends of molecules, suggests the occurrence of additional minor fracture reactions associated with gas formation. A likely reaction scheme of this type, which would be expected to yield a ratio of double bonds to fractures in excess of unity, stems from the cleavage[25] of CH_3 or H, both of which are represented by A in the schematic reaction (8). The resulting type of reaction scheme (8–10) has been suggested by Wall,[2] who has offered good reasons for supposing that the sterically strained polymer radicals from polyisobutene would undergo β-bond scission [eq. (10)]. The occurrence of these reactions would provide a ready explanation of the observed decrease in the rates of formation of gas, double bonds, and fractures by postulating that A· is scavenged by double bonds (Fig. 1).

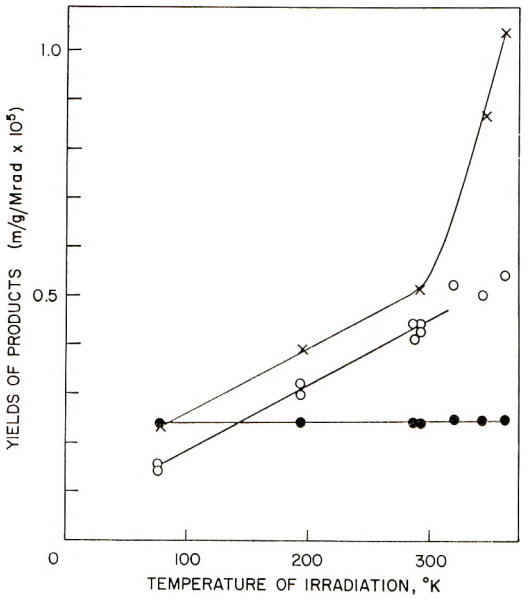

Fig. 4. Influence of temperature on yields of fractures and gas: (×) yields of fractures calculated from Table 2 of the paper by Alexander et al. for Co^{60} γ-irradiation; (O) yields of fractures (6–12 Mrad); (●) yields of gas volatile at −196°C. (6–14 Mrad).

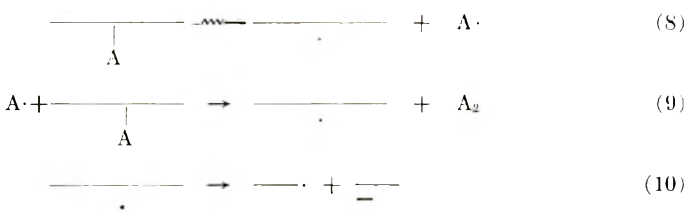

(8)

(9)

(10)

From the above considerations it seems unlikely that all the gas can be associated with the fracture reactions. In addition, reference to the simple stoichiometric relationship [eq. (11)] suggests that some of the gas is not

$$\underset{4.1}{G\ (F)} + \underset{2.1}{G\ (\text{Gas})} = \underset{5.3}{G\ (\text{C—C})}$$

associated with double bond formation. By default, it is possible that some gas is associated with the linking of carbon atoms and, as G (cross-links) <0.2,[5] to the formation of intramolecular cyclic structures. This possibility appears reasonable on examination of molecular models.

This work was begun in the laboratories of The Natural Rubber Producers' Research Association. Irradiation facilities were provided by the Technological Irradiation Group at Wantage Research Laboratories (A.E.R.E.) with the kind cooperation of Dr. R. Roberts and his colleagues. Mr. G. T. Jones is thanked for help with the experiments.

References

1. Alexander, P., and R. M. Black, and A. Charlesby, *Proc. Roy. Soc. (London)*, **A232,** 31 (1955).
2. Wall, L. A., *J. Polymer Sci.*, **17,** 306 (1955).
3. Chapiro, A., *J. Chim. Phys.*, **53,** 306 (1956).
4. Shultz, A. R., *J. Polymer Sci.*, **35,** 369 (1959).
5. Turner, D. T., unpublished work.
6. Shuler, R. H., and A. O. Allen, *J. Am. Chem. Soc.*, **77,** 5 (1955).
7. Lee, T. S., I. M. Kolthoff, and M. A. Mains, *J. Polymer Sci.*, **3,** 66 (1948).
8. Lee, T. S., I. M. Kolthoff, and E. Johnson, *Anal. Chem.*, **22,** 995 (1950).
9. Barnard, D., *J. Polymer Sci.*, **22,** 213 (1956).
10. Moore, C. G., and W. F. Watson, *J. Polymer Sci.*, **19,** 237 (1956).
11. Campbell, N. R., *Proc. Phys. Soc.*, **33,** 287 (1921).
12. Farkas, A., and H. W. Melville, *Experimental Methods in Gas Reactions*, London, 1939, p. 79.
13. Fox, T. G, and P. J. Flory, *J. Phys. Colloid Chem.*, **53,** 197 (1949).
14. Flory, P. J., *Principles of Polymer Chemistry*, Cornell Univ. Press, Ithaca, N. Y., 1953, p. 313.
15. Karpov, V. L., *Conf. Acad. Sci. USSR, Peaceful Uses At. Energy, Moscow, 1955, Sess. Div. Chem. Sci.*, **3,** 22 (1955).
16. Henglein, A., and C. Schneider, *Z. Physik. Chem. (Frankfurt)*, **19,** 367 (1959).
17. Rehner, J., Jr., *Ind. Eng. Chem.*, **36,** 118 (1944).
18. Hardwick, T. J., *J. Phys. Chem.*, **64,** 1623 (1960).
19. Dewhurst, H. A., *J. Am. Chem. Soc.*, **80,** 5607 (1958).
20. Madorsky, S. L., S. Straus, D. Thompson, and L. Williamson, *J. Polymer Sci.*, **4,** 639 (1949).
21. Dainton, F. S., and K. J. Ivin, *Trans. Faraday Soc.*, **46,** 331 (1950).
22. Charlesby, A., and W. H. T. Davison, *Chem. Ind. (London)*, **1957,** 232.
23. Turner, D. T., *Polymer*, **1,** 27 (1960).
24. Lawton, E. J., J. S. Balwit, and R. S. Powell, *J. Polymer Sci.*, **32,** 257 (1959).
25. Burton, M., *Actions Chimiques et Biologiques des Radiations*, Vol., Haissinsky Ed., 1958, p. 39.

Résumé

Du polyisobutène purifié, ayant une distribution des poids moléculaires à peu près statistique et un poids moléculaire moyen en nombre de 3.5×10^5, a été irradié sous vide à 25°C avec des électrons de 25 Mev. On a étudié la dégradation de ce polymère par osmométrie et par viscosimétrie et on a trouvé comme valeur de G (rupture) 4.1. Une méthode chimique appropriée pour les oléfines branchées au voisinage de la liaison double a permis de trouver pour G la valeur de 5.3 pour une insaturation totale. L'ozonolyse du polymère irradié n'a revèlé aucune ou presqu'aucune insaturation interne. L'hydrogène et le méthane étaient formés avec des valeurs de G de 1.3–1.6 et 0.8–0.5 respectivement. A des doses supérieures à 10 Mrad, toutes les valeurs de G diminuaient. La valeur de G pour la formation de l'isobutène (≤ 0.1) restait constante jusqu'à une dose d'au moins 150 Mrad. En abaissant la température d'irradiation à -196°C, la quantité de produits de rupture diminuait considérablement, tandis que la quantité d'hydrogène et de méthane était à peine influencée. On a interprête ceci comme preuve du fait que la dégradation est due principalement à la rupture directe des liaisons C—C, plutôt qu'à une réaction associée à la formation d'un gaz. On a démontré que le rapport observé entre les quantités de doubles liaisons et de produits de dégradation correspond avec cette interprétation.

Zusammenfassung

Gereinigtes Polyisobuten mit annähernd statistischer Molekulargewichtsverteilung und einem Molekulargewichtszahlenmittel von $3,5 \times 10^5$ wurde im Vakuum bei 25°C mit Elektronen von 4 MeV bestrahlt. Der Abbau des Polymeren wurde osmometrisch und viskosimetrisch untersucht und ein G-Wert (Spaltung) von 4,1 gefunden. Mit einer für Olefine mit zur Doppelbindung benachbarten Verzweigungen geeigneten chemischen Methode wurde der G-Wert für die Gesamtzahl der Doppelbindungen zu 5,3 bestimmt. Bei der Ozonolyse des bestrahlten Polymeren wurden nur geringe oder gas keine inneren Doppelbindungen gefunden. Die der Bildung von Wasserstoff und Methan entsprechenden G-Werte waren 1,3–1,6 bzw. 0,8–0,5. Bei grösseren Dosen als 10 Mrad trat ein Absinken aller angeführten G-Werte ein. Der G-Werte für die Isobutenbildung ($\leq 0,1$) blieb bis zu Dosen von mindestens 150 Mrad konstant. Wurde die Bestrahlungstemperatur auf −196°C erniedrigt, so sank die Spaltungsausbeute deutlich, während die Gesamtausbeute an Wasserstoff und Methan kaum beeinflusst wurde. Dies wird als Beweis dafür angesehen, dass der Abbau viel eher auf einer direkten Spaltung von Kohlenstoff-Kohlenstoff-Bindungen als auf einer unter Gasbildung verlaufenden Reaktion beruht. Das beobachtete Verhältnis Doppelbindungen:Spaltungen steht mit dieser Interpretation im Einklang.

Received March 4, 1963

JOURNAL OF POLYMER SCIENCE: PART A VOL. 2, PP. 1713–1719 (1964)

Radiolysis of Polyisobutene. Part II. Infrared and Ultraviolet Absorption Spectra

G. M. C. HIGGINS, *The Natural Rubber Producers' Research Association, Welwyn Garden City, Herts, England,* and D. T. TURNER, *Camille Dreyfus Laboratory, Research Triangle Institute, Durham, North Carolina*

Synopsis

Purified polyisobutene was irradiated *in vacuo* with 4 M.e.v. electrons and the changes in infrared and ultraviolet absorption recorded. $R_1R_2C{=}CH_2$ groups accounted for about 60% of the total unsaturation, and evidence could be adduced for the formation of $R_1R_2C{=}CHR_3$ groups. About one *tert*-butyl group was formed per double bond. Qualitative evidence was obtained for formation of the group $R_1{-}CH_2{-}CH_2{-}R_2$. Conjugated diene groups are formed proportional to the dose up to the maximum investigated of 1400 Mrad (G value about 0.1).

Changes produced in the infrared and ultraviolet spectra of polyisobutene on exposure to radiation from an atomic pile have been reported by Alexander, Black, and Charlesby.[1] Infrared spectroscopic data were interpreted as providing qualitative evidence for the formation of $R_1R_2C{=}CH_2$ groups. Ultraviolet data revealed the formation of a chromophore with an absorption maximum at 240–270 mμ, varying in a rather erratic manner with radiation dose. The yield of this chromophore was found to increase roughly linearly with dose.

In the present paper more extensive spectroscopic data are reported for a purified polyisobutene irradiated *in vacuo*.

EXPERIMENTAL RESULTS

A purified polyisobutene of number-average molecular weight 3.5×10^5 was carefully degassed and sealed *in vacuo* in tubes. The tubes were exposed with water cooling to a 4 M.e.v. beam of electrons from a linear accelerator at Wantage Radiation Laboratory. Mean dose rates ranged from 1 to 5 Mrad/min. Doses greater than 500 Mrad were built up in stages, the successive increments being administered after intervals of about two weeks.

More details concerning the above procedures have been given previously.[2]

Thin films of the polymer and solutions in analytical reagent carbon disulfide were examined with a Hilger H.800 double-beam spectrometer fitted

with a sodium chloride prism. Ultraviolet absorption spectra of the polymer in spectroscopically pure cyclohexane were measured with a Hilger Uvispec spectrophotometer.

2,2,4-Trimethylpent-1-ene (Phillips Petroleum Company) shown by gas-liquid chromatography to be 99% pure was used as a reference compound.

Figure 1 shows the infrared absorption of the polymer before and after the maximum dose investigated of 1400 Mrad. Figure 2 shows changes occurring in the region 1400–700 cm.$^{-1}$ as a function of radiation dose. The overall degradation of the polymer with increasing dose is reflected in the gradual decrease of various bands. Those at 1380 and 1358 cm.$^{-1}$ have

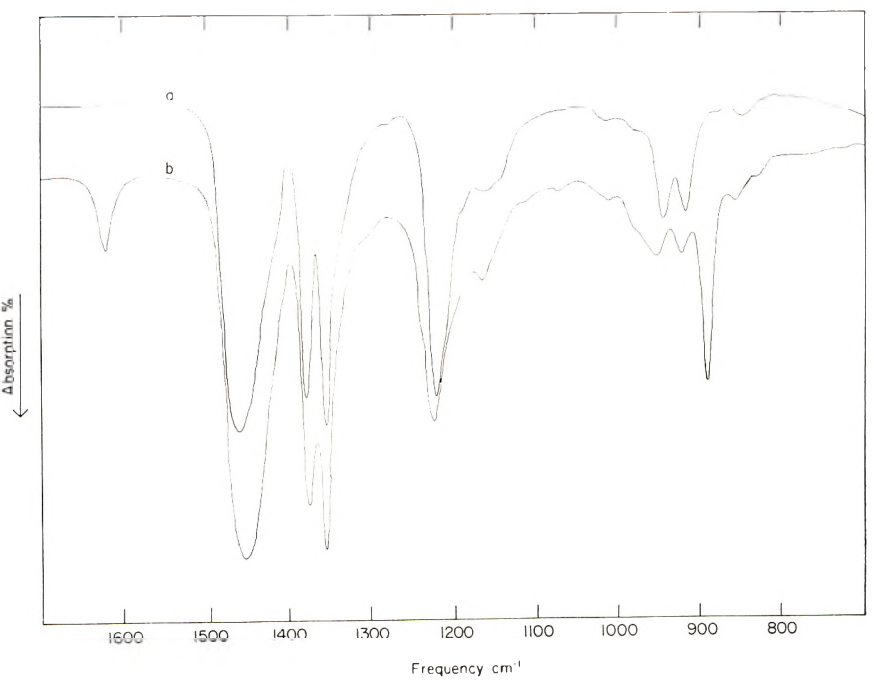

Fig. 1. Infrared absorption spectra of polyisobutylene (*a*) before and (*b*) after a dose of 1400 Mrad.

been assigned to the symmetrical deformation vibration of a pair of methyl groups on a single carbon atom and those at 1225, 950, and 925 cm.$^{-1}$ to vibrations of the distorted carbon tetrahedron.[3] The increased absorption at 899 cm.$^{-1}$ due to the out-of-plane deformation vibration of hydrogen atoms in the group $R_1R_2C{=}CH_2$[4] was used to determine this group quantitatively by reference to 2,2,4-trimethylpent-1-ene (Fig. 3).

Use of a differential spectroscopic technique in the region 1500–1350 cm.$^{-1}$, after a dose of 1400 Mrad, revealed that in addition to the expected decrease of absorption at 1485 cm.$^{-1}$ due to the bending frequency of polyisobutene methylene groups there was also increased absorption at 1450 cm.$^{-1}$.

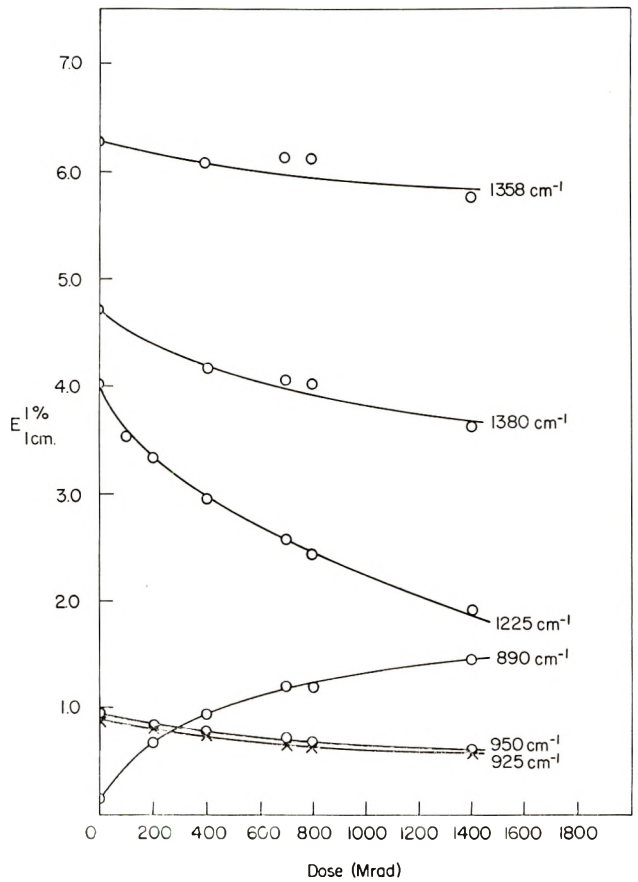

Fig. 2. Change of intensity of absorption bands with dose.

DISCUSSION

Infrared Absorption

The $R_1R_2C{=}CH_2$ group accounts for only about 60% of the total unsaturation as previously determined, by addition of iodine monochloride,[2] up to a dose of 150 Mrad (Fig. 3). As experiments at low doses (<10 Mrad) indicate that little or no internal unsaturation is formed on irradiation of polyisobutene,[2] this unaccounted unsaturation may be largely assigned to terminal groups of the type $RHC{=}C(CH_3)_2$. On account of their intrinsically weak absorption such groups would be difficult to detect in low concentration, although there is a very weak band[4] at approximately 820 cm.$^{-1}$ which is consistent with their formation (Fig. 1). The predominant mechanism of polymer degradation by the direct fracture of the main chain of carbon atoms[2] may therefore be represented by reactions (1) and (2). Additionally, there would probably be a smaller contribution to these unsaturated groups as a result of the β-bond scission of

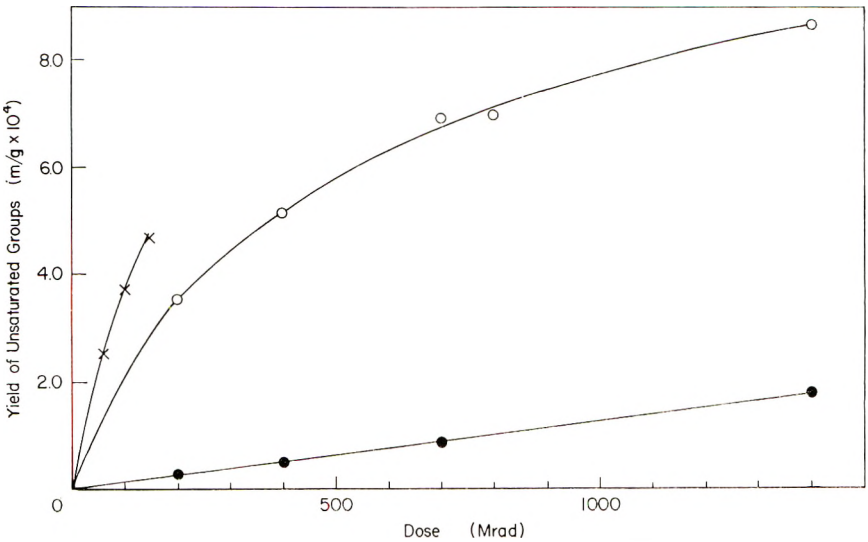

Fig. 3. Yield of unsaturated groups on irradiation of polyisobutene: (×) total unsaturation; (○) $R_1R_2C{=}CH_2$; (●) conjugated diene.

polymer radicals formed by the primary fracture of C—H and C—CH_3 bonds.[2]

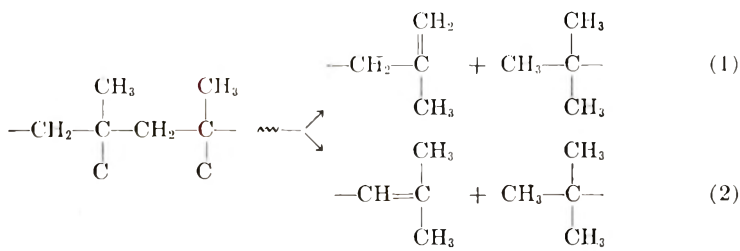

Reactions (1) and (2) require the formation of *tert*-butyl end groups which may be detected[5] in polyisobutenes by absorption at 1250 and 1193 cm.$^{-1}$, although these bands are largely obscured by the previously mentioned band at approximately 1225 cm.$^{-1}$ if the polymer is of too high molecular weight.[6] This is evidently the case with even the lowest molecular weight polymer, obtained after a dose of 1400 Mrad, but nevertheless the spectrum does show an inflection at 1240 cm.$^{-1}$ which could be assigned to the *tert*-butyl group (Fig. 1). In order to assess the quantitative significance of this absorption, the extinction coefficient of the band at 1235 cm.$^{-1}$ in 2,2,4-trimethylpent-1-ene was determined and used to estimate the concentration of *tert*-butyl groups in the polymer as about 10^{-3} mole/g. Reference to Figure 3 (1400 Mrad) indicates that this value is consistent with the equimolar relationship with terminal double bonds required by reactions (1) and (2).

The increased absorption at 1450 cm.$^{-1}$ may be assigned to the formation of sterically strained $R_1CH_2CH_2R_2$ groups on the grounds that methylene

groups in cyclopentane[4] similarly have a bending frequency at 1455 cm.$^{-1}$. Such groups might be formed intramolecularly by reaction (3), which would help to account for hydrogen formation,[2] or by various intermolecular reactions such as reaction (4).

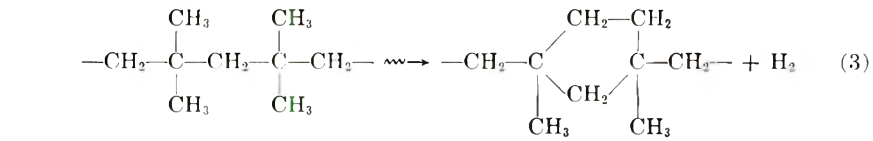

(3)

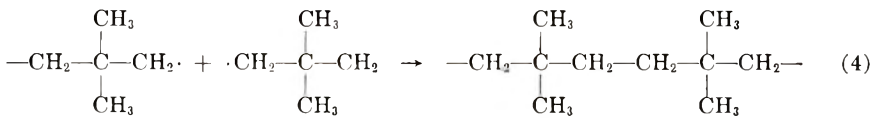

(4)

Ultraviolet Absorption

A puzzling feature of the ultraviolet absorption data of irradiated polyisobutene reported by Alexander et al. is that the absorption maximum varies in an erratic manner with radiation dose in the region of 240–270 mμ. This absorption was reasonably attributed to "a very small number

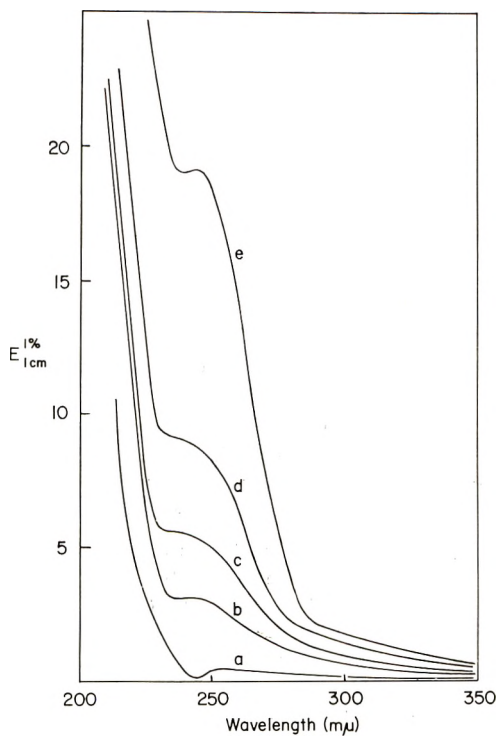

Fig. 4. Change in ultraviolet absorption on irradiation: (*a*) 0 Mrad; (*b*) 200 Mrad; (*c*) 400 Mrad; (*d*) 800 Mrad; (*e*) 1400 Mrad.

of conjugated double bonds," but the variation of the maximum was not explained satisfactorily.

The present results differ from those mentioned above in that even up to the much higher dose of 1400 Mrad the absorption maximum occurs in the narrow range of 242 ± 2 mμ (Fig. 4). As the polymer was irradiated *in vacuo* the presence of oxygenated groups may be definitely excluded and the chromophore assigned to conjugated diene. A simple conjugated diene has an absorption maximum at <230 mμ, but a bathochromic shift of the extent observed is to be expected[7] in one formed from a molecule of polyisobutene on account of its considerable steric strain.[8] Quantitative estimates of the yield of conjugated diene were made by assuming an extinction coefficient of $\epsilon = 10{,}000$ which, by reference to similar chromophores,[7] is unlikely to lead to an error greater than a factor of two (Fig. 3).

A most striking feature of the formation of conjugated diene is that its concentration is proportional to the dose up to the maximum investigated of 1400 Mrad. As pointed out by Alexander et al., a linear dependence on dose seems to rule out the possibility of a superimposition of damage by further absorption of energy and therefore it is suggested that double damage can occur following a single absorption of energy as has been suggested previously to account for similar features in isobutene formation.[2] For example, some olefin groups may be formed with sufficient excess energy to eliminate a molecule of methane [eq. (5)].

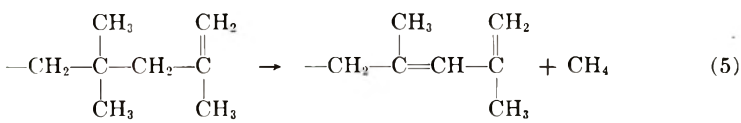

(5)

As no conjugated triene is detected by the appearance of an absorption maximum in the—region beyond 275 mμ the reaction apparently stops at this stage although in order to account for the slight coloration of the irradiated polymer, also observed by Alexander et al., it might be supposed that occasionally it proceeds further to yield a conjugated polyene.

Note: Since this paper was completed the authors have learned of the earlier work of Slovokhotova.[9] Changes observed in the infrared spectrum of polyisobutene after exposure *in vacuo* γ-radiation (900 Mrad) from a Co^{60} source were consistent with a decrease in the number of $>C(CH_3)_2$ groups and the formation of the groups $R_1R_2C{=}CH_2$ and $R_1R_2C{=}CHR_3$. It is, however, disturbing to note that the spectra apparently were obtained only on relatively thick films of carbon tetrachloride solutions implying intense absorption by the solvent in the region 850–700 cm.$^{-1}$. In these circumstances, and in the absence of any supporting evidence, the assignment of a band at 770 cm.$^{-1}$ to ethyl groups must be regarded as not proven.

This work was begun in the laboratories of The Natural Rubber Producers' Research Association. Irradiation facilities were provided by the Technological Irradiation Group at Wantage Research Laboratories (A.E.R.E.) with the kind cooperation of Dr. R. Roberts and his colleagues.

References

1. Alexander, P., R. M. Black, and A. Charlesby, *Proc. Roy. Soc. (London)*, **A232**, 31 (1955).
2. Turner, D. T., *J. Polymer Sci.*, **A2**, 1701 (1964).
3. Thompson, H. W., and P. Torkington, *Trans. Faraday Soc.*, **41**, 246 (1945).
4. Jones, R. N., and C. Sandorfy, *Chemical Applications of Spectroscopy*, New York, 1956.
5. Dainton, F. S., and G. B. B. M. Sutherland, *J. Polymer Sci.*, **4**, 37 (1949).
6. Kozyreva, M. S., *Opt. Spektroskopiya*, **6**, 479 (1959).
7. Gillam, A. E., and E. S. Stern, *An Introduction to Electronic Absorption Spectroscopy in Organic Chemistry*, 1960, Chap. 7.
8. Flory, P. J., *Principles of Polymer Chemistry*, Cornell Univ. Press, Ithaca, N. Y., 1953, p. 246.
9. Slovokhotova, N. A., *Trudy 1 Vsesoyuznogo Soveshchaniya po Radiatsionnoi Khimii*, Academy of Sciences of the U.S.S.R., Moscow, 1958, p. 263.

Résumé

Du polyisobutène purifié a été irradié sous vide avec des électrons de 4 Mev, et on a suivi les changements de l'absorption I.R. et U.V. Les groupements $R_1R_2C{=}CH_2$ constituaient environ 60% de l'insaturation totale, et on pouvait prouver la formation de groupements $R_1R_2C{=}CHR_3$. Il se formait à peu près un groupe *tert*-butyle par double liaison. On trouvait une preuve qualitative de la formation du groupement $R_1{-}CH_2{-}CH_2{-}R_2$. Des groupements diéniques conjugués se formaient proportionnellement à la dose d'irradiation jusqu'à la dose maximum qui était examinée, c'est à dire 1400 Mrad (valeur de G. environ, 0.1).

Zusammenfassung

Gereinigtes Polyisobuten wurde im Vakuum mit Elektronen von 4 MeV bestrahlt und die Veränderungen in der IR- und UV-Absorption bestimmt. 60% der Gesamtzahl der Doppelbindungen waren $R_1R_2C{=}CH_2$-Gruppen. Die Bildung von $R_1R_2C{=}CHR_3$-Gruppen wurde nachgewiesen. Pro Doppelbindung wurde ungefähr eine *tert.*-Butylgruppe gebildet. Die Bildung der $R_1CH_2{-}CH_2R_2$-Gruppe konnte qualitativ nachgewiesen werden. Die Bildung konjugierter Diengruppen ist bis zur höchsten untersuchten Dosis von 1400 Mrad der Dosis proportional (G-Wert etwa 0,1).

Received March 4, 1963

JOURNAL OF POLYMER SCIENCE: PART A VOL. 2, PP. 1721–1729 (1964)

Radiolysis of Polyisobutene. Part III. Effect of Additives

D. T. TURNER,* *Camille Dreyfus Laboratory, Research Triangle Institute, Durham, North Carolina*

Synopsis

The effect of various liquid additives on the degradation of polyisobutene exposed to 4 M.e.v. electrons has been studied by solution viscometry and by measurement of gas volatile at −196°C. At a concentration of about 10^{-4} mole/g. some additives result in an increased yield of fractures, the maximum observed being about 20% with nitrobenzene, presumably due to the scavenging of polymer radicals which otherwise would combine. At higher concentrations most additives result in a decrease in the yield of fractures. Thus, 2×10^{-3} mole/g. thiophenol decreases the yield by about two-thirds and itself suffers sensitized decomposition as evidenced by an increase in the yield of gas from the irradiated mixture. In the simplest case, di-*n*-butyl disulfide has a symmetrical effect in suppressing part of the yield of fractures and gas. This is consistent with the view that a proportion of the fractures is associated with gas formation.

The influence of additives on a polymer which degrades on irradiation has been studied previously for the case of polymethyl methacrylate. Alexander, Charlesby, and Ross[1] incorporated solid additives into the polymer by casting films from solution and calculated molecular weights after irradiation from solution viscosity measurements. These additives were found to reduce radiation-induced degradation of the polymer and subsequently further additives were found to be similarly effective and investigated in most detail by Alexander and Toms.[2]

No work has been reported on the effect of a range of additives on the radiolysis of polyisobutene, but a number of related studies should be noted. Alexander and Charlesby[3] showed that isobutene units were protected by styrene units in the radiolysis of copolymers. Henglein and Schneider[4] studied the radiation-induced degradation of polyisobutene in solution and showed that some solvents protect the polymer whereas others cause increased degradation. Lastly, in a study of the γ-initiated polymerization of styrene mixed with polyisobutene Sebban-Danon[5] has obtained data which show that the polymer is protected by the monomer.

The present paper describes a survey of the influence of varying concentrations of a range of liquid additives on the radiolysis of polyisobutene.

* Post-Doctoral Fellow on leave from The Natural Rubber Producers' Research Association, Welwyn Garden City, Herts, England.

Polymer degradation was followed by viscometry and additional data has been obtained on yields of hydrogen plus methane.

EXPERIMENTAL

The purified polyisobutene had a number-average molecular weight of 3.5×10^5 and approximately a random molecular weight distribution.

The liquids used as additives or solvents were whenever possible of analytical reagent grade and in other cases of laboratory reagent grade.

Liquids were added to the degassed polymer (1 g.) in glass tubes with a micrometer syringe or pipet and thoroughly degassed by freezing and melting *in vacuo*. The tubes were sealed at $< 10^{-4}$ mm. Hg pressure.

The tubes for any one experiment were irradiated simultaneously with water cooling by a 4 M.e.v. electron beam from a linear accelerator. The mean dose rate ranged from 1 to 4 Mrad/min. throughout all the experiments.

Measurement and Interpretation of Viscosity Results

The tubes were opened two or more days after irradiation. In some cases the additive was pumped off but generally the total contents were dissolved in toluene or carbon tetrachloride (100 ml.) and the limiting viscosity number $[\eta]$ determined by measurements of intrinsic viscosity at three concentrations or else at one low concentration, c, by using eq. (1)[6]

$$[\eta] = c^{-1} \ln (f/f_0) \tag{1}$$

in which f and f_0 are the flow times of the solution and solvent, respectively.

The viscosity-average molecular weight, M_v, was calculated from either eq. (2) or (3)[7] and the number-average molecular weight from eq. (4),[8] which applies for a random molecular weight distribution.

$$[\eta]_{25°C.} = 2.9 \times 10^{-4} M^{0.68} \text{ (carbon tetrachloride)} \tag{2}$$

$$[\eta]_{25°C.} = 2.15 \times 10^{-4} M^{0.67} \text{ (toluene)} \tag{3}$$

$$M_v/M_n = 1.85 \tag{4}$$

The number of moles of fractures per gram of polymer, F, was calculated from eq. (5), in which M_0 and M_n represent, respectively, the number-average molecular weight of the polymer before and after irradiation.

$$F = M_n^{-1} - M_0^{-1} \tag{5}$$

The percentage decrease in the yield of fractures due to the additive was obtained from eq. (6), in which F_0 and F represent, respectively, the yield of fractures in the absence and in the presence of additive.

$$\% \text{ decrease in yield of fractures} = \frac{F_0 - F}{F_0} \times 100 \tag{6}$$

Expression (6) is numerically equivalent to the percentage protection previously defined in similar work on polymethyl methacrylate,[2] but differs in that it does not assume independence of the dose.

Determination of Gaseous Yields

The irradiated polymer was thoroughly outgassed and the volatiles at $-196°C.$ ($H_2 + CH_4$) determined with a manometer.

More details concerning the conditions of irradiation and experimental procedure have been given in a previous paper.[9]

RESULTS AND DISCUSSION

As thermal radicals are readily scavenged by very low concentrations of scavenger, a preliminary experiment was undertaken with 2×10^{-5} mole/g. of additive and the dose kept low to minimize any additive depletion. Under these conditions the yield of fractures was reduced by up to about 10% (Table I). Greater reductions in the yield of fractures were obtained with larger amounts of additives (about 5%), the maximum effect being a 42% decrease with thiophenol (Table II). This degree of protection appears to be less than in polymethyl methacrylate,[2] as may be judged from the 80% protection reported for the following concentrations of additives: benzoic acid (1%), α-naphthylamine (3%), and α-naphthol (6%). However, the two sets of results are not strictly comparable, as those for polymethyl methacrylate were obtained with the use of solid additives and by exposure to γ-radiation.

An observation from Table II which has no parallel in the work reported for polymethyl methacrylate is that some additives increase the degradation of the polymer. Such additives are generally only partly miscible with polyisobutene and hence are present in lower concentration than the amount actually added. A study of the effect of the concentration of additive on the yield of fractures reveals that increased degradation may also be observed with low concentrations of additives such as benzene and toluene which protect at higher concentrations (Fig. 1). Conversely, there

TABLE I
Decrease in the Yield of Fractures for Low Concentrations of Additives at Low Doses

Additive (2×10^{-5} mole/g.)	Decrease in fractures, %	
	1.5 Mrad	3 Mrad
Benzene	−1	−4
Toluene	6	9
Trichlorobromomethane	−1	1
Di-*n*-butyl disulfide	9	6
Methyl iodide	7	3
Di-*n*-butyl monosulfide	8	10
n-Butyl mercaptan	7	−1

TABLE II
Decrease in the Yield of Fractures for Higher Concentrations of Additive[a]

Additive (0.05 mole/g.)	Decrease in fractures, %
Thiophenol	42
Iodobenzene	39
Thiophene	38
Methyl iodide	32
Di-*n*-butyl disulfide	30
Dimethylaniline[b]	28
Anisole	17
Toluene	15
Di-*n*-butyl monosulfide	14
n-Butyl mercaptan	10
Benzene	7
Petroleum ether	1
n-Decane	−1
Cyclohexane	−1
Trichlorobromomethane	−7
Methyl phenyl ketone[b]	−11
Benzonitrile[b]	−12
Benzaldehyde[b]	−16
Nitrobenzene[b]	−18

[a] Dose: 5 Mrad.
[b] Only partly miscible with polymer.

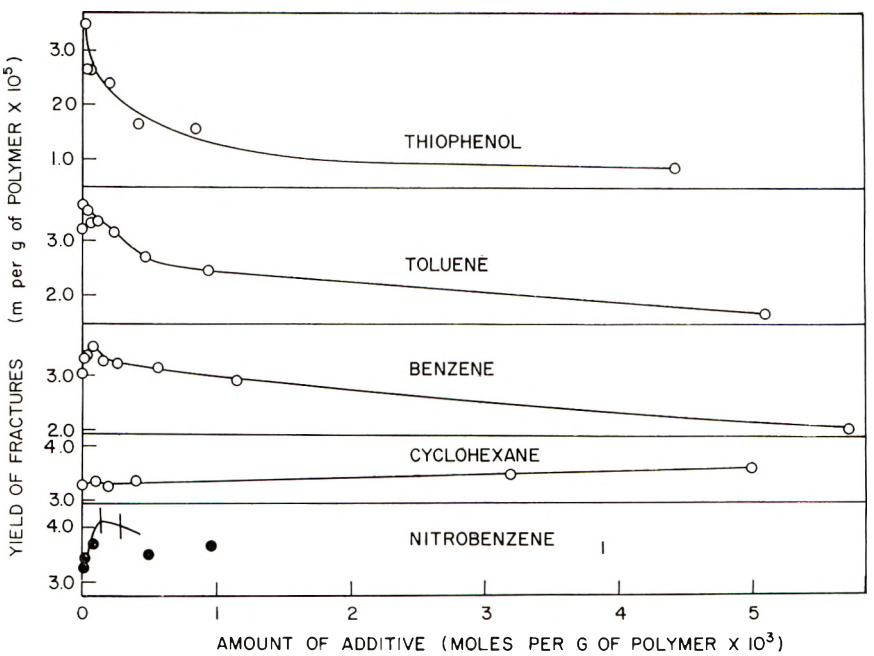

Fig. 1. Effect of concentration of various additives on the yield of fractures. Dose: 8 Mrad. Vertical lines indicate extent of degradation during certain viscosity measurements.

are indications that an additive such as nitrobenzene which causes increased degradation according to the results in Table II might protect the polymer if the two were more miscible.

A unique difficulty encountered with nitrobenzene as an additive was that solutions prepared from the irradiated polymer degraded during viscosity measurements. This effect was not always detected and subsequent to obtaining the results in Figure 1 it was found that it could be prevented by an initial extraction of the irradiated polymer with cold acetone. Previously, post-irradiation degradation has been reported only after irradiation of polymethyl methacrylate in air.[10]

An additive which is miscible with polyisobutene and yet appears to cause increased degradation according to Table II is trichlorobromoethane. In a more extensive experiment with a number of halogen compounds it was found that for a concentration of 1.5×10^{-3} mole/g. and a dose of 25 Mrad increased degradation was observed only with aliphatic bromine compounds and not with chlorides or iodides (Table III).

It was convenient to vary the dose according to the experiment and evidence that this would not seriously distort the overall picture was provided

TABLE III
Decrease in Yield of Fractures for Halogen Compounds[a]

Additive (1.5×10^{-3} mole/g.)	Decrease in fractures, %
Methyl iodide	45
Iodobenzene	41
Chlorobenzene	41
Bromobenzene	39
Carbon tetrachloride	2
Propyl chloride	1
Trichlorobromomethane	−27
sec-Octyl bromide	−32
Propyl bromide	−33
Cyclohexyl bromide	−40

[a] Dose: 25 Mrad.

TABLE IV
Effect of Additives after Various Doses

Dose, Mrad	Fractures without additive, mole/g. fractures $\times 10^4$	Decrease in fractures with additives, %[a]	
		Thiophenol	Nitrobenzene
6	0.25	40	−8
12	0.44	35	−14
18	0.56	28	−12
24	0.72	31	−8
30	0.83	29	−15
36	0.97	26	−13

[a] Initial concentration of additive: 1.7×10^{-4} mole/g.

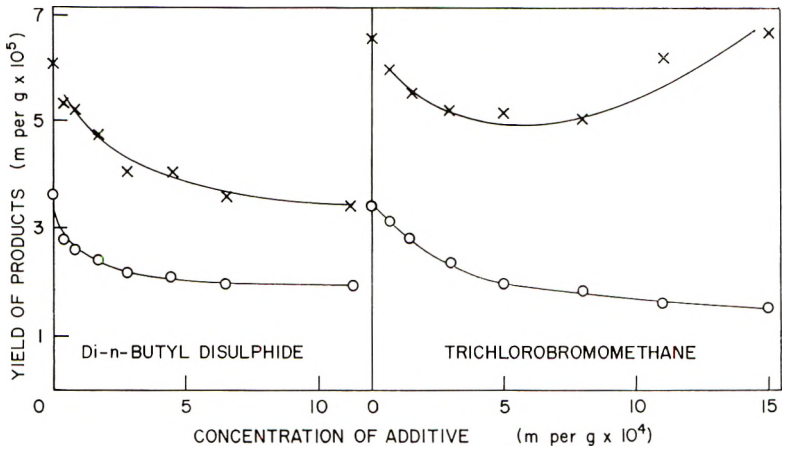

Fig. 2. Effect of additives on the yields of gas and fractures: (×) fractures; (O) gas volatile at −196°C. Dose: 15 Mrad.

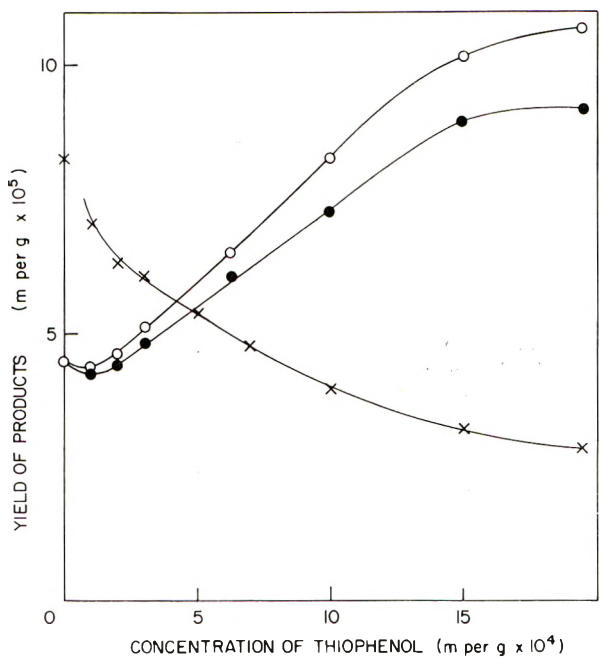

Fig. 3. Effect of thiophenol on the yields of gas and fractures: (×) fractures; (O) gas volatile at −196°C.; (●) gas volatile at −196°C. minus gas calculated to come from direct radiolysis of thiophenol. Dose: 25 Mrad.

by studying the effect of dose on polyisobutene containing small concentrations (1.7×10^{-4} mole/g.) of additive. Thiophenol and nitrobenzene were chosen as representing the extremes of behavior observed in Table II, and the results in Table IV provide evidence of some depletion of the former additive but not the latter. A decrease of protective power after

high doses has previously been reported[2] in the case of 8-hydroxyquinoline in polymethyl methacrylate.

Figures 2 and 3 show the effect of additives on the yield of gas volatile at −196°C. as well as on the yield of fractures. The simplest results were obtained with trichlorobromoethane which cannot itself contribute to the yield of gas which is decreased by some 50%. Similar results with di-*n*-butyl disulfide would require a correction for the contribution of any gas formed from the additive although this would probably be relatively small.

With large concentrations of thiophenol the yield of gas from the mixture is increased (Fig. 3). Values of the G(gas) value for the irradiation of thiophenol alone (1 g.) were determined after doses of 5 and 30 Mrad as 4.2 and 4.1, respectively. Even after using these G values to allow for a contribution to the gaseous yield through direct radiolysis of thiophenol, an increased yield was still evident at the higher concentrations from the mixture.

With low concentrations of thiophenol ($<10^{-4}$ mole/g.), the yield of gas from the mixture is decreased. Experiments[11] with tritiated thiophenol have shown that the polymer is tritiated on irradiation and therefore it may be inferred that as a consequence small concentrations of thiophenol would be largely converted to diphenyl disulphide. By analogy with the results obtained with an aliphatic disulfide (Fig. 2) it may be further inferred that an aromatic disulfide would depress the yield of gas and so account for the initial decrease in Figure 3. Direct experiments with diphenyl disulphide were not undertaken, as it is a solid and not very miscible with the polyisobutene.

Relationship Between Effects on Gas and Fractures

The degradation of polyisobutene on irradiation is predominantly by direct fracture of the main chain of carbon atoms, represented schematically by reaction (7). However, there are also indications that some fractures are associated with a part of the gas formed, possibly by reactions (8)–(10), in which A represents H or CH_3.[9]

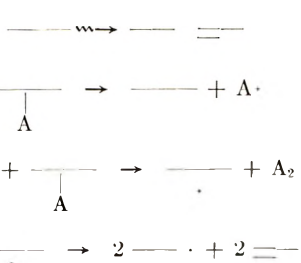

(7)

(8)

(9)

(10)

Consistent with these reactions it is found that a part of the gas, some 50%, is suppressed[12] by additives (Fig. 2) and that in the case of di-*n*-butyl disulfide there is a symmetrically related suppression of fractures. More complicated fracture results are obtained with trichlorobromomethane but these

may be attributed to the formation of radicals which attack and degrade the polymer (cf. Table III). This type of reaction is known to occur when polyisobutene is heated with peroxides[13] and also is in line with the report that bromine rapidly degrades butyl rubber,[14] a copolymer of isobutene with small amounts of diolefin.

No precise quantitative significance is attached to the relationship between the suppressed yields of gas and fractures because the latter effect probably includes a contribution due to the suppression of reaction (7). Suppression of reaction (7) must be invoked in order to account for marked protection by thiophenol which can reduce the yield of fractures by as much as two-thirds (Fig. 3). To account for the symmetrical relationship between the decrease in the yield of fractures and the increase in the yield of gas it may be postulated that thiophenol deactivates[12] an intermediate in reaction (7) and as a result itself suffers sensitized decomposition.

Increased Degradation in the Presence of Scavengers

Polymer radicals are formed on irradiation of polyisobutene, G(radical) = 7.4,[11] and the question arises as to whether these participate in combination reactions which offset degradation. As very low concentrations of additive do not increase the yield of fractures (Table I), it may be supposed that the contribution of randomly distributed radicals to such reactions is unimportant. However, the increased degradation which is observed with some additives, which would be expected to scavenge hydrocarbon radicals, at a much higher concentration of about 10^{-4} mole/g. suggests competition for radicals which are formed close together.[15] The largest effect observed is an increase in fractures of about 20% with nitrobenzene (calculated with reference to the lower extremities of the vertical lines in Fig. 1) although the quantitative significance of this and other results (Table II and IV) is open to question because of an overlapping protective effect.

This work was begun in the laboratories of The Natural Rubber Producers' Research Association. Irradiation facilities were provided by the Technological Irradiation Group at Wantage Research Laboratories (A.E.R.E.) with the kind cooperation of Dr. R. Roberts and his colleagues. Mr. G. T. Jones is thanked for help with the experiments.

References

1. Alexander, P., A. Charlesby, and M. Ross, *Proc. Roy. Soc. (London)*, **A223**, 392 (1954).
2. Alexander, P., and D. Toms, *Radiation Res.*, **9**, 509 (1958).
3. Alexander, P., and A. Charlesby, *Proc. Roy. Soc. (London)*, **A230**, 136 (1955).
4. Henglein, A., and C. Schneider, *Z. Physik. Chem. (Frankfurt)*, **19**, 367 (1959).
5. Sebban-Danon, J., *J. Chim. Phys.*, **57**, 1123 (1960).
6. Kraemer, E. O., *Ind. Eng. Chem.*, **30**, 1200 (1938).
7. Fox, T. G, and P. J. Flory, *J. Phys. Colloid. Chem.*, **53**, 197 (1949).
8. Flory, P. J., *Principles of Polymer Chemistry*, Cornell Univ. Press, Ithaca, N. Y., 1953, p. 313.
9. Turner, D. T., *J. Polymer Sci.*, **A2**, 1701 (1964).

10. Wall, L. A., and D. W. Brown, *J. Phys. Chem.*, **61**, 129 (1957).
11. Ayrey, G., and D. T. Turner, *J. Polymer Sci.*, **B1**, 185 (1963).
12. Burton, M., *Actions Chimiques et Biologiques des Radiations*, Vol. 3, Haissinsky, Ed., 1958, p. 39.
13. Thomas, D. K., *Trans. Faraday Soc.*, **57**, 511 (1961).
14. Thomas, R. M., and W. J. Sparks, *Synthetic Rubber*, G. S. Whitby, Ed., 1954, p. 813.
15. Prevot-Bérnas, A., A. Chapiro, C. Cousin, Y. Landler, and M. Magnet, *Discussions Faraday Soc.*, **12**, 98 (1952).

Résumé

L'effet de différents additifs liquides sur la dégradation du polyisobutène, exposé à des électrons de 4 Mev, a été étudié par viscosimétrie de la solution et par la mesure de volatilité gazeuse à −196°C. Pour une concentration d'environ 10^{-4} moles/gr quelques additifs entraînent une augmentation de rupture, le maximum observé est d'environ 20% avec le nitrobenzène, probablement par suite de la capture des radicaux polymères, qui autrement se recombinent. À des concentrations plus élevées, la plupart des additifs entraînenet une diminution dans le pourcentage de rupture. 2×10^{-3} moles/g de thiophénol diminuent le pourcentage à environ deux tiers et le thiophénol même subit une décomposition sensibilisée, ce qui est démontré par une augmentation dans le pourcentage de gaz du mélange irradié. Dans le cas le plus simple, le disulfure de *n*-butyle a un effet symétrique en supprimant une partie du pourcentage des ruptures et du gaz. Ceci est compatible avec l'idee qu' une partie des ruptures est associée à la formation de gaz.

Zusammenfassung

Der Einfluss verschiedener flüssiger Zusätze auf den Abbau von Polyisobuten bei der Bestrahlung mit Elektronen von 4 MeV wurde durch Lösungsviskosimetrie und durch Bestimmung des bei −196°C flüchtigen Gases untersucht. In einer Konzentration von etwa 10^{-4} Mol/g führen gewisse Zusätze zu einer erhöhten Spaltungsausbeute. Die grösste Erhöhung—etwa 20%—wurde beim Nitrobenzol beobachtet, was vermutlich darauf zurückgeht, dass Polymerradikale abgefangen werden, die andernfalls rekombinieren würden. In höheren Konzentrationen führen die meisten Zusätze zu einer Abnahme der Spaltungsausbeute. So erniedrigt Thiophenol in einer Konzentration von 2×10^{-3} Mol/g die Ausbeute um etwa zwei Drittel und erleidet dabei selbst eine sensibilisierte Zersetzung, wie die Erhöhung der Gasaubeute bei der Bestrahlung der Mischung zeigt. Der einfachste Fall liegt beim Di-*n*-butylsulfid vor, welches die Spaltungs- und Gasausbeute in gleichem Masse erniedrigt. Dies stimmt mit der Auffassung überein, dass ein bestimmter Anteil der Spaltungen von Gasbildung begleitet ist.

Received March 4, 1963

JOURNAL OF POLYMER SCIENCE: PART A VOL. 2, PP. 1731–1748 (1964)

Permanganate–Oxalic Acid as a Redox Initiator of Acrylonitrile Polymerization in Aqueous Media. Part III. Kinetics and DP

RANJIT S. KONAR and SANTI R. PALIT, *Indian Association for the Cultivation of Science, Jadavpur, Calcutta, India*

Synopsis

The kinetics of the aqueous polymerization of acrylonitrile initiated by the permanganate–oxalic acid redox pair have been studied gravimetrically at 32 ± 0.2°C. The rate of polymerization is independent of oxalic acid concentration over a small range. The catalyst exponent varies continuously with the catalyst concentration, being 0.9 at low catalyst concentration and 0.27 at high catalyst concentration at a monomer concentration of 0.30*M*. The monomer exponent is nearly unity in the concentration range 0.30*M* and above. The molecular weight of the polymer is independent of oxalic acid concentration in the range where the rate of polymerization is independent of the oxalic acid concentration but decreases at higher concentration of oxalic acid with increasing concentration of catalyst and temperature. The overall activation energy was found to be 8.6 kcal./mole. Addition of salts such as Na_2SO_4 depresses the rate of polymerization, but the addition of $MnSO_4$ at low concentrations increases the rate, whereas at higher concentration the initial rate falls. It has been suggested that hydrated Mn^{3+} ions cause oxidative chain termination of polyacrylonitrile radicals. Complexing agents, such as fluoride ions, ethylene-diaminetetraacetic acid, etc., decrease the rate of polymerization, whereas addition of detergents enhances it.

The initiating power of the permanganate–oxalic acid system for polymerization of methyl methacrylate, acrylonitrile, vinyl acetate, and methyl acrylate has been reported briefly,[1] and detailed studies of polymerization of methyl methacrylate have also been published.[2] The present paper reports the results of a similar study with acrylonitrile as the monomer.

GENERAL FEATURES AND MECHANISM OF THE INITIATION OF POLYMERIZATION

Permanganate–oxalic acid is a powerful initiator, and the polymer separates out as a colloidal suspension or precipitate, depending on the concentration of the activator, the catalyst, and the monomer, the lower the concentration the stabler being the separating phase. In this system, there are two consecutive redox reactions,[3] viz., (1) that between permanganate (oxidant) and monomer (reductant) and (2) that between the separated hydrated manganese dioxide (oxidant) and oxalic acid (reductant). The reactions involved in (2) are probably the same as reported by

Launer and Yost[4] but no detailed study of reaction (1) is available. On addition of permanganate to an aqueous solution of acrylonitrile, the following changes are observed: (a) permanganate is immediately reduced and a brownish black colloidal suspension, probably of MnO_2, is formed; (b) a faint turbidity is observed; (c) the solution becomes alkaline. The fact that turbidity is seen suggests that permanganate alone initiates aqueous polymerization of acrylonitrile. The reactive species is not known but may be a hydrated form of the higher valent manganese ion. The overall reaction between the permanganate and the monomer appears to be

$$MnO_4^- + 3\ CH_2{=}CHCN + H_2O \rightarrow MnO_2 + 3\ \underset{\underset{OH}{|}}{CH_2{-}\dot{C}HCN} + OH^-$$

Polymethyl methacrylate initiated by the MnO_4^-–$H_2C_2O_4$ redox system has been found to contain carboxyl and hydroxyl endgroups.[3,5] The incorporation of OH endgroups in the polymer may be partly due to the above reaction. Again the fact that the oxidation of olefinic compounds by permanganate in acid[6] or alkaline media involves hydroxylation suggests the possibility of the occurrence of the above reaction, which is similar to the initiation reaction of vinyl monomers initiated by cobaltic salts in aqueous media, proposed by Baxendale et al.[7] The reactive species in the permanganate–oxalic acid reaction is undoubtedly "active" oxalic acid[8,9] ($C_2O_4^-$) or the carboxyl radical ion ($\dot{C}OO^-$) or both. The existence of carboxyl endgroups in polymers[3] initiated by permanganate–oxalic acid clearly demonstrates the existence of these species as intermediate products in this redox reaction. We assume that these species also initiate acrylonitrile polymerization because so far it has not been possible to identify these initiator fragments as polymer endgroups in polyacrylonitrile by the dye tests as the latter are inapplicable to polyacrylonitrile due to the insolubility of the polymer in benzene.

Permanganate is also a powerful initiator in presence of the disodium salt of ethylenediaminetetraacetic acid (EDTA). No brownish-black precipitate of manganese dioxide separates out. The colloidal MnO_2 dissolves very quickly to form a highly effective initiator, a light violet solution of a complex of higher valent manganese and EDTA. Polymerization continues usually as long as the solution is colored. The behavior of the initiator will be reported elsewhere.[5]

EXPERIMENTAL

The quality of the reagents and the details of the experimental procedure for rate measurements by the gravimetric method have been described in Part II.[2] The results are quite reproducible.

RESULTS AND DISCUSSION

The yield versus time curve shows linearity after the initiation of polymerization, but this region in the yield–time curve probably does not exist

at sufficiently low monomer concentration (0.075M or below) (Figs. 1 and 3) or if it exists, it thus persists for a very short period which is difficult to diagnose by the gravimetric method of rate measurement.

Rate Dependence on Oxalic Acid Concentration

Yield–time curves at various concentrations of oxalic acid are shown in Figures 1 and 2. At low monomer concentration the rate of polymerization R_p as well as the yield remains practically constant over a wide range of oxalic acid concentration. The rate tends to increase at oxalic acid concentration when the separating phase is colloidal, but tends to fall at relatively high concentration of the activator (viz., oxalic acid), the separat-

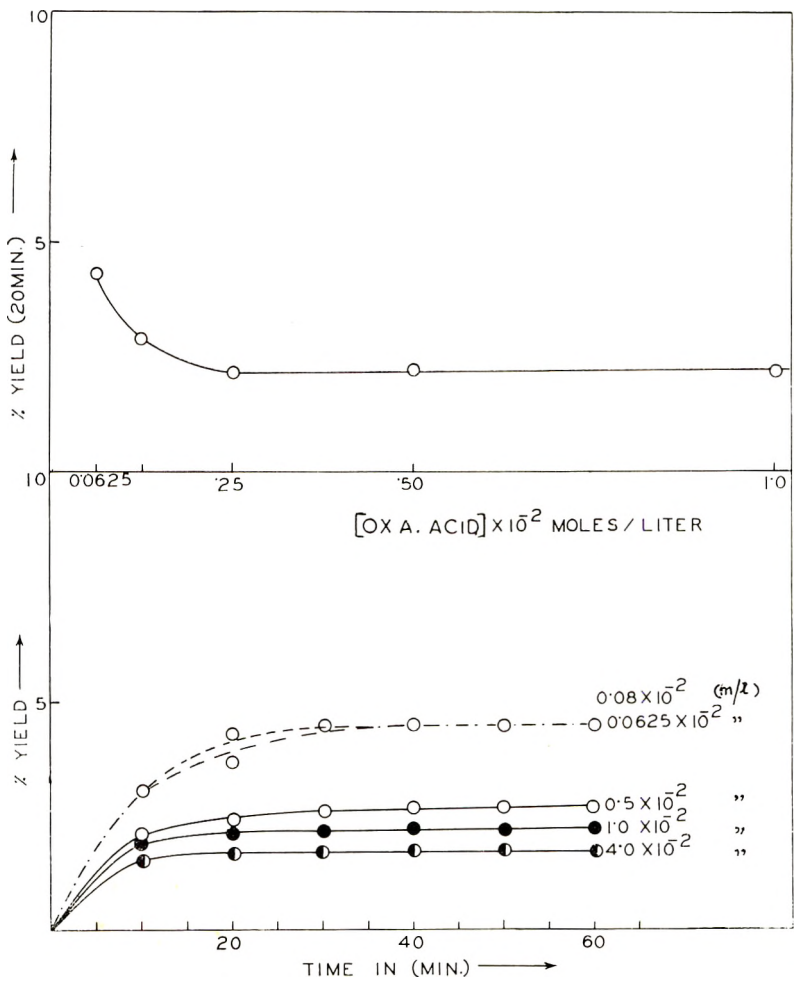

Fig. 1. Yield and rate curves in the aqueous polymerization of acrylonitrile (0.075M) with permanganate–oxalic acid initiation at $KMnO_4$ concentration of $1.26 \times 10^{-4}M$ and varying concentrations of oxalic acid.

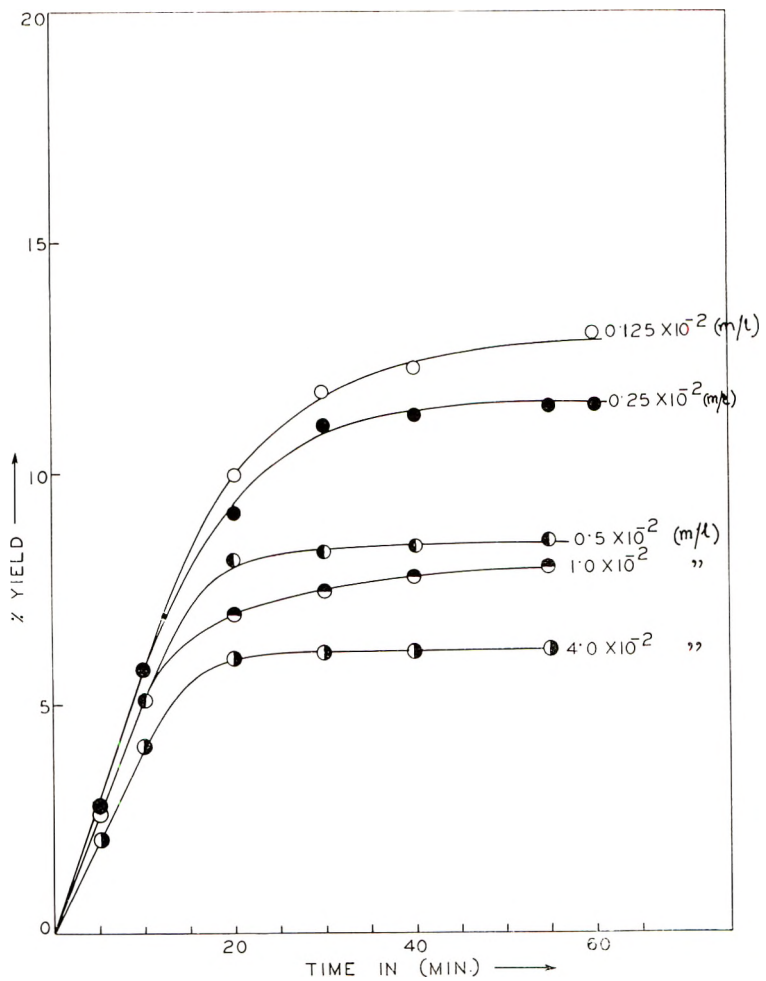

Fig. 2. Yield curves at acrylonitrile concentration of 0.30M, $KMnO_4$ concentration of $1.26 \times 10^{-4}M$, and varying concentrations of oxalic acid.

ing phase being a precipitate. At relatively high monomer concentration, R_p is independent of oxalic acid concentration over a wider range, but the yield tends to fall (Fig. 2). In general in a redox-initiated system, an increase of the activator concentration enhances the rate of generation of primary radicals which, in turn, increases the rate of polymerization. Therefore it is expected that the rate of polymerization should increase with the increase in the concentration of the activator (oxalic acid), the concentration of the catalyst (permanganate) remaining constant. However, the increase in concentration of oxalic acid increases the electrolyte concentration as well as the H^+ ion concentration of the medium. This, on the other hand, enhances the rate of coagulation of the separating phase and thus lowers the rate of polymerization. Therefore, these two opposite

effects on the kinetics of polymerization would strike a balance over a certain range of concentration and the rate of polymerization will be independent of activator concentration over this range of oxalic acid concentration. At high concentration of oxalic acid the pH effect probably predominates and so the rate falls. At very low concentration of the activator, the rate rises due to the colloidal stability of the separating phase.[10] The variation in the yield of the polymer (Fig. 2) in the concentration range of oxalic acid where the initial rate remains almost constant, is again due to the stability of the latex particles. Initially, the polymer separates as a colloid, the stability of which depends on pH of the solution. In fact, at low concentration of oxalic acid ($0.0625 \times 10^{-2}M$), the separating phase is very unstable colloid which coagulates on shaking in this case, whereas at higher concentration of the acid, the polymer coagulates during the course of the reaction. The lower the pH, the faster is the rate of coagulation. Several workers[11] have reported similar independence of rate over a wide range of activator.

Rate Dependence on Catalyst Concentration

Figures 3 and 4 show that the rate of polymerization and the yield increase with increase in the concentration of the catalyst (oxidant, $KMnO_4$) and the variation of the initial rate R_{ini} (taken from the slopes at zero time) with the concentration of the catalyst is shown in Figure 5, while the variation of the steady-state rate (R_p) with catalyst concentration is shown in Figure 6. At low concentration of monomer ($0.075M$), the catalyst exponent is nearly unity, i.e., rate α [catalyst]. At relatively high monomer concentration ($0.30M$), the catalyst exponent continuously decreases with the concentration of the catalyst from 0.9 to 0.27. This probably suggests that the nature of the termination reaction also changes with catalyst concentration. It is customary to interpret the usual kinetic data in the classical way, viz. (a) when the catalyst exponent is unity, termination takes place unimolecularly either by degradative chain transfer or by dissolved metal ions or by occlusion of the growing radicals in the cage of polymer coils; (b) when the exponent is 0.5, the termination is due to the bimolecular collision process of two growing polymeric radicals; (c) when the catalyst exponent is less than 0.5, termination partly by primary radicals take place, and when the catalyst exponent is zero, termination is then only due to primary radicals,[12] assuming stationary state kinetics in all cases.

However in a precipitating medium, the kinetic data can also be interpreted in a different way. It is well known that in precipitating media, the polymer molecules will be tightly coiled and the growing ends will be occluded in the coils, and so the termination is likely to be unimolecular as indicated by the catalyst exponent (unity). With the increase in the concentration of the catalyst, the rate of generation of primary radicals and also its concentration increase. During the polymerization reaction, the primary radicals will distribute themselves in the two phases, i.e., aqueous

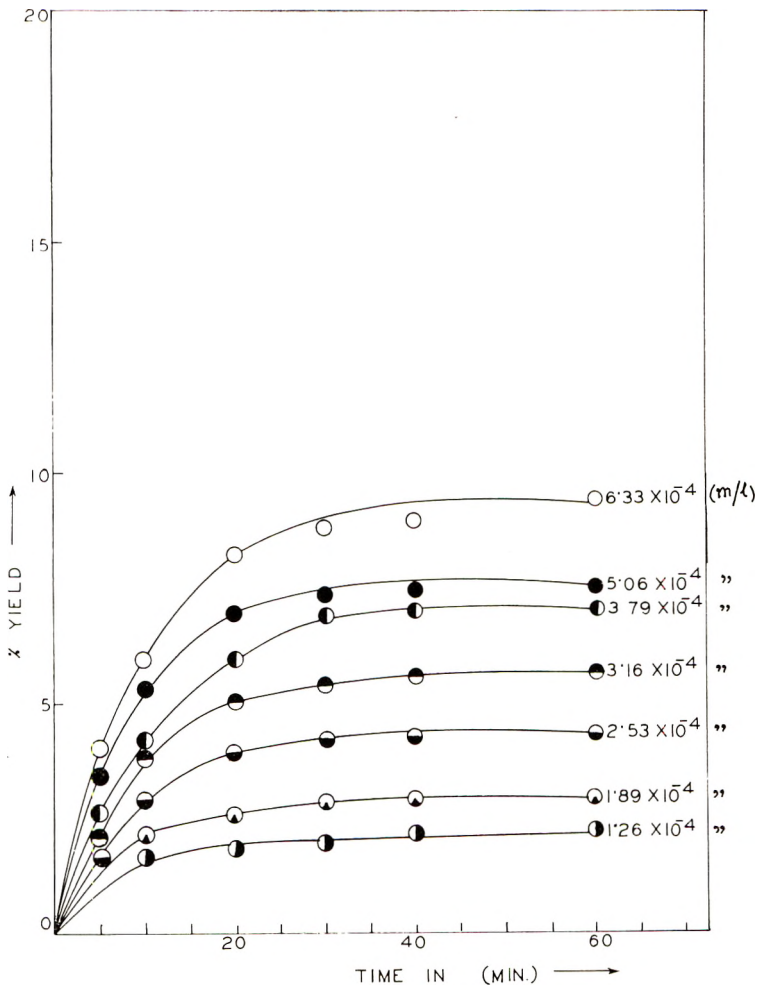

Fig. 3. Yield curves at acrylonitrile concentration of 0.075M, oxalic acid concentration of 0.8 $\times$ $10^{-2}M$, and varying concentrations of $KMnO_4$.

phase and polymer phase containing trapped radicals. Thus the termination by primary radicals is a possibility and becomes more and more important as the catalyst exponent falls. When the overall catalyst exponent becomes 0.5 in a precipitating medium, termination may be partly by unimolecular process and partly by primary radicals rather than the mutual annihilation process, as the mobility of the growing chain in a precipitate has been reduced to a considerable extent. In other words, termination in a precipitating medium takes place either unimolecularly or by primary radicals or by both, depending on the concentration of the catalyst. It has been demonstrated clearly by Palit and co-workers[5] that as the catalyst exponent changes gradually from unity to zero with the increase in the catalyst (permanganate) concentration in the aqueous polymeriza-

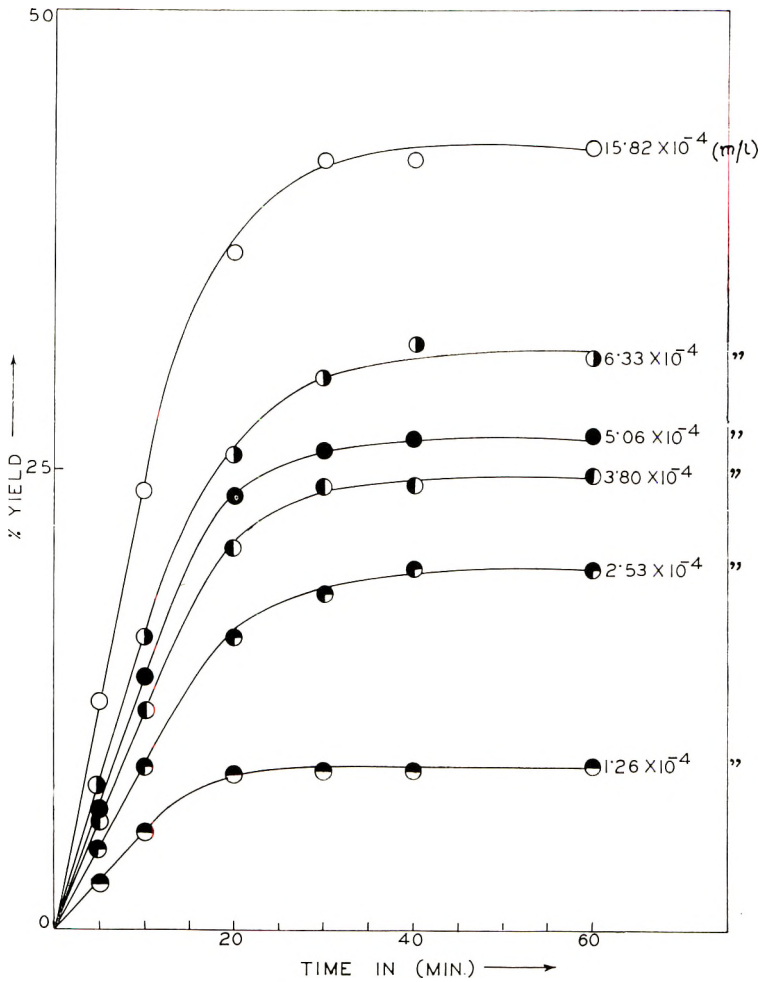

Fig. 4. Yield curves at acrylonitrile concentration of 0.30M, oxalic acid concentration of 0.8 $\times$ $10^{-2}M$, and varying concentrations of $KMnO_4$.

tion of methyl methacrylate initiated by MnO_4^-–$H_2C_2O_4$ redox system, the average number of endgroups per polymer molecule increases gradually from one to two. This probably confirms our conclusion that in the heterogeneous polymerization where the separating polymer is a precipitate, termination takes place unimolecularly at low initiator concentration (initiator exponent being unity), solely by primary radicals (initiator exponent being zero) and due to their joint action at concentrations of the initiator lying between these two limits.

However, this does not overthrow the concept of bimolecular collision process when the catalyst exponent is 0.5. In fact, when sustained coexistence of radicals in a coagulum is possible (gel effect), termination by mutual collision between two growing chains is highly probable[2] due to the

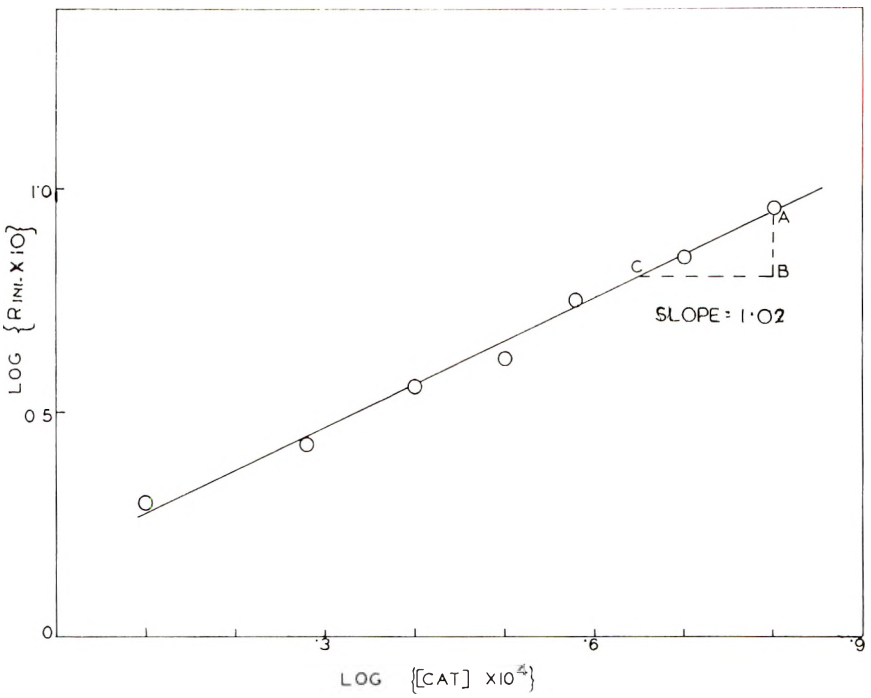

Fig. 5. Plot of the logarithm of the initial rate R_{ini} (in per cent polymerized/minute) vs. the logarithm of the initiator ($KMnO_4$) concentration at acrylonitrile concentration of 0.075M and oxalic acid concentration of $0.8 \times 10^{-2}M$.

internal Brownian motion of the polymer molecules which does not even vanish in a three-dimensional crosslinked polymer.[13] Apart from the catalyst concentration, termination also depends on monomer concentration. When the monomer concentration is very low (0.075M) the catalyst exponent is 1.0. This result is to be taken with caution, because at high catalyst concentration water-soluble oligomers will be formed, and they escape estimation by the gravimetric method. However, at low concentration of the monomer the catalyst exponent, unity, may arise from the nonstationary-state kinetics.

Dainton and co-workers[14] reported similar results. They concluded that in aqueous acrylonitrile polymerization when the separating phase is a very unstable colloid, the rate of polymerization R_p and the nature of chain termination depends on monomer concentration, [M], and the rate of initiation.

$$R_p = K[\mathrm{M}]\,[\mathrm{Cat}]^{1/2} \qquad [\mathrm{M}] > 0.5 \text{ mole/l.}$$

and

$$R_p = K[\mathrm{M}]^2\,[\mathrm{Cat}]^x \qquad [\mathrm{M}] < 0.5 \text{ mole/l.}$$

where $0.2 < x < 0.9$.

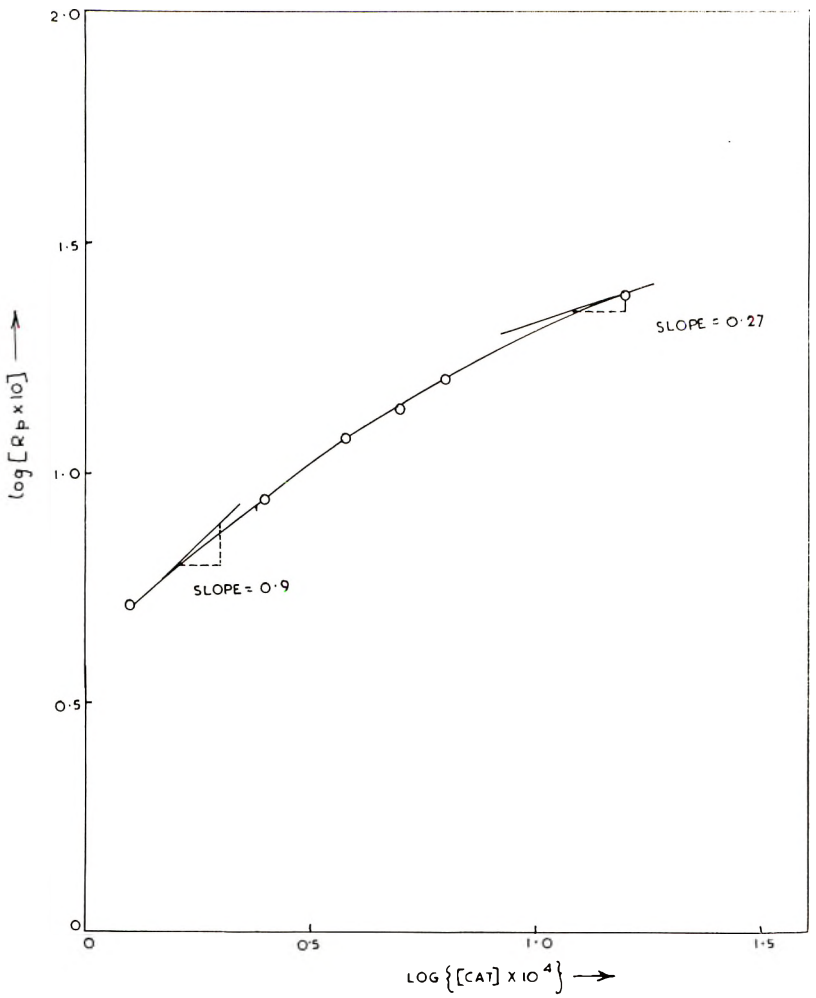

Fig. 6. Plot of the logarithm of the steady-state rate R_p (in per cent polymerized/minute) vs. the logarithm of $KMnO_4$ concentration at acrylonitrile concentration of 0.30M and oxalic acid concentration of $0.8 \times 10^{-2}M$.

Initiator Injection Experiment and Locus of Polymerization

Injection of catalyst late in a run increases both the rate and the yield (Fig. 7). This is to be expected because the injection of catalyst in a precipitating medium will be tantamount to fresh initiation, as the new primary radicals generated from the injected initiator will distribute themselves in the two existing phases, e.g., aqueous phase and polymer phase.[2] Thus the rate will increase but the DP must fall due to premature chain termination by primary radicals. This is borne out by the data in Table I. Since the rate increases due to the injected initiator, the locus of polymerization still exists in the aqueous phase. In other words, the locus of polymerization remains in both the phases.

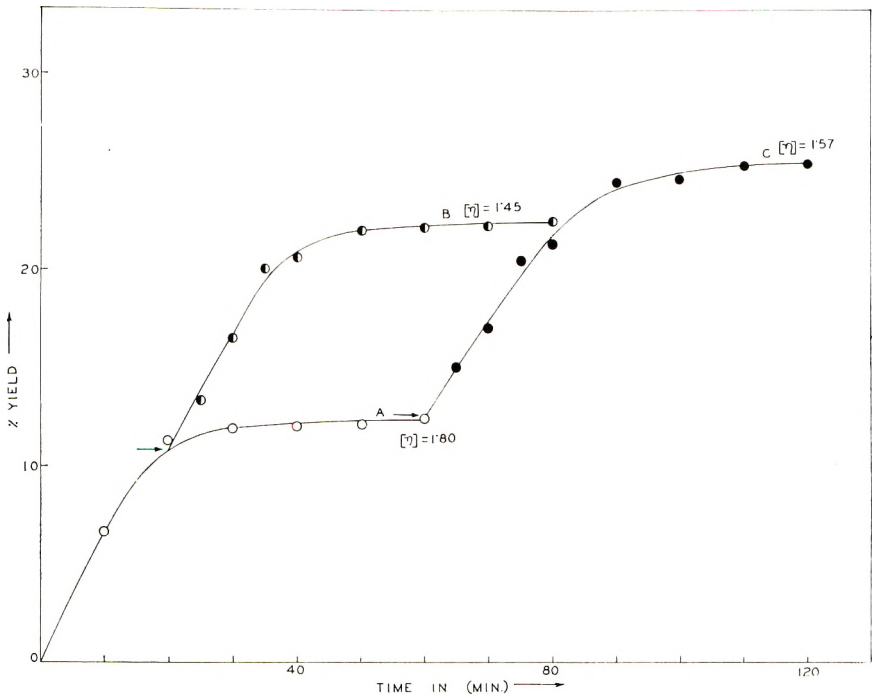

Fig. 7. Effect of initiator ($KMnO_4$) injected late in a run at a concentration of oxalic acid of $0.4 \times 10^{-2}M$, permanganate concentration of $1.26 \times 10^{-4}M$, and acrylonitrile concentration of $0.30M$: (*A*) control; (*B*) $1.26 \times 10^{-4}M$ $KMnO_4$ injected after 20 min.; (*C*) $1.26 \times 10^{-4}M$ $KMnO_4$ injected after 60 min. The arrows indicate the points of injection.

TABLE I
Initiator Injection Experiment[a]

Time of injection of catalyst after the initiation of polymerization, min.	Amount of catalyst injected, mole $\times 10^4$	$[\eta]$, 100 ml./g.
Control	nil	1.80
20	1.26	1.45
60	1.26	1.57

[a] Acrylonitrile = 0.30 mole/l.; catalyst = 1.26×10^{-4} mole/l.; activator = 0.4×10^{-2} mole/l.

Rate Dependence on Monomer Concentration

The yield versus time curve at different monomer concentrations is shown in Figure 8. We find that the steady-state rate varies approximately linearly at relatively high monomer concentration ($0.30M$ and above). At very low monomer concentration ($0.075M$) possibly a steady state is not attained, or if so, it persists for a very short period and so the steady-state rate is difficult to measure gravimetrically in this case.

Rate Dependence on Temperature

The initial rate of polymerization rises with temperature, attains a maximum value at about 45°C., and then falls with further rise in temperature; a similar feature has also been observed with methyl methacrylate as

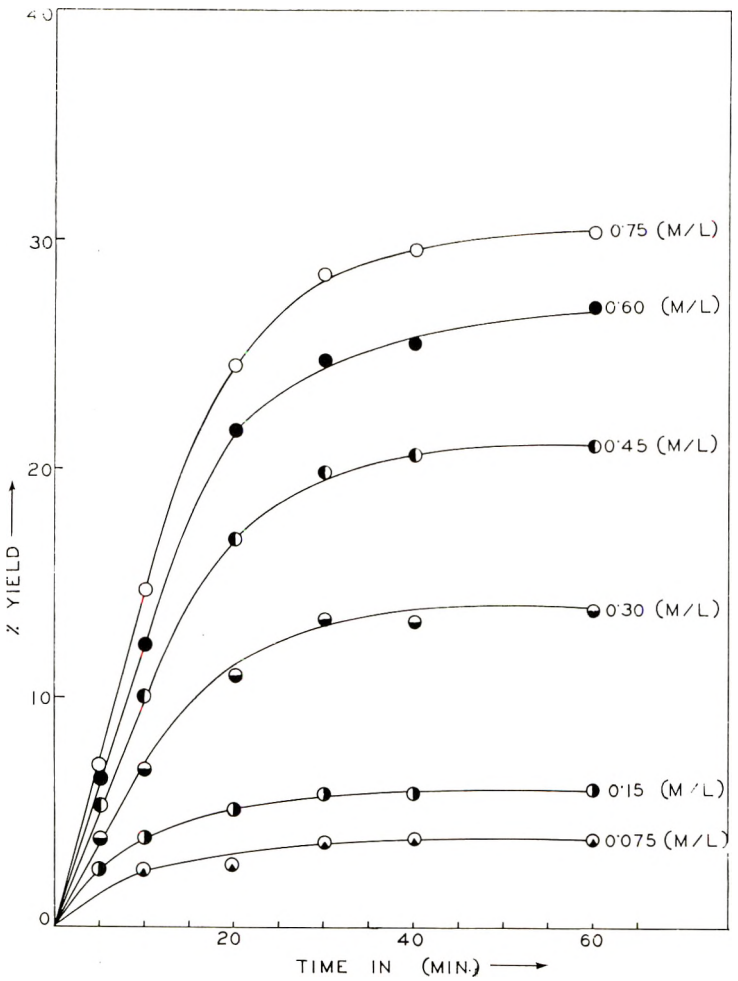

Fig. 8. Yield curves at oxalic acid concentration of $0.08 \times 10^{-2}M$, permanganate concentration of $1.26 \times 10^{-4}M$, and varying concentrations of acrylonitrile.

monomer.[2] The yield, however, decreases with increasing temperature (from 25°C. on) (Table II). The fall in the initial rate at higher temperature (above 45°C.) is evidently due to the instability of the primary radicals ($C_2O_4^-$ or COO^-), and the fall in the yield with increasing temperature is probably due to the fact that a good portion of the primary radicals undergoes side reactions such as

$$C_2O_4^- + Mn^{3+} \rightarrow 2CO_2 + Mn^{2+}$$

i.e., the reaction of Mn^{3+} or Mn^{4+} with oxalic acid becomes faster. Higher temperature will also coagulate the polymer rapidly, and so the rate and yield may fall at 50°C. and above. The overall activation energy in the temperature range 20–45°C. has been found to be 8.6 kcal./mole.

TABLE II
Rate Dependence on Temperature[a]

Temp., °C.	Initial rate, % polymerized/min.	Limiting conversion (in 1 hr.), %	$[\eta]$, 100 ml./g.	Overall activation energy, kcal./mole
20	0.27	12.9	1.87	
25	0.32	14.4	2.08	
30	0.40	11.4	1.82	8.61
35	0.55	8.0	1.05	
40	0.70	5.6	0.97	
45	0.80	4.3	0.68	
50	0.61	3.1	—	
55	0.41	2.5	—	

[a] Acrylonitrile = 0.22 mole/l.; $KMnO_4 = 1.26 \times 10^{-4}$ mole/l.; $H_2C_2O_4 = 0.08 \times 10^{-2}$ mole/l.

Rate Dependence on Additives

a. Salts. Addition of neutral salts such as sodium sulfate depress the rate of polymerization (Fig. 9). This is evidently due to the coagulating effect of the added electrolyte.[10] However, the addition of $MnSO_4$ in small quantities enhances the rate of polymerization except at relatively high concentration. It is well known that Mn^{2+} ions undergo a disproportionation reaction with Mn^{4+} ions and produce Mn^{3+} ions at a rapid rate; in other words, the rate of carboxyl radical ion-producing reaction increases, and hence the rate of polymerization rises. The increase in the yield may be due to polymerization initiated by the Mn^{3+}–oxalate complex which persists even after the initiation of polymerization as indicated by the light violet color of the solution, and the higher the concentration of the added Mn^{2+} ions, the greater is the duration period of the complex.

It is difficult to explain the fall in the initial rate at relatively high concentration of added Mn^{2+} ions. It may be that under these conditions the concentration of Mn^{3+} ions becomes very high, and all of the Mn^{3+} ions do not find time to form a complex with oxalate ions; a fraction of the hydrated Mn^{3+} ions probably causes oxidative chain termination of polyacrylonitrile radicals which is known to occur with hydrated Fe^{3+} ions.[15,16]

b. Detergents. Two types of detergents were used: (*1*) anionic, e.g., sodium cetyl sulfate, and (*2*) cationic, e.g., cetyl trimethylammonium bromide (CTAB); the results are shown in Figure 10. In presence of detergents, the separating phase is a colloidal latex and, as expected, the rate of polymerization increases. This gives additional experimental evidence to

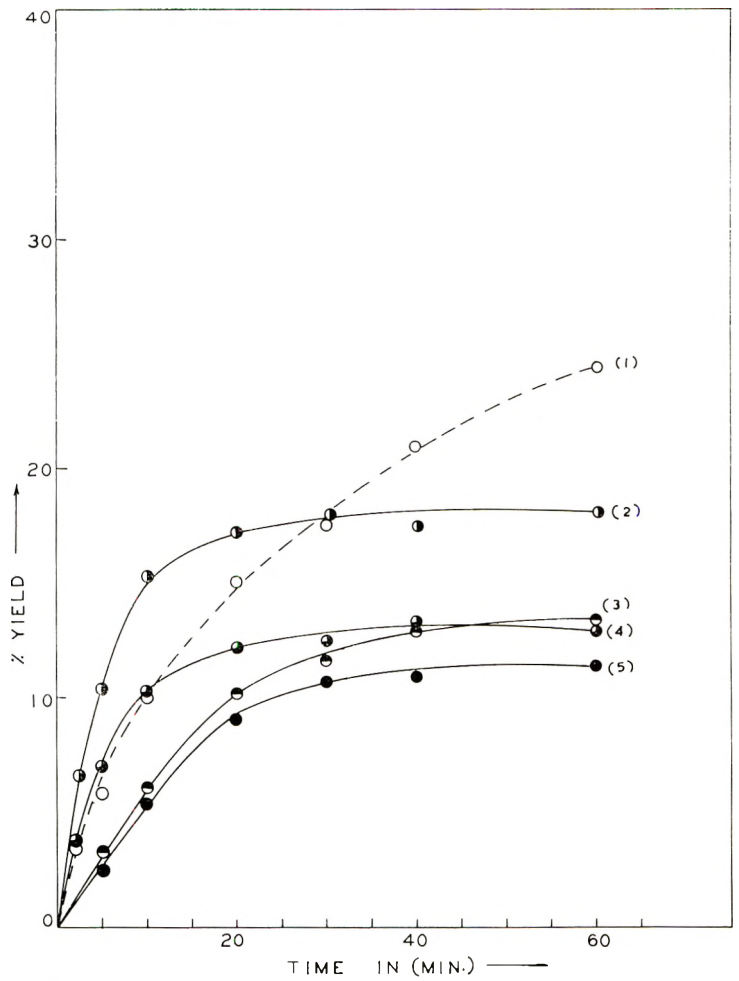

Fig. 9. Effect of inorganic salts on the rate of polymerization at monomer concentration of 0.30M, oxalic acid concentration of 0.08 $\times$ $10^{-2}M$, and permanganate concentration of 1.26 $\times$ $10^{-4}M$: (*1*) 4.0 $\times$ $10^{-2}M$ manganous sulfate; (*2*) 2.0 $\times$ $10^{-2}M$ manganous sulfate; (*3*) control; (*4*) 1.0 $\times$ $10^{-2}M$ manganous sulfate; (*5*) 4.0 $\times$ $10^{-2}M$ sodium sulfate.

support the conclusion of Palit and Guha[10] that in heterogeneous aqueous polymerization the rate of polymerization depends on the colloidal stability of the polymer. Baxendale and Madaras[17] also made a similar observation and reported that the rate of aqueous acrylonitrile polymerization increases in presence of CTAB. It is to be noted that the anionic detergent is a better peptizer than the cationic one.

c. Complexing Agents. Some species, such as fluoride and ethylenediaminetetraacetic acid, form complexes with higher valent manganese ions, and as a result the rate of carboxyl radical ion-producing reaction is suppressed and so the rate falls (Fig. 11). Weiss[9] also noted that the ad-

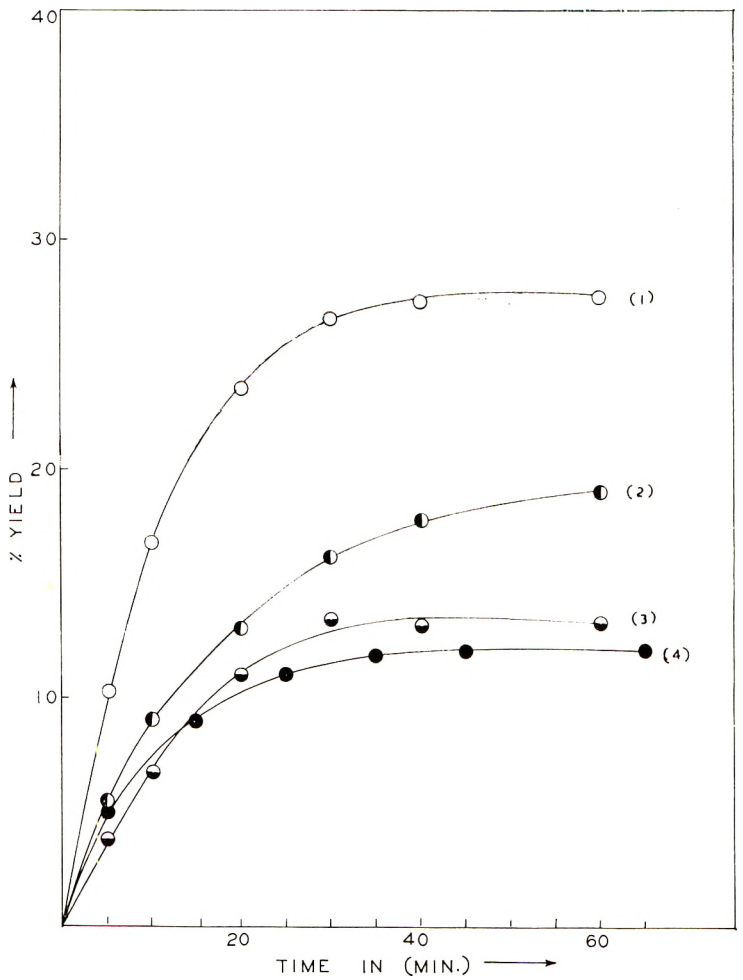

Fig. 10. Effect of detergents on the rate of polymerization at permanganate concentration of $1.26 \times 10^{-4}M$, oxalic acid concentration of $0.08 \times 10^{-2}M$, and acrylonitrile concentration of $0.30M$: (*1*) 0.01% sodium cetyl sulfate; (*2*) 0.1% cetyltrimethylammonium bromide; (*3*) control; (*4*) 0.01% cetyltrimethylammonium bromide.

dition of fluoride ions in the system containing Hg^{2+}, $H_2C_2O_4$, and MnO_4^- ions decreases the rate of production of Hg^+ ions, and attributed this to the fall in the rate of generation of "active" oxalic acid ($C_2O_4^{\cdot-}$).

Degree of Polymerization

The intrinsic viscosity of the polymer remains constant within experimental error in the range of oxalic acid concentration where the rate of polymerization is independent of activator concentration (Table III). A similar observation was made with methyl methacrylate polymerization.[2] In the $S_2O_8^{=}$–HSO_3^--initiated polymerization, Whitby et al.[11(a)] also got

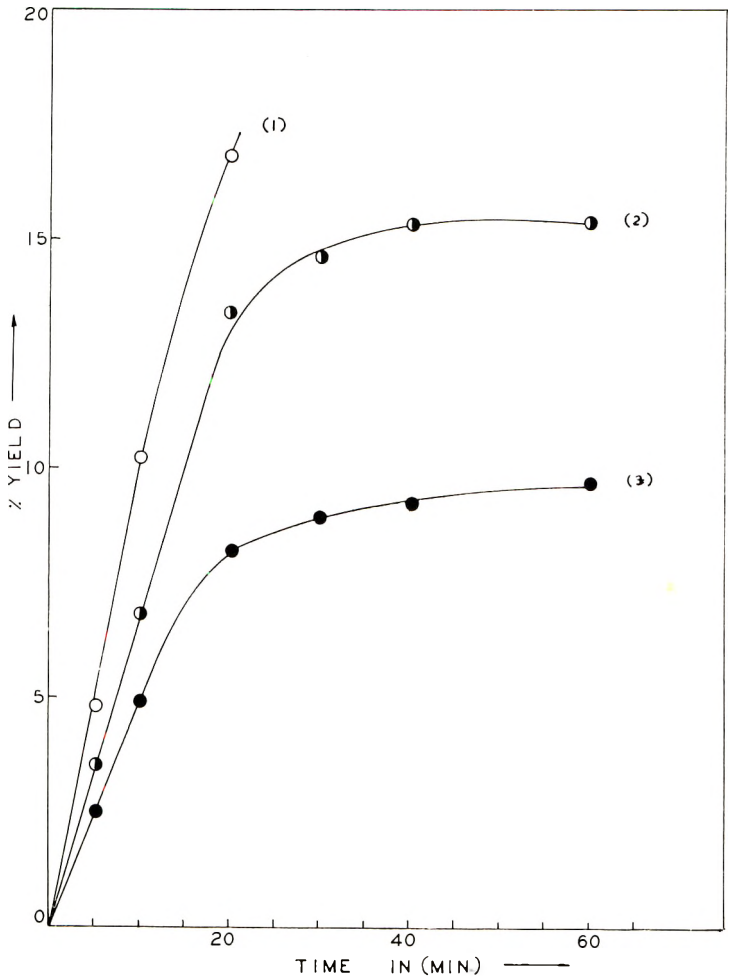

Fig. 11. Effect of complexing agents on the polymerization rate at monomer concentration of 0.30M, permanganate concentration of 31.65 $\times$ $10^{-5}M$, and oxalic acid concentration of 0.8 $\times$ $10^{-2}M$: (*1*) control; (*2*) 0.025% EDTA [disodium salt]; (*3*) 4.0 $\times$ 10^{-2} M NaF.

similar results. The molecular weight of the polymer however falls with further rise in oxalic acid concentration (Table III).

The reciprocal of the intrinsic viscosity varies approximately linearly with the square root of the catalyst concentration (Fig. 12). With the rise of temperature, the molecular weight of polymer falls (Table II).

When this work had been completed, we came across a recent paper by Yuguchi and Watanabe[18] who studied dilatometrically the aqueous acrylonitrile polymerization initiated by the permanganate–oxalic acid redox pair, and gave the rate of polymerization R_p by

$$R_p = k\,[KMnO_4]_0^{0.75}[H_2C_2O_4]_0^{0}[AN]^{1.9-2.0}$$

TABLE III
Variation of Intrinsic Viscosity with Oxalic Acid Concentration[a]

Oxalic acid concentration, mole/l. $\times 10^2$	$[\eta]$, 100 ml./g.
0.0625	2.35
0.125	2.40
0.25	1.89
0.50	1.80
1.0	1.63
4.0	1.60

[a] Acrylonitrile = 0.30 mole/l.; $KMnO_4 = 1.26 \times 10^{-4}$ mole/l.

The overall activation energy was found to be 9.3 kcal./mole. Unimolecular termination has been suggested. The degree of polymerization decreased with the rise of catalyst concentration, temperature, and with the

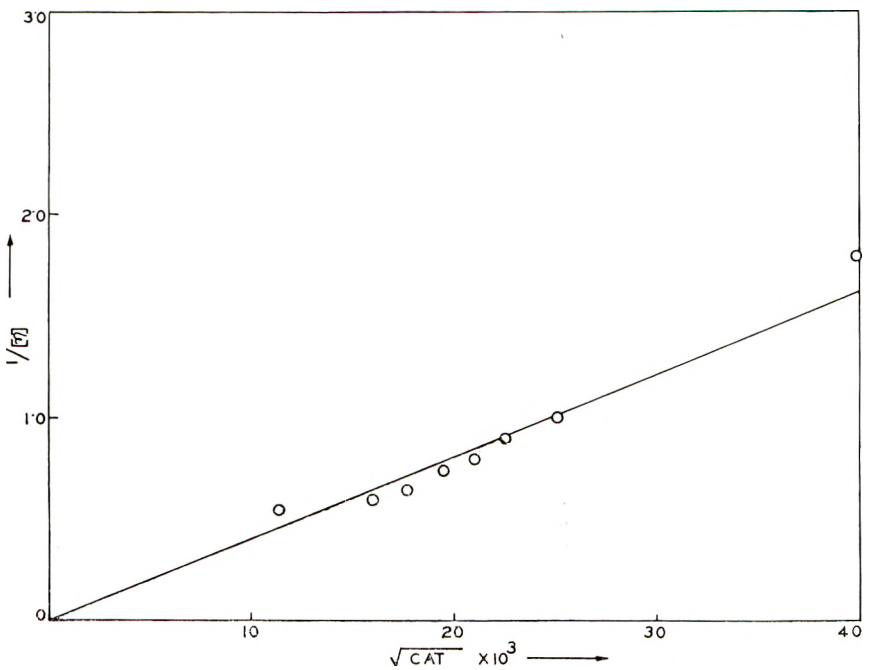

Fig. 12. Variation of the reciprocal of the intrinsic viscosity at 35 ± 0.05°C. with the square root of the catalyst ($KMnO_4$) concentration.

decrease in monomer concentration. Their results differ significantly from those of ours in some respects, but strongly support our conclusion on unimolecular chain termination in a precipitating medium.

Thanks are due to the C.S.I.R. (India) for giving financial assistance to one of us (R.S.K.) in the form of a senior research fellowship.

References

1. Konar, R. S., and S. R. Palit, *Proc. Symp. Redox Processes Allahabad Univ., India, February 1961*, Chemical Research Committee, C.S.I.R., New Delhi, p. 24.
2. Palit, S. R., and R. S. Konar, *J. Polymer Sci.*, **58**, 85 (1962).
3. Palit, S. R., and R. S. Konar, *J. Polymer Sci.*, **57**, 609 (1962).
4. Launer, H. F., and D. M. Yost, *J. Am. Chem. Soc.*, **56**, 2571 (1934).
5. Palit, S. R., A. R. Mukherjee, and R. Mitra, unpublished results.
6. Dean, W. R., V. Perera, and J. Glazer, *Trans. Faraday Soc.*, **53**, 679 (1957).
7. Baxendale, J. H., and C. F. Wells, *Trans. Faraday Soc.*, **53**, 800 (1957).
8. Ludbury, J. W., and C. F. Cullis, *Chem. Revs.*, **58**, 403 (1958).
9. Weiss, J., *Discussions Faraday Soc.*, **2**, 188 (1947).
10. (a) S. R. Palit and T. Guha, *J. Polymer Sci.*, **34**, 243 (1959); (b) M. Biswas and S. R. Palit, *J. Sci. Ind. Res. (India)*, **20B**, 160 (1961).
11. (a) G. S. Whitby, M. D. Gross, J. R. Miller, and A. J. Costanza, *J. Polymer Sci.*, **16**, 549 (1955); (b) D. Josefwitz and H. Mark, *Polymer Bull.*, **1**, 140 (1945); (c) L. B. Morgan, *Trans. Faraday Soc.*, **42**, 169 (1946).
12. Burnett, G. M., and G. L. Duncan, *Makromol. Chem.*, **51**, 154 (1962).
13. Brass, A. M., and H. P. Broida, *Formation and Trapping of Free Radicals*, Academic Press, New York, 1960, p. 369.
14. (a) F. S. Dainton, P. H. Seaman, D. G. L. James, and R. S. Eaton, *J. Polymer Sci.*, **34**, 209 (1959); (b) F. S. Dainton and P. H. Seaman, *ibid.*, **39**, 279 (1959).
15. Dainton, F. S., and D. G. L. James, *Trans. Faraday Soc.*, **54**, 649 (1958).
16. Dainton, F. S., and D. G. L. James, *J. Polymer Sci.*, **39**, 299 (1959).
17. Baxendale, J. H., and G. W. Madaras, *J. Polymer Sci.*, **19**, 171 (1956).
18. Yuguchi, S., and M. Watanabe, *Kobunshi Kagaku*, **18**, 273 (1961); *Chem. Abstr.*, **55**, 27945 (1961).

Résumé

On a étudié par gravimétrie la polymérisation de l'acrylonitrile, en milieu aqueux, initiée par le système redox permanganate-acide oxalique (32 ± 0.2°C.) La vitesse de polymérisation est indépendante de la concentration en acide oxalique dans un petit domaine de concentration. L'exposant du catalyseur varie d'une façon continue avec la concentration de celui-ci: il passe de 0.9 à basse concentration en catalyseur à 0.27 à concentration élevée en catalyseur pour une concentration en monomère de 0.3*M*. L'exposant du monomère est proche de l'unité dans le domaine des concentrations égales et supérieures à 0.3*M*. Le poids moléculaire du polymère est indépendant de la concentration en acide oxalique dans la région où la vitesse de polymérisation ne dépend pas de la concentration de celui-ci mais il décroît aux concentrations plus élevées en acide oxalique lorsque la concentration en catalyseur et la température augmentent. L'énergie d'activation totale est de 8.6 kcal/mole. L'addition de sels tels le Na_2SO_4, abaisse la vitesse de polymérisation mais l'addition de $MnSO_4$ à basse concentration augmente la vitesse, tandis qu'à concentration plus élevée, la vitesse initiale tombe. On suppose que les ions Mn^{+3} hydratés produisent une terminaison de chaîne oxydante des radicaux polyacrylonitriliques. Des agents complexants, tels les ions fluorures, l'acide tétraacétique de l'éthylène diamine etc., abaissent la vitesse de polymérisation tandis que l'addition de détergents produit l'effet contraire.

Zusammenfassung

Die Kinetik der wässrigen, durch das Redoxpaar Permanganat-Oxalsäure gestarteten Polymerisation von Acrylnitril wurde bei (32 ± 0,2)°C. gravimetrisch untersucht. Die Polymerisationsgeschwindigkeit ist von der Oxalsäurekonzentration in einem kleinen Bereich unabhängig. Der Katalysatorexponent ändert sich bei einer Monomerkonzentration von 0,30 M kontinuierlich mit der Katalysatorkonzentration und zwar von 0,9 bei niedriger bis 0,27 bei hoher Katalysatorkonzentration. Der Monomerexponent ist

im Konzentrationsbereich von 0,30 M und darüber fast eins. In demjenigen Bereich, in welchem die Polymerisationsgeschwindigkeit von der Oxalsäurekonzentration unabhängig ist, gilt das gleiche auch für das Molekulargewicht, doch sinkt dieses bei höheren Oxalsäurekonzentrationen mit steigender Katalysatorkonzentration und Temperatur ab. Die Bruttoaktivierungsenergie ist 8,6 kcal./Mol. Zusatz von Salzen wie Na_2SO_4 erniedrigt die Polymerisationsgeschwindigkeit. Dagegen führt ein Zusatz von $MnSO_4$ in niedriger Konzentration zu einer Erhöhung der Geschwindigkeit, während bei höheren Konzentrationen die Anfangsgeschwindigkeit absinkt. Es wird angenommen, dass hydratisierte Mn^{3+}-Ionen den oxydativen Kettenabbruch der Polyacrylnitrilradikale bewirken. Komplexierende Agenzien wie Fluoridionen, Äthylendiamintetraessigsäure etc. erniedrigen die Polymerisationsgeschwindigkeit, während der Zusatz von Detergentien sie erhöht.

Received March 8, 1963

JOURNAL OF POLYMER SCIENCE: PART A VOL. 2, PP. 1749–1764 (1964)

Structures of Vinylidene Chloride–Vinyl Chloride Copolymers

KENSUKE OKUDA, *Kureha Chemical Industry Co., Ltd., Tokyo Laboratory, Tokyo, Japan*

Synopsis

The relationships between composition and structure of vinylidene chloride (VDC)–vinyl chloride (VC) copolymer were investigated by various methods such as x-ray wide-angle and small-angle scattering, electron diffraction and microscopy, thermal analysis, and high resolution nuclear magnetic resonance. The copolymers used were made by suspension copolymerization below 5% conversion. The crystalline regions are fundamentally ismorphous to polyvinylidene chloride (PVDC) for the VDC–VC copolymers in the composition range from 1 to 0.560 in terms of the molar fraction of VDC (0.560 VDC). In the composition range below 0.145 VDC, the copolymers form crystallites isomorphous to polyvinyl chloride. The copolymers having the intermediate compositions are amorphous. In the composition range above 0.560 VDC, the average crystallite sizes of the uniaxially oriented specimens are almost constant; on the contrary, the long periods increase with decrease of the molar fraction of VDC. The intensities of the long-period diffraction peaks show a maximum for the copolymer in which the molar fraction of VDC is 0.685. The crystallinities, which were estimated from the x-ray method, decrease with decrease of the VDC fraction. The melting point depression is so small that it cannot be explained by Flory's equation. The results of NMR indicate that a large percentage of VC monomer units exists as sequences even in VDC-rich copolymers. PVDC and the VDC–VC copolymers higher than 0.745 VDC crystallize in the form of layer crystal aggregates from monochlorobenzene solutions. The molecules are sharply folded within these layers. The average crystallite sizes and long periods of the solution growth crystals are almost constant. These experimental facts cannot be interpreted in the terms of the structure which is expected by the copolymerization theory, but may be explained only on the basis of the molecular structure model which means the copolymer has a kind of block-type structure.

INTRODUCTION

It is well known that structures and physical properties of copolymers are influenced predominantly by their compositions. There have been so far many papers on the melting and glass transitions of copolymers. On the other hand, with respect to the crystallographic studies, there have been reported only a few papers which discussed the relationships between the compositions and crystal structures of copolymers such as ethylene–carbon monoxide copolymer (Polyketone),[1] 3-methyl-1-butene–4-methyl-1-pentene copolymer;[2] also a few papers[3,4] on the relationships between the compositions and diffraction patterns have been published. On some aspects

of the molecular configuration of copolymers, for instance, investigations by means of nuclear magnetic resonance spectroscopy of vinylidene fluoride–hexafluoropropylene copolymer,[5] and some studies by means of infrared absorption spectroscopy of vinylidene chloride–vinyl chloride copolymer[6] and ethylene–propylene copolymer[7] have been recently reported.

The relationship between composition and structure of the copolymer, in particular vinylidene chloride–vinyl chloride copolymer, has not been systematically investigated in spite of its practical importance.

The purpose of this study is to scrutinize the above-mentioned problem. Various methods, such as x-ray wide-angle and small-angle scattering, electron diffraction and microscopy, thermal analysis, infrared absorption, and high resolution nuclear magnetic resonance were applied in this work.

EXPERIMENTAL AND RESULTS

Samples

Copolymerizations were carried out below 5% conversion in a 10-liter autoclave at 50°C., because a large quantity of the samples of vinylidene chloride (VDC)–vinyl chloride (VC) copolymers of different compositions with narrow distributions were needed for the experiments. Copolymerization conditions were as follows: lauroyl peroxide (0.1% to monomer) was used as catalyst; the ratio of monomer to water was 1/2; a methanol solution of guaiacol (0.05% to monomer) was used as stopper reagent. The copolymers obtained were dissolved in tetrahydrofuran and precipitated with methanol, after Soxhlet extraction with methanol. The purified copolymers were dried at 40°C. under reduced pressure. The compositions of the copolymers were determined from chlorine analysis.

Polyvinylidene chloride (PVDC) was made under the same conditions.

Uniaxially oriented filaments of PVDC and VDC–VC copolymers were made by the following procedure. The monofilaments, from resins containing 3% plasticizer were extruded through a die (1 mm. diameter) at temperatures of 140–200°C. and then immediately quenched in a methanol bath (at −78°C.), were drawn to their maximum elongation at room temperature (about 15°C.), and were annealed at temperatures given in Table II.

As reference materials, vinylidene chloride–methyl acrylate (MA) copolymers and vinylidene chloride–octyl acrylate (OA) copolymers which had different compositions were copolymerized under nearly the same conditions as those of PVDC.

X-Ray Wide-Angle Diffraction

Powder patterns of PVDC and the VDC–VC copolymers were measured with a diffractometer using Ni-filtered CuKα radiation. For the uniaxially oriented filaments, photographs were taken with a cylindrical camera. In this case the fiber axis was tilted to the incident beam to permit observation of the (020) reflection,[8] beside the usual perpendicular position. The

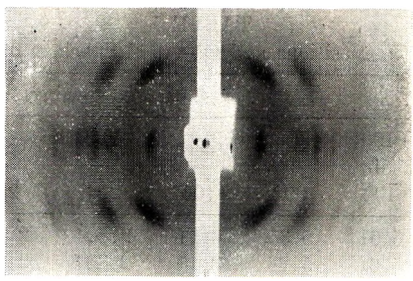

Fig. 1. Fiber photograph of cold-drawn PVDC.

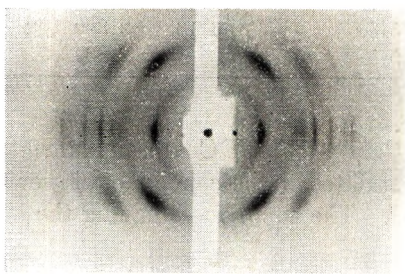

Fig. 2. Fiber photograph of cold-drawn VDC–VC copolymer (0.685 VDC).

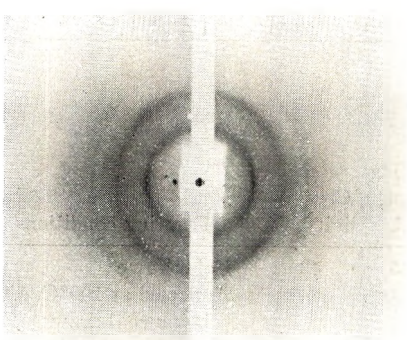

Fig. 3. Fiber photograph of cold-drawn VDC–VC copolymer (0.560 VDC).

x-ray beam used for these photographs was CuKα radiation monochromatized by a LiF single crystal.

Unit cell dimensions of PVDC and its copolymers (isomorphous to PVDC) have been given:[8] a = 6.73 A., b = 4.68 A. (fiber axis), c = 12.54 A., β = 123°35′, z = 4, monoclinic system, space group; C_2^2–P_{2_1}. The crystal structure will be reported in a following paper.[8]

Fiber photographs of PVDC, the VDC–VC copolymer, 0.685 in terms of the molar fraction of VDC (0.685 VDC), and the VDC–VC copolymer (0.560 VDC) are shown in Figures 1–3. These photographs were taken with a cylindrical camera using CuKα radiation monochromatized by LiF. The observed spacings are listed in Table I. It may be concluded from the results of the wide-angle diffraction that the crystalline regions of VDC–VC

TABLE I
Relationship between Compositions and Observed Spacings of VDC–VC Copolymers

Composition (molar fraction of VDC)	Observed spacings, A.						
	100 + $\bar{1}02$	002	104	200 + 204	$\bar{1}05$ + 205	005 + $\bar{3}05$	020
1.000 (PVDC)	5.61	5.35	3.11	2.804	2.440	2.081	2.343
0.905	5.61	5.28	3.10	2.804	2.440	2.089	2.343
0.820	5.63	5.28	3.11	2.809	2.443	2.086	2.343
0.745	5.61	5.28	3.11	2.809	2.443	2.086	2.343
0.685	5.63	5.28	3.11	2.809	2.450	2.089	2.350
0.603	5.63		3.13	2.809	2.450	2.089	2.343
0.560	5.57			2.809			2.350

copolymers higher than 0.560 VDC are fundamentally isomorphous to PVDC, and the crystallites of the copolymers lower than 0.145 VDC are isomorphous to PVC. The copolymers having the intermediate compositions are amorphous.

TABLE II
Relationship between Composition and Crystalline Parameters of VDC–VC Copolymers

Composition (molar fraction of VDC)	Melting point, °C.	Crystallinity, %	Drawing conditions	Average crystallite size along fiber axis, A.	Long period A.
1.000 (PVDC)	195	43	Cold-drawn	45	76
			Annealed at 100°C. after being cold-drawn[a]	48	90
0.905	192	34	Cold-drawn	45	80
			Annealed at 100°C. after being cold-drawn	48	96
0.820	188	33	Cold-drawn	45	84
			Annealed at 100°C. after being cold-drawn	47	96
0.745	185	28	Cold-drawn	45	87
			Annealed at 100°C. after being cold-drawn	47	100
0.685	183	22	Cold-drawn	41	103
			Annealed at 90°C. after being cold-drawn	43	119
0.603	183	19	Cold-drawn	41	135
			Annealed at 70°C. after being cold-drawn	43	142
0.560	183	20	Cold-drawn	42	—

[a] Annealing was carried out under constant length, for 10 min., in a water bath.

In this paper, the VDC–VC copolymers which are 1 to 0.560 VDC in their compositions will be discussed.

The x-ray measurements of crystallinity were carried out in powder state with a diffractometer, because it was impossible to apply other methods in this case.

The scattering due to continuous x-ray was removed by using the balanced-filter method.[9] The Compton scattering was neglected.

Separation of the crystalline and amorphous components from whole diffraction curves was carried out according to Hermans' method.[10] The per cent crystallinity shown in Table II was calculated from the integrated intensities of both components in the angle range between 10° and 50°.

The radial broadness of the (020) reflection in the tilt photographs was measured with a microphotometer; the average crystallite sizes, D_{020}, in the direction parallel to the fiber axis were calculated by using Scherrer's line broadening equation:[11]

$$D_{hkl} = K \cdot \lambda / (\beta \cdot \cos \theta)$$

where D_{hkl} is the average size of the crystallites perpendicular to the (hkl) planes in angstroms, K is a constant (0.9[11] used here), and β is the pure breadth at half-maximum intensity of the (hkl) reflection having wavelength λ and Bragg angle θ. In this case, corrections for the instrumental broadening were neglected,[12] because $b/B < 0.1$, where b is the breadth due to instrumental conditions obtained by using finely powdered quartz, and B is the experimentally observed breadth of the (hkl) reflection. As well known, the crystallite size derived from the line broadening of x-ray diffraction always includes some amounts of error due to lattice imperfection.

As a measure of the average crystallite sizes in the direction perpendicular to the fiber axis, D_{h0l} were measured in a similar way by using the equatorial reflection in which the $(\bar{2}04)$ reflection were superposed on the (200) reflection. The intensity of the (200) reflection is five times greater than that of the $(\bar{2}04)$ reflection.[8] The average crystallite sizes measured with that reflection, therefore, may be regarded as D_{200}. It was impossible to measure the average sizes in other equatorial directions, because of superposition or weakness of the intensities of other reflections.[8]

For reference, the degrees of parallelity of the uniaxially oriented filaments used were estimated from their fiber photographs (taken with a flat camera), as a measure of crystallite orientation. The degree of parallelity, π, was defined by the following equation:[13]

$$\pi = (180 - \beta)/180$$

where β is the breadth at half-maximum intensity along the Debye ring of the (hkl) reflection in degrees, the reflection used here in which the (100) and $(\bar{1}02)$ reflections were mutually superposed.

The degrees of parallelity of these filaments were about 0.94, except for the VDC–VC copolymer (0.560 VDC) (0.90).

X-Ray Small-Angle Scattering

The small-angle scattering photographs were obtained with an unfiltered x-ray beam through a pin hole slit system with a flat plate at a distance of 180 mm. from the specimen. The uniaxially oriented filaments of PVDC and the VDC–VC copolymers higher than 0.603 VDC show a typical long-

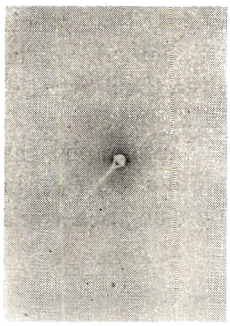

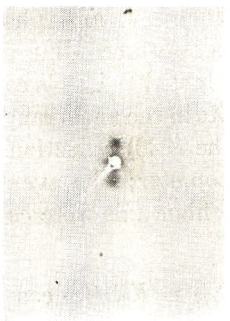

Fig. 4. Small-angle scattering photograph of cold-drawn PVDC. Fiber axis vertical.
Fig. 5. Small-angle scattering photograph of cold-drawn VDC–VC copolymer (0.685 VDC). Fiber axis vertical.
Fig. 6. Small-angle scattering photograph of cold-drawn VDC–VC copolymer (0.560 VDC). Fiber axis vertical.

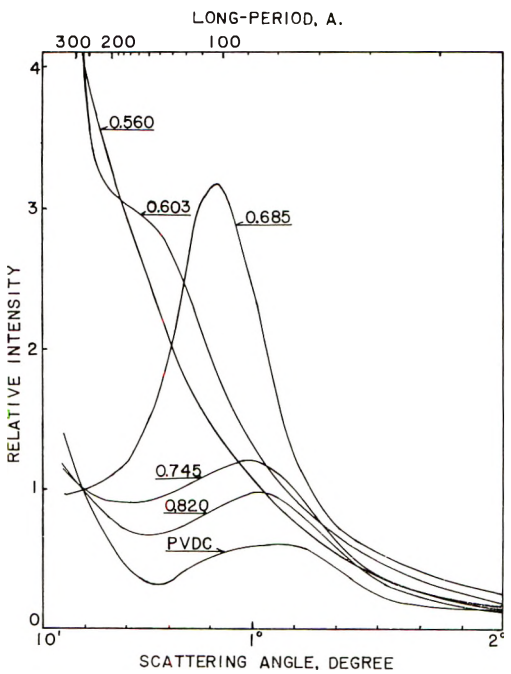

Fig. 7. Relative long-period diffraction curves of VDC–VC copolymers (cold-drawn). Numbers in the figure represent the molar fraction of VDC of the copolymers.

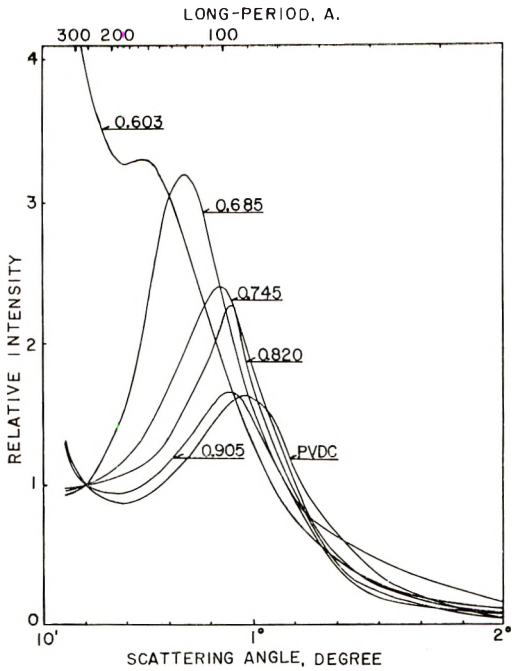

Fig. 8. Relative long-period diffraction curves of VDC–VC copolymers (heat-treated after being cold-drawn). Numbers in the figure represent the molar fraction of VDC of the copolymers.

period diffraction, as seen in Figure 4 and 5, but the VDC–VC copolymer (0.560 VDC) shows a continuous scattering (Fig. 6).

Furthermore, the long-period diffraction was measured by means of fixed count method with a small-angle diffractometer (Rigaku-Denki Co., Ltd.). The guard slit was not used, because it was required to fix specimens directly on the second slit.

Figures 7 and 8 are the relative long-period diffraction curves of the cold-drawn and the heat-treated filaments obtained with Ni-filtered CuKα radiation. In these curves, the scatterings from both air and the slit edges were experimentally eliminated, but the collimation error was not corrected. The long periods which were calculated by Bragg's equation from the positions of maximum intensities of these curves are given in Table II. The long periods of the heat-treated specimens are longer than those of the cold-drawn ones over the entire composition range under consideration. This phenomenon is not unusual, and may be explained by the similar phenomenon in D_{020}.[14]

Thermal Analysis

The specific heats of PVDC and its copolymers were measured in the powder state with an automatic recording differential thermal analyzer and adiabatic calorimeter (Rigaku-Denki Co., Ltd., Japan).

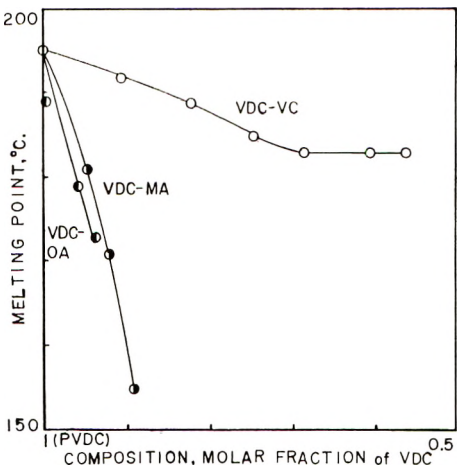

Fig. 9. Melting points vs. compositions for VDC–VC, VDC–MA, and VDC–OA copolymers.

In the cases of PVDC, the VDC–VC copolymers, the VDC–MA copolymers, and the VDC–OA copolymers (higher than 0.745, 0.917, and 0.935 VDC, respectively), two peaks are observed in the specific heat versus temperature curves. The lower peaks obviously disappear when the samples are annealed at temperatures just above the temperatures of the lower peaks, but no difference can be found between the x-ray diagrams of the untreated and the annealed powder, and it is impossible to find at the annealing temperatures the macroscopic features of melting. Similar phenomena have been reported by Dole,[15] but at present it is very difficult to

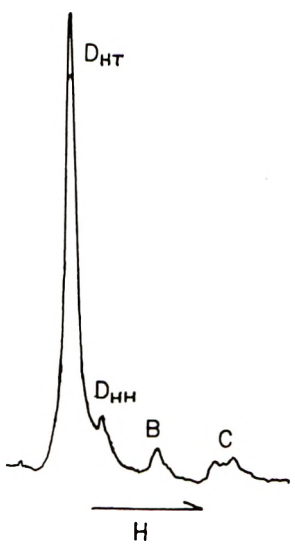

Fig. 10. NMR absorption spectrum of VDC–VC copolymer (0.820 VDC).

explain the lower peaks. It is evident that the higher peaks correspond to the melting of crystallites having normal structure. It was found by thermogravimetric analysis that a decrease in weight—probably due to dehydrochlorination—occurred after melting. The melting points of PVDC and the VDC–VC copolymers are given in Table II and Figure 9 and those of the VDC–MA copolymers and the VDC–OA copolymers in Figure 9.

High Resolution Nuclear Magnetic Resonance

The proton magnetic resonance of solutions of PVDC and the VDC–VC copolymers in *o*-dichlorobenzene (10%) was measured with a Varian Associates Model V-4311 high resolution NMR spectrometer operating at 60 mcycles/sec. equipped with a variable temperature probe accessory, Model V-4340, at a high temperature (about 100°C.) to get better solubility of the polymers and to attain better resolution of the spectra. One of the spectra is illustrated in Figure 10. The peak C is assigned as the resonance effect due to the methylenic protons in VC sequences, from the information obtained on PVC and its model compounds; the assignments of other peaks is not decided at present.[16]

Solution Growth Crystals

For the purpose of this investigation, powders of PVDC and the VDC–VC copolymers were dissolved in monochlorobenzene (at 132°C.) and crystallized in the form of a suspension by lowering slowly the temperature of the solutions (0.01% to 0.1%) to room temperature.

The suspension was picked up on a collodion film and was directly examined under a electron microscope, JEM-5Y (Japan Electron Optics Laboratory Co., Ltd.). The crystals grown from the solutions of PVDC and the VDC–VC copolymers higher than 0.745 VDC were obtained in many cases in the form of layerlike aggregates as seen in Figure 11. Single

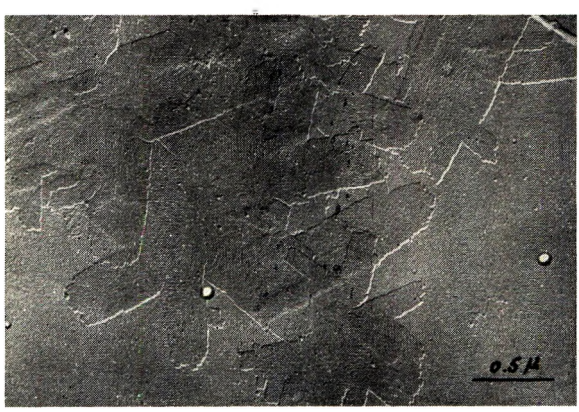

Fig. 11. Electron micrograph of solution growth crystals of VDC–VC copolymer (0.905 VDC). Crystallized in the form of a suspension from 0.015% monochlorobenzene solution, Pt shadowed, ×30,000.

crystals with well-defined faces equivalent to that observed, for example, in polyethylene[17] have not yet been obtained. It is thought to be due to solubility that such crystals of VDC–VC copolymers lower than 0.685 VDC cannot be obtained under that condition. The direction of molecules was examined by selected area electron diffraction. These electron diffraction photographs, however, showed only a pattern due to twin structure in spite of the similarity in appearance to single crystal material.

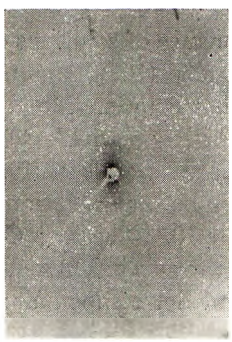

Fig. 12. Small-angle scattering photograph of solution growth crystal sediment of VDC–VC copolymer (0.745 VDC). Fiber axis vertical.

When the suspension was filtered slowly,[18] the sedimenting crystals formed a film. These films could be used for x-ray examinations. When the beam was perpendicular to the film surface, the wide-angle diffraction diagram consisted of continuous rings. On the other hand, when the beam was parallel to the film surface, a diagram of fiber symmetry was obtained. The average crystallite sizes on the D_{020} of these films were measured by the method described above. The results are given in Table III. The small-angle scattering photographs of such films were also taken with the camera previously described. As seen in Figure 12, these photographs gave weak but sharply defined diffractions corresponding to the lattice planes parallel to the film surface with the Bragg spacings given in Table III.

TABLE III
Relationship between Compositions and Periodicities of Solution Growth Crystals of VDC–VC Copolymers

Composition (molar fraction of VDC)	Long period, A.	Average crystallite size along fiber axis, A.
1.000 (PVDC)	76	50
	74[a]	53[a]
0.905	78	54
0.820	76	44
	78[a]	50[a]
0.745	72	45

[a] Heat-treated at 100°C. for 20 min., in an air bath.

These experiments suggest that the molecules are either perpendicular to these layers or nearly so and must be sharply folded within these layers. The long period is smaller than the folding period, i.e., the layer thickness which was assessed from the shadows in the electron micrographs. A more detailed report on the morphological investigations will be published at a later date.

DISCUSSION

The melting point depression in copolymers can be expressed by Flory's equation:[19]

$$1/T_m - 1/T_m^\circ = -(R/\Delta H_u)\ln p$$

where T_m° and T_m are the melting points of the homopolymer composed of A units (i.e., VDC units in this study) and the copolymer, respectively, R is the gas constant, ΔH_u is the heat of fusion per mole of A units, and p is the probability that in the copolymer an A unit is succeeded by another A unit, independent of the number of A units preceding the given one. For a random copolymer, $p = X_A$, where X_A is the molar fraction of A units, while for a vinyl copolymer $p \geqq X_A$. For the VDC–MA copolymers and the VDC–OA copolymers which can be regarded as random copolymers,[20] ΔH_f, the true heat of fusion per gram of PVDC obtained from Flory's equation, was 11–15 cal./g. In the case of the VDC–VC copolymers which are not random copolymers,[20] ΔH_f values more than 100 cal./g. were obtained.

From the experiment on the melting point depression of PVDC by α-methyl benzyl ether as a diluent,[19] we obtained about 14 cal./g. as ΔH_f. The ΔH_f value obtained from the calorimetric measurement was about 15 cal./g.; 0.43 was used as the weight fraction of crystallinity.[21]

These results indicate that the melting point depression of the VDC–VC copolymers cannot be explained by Flory's equation.

The average crystallite sizes in the direction parallel to the fiber axis of the uniaxially oriented filaments of the VDC–VC copolymers are almost constant; D_{020} = 40–50 A., in the composition range from 1 to 0.560 in terms of the molar fraction of VDC (Table II). This result means that the scattered x-rays are in phase among about twenty monomer units in the direction parallel to the molecular axis. Simply considered, it is supposed that the majority of VDC units exists as VDC sequences having more than twenty monomer units, in other words, the VDC–VC copolymers are block-type copolymers, and the crystallites are almost all composed of VDC units. This view is supported by two facts: one is the smaller melting point depression, which means the copolymer is a block-type copolymer;[22] the second is the results of NMR. As seen in Figure 10, the intensity of the absorption by VC sequences indicates that a large percentage of VC monomer units exists as sequences even in such VDC-rich copolymer.

The above view, however, is rejected by the copolymerization theory[20,23] and the infrared study of VDC–VC copolymers.[6] The average sequence

length of VDC units of the VDC–VC copolymer (0.560 VDC) calculated by the theory is about 2; values used for the monomer reactivity ratios, r_1 and r_2, were 3.2 and 0.3,[20] respectively. The infrared study leads to similar results. These facts may suggest that VC monomer units are included, as a fault, in the copolymer crystallites isomorphous to PVDC. On the inconsistency between these models, the results of the small-angle scattering will give a solution.

There have been so far presented many theories on the long-period diffraction of fiber substance, such as the theories of Kratky and Porod[24] and Hess and Kiessig[25] and Hosemann's recent review on this problem.[26] However, it is generally difficult to find an interpretation applicable in any case.[27] In this case, therefore, the interpretations of small-angle scatterings were forced to be limited in some particular conceptions. For instance, it may be possible to discuss qualitatively the scatterings on the basis of the lamella-packing model of Kratky.[24]

The long periods considerably increase with decrease of the molar fraction of VDC, as seen in Table II. On the contrary, increases of crystallite sizes on the D_{020} are very small as compared with those of the long periods. These results indicate that referring to the Kratky's theory, the x-ray scattering systems of the uniaxially oriented filaments continuously change from densely packed particle systems to dilute particle systems, as the molar fraction of VDC decreases. This change is also shown by the decreasing crystallinities of the powder samples, as seen in Table II. This is reasonable at least qualitatively, although the per cent crystallinities of the filaments cannot be discussed on the same basis as those of the powder samples.

The intensities of the long-period diffraction peaks show maxima for the specimens in which the molar fraction of VDC is 0.685, for both the cold-drawn and the heat-treated system, as seen in Figure 7 and 8. A decrease in the scattering intensity for the copolymers in the composition range from 0.685 to 0.560 VDC is explained as due to a change of density inhomogeneity in the specimens from densely packed particle systems into dilute particle systems.[24,27] The nature of the scattering intensity curves for the specimens in the composition range from 1 to 0.685 VDC cannot be interpreted in the above point of view. The decrease of the intensity of the scattering maximum may be also due to the increase of the relative fluctuation of the interparticle distance.[24] It is, however, very difficult to conclude that the relative fluctuations decrease with decrease of the molar fraction of VDC, because this fact is somewhat incompatible with the copolymerization theory.[23] Such a nature of the scattering intensity curves for the copolymers in the composition range from 1 to 0.685 VDC cannot be explained by the relative fluctuation only. It is evident that the intensity of the small-angle scattering is proportional to the square of the difference of electron densities between particles and media, i.e., crystallites and the amorphous regions.[27] Such a nature of the scattering intensity curves for the copolymers over the entire composition range, therefore, should be interpreted not only from the periodicity in density in-

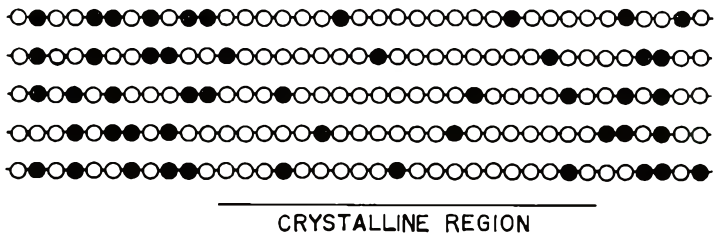

Fig. 13. A schematic model of molecular structure and fine texture of VDC–VC copolymer: (O) VDC units; (●) VC units.

homogeneity in the scattering systems but also from the difference of electron densities between crystallites and the amorphous regions.

From this point of view, such a difference of the electron densities may be interpreted by a model in which the composition of the crystalline regions is rich in VDC as compared with the overall composition of the copolymer; on the contrary, the composition of the amorphous regions is rich in VC. By this model, the difference of electron densities between both regions becomes greater with decrease of the molar fraction of VDC, if the compositions of the crystalline regions are approximately equal to each other, independently of the overall compositions of the copolymers. This model may be realized only by the molecular structure satisfying the following conditions: (*1*) the average sequence lengths of VDC units, of course, become shorter with decrease of the molar fraction of VDC; (*2*) VDC sequences have a distribution in the lengths; and (*3*) longer VDC sequences exist as blocks in the molecular chains. Under considerations of these conditions, a schematic model of molecular structure and fine texture of the copolymer is illustrated in Figure 13.

The periodicity in density inhomogeneity is easily understood from this model, that is, the average distances between crystallites in the direction parallel to the fiber axis should increase with decrease of the molar fraction of VDC, because the average crystallite sizes in that direction are considered almost constant.

In this molecular structure model, the crystallites of the VDC–VC copolymers are assumed to be composed predominantly of blocks of longer VDC sequences. On the contrary, in the amorphous regions, blocks of shorter VDC sequences may be predominant. This assumption may be supported by the following facts. Firstly, results of the wide-angle diffraction studies show that the average crystallite size in the direction parallel to the fiber axis is almost constant, and the average crystallite size in the direction perpendicular to the (200) planes is of the order of several tens of Angstroms over the entire composition range under consideration. The latter result also is believed to be evidence to support the model, because more than ten molecules should be regularly aggregated in the direction perpendicular to the (200) planes even in the VDC–VC copolymer (0.560 VDC). Secondly, a decrease of the per cent crystallinity in the

diffraction curves of powder samples is attributed mainly to the increase of the background scattering for the samples in the composition range from 1 to 0.745 VDC and also to the decrease of the lattice component of the scattering for the copolymers in the composition range from 0.745 to 0.560 VDC. The decrease of the lattice component is appreciable on the others than the (h00) reflection, as seen in Table I and Figure 1–3. This fact leads us to the following speculations. The molecules may form a crystallite including a small number of VC units in it; then, such VC units in the crystallites increase more and more with decrease of the molar fraction of VDC, and finally become too many to permit formation of a regular lattice. The third fact supporting the molecular model is the smaller melting point depression. Fourth, the average crystallite sizes in the fiber direction of the uniaxially oriented VDC–VC copolymers are almost equal to or somewhat greater than those of the uniaxially oriented VDC–MA copolymers and VDC–OA copolymers in which the molar fractions of VDC are nearly equal to those of the corresponding VDC–VC copolymers and which were spun under the same conditions as the VDC–VC copolymers. On the other hand, the long periods of the former are smaller than those of the latter. The intensities of the long-period diffraction peaks of the latter are generally stronger than those of the former. This is an evidence for the model, because electron densities of MA units and OA units are estimated as to be smaller than those of VC units.

As seen in Table III, the average crystallite sizes in the fiber direction of the solution growth crystals decrease somewhat with decreasing molar fraction of VDC and are almost equal to those of the drawn samples. The long periods are almost constant, in spite of the variations of the molar compositions. It seems that the intensities and sharpness of the long-period diffraction peaks do not change much. On heat treatment, the average crystallite sizes increase a fair amount, but the long periods scarcely increase, as indicated in Table III. This is also evidence for the above mentioned arguments.

As described above, all the experimental results in this paper were explained only on the basis of the molecular structure model proposed here. In Figure 10 a peak, D_{III} is assigned as the resonance effect due to the methylenic protons in VDC units bonded in head-to-head sequence.[16] This peak is not observed in the spectrum of PVDC. The absorption intensity of this peak increases with decrease of the molar fraction of VDC. Therefore, if the head-to-head bonds of VDC units exist in the shorter sequences, our model may be compatible with the NMR investigation[16] too. This model, also, is believed to be not inconsistent with the results of the infrared study,[6] if distributions in the sequence lengths are taken into consideration in the interpretation of those results.

It may be concluded that VDC–VC copolymer made by the usual suspension copolymerization is a kind of block copolymer in which longer VDC sequences are aligned as blocks in the molecular chains, although this

structure may be inconsistent with the structure which is expected by the copolymerization theory.[20,23]

The author would like to express his thanks to Prof. M. Kakudo of Osaka University and Dr. M. Asahina of this Laboratory for their helpful advice, and also to Mr. A. Aida who kindly provided the copolymer samples.

References

1. Chatani, Y., T. Takizawa, and S. Murahashi, paper presented at the 15th Annual Meeting of The Chemical Society of Japan, Kyoto, April 1962.
2. Redding, F. P., and E. R. Walter, *J. Polymer Sc.*, **37**, 555 (1959).
3. Kargin, V. A., and G. S. Markova: *Zhur. Fiz. Khim.*, **27**, 1525 (1953).
4. Beevers, R. B., E. F. T. White, and L. Brown, *Trans. Faraday Soc.*, **56**, 1535 (1960).
5. Fergson, R. C., *J. Am. Chem. Soc.*, **82**, 2416 (1960).
6. Enomoto, S., *J. Polymer Sci.*, **55**, 95 (1961).
7. van Schooten, J., E. W. Duck, and R. Berkenbosh, *Polymer*, **2**, 357 (1961).
8. Okuda, K., paper presented at the 10th Annual Meeting of The Society of Polymer Science, Japan, Tokyo, May 1961.
9. Ross, P. A., *J. Opt. Soc. Am.*, **16**, 433 (1928).
10. Hermans, P. H., and A. Weidinger, *J. Appl. Phys.*, **19**, 491 (1948); *J. Polymer Sci.*, **4**, 135 (1949).
11. Saitô, Y., in *X-Sen Kesshô-Gaku*, Vol. II, I. Nitta, Ed., Maruzen, Tokyo, 1961, p. 489.
12. Alexander, L. E., and H. P. Klug, *J. Appl. Phys.*, **21**, 137 (1950).
13. Go, Y., and K. Kubo, *Kogyo Kagaku Zasshi*, **39**, 929 (1936).
14. Statton, W. O., *J. Polymer Sci.*, **41**, 143 (1959).
15. Dole, M., *Fortschr. Hochpolymer. Forsch.*, **2**, 221 (1960).
16. Chûjô, R., unpublished data.
17. Keller, A., *Phil. Mag.*, **2**, 1171 (1957).
18. Keller, A., and A. O'Connor, *Nature*, **180**, 1289 (1957).
19. Flory, P. J., *J. Chem. Phys.*, **17**, 223 (1949).
20. Alfrey, T., J. J. Bohrer, and H. Mark, *Copolymerization*, Interscience, New York, 1952.
21. Dole, M., and B. Wunderlich, *Makromol. Chem.*, **34**, 29 (1959).
22. Mandelkern, L., *Chem. Revs.*, **56**, 903 (1956).
23. Bamford, C. H., W. G. Barb, A. D. Jenkins, and P. F. Onyon, *The Kinetics of Vinyl Polymerization by Radical Mechanisms*, Butterworths, London, 1958, p. 148.
24. Kratky, O., and G. Porod, *J. Colloid Sci.*, **4**, 35 (1949); G. Porod, *Kolloid-Z.*, **124**, 83 (1951).
25. Hess, K., and H. Kiessig, *Z. Physik. Chem.*, **193**, 196 (1944).
26. Hosemann, R., *Polymer*, **3**, 349 (1962).
27. Kakudo, M., in *X-Sen Kesshô-Gaku*, Vol. II, I. Nitta, Ed., Maruzen, Tokyo, 1961; p. 517; A. Guinier, and G. Fournet, *Small-Angle Scattering of X-Rays*, Wiley, New York–London, 1955.

Résumé

On a étudié les relations entre les compositions et les structures du copolymère de chlorure de vinylidène (VDC) et chlorure de vinyle (VC) par diverses méthodes telles que la diffusion des rayons-X à grand et petit angle, diffraction des électrons et microscopie, analyse thermique, et résonance magnétique nucléaire à haute résolution. Les copolymères utilisés ont été préparés par copolymérisation en suspension, le degré de conversion étant inférieur à 5%. Les régions cristallines sont fondamentalement ismorphes au chlorure de polyvinylidène (PVDC) pour les copolymères de VDC–VC dans le domaieu

de composition de 1 à 0.560 fraction molaire de VDC (0.560 VDC). Dans le domaine de composition en-dessous de 0.145 VDC, les copolymères forment des cristallites isomorphes au chlorure de polyvinyle. Les copolymères ayant des compositions intermédiaires sont amorphes. Dans le domaine de composition au-dessus de 0.560 VDC les dimensions moyennes des cristallites des spécimens orientés de façon non-axiale sont presque constantes, au contraire les longues séquences croîssent lorsque la fraction molaire de VDC décroît. Les intensités des pics de diffraction des longues séquences montrent une valeur maximum dans le copolymère dont la fraction molaire en VDC est 0.685. Les cristallinités, estimés au moyen de la méthode des rayons-X, décroîssent bien sûr, lorsque décroît la fraction de VDC. La dépression du point de fusion est si faible qu'elle ne peut pas être expliquée par l'équation de Flory. Les résultats de NMR indiquent qu'il existe, même dans les copolymères riches en VDC, un grand pourcentage d'unités monomériques VC séquencées. Le PVDC et les copolymères de VDC–VC avec plus de 0.745 VDC cristallisent sous forme d'aggrégats de couches cristallines à partir de leurs solutions dans le monochlorobenzène. Les molécules sont en plis serrés à l'intérieur de ces couches. Les dimensions moyennes des cristallites et les longues séquences des cristaux développés à partir de la solution sont presque constantes. Ces faits expérimentaux ne peuvent pas être interpêtés en termes de structure selon la théorie de la copolymerisation, mais peuvent uniquement être expliqués sur base du modèle de structure moléculaire qui implique que le copolymère se presente sous forme d'une sorte de copolymère séquencé.

Zusammenfassung

Die Beziehungen zwischen Zusammensetzung und Struktur wurden an Vinylidenchlorid (VDC)–Vinylchlorid(VC)–Copolymeren mit Hilfe verschiedener Methoden, wie Röntgenbeugung bei grossen und kleinen Winkeln, Elektronenbeugung und mikroskopie, thermische Analyse und magnetische Kernresonanz hoher Auflösung untersucht. Die Copolymeren wurden durch Suspensions-Copolymerisation zu Umsätzen unter 5% hergestellt. Im Bereich des VDC-Molenbruches von 1 bis 0,560 (0,560 VDC) sind die kristallinen Bereiche der VDC–VC-Copolymeren grundsätzlich isomorph mit Polyvinylidenchlorid (PVDC). Im Bereich unter 0,145 VDC sind die von den Copolymeren gebildeten Kristallite isomorph mit Polyvinylchlorid. Copolymere mit dazwischen liegender Zusammensetzung sind amorph. Im Zusammensetzungsbereich über 0,560 VDC ist die mittlere Kristallitgrösse der in einer Richtung orientierten Proben fast konstant, dagegen steigen die Langperioden mit abnehmendem VDC-Molenbruch an. Die Intensität der Beugungsmaxima der Langperioden hat bei Copolymeren mit einem VDC-Molenbruch von 0,685 ein Maximum. Die mittels der Röntgenmethode bestimmte prozentuelle Kristallinität nimmt natürlich mit abnehmendem VDC-Molenbruch ab. Die Schmelzpunktserniedrigung ist kleiner als der Flory-Gleichung entsprechen würde. Die NMR-Ergebnisse zeigen, dass auch in VDC-reichen Copolymeren ein Grossteil der VC-Monomereinheiten in Sequenzen vorliegt. PVDC und die VDC–VC-Copolymeren mit höherem VDC-Molenbruch als 0,745 kristallisieren aus ihrer Lösung in Monochlorbenzol in Form von Schichtkristallaggregaten. Innerhalb dieser Schichten sind die Moleküle scharf gefaltet. Die mittlere Kristallitgrösse und die Langperioden der aus der Lösung gewachsenen Kristalle sind fast konstant. Diese experimentellen Ergebnisse können nicht durch die nach der Copolymerisationstheorie zu erwartenden Strukturen erklärt werden, sondern nur auf der Basis eines Molekülstrukturmodelles, nach welchem das Copolymere eine Art Block-Copolymeres ist.

Received March 11, 1963

JOURNAL OF POLYMER SCIENCE: PART A VOL. 2, PP. 1765–1784 (1964)

The Chemistry of Poly(vinyl Chloride) Stabilization. III.* Organotin Stabilizers Having Radioactively Tagged Alkyl Groups

ALFRED H. FRYE, RAYMOND W. HORST, and MARKO A. PALIOBAGIS, *The Cincinnati Milling Machine Company, Cincinnati, Ohio, and The Advance Division of the Carlisle Chemical Works, New Brunswick, New Jersey*

Synopsis

The stabilizing action of a representative group of organotin compounds of the formula Bu_2SnY_2 has been studied by a radioactive tracer technique, the tags (^{14}C) being located in the butyl group's C_1-position. The Y groups of the chosen organotin compounds were: monomethyl maleate, oxoöctyl thioglycolate, β-mercaptopropanoate, and 2-ethylhexanoate. It was found that after a sequence of two dissolution and precipitation cycles (using tetrahydrofuran and methanol) an appreciable portion of radioactivity is retained by the resin, the resins having been previously admixed with the tagged stabilizer, milled into films and then subjected to carefully controlled heat treatments. Under these conditions it was found that the amount of radioactivity retained by the resin was determined by the nature of the Y group and the duration of the heat treatment. Further, it was found that for a given Y group, the amount of retention first increases with increase in the duration of the heat treatment, reaches a maximum, and then drops off. However, the amount of radioactivity retained by such a resin was not found to be constant when the sample was subjected to further dissolution–precipitation cycles, but, within the limits of the present experiments, to decrease markedly with each successive cycle. It is suggested that the major portion of this retention is due to the formation of an associative link between the polymer and the organotin compound and that this linkage is partially ruptured by the tetrahydrofuran–methanol treatment. It is also shown that only a very minor portion of the radioactivity retained by the precipitated resin can be due to actual butylation of the resin as preposed by Kenyon, and that it is unlikely that it could contribute appreciably to the resin's stabilization. It is suggested that the formation of an associative complex between the resin and the organotin compound functions as a precursor wherein certain relatively labile centers in the polymer chain can be altered, possibly by a displacement reaction involving the organotin compound's Y group, and int his way retard or inhibit the zipperlike elimination of hydrogen chloride which is the initial phase of the polymer's degradation.

INTRODUCTION

The deterioration of poly(vinyl chloride) by the action of heat and light, as well as the retardation of that deterioration by the inclusion of chemical additives, are subjects of considerable practical and theoretical interest.

* For Parts I and II of this series, see Frye and Horst.[1,2]

Over the course of the past twenty-five or so years, many substances and combinations of substances have been found which have proved remarkably effective in retarding such deterioration. In most instances the discovery of these stabilizing additives has been the result of simple trial and error experimentation, and, until recently, little was actually known concerning the chemistry of their stabilizing action.

In Parts I and II[1,2] of this series, we presented evidence in support of our theory that the stabilizing action of the barium, cadmium, and zinc carboxylate class of stabilizers results, at least in part, from the displacement of certain of the polymer's relatively labile chlorine atoms by the stabilizer's carboxylate moiety.

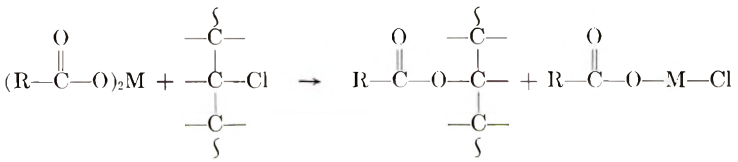

There is evidence which indicates[3] that the resulting carboxylate ester is more resistant toward pyrolytic elimination than the original chloride from which it was derived.

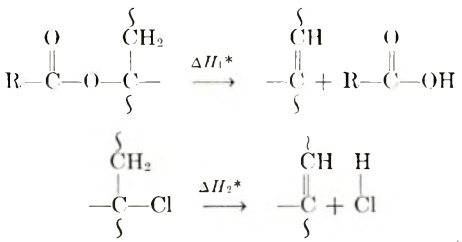

($\Delta H_1^* > \Delta H_2^*$)

In its early stages, the deterioration is known to proceed through a rapid and sequential elimination of hydrogen chloride along a length of polymer chain giving rise to a chromophoric and easily oxidizable polyene structure.[1,2] The ease of this zipperlike elimination, once it has been initiated, is readily understood in terms of the allylic effect of an olefinic group upon an adjoining chlorine-bearing carbon atom. Accordingly, it is reasonable to expect that, other things being equal, an agent which can either inhibit the introduction of such a labile group, or, if such a group be already present, alter it to a more stable one, can thus serve to stabilize the resin. In the present series of papers,[4,5] we report on our investigations into the stabilizing action of a representative group of organotin stabilizers and offer some interpretations of these findings in terms of our theory of stabilization.

The stabilizing action of certain organotin compounds on poly(vinyl chloride) resins was discovered by Yngve in 1936, for which discovery he was subsequently issued a series of patents.[6] Since Yngve's initial discovery, hundreds of structurally modified organotin compounds have been prepared and tested for their stabilizing action and it is now clear that a wide range of

effectivity is possible as a function of the organotin compound's molecular structure and of the concentration in which it is used. Some generalizations are also possible. Thus, the most effective compounds (compared on the basis of equal tin concentrations) are of the general formula $[R_xSnY_{(4-x)}]_n$, where R is alkyl and Y is a more complex organic moiety. Although the published information[7-9] on the way in which variation in the size and structure of the R group affects the stabilizing action of $[R_xSnY_{(4-x)}]_n$ is not exhaustive, it is in accord with our own fragmentary observations, viz., that for alkyl and alicyclyl groups in the C_3–C_{10} range, and for a given Y group, the effects are relatively minor. We have also observed that for given R and Y groups, where x is 1, 2, or 3, the stabilizing activities of the mono- and dialkyl compounds are essentially equivalent and considerably greater than that of the trialkyl analogs. Curiously enough, it appears that compounds in which x is zero (i.e., SnY_4) exert a quite deleterious action upon poly(vinyl chloride)'s thermal stability. However, it is the nature of the Y group which most profoundly affects the stabilizing efficiency of the organotin compound and a useful summary of this facet has been recently presented by H. V. Smith.[10] Among the more frequently encountered Y groups are the carboxylates of fatty acids, and especially of α,β-unsaturated dibasic acids and their half-esters, mercapto-substituted carboxylic acids and esters thereof, alkoxides, and mercaptides. Finally, it is also possible that at least some of the organotin stabilizers corresponding to the formula $[R_xSnY_{(4-x)}]_n$ may actually be oligomeric rather than monomeric (n may have values greater than unity). Thus, the known tendency of tin toward octahedral or trigonal bipyramidal coordination,[11-14] together with the fact that the Y groups invariably contain at least one donor atom, open numerous possibilities for oligomeric association. This, however, is an area upon which factual information is almost entirely lacking.

PLAN OF THE INVESTIGATION

In planning the investigations summarized in this series of papers, we sought to learn the following things: (*1*) do any chemical reactions occur between the organotin stabilizers and the polymer in the course of milling and heat treatment; (*2*) if so, what are their natures; (*3*) do the reactions contribute significantly to the polymer's stabilization? From the viewpoint of mechanistic organic chemistry, chemical reactions in general may be classed as elimination reactions, displacement reactions, or addition reactions (or their combinations in sequence). The fact that the primary event in the deterioration of poly(vinyl chloride) is the elimination of hydrogen chloride, renders it highly unlikely that organotin compounds could promote the elimination of hydrogen chloride (or any other moiety) and by so doing enhance the polymer's stability. Accordingly, one may confidently assume that any stabilizing chemical reactions which may occur between the polymer and the organotin additives will be reactions involving displacements and/or additions upon the polymer. The problem then becomes

one of detecting whether or not portions of the organotin additives become, in the course of the milling and heat treatment operations, chemically bound to the polymer, and secondly of determining whether the reaction or reactions have been displacements or additions, or both. For these purposes the method employing radioactively tagged stabilizers, as used in our earlier work,[2] is particularly well suited, since it can furnish unequivocal evidence of chemical reaction under conditions identical with those used industrially in the screening and evaluation of resin-stabilizer systems.

In principle, the method consists in the preparation of milled poly(vinyl chloride) films into which the radioactively tagged stabilizers have been incorporated. After subjecting the films to rigorously controlled heat treatment, each is put through a sequence of dissolutions in tetrahydrofuran and precipitations with methanol. The dry precipitated resins are then assayed for retained radioactivity. If a resin sample retains an appreciable and effectively constant amount of radioactivity through a sequence of three or more successive cycles, it is taken as definitive evidence of chemical bonding between the radioactively tagged portion of the stabilizer and the polymer. This conclusion is warranted by the fact that when unstabilized poly(vinyl chloride) resins, either virgin or milled and heat treated, are dissolved in tetrahydrofuran and the radioactively tagged stabilizers are then added to the solutions, the methanol precipitated resins exhibit but slight radioactivity.

Our choice as to the particular organotin stabilizers to be studied was based upon the following considerations: (*1*) the stabilizers should be representative of the various important types used industrially; (*2*) their radioactively tagged modifications should not be unduly difficult or costly to prepare; (*3*) their molecular structures should be reasonably well established. The compounds chosen were: dibutyltin β-mercaptopropanoate*

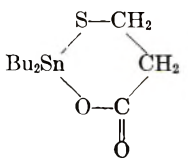

dibutyltin bis(oxoöctyl thioglycolate), $Bu_2Sn(SCH_2CO_2C_8H_{17})_2$;† dibutyltin bis(monomethyl maleate), $Bu_2Sn(O_2CCH{=}CHCO_2CH_3)_2$;‡ and dibutyltin bis(2-ethylhexanoate), $Bu_2Sn[O_2CCH(C_2H_5)C_4H_9]_2$.

To obtain reasonably unambiguous information bearing on the stated objectives, our plans called for the synthesis of three differently tagged

* The structure of dibutyltin β-mercaptopropanoate has been assigned on the basis of its elementary analysis and method of synthesis; however, molecular weight determinations (ebullioscopic) indicate it to be more complex.

† The octyl alcohol employed in the synthesis of this material was a complex mixture of isomeric primary octanols produced commercially by reduction of oxo-process octanals.

‡ Dibutyltin bis(monomethyl maleate) is considerably less effective as a stabilizer than the industrially used dibutyltin bis(monobutyl maleate); however, the ready availability and comparative cheapness of methanol-C^{14} dictated this choice.

radioactive modifications of each of the above compounds: one having the tag in the butyl group, another having it in the tin atom, and a third having it in the Y group. In the studies reported in the present paper, the butyl groups were tagged with ^{14}C in their C_1-positions. The syntheses are summarized in the eqs. (1)–(7). Details of these syntheses will be reported elsewhere [23]

$$CH_3CH_2CH_2\overset{*}{C}H_2Cl + Mg \xrightarrow[Et_2O]{n\text{-}C_7H_{15}} CH_3CH_2CH_2\overset{*}{C}H_2MgCl \quad (1)$$

$$4CH_3CH_2CH_2\overset{*}{C}H_2MgCl + SnCl_4 \rightarrow (CH_3CH_2CH_2\overset{*}{C}H_2)_4Sn + 4MgCl_2 \quad (2)$$

$$(CH_3CH_2CH_2\overset{*}{C}H_2)_4Sn + SnCl_4 \rightarrow 2(CH_3CH_2CH_2\overset{*}{C}H_2)_2SnCl_2 \quad (3)$$

$$(CH_3CH_2CH_2\overset{*}{C}H_2)_2SnCl_2 + 2NaHCO_3 + 2HSCH_2CO_2C_8H_{17} \rightarrow (CH_3CH_2CH_2\overset{*}{C}H_2)_2Sn(SCH_2CO_2C_8H_{17})_2 + 2NaCl + 2CO_2 + 2H_2O \quad (4)$$

$$(CH_3CH_2CH_2\overset{*}{C}H_2)SnCl_2 + 2NaHCO_3 + HSCH_2CH_2CO_2H \rightarrow$$

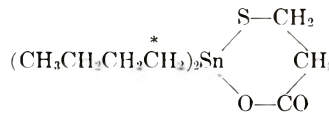

$$(CH_3CH_2CH_2\overset{*}{C}H_2)_2Sn \quad CH_2 + 2NaCl + 2CO_2 + 2H_2O \quad (5)$$

$$(CH_3CH_2CH_2\overset{*}{C}H_2)SnCl_2 + 2KO_2CCH{=}CHCO_2CH_3 \rightarrow (CH_3CH_2CH_2\overset{*}{C}H_2)_2Sn(O_2CCH{=}CHCO_2CH_3)_2 + 2KCl \quad (6)$$

$$(CH_3CH_2CH_2\overset{*}{C}H_2)_2SnCl_2 + 2NaO_2C\underset{\displaystyle C_2H_5}{\underset{|}{C}}HC_4H_9 \rightarrow (CH_3CH_2CH_2\overset{*}{C}H_2)_2Sn(O_2C\underset{\displaystyle C_2H_5}{\underset{|}{C}}HC_4H_9)_2 + 2NaCl \quad (7)$$

EXPERIMENTAL

Materials

The poly(vinyl chloride) used in these experiments was Geon 101-EP manufactured by the B. F. Goodrich Co.

Although we have no direct quantitative measure of the amount of radioactivity present in each of the final organotin stabilizers, the following facts are pertinent. Dibutyltin dichloride (b.p. 113–114°C./2 Torr) was obtained in 91% overall conversion from a mixture of radioactive butyl-1-^{14}C chloride (46 mg., 2.0 mc./mmole, New England Nuclear Corp.) and ordinary butyl chloride (17.2 g.) by the sequence of reactions outlined in the eqs. (1)–(3), given above. Dibutyl-1-^{14}C-tin β-mercaptopropanoate (m.p. 120–123°C.) was obtained from a portion of the radioactive dibutyltin dichloride in 82% conversion. Dibutyl-1-^{14}C-tin bis(oxoöctyl thioglycolate) was obtained in 97.5% conversion from a second portion of the radioactive dibutyltin dichloride. A third portion of the radioactive dibutyltin dichloride was used to prepare the dibutyltin-1-^{14}C-tin bis(monomethyl maleate) (98% conversion). The dibutyl-1-^{14}C-tin bis(2-ethylhexoanoate) was obtained in essentially quantitative conversion.

Film Preparation

The films were prepared from mixtures of Geon 101-EP resin (100 g.), the organotin stabilizer (3.34 mmole), and mineral oil (0.5 g.). They were milled on a Wm. R. Thropp Sons mill having a pair of oil-heated chromium plated rollers, one with speed 18 rpm and the other with speed 26 rpm. Prior to the milling of each film, the rollers were carefully cleaned with mineral oil and their separation adjusted to furnish films having thicknesses in the range of 0.016–0.018 in. The temperature of the rollers was maintained at 160°C. and each film was milled for 5 min.

Heat Treatment

Heat treatment of the films was done in a thermostatically controlled, forced-draft oven. (Precision Scientific Co., Model 18). Each of the experimental films was cut into sections measuring 3.5 × 3.5 in. Along one side of each section a pair of $^1/_8$ in. holes was drilled, 1.5 in. apart and approximately 0.5 in. from the films edge. These holes permitted a number of films to be mounted (about 0.5 in. from each other) on the spikes of a small metal rack (Fig. 1) and the rack and films centrally placed in the oven. This device insured effectively uniform heat treatment conditions for a series of films (as demonstrated by control tests) and, at the same time, permitted the expeditious withdrawal of individual specimens at predetermined

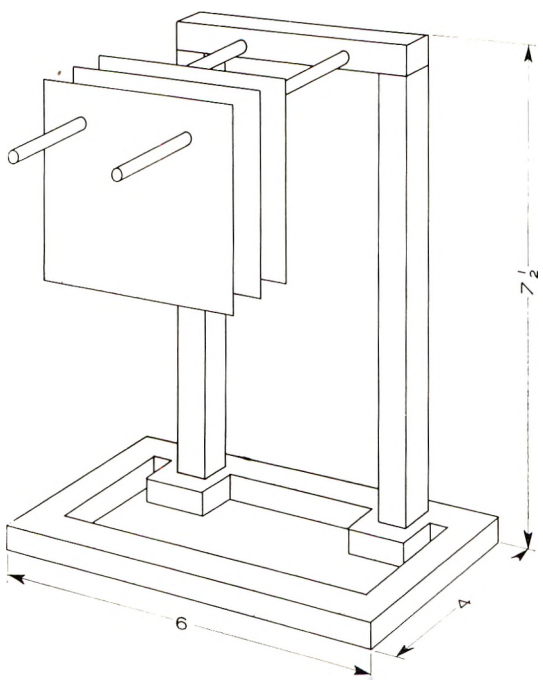

Fig. 1. Rack for film heat treatment.

intervals. The temperature of the oven during heat treatment was maintained at 175 ± 1°C.

Film Work-Up

The individual film sections (3.5 × 3.5 in.) were cut into $^1/_4$–$^1/_8$ in. squares with scissors (in order to facilitate dissolution), dissolved with stirring in 85 ml. of tetrahydrofuran contained in a Waring Blendor, and the clear solution then diluted with 210 ml. of absolute methanol added dropwise over the course of 30 min. accompanied by vigorous stirring. The precipitated material was collected by suction filtration, washed repeatedly with small portions of methanol, and then dried in air overnight. Prior to measurement of their retained radioactivity, the individual dry and powdery resins were placed in a vacuum desiccator for 2.5 hr., the pressure therein being reduced to approximately 0.1 Torr by a continuously operating vacuum pump.

Measurement of Radioactivity

Radioactivity measurements were made with a decade scaler (Model 1070-A, Atomic Instruments Co.) in conjunction with a gas flow proportional counter. The chamber of this counter was especially designed and constructed so that it could accommodate relatively large samples—film sections (3.5 × 3.5 in.) or shallow brass trays (3 × 4 × $^1/_4$ in.) containing the precipitated resin powders—thus permitting a greater degree of precision in counting than is possible with smaller samples and their cor-

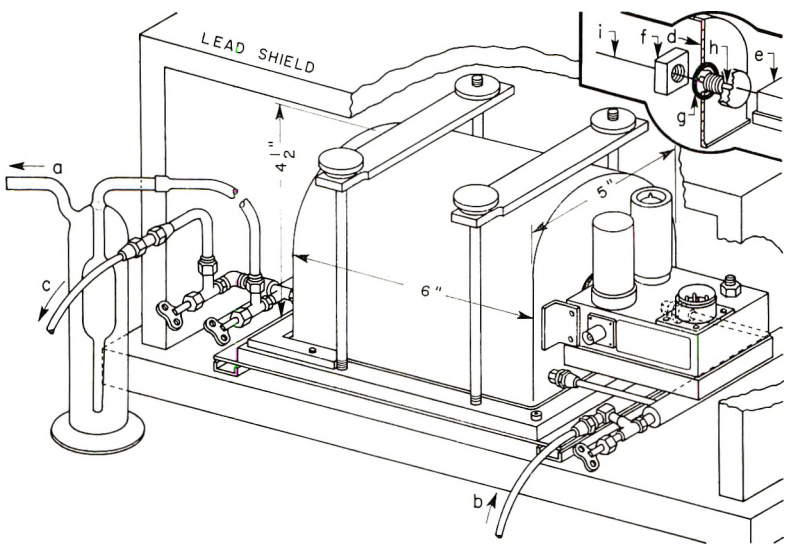

Fig. 2. Counting chamber: (*a*) to atmosphere, (*b*) inlet for P-10 gas; (*c*) to vacuum pump, (*d*) chamber wall, (*e*) preamplifier case, (*f*) nylon insulator, (*g*) O-ring, (*h*) hypodermic needle, (*i*) counterwire.

respondingly reduced area of effective radiating surface. The chamber was made of $^1/_8$ in. stainless steel in hemicylindrical shape (Fig. 2) having a $^3/_8$ in. flange on its bottom surface to which was cemented a Neoprene gasket. The base-plate of the chamber was made of 0.5 in. stainless steel into which was milled a rectangular groove, $^3/_8$ in. deep and $^1/_2$ in. in width, the overall dimensions of the groove being such as to coincide with the hemicylinder's flanged surface. A silicone rubber gasket (Silastic RTV-11, Dow Corning Corp.) was formed *in situ* in the base-plate's groove. By means of a pair of metal clamps the hemicylinder could be easily and securely positioned on the base-plate.

In one of the hemicylinder's ends was drilled a set of three holes, one having a $^1/_2$ in. diameter and centered $1^3/_4$ in. from the flanged surface. The other two holes ($^3/_{16}$ in. diam.) were symmetrically placed below and on either side of the central hole, $^1/_2$ in. above the flange and 3 in. apart. A pair of holes was drilled into the hemicylinder's other end: one, of $^1/_2$ in. diameter, was placed directly opposite the hole of that same diameter in the opposite end, the other, of diameter $^3/_{16}$ in., was located directly below the first and $^1/_2$ in. from the flange. Each of the $^1/_2$ in. holes was fitted with a nylon insulator having an O-ring seal (see inset, Fig. 2). One of the insulators was pierced with a stout hypodermic needle serving as a canal through which the 0.008 in. diameter tungsten counterwire was passed. A second hypodermic needle was firmly embedded in the other nylon insulator and served as the terminus of the counterwire. The wire was made taut and firmly soldered into these needles. The preamplifier (Model 851–13, Victoreen Co.) was mounted on the external wall of the chamber and as close as possible to the emerging counterwire in order to provide an electrical path of minimum distance between the collecting wire and the preamplifier. The signal from the preamplifier was relayed, via a linear amplifier (Model 851-A, Victoreen Instrument Co.) and an integral and differential pulse height analyzer (Model DD2, Victoreen Instrument Co.) to the decade scaler. The hemicylinder's remaining three holes were threaded to accept fittings for $^1/_4$-in. o.d. copper tubing bearing the various connections and needle valves shown in Figure 2. This latter assembly served to evacuate air from the chamber and to replace it with P-10 counting gas (90% methane, 10% argon).

In order to reduce to a minimum the relatively large background count to be expected for a counter having the specified dimensions, the apparatus was entirely enclosed with a 2 in. lead brick shielding. Access to the counter for loading and unloading was facilitated by mounting its base on a set of roller bearing slide-ways, an arrangement which permitted the counter to be rolled out of the lead enclosure upon removal of four of the front bricks. We found that with this set-up we obtained an average background of 280 counts/min.

The following procedure was followed in assaying the radioactivity of our samples. The sample to be assayed was symmetrically placed on the chamber's base-plate and the hemicylinder properly positioned and firmly se-

cured with the pair of metal clamps. The various needle valves were than set so that the chamber was subjected to the action of a vacuum pump for a 10-min. period, at the end of which time the pressure inside the chamber was reduced to about 25 μ. Next, the valves were adjusted to close off the vacuum pump and carefully admit the counting gas until the pressures inside and outside the chamber were equal. Then, the valves to the vacuum pump were carefully reopened and the atmosphere inside the chamber again evacuated by a second 10-min. pumping period. Finally the vacuum pump valves were closed and counting gas again readmitted until the pressure inside the chamber was just slightly greater than the external pressure, a condition readily achieved by the use of a simple monostat bubbler (Fig. 2). We found that $^1/_4$-in. o.d. nylon tubing proved most satisfactory in making the connections between the counter, the vacuum pump, and P-10 gas cylinder.

The counter was operated at the β-plateau region, attained by applying approximately 2800 v. on the counterwire, and had a slope of about 10% per 100 v. The selected counting interval was such that a precision of $\pm 5\%$ (based on 90% confidence limits) was obtained. Before each day's run and at several intervals throughout that day, the instrument's performance was checked against a standard ^{60}Co source and, at the same time, a count of the background was made. This information then permitted the appropriate corrections to be made to the data collected in the ensuing interval. In order to compensate for any effects caused by the brass tray used to contain the precipitated powders, the background count was made with an empty tray in the counter chamber.

RESULTS AND DISCUSSION

Figure 3 summarizes our findings in the experiments designed to determine the extent of radioactivity retained by the precipitated resins from a set of four films, each stabilized with a different organotin compound (all tagged in the butyl group), as a function of the duration of the film's heat treatment at 175°C. The summarized data refer to the assays made after a sequence of two dissolution–precipitation cycles. The organotin stabilizers used in these experiments were: dibutyl-1-^{14}C-tin bis(monomethyl maleate), dibutyl-1-^{14}C-tin β-mercaptopropanoate, dibutyl-1-^{14}C-tin bis–(oxoöctyl thioglycolate), and dibutyl-1-^{14}C-tin bis(2-ethylhexanoate).

Perhaps the first feature which one notices in inspecting Figure 3 is the fact that each of the retention curves rises with increase in the duration of heat treatment, passes through a maximum, and then drops off. Behavior of this same sort was encountered in our earlier studies on stabilization by barium, cadmium, and zinc carboxylates.[1,2] In all instances the blackening of the films sets in on the descending portions of the curves (indicated in Figure 3 by a pair of intercepting slashes). The appearance of early color for the poorer stabilizers occurs on the ascending portions of the curves (indicated by a single slash), while for the better stabilizers it is on the

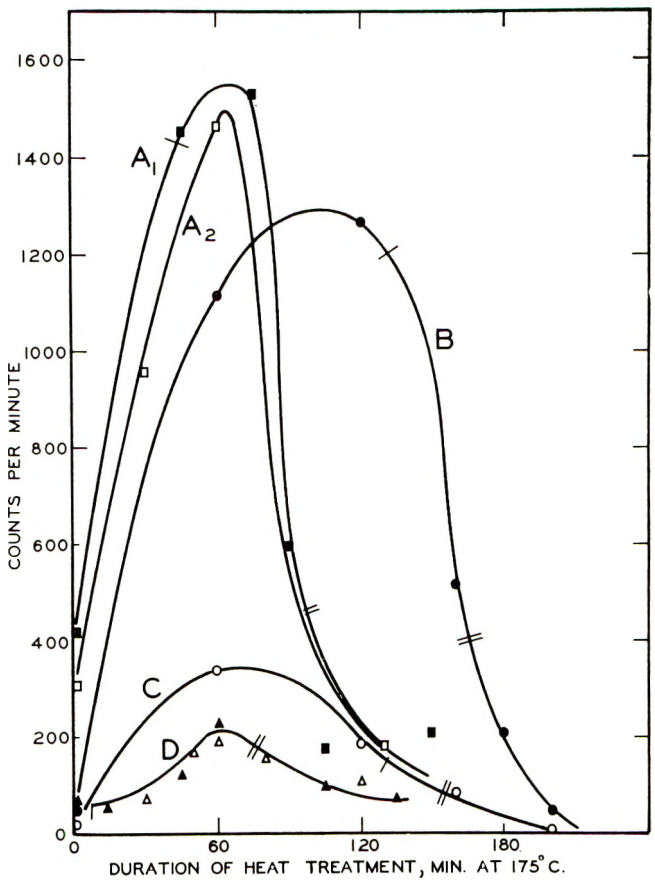

Fig. 3. Effect of heat treatment on the retention of radioactivity by poly(vinyl chloride) resin after two dissolution-precipitation cycles, the resins having been milled with: (A_1 and A_2) dibutyl-1-^{14}C-tin bis(monomethyl maleate), (*B*) dibutyl-1-^{14}C-tin β-mercaptopropanoate, (*C*) dibuytl-1-^{14}C-tin bis(oxoöctyl thioglycolate), (*D*) dibutyl-1-^{14}C-tin bis(2-ethylhexanoate).

curve's descending portion. (Dibutyltin bis(2-ethylhexanoate), although it delays the film's blackening, has little or no effect on early color.) One might also anticipate that the heights of the curves' origins and maxima could be correlated with the effectiveness of the stabilizers.* If such a correlation does indeed exist, it is not apparent to us. Its absence, we are confident, finds explanation in certain other findings to which we now turn our attention.

As we have pointed out above, if the retention of radioactivity by the precipitated resin is due to the formation of a stable chemical bond between the resin and the stabilizer, or a radioactively tagged portion of that

* Since all of our organotin compounds were prepared from the same batch of dibutyl-1-^{14}C-tin dichloride, they must all have the same concentration of radioactivity per mole of stabilizer.

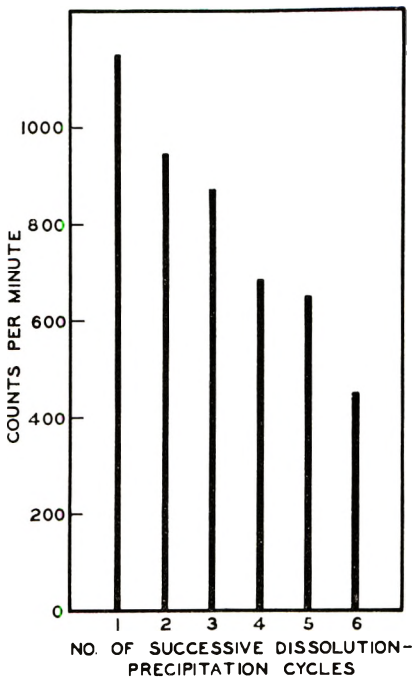

Fig. 4. Effect of repeated dissolution and precipitation on the retention of radioactivity by a resin milled with dibutyl-1-^{14}C-tin bis(monomethyl maleate).

stabilizer, then it is reasonable to conclude that that retention should remain effectively constant through successive dissolution and precipitation cycles.

To obtain information bearing on this point we selected a section of dibutyl-1-^{14}C-tin β-mercaptopropanoate-stabilized film which had been subjected to heat treatment at 175°C. for 60 min. (near the maximum of curve *B*, Fig. 3) and put this material through a sequence of six dissolution–precipitation cycles, the precipitates being assayed for retained radioactivity at the close of each cycle. Figure 4 summarizes the resultant data and shows that within the limit of these experiments the retention is not constant but decreases as a function of the number of successive dissolution–precipitation cycles to which the resin is subjected.

The question that next arises is whether the sort of retention with which we are here dealing is the result of physical occlusion of the stabilizer by the precipitated polymer, or to a relatively weak associative link between the resin and the stabilizer, which link is disrupted by the action of the tetrahydrofuran, the methanol, or both. In a set of experiments reported in the subsequent paper,[4] we show that when a radioactively-tagged stabilizer is added to a tetrahydrofuran solution of poly(vinyl chloride)—either virgin resin or resin which had been milled and heat treated—and the solution then diluted with methanol in the usual manner, it is found that the amount of radioactivity retained by the precipitated resin is so very much less than that observed in the present experiments that there can be no reasonable

doubt about the existence of such an associative link between the polymer and the stabilizer. (In the cited experiments the particular stabilizer used was dibutyl-^{113} tin β-mercaptopropanoate rather than dibutyl-1-^{14}C-tin β-mercaptopropanoate, as one might *a priori* deem more appropriate. However, evidence yet to be presented shows convincingly that under the experimental conditions involved all but a very small portion of the butyl groups remain firmly bound to their respective tin atoms.)

The above findings contrast most surprisingly with certain studies briefly reported by Kenyon[15] more than a decade ago on the photostabilization of poly(vinyl chloride) by dibutyltin diacetate. Although Kenyon gave no experimental details, he stated that "when polyvinyl chloride is irradiated by light of wavelengths greater than 2700 A. in the presence of C-14 butyl-labeled dibutyltin diacetate, there is observed an increase in the retained β-activity with time of irradiation. After irradiation the stabilizer was extracted by dissolving and reprecipitating the polymer a number of times until constant retained activity was observed in the polymer film." Kenyon proposed that the stabilizing action of the dibutyltin diacteate was due to its ability to donate a butyl group to a polymer radical (R·),

$$R\cdot + (C_4H_9)_2Sn(AC)_2 \rightarrow RC_4H_9 + C_4H_9\dot{S}n(AC)_2$$

that radical having been formed by the "extraction of a hydrogen atom from the polyvinyl chloride." If it is true, as has frequently been proposed,[16–18] that the thermal degradation of poly(vinyl chloride) is also a free radical process, it is difficult to understand why in our experiments using such truly effective stabilizers as dibutyltin β-mercaptopropanoate and dibutyltin bis(oxoöctyl thioglycolate) we find no constant retention of radioactivity even after a sequence of six dissolution–precipitation cycles.

In the hope of obtaining some more definitive information on this point we resorted to a more drastic series of experiments. In these experiments, the precipitated resins, which served to establish curve A_2 of Figure 3, were separately redissolved in tetrahydrofuran and their solutions slowly made saturated with anhydrous hydrogen chloride (1–2 hr.) at room temperature. The solutions were allowed to stand overnight and the resins then reprecipitated in the usual manner with methanol. After being allowed to dry in air, the precipitated resins were subjected to a second dissolution–precipitation cycle and then assayed for retained radioactivity in the usual manner. Figure 5 summarized the results of these assays and shows that a very greatly diminished, but nevertheless definite, amount of radioactivity is retained even after this drastic treatment. Finally, in order to gain evidence as to whether or not this small amount of retained radioactivity is due to butylation of the polymer as proposed by Kenyon, we again subjected one of the hydrogen chloride-treated resins (arrowed specimen in Fig. 5) to an additional HCl-treatment and a sequence of two further dissolution–precipitation cycles. A radioactivity assay of the thus treated resin showed it to have effectively the same amount of retained radioactivity (95 counts/min.) as it had before the second HCl treatment.

One further finding is also pertinent here. When the above hydrogen chloride-treated resin specimen was analyzed by emission spectroscopy, no trace of tin was evident. Accordingly, we must conclude that butylation of the resin does occur. However, in view of the absence of tin, one must

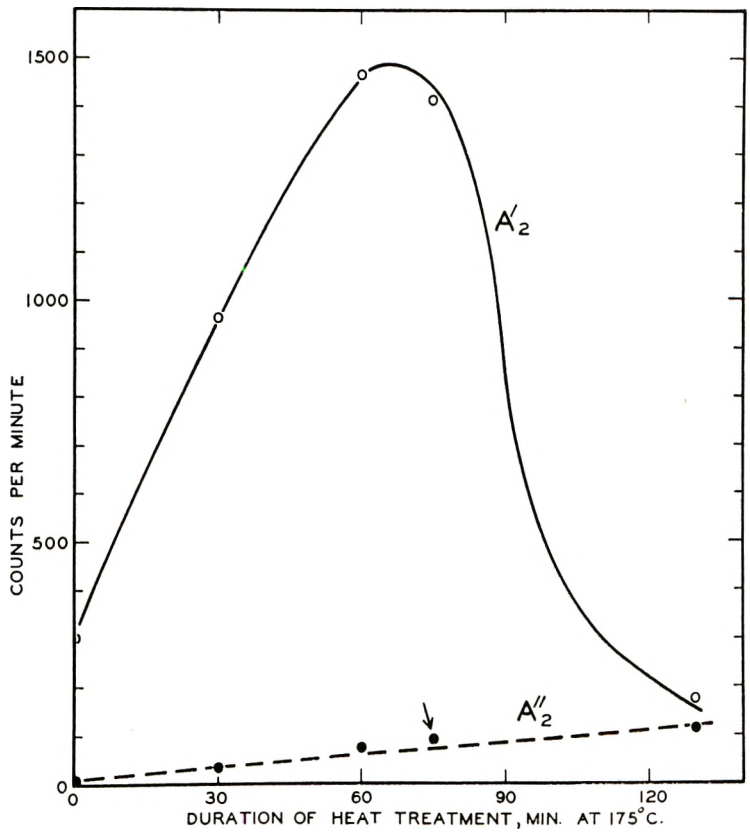

Fig. 5. Radioactivity retained by a resin stabilized with dibutyl-1-^{14}C-tin bis-(monomethyl maleate) (A) before and (A_2) after treatment with HCl in tetrahydrofuran

regard as unlikely the suggestion that this butylation is the result of an addition reaction of the sort,

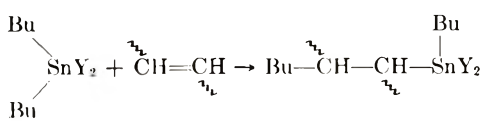

This conclusion is substantiated by the fact that when model compounds, such as dibutyltin dichloride, are subjected to the action of hydrogen chloride in tetrahydrofuran, no cleavage of the carbon–tin bonds occur. Hence,

the explanation that the absence of tin in the polymer is due to hydrogen chloride cleavage:

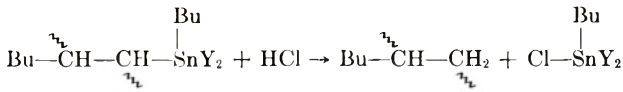

is untenable. The question which next arises is whether the observed butylation of the polymer is indeed responsible for all or a part of the stabilizing action of the organotin additive. In seeking a plausible answer to this question, it is helpful to know something about the extent to which it occurs. Although we have no direct measurements of this, evidence of an indirect sort obtained in connection with our ^{113}Sn-tracer studies[5] indicates that the amount of organotin compound retained by a dibutyltin bis(monomethyl maleate)-stabilized film which had been heat treated at 175°C. for 75 min. and then subjected to two successive dissolution–precipitation cycles is only about 18% of the 3.34 mmoles which had been initially added per 100 g. of resin. After hydrogen chloride treatment, the radioactivity of this resin drops from 1400 to 95 counts/min., a decrease of approximately 95%. On the basis of these figures, it appears that only about 1% of the butyl groups present in the initially added dibutyltin bis(monomethyl maleate) or 0.0334 mmole become covalently bound to the polymer chain as proposed by Kenyon. Geon 101-EP is reported to have an average molecular weight of approximately 75,000; accordingly 100 g. of that resin corresponds to about 1.3 mmole. Thus, under the condition of our experiment only an average of one out of every 40 polymer molecules is butylated and, according to the Kenyon mechanism, has its unzippering chain terminated at some stage prior to that which would have obtained in the absence of the stabilizer. Clearly, this disparity creates serious difficulties for the Kenyon mechanism. Further, recent kinetic studies by Guyot and Benevise,[19] employing a highly refined measuring technique, have shown that at 170°C. in an atmosphere of air a commercial poly(vinyl chloride) resin, with a number-average molecular weight of 65,000 eliminates approximately 2.2% of its weight as hydrogen chloride in 75 min., which is equivalent to an average of about 40 molecules of HCl per molecule of polymer. Yet visual inspection of the stabilized and unstabilized films at the end of 75 min. at 175°C. shows the former to have only a pale straw color whereas the latter is a deep brownish red. Even at the end of 45 min. the unstabilized film showed strong coloration. Taken together, these facts make it seem highly unlikely that the Kenyon mechanism contributes anything but a very minor role to the stabilizing action of the organotin additive. This view is also readily rationalized by the apparent zero order of the polymer butylation reaction (Fig. 5).

It yet remains for us to offer some clarification of the nature of the associative link which we propose is formed between the polymer and the organotin stabilizer in the course of the milling and heat treatment operations.

We suggest that one (or possibly two) of the polymer molecule's chlorine atoms forms a dative bond with the tin atom.

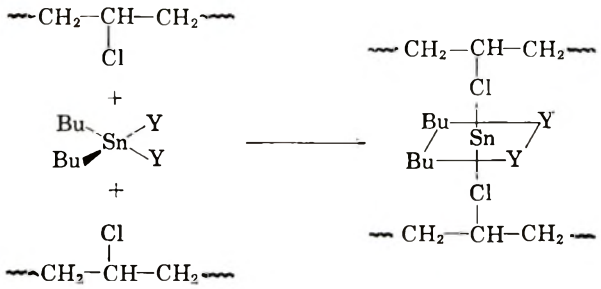

Such a complex might serve as a precursor by means of which the displacement of certain relatively labile halogen atoms can be affected by Y groups.

Such a process would involve an activation energy sufficient to account for the ascending portion of the curves in Figure 3. The fact that the retention of radioactivity by the polymer is not constant but decreases through a sequence of dissolution–precipitation cycles might be the result of solvolytic displacement of the Y or Cl functions by the tetrahydrofuran, the methanol, or both.

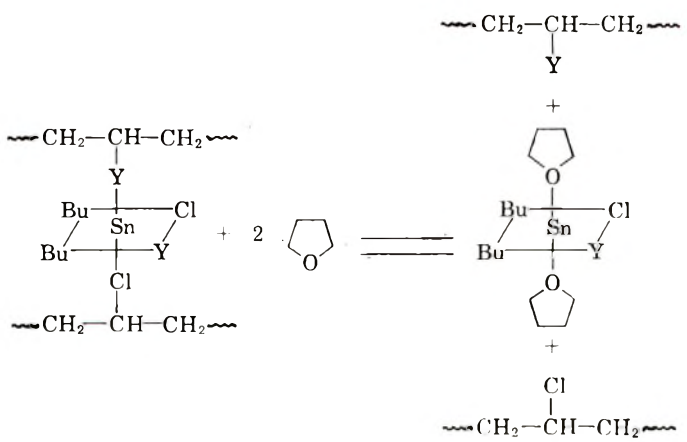

Evidence in support of such coordinative organotin complexes has recently been given by Gol'dshtein[20] and his co-workers. Other evidence is the fact that if we increase the volume of tetrahydrofuran used for dis-

solution of the resin (or, alternatively, use an equal volume of cyclohexanone, a stronger nucleophile) the amount of radioactivity retained by the subsequently precipitated resin can be markedly decreased.

Finally, the descending branches of the curves in Figure 3 find a plausible explanation in terms of the cleaving action of eliminated hydrogen chloride upon the organotin–polymer complex. (See following paragraph.)

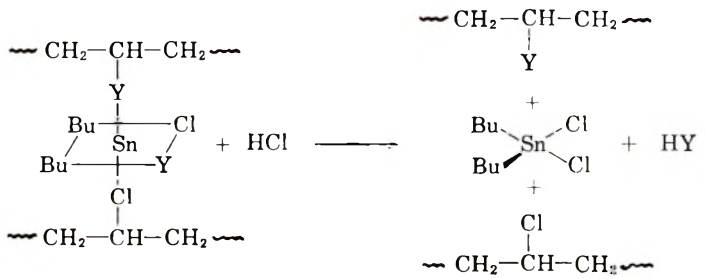

Supplementing this action, a certain amount of pyrolytic elimination of the complexed organotin moiety may also take place.

There remain several other experiments of ours which are informative. In one of these we sought to determine whether the resins obtained from films which had been milled with dibutyl-^{14}C-1-tin dichloride, heat-treated, and then subjected a sequence of two dissolution–precipitation cycles, exhibited any retention of radioactivity. Curve *F* in Figure 6 summarizes our findings and shows that only after about 75 min. at 175°C. (when the film is quite dark in color) is there any convincing evidence of retention by the resin. It is also pertinent to point out that in the concentration in which we employed the dibutyltin dichloride (3.34 mmoles/100 g. of resin) it causes only a very slight or negligible stabilizing action. Apparently, dibutyltin dichloride forms no associative links with the undegraded polymer, or if such links are formed, they are very readily broken by the tetrahydrofuran and methanol.

It has been suggested[21] that organotin compounds of the type $R_2Sn(SR)_2$ may perform their stabilizing function by acting as a generating source for mercaptans.

$$R_2Sn(SR)_2 + HCl \rightarrow R_2Sn(SR)Cl + HSR$$

The thus liberated mercaptan might thereafter act as an antioxidant, chain terminator, etc. However, we have found that mixture of dibutyltin dichloride and either β-mercaptopropanoic acid or oxoöctyl thioglycolate, taken in a 1:2 molar ratio, exerts but very little stabilizing action and this only during the milling operation. Moreover, if films are prepared which contain only the mercaptan entity and no dibutyltin dichloride, then no stabilization is observable. It is, however, not to be denied that the observed ineffectivity of the added free mercaptans might be due to their loss by volatilization during the milling operation, however, their relatively high boiling points (β-mercaptopropanoic acid, 110°C./15 Torr; oxoöctyl thio-

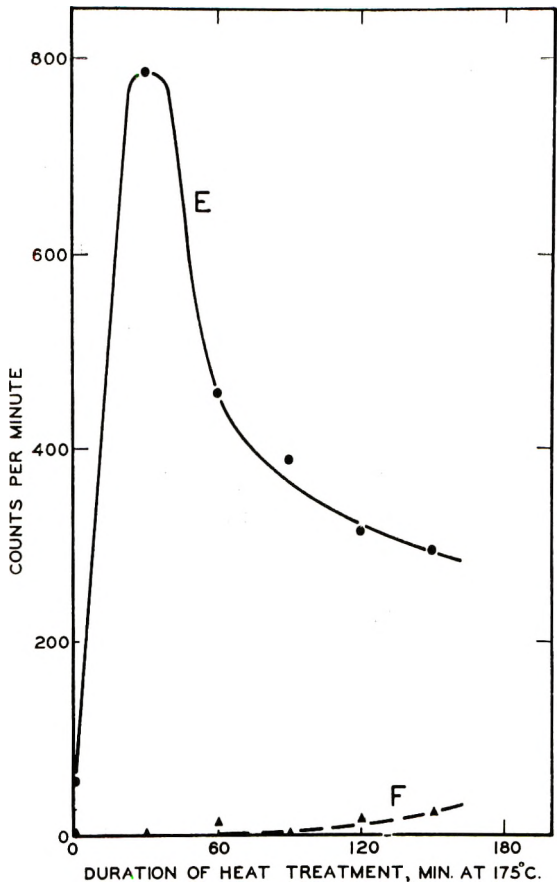

Fig. 6. Radioactivity retained by a resin stabilized with (*E*) a mixture of dibutyl-1-^{14}C-tin dichloride and disodium β-mercaptopropanoate and (*F*) dibutyl-1-^{14}C-tin dichloride.

glycolate, 125°C./17 Torr) makes this argument somewhat less than convincing. One might, of course, attribute the feeble stabilization observed when mixtures of dibutyltin dichloride and the free mercaptan are used to an associative complex between the two which inhibits the volatilization of the mercaptan.

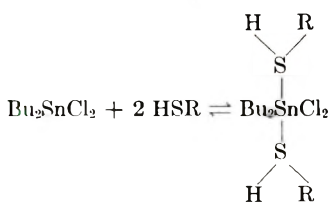

We have also examined the possibility that a mixture of dibutyltin dichloride and the disodium salt of β-mercaptopropanoic acid may affect stabilization. We found that the mixture was very definitely effective, however

considerably less effective than dibutyltin β-mercaptopropanoate. It is not unlikely that in this case the stabilization results from the generation *in situ* in some dibutyltin β-mercaptopropanoate.

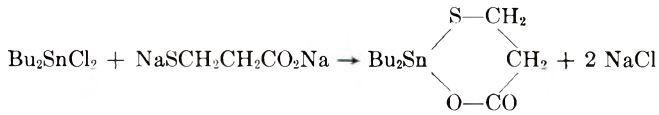

Curve *E* (Fig. 6) summarizes our findings in a set of tracer studies on a film milled with a mixture of dibutyl-1-^{14}C-tin dichloride and disodium β-mercaptopropanoate and which had been subjected to our standard heat treatment and dissolution–precipitation procedure. It is evident that in the presence of the sodium salt there is a very appreciable amount of radioactivity retained by the resin after a sequence of two dissolution–precipitation cycles. Finally, we have examined the stabilizing action of a mixture of oxoöctyl thioglycolate with either dibutyltin bis(2-ethylhexoanoate) or dibutyltin bisacetate. By themselves these latter compounds are quite poor stabilizers—indeed, the acetate compound appears to affect some slight destabilization. Curiously enough, the stabilizing actions of the mixtures (2 moles of mercaptan per mole of dibutyltin compound) are essentially equivalent and almost equal to that of dibutyltin bis(oxoöctyl thioglycolate) itself.[22] This, of course, suggests that the following interaction occurs.

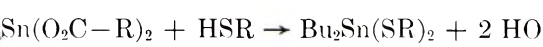

References

1. Frye, A. H., and R. W. Horst, *J. Polymer Sci.*, **40,** 419 (1959).
2. Frye, A. H., and R. W. Horst, *J. Polymer Sci.*, **50,** 1 (1960).
3. DePuy, C. H., and R. W. King, *Chem. Revs.*, **60,** 451 (1960).
4. Frye, A. H., R. W. Horst, and M. A. Paliobagis, *J. Polymer Sci.*, **A2,** 1791 (1964).
5. Frye, A. H., R. W. Horst, and M. A. Paliobagis, *J. Polymer Sci.*, **A2,** 1803 (1964).
6. Yngve, V., U. S. Pat. 2,219,463 (Oct. 29, 1941); U. S. Pats. 2,267,777 and 2,267,779 (Dec. 30, 1942); U. S. Pat. 2,307,092 (Jan. 5, 1943); Brit. Pat. 497,879 (Dec. 30, 1938); cf. E. W. Rugely and W. B. Quattlebaum, U. S. Pat. 2,344,002 (Mar. 14, 1949).
7. Jasching, W., *Kunststoffe*, **52,** 458 (1962).
8. Luijten, J. G. A., and S. Pezarro, *Brit. Plastics*, **30,** No. 5, 183 (1957).
9. van Egmond, J. C., M. J. Janssen, J. G. A. Luijten, G. J. M. van der Kerk, and G. M. van der Want, *J. Appl. Chem.*, **12,** 17 (1962).
10. Smith, H., Verity, *The Development of the Organotin Stabilizers*, Tin Research Institute, Green Ford, Middlesex, England, 1959, p. 9.
11. Holmes, J. R., and H. D. Kaes, *J. Am. Chem. Soc.*, **83,** 3403 (1961).
12. Beattie, I. R., and T. Gilson, *J. Chem. Soc.*, **1961,** 2585.
13. Beattie, I. R., G. P. McQuillan, and R. Hulme, *Chem. Ind. (London)*, **1962,** 1429.
14. Brown, T. L., and M. Kubota, *J. Am. Chem. Soc.*, **83,** 331 (1961).
15. Kenyon, A. S., *Natl. Bur. Standards (U. S.), Circ.*, **No. 525,** 91 (1953).
16. Stromberg, R. R., S. Straus, and B. G. Achhammer, *J. Polymer Sci.*, **35,** 355 (1954).
17. Winkler, D. E., *J. Polymer Sci.*, **35,** 3 (1959).
18. Baum, B., and L. H. Wartman, *J. Polymer Sci.*, **28,** 537 (1958).
19. Guyot, A., and J. P. Benevise, *J. Appl. Polymer Sci.*, **6,** 489 (1962).

20. Gol'dshtein, I. P., E. N. Gur'yanova, E. D. Delinskaya, and K. A. Kocheskov, *Doklady Akad. Nauk SSSR*, **136**, 1079 (1961).
21. Rieche, A., A. Grimm, and H. Mucke, *Kunststoffe*, **52**, 398 (1962).
22. Luz, W. D., Brit. Pat. 874,574 (Aug. 10, 1960).
23. Frye, A. H., and R. W. Horst, *Intern. J. Appl. Radiation Isotopes*, in press.

Résumé

L'action stabilisatrice d'un groupe représentatif de composés organostanniques de formule Bu_2SnY_2 a été étudiée par le technique des traceurs radioactifs; l'atome traceur ^{14}C est localisé en position C_1 du groupement butyle. Les groupements Y des composés organostanniques choisis étaient (1) le maléate de monométhyle, (2) le thioglycolate d'oxooctyle, (3) le β-mercaptopropanoate, et (4) le 2-éthylhexanoate. On a trouvé qu'après une série de 2 cycles de dissolution et précipitation (au moyen de tétrahydrofuranne et de méthanol), une fraction appréciable de radioactivité est retenue par la résine, celle-ci ayant été au préalable mèlée au stabilisateur marqué, mise sous forme de film et soumise à des traitements thermiques soigneusement contrôlés. Dans le telles conditions, on a trouvé que la quantité de radioactivité retenue par le résine est déterminée par la nature du groupe Y et par la durée du traitement thermique. De plus, on a trouvé que pour un groupe Y donné, la quantité de matériau retenu commence par augmenter lorsqu'on accroît la durée de traitement thermique, puis atteint un maximum et enfin diminue. Cependant on a trouvé que la quantité de radioactivité retenue par une telle résine ne reste pas constante lorsqu'on soumet l'échantillon à de nouveaux cycles de dissolution–précipitation mais que, dans les limites des expériences actuelles, elle décroît notablement à chaque cycle. On émet l'hypothèse que la majeure partie de cette rétention est due à la formation d'associations entre le polymère et le composé organostannique et que ces liaisons sont en partie détruites par le traitement au tétrahydrofuranne et au méthanol. On montre aussi qu'il n'y a quîune très faible partie de la radioactivité retenue par la résine précipitée, que peut être attribuée à une butylation réelle de la résine, comme le propose Kenyon et qu'il est peu probable que cela puisse contribuer à la stabilisation de la résine d'une façon appréciable. On suppose que la formation d'un complexe d'association entre la résine et le composé organostannique constitue un premier intermédiaire dans lequel certains centres relativement labiles de la chaîne polymérique peuvent subir des altérations, peut-être par une réaction de déplacement faisant intervenir le groupement Y du composé organostannique; de cette façon l'élimination en série contigue d'acide chlorhydrique qui constitue le phase initiale de la dégradation du polymère est retardée ou inhibée.

Zusammenfassung

Die stabilisierende Wirkung einer repräsentativen Gruppe von Organozinnverbindun, gen der Formel Bu_2SnY_2 wurde mittels einer radioaktiven Tracer-Technik untersucht-wobei die Butylgruppen in der C_1-Stellung mit ^{14}C markiert waren. Die Y-Gruppen der ausgewählten Organozinnverbindungen waren (1) Monomethylmaleat, (2) Oxooctylthioglycolat, (3) β-Mercaptopropionat, (4) 2-Äthylhexanoat. Nach einer Folge von Umfällungen (mit Tetrahydrofuran als Lösungs- und Methanol als Fällungsmittel) wird ein merklicher Teil der Radioaktivität durch das Harz zurückgehalten, wenn die Harze vorher mit dem markierten Stabilisator vermischt, zu Filmen gewalzt und dann einer sorgfältig kontrollierten Hitzebehandlung unterworfen worden waren. Unter diesen Bedingungen hängt die Menge der vom Harz zurückgehaltenen Radioaktivität von der Art der Y-Gruppe und der Dauer der Hitzebehandlung ab. Bei einer gegebenen Y-Gruppe stieg das Ausmass der Retention mit steigender Dauer der Hitzebehandlung zuerst an, erreichte ein Maximum und fiel dann wieder ab. Die Menge der von einem solchen Harz zurückgehaltenen Radioaktivität blieb jedoch nicht konstant, wenn die Probe weiteren Umfällungen unterworfen wurde, sondern nahm im Bereich der vorliegenden Experimente mit jeder weiteren Umfällung deutlich ab. Es wird angenommen,

dass der Grossteil dieser Retention auf die Bildung einer associativen Bindung zwischen dem Polymeren und der Organozinnverbindung beruht und dass diese Bindung durch die Tetrahydrofuran-Methanol-Behandlung teilweise gespalten wird. Es wird ferner gezeigt, dass nur ein sehr kleiner Teil der vom gefällten Harz zurückgehaltenen Radioaktivität auf eine tatsächliche Butylierung des Harzes zurückgehen kann, wie sie von Kenyon vorgeschlagen wurde, und dass es unwharscheinlich ist, dass eine solche zur Stabilisierung des Harzes merklich beiträgt. Es wird angenommen, dass die Bildung eines assoziativen Komplexes zwischen Harz und Organozinnverbindung als Vorstadium auftritt, in welchem bestimmte relativ labile Zentren im Polymeren durch eine Verdrängungsreaktion under Beteiligung der Y-Gruppe der Organozinnverbindung verändert werden können, und dass auf diese Weise die zipper-artige Abspaltung von HCl gehemmt oder inhibiert wird, die den Beginn des Polymerabbaues darstellt.

Received March 15, 1963

JOURNAL OF POLYMER SCIENCE: PART A VOL. 2, PP. 1785–1799 (1964)

The Chemistry of Poly(vinyl Chloride) Stabilization. IV. Organotin Stabilizers Having Radioactively Tagged Tin Atoms

ALFRED H. FRYE, RAYMOND W. HORST, and MARKO A. PALIOBAGIS, *The Cincinnati Milling Machine Company, Cincinnati, Ohio, and The Advance Division of the Carlisle Chemical Works, New Brunswick, New Jersey*

Synopsis

The chemistry of poly(vinyl chloride) stabilization by organotin compounds has been studied by the use of a radioactive tracer technique. The stabilizers studied were of the type $[R_2SnY_2]_n$, where R was either butyl or octyl, Y either monomethyl maleate, oxo-octylthioglycolate, or β-mercaptopropanoate, and ^{113}Sn was the radioactive tag. It was found that resins milled into films with the tagged stabilizers retain an appreciable amount of radioactivity after the films have been subjected to the conditions of accelerated thermal degradation, dissolution in tetrahydrofuran, and thereafter precipitated from solution by the addition of methanol. The amount of retained radioactivity varies with the duration of the heat treatment and with the nature of the Y group in a manner that parallels our findings in a previously reported study using a ^{14}C tag in the stabilizers' butyl groups. We have also found that the amount of radioactivity retained by the precipitated resins decreases in a regular manner when the resins are subjected to a sequence of repeated dissolutions and precipitations. However, in the case of the resin stabilized with dibutyltin-^{113}Sn bis(monomethyl maleate) at least, the loss of radioactivity with repeated dissolution and precipitation appears to level off after 13–14 cycles and approach a constant value of retention. Treatment of the radioactive resins with anhydrous hydrogen chloride results in the loss of essentially all their radioactivity. On the basis of these findings, we suggest that in the performance of their stabilizing action, the organotin compounds undergo little or no cleavage of their carbon–tin bonds. Further, the observed retention of radioactivity by the resin is best rationalized as due to the existence of a coordinative linkage formed between the stabilizer's tin atom and some donor atom present in polymer's molecular structure.

INTRODUCTION

In Part III of this series[1] we reported our findings on a set of experiments designed to determine whether poly(vinyl chloride) is butylated by organotin stabilizers of the general type $[Bu_2SnY_2]_n$ under the conditions normally used to study the thermal degradation of the polymer. In those studies the butyl groups were radioactively tagged with ^{14}C at the 1-position. The Y groups were either monomethyl maleate, oxoöctyl thioglycolate, β-mercaptopropanoate, or 2-ethylhexanoate, and were chosen because they are representative of the various types of organotin stabilizers commonly encountered in industrial usage. In this part we report our findings on the

second phase of the study wherein the same stabilizers are used, but in which the tin atoms, rather than the butyl groups, bear the radioactive tag. In Part V of this series[2] we report on our studies with the stabilizers having their Y groups tagged.

The principle underlying the use of radioactively tagged stabilizers in these studies is simply this: if one finds that a sample of poly(vinyl chloride) after treatment with a radioactively tagged stabilizer acquires and retains an effectively constant amount of radioactivity through a sequence of dissolution–precipitation cycles, then that moiety of the stabilizer in which the tag was localized has, perforce, become chemically bound to the polymer molecule. The treatment involved consists in the preparation of poly(vinyl chloride) films into which the stabilizers are incorporated by a milling operation. The films are carefully heat treated, dissolved in tetrahydrofuran, and the resins precipitated from solution by the addition of methanol. The precipitated resins are then assayed for their radioactive content.

The radioactive tin required for the present group of experiments was obtained by subjecting a specimen of high purity tin to neutron bombardment which resulted in the formation of the unstable isotope, ^{113}Sn.

$$^{112}Sn + {}^{1}n^{0} \rightarrow {}^{113}Sn + \gamma$$

The resultant radioactive metal was next converted to tin tetrachloride by reaction with chlorine and the product diluted with a quantity of nonradioactive $SnCl_4$. By means of a redistribution reaction with tetrabutyltin, the diluted radioactive tin tetrachloride was transformed to dibutyltin dichloride.

$$^{113}SnCl_4 + Bu_4Sn \rightarrow Bu_2{}^{113}SnCl_2 + Bu_2SnCl_2$$

The radioactive dibutyltin dichloride was then used to prepare the various organotin stabilizers by the methods outlined in Part III[1] of this series.

EXPERIMENTAL

Materials

The poly(vinyl chloride) used in these experiments was Geon 101-EP manufactured by the B. F. Goodrich Company.

The tin used for neutron bombardment was Tin E, Sample No. 435, obtained from the U. S. National Bureau of Standards. To facilitate its handling, the metal was cast in the form of 3-mm. diameter wire by drawing the molten metal into a length of glass tubing having that same diameter. The wire was then cut into four small sections, each weighing approximately 0.2 g. Each section was then sealed in a small quartz ampule. The neutron bombardment was performed in the "swimming pool" reactor of the Battelle Memorial Institute at West Jefferson, Ohio. After irradiation, the four ampules and their contents at a distance of 1 m. had an activity

of 690 counts/min. This material (0.8 g., 0.067 atom) was converted quantitatively to tin tetrachloride by reaction with chlorine and the product diluted with nonradioactive $SnCl_4$ (25 g., 0.096 mole). (The detailed experimental procedure for this and the other preparations will be reported elsewhere.[5]) A portion of the resultant radioactive tin tetrachloride (18.93 g., 0.073 mole) was then equilibrated with tetrabutyltin (24.97 g., 0.072 mole) to furnish dibutyltin dichloride. After distillation (135°C./7 Torr) there was obtained 39.2 g. (0.137 mole) of product melting at 43°C. Another portion of the radioactive tin tetrachloride (7.8 g., 0.03 mole) was allowed to react with tetraoctyltin (17.1 g., 0.03 mole) to furnish, after recrystallization from petroleum ether, 11.85 g. of dioctyltin dichloride melting at 48°C.

The preparation of the organotin-^{113} Sn-stabilized poly(vinyl chloride) films, their heat treatment, and subsequent work-up was performed as detailed in Part III.[1]

Measurement of Radioactivity

Isotope ^{113}Sn decays by the process of K-electron capture to yield a metastable indium isotope, a process having a half-life of 112 days.

$$^{113}\mathrm{Sn} + {}^{0}e^{-1} \xrightarrow[112\ \mathrm{d.}]{} {}^{113m}\mathrm{In} + \gamma'$$

The indium isotope thus generated in turn undergoes rapid decay to a stable isotope of that same element. This latter process has a half-life period of 1.73 hr.

$$^{113m}\mathrm{In} \xrightarrow[1.73\ \mathrm{hr.}]{} {}^{113}\mathrm{In} + \gamma''$$

These two processes are accompanied by the emission of γ-rays of widely differing energies—24 K.e.v. for the ^{113}Sn decay and 392 K.e.v. for ^{113m}In. For the purposes of our present studies we chose to measure the 392 K.e.v. radiation.

The metastable indium, formed by the decay of the ^{113}Sn atoms, is insoluble in the tetrahydrofuran–methanol mixture and, as a consequence, all of that element present in the film at the time of its dissolution will be collected along with the precipitated resin in the filtration step. This will be true whether the individual radioactive indium atom has originated from a tin atom which is chemically bound to the polymer or from one which is in no way bound to the polymer. Obviously, if our studies were to be meaningful, a way had to be found to circumvent this difficulty. The way proved to be quite simple and consisted in simply allowing the filtered resin to stand for a period of 20–24 hr. before attempting to assay its radioactivity. During this interval, which amounts to about 12–13 half-life periods, more than 99% of the radioactive indium present at the time of filtration will have been transformed to the nonradioactive species. Twenty-four hours after filtration essentially all the 392 K.e.v. radiation emitted by the resin will be originating from ^{113m}In atoms which have been generated from

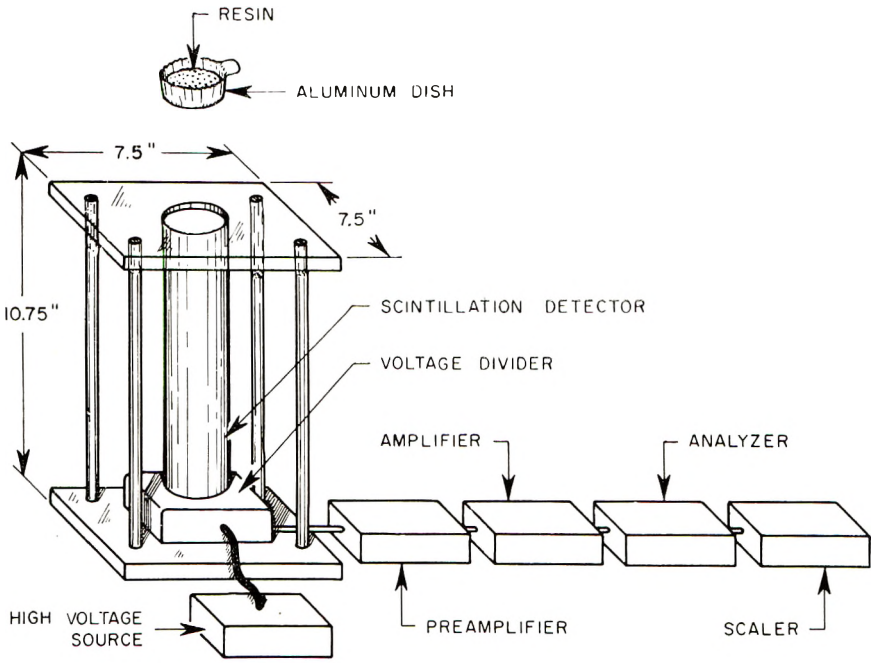

Fig. 1. Semischematic diagram of scintillation counter.

^{113}Sn atoms that were chemically bound to (or coordinatively associated with) the resin at the time of its precipitation.

Detection of the 392 K.e.v. radiation was made by means of a thallium-activated sodium iodide scintillation phosphor (crystal diameter 2 in., crystal thickness 2 in.) coupled to a 2-in. photomultiplier tube (Assembly 8S8/2, Harshaw Chemical Co.), the power required for the photomultiplier tube being furnished by a stable high voltage supply unit (Model 683, Victoreen Instrument Co.) The signal from the photomultiplier tube was transmitted in sequence to a preamplifier (Model 851-15, Victoreen), a nonoverload linear amplifier (Model 851A, Victoreen), an integral-differential single-channel pulse height analyzer (Model DD2, Victoreen), and finally to a scaler (Model 1050A, Atomic Instrument Co.). The entire assembly is shown semischematically in Figure 1. The scintillation detector was mounted in a small metal stand having a base made of 0.5 in. aluminum plate and a Plexiglas top supported by four aluminum rods. In the center of the Plexiglas top was located a circular aperture (diameter upper portion 2.31 in.) having a 0.25 in. shoulder on its lower edge, the aperture thus being able to function as a receptacle for aluminum foil sample dishes (diameter 2.25 in.). The Plexiglas shelf also permitted us to measure directly the radioactivity of an intact section of poly(vinyl chloride) film. This we did by symmetrically placing the film directly over the aperture, covering it with a second Plexiglas plate and compressing the resultant "sandwich" with a set of four pinch clamps.

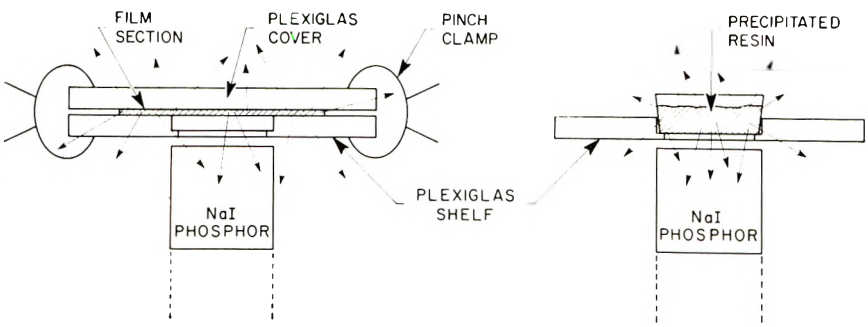

Fig. 2. The differing geometries involved in the scintillation counting of samples as milled films and as precipitated resins.

In order to obtain meaningful data on the radioactivity of our samples, it was necessary to make certain corrections on our experimentally observed measurements. Thus, in addition to the usual correction for background count, it was necessary to correct for the decay of ^{113}Sn occurring in the interval between some initial "zero" time and the time at which the particular sample was actually counted. This was done empirically by employing a standard reference sample, prepared by evenly distributing a layer of finely powdered ^{113}Sn-tagged dibutyltin β-mercaptopropanoate on the bottom of a standard aluminum foil dish. The powder was made to adhere to the dish by careful application of several coats of acrylic spray (Krylon). The activity of this reference sample was carefully determined at a date (our zero time) prior to measurement of the activity of all other experimental samples. Its activity was also determined each day that experimental samples were to be assayed. Then, by application of a simple proportion, the activities of the various experimental samples could be corrected back to their values at zero time, thus providing a meaningful basis of comparison.

In a number of the experiments we also undertook to estimate the amount of radioactivity present in a sample of precipitated resin relative to the amount of radioactivity in the original intact film. This we did by measuring the activity, A_f, of the film prior to its heat treatment, dissolution, and precipitation, and then later measuring the activity, A_r, of it's precipitated resin. The quotient of these two values, A_r/A_f, (both corrected for background and decay) was multiplied by an empirically determined geometry factor, F_g, and by 100 to give the sought for relationship in terms of the percentage of the initially added stabilizer retained by the precipitated resin.

$$\text{Per cent retention} = (A_r/A_f)F_g \times 100$$

The necessity for a geometry correction factor can be readily understood by reference to Figure 2, which shows schematically the geometry involved in the film and precipitated resin counting operations. Clearly, of the total

number of γ-particles emitted by a sample in a given interval of time, only those which strike the sodium iodide phosphor are detected. Further, for a sample of some particular total activity, the magnitude of that detectable fraction can be made to vary by alteration of the sample's shape or placement on the Plexiglas top of the counting stand. Our empirical correction factor for this difference was determined as follows. A section of dibutyltin-^{113}Sn bis(monomethyl maleate)-containing film was assayed for activity as outlined above. It was then subjected to dissolution in tetrahydrofuran and precipitation by methanol, the precipitated resin being collected, washed, and dried in the usual manner. However, the filtrate and the washings, instead of being discarded, were combined and carefully concentrated to a volume of about 3–5 ml. The dry resin was placed in an aluminum foil counting dish and the concentrated mother liquors carefully added from a micropipet in small droplets in such a way as to insure as homogeneous a distribution as possible. To minimize any losses in transfer, the concentrating vessels and the micropipet were washed with small portions of methanol and these washings added to the resin sample. The dish and its contents were then placed in position on the counting stand, assayed for radioactivity, and the geometry factor calculated by means of the relationship

$$F_g = \frac{\text{Activity of the film section}}{\text{Activity of the ppt. resin} + \text{conc'd filtrate}}$$

Two independent determinations of F_g furnished values of 0.6038 and 0.6881. For our calculations we employed their average, 0.6460.

RESULTS AND DISCUSSION

Figure 3 summarizes our findings pertaining to the retention of radioactivity by a poly(vinyl chloride) resin which has been milled with various ^{113}Sn-tagged organotin stabilizers, the films subjected to heat treatment at 175°C. and then to a sequence of two dissolution–precipitation cycles. When one compares these results with those obtained for the corresponding butyl-tagged stabilizers,[1] it is seen that certain similarities are clearly evident.* Thus, both of the monomethyl maleate curves rise steeply,

* In comparing the curves of Figure 3 in this paper with the curves of Figure 3 in the preceding paper,[1] one should note that in the present paper we have plotted the percentage of the originally added stabilizer which is retained by the precipitated resin, whereas in the earlier paper we have plotted the actually measured counts per minute. Since the same batch of radioactive tin tetrachloride was used to prepare all of our ^{113}Sn-tagged stabilizers, their radioactivities per millimole will be equal. Similarly, in our butyl-tagged studies, the same batch of dibutyl-1-^{14}C-tin dichloride was used to prepare the different stabilizers used in that work hence their radioactivities per millimole must also be the same. Unfortunately, our supply of ^{113}Sn-tagged dibutyltin dichloride was insufficient to enable us to prepare an adequate amount of the correspondingly tagged dibutyltin bis(2-ethylhexanoate) for study of its retention by poly(vinyl chloride).

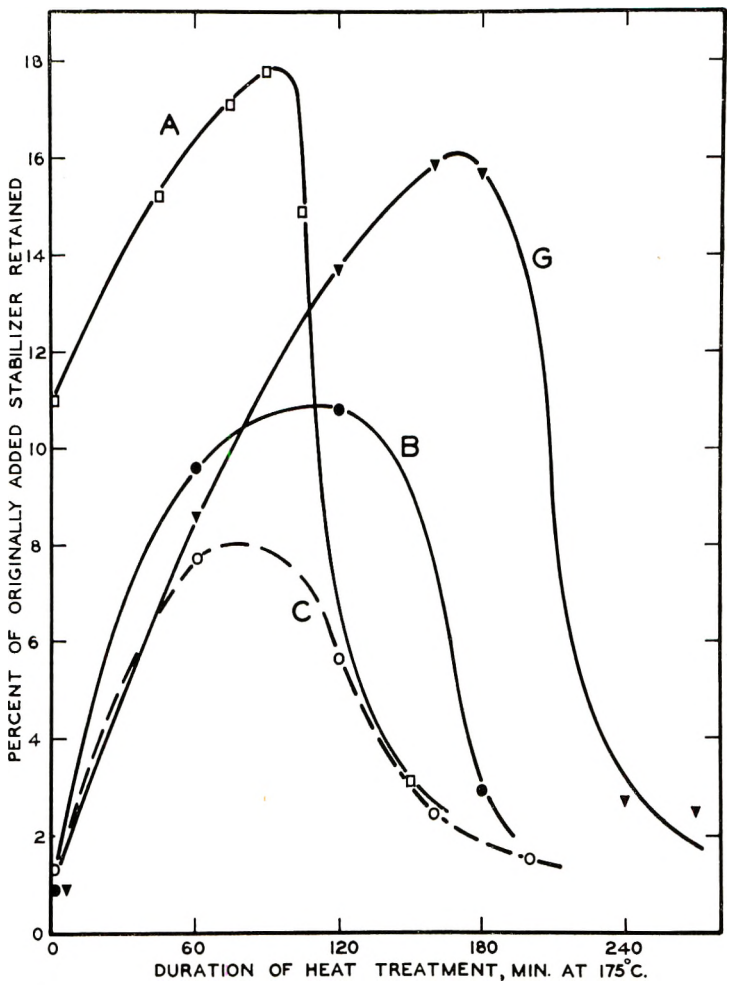

Fig. 3. Effect of heat treatment on the retention of radioactivity by poly(vinyl chloride) resin after two dissolution-precipitation cycles, the resins having been milled with: (*A*) dibutyltin-^{113}Sn bis(monomethyl maleate); (*B*) dibutyltin-^{113}Sn (β-mercaptopropanoate; (*C*) dibutyltin-^{113}Sn bis(oxoöctyl thioglycolate; (*G*) dioctyltin-^{113}Sn β-mercaptopropanoate.

reach relatively sharp maxima, and then steeply descend. The pair of curves which characterize the retention of radioactivity from the butyl-tagged and the ^{113}Sn-tagged dibutyltin β-mercaptopropanoates are especially similar in both their shape and displacement. Although the two curves for the differently tagged species of dibutyltin bis(oxoöctyl thioglycolate) do not match each other quite so well as do the curves for the β-mercaptopropanoates, there is, nevertheless, an obvious similarity. Finally, when one compares the relative heights of the maxima, it is clear that the same general relationships obtain for the stabilizers tagged in the butyl group as for the stabilizers tagged in the tin atom. Thus, the rela-

tive heights of the maxima of the A, B, and C curves are $A > B > C$, whereas the displacements of those maxima along the abscissa are $A \simeq C < B$.

These facts, as well as certain others about to be discussed, suggest that in the performance of their stabilizing functions the organotin compounds undergo little or no cleavage of their carbon–tin bonds. True, if this postulate is correct, then the displacements of the maxima along the abscissa for a given stabilizer should be the same when the tag is in the butyl group as when it is in the tin atom. Further, the relative heights of the maxima for the different stabilizers as revealed by the butyl-tagging should be equivalent to the relative heights of the maxima for those stabilizers as revealed by the ^{113}Sn-tagging. However, the accumulation of experimental errors inherent in the various operations, as well as the fact that the positions assigned to the maxima were arrived at by extrapolation from only two or three experimentally determined points, may reasonably be expected to result in some discrepancies. Thus, it appears that for the ^{113}Sn-tagged studies with dibutyltin bis(monomethyl maleate) the maximum retention of radioactivity by the resin coincides with approximately 90 min. of heat treatment, whereas the butyl-tagged studies indicate that the maximum retention occurs at about 60 min.

Figure 3 has one other curve which merits some attention viz., curve G, which was obtained from a film that had been milled with dioctyltin ^{113}Sn β-mercaptopropanoate. It is generally recognized that the toxicities of dioctyltin stabilizers are considerably less than that of their butyl analogs.[3] Further, the dioctyl compounds appear to be equal, or perhaps somewhat superior, to the dibutyl analogs with respect to their stabilizing action. These advantages notwithstanding, the industrial usage of the dioctyltin compounds remains relatively minor, chiefly because of their increased costliness. It was of interest, nevertheless, to learn whether under our experimental conditions a dioctyltin compound might show a greater degree of retention by the resin than its dibutyl analog. For this purpose we chose to compare the β-mercaptopropanoate derivatives. Curves B and G (Fig. 3) show that appreciable differences do exist after the films have been heated for approximately 2 hr. at 175°C., the dioctyl compound being more strongly retained. During the earlier stages, however, the difference in retention is slight or nonexistent.

The information summarized in Figure 3 relates to the retention of radioactivity by the resin after a sequence of two dissolution–precipitation cycles. In order to gain insight into the nature of this retention, it is essential to know whether it remains effectively constant when the resin is subjected to further cycles of dissolution and precipitation, or whether that treatment will result in further decrease. Figure 4 summarizes our findings for a film containing dibutyltin-^{113}Sn bis(monomethylmaleate) which had been heat treated at 175°C. for 75 min. It is clearly evident that during the first 10–11 cycles the amount of retention decreases markedly with each successive cycle. However, in the latter cycles the differences become

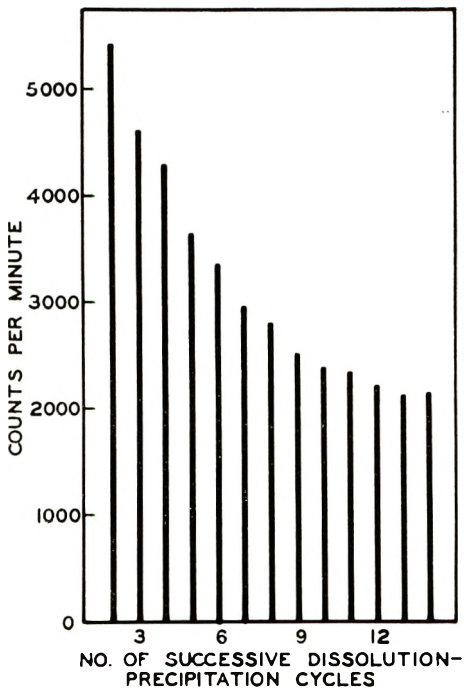

Fig. 4. Effect of repeated dissolution and precipitation on the retention of radioactivity by a resin milled with dibutyltin-^{113}Sn bis(monomethyl maleate).

smaller and smaller and there is reason to think a constant value in the neighborhood of 2000 counts/min. is being approached. If our postulate that organotin compounds undergo little or no cleavage of their carbon–tin bonds in the performance of their stabilizing function is indeed valid, then it follows that in our experiment[1] involving the repeated dissolution and precipitation of the dibutyl-1-^{14}C-tin bis(monomethyl maleate)-stabilized resin, a sequence of ten or more successive dissolution–precipitation cycles, rather than six, would have revealed a similar leveling off.

Curve *K* in Figure 5 summarizes our findings in a supplementary experiment with a dibutyltin-^{113}Sn β-mercaptopropanoate-stabilized film which had been heat-treated at 170°C. for 75 min. It is seen that for this particular resin-stabilizer system a sequence of 11 dissolution–precipitation cycles shows only a continuous decrease in retained radioactivity with no indication of a leveling off at some effectively constant value. Whether, upon continued dissolution and precipitation, such a leveling off might be revealed can only be conjectured. But should that prove to be the case, the value at constant retention, it would seem, would be considerably less than the value of 2000 counts/min. indicated for the monomethyl maleate analog. The other two curves in Figure 5 relate to experiments in which dibutyltin-^{113}Sn β-mercaptopropanoate (ca. 0.25 mmole) was added to a solution of either virgin resin (5.17 g., curve *L*) or milled and heat treated

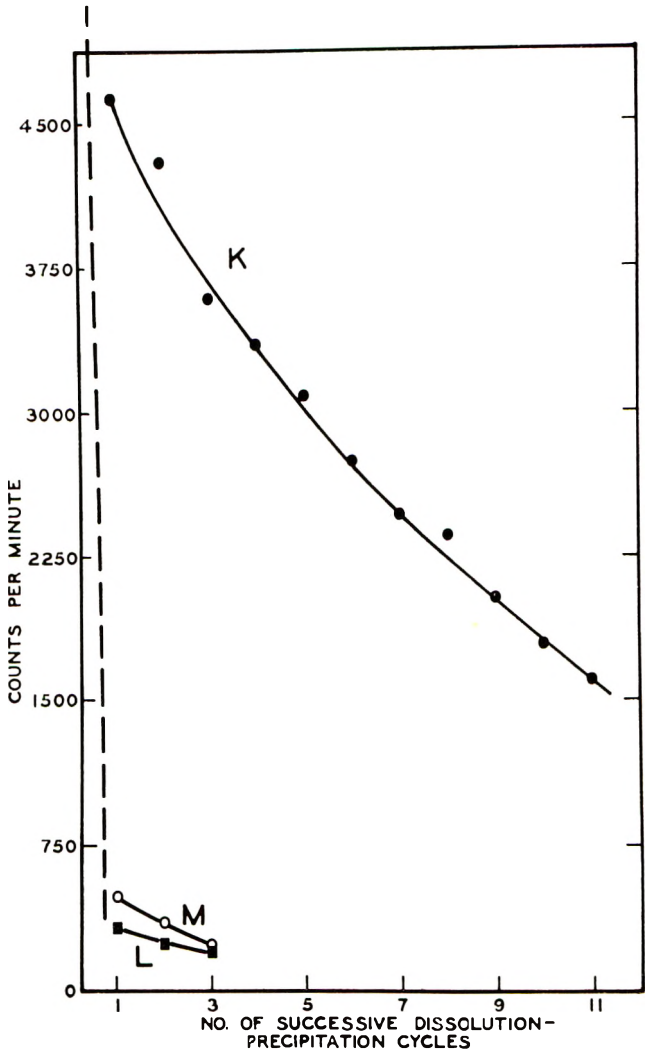

Fig. 5. Effect of repeated dissolution and precipitation on the retention of radioactivity by: (*K*) a resin milled with dibutyltin-^{113}Sn β-mercaptopropanoate and heat treated at 170°C. for 75 min.; (*L*) a virgin resin to whose solution in tetrahydrofuran dibutyl-tin-^{113}Sn β-mercaptopropanoate was added; (*M*) a milled and heat-treated resin to whose solution in tetrahydrofuran dibutyltin-^{113}Sn β-mercaptopropanoate was added.

resin (5.17 g. of film, 30 min. at 175°C., curve *M*) in tetrahydrofuran (85 ml.) and the resins thereafter precipitated and assayed for retained radioactivity. It is seen that in both cases the amount of radioactivity retained by the precipitated resins is very much less than that found in the experiment relating to curve *K*. In the former cases it seems probable that the activity of the precipitated resins is primarily the result of physical occlusion. The very magnitudes of the differences between curve *K* and curves *L* and *M* are such as to render extremely unlikely the possibility that the re-

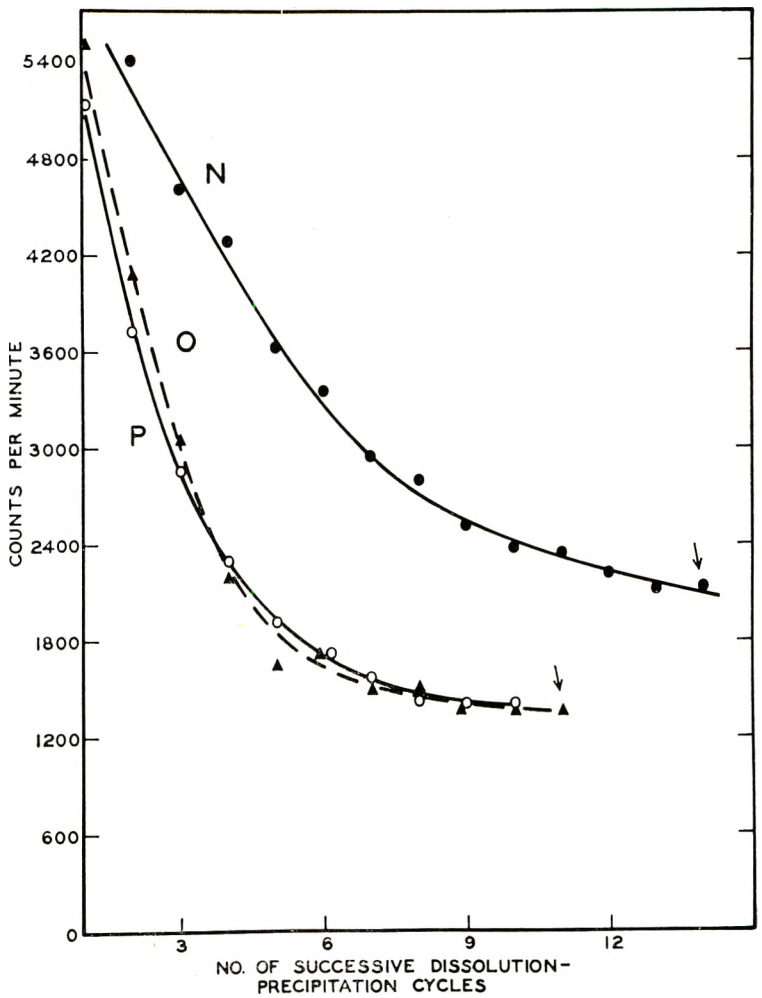

Fig. 6. Retention of radioactivity by a resin milled with dibutyltin-^{113}Sn bis(monomethyl maleate) and subjected to repeated dissolution and precipitation using: (*N*) the standard volumes of tetrahydrofuran and methanol; (*O*) 2.5 times that amount of tetrahydrofuran and methanol; (*P*) standard volumes of cyclohexanone and methanol.

tention represented by curve *K* can also be the result of simple physical occlusion.

Figure 6 summarizes some further findings on the retention of radioactivity by a dibutyltin-^{113}Sn bis(monomethyl maleate)-stabilized resin. Curve *N* in Figure 6 restates the information given in Figure 4 as a bar graph and indicates an approaching leveling off of retention at about 2000 counts/min. In that experiment we employed our standard volumes of tetrahydrofuran (85 ml.) and methanol (220 ml.) to affect the dissolution and precipitation of the resin in a standard section of film (3.5 × 3.5 in., ca. 5.2 g.). The particular specimen of film used was one which had been

heated at 175°C. for 75 min., and which, after a sequence of two dissolutions and precipitations was found to retain approximately 17.8% of the initially added radioactively tagged stabilizer (3.34 mmoles/100 g. resin). At that stage, the resin had a radioactivity of 5400 counts/min. This activity fell, after a sequence of 14 dissolutions and precipitations, to 2100 counts/min., which is equivalent to a retention of approximately 6.9% of the initially added stabilizer (or a tin-containing moiety thereof). Curve *O* Figure 6, relates to an experiment in which another sample of the same dibutyltin-^{113}Sn bis(monomethyl maleate)-stabilized film was subjected to a sequence of 11 dissolution and precipitation cycles, but in which the volumes of tetrahydrofuran and methanol used were increased by a factor of 2.5. It is seen that under these conditions the initial cycles reveal a much sharper decrease in retained radioactivity and that the latter cycles show a leveling off of about 1350 counts/min., which is equivalent to a retention of approximately 4.5% of the initially added tin. Curve *P* refers to a third experiment in which the standard volume of tetrahydrofuran was replaced by an equal volume of cyclohexanone, and shows that under these conditions one obtains essentially the same results as when the standard volumes of tetrahydrofuran and methanol are increased by a factor 2.5. Clearly, these experiments leave no doubt as to the reality of the leveling off of retention in resins stabilized with dibutyltin-^{113}Sn bis(monomethyl maleate). One is, of course, tempted to conclude that curve *N*, if the experiment had been further continued, would show a leveling off at the same value as found for curves *O* and *P*. But this, if correct, remains to be proved.

Two further experiments are pertinent here. We found that when the resin samples which correspond to the pair of "arrowed" points in Figure 6 were dissolved in tetrahydrofuran (85 ml.), their solutions slowly saturated at room temperature with anhydrous hydrogen chloride and then allowed to stand for 24 hrs. before precipitation with methanol, the measured activities of the resins were essentially zero (21 and 42 counts/min.). This finding is consistent with our earlier one,[1] which showed by spectroscopic means the absence of tin in a dibutyltin bis(monomethyl maleate)-stabilized resin which had been subjected to a similar treatment. Since such hydrogen chloride treatment causes extremely little or no carbon–tin bond cleavage when applied to tetrabutyltin, dibutyltin dichloride, or dibutyltin β-mercaptopropanoate, we conclude that the retention of radioactivity by the resin cannot be due to the presence of carbon–tin bonds linking the polymer to the stabilizer. Instead, the accumulated evidence is most plausibly accounted for by the presence of coordinative linkages between the tin atoms and certain donor atoms covalently bound to the polymers backbone (viz., chlorine, oxygen, and/or sulfur). Such linkages could be ruptured by the action of tetrahydrofuran, methanol, cyclohexanone and, most readily, by hydrogen chloride. The proposed reactions can be visualized by the following equations in which Z is a donor present in the Y moiety (W + Z = Y).

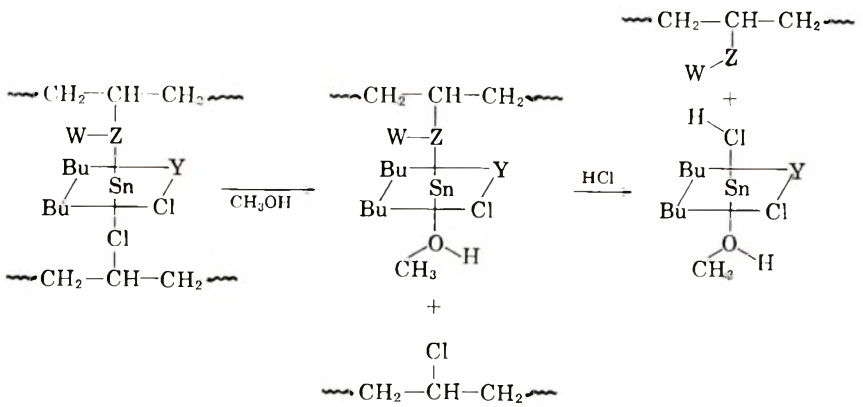

For the particular case of the dibutyltin-^{113}Sn bis(monomethyl maleate)-stabilized resin, which furnished unequivocal evidence of constant retention of radioactivity equivalent to approximately 4.5% of the initially added tin, one may rationalize the findings in terms of the often suggested[4] Diels-Alder addition to a degraded section of the polymer

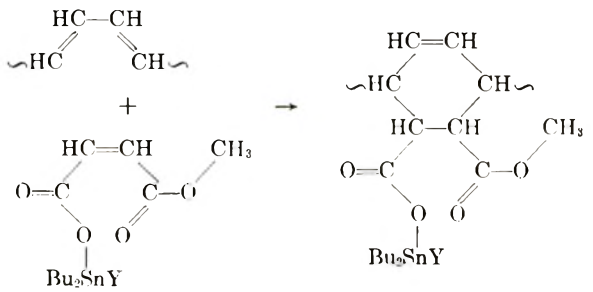

where Y is monomethyl maleate or chlorine. The fact that treatment of the resin with hydrogen chloride in tetrahydrofuran results in the loss of essentially all of the resin's radioactivity, is then readily accounted for in the following way.

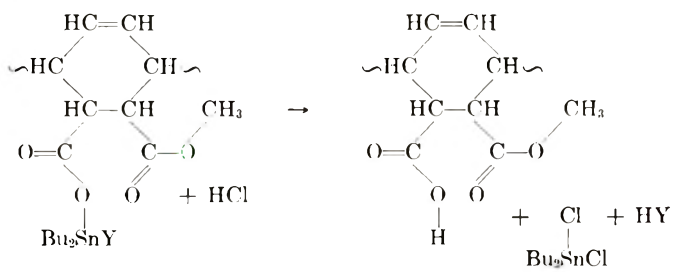

Attractive as these ideas may be, the question yet remains as to whether such a Diels-Alder addition, if it does indeed occur, accounts for in whole or in part the stabilizing action of the organotin maleates.

References

1. Frye, A. H., R. W. Horst, and M. A. Paliobagis, *J. Polymer Sci.*, **A2**, 1765 (1964).
2. Frye, A. H., R. W. Horst, and M. A. Paliobagis, *J. Polymer Sci.*, **A2**, 1801 (1964).
3. Lewis, W. R., and E. S. Hedges in *Metal-Organic Compounds*, No. 23, Advances in Chemistry Series, American Chemical Society, Washington, D. C., 1959, p. 193.
4. Chevassus, F., and R. de Broutelles, *La Stabilisation des Chlorures de Polyvinyle*, Amphora, Paris, 1957, p. 61.
5. Frye, A. H., and R. W. Horst, *Intern. J. Appl. Radiation Isotopes*, in press.

Résumé

On a étudié la chimie de la stabilisation du chlórure de polyvinyle par les composés organostanniques en utilisant la technique des traceurs radioactifs. Les stabilisateurs étudiés sont du type $(R_2SnY_2)_n$ où R est soit butyl ou octyl, Y maléate de monomethyle, oxoöctylthioglycolate ou β-mercaptopropanoate et ou l'étain 113 constitue l'atome traceur. On a trouvé que des résines calendrées sous forme de film avec des stabilisateurs marqués retiennent une quantité appréciable de radioactivité après qu'on ait placé les films dans des conditions de dégradation thermique accélérée, qu'on les ait dissous dans le tétrahydrofuranne et ensuite précipités de leur solution par addition de méthanol. La quantité de radioactivité retenue varie avec la durée du traitement thermique et avec la nature du groupement Y d'une façon comparable à ce que l'on avait trouvé dans une étude précédente où le groupement butyle du stabilisateur était marqué au ^{14}C. Nous avons également trouvé que la quantité de radioactivité retenue par la résine précipitée décroît régulièrement quand on soumet la résine à une suite de dissolution et de précipitation. Cependant, dans le cas de la résine stabilisée avec le dibutyl-^{113}Sn bis(monométhyl maléate), la perte de radioactivité causée par les dissolutions et les précipitations répétées, semble s'arrêter après 13 à 14 cycles et conserver une valeur constante de rétention. Le traitement des résines radioactives par l'acide chlorhydrique anhydre provoque la perte de presque toute la radioactivité. Sur la base de ce fait, nous supposons, que lors de leur action stabilisatrice, les composés organostanniques ne subissent que peu ou pas de rupture de leur liaison carbone-étain. Ultérieurement la rétention de radioactivité observée sur la résine s'explique le mieux en supposant l'existence d'un lien de coordination entre l'atome d'étain du stabilisateur et quelqu'atome donneur présent dans la structure moléculaire du polymère.

Zusammenfassung

Der Chemismus der Stabilisierung von Polyvinylchlorid durch Organozinnverbindungen wurde mittels einer radioaktiven Tracer-Technik untersucht. Die untersuchten Stabilisatoren waren vom Typ $[R_2SnY_2]_n$, wobei R Butyl oder Octyl, Y Monomethylmaleat, Oxoöctylthioglykolat oder β-Mercaptopropionat war und ^{113}Sn als radioaktive Markierung verwendet wurde. Die mit den markierten Stabilisatoren zu Filmen gewalzten Harze hielten eine merkliche Menge Radioaktivität zurück, nachdem sie einem beschleunigten thermischen Abbau unterworfen, in Tetrahydrofuran gelöst und durch Zusatz von Methanol aus der Lösung gefällt worden waren. Die Menge der zurückgehaltenen Radioaktivität variiert mit der Dauer der Hitzebehandlung und mit der Art der Y-Gruppe in einer Weise, die zu unseren Befunden bei einer früheren Untersuchung mit einem in den Butylgruppen mit ^{14}C markierten Stabilisator parallel verläuft. Die Menge der von den gefällten Harzen zurückgehaltenen Radioaktivität sinkt bei wiederholter Umfällung der Harze stetig ab. Jedoch scheint wenigstens im Falle des mit Dibutylzinn-^{113}Sn-bis(monomethylmaleat) stabilisierten Harzes, dieser Radioaktivitätsverlust bei wiederholtem Umfällen nach 13–14 Umfällungen aufzuhören und sich ein konstanter Retentionswert einzustellen. Die Behandlung der radioaktiven Harze mit wasserfreiem Chlorwasserstoff führt zum Verlust praktisch ihrer gesamten Radioaktivität. Auf Grund dieser Befunde nehmen wir an, dass die Organozinnverbindungen

bei ihrer stabilisierenden Wirkung nur geringe oder gar keine Spaltung ihrer Kohlenstoff–Zinn-Bindung erlieiden. Ferner lässt sich die beobachtete Retention der Radioaktivität durch das Harz am einfachsten durch das Vorliegen einer koordinativen Bindung zwischen dem Zinnatom des Stabilisators und irgendeinem in der Molekülstruktur des Polymeren vorhandenen Donatoratom deuten.

Received March 15, 1963

JOURNAL OF POLYMER SCIENCE: PART A VOL. 2, PP. 1801–1814 (1964)

The Chemistry of Poly(vinyl Chloride) Stabilization. V. Organotin Stabilizers Having Radioactively Tagged Y Groups

ALFRED H. FRYE, RAYMOND W. HORST, and MARKO A. PALIOBAGIS, *The Cincinnati Milling Machine Company, Cincinnati, Ohio, and The Advance Division of the Carlisle Chemical Works, New Brunswick, New Jersey*

Synopsis

Experiments with a select group of radioactively tagged organotin stabilizers of the general formula Bu_2SnY_2, in which the radioactive atoms (^{14}C) are located in the Y groups, have shown, that, under the conditions normally employed to evaluate and screen poly(vinyl chloride) heat stabilizers, a portion of that radioactivity becomes firmly associated with the resin. Under standard conditions, the extent of this association has been found to be dependent upon the nature of the Y group and the duration of the heat treatment. It is suggested that the stabilizing action of these organotin compounds arises in part from reactions between the polymer and the stabilizer wherein certain of the polymer's chlorine atoms are exchanged for the stabilizer's Y groups (or a portion thereof), the resulting structure being more stable toward degradative elimination. Other possibilities for reaction between the polymer and the stabilizer are also considered and it is shown how these can further supplement the organotin compound's stabilizing action and yet be rationalized within the experimental evidence.

INTRODUCTION

In Parts III[1] and IV[2] of this series we reported the results of our radioactive tracer studies on the stabilizing action of a group of organotin compounds of the class $[R_2SnY_2]_n$, with tags in the alkyl groups (^{14}C) and in the tin atoms (^{113}Sn). The alkyl groups of the stabilizers chosen for study were, with one exception, butyl groups, while the Y groups were monomethyl maleate, β-mercaptopropanoate, oxoöctyl thioglycolate, or 2-ethylhexanoate. In the one exception the stabilizer's alkyl groups were octyl. These studies showed that a resin milled with a tagged stabilizer, and thereafter subjected to the conditions normally used to affect the accelerated thermal degradation of the polymer, retains a significantly large amount of radioactivity when the milled film is dissolved in tetrahydrofuran and the resin then precipitated by the addition of methanol. The amount of radioactivity retained by the resin varies with the nature of the stabilizer's Y group and with the duration of the film's heat treatment, and is very much greater than can reasonably be accounted for by physical

occlusion of the stabilizer in the precipitated polymer. It was also found, that the amount of radicactivity retained by the precipitated resins decreases in a regular way when the resins are subjected to successive cycles of dissolution and precipitation. In one instance at least—a resin stabilized with dibutyltin-^{113}Sn bis(monomethyl maleate)—the loss of radioactivity with successive dissolutions and precipitations leveled off at a relatively low but constant value. Of particular interest was the marked parallelism evident between the curves in the butyl-tagged experiments with those of the tin-tagged series, a parallelism which indicates that in the performance of their stabilizing action organotin compounds undergo little or no cleavage of their carbon–tin bonds. It was suggested that these and other findings are best rationalized in terms of a coordinative linkage formed between the stabilizer's tin atom and donor atoms present in the polymer's molecular structure.

In the present paper we report our experiments involving the same set of organotin stabilizers, but with the radioactive tags in the Y groups. The syntheses of the required radioactive intermediates and their conversion to the final stabilizers are outlined in eqs. (1)–(11).

Dibutyltin bis(monomethyl-^{14}C maleate):

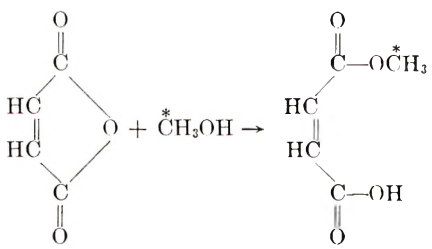

(1)

$$2\ \overset{*}{C}H_3O_2CCH{=}CHCO_2H + K_2CO_3 \rightarrow 2\ \overset{*}{C}H_3O_2CCH{=}CHCO_2K + CO_2 + H_2O \quad (2)$$

$$Bu_2SnCl_2 + 2\ KO_2CCH{=}CHCO_2\overset{*}{C}H_3 \rightarrow Bu_2Sn(O_2CCH{=}CHCO_2\overset{*}{C}H_3)_2 + 2\ KCl \quad (3)$$

Dibutyltin β-Mercaptopropanoate-3-^{14}C:

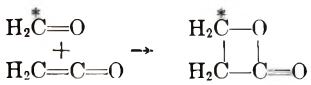

(4)

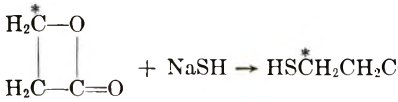

(5)

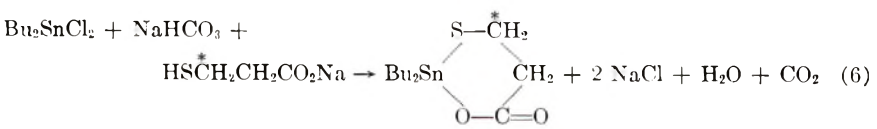

(6)

Dibutyltin bis(oxoöctyl thioglycolate-1-^{14}C):

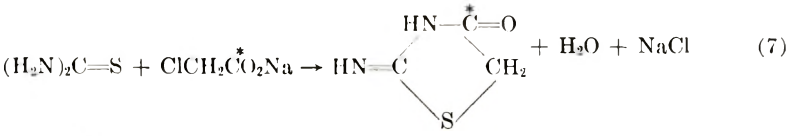

(7)

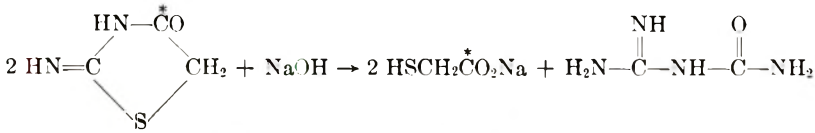

(8)

(9)

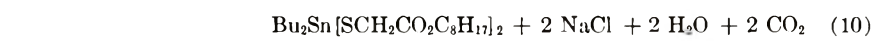

(10)

Dibutyltin bis(2-ethylhexanoate-1-^{14}C):

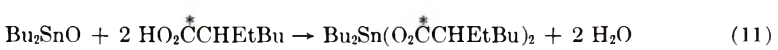

(11)

EXPERIMENTAL

Materials

The poly(vinyl chloride) used in these experiments was the same as used in parts III[1] and IV.[2]

The detailed procedures for the preparation of the radioactive stabilizers will be reported elsewhere;[9] however, the following data will serve to provide information pertinent to the relative radioactivities of the stabilizers and the per cent conversions in which they were obtained. Dibutyltin bis-(monomethyl-^{14}C maleate) was prepared from a mixture of 16 mg. of methanol-^{14}C (2.0 mc./mmole, Volk Radio-Chemical Co.) and 830 mg. of nonradioactive methanol. The end product was obtained in a 96% overall conversion and was found by assay to have an activity of 32 μc./mmole. The dibutyltin β-mercaptopropanoate-3-^{14}C was prepared from a mixture of 60 mg. of paraformaldehyde-^{14}C (0.5 mc./mmole, Volk Radio-Chemical Co.) and 2670 mg. of the nonradioactive material. From this the dibutyltin β-mercaptopropanoate-3-^{14}C was obtained in 43.2% overall conversion with a calculated activity of 11 μc./mmole. From a mixture of 57 mg. of monochloroacetic-1-^{14}C acid (1.64 mc./mmole, Nuclear-Chicago Co.) and 5460 mg. of the nonradioactive acid we obtained dibutyltin bis(oxoöctyl thioglycolate-1-^{14}C) in 62.6% overall conversion, the products' calculated activity being 34 μc./mmole. Dibutyltin bis(2-ethylhexanoate-1-^{14}C) was prepared in essentially quantitative conversion from a mixture of 78 mg. of 2-ethylhexanoic acid (1 mc./mmole, Nuclear Chicago Co.) and 5480 mg. of the nonradioactive acid, the calculated activity of the product being 28 μc./mmole.

Procedures and Radioactive Measurements

The various experimental films were prepared as detailed in Part III[1] of this series, each having 3.34 mmole of stabilizer per 100 g. of resin. The films were than subjected to the same standard procedures of heat treatment, dissolution and precipitation, and radioactive assay as also described therein.

RESULTS AND DISCUSSION

Unlike the experiments in Parts III and IV of this series, in which the different stabilizers had equal radioactivities per millimole, the stabilizers employed in the present experiments have unequal radioactivities. Thus, in the experiments in which the stabilizers' butyl groups were tagged with ^{14}C, all had identical radioactivities per millimole (ca. 11 μc./mmole) because they were prepared from the same batch of dibutyl-1-^{14}C-tin dichloride. Similarly, the ^{113}Sn-tagged stabilizers had equal radioactivities because they were prepared from the same batch of dibutyltin-^{113}Sn dichloride (although here we have no specific measure of the degree of that radioactivity). In the present experiments involving the Y-tagged stabilizers, such uniformity no longer obtains and, as a consequence, an additional element of uncertainty is introduced into the interpretation of our findings. Although we have data which permit us to calculate the activities of our different Y-tagged stabilizers, those data involve a number of uncertainties. Hence we offer the following values in full realization of their possible error: dibutyltin bis(monomethyl-^{14}C maleate), 32 μc./mmole; dibutyltin β-mercaptopropanoate-3-^{14}C, 11 μc./mmole; dibutyltin bis(oxoöctyl thioglycolate-1-^{14}C), 34 μc./mmole; dibutyltin bis(2-ethylhexanoate-1-^{14}C), 28 μc./mmole.

Figure 1 summarizes our data on the retention of radioactivity by Geon 101–EP poly(vinyl chloride) resin stabilized with the above Y-tagged organotin compounds, the radioactive assays having been made after the milled resin's heat treatment and a sequence of two dissolution and precipitation cycles. The data present a number of surprises; however, before we proceed with their analyses, it is advantageous to examine our findings regarding the effect of repeated dissolution and precipitation on the retention of radioactivity in these same resin–stabilizer systems. Figure 2 shows that none of the four resin–stabilizer systems gives evidence of a continued loss of radioactivity when the precipitated resins are subjected to further dissolution-precipitation cycles. True, each shows a considerable amount of irregular fluctuation from assay to assay, but these are of a nature and magnitude as to be accounted for by experimental inaccuracies. From these data we conclude that the observed retention of radioactivity by the resin is due to the incorporation of the respective Y groups (or a portion thereof) into the polymer's molecular structure.

Perhaps the greatest surprise disclosed by Figure 1 is the relatively small amount of radioactivity retained by the resin stabilized with dibutyltin

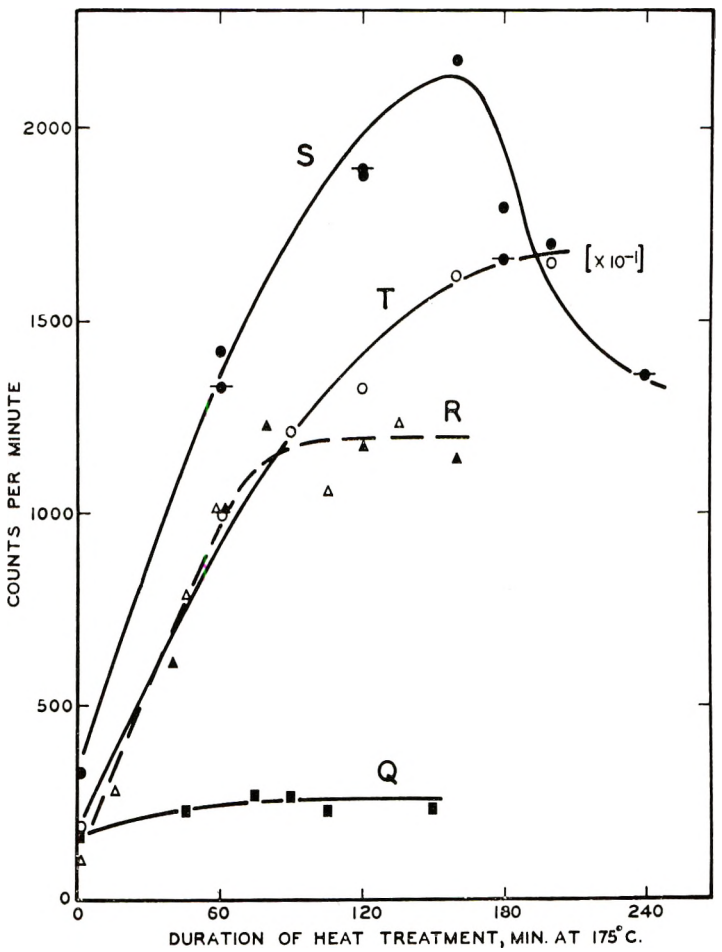

Fig. 1. Effect of heat treatment on the retention of radioactivity by poly(vinyl chloride) resin after two dissolution precipitation cycles, the resin having been milled with: (*Q*) dibutyltin bis(monomethyl-^{14}C maleate; (*R*) dibutyltin bis(2-ethylhexanoate-^{14}C; (*S*) dibutyltin β-mercaptopropanoate-3-^{14}C; (*T*) dibutyltin bis(oxoöctyl thioglycolate-1-^{14}C). Note that ordinate of curve T has been diminished by a factor of 10^{-1}.

bis(monomethyl-^{14}C maleate). We find this surprising because in our previous studies involving these same stabilizers, but in which the butyl groups and then the tin atoms bore the radioactive tags, the amount of radioactivity retained by a resin containing the monomethyl maleate stabilizer was, on the whole, greater than that for the other resin–stabilizer systems. In the original design of the investigation, our first thought was to prepare a dibutyltin maleate compound in which the ^{14}C-tag would be located in the acyl moiety of the half-ester rather than in the alkyl moiety. We were dissuaded from this, however, by the work involved in the synthesis of a ^{14}C-tagged maleic acid, and chose instead to tag the alkyl moiety.

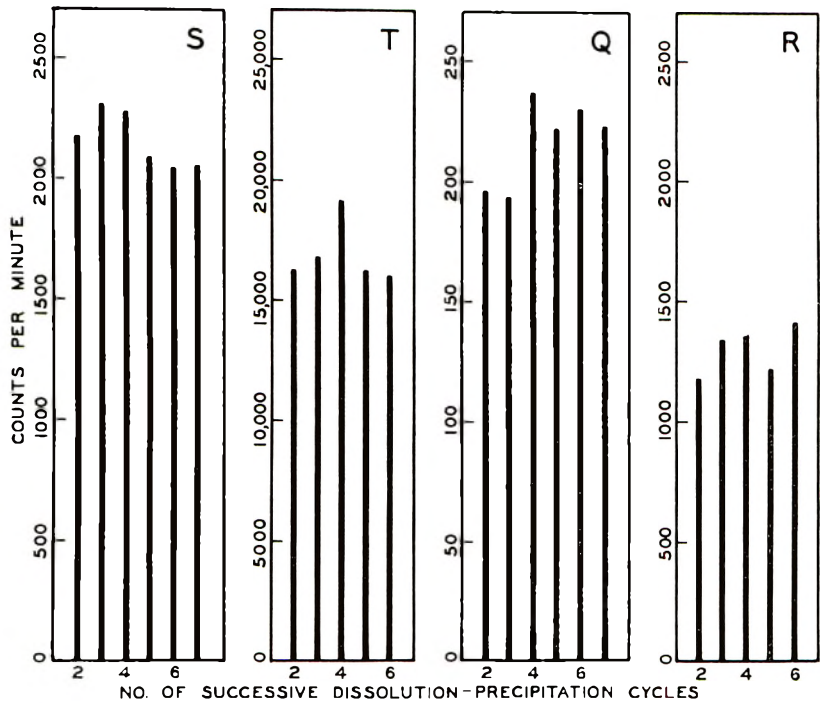

Fig. 2. Effect of repeated dissolution and precipitation on the retention of radioactivity by a resin milled with: (*S*) dibutyltin β-mercaptopropanoate-3-^{14}C; (*T*) dibutyltin bis(oxoöctyl thioglycolate-1-^{14}C); (*Q*) dibutyltin bis(monomethyl-^{14}C maleate); (*R*) dibutyltin bis(2-ethylhexanoate-1-^{14}C).

This choice was made in full awareness of two possible consequences: (*1*) half-esters of maleic acid are prone to undergo thermal cleavage to the anhydride and alcohol; (*2*) in the dissolution-precipitation phase of the work one might incur ester exchange with the methanol used for precipita-

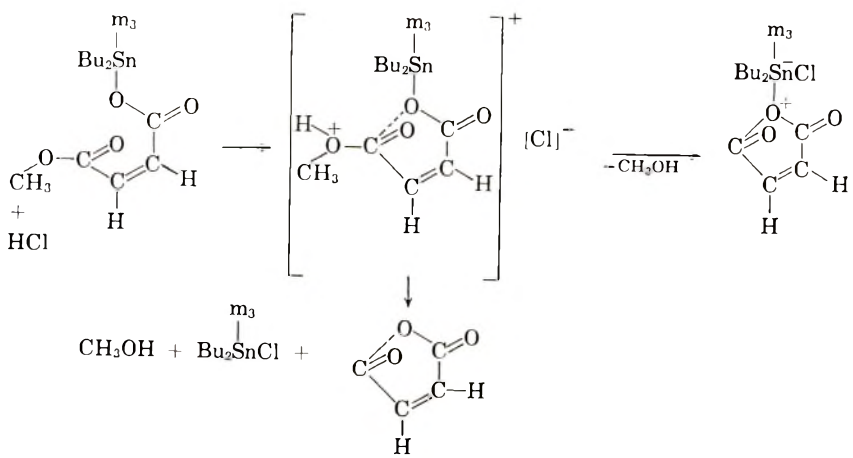

tion. The latter of these two possibilities is discredited by the fact that the retention of radioactivity by a dibutyltin bis(monomethyl-^{14}C maleate)-stabilized resin remains effectively constant through a sequence of seven dissolution–precipitation cycles (Fig. 2). The other possibility (thermal cleavage of the half-ester) appears to account most plausibly for our present results as shown in the following equations, in which we depict the reaction as being promoted by eliminated hydrogen chloride. Here m_3 represents monomethyl maleate.

The maleic anhydride thus liberated might then undergo a Diels-Alder addition with a segment of olefinically degraded polymer chain.

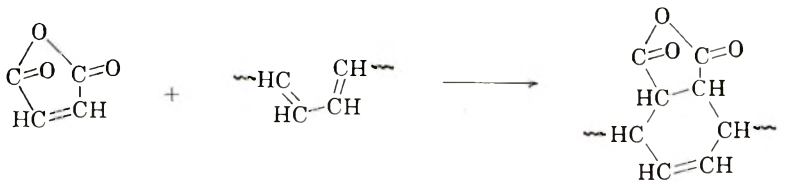

Such a reaction might well serve to "mend" or "heal" an injured section of the polymer, the structure of the adduct, relative to that of the conjugated polyene from which it was derived, being less chromophoric and, at the same time, of enhanced stability toward further reaction. Alternatively, a Diels-Alder addition might occur between the postulated maleic anhydride–dibutyltin chloride monomethyl maleate complex and the polymer:

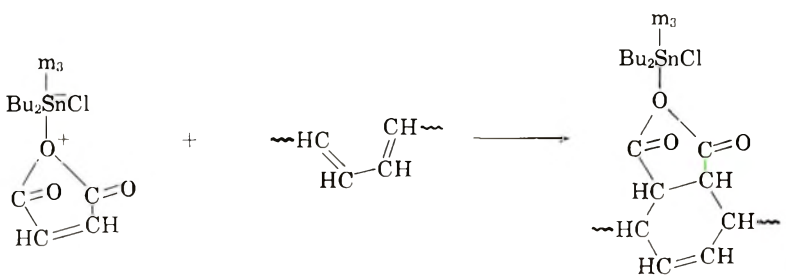

It should be noted that the first of these two possibilities does not provide (at least specifically) for the retention of radioactivity in either the Y-tagged, the tin-tagged, or the butyl-tagged experiments, whereas the second does. Before we consider any further possibilities for reaction between dibutyltin bis(monomethyl maleate) and the polymer, it is advantageous to consider the case of dibutyltin bis(2-ethylhexanoate-1-^{14}C).

The retention of radioactivity for this stabilizer is most plausibly rationalized in terms of an esterifying displacement of certain of the polymer's halogen atoms by the organotin compound's carboxylate moiety, a reaction which we have shown to occur with the barium, cadmium, and zinc carboxylate stabilizers.[3,4]

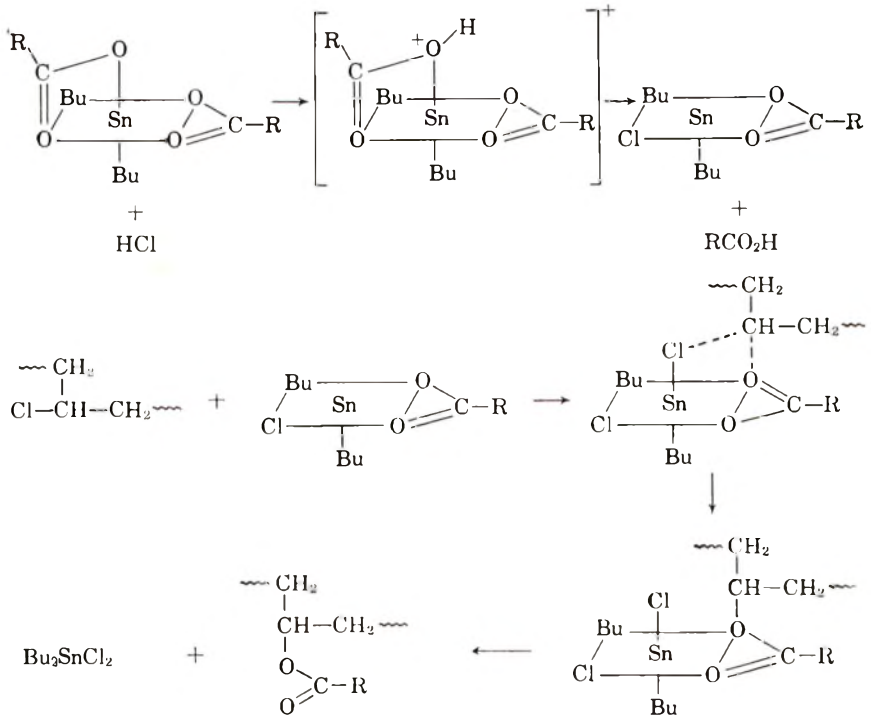

This suggests that similar displacements might be possible for the maleate stabilizer

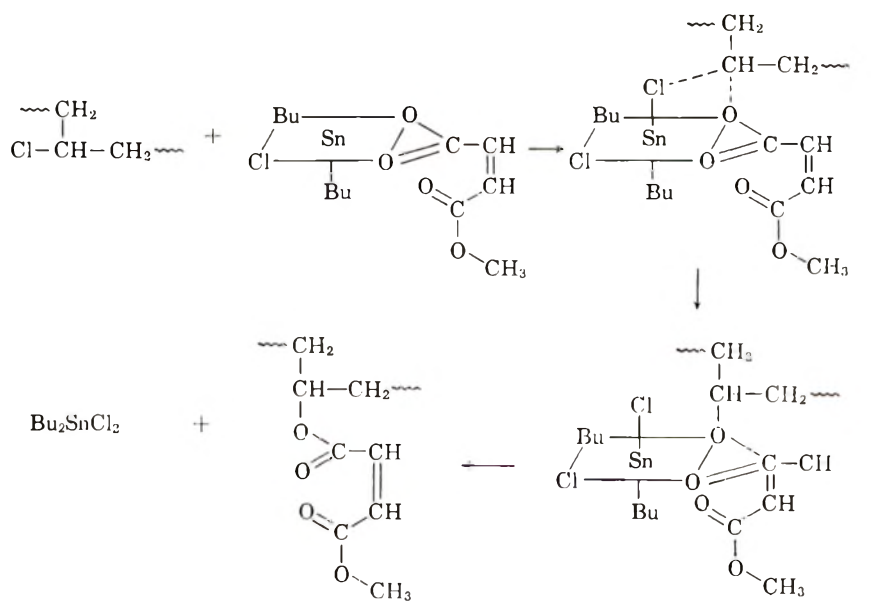

and for the β-mercaptopropanoate as well.

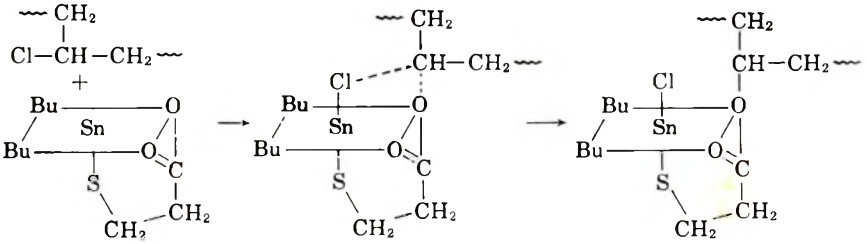

These displacements, like those of the barium, cadmium, and zinc carboxylates, would serve to stabilize the resin when the resulting carboxylate ester is less prone toward elimination than the halide from which it was derived, an aspect of the problem to be discussed more fully below.

Finally, we come to the case of dibutyltin bis(oxoöctyl thioglycolate). Clearly, for this stabilizer some other mode of reaction must be invoked. One which appears quite plausible, is the following wherein a thioether group replaces a chlorine atom on the polymer's backbone.

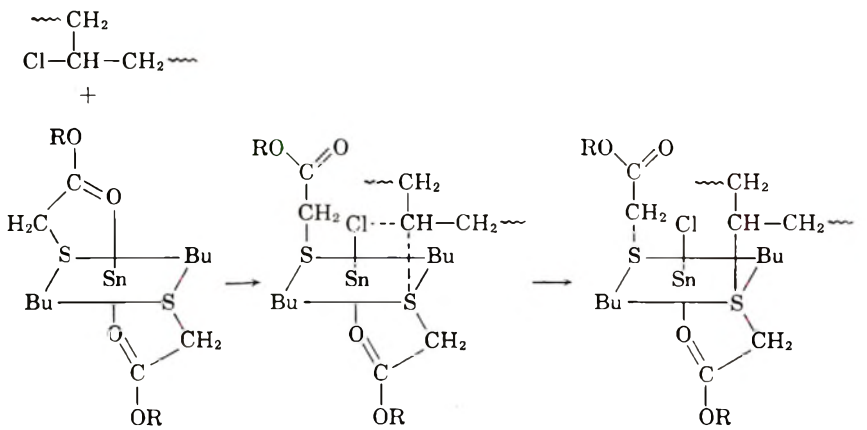

This, of course, suggests that a similar reaction might also be possible for the β-mercaptopropanoate and might even lead to crosslinking between polymer chains (or cyclization).

The above suggestions as to possible modes of reaction between the polymer and the various Y groups require, of course, their further experimental verification. In this connection it is pertinent to note that our examination of the infrared spectrum of a dibutyltin bis(2-ethylhexanoate)-stabilized resin failed to reveal any convincing evidence of a band at 5.75 μ (the carbonyl stretching frequency of aliphatic esters). This is somewhat surprising in view of the fact that our earlier studies[3] with the barium, cadmium, and zinc carboxylates showed marked absorption at this region. We suggest that this may be due to a lesser degree of esterification in the case of the dibutyltin bis(2-ethylhexanoate) than for the barium, cadmium, and zinc 2-ethylhexanoates, and that the amount of esterification which did

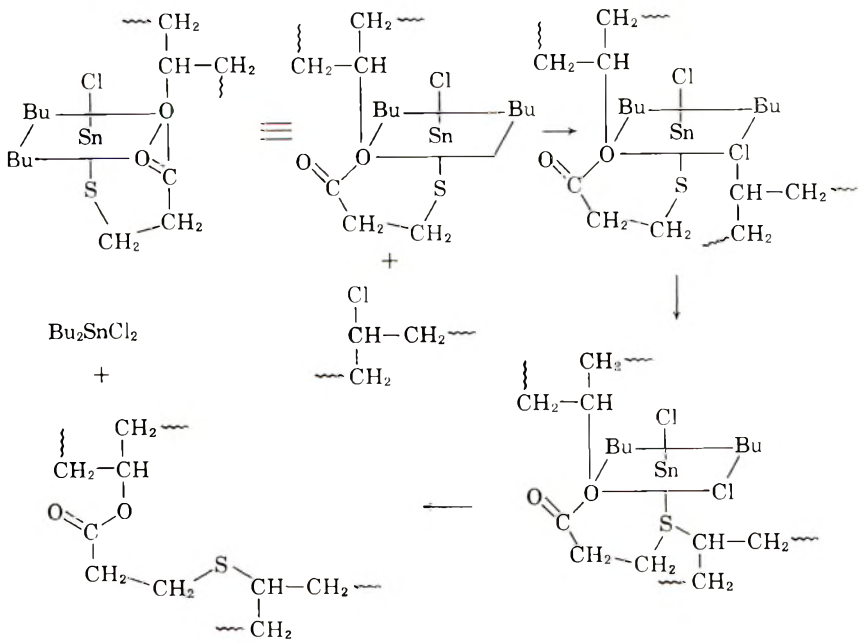

occur was not sufficient to permit spectroscopic detection. If this is correct, one then is obliged to explain why such a surprisingly high degree of retained radioactivity was found in our experiments with the dibutyltin bis(2-ethylhexanoate-1-^{14}C), as indicated in Figure 1. One possibility which we are inclined to favor is that the actual radioactivity of our dibutyltin bis(2-ethylhexanoate-1-^{14}C) was considerably greater than the 28 μc./mmole which we have assigned to it. If this is true, it would also serve to explain the curious fact that our butyl-tagged experiments with that same stabilizer showed only relatively weak retention of radioactivity. Finally, one wonders why the retention curve for dibutyltin bis(2-ethylhexanoate-1-^{14}C) does not descend after reaching a maximum, as we found both in our butyl-tagged studies and in our infrared and tracer studies with the barium cadmium and zinc carboxylates. In the case of the butyl-tagged studies we suggest that the descending branch of the curve results from the attack of eliminated hydrogen chloride on the coordinatively associated polymer–dibutyltin bis(2-ethylhexanoate) complex giving rise to dibutyltin dichloride which is readily displaced by the tetrahydrofuran (or methanol). That our Y-tagged experiments with dibutyltin bis(2-ethylhexanoate), or with dibutyltin bis(monomethyl maleate), or dibutyltin bis(oxoöctyl thioglycolate), show no descending branches may be due to the fact that dibutyltin dichloride, unlike either barium, cadmium, or zinc dichloride, causes little or no deleterious action on poly(vinyl chloride).[1] Of course, the question then arises as to why the β-mercaptopropanoate alone exhibits a definite and sharply descending branch in its retention curve. A number of explanations are reasonably plausible; however, the one which we prefer is based on the assumption that reaction between the

polymer and the stabilizer has resulted in at least a number of tin-containing β-mercaptopropanoic ester groupings which, by the action of eliminated hydrogen chloride, first lose their organotin moieties, and then pyrolytically eliminate β-mercaptopropanoic acid.

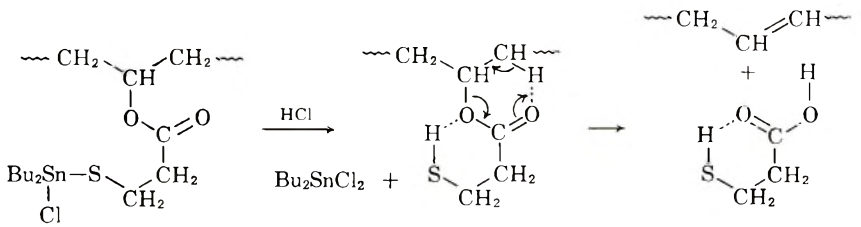

One other aspect of this work warrants some comment. In Part III[1] in which we dealt with the butyl-tagged stabilizers, we pointed out the dissimilarity of our findings on thermal stabilization to those of Kenyon[5] on photostabilization. The present Y-tagged experiments have revealed another dissimilarity. Whereas Kenyon found that under the conditions of his experiments, dibutyltin diacetate (tagged with ^{14}C in the acetate moiety) showed "no change in the retained β-activity with time of irradiation" permitting him to conclude "that the acetate groups are not involved in the reaction," we find that without particular stabilizers under conditions of thermally accelerated degradation the Y groups do become part of the polymer's molecular structure.

It is now generally accepted that the thermal instability of ordinary poly(vinyl chloride) is due primarily to deviations from structural ideality—to chain branching, to unsaturated chain endings, and to certain incidentally incorporated oxygen functions such as hydroperoxy groups—and that these are the sites at which the zipperlike elimination of hydrogen chloride is initiated. Baum and Wartman[6] have presented evidence which suggests that at temperatures up to about 150°C. initiation proceeds principally from unsaturated chain endings, but that at 190°C. chlorine atoms bound to tertiary carbon atoms also become important initiating sites. Sönnerskog,[7] on the other hand, maintains that incidentally incorporated hydroperoxy groups are the prime centers at which degradation is initiated. We have suggested that our present findings with organotin stabilizers, as well as our earlier findings with the barium, cadmium, and zinc carboxylate class of stabilizers, can be rationalized in terms of displacement reactions between the stabilizers and the poylmer wherein some of the polymers chlorine atoms are replaced by the stabilizer's Y groups, in the case of the organotin compounds, and the carboxylate groups in the case of the metal carboxylates. Such reactions would serve to stabilize the polymer when the resulting structure is more resistant toward elimination than its predecessor. Thus, the replacement of a tertiary chlorine atom by a carboxylate group must result in stabilization if, as present evidence indicates,[8] the activation energy for elimination of hydrogen chloride from a tertiary alkyl halide is less than that for the elimination of carboxylic acid from the ester

analog. Although no activation energy data appear to be available for allylic compounds, it is not unlikely that the replacement of an allylic chlorine by means of a Y group could also affect a measure of stabilization. In this connection, the possibility of an allylic rearrangement attending the displacement also arises.

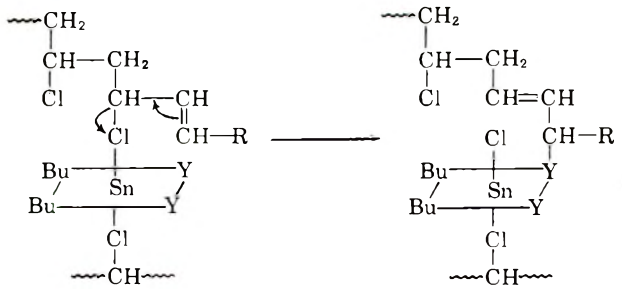

This is particularly attractive since the resulting homo-allylic structure would be considerably less prone toward elimination.

There yet remains the possibility that the superior effectivity of certain of the organotin compounds as stabilizers derives in part from their ability to inactivate deleterious hydroperoxide functions which may have been incidentally incorporated into the polymer's structure. Thus, the superior stabilizing action of dibutyltin bis(oxoöctyl thioglycolate) might result from a reaction in which the oxoöctyl thioglycolate groups are oxidized to the disulfide compound.

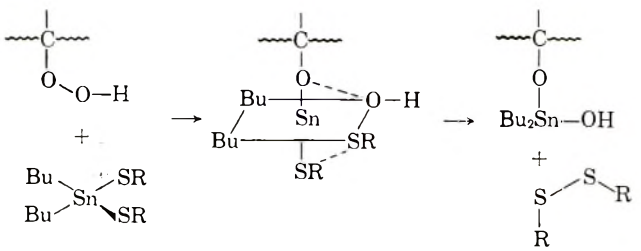

Such a reaction would not, of course, account for the observed retention of the oxoöctyl thioglycolate groups by the polymer, although it does suggest the possible retention of some dibutyltin groups. Although the assigned structure of dibutyltin β-mercaptopropanoate does not appear to permit a directly analogous reaction, other courses of reaction are possible, e.g.,

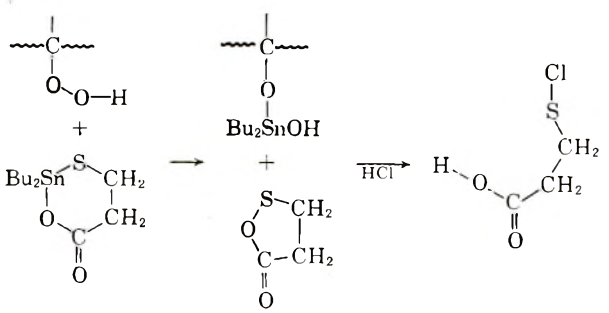

The sulfenyl chloride thus generated might further stabilize both itself and the polymer by addition to the polymer at a point of unsaturation.

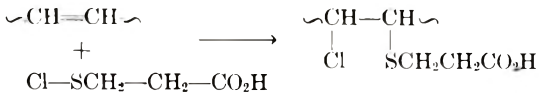

Finally, there is the possibility that the monomethyl maleate stabilizer might also deactivate hydroperoxy groups, perhaps by oxidation to a tartaric acid derivative.

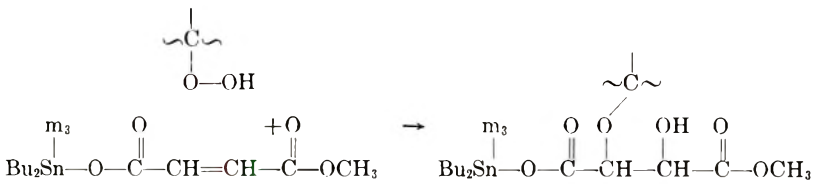

References

1. Frye, A. H., R. W. Horst, and M. A. Paliobagis, *J. Polymer Sci.*, **A2, 1767** (1964).
2. Frye, A. H., R. W. Horst, and M. A. Paliobagis, *J. Polymer Sci.*, **A2,** 1785 (1964).
3. Frye, A. H., and R. W. Horst, *J. Polymer Sci.*, **40,** 419 (1959).
4. Frye, A. H., and R. W. Horst, *J. Polymer Sci.*, **45,** 1 (1960).
5. Kenyon, A. S., *Nat'l. Bur. Standards (U. S.), Circ.*, **No. 525,** 91 (1953).
6. Baum, B., and L. H. Wartman, *J. Polymer Sci.*, **28,** 537 (1958).
7. Sönnerskog, S., *Acta Chem. Scand.*, **13,** 1634 (1959); *ibid.*, **14,** 491 (1960); also see C. F. Bersch, R. M. Harvey, and B. G. Achhammer, *J. Res. Natl. Bur. Std.*, **60,** 481 (1958).
8. DePuy, C. H., and R. W. King, *Chem. Revs.*, **60,** 451 (1960).
9. Frye, A. H., and R. W. Horst, *Intern. J. Appl. Radiation Isotopes*, in press.

Résumé

Des expériences ont été effectuées avec une série choisie de stabilisateurs marqués radioactivement, de formule générale Bu_2SnY_2, dans lesquels les atomes radioactifs (^{14}C) sont localisés dans les groupements Y et on a montré que, dans les conditions normales utilisées pour évaluer et protéger les stabilisateurs thermiques du chlorure de polyvinyle, une partie de la radioactivité demeure fermement associée à la résine. Dans des conditions déterminées, l'importance de cette association dépend de la nature des groupements Y et de la durée du traitement thermique. On émet l'hypothèse que l'action stabilisatrice de ces composés organostanniques provient en partie de réactions entre le polymère et le stabilisateur au cours desquelles certains atomes de chlore du polymère sont échangés avec des groupements Y du stabilisateur (ou avec une partie de ceux-ci); la structure qui en résulte étant plus résistante à une élimination dégradante. On considère également d'autres possibilités de réactions entre le polymère et le stabilisateur et on montre comment elles peuvent compléter ultérieurement l'action stabilisatrice des composés organostanniques et rendre compte des observations expérimentales.

Zusammenfassung

Versuche mit einer ausgewählten Gruppe radioaktiv markierter Organozinn-Stabilisatoren der allgemeinen Formel Bu_2SnY_2, in denen sich die radioaktiven Atome (^{14}C) in den Y-Gruppen befinden, haben gezeigt, dass unter den normalerweise bei der Auslese von Polyvinylchlorid-Hitzestabilisatoren vorliegenden Bedingungen ein Teil dieser

Radioaktivität fest mit dem Harz assoziiert wird. Unter Standardbedingungen hängt das Ausmass dieser Assoziation von der Art der Y-Gruppe und der Dauer der Hitzebehandlung ab. Es wird angenommen, dass die stabilisierende Wirkung dieser Organozinnverbindungen zum Teil auf Reaktionen zwischen dem Polymeren und dem Stabilisator beruht, bei welchen bestimmte Chloratome des Polymeren gegen die Y-Gruppen (oder einen Teil derselben) des Stabilisators ausgetauscht werden und dabei eine gegen Abspaltung und Abbau beständigere Struktur entsteht. Es werden auch andere Möglichkeiten für Reaktionen zwischen Polymeren und Stabilisator in Betracht gezogen. Diese können die Stabilisierungswirkung der Organozinnverbindung in einer Weise fördern, die mit den experimentellen Befunden in Einklang gebracht werden kann.

Received March 15, 1963

JOURNAL OF POLYMER SCIENCE: PART A VOL. 2, PP. 1815–1823 (1964)

Stereochemical Configurations of Polypropenes by High Resolution Nuclear Magnetic Resonance

FERDINAND C. STEHLING, *Research and Development, Humble Oil and Refining Company, Baytown, Texas*

Synopsis

High resolution hydrogen NMR spectra of amorphous, stereoblock, and isotactic fractions of polypropylene show distinct differences. The spectra are complex but those of polypropene-2-d_1 and polypropene-2,3,3,3-d_4 are simple and easily interpreted. The differences in the spectra of the amorphous, stereoblock and isotactic fractions of the polymers is the result of a difference in the chemical shifts of isotactic and syndiotactic type methylenes. The ratio of the types of methylenes can be estimated from the spectra of polypropene-2,3,3,3-d_4. In isotactic polymer the concentration of syndiotactic type methylenes is below the limit of detection. Assuming that the inversions in stereochemical configuration are randomly distributed along the polymer chain, the average length of sterically identical segments in stereoblock polymer is about fifteen monomer units. In amorphous polymer the ratio of isotactic to syndiotactic type sequences is approximately one. The spectra of the deuterated polymers show no detectable rearrangement of hydrogen and deuterium atoms in the polymerization.

The stereochemical configurations and conformations of crystalline isotactic[1] and syndiotactic[2] polypropene have been determined by Natta using x-ray diffraction. However, x-ray diffraction, as well as infrared[3] and melting point measurements,[4] has given little definitive information concerning the structure of the amorphous and stereoblock forms of this polymer. High resolution NMR has been demonstrated to be a very useful technique for ascertaining the tacticity of polymers of methyl methacrylate,[5] trifluorochloroethylene,[6] α-methylstyrene,[7] and styrene.[8] This paper describes the first application of high resolution NMR to the study of the stereochemical structure of a saturated polymer derived from an alkene. Although the chemical shift differences observed in the spectra of polypropenes are small, useful information concerning the stereochemical configuration of the polymers can be obtained.

Experimental

The polypropene used in this study was commercial polymer. Deuterated polymers were prepared from Merck propene-2-d_1 (isotopic purity > 96%) and propene-2,3,3,3-d_4 (isotopic purity > 98%) by means of a typical Ziegler catalyst. The polymers were separated into three fractions by successive extraction with diethyl ether and n-heptane by using a procedure

similar to that described by Natta.[9] According to Natta, this treatment separates the polymer into three fractions with different stereoisomeric composition, namely: (*1*) an amorphous fraction (the ether-soluble extract) with a structure approximating that of an atactic polymer, (*2*) a stereoblock fraction (insoluble in ether but soluble in *n*-heptane) consisting of molecules with relatively long segments of monomer units having the isotactic configuration, and (*3*) an isotactic fraction (the residue remaining after extract with ether and *n*-heptane) approximating the structure of an ideal isotactic polymer. After the extraction steps the polymer fractions dried at 100°C. under vacuum to remove the solvent.

Hydrogen NMR spectra were obtained at elevated temperatures with a modified 60 cycle Varian HR-60 NMR spectrometer equipped with proton control of the magnetic field and with variable temperature facilities. *p*-Dichlorobenzene was used as a solvent for the polypropene samples and 2-chlorothiophene for the deuterated polymers. Hexamethyldisiloxane was added as an internal standard, and the chemical shift of the methyl resonance in this compound is defined as 10.0 ppm. Specific operating conditions are shown on the spectra. The spectrum of isotactic polypropene-2,3,3,3-d_4 was also obtained at 40 Mcycles by using the audio sideband technique to measure peak separations.

Experimental Results and Interpretations of Spectra

The 60 Mcycles spectra of the isotactic, stereoblock, and amorphous fractions of polypropene-2,3,3,3-d_4, together with the spectrum of the unseparated polymer, are shown in Figures 1*a*, 1*b*, 1*c*, and 1*d*, respectively. The key to the interpretation of these spectra is the spectrum of the isotactic fraction, 1*a*. Assuming no hydrogen–deuterium exchange in polymerization, the propene-2,3,3,3-d_4 monomer should yield a polymer with hydrogen atoms present only in the methylene groups. Spectrum 1*a* has the appearance of a typical AB pattern given by two nonequivalent hydrogen atoms.[10] In isotactic polypropene, the methylene hydrogens are nonequivalent from geometrical considerations. Therefore, the hydrogen NMR spectrum of polypropene-2,3,3,3d_4 would be expected to be a perturbed AB pattern, the perturbaton being caused by relatively small hydrogen-deuterium couplings.

There are two difficulties with an AB interpretation, however. The separation between the two low field peaks and the two high field peaks should be exactly equal. However, repetitive measurements gave an average separation of 13.5 cycles/sec. for the low field pair and 12.9 cycles/sec. for the high field pair. Statistical analysis of the data leads to the conclusion (94% confidence level) that the separations are not equal. The relative peak heights also do not agree exactly with the relative intensities calculated for an AB pattern with the observed separations. If this is an AB pattern the coupling constant, J, is about 13.2 cycles/sec. and the chemical shift difference δ is about 23.2 cycles/sec. or 0.39 ppm. The relative intensities of an AB spectrum calculated using these parameters

are 0.34:1.00:1.00:0.34, whereas the relative peak heights in the experimental spectrum are 0.46:1.00:1.00:0.46. In order to confirm the AB assignment a 40 Mcycles spectrum was obtained. The 40 Mcycles spectrum predicted from the 60 Mcycles spectrum for $J = 13.2$ cycles/sec. and $\delta = 23.2$

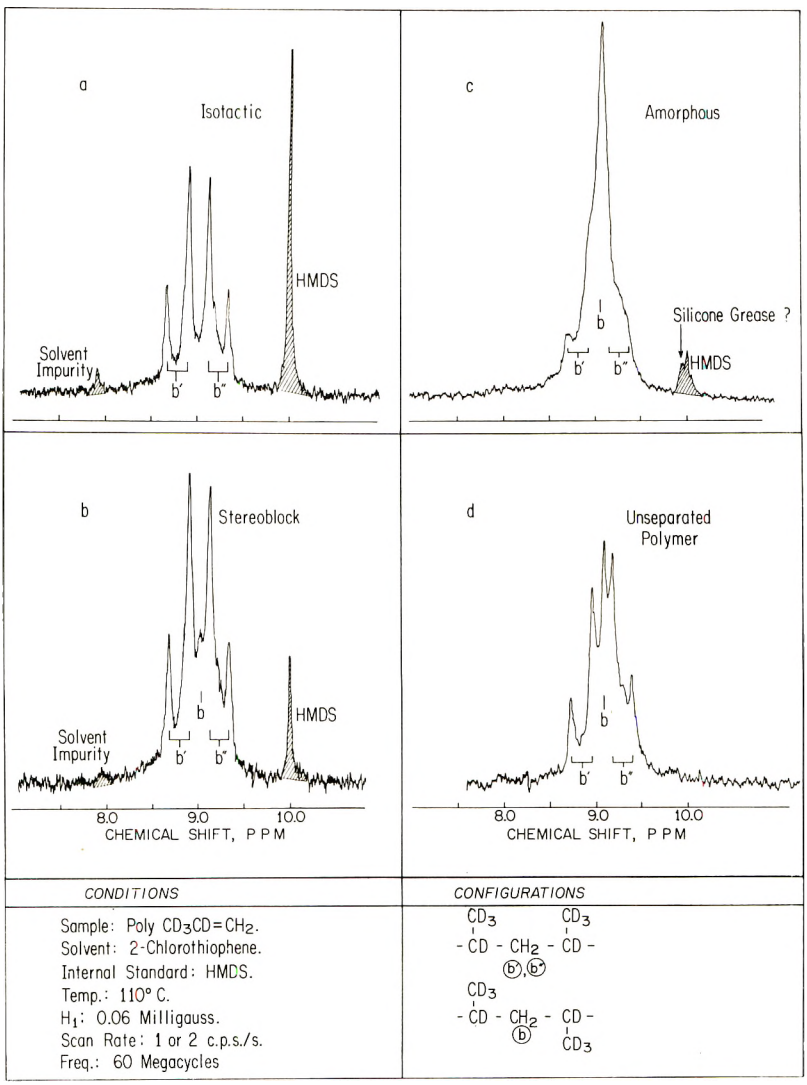

Fig. 1. NMR spectrum of polypropene-2,3,3,3-d_4.

cycles/sec. is compared with the experimental 40 Mcycles spectrum in Table I. The good agreement between the predicted and observed spectra is compelling evidence for the validity of the AB interpretation. The deviation of the 60 Mcycles and the 40 Mcycles spectra from an exact AB pattern is probably caused by the hydrogen–deuterium couplings.

Spectrum 1*b* is very similar to 1*a* except that an additional peak is present. This peak is even more apparent in spectra 1*c* and 1*d*. The quadruplet is again assigned to isotactic type methylenes, i.e., to methylenes in *dd* and *ll* sequences, and the singlet is attributed to syndiotactic type

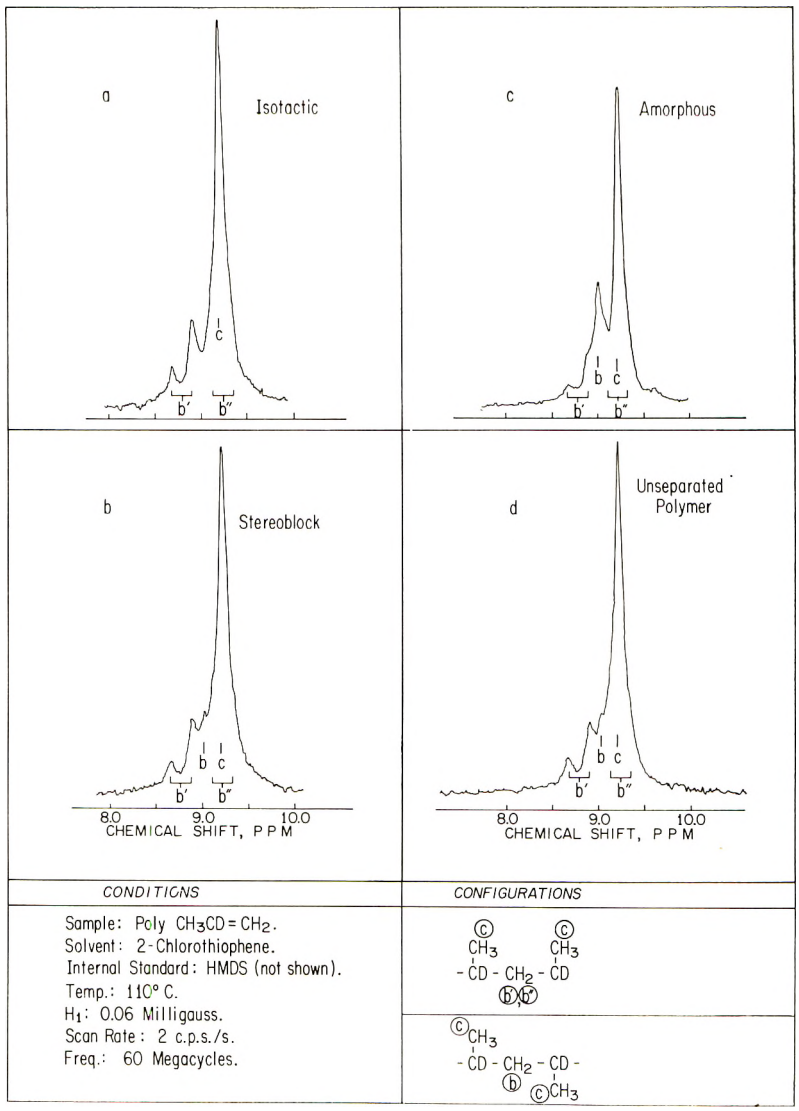

Fig. 2. NMR spectra of polypropene-2-*d*.

methylenes, i.e., to methylenes in *dl* and *ld* sequences. In syndiotactic polymer methylene hydrogens are equivalent. Therefore, in polypropene-2,3,3,3-d_4 syndiotactic type methylenes give a single band broadened slightly by hydrogen–deuterium couplings.

The spectra of polypropene-2-d_1 samples (Figs. 2*a*, 2*b*, 2*c*, and 2*d*) are entirely analogous to those of the corresponding polypropene-2,3,3,3-d_4 samples except that an additional band caused by the methyl hydrogens is present. Methyl groups in polymer segments having different stereo-

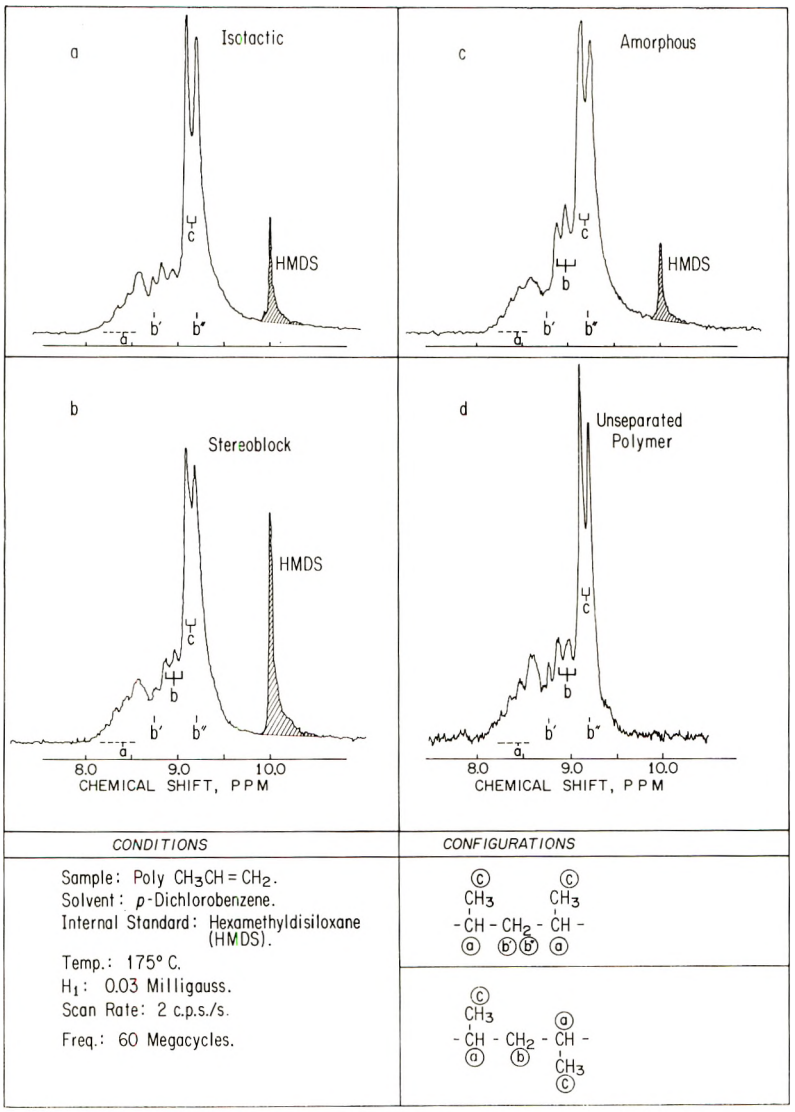

Fig. 3. NMR spectra of polypropene.

chemical configurations are theoretically nonequivalent, but they are not resolved in these spectra. The spectra of polypropene (Figs. 3*a*, 3*b*, 3*c*, and 3*d*) fractions are much more complex than those of the deuterated polymers and only a partial interpretation of these spectra is given. The

TABLE I
Comparison of Predicted and Experimental 40 mc. NMR Spectra of Isotactic Polypropene-2,3,3,3-d_4

	Predicted, cps	Experimental, cps
Separation between low field pair of bands	13.2	13.7
Separation between central pair of bands	7.2	7.2
Separation between high field pair of bands	13.2	13.0
Relative Intensities	0.21:1.00:1.00:0.21	0.25:1.00:1.00:0.25

methylene and methyl resonances of the amorphous fractions are very similar to those of 2,4-dimethylpentane (Fig. 4). As in syndiotactic polypropene sequences, the methylene hydrogens in this compound are equivalent and are coupled to two tertiary hydrogen atoms. The methylene resonance *b* in Figure 4 is a triplet with the high field member obscured by the methyl doublet. In amorphous polypropene the two down

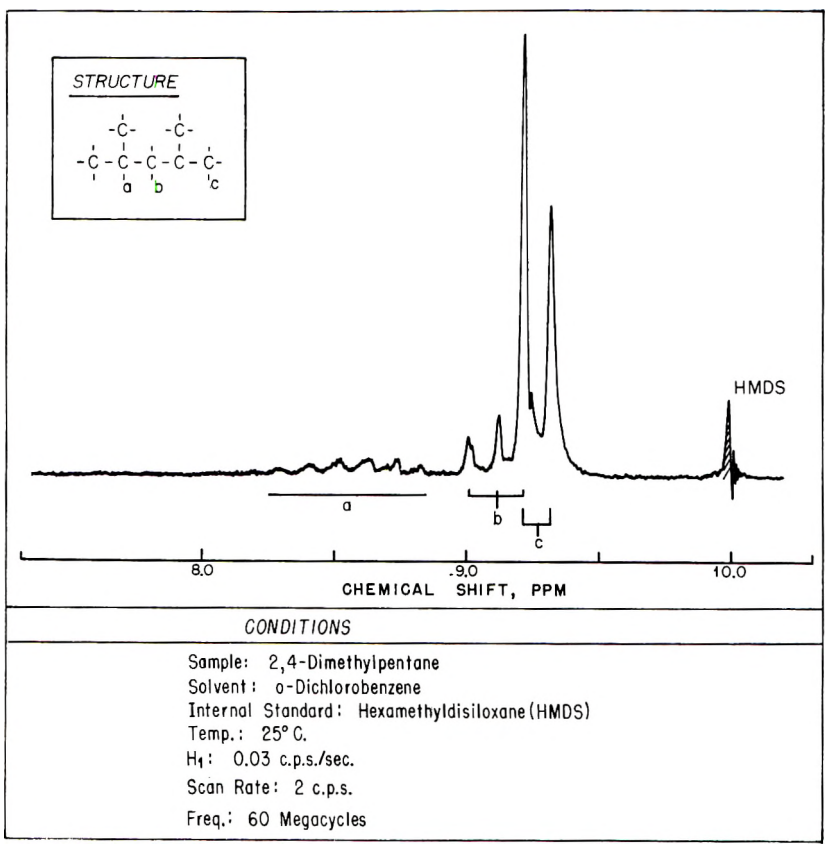

Fig. 4. NMR spectrum of 2,4-dimethylpentane.

field members of the triplet given by syndiotactic methylenes can also be clearly discerned. In stereoblock polymer this band is considerably less intense. Thus, the relative intensity of the *b* band of polypropene may be used as a qualitative measure of the tacticity of the polymer. In syndiotactic polymer the relative intensity of this band would be expected to be about twice that shown in Figure 3*c*.

Discussion

The preceding spectra and interpretations lead to conclusions concerning the mechanism of polymerization and the stereochemical configuration of the polymers. In none of the spectra of the deuterated polymers is there any evidence of hydrogen-deuterium exchange. The polymerization therefore occurs without rearrangement of hydrogen-deuterium atoms.

The most important result of this investigation is that it provides a means for estimating the ratio of isotactic (*dd* and *ll*) to syndiotactic (*dl* and *ld*) sequences in the various fractions of polypropene-2,3,3,3-d_4. The ratio of the area of the quadruplet to that of the singlet is equal to the ratio of (*dd* and *ll*) to (*dl* and *ld*) sequences. This ratio, hereafter referred to as i/s, gives information concerning the stereochemical configuration of the polymer. Thus, for an ideal isotactic polymer, $i/s = \infty$; for an ideal syndiotactic polymer, $i/s = 0$; and for an ideal atactic polymer $i/s = 1$. Of course, the i/s ratio gives no information concerning the distribution of inversions in configuration along the polymer chain.

The i/s values determined for the various fractions of polypropene-2,3,3,3-d_4 are presented in Table II. The possible error of these measurements is large because of extensive band overlap. For the amorphous polymer the indicated ratio may be in error by as much as a factor of two and for the other two fractions by as much as a factor of about 1.5. In the isotactic polymer there is no evidence for any *dl* and *ld* sequences. Assuming that the inversions in steric configuration are randomly distributed along the polymer chain the average length of sterically identical segments in stereoblock polymer is about fifteen monomer units. In amorphous polymer there appear to be about as many *dl* and *ld* sequences as there are *dd* and *ll* sequences.

Natta has determined a parameter n which is related to i/s.[4] n is defined as the fraction of irregularities with respect to the number of

TABLE II
Comparison of Stereochemical Configurations of Polypropene Derived by NMR and by Melting Point Measurements

Sample	i/s by NMR	n by NMR	n by melting point
Isotactic polymer	>20	<0.05	<0.02
Stereoblock polymer	15	0.07	0.02–0.2
Amorphous polymer	1	—	>0.25

monomeric units in the chain. The value of n was determined for polypropene from the melting point of the polymer by an extension of Flory's copolymer melting point depression theory.[11] Assuming that the inversions in configuration are randomly distributed along the polymer chain, it is possible to convert i/s to n. For larger i/s, as in isotactic and stereoblock polymer, $i/s \sim 1/n$. In Table II it can be seen that for these fractions the agreement between the two methods for ascertaining n is good. When i/s is of the order of one, as in the amorphous polymer, the conversion to n is mathematically complicated and has not been made. The i/s ratio for this fraction is, however, consistent with the highly irregular structure proposed by Natta.

Natta[12] has shown that *cis*-propene-1-*d* and *trans*-propene-1-*d* yield different, i.e. *threo* and *erythro*, diisotactic polymers. The hydrogen NMR spectra of the heptane-insoluble portions of poly(*cis*-propene-1,2,3,3,3-d_5) and poly(*trans*-propene-1,2,3,3,3-d_5) would thus be expected to consist of a single bond band slightly broadened by hydrogen–deuterium coupling. The observation of such a singlet would provide graphic confirmation of Natta's proposal. The hydrogen resonance from one of these polymers would occur at 8.8 ppm and at 9.2 ppm from the other. In fractions containing syndiotactic type sequences overlap between i and s type hydrogens would be greatly reduced, and much more accurate i/s ratios could probably be obtained.

These results demonstrate the utility of high resolution NMR spectroscopy for ascertaining the stereochemical configurations of saturated polymers derived from alkenes. In such polymers the chemical shift differences will be small, so it will generally be necessary to study the partially deuterated polymers in order to simplify and interpret the spectra.

The author wishes to express his appreciation to Mr. N. F. Chamberlain for helpful discussions of the spectra, to Messrs. R. K. Saunders and T. J. Denson for obtaining the 60 Mcycles spectra, to Dr. Leonard Reeves of the University of British Columbia for running the 40 Mcycles spectrum, to Dr. B. H. Johnson and Mr. G. C. McCollum for preparing the deuterated polymers, and to Dr. L. Westerman and Mr. J. O. Brewer for separating the polymer into the various fractions.

References

1. Natta, G., et al., AH: *Accad. Nazl. Lincei, Rend. Classe Sci. Fis. Mat. Nat.*, **21**, 365 (1956).

2. Natta, G., et al., *Atti Accad. Nazl. Lincei, Rend. Classe Sci. Fis. Mat., Nat.*, **28**, 539 (1960).

3. Luongo, J. P., *J. Appl. Polymer Sci.*, **3**, 302 (1960).

4. Natta, G., *Atti Accad. Nazl., Lincei, Rend. Classe Sci. Fis. Mat. Nat.*, **24**, 246 (1958).

5. Bovey, F. A., and G. V. D. Tiers, *J. Polymer Sci.*, **44**, 173 (1960).

6. Bovey, F. A., and G. V. D. Tiers, paper presented to the Division of Polymer Chemistry, 143rd National Meeting American Chemical Society, Atlantic City, September 1962.

7. Brownstein, S., et al., *Makromol. Chem.*, **48**, 127 (1961).

8. Brownstein, S., *J. Phys. Chem.*, **66**, 2067 (1962).

9. Natta, G., et al., *Gazz. Chim. Ital.*, **87**, 528 (1957).
10. Pople, J. A., W. G. Schneider, and H. J. Bernstein, *High Resolution Nuclear Magnetic Resonance*, McGraw-Hill, New York, 1959, p. 119.
11. Flory, P. J., *Principles of Polymer Chemistry*, Cornell Univ. Press, Ithaca, N. Y., 1953, p. 237.
12. Natta, G., paper presented at 15th Annual Technical Conference of the Society of Plastics Engineers, Jan. 1959.

Résumé

Les spectres RMN protonique à haute résolution des fractions amorphes à stéréoblocs et isotactiques de polypropylène montrent des différences distinctes. Les spectres sont complexes, mais ceux du polypropène-2-d_1 et du polypropène-2,3,3,3-d_4 sont simples et facilement interprétables. Les différences spectrales entre les fractions copolymères amorphes à stéréoblocs et isotactiques sont le résultat d'une différence dans les déplacements chimiques des méthylènes types isotactique et syndiotactique. Le rapport des types de méthylènes peut être estimé au départ des spectres du 2,3,3,3-d_4-polypropène. Dans les polymères isotactiques la concentration en méthylènes du type syndiotactique est en dessous de la limite de détectabilité. En admettant que les inversions de la configuration stéréochimique sont distribuées statistiquement tout au long de la chaîne polymérique, la longueur moyenne des segments stériquement identiques dans le polymère à stéréobloc est environ de 15 unités monomériques. Dans le polymère amorphe, le rapport des séquences du type isotactique et celles du type syndiotactique est approximativement unitaire. Les spectres des polymères deutérés n'accusent aucun réarrangement entre les atomes d'hydrogène et de deutérium au cours de la polymèrisation.

Zusammenfassung

Hochauflösende Wasserstoff-NMR-Spektren von amorphen, Stereoblockund isotaktischen Polypropylenfraktionen unterscheiden sich deutlich voneinander. Im allgemeinen sind die Spektren komplex, diejenigen von Polypropen-2-d_1 und Polypropen-2,3,3,3,-d_4 jedoch einfach und leicht zu interpretieren. Die Unterschiede zwischen den Spektren von amorphen, Stereoblock- und isotaktischen Fraktionen gehen auf eine unterschiedliche chemische Verschiebung der Methylene in isotaktischen und syndiotaktischen Strukturen zurück. Aus dem Spektrum von Polypropen-2,3,3,3,-d_4 kann das Verhältnis der Methylentypen bestimmt werden. Im isotaktischen Polymeren liegt die Konzentration von syndiotaktischem Methylen unter der Erfassberkeitsgrenze. Unter der Annahme, dass die Umkehrungen der stereochemischen Konfiguration statistische über die Polymerkette verteilt sind, bestehen die sterisch identischen Teilstücke in Stereoblockpolymeren aus durchschnittlich 15 Monomereinheiten. In amorphen Polymeren ist das Verhältnis von isotaktischen zu syndiotaktischen Sequenzen etwa eins. Die Spektren der deuterierten Polymeren lassen nicht auf eine merkliche Umlagerung von Wasserstoff- und Deuteriumatomen bei der Polymerisation schliessen.

Received March 18, 1963

JOURNAL OF POLYMER SCIENCE: PART A VOL. 2, PP. 1825–1832 (1964)

Metal Chelates of Polyhydrazides

A. H. FRAZER and F. T. WALLENBERGER, *Pioneering Research Division, Textile Fibers Department, E. I. du Pont de Nemours & Company, Inc., Experimental Station, Wilmington, Delaware*

Synopsis

Two all-aromatic polyhydrazides have been investigated with respect to their propensity to form metal-chelate bulk polymer, films, and fibers. The aromatic polyhydrazide derived from isophthalic acid was found to give chelate bulk polymer with Ni^{+2}, Ca^{+2}, Ag^{+1}, Hg^{+2}, Pb^{+2}, Zn^{+2}, Cd^{+2}, and Cu^{+2} which analyze for a 1:1 ratio of hydrazide link:metal ion. Films of the polyhydrazide–metal chelate were prepared by soaking polyhydrazide films in dimethylformamide solutions of metal salts. Tough fibers of the polyhydrazide–metal chelates with such metal ions as Cr^{+3}, Co^{+2}, and Ag^{+1} were prepared by passing polyhydrazide fiber through dimethylformamide solutions of these metal salts.

INTRODUCTION

Technological development in the past few years has resulted in renewed interest in polymers which would possess high thermal stability. Comprehensive reviews list the preparation of organic[1] and of coordination[2] polymers which withstand prolonged exposure to 350–400°C. without decomposition. These polymeric materials could be fabricated and resulting films and fibers were usually weak and brittle.

More recently, however, tough and high temperature-resistant films or fibers were obtained from polybenzimidazoles[3] by Vogel and Marvel,[4,5] from poly-1,3,4-oxadiazoles by Frazer and Wallenberger[6] and from polythiosemicarbazide chelates by Campbell and Tomic.[7]

It is known that dibenzoylhydrazine chelates[8,9] quite readily with a variety of metals. This suggested that aliphatic[10] and aromatic[11] polyhydrazides, which we had prepared in high molecular weight by a new synthetic route, should be extremely effective chelating agents. It was therefore of interest to prepare and characterize this new class of organometallic polymers and to determine their utility as thermally stable fibers and films.

EXPERIMENTAL

Polymer melt temperatures and inherent viscosities were obtained by standard methods of polymer characterization as recommended by Beaman and Cramer[12] and by Sorenson and Campbell.[13]

Codes and Abbreviations

The polyhydrazide derived from isophthalic dihydrazide and isophthaloyl chloride and the alternating copolyhydrazide derived from isophthalic dihydrazide and terephthaloyl chloride have been coded O-I and O-I-O-T, respectively. Solvents often referred to are *N*,*N*-dimethylacetamide (DMAc), *N*,*N*-dimethylformamide (DMF), and dimethyl sulfoxide (DMSO). Fiber properties are recorded as T (tenacity, g./den.), E (% elongation), and M_i (initial modulus, g./den.).

Preparation of Polyhydrazides and Fibers

The two polyhydrazides used in this study, O-I and O-I-O-T, were conveniently prepared by low temperature solution polymerizations.[11] O-I-O-T was spun to give strong fibers with high degree of orientation and crystallinity.[11]

Preparation of Polyhydrazide–Chelate Bulk Polymer

To a solution containing 1.0 g. of metal salt dissolved in 50 ml. of dimethyl sulfoxide was rapidly added 10 ml. of a solution containing 1.0 g. O-I. Instantaneously, a highly swollen gel precipitated from the reaction mixture. This gel was collected by filtration, washed repeatedly with water, and dried at 120°C. at 25 mm. for 74 hr.

TABLE I
O-I Chelate: Bulk Polymer

Metal	Reactant	Metal, %		H, %		Infrared spectra[a] x = 0, cm.$^{-1}$[a]	Color
		Found	Calc.	Found	Calc.		
Ni	$NiCl_2$	24.4	26.64	1.63	1.84	1636[b]	Purple[c]
Ca	$Ca(OH)_2$	16.7	13.35	1.69	1.34	1635	Grey
Ag	$AgNO_3$	54.7	40.10	0.99	1.87	1636	Black
Hg	$Hg(OAc)_2$	54.1	55.46	1.10	1.10	1604	Tan[c]
Pb	$Pb(NO_3)_2$	51.6	56.25	1.05	1.09	1636	Grey[c]
Zn	$ZnCl_2$	26.4	28.99	1.13	1.58	1635	White
Cd	$CdCl_2$	37.6	41.24	1.33	1.47	1629	White
Cu	$CuCl_2$	25.4	28.40	1.67	1.80	1638	Brown

[a] All products show absence of NH absorption at 3300 cm.$^{-1}$.
[b] The carbon absorption of O-I is 1646 cm.$^{-1}$.
[c] Precipitates from DMSO solution best in presence of tertiary amine.

The dried product was analyzed for metal and hydrogen, and the NH absorption and shift in carbonyl absorption were determined by examination of the infrared absorption in the 3300 cm.$^{-1}$ and 1646 cm.$^{-1}$ regions, respectively.

With metal ions such as Ni^{+2}, Hg^{+1}, and Pb^{+2}, 5 ml. of triethylamine was added to the salt solution to insure complete precipitation of the metal-

chelate. With Hg^{+2}, Cu^{+2}, and Co^{+2}, essentially quantitative precipitation of the metal-chelate occurred irrespective of pH.

The poly(hydrazide–chelate) prepared and pertinent analytical data are summarized in Table I.

Polyhydrazide/$HgCl_2$ Chelate Film

O-I-O-T, 0.75 g. was dissolved in 3 ml. DMAc and diluted to 10 ml. To this solution was added 1.3 g. (0.0048 mole) mercuric chloride which dissolved. The faint yellow color of the solution disappeared simultaneously. On the addition of 0.3 ml. of triethylamine the solution viscosity increased and became an intense yellow color. This solution, after dilution, yielded, an evaporation of solvent, a tough, colorless film of the chelate; this was used in further evaluations.

Polyhydrazide–Chelate Fibers

O-I-O-T yarn was passed through a DMF bath containing 10% metal salt at 100 ± 5°C., with a 4 sec. contact time and dried in a vacuum oven at 85°C. In some experiments the basicity of the bath was varied by the addition of a small amount of *N,N*-dimethylaniline (DMA).

Since the addition of *N,N*-dimethylaniline to a $AgNO_3$ solution in DMF caused a violent reaction which results in the depositing of Ag^0, the yarn was passed through a DMF/$AgNO_3$ bath at 100 ± 5°C. and then through a subsequent *N,N*-dimethyl-aniline–DMF bath.

RESULTS AND DISCUSSION

Stolle and Benrath[8] and later Benrath, Giesler, and Gärtner[9] studied the preparation of salts of dibenzoylhydrazine. Most of these metal derivatives were prepared in basic solutions and were presumed to be derived from the enol form:

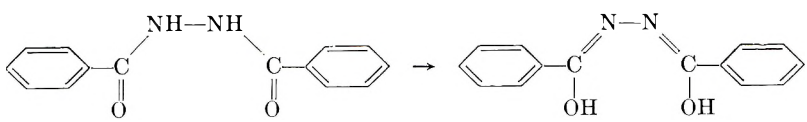

They were described as colored compounds, analyzed correctly for a 1:1 ratio of metal to hydrazide link, and were thermally stable. Two unusual chelates[8,9] were derived from $HgCl_2$. The first did not contain chlorine, analyzed correctly for $(C_{10}H_{11}N_2O_2)$-Hg-$(C_{10}H_{11}N_2O_2)$, and was the only compound described as thermally unstable. It decomposed[9] on heating into nitrogen, Hg^0, benzil, and dibenzoylhydrazine. The second derivative of $HgCl_2$, namely $HgCl(C_{10}H_{11}N_2O_2)$, was its precursor.

Many of the above observations are relevant to the present work on polyhydrazides. While the adsorption of metal ions may occur by chela-

tion or by ion exchange,[2,7] it appears reasonable to assume chelate formation, in agreement with monomeric[8,9] reaction:

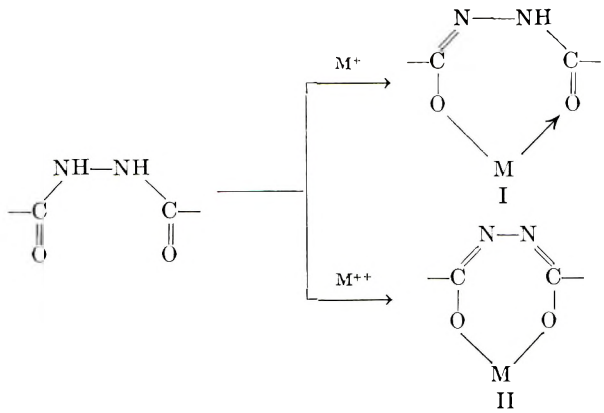

The possibility of a certain amount of crosslinking as has been observed[9] with the monomeric chelate $(C_{14}H_{11}N_2O_2)$-Hg-$(C_{14}H_{11}N_2O_2)$ may occur.

1. Poly(hydrazide-chelates) Bulk Polymer Based on O-I

The poly(hydrazide-chelates) prepared from O-I (Table I) were high melting solids, with polymer melt temperatures in excess of 350°C. These organo-inorganic materials, with the exception of the Zn^{+2} and Cd^{+2} chelates, were highly colored, the color being characteristic of the metal ion used. As would be expected, these chelates were quite intractable, dissolving in concentrated H_2SO_4 with degradation.

Based on metal and hydrogen analyses, along with the absence of NH absorption and the shift to shorter wavelength for the carbonyl absorption in the infrared spectra, it would appear that the operational models (I and II), are correct. For divalent metal ions, the metal and hydrogen values are in excellent agreement for one metal ion per hydrazide linkage. This, coupled with the absence of NH absorption and the more single bond character of the carbonyl, suggests that for these metal ions the structure should be as shown in III.

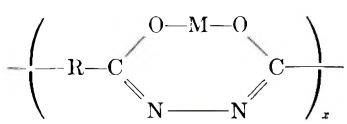

III

In the case of the chelates from monovalent ions, such as Ag^+ and Cu^+, even though the hydrogen analysis is 90% or better of the theoretical, the metal analysis corresponds to more than one metal ion per hydrazide linkage. This suggests that these structures should be as shown in IV.

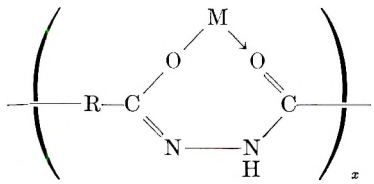

IV

2. Films of Poly(hydrazide-chelates) Based on O-I and O-I-O-T

Films of the poly(hydrazide-chelates) were most conveniently prepared by soaking films of the polyhydrazides O-I and O-I-O-T in metal salt solutions containing Cu^{+1} and Co^{+2}. The chelate films from O-I had polymer melt temperature in excess of 350°C. (O-I control, = 320–325°C.), whereas those from O-I-O-T had polymer melt temperatures in excess of 400°C. (O-I-O-T = 400°C.). All of these metal–chelate films from both O-I and O-I-O-T rapidly embrittled and decomposed on exposure to temperatures in excess of 350°C.

The chelate films were colored, insoluble in dimethyl sulfoxide, and soluble in concentrated H_2SO_4 with degradation. Unlike the bulk chelates, the films analyzed for less than the theoretical amount of metal.

The only colorless, transparent film prepared in this work was derived from O-I-O-T and $HgCl_2$ and was obtained from a *N,N*-dimethylacetamide solution. Under vacuum, the film remained colorless and transparent even after exposure for 60 hr. at 80°C. The same film discolored in air after 1/2 hr. exposure to 250°C. Another sample of this colorless $HgCl_2$ chelate film on exposure to an ultraviolet light turned dark gray, presumably by release of Hg°, and became very brittle after 150 hr. of exposure. Both types of degradation are reminiscent of the decomposition of Benrath's unusual Hg salt that yielded Hg°, N_2, benzil, and dibenzoylhydrazine.

Another type of chelation was observed from O-I-O-T films cast from DMF or DMAe on aluminum or brass plates. These films which adhered tenaciously, were stable to boiling water. The film on brass adhered for 4 hr.; the film on aluminum, for 3–4 days. Discoloration of the O-I-O-T, which occurred simultaneously, was taken as an indication of metal ion chelation.

3. Fabrication of Chelate Fibers

O-I-O-T fibers were chelated with ions such as cobalt, chromium, silver, tin, and copper. For Ag^{+1} in DMF, a straw-colored O-I-O-T/$AgNO_3$ fiber was obtained (Table III, Sample 5). When this fiber was run through a subsequent *N,N'*-dimethylaniline (DMA) bath, the tertiary amine reduced Ag^{+1} on O-I-O-T to give Ag°/O-I-O-T fibers which had a silvery grey or black appearance, depending upon such conditions as temperature, exposure time, and concentration of salt solutions (Table II, samples 6–8).

TABLE II
O-I-O-T Chelate Fiber Properties

Sample[a]	Chelate structure[b]	DMF Bath I	Bath II	Color of dry yarn	$T/E/M_i$[c]	X-ray crystallinity
1	II	13.9% $CoCl_2$	—	Dk. green	0.5/16/22	Amorphous
2	II	13.2% $CoCl_2$ + 4.7% DMA	—	Lemon	1.1/96/38	Crystalline
3	II	9.7% $CrCl_3$	—	Olive	1.2/82/37	Amorphous
4	II	9.2% $CrCl_3$ + 4.9% DMA	—	Green	1.2/90/38	Trace crystallinity
5	I	16.7% $AgNO_3$	—	Straw	0.7/5/32	Crystalline (random)
6	I	9.7% AgNO	DMA	Black (Ag°)	0.9/65/34	Crystalline
7	I	9.7% $AgNO_3$	DMA	Dk. grey (Ag°)	1.3/99/36	Figure 1
8	I	10.6% $AgNO_3$[d]	DMA	Silvery (Ag°)	1.3/101/36	Trace crystallinity

[a] O-I-O-T fiber used: $T/E/M_i$ = 3.2/27/61 (oriented fiber).

[b] Structure II:

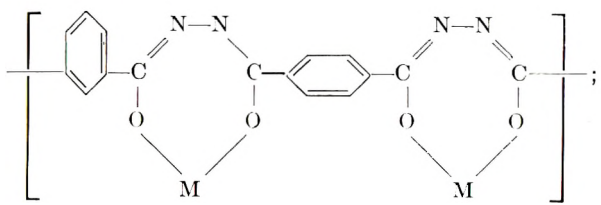

structure I:

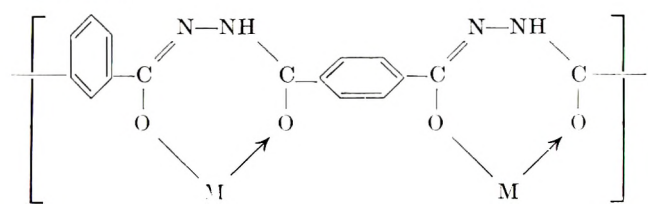

[c] Reference: $T/E/M_i$ = 1.8/118/41, amorphous O-I-O-T fiber

[d] Short contact time.

TABLE III
High Tenacity Chelate Fibers

$CoCl_2$ Bath	O-I-O-T Fiber $T/E/M_i$	Chelate Fiber $T/E/M_i$	X-ray crystallinity	Color of fiber
DMF	5.2/24/80	2.3/15/55	—	Green
DMF + DMA	5.2/24/80	3.4/27/59	Figure 1	Olive

For Co^{+2} in DMF, when amorphous O-I-O-T fiber was used, there was no change in fiber properties ($T/E/M_i$ = 1.0/96/39 → 0.8/100/39) in chelation. When oriented, amorphous O-I-O-T fiber ($T/E/M_i$ = 3.2/27/61) was used, the resulting fiber properties, after chelation, were nearly identical with those unoriented O-I-O-T fiber[13] ($T/E/M_i$ = 1.8/118/41). Entirely different results were observed when crystalline and oriented O-I-O-T fiber[13] was chelated (Table III). The chelated yarn, in this instance, lost its original crystallinity and orientation, but had fiber properties comparable to those of oriented O-I-O-T fiber ($T/E/M_i$ = 3.2/27/61).

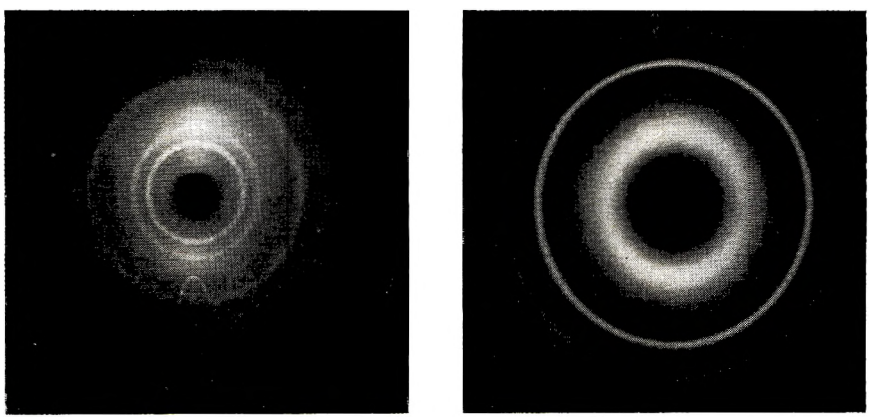

Fig. 1. X-ray diffraction patterns of O-I-O-T/Chelate fibers: (*a*) O-I-O-T/Co fiber; (*b*) O-I-O-T/Ag fiber.

Figure 1 shows the x-ray diffraction patterns of two chelate fibers. The O-I-O-T/Co fiber (Table III) was obtained from oriented and crystalline O-I-O-T fiber, and the O-I-O-T/Ag fiber (Table II) was obtained from oriented but not crystalline yarn. In both cases, the x-ray patterns of the chelate fibers are characteristic only of the crystallinity of the additive while the fiber itself is essentially amorphous.

The fibers were generally found to analyze for about 10% of the theoretical amount of metal chelate. This in conjunction with bulk chelate studies (Table II) indicates that successful chelating occurs readily at the fiber surface but complete penetration of the metal ion to the core of the fiber is prevented.

These chelate fibers have higher polymer melt temperatures than the corresponding O-I-O-T fibers but show no marked improvement in thermal

stability. All the metal chelate fibers, irrespective of the nature of the metal ion used, decomposed rapidly (<1 hr.) at temperatures in excess of 350°C.

This work was carried out, in part, under AF 33(616)-8253, Project No. 7340 by the Directorate of Materials and Processes, ASD, Air Force Systems Command, Wright-Patterson Air Force Base, Ohio.

The authors wish to express their appreciation to Messrs. S. H. Catts, W. F. Holley, and A. J. Prucino for their excellent technical assistance.

References

1. Koton, M. M., *J. Polymer Sci.*, **52**, 97 (1961).
2. Kenny, C. N., *Chem. and Ind. (London)*, **1960**, 880.
3. Brinker, K. C., and I. M. Robinson, (to E. I. du Pont de Nemours & Co., Inc.), U. S. Pat. 2,895,948 (7/1/59).
4. Vogel, H., and C. S. Marvel, *J. Polymer Sci.*, **50**, 511 (1961).
5. Vogel, H., and C. S. Marvel, *J. Polymer Sci.*, **A1**, 1531 (1963).
6. Frazer, A. H., and F. T. Wallenberger, *J. Polymer Sci.*, **A2**, 117 (1964).
7. Campbell, T. W., and E. A. Tomic, *J. Polymer Sci.*, **62**, 379 (1962).
8. Stolle, R., and A. Benrath, *J. Prakt. Chem.*, **70**, 263 (1904).
9. Benrath, A., P. Giesler, and O. Gärtner, *J. Prakt. Chem.*, **107**, 211 (1924).
10. Frazer, A. H., and F. T. Wallenberger, *J. Polymer Sci.*, **A2**, 1137 (1964).
11. Frazer, A. H., and F. T. Wallenberger, *J. Polymer Sci.*, **A3**, 1147 (1964).
12. Beaman, R. G., and F. B. Cramer, *J. Polymer Sci.*, **21**, 223 (1956).
13. Sorenson, W. R., and T. W. Campbell, *Preparative Methods of Polymer Chemistry*, Interscience, New York, 1961, pp. 33–55.

Résumé

Deux polyhydrazides polyaromatiques ont été étudiés en ce qui concerne leur aptitude à former des chélates polymériques métalliques en émulsion, des films et des fibres. On a trouvé que le polyhydrazide aromatique dérivé de l'acide isophtalique donne un chélate polymérique avec Ni^{+2}, Ca^{+2}, Ag^{+1}, Hg^{+2}, Pb^{+2}, Zn^{+2}, Cd^{+2}, et Cu^{+2} dont l'analyse révèle un rapport 1:1 entre un lien hydrazide et l'ion métallique. Des films du chélate métallique du polyhydrazide ont été préparés en plongeant des films de polyhydrazide dans des solutions de diméthylformamide des sels métalliques. Ainsi des fibres de chélates polyhydrazide–métal avec des ions tels que Cr^{+3}, Co^{+2}, et Ag^{+1} ont été préparés en passant la fibre de polyhydrazide à travers des solutions de diméthylformamide de ces sels métalliques.

Zusammenfassung

Zwei vollaromatische Polyhydrazide wurden hinsichtlich ihrer Fähigkeit zur Bildung von Metallchelat-Polymerenmassen, filmen und -fasern untersucht. Das von Isophthalsäure abgeleitete aromatische Polyhydrazid liefert mit Ni^{+2}, Ca^{+2}, Ag^{+1}, Hg^{+2}, Pb^{+2}, Zn^{+2}, Cd^{+2} und Cu^{+2} Chelat-Polymermassen deren Analyse ein Verhältnis Hydrazidbindung:Metallion von 1:1 ergibt. Polyhydrazid-Metallchelat-Filme wurden durch Tränkung von Polyhydrazidfilmen mit Dimethylformamidlösungen von Metallsalzen hergestellt. Zähe Fasern aus Polyhydrazid-Metallchelaten mit Metallionen wie Cr^{+3}, Co^{+2} und Ag^{+1} wurden durch eine Passage von Polyhydrazidfasern durch Dimethylformamidlösungen dieser Metallsalze hergestellt.

Received March 11, 1963

JOURNAL OF POLYMER SCIENCE: PART A VOL. 2, PP. 1833–1838 (1964)

Polyesters and Polyurethanes of Dihydroxymethylxylitol and Glucitol*

WILLIAM E. DICK, JR., and ROY L. WHISTLER, *Department of Biochemistry, Purdue University, Lafayette, Indiana*

Synopsis

Several linear polyesters and polyurethanes containing 2,3,4-tri-*O*-methylxylitol, or 2,3,4,6-tetra-*O*-methyl-D-glucitol, were prepared. Solution polymerization of either of the methylated derivatives with methylenebis(4-phenyl isocyanate) affords polyurethanes having molecular weights of about 30,000. Thermal polymerization of either methylated derivative with terephthaloyl chloride or mixtures of terephthaloyl chloride and sebacoyl chloride yields polyesters in the 4000–7000 molecular weight range. Films from these polyesters are brittle, with tensile strengths up to 32 kg./mm.^{2}

INTRODUCTION

Synthesis of condensation polymers from carbohydrates is of continuing industrial interest.

Haworth, Heath, and Wiggins[1] reported the polycondensation of 1,6-diamino-1,6-dideoxy-2,4:3,5-di-*O*-methylene-D-mannitol with adipic, sebacic, and 2,4:3,5-di-*O*-methylene-D-glucaric acids. In a later communication, Wiggins[2] reported the condensation of 1,2:5,6-dianhydro-3,4-*O*-isopropylidene-D-mannitol with 1,6-diamino-1,6-dideoxy-di-*O*-methylene-D-mannitol, and with phthalic acid. Mehltretter and Mellies[3] polymerized 2,4:3,5-di-*O*-methylene-D-gluconic acid in pyridine containing benzoyl chloride. A polyamide was prepared by Wolfrom, Toy, and Chaney,[4] using 2,3,4,5-tetra-*O*-acetyl-galactaroyl dichloride and ethylenediamine. Overend, Shafizadeh, and Stacey[5] obtained low molecular weight polymers by the thermal condensation of methyl 2-deoxy-β-D-galactofuranoside. Glycans from the action of acidic catalysts on D-glucose and derivatives is well documented. Kent[6] thermally polymerized D-glucose, using thionyl chloride as a catalyst. Glycans containing D-glucose, D-galactose, or D-maltose were similarly obtained by Ricketts and Rowe,[7] using hydrogen chloride. O'Colla and Lee[8] used cation exchange resins to polymerize D-glucose, and with McGrath[9] polymerized 1,2,3,4-tetra-*O*-acetyl-β-D-glucopyranose, using zinc chloride. Thermal condensation of D-glucose, using phosphorous acid, was demonstrated by Mora and Wood,[10] and with McFarland[11] they outlined procedures for thermal condensation of other

* Journal Paper No. 2084 of the Purdue University Agricultural Experiment Station.

aldoses. Schramm, Grötsch, and Pollmann[12] claimed the preparation of regular, synthetic polysaccharides from D-glucose, in the presence of polyphosphoric acid ester. A linear polymer has been achieved also by Micheel and Böckmann[13] from 2,3,6-tri-*O*-methyl-D-glucopyranose and an acid catalyst, using procedures similar to those developed earlier with Gresser.[14] Durand, Dull, and Tipson[15] obtained low molecular glucans using metaboric acid and α-D-glucopyranose. A novel polyester synthesis involving ring scission of cyclic acetals was reported by Bonner, Bourne, and Saville,[16] who used trifluoroacetic anhydride to open the 1,3 and 5,6 rings of 1,3:2,4:5,6-tri-*O*-methylene-D-glucitol, and induced polyesterification with adipic acid. Sucrose polycarbonates were prepared and investigated by Theobald.[17] Recently, Micheel and Hallerman[18] prepared glycans from the 1-fluoro derivatives of D-glucose, D-arabinose, and D-xylose. Bird and co-workers[19] obtained fiber-forming nylons when sebacoyl chloride was reacted with 1,6-diamino-1,6-dideoxy-2,4:3,5-di-*O*-methylene-D-mannitol, and 1,6-diamino-1,6-dideoxy-D-mannitol, respectively.

EXPERIMENTAL

Materials

The method of Hibbert and co-workers[20] was used to prepare 2,3,4,6-tetra-*O*-methyl-D-glucose, and 2,3,4-tri-*O*-methyl-D-xylose, which spontaneously crystallized after distillation under reduced pressure.

These derivatives were hydrogenated by a modification of the method of Freundenberg and Sheehan.[21] Temperature and pressure were maintained at 145°C. and 2600 psi (final) for 12 hr. in the presence of 1 g. of Raney nickel for each 1 g. of sugar derivative.

On distillation, the D-glucitol derivative showed b.p. 130–140°C. at 0.01 mm., and the xylitol derivative showed a b.p. 140–145°C. at 0.005 mm. pressure.

Terephthaloyl chloride was prepared by refluxing 100 g. of terephthalic acid with 500 ml. of thionyl chloride and 2 ml. of pyridine, for 12 hr. The product was freed of thionyl chloride by placing it under reduced pressure and subsequent crystallization from dry hexane.

Sebacoyl chloride was prepared by refluxing sebacic acid with thionyl chloride and pyridine for 6 hr. and was purified by rapid distillation under reduced pressure.

Polyurethane Preparation

Following a procedure modified from that of Lyman,[22] polyurethanes were made by reaction of each glycitol with methylenebis(4-phenyl isocyanate). Thus, 0.02 mole of the particular glycitol was stirred with 0.02 mole of methylenebis(4-phenyl isocyanate) in 16 ml. of 4-methylpentanone-2-dimethyl sulfoxide mixture (1:1 v/v) at 115°C. for 2 hr.

The resulting poly[2,3,4-tri-*O*-methylxylitol methylenebis(4-phenyl carbamate)], or poly[2,3,4,6-tetra-*O*-methyl-D-glucitol methylenebis(4-

phenyl carbamate)] was precipitated in water, using a Waring Blendor, and dried under reduced pressure at 70°C. On solution in tetrahydrofuran and dialysis in cellophane, 90% of each polymer was nondialyzable.

Polyester Preparation

The melt polyesterification procedures of Flory and Leutner[23] were adapted for use with the methylated glycitols. Reactions were conducted in a 20-ml. round-bottomed flask equipped with a close-fitting, four-blade glass stirrer. Side arms permitted nitrogen to be passed through the reaction mass.

The flask was charged with 0.02 mole of glycitol derivative, and 0.02 mole of terephthaloyl chloride. A dry nitrogen stream was admitted, and the stirrer started. After 1 hr., an oil bath at 75°C. was raised to a point where the oil level was above the liquid level in the flask, and the temperature increased to 150°C. over a period of 3 hr. and maintained at this temperature for an additional 3 hr.

The polymer was cooled to 25°C. under a stream of nitrogen and dissolved in 100 ml. of acetone containing 1 ml. of pyridine and 1 ml. of water. This solution was concentrated under reduced pressure, 100 ml. of 99.5% ethanol was added, and distilled. Then 100 ml. of diethyl ether was added and after 12 hr. removed by decantation. The remaining polymer was dried under reduced pressure at 40°C., yielding poly(2,3,4-tri-*O*-methylxylitol terephthalate), or poly(2,3,4,6-tetra-*O*-methyl-D-glucitol terephthalate), in overall yields of 50–60%. On solution in acetone and dialysis through cellophane, 90% of each polymer was nondialyzable.

Polyesters containing both terephthalate and sebacate were also prepared, using the above procedure. Six mixed polyesters were prepared, four containing the xylitol derivative and two containing the glucitol derivative. In preparation of poly(2,3,4-tri-*O*-methylxylitol terephthalate cosebacate)s, the terephthalate:sebacate mole ratios were 90:10, 88:12, 85:15, and 50:50, respectively, while in the corresponding poly(2,3,4,6-tetra-*O*-methyl-D-glucitol terephthalate cosebacate)s the ratios were 85:15, and 80:20.

Molecular Weights

Molecular weights of the polyurethanes were determined in a modified[24] Zimm-Myerson osmometer equipped with American Viscose gel cellophane membranes, *N*,*N*-dimethylformamide being used as a solvent.

The endgroup assay method of Ogg and co-workers[25] was used for molecular weight determinations of the polyesters.

Viscosities

Viscosity measurements were made in an Ubbelohde viscometer, *N*,*N*-dimethylformamide serving as the polyurethane solvent, and 1,1,2,2-tetrachloroethane for the polyesters.

TABLE I
Polymers From Xylitol

Copolymer	Copolymer mole ratio	Intrinsic viscosity	Molecular weight
Methylenebis(4-phenyl isocyanate)		0.323	30,200
Terephthalic		0.152	6,100
Terephthalic–sebacic	90:10	0.233	10,500
Terephthalic–sebacic	88:12	0.195	4,600
Terephthalic–sebacic	85:15	0.300	5,000

TABLE II
Polymers From Glucitol

Copolymer	Copolymer mole ratio	Intrinsic viscosity	Molecular weight
Methylenebis(4-phenyl isocyanate)		0.300	29,700
Terephthalic		0.117	4,600
Terephthalic–sebacic	85:15	0.175	7,500
Terephthalic–sebacic	80:20	0.123	4,400

DISCUSSION AND RESULTS

Solution polymerization of either methylated glycitol with methylenebis-(4-phenyl isocyanate) proceeds smoothly. Although polymers from either 2,3,4-tri-*O*-methylxylitol or 2,3,4,6-tetra-*O*-methyl-D-glucitol, had molecular weights of about 30,000, their film properties were quite different. Polyurethane containing xylitol yielded clear films of moderate tensile strength, while the corresponding films containing glucitol, though clear, were brittle.

Melt polymerization of either of the methylated glycitols with terephthaloyl chloride produced brittle films, but the use of sebacoyl chloride with terephthaloyl chloride in the polymerization produced polymers which were easily cast into films exhibiting 6–7% elongation at break (Table III).

TABLE III
Film Tensile Strength of Polymers From Xylitol

Copolymer	Copolymer mole ratio	Elongation, %	Tensile strength, kg./mm.^{2}
Polyurethane		0.0	115.5
Polyester	88:12	7.5	29.1
Polyester	85:15	6.1	32.3

Terephthalate and sebacate were employed in several molar ratios, from 90:10 to 50:50, in order to determine the combination producing polyester

films of greatest strength. When polymerized with the xylitol derivative, polyester films were obtained at acid ratios of 90:10, 88:12, and 85:15, but a heavy liquid resulted from the 50:50 mixture of acyl chlorides. Though initially flexible, the 90:10 and 88:12 films became brittle after several weeks, while the 85:15 remained flexible for several months.

Two polyesters containing the glucitol derivative were prepared, with component acyl chloride ratios of 85:15 and 80:20. Both ratios produced brittle films.

Polyester molecular weights were in the 4000–7000 range, as determined by endgroup assay.

As noted in Table III, the polyurethane containing xylitol units had a tensile strength approximately four times those of the polyesters.

The authors wish to express their gratitude for National Science Foundation and Regional Research Funds which helped to support this work.

References

1. Haworth, W. N., R. L. Heath, and L. F. Wiggins, *J. Chem. Soc.*, **1944**, 155.
2. Wiggins, L. F., *J. Chem. Soc.*, **1946**, 384.
3. Mehltretter, C. L., and R. L. Mellies, *J. Am. Chem. Soc.*, **77**, 427 (1955).
4. Wolfrom, M. L., M. S. Toy, and A. Chaney, *J. Am. Chem. Soc.*, **80**, 6328 (1958).
5. Overend, W. G., F. Shafizadeh, and M. Stacey, *J. Chem. Soc.*, **1951**, 994.
6. Kent, P. W., *Biochem. J.*, **55**, 361 (1953).
7. Ricketts, C. R., and C. E. Rowe, *J. Chem. Soc.*, **1955**, 3809.
8. O'Colla, P. S., and E. Lee, *Chem. Ind. (London)*, **1956**, 522.
9. O'Colla, P. S., E. E. Lee, and D. McGrath, *Chem. Ind. (London)*, **1962**, 178.
10. Mora, P. T., and J. W. Wood, *J. Am. Chem. Soc.*, **80**, 685 (1958).
11. Mora, P. T., J. W. Wood, and V. W. McFarland, *J. Am. Chem. Soc.*, **82**, 3418 (1960).
12. Schramm, G., H. Grötsch, and W. Pollmann, *Angew. Chem. (Internat. Ed.)*, **1** 1 (1962).
13. Micheel, F., and A. Böckmann, *Makromol. Chem.*, **51**, 102 (1962).
14. Micheel, F., and W. Gresser, *Chem. Ber.*, **91**, 1214 (1958).
15. Durand, H. W., M. F. Dull, and R. S. Tipson, *J. Am. Chem. Soc.*, **80**, 3691 (1958).
16. Bonner, T. G., E. J. Bourne, and N. M. Saville, *J. Chem. Soc.*, **1960**, 2914.
17. Theobald, R. S., *J. Chem. Soc.*, **1961**, 5359, 5365, 5370.
18. Micheel, F., and G. Hallerman, *Tetrahedron Letters*, **1962**, 19.
19. Bird, T. P., W. A. P. Black, E. T. Dewar, and D. Rutherford, *Chem. Ind. (London)*, **1960**, 1331.
20. Hibbert, H., T. H. Evans, I. Levi, and W. L. Hawkins, *Can. J. Res.*, **20B**, 175 (1942).
21. Freundenberg, W., and J. T. Sheehan, *J. Am. Chem. Soc.*, **62**, 558 (1940).
22. Lyman, D. J., *J. Polymer Sci.*, **45**, 49 (1960).
23. Flory, P. J., and F. S. Leutner, U. S. Pat. 2,623,034 (December 23, 1952).
24. Riesel, E., and A. Berger, *J. Polymer Sci.*, **32**, 337 (1959).
25. Ogg, C. L., W. L. Porter, and C. O. Willits, *Ind. Eng. Chem., Anal. Ed.*, **17**, 394 (1945).

Résumé

On a préparé plusieurs polyesters et polyuréthanes linéaires, contenant des unités de 2,3,4-tri-*O*-méthyl-xylitol, ou de 2,3,4,6-tétra-*O*-méthyl-D-glucitol. La polymérisation

en solution de chacun des dérivés méthylés avec l'isocyanate de méthylènebis(4-phényle), fournit des polyuréthannes avec un poids moléculaire d'environ 30.000. La polymérisation thermique de chacun des dérivés méthylés avec le chlorure de téréphtaloyle ou avec des mélanges du chlorure de téréphtaloyle et du chlorure de sébacoyle, fournit des polyesters avec un poids moléculaire de 4000 à 7000. Des films de ces polyesters sont fragiles. Les résistances à la traction ont des valeurs jusqu'à 32 kg/mm^2.

Zusammenfassung

Es wurden einige lineare Polyester und Polyurethane hergestellt, die 2,3,4-Tri-*O*-methyl-xylit oder 2,3,4,6-Tetra-*O*-methyl-D-sorbit enthielten. Die Lösungspolymerisation eines jeden der beiden methylierten Derivate mit Methylen-bis(4-phenylisocyanat) ergibt Polyurethane mit Molekulargewichten von etwa 30000. Thermische Polymerisation eines jeden der methylierten Derivate mit Terephthaloylchlorid oder mit Mischungen von Terephthaloyl- und Sebazoylchlorid ergibt Polyester mit Molekulargewichten zwischen 4000 und 7000. Filme aus diesen Polyestern sind spröde und haben Zugfestigkeiten bis zu 32 kg/mm^2.

Received March 13, 1963

JOURNAL OF POLYMER SCIENCE: PART A VOL. 2, PP. 1839–1845 (1964)

Bis(imidazolato)-Metal Polymers*

G. P. BROWN and S. AFTERGUT, *Advanced Technology Laboratories, General Electric Company, Schenectady, New York*

Synopsis

The reaction of imidazole and the sulfates of Cu(II), Zn(II), and Co(II) in aqueous $NaHCO_3$ gave products whose analysis corresponded to two imidazole residues per metal atom. The products were insoluble in common organic solvents and had very high melting points. Thermogravimetric analyses revealed that the Co- and Zn-containing materials had unusually high thermal stability, as no loss in weight could be detected below 500–575°C. when heated in nitrogen. The properties led to their formulation as metal coordinate polymers. The electrical resistivity of the products was in excess of 10^{15} ohm-cm. at 140°C.

INTRODUCTION

One of the structural features frequently present in semiconducting organic substances is a multitude of conjugated double bonds. As the length of the conjugated system increases, there is a trend toward lower resistivities and energy gaps. It was, therefore, proposed to attempt the synthesis of polymers of the type shown in I with the expectation that, owing to the extensive conjugation, such polymers should display semiconductivity.

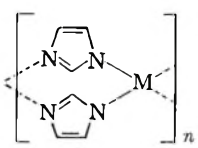

I

Coordination compounds of imidazole and benzimidazole and their derivatives with metal ions in solution have been widely investigated,[1–4] but little work has been reported on solid complexes other than salts.[5–8] In a few instances, speculation was advanced as to the possible polymeric nature of these materials[9] but recently reference has been made to x-ray crystallographic evidence which indicates that bisimidazolatozinc is polymeric.[10]

The present work reports on the synthesis of polymers from imidazole

* This work was supported by the Aeronautical Systems Division, Air Force Systems Command, U. S. Air Force.

and Cu(II), Zn(II), and Co(II) and on their electrical properties and thermal stability.

EXPERIMENTAL

Preparation of Materials

Poly[bis(imidazolato)-Cu(II)] (I, M = Cu). To a hot solution (heated over the steam bath) of 13.6 g. (0.2 mole) of imidazole and 66 g. (0.8 mole) of sodium bicarbonate in 500 ml. of water was added dropwise with stirring a solution of 25 g. (0.1 mole) of cupric sulfate pentahydrate in 125 ml. of water. The agitated mixture was kept 1 hr. over the steam bath and three days at room temperature. The blue precipitate was collected, washed with about 2 l. of water and dried at 110° overnight. The product weighed 16 g. and had m.p. 278–279°C. (dec.). It did not sublime at 250°C. (0.01 mm.) but decomposed to give a trace of imidazole and an unidentified compound melting at 170–2°.

ANAL. Calcd. for $(C_3H_3N_2)_2Cu$: C, 36.5%; H, 3.1%; N, 28.3%; Cu, 32.1%. Found: C, 36.7%; H, 2.9%; N, 28.4%; Cu, 32.5%.

An x-ray powder diffraction pattern gave the following d values (most intense lines are starred (*)): 6.90*, 5.10*, 4.60*, 4.51, 3.80, 3.72, 3.55, 3.42, 3.15, 3.00, 2.74, 2.63, 2.46, 1.90, 1.82.

Poly[bis(imidazolato)-Zn(II)] (I, M = Zn). This product was similarly prepared using zinc sulfate heptahydrate. It did not melt below 360°C. nor did it sublime at 300°C. (0.01 mm.).

ANAL. Calcd. for $(C_3H_3N_2)_2Zn$: C, 36.12%; H, 3.03%; N, 28.08%; Zn, 32.77%. Found: C, 36.0%; H, 3.0%; N, 28.1%; Zn, 32.4%.

The x-ray powder diffraction pattern had the following d values, (most intense lines are starred (*)): 5.90*, 5.51, 5.45, 4.75, 4.25, 4.12*, 3.70, 3.50, 3.32, 3.10, 2.98, 2.92, 2.82, 2.73, 2.67, 2.53, 2.47, 2.42, 2.36, 2.28, 2.25, 2.18, 2.15, 2.12, 2.05, 2.00, 1.94, 1.91, 1.86, 1.83, 1.75, 1.72, 1.68, 1.65, 1.60, 1.56, 1.45.

Poly[bis(imidazolato)-Co(II)] (I, M = Co). This was prepared from 0.15 mole of imidazole, 0.4 mole of sodium bicarbonate and 0.05 mole of cobaltous sulfate heptahydrate. It did not melt below 360°C.

ANAL. Calcd. for $(C_3H_3N_2)_2Co$: C, 37.32%; H, 3.13%; N, 29.01%; Co, 30.52%. Found: C, 37.5%; H, 3.0%; N, 29.9%; ash, 41.7, 40.7%. Assuming that the ash is Co_3O_4, the per cent Co is 30.6 and 29.9% for the two determinations.

The x-ray powder diffraction pattern gave the following d values (most intense line starred (*)): 5.85*, 5.55, 5.08, 4.75, 4.50, 4.10, 3.70, 3.50, 3.35, 3.10, 2.92, 2.82, 2.75, 2.66, 2.49, 2.19, 2.06, 1.92, 1.84.

Electrical Measurements

Resistance measurements (d.c.) were made with a Keithley Model 200B electrometer with accompanying power supply and shunt. The outputs of

the electrometer and the thermocouple were fed into an X–Y recorder to plot the changes in resistance with temperature. The test specimens consisted of disks having a diameter of 1 in. and a thickness of 0.03–0.07 in. They were prepared by compaction of the polycrystalline materials in a scrupulously cleaned mold at a pressure of about 44,500 psi at room temperature. The resistance of the disk specimens was measured in a sample holder consisting of two L-shaped pieces of glass tubing, each terminating in a spherical socket joint at one end. The sample disk was clamped in a vertical position between the two joints and the glass tubes were filled with mercury. A thermocouple well was located near one of the socket joints. The whole assembly was enclosed in a glass vessel which had provisions for inserting leads and for maintaining an inert atmosphere. In this setup, only the edge of the disk was exposed to the ambient which was nitrogen. A guard ring arrangement was used to eliminate surface conduction.

RESULTS AND DISCUSSION

The reaction of two moles of imidazole with one mole of copper and zinc sulfate in aqueous sodium bicarbonate gave products whose analysis corresponded to two imidazolyl groups per metal atom. Reaction under similar stoichiometric conditions with cobalt sulfate did not furnish an analogous product. The desired product was obtained by the reaction of a 50 mole-% excess of imidazole with $CoSO_4$. The products were crystalline powders, extremely insoluble in water and in common organic solvents which precluded the cryoscopic determination of their molecular weights. X-ray powder diffraction spectra confirmed their crystallinity.

The complexes had very high melting points. Thus, the copper complex melted at 279°C. and the cobalt and zinc complexes did not melt below 360°C. None of the materials could be sublimed in high vacuum. Thermogravimetric analyses (Fig. 1) revealed that the cobalt and zinc complexes had unusually high thermal stability, as no loss of weight could be detected below about 500–575°C. when heated in an atmosphere of nitrogen. On the other hand, the copper complex underwent a stepwise degradation starting at 250°C. The thermal behavior as well as the insolubility of the three products are not consistent with their formulation as sandwich compounds or simple covalent compounds.

The infrared spectra of the Zn and Co complexes were virtually identical, and were only slightly different from that of the Cu complex. The spectrum of the Zn complex, shown in Figure 2, lacks the characteristic absorptions of imidazole in the 3–4 μ region attributable to associated N–H (hydrogen bonding), confirming the replacement of the imino hydrogen. However, the peak at 3.25 μ attributable to C—H stretching is still present. For comparison, the spectrum of the sodium salt of imidazole (Fig. 3) was also determined. It is almost entirely different from those of imidazole and the metal complexes. It should be noted that the vestiges of associated N—H absorption present in the 3–4 μ region of the sodium salt are

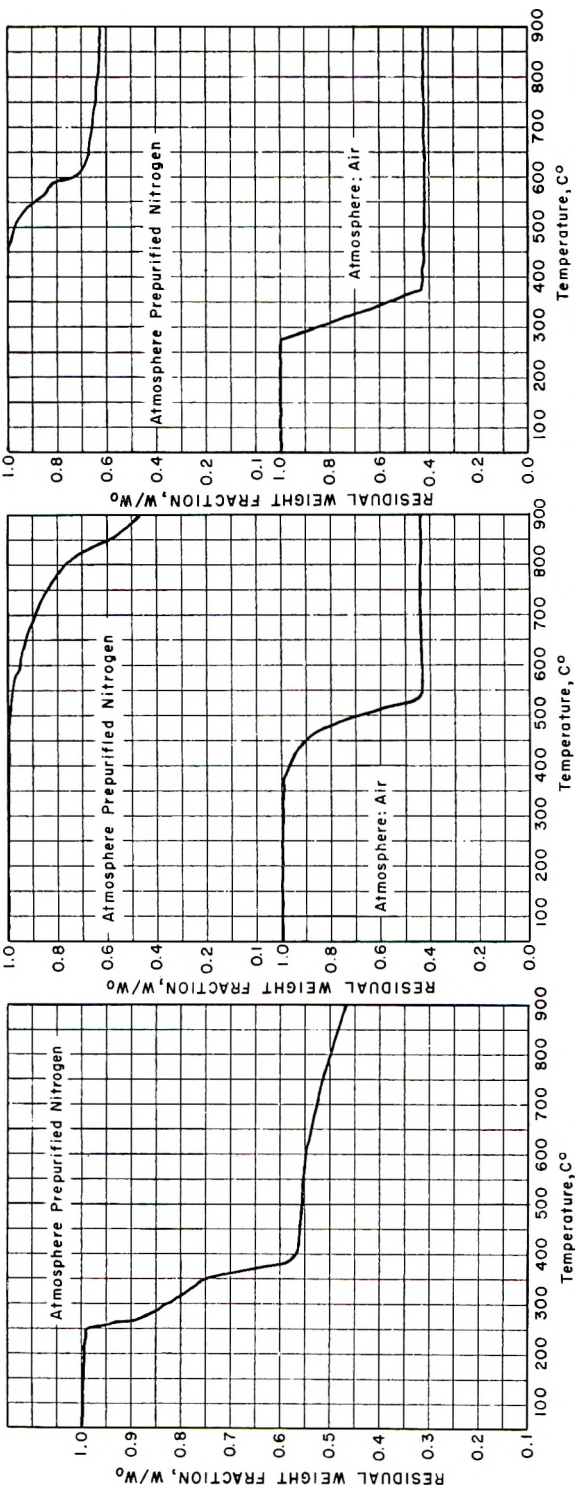

Fig. 1. Thermogravimetric analysis of metal–imidazole complexes: (*a*) poly[bis(imidazolato)-Cu(II)]; (*b*) poly[bis(imidazolato)-Zn(II)]; (*c*) poly[bis(imidazolato)-Co(II)].

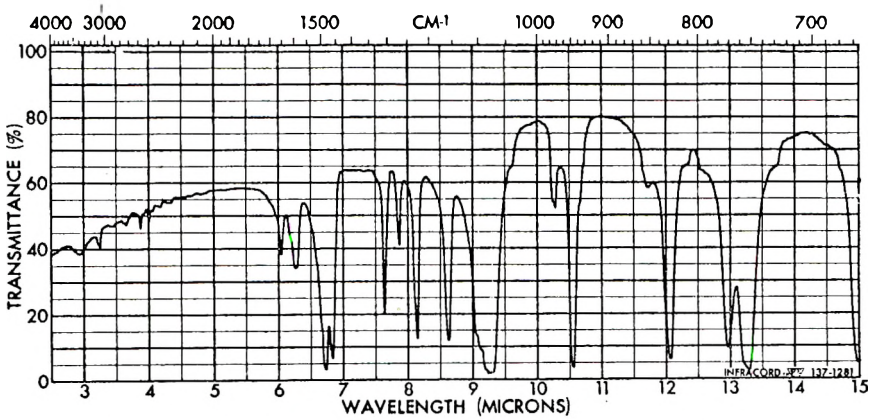

Fig. 2. Infrared spectrum of poly[bis(imidazolato)-Zn(II)]; KBr disk.

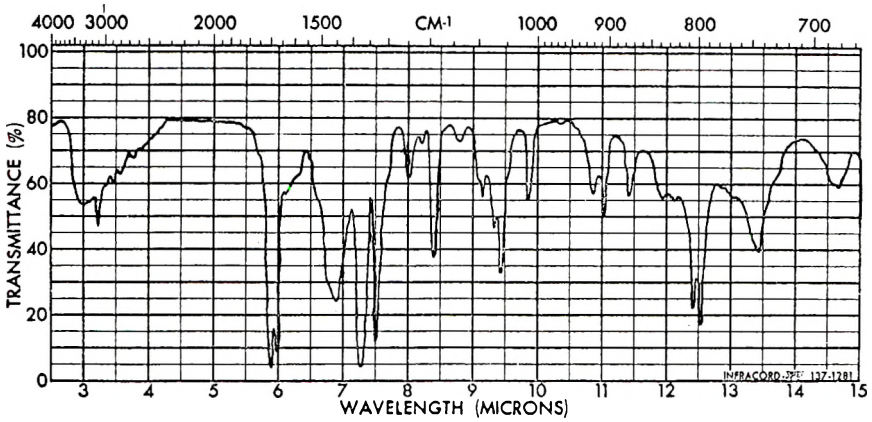

Fig. 3. Infrared spectrum of sodium salt of imidazole; KBr disk.

probably due to free imidazole arising as a consequence of its extreme hydrolytic instability. Furthermore, the absorptions at 6.9 and 11.4 μ in the sodium salt are enhanced by the presence of sodium hydroxide which was used in slight excess in its preparation. The differences in the spectra between the sodium salt and the metal complexes suggest that the latter are not simple ionic lattices. The spectral evidence does not warrant a conclusion concerning the relative contribution of ionic and covalent bonding. An assessment of the various physical properties, however, make it apparent that the structure of the complexes is polymeric.

The electrical resistivity of the products was measured on compacted polycrystalline specimens sandwiched between mercury electrodes in an atmosphere of nitrogen. The cobalt-imidazole polymer had a resistivity of 10^{17} ohm-cm. at 114°C. which decreased exponentially with an increase in temperature according to $\rho = \rho_0 \exp \{E/kT\}$ with an activation energy E of 1.55 e.v. in the range of 114–149°C. The cobalt– and zinc–imidazole

polymers had resistivities of 10^{15} ohm-cm. at 150°C. and 10^{15} ohm-cm. at 140°C., respectively.

The resistivity of these polymers is many orders of magnitude higher than that of imidazole (10^{11} ohm-cm. at 27°C.), measured in similar fashion.[11] The relatively low resistivity of the latter has been ascribed to favorable molecular orbital overlap provided by intermolecular hydrogen bonding. Assuming that the complexes of imidazole with copper, zinc, and cobalt are polymeric, there may be various reasons for their high resistivities. One of these is that conduction in imidazole is by proton migration and that due to the absence of protons, this mechanism is not available to the complexes. In view of Zimmermann's findings[12] that the structure of imidazole is best described by hydrogen-bonding in which the hydrogen is equidistant to two nitrogen atoms, there is no need to postulate transfer of charge by proton migration. Another possibility is that the actual manner of coordination (apparently tetrahedral in the zinc and cobalt complexes) between the metal atoms and the imidazole residues may not be conducive to the type of conjugation required for electrical conductivity. A further possibility is that hydrogen bonding is considerably more effective than coordination to a metal in facilitating the transport of charge involved in semiconduction.

The authors gratefully acknowledge the assistance of Mr. J. D. Howard in the synthesis phase, Mr. W. T. Doyle in metal analyses and in obtaining infrared spectra, Mr. J. A. Hill in obtaining x-ray spectra and Mr. E. J. McGowan in measurement of the electrical properties.

References

1. Tanford, C., and M. L. Wagner, *J. Am. Chem. Soc.*, **75**, 434 (1953).
2. Edsall, J. T., G. Felsenfeld, D. S. Goodman, and F. R. N. Gurd, *J. Am. Chem. Soc.*, **76**, 3054 (1954).
3. Li, N. C., J. M. White, and E. Doody, *J. Am. Chem. Soc.*, **76**, 6219 (1954).
4. Nozacki, Y., F. R. N. Gurd, R. F. Chen, and J. T. Edsall, *J. Am. Chem. Soc.*, **79**, 2123 (1957).
5. Holmes, F., K. M. Jones, and E. G. Torrible, *J. Chem. Soc.*, **1961**, 4790.
6. Goodgame, M., and F. A. Cotton, *J. Am. Chem. Soc.*, **84**, 1543 (1962).
7. Terlon, C., and J. Brigando, *Compt. Rend.*, **253**, 2069 (1961).
8. Hatem-Champy, S., *Compt. Rend.*, **253**, 2791 (1961).
9. Brooks, P., and N. Davidson, *J. Am. Chem. Soc.*, **82**, 2118 (1960).
10. Ref. 6, footnote 16a.
11. Brown, G. P., and S. Aftergut, *J. Chem. Phys.*, **38**, 1356 (1963).
12. Zimmermann, H., *Z. Elektrochem.*, **65**, 821 (1961).

Résumé

Les réactions de l'imidazole et de sulfate, de Cu(II), Zn(II) et de Co(II) dans une solution aqueuse de bicarbonate de soude fournissent des produits dont les analyses correspondent à deux résidus imidazoliques par atome de métal. Les produits sont insolubles dans les solvants organiques usuels et ont de très hauts points de fusion. Par analyse thermogravimétrique on a montré que les matériaux contenant du Co et du Zn possèdent une stabilité thermique très élevée car on n'a pu détecter aucune perte de poids

par chauffage de ces substances sous azote en-dessous de 500–575°C. Les propriétés observées amènent à formuler ces substances comme des polymères de coordination. La résistivité électrique des produits est en excès de 10^{14} ohm/cm à 140°C.

Zusammenfassung

Die Reaktion von Imidazol mit den Sulfaten von Cu(II), Zn(II) und Co(II) in wässrigem $NaHCO_3$ ergab Produkte, deren Zusammensetzung zwei Imidazolresten pro Metallatom entspricht. Die Produkte waren in den üblichen organischen Lösungsmitteln unlöslich und hatten sehr hohe Schmelzpunkte. Thermogravimetrische Analysen zeigten eine ungewöhnlich hohe thermische Stabilität der Co- und Zn-hältigen Produkte, da beim Ehritzen in Stickstoff bis 500–575° kein Gewichtsverlust festgestellt werden konnte. Diese Eigenschaften sprechen für ein Vorliegen von Metallkoordinationspolymeren. Der spezifische elektrische Widerstand der Produkte war bei 140° grösser als 10^{15} Ω cm.

Received March 14, 1963

JOURNAL OF POLYMER SCIENCE: PART A VOL. 2, PP. 1847–1862 (1964)

Clay-Catalyzed Reactions of Olefins. II. Catalyst Acidity and Mechanism*

JAMES A. BITTLES, A. K. CHAUDHURI,† and SIDNEY W. BENSON,‡ *Department of Chemistry, University of Southern California, Los Angeles, California*

Synopsis

Evidence is presented for the heterogeneity of olefin reactions on acid clay surfaces and for the inherent acidity of the catalyst. Catalyst activity was shown to be due to an active proton probably associated with tetrahedral aluminum. Deactivation of catalyst was observed with proton accepting contaminants such as water, amines, and basic olefins. Surface acidities and total exchangeable hydrogen in the catalyst were determined by gas phase absorption and by deuterium analysis, respectively. The measurements were correlated with previous acidity measurements, styrene polymerization rates, and polymerization mechanism. Polymerization rates were measured by time–temperature observations and by analyses of monomer. Exchangeable hydrogen was determined by deuterium exchange and density measurements. Exchange was 90% complete before polymerization began. The equilibration of a classical carbonium ion from styrene by a sorption–desorption process was definitely indicated and we propose that these ions are the active intermediates in the initiation, propagation, transfer, and solvent termination processes.

INTRODUCTION

Naturally occurring clays have been known for a long time to "catalyze" a large number of chemical reactions. These are cracking reactions of hydrocarbons,[1,2] hydration of olefins,[1,2] polymerization of olefins,[1–3] ion exchange, and formation of acid aqueous suspensions. Jurinak and Volman[4] have recently reported that the olefins isobutene and chloroethylene are irreversibly absorbed by kaolin. These phenomena are collectively evidence of the acidic nature of clay catalysis.

The surface acidity of clay cracking catalysts has been measured by several liquid phase methods[5–7] and by amine absorption from the gas phase.[8–10] The surface acidities have been found to be mildly dependent upon desorption temperature, basicity of adsorbed agent, and surface area of solid.[10] Gas phase acidity measurements certainly appear to be dif-

* This work has been supported by grants from the Goodyear Tire and Rubber Company, Akron, Ohio.

† Present address: Indian Association for the Advancement of Science, Calcutta, India.

‡ Present address: Standford Research Institute, Menlo Park, California.

fusion-controlled.[10] An accumulation of data on acidities of clays indicated acid site concentrations of a fraction of a millimole per gram of solid.

The measurements of acidity reported here were in general agreement with previous findings, and the results were employed to explain the acidity of the catalyst, the nature of the reactions involved with olefins, and to propose a mechanism.

It became evident that in the reactions with olefins, sorption-desorption phenomena were involved as has been indicated by Volman.[4] Further it was evident that the reaction was heterogeneous. Heterogeneous polymerization of olefins with clays has been observed,[3,11] and we have reported the polymerization of styrene with acid clays[12] and will report condensation of other olefins.

EXPERIMENTAL

The acid clay polymerization of styrene has been studied in this laboratory and the polymer characteristics, endgroup analyses, and polymer molecular weights have been reported.[12]

Acid Clay Catalyst

The catalyst used was Filtrol Corporation Grade 13 SV7494 (Neutrol 40) fluid catalytic cracking catalyst. This material was prepared commercially from natural clays in which the active mineral is montmorillonite (a silica–alumina). It is processed, washed with acid, and calcined at about 450°C.

Activation and Handling of Acid Clay Catalyst

The catalyst as processed is inactive in most cracking and polymerization reactions without strong heating (heating which removes physically adsorbed water).

The catalyst employed in this study was activated by heating in a glass ampule *in vacuo* at 10^{-5} mm. Hg pressure and at 280°C. The detailed procedure is described in the preceding paper.[12] Catalyst was employed immediately after activation for consistent results and stored under anhydrous conditions. Maximum activity after long storage was obtained by reheating *in vacuo* at 280°C.

Analysis of Catalyst

A fluid cracking catalyst is of the approximate composition $(SiO_2)_x$-$(Al_2O_3)_y$,[11,13–15] in which Al_2O_3 is approximately 16% by weight, silica 71% by weight. A typical product analysis of Filtrol Corporation cracking catalyst was as follows SiO_2, 71.2%; Al_2O_3, 16.5%; MgO, 4.3%; SO_3, 4.6%; Fe_2O_3, 1.4%; CaO, 1.6%; K_2O, 0.4%; TiO_2, 0.4%. The analytical data were obtained from the manufacturer (Filtrol Corporation, Los Angeles, Calif.). These analyses were representative of volatiles-free solids, the volatiles being removed by calcination at 900°C. There

was apparently no hydrogen in the material, at least within the limits of the analytical measurements (i.e. 0.1%).

Catalyst after calcining was hygroscopic and absorbed approximately 20% of moisture by weight on a dry basis. Our weighing experiments have agreed well with this figure. This absorbed or uncombined water was removed by the activation process.

Extractable Sulfate

Extractable sulfate in the catalyst was determined by washing the clay with water until no precipitate was obtained, and then precipitating and weighing barium sulfate. In this manner there was obtained an average of 5.57% of sulfuric acid (5.47 and 5.68%). This was equivalent to 1.14×10^{-3} equiv. of acid per gram of catalyst or to 4.54% SO_3. In view of the uncertain source and exact nature of such a clay the agreement is good.

This catalyst remained active after washing free of sulfate ion, indicating that activity (acidity) was inherent and was not due to desorption of acid into the liquid phase or to reaction with adsorbed sulfuric acid. Since catalyst acidity was of the order of 0.27 mequiv./g., sulfate was apparently absorbed as $SO_4^=$ in combination with another positive ion.

Catalyst Activity

Catalyst obtained by washing free of sulfate ion and before activation failed to initiate polymerization or condensation. This catalyst was activated by water removal *in vacuo* at 280°C. and was deactivated by absorption of basic impurities such as water.

Sulfate-free catalyst, weighing 8.0458 g., was activated by heating *in vacuo* at 280°C. Activated catalyst (6.1126 g.) was employed in the following experiment. A 0.5*M* solution of monomer in benzene was prepared from 17.4 ml. (15.7 g.) of freshly double distilled styrene and 282.6 ml. of sodium-dried benzene. The polymerization was run adiabatically commencing at ambient temperature. The measured time–temperature data are shown in Table I.

TABLE I
Polymerization Rate of Sulfate-Free Catalyst (0.5*M* in Benzene)

Time, min.	Temp., °C.
0	25
1	40
2	43
3	44
4	42
8	42
16	41
32	39

The maximum temperature rise during polymerization was 17°C. in the first 3 min. which is the expected reaction time for 100% conversion. The calculated T_{max} was 17.8°C. calculated from the equation:

$$\Delta T_{max} = m\Delta H/V_s d_s C_v$$

where ΔH is the molar heat of polymerization, d_s is the density of the solution, C_v is the specific heat, V_s is the volume of the solution in cubic centimeters, and m is the number of moles of monomer. A comparison with a polymerization using unwashed catalyst was made. A time–temperature measurement of such a run is shown in Table II. The weight of catalyst employed was 6.1930 g., and the benzene solution was 0.5M in styrene.

TABLE II
Polymerization Rate of Sulfate-Containing Catalyst (0.5M in Styrene)

Time, min.	Temp., °C.
0	25
0.5	35
1	41
2	42
3	41
4	40
8	37
16	34
32	30

The rate of temperature rise was that of sulfate-free catalyst and was that expected of a 0.5M solution (300 cc.) under adiabatic conditions. Polymer yield from sulfate-free catalyst was 30% and the molecular weight was 1065. Polymer yield from unwashed catalyst was 40% and molecular weight was approximately 1200. In both cases monomer conversion was 100%, and the bulk of this was in the form of low molecular weight material. No effort was made to obtain maximum yields of polymer.

Inherent Activity of Sulfate-Free Catalyst

The sulfate-free catalyst employed in the previous experiment was recovered, and activated by degassing in the usual manner. The following experiment was run with 5.73 g. of catalyst. A 0.1M solution of styrene in 300 cc. of benzene was prepared and the polymerization run adiabatically. A time–temperature observation was made, and monomer conversion was determined. These results are shown in Table III.

Monomer analyses were performed by titration of aliquots with solutions of bromine in acetic acid.

The inherent and repeated acidic activity of the clay catalyst was indicated by these and the previous results.

TABLE III
Sulfate-Free Reactivated Catalyst (0.1*M* Styrene in Benzene)

Time, min.	Temp., °C.	Monomer conversion, %
0	28	0
1	28	
2.33	28	15.3
4.0	29	
7.0	29	
11.0	30	
16.0	31	
32.0		
1440		97.1

Organic Solvent Washing of Catalyst

Activated and degassed catalyst (10.09 g.) was extracted with 50 cc. of benzene (not dried) at ambient temperature. The benzene extract was found to contain no sulfate and the solvent extract was inactive in polymerization. The remaining solid catalyst upon activation was active in polymerization.

Pepper and Hayes[16] have reported styrene polymerization by sulfuric acid in 1,2-dichloroethane. They further show that sulfuric acid is distributed between aqueous acid phase and organic solvent.[17] Ionized sulfuric acid is no doubt responsible for the observations, but the above experiments show that the acid clay system is not of this type. On the contrary, these results indicate surface polymerization and show that polymerization does not occur homogeneously by solution equilibration of sulfuric acid from the catalyst itself. Further it appears that any "free" sulfuric acid should be in the solvent phase.

Catalyst Activity at −70°C.

Activated clay catalyst weighing 8.15 g. was employed in the polymerization of a 0.73*M* solution of styrene in toluene. The reaction mixture was cooled in solid CO_2–acetone and run at −70°C. Monomer conversions versus time is shown in Table IV.

TABLE IV
Catalyst Activity at −70°C.

Time, min.	Monomer concn., *M*
0	0.73
190	0.63
485	0.62
1335	0.59

Catalyst activity was observable at −70°C., though much slower, and polymer was of molecular weight 1200 (average). The common observation

in cationic homogeneous solution reactions is a small temperature coefficient for the rate* or a complete stoppage of reaction[18] due to freezing out of the catalyst complex. The slow but observable rate indicates heterogeneity. (The most convincing demonstration of the heterogeneity of the process comes from our dilatometer measurements where we found that when stirring stopped, the catalyst settled to the bottom of the tube and reaction quickly stopped. Upon restoring the suspension of the catalyst, polymerization resumed.)

Inactivation of Catalyst (Poisoning)

Inactivation of catalyst was observed experimentally by qualitative measurements of polymerization rates in the presence of basic substances. Polymer was isolated and characterized.

Water. Activated catalyst (4.13 g.) was employed in the polymerization of a 0.5*M* solution of styrene in 1,2-dichloroethane. Water was present in the solvent to the extent of an estimated 0.1%. The polymerization was conducted isothermally at 0°C. and monomer conversions determined. Polymer isolated from this experiment was of molecular weight 1400. The rate data are shown in Table V.

TABLE V
Rate of Water-Inhibited Polymerization

Time, min.	Monomer conc., *M*
0	0.5
5	—
10	0.49
20	0.48
30	0.47
42	—
90	0.45
2400	0.22

These results show a halflife of polymerization slightly less than 40 hr. for this quantity of catalyst. An uninhibited polymerization under identical conditions with this quantity of catalyst has a halflife of 1.5 hr.[19] Polymer molecular weight in both cases was 1400.

Further depressions in rate were observed by addition of moisture and complete inhibition occurred by catalyst containing 20% of water before activation. Polymerizations were also quenched at definite time intervals by addition of water.

Dimethylamine. The deactivation effect of dimethylamine was shown by measuring crude polymerization rates after exposure to the base. Acid silica–alumina cracking catalyst was partially neutralized with varying quantities of the base. Samples (2 g.) of degassed catalyst were exposed to predetermined quantities of dimethylamine from a gas buret. Then

* The activation energy of polymerization will be discussed in a future communication.

0.15 g. of activated neutralized catalyst was used to polymerize 10 ml. of 0.82*M* styrene in benzene. The reaction was quenched after 400 sec. and yields of polymer determined. The results of six neutralizations are shown in Table VI.

TABLE VI
Inhibition by Dimethylamine[a]

$(CH_3)_2NH$, mmole/g. catalyst	Wt. of polymer, g./g. monomer	Monomer conversion, %
0.27	0	0
0.22	0	0
0.18	0	0
0.16	0	0
0.13	0.080	8
0.02	0.060	6

[a] We are indebted to Dr. S. Kessar for these measurements.

Active catalyst neutralized with dimethylamine failed to initiate polymerization and catalyst 50% neutralized (0.13 mmole) gave only low yields of polymer. Apparently less than 10% neutralization of acid sites (0.02 mmole) was sufficient to prevent normal polymerization. In a 400 sec. reaction time at ambient temperature the polymerization would be expected to be 90% complete. The halflife of a 1*M* solution of styrene in benzene at ambient temperature is approximately 120 sec.[24]

α-Methylstyrene. Inhibition by α-methylstyrene was estimated by employing a dilatometric method which will be described later. Dry and distilled α-methylstyrene (6.5 mg.) was added to 10 cc. of 0.1*N* styrene in toluene, and this solution polymerized with the use of 0.275 g. of catalyst. The time to 50% monomer conversion was about 250 min. compared to the normal halflife of 10 min.

Catalyst Acidity Measurement

The acidities of Filtrol cracking catalyst are reported in the literature to be 0.1–0.15 mequiv. acid/g. catalyst.[21] Acidity values were obtained in this laboratory by exposure to dimethylamine. A sample of catalyst was degassed at 150°C. and then exposed to dimethylamine vapor at a pressure

TABLE VII
Catalyst Acidity Measurement

Run No.	Wt. of samples, g.	Wt. of amine, g.	Acidity, mequiv./g.
1	2.0905	0.0255	0.27
2	2.1901	0.0253	0.265
3	2.3022	0.0271	0.26
4	4.2051	0.0529	0.28
		Avg.	0.27

of 600 mm. for 5 hr. The sample was again degassed *in vacuo* at 150°C. for 24 hr. The data obtained in these experiments are shown in Table VII.

The acidity of fresh Davidson DA-1 fluid cracking catalyst (similar to Filtrol cracking catalyst) has been measured by Richardson and Benson[10] using trimethylamine and pyridine in the gas phase. The acidities were 0.14–0.18 mequiv./g. when pyridine was employed and final degassing was done at 300°C. and acidities were 0.23–0.33 mequiv./g. with trimethylamine when degassing was done at 300 and 200°C., respectively. The acidity of the catalyst was dependent upon the temperature of degassing. The value of 0.33 mequiv./g. checks with our value of 0.27 mequiv./g. obtained by degassing at 150°C.

The acidity of catalyst measured by titration with alkali hydroxide was 1.02 mequiv./g. The higher value was due to the greater basicity of hydroxide ion and the leveling effect of water. Since strong acid sites are required for reaction with olefins such as styrene the effective acidity of the catalyst in these reactions is probably about 0.15 mequiv./g. rather than the higher value obtained with OH^-.

Deuterium Exchange with Catalyst

Exactly 33.3 g. of Filtrol cracking catalyst containing adsorbed water was activated on the vacuum line at 280°C., and 50 cc. of heavy water assaying 99.5% D_2O was added to the catalyst. The catalyst mixture was then stirred for 68 hr. at ambient temperatures. The sample was filtered and activated by heating, and employed in the polymerization of styrene. After being employed in a polymerization experiment the sample was recovered and treated with 50 cc. of 99.5% D_2O. Exactly 20.36 g. of catalyst was exchanged in this manner The sample was again activated by heating and treated with 10 cc. of boiled distilled water at ambient temperature for 16 hr. The exchanged water was collected *in vacuo* and analyzed* for heavy water content by the falling drop method.[22]

Deuterium Exchange with Monomer

The deuterated catalyst (33.3 g.) was activated by heating. The catalyst now weighed 26.64 g. This was employed in the polymerization of 11.6 cc. (10.4 g.) of styrene in 990 cc. of 1,2-dichloroethane at 0°C. The polymerization was run for 600 sec. which was estimated from rate measurements to be the halflife of the polymerization. The run was stopped by the addition of 1 cc. of water. Unconverted monomer was recovered by fractionation *in vacuo* at 26 mm. Hg. There was recovered 6.78 g. of styrene which was a conversion of 34.8%. Approximately 3 g. of polymer was isolated from the precipitation placing the overall recovery at 94%. Monomer was analyzed for deuterium content.

* We are indebted to Mr. J. C. Mayfield for some of these experiments.

Deuterium Analysis

The deuterium content of the clay catalyst was determined in the following manner. Deuterated clay was treated with 10 cc. of water as described and the water collected. The sample (1.0250 g.) was assayed for D_2O content by the falling drop method for a determination of density. It was the method originally employed by Barbour and Hamilton and described by Kirshbaum.[22] A mixture of bromobenzene and kerosene was used in the drop tube in a thermostat at 30.25°C. The difference between reciprocal drop times of the sample and boiled distilled water were compared with a calibration curve. The calibration curve was determined from samples of known D_2O content. The size of the drops was controlled by a microburet ($\simeq$0.02 cc.) and readings were taken on drops of uniform cross section. The times could be controlled within limits by adjusting the ratio of bromobenzene–kerosene. The drop times of boiled distilled water were determined frequently since $(1/t) - (1/t_{H_2O})$ was plotted against D_2O content and $1/t_{H_2O}$ was the critical variable. The method worked well when drop sizes were controlled uniformly and drop times were of the order of 150–250 sec.

The sample from deuterated catalyst was 4.56 mole-% D_2O. Since 0.553 mole of water (9.956 g.) and 16.3 g. of catalyst on a dry basis were used, there was 3.09 mequiv. of exchangeable H^+ per gram of catalyst.

The deuterium content of monomer obtained by exchange with deuterated catalyst was determined by analysis of the combustion products of the styrene sample. A sample of deutero styrene was burned in a micro combustion train* and the water collected in a series of Dry Ice–acetone traps. The water was distilled six times *in vacuo* until carbon dioxide was completely removed. Styrene which had not been deuterated was subjected to the same procedure and the water purity determined by a drop time measurement. The experiment showed the sample to be free of carbon dioxide and the purification process workable.

Analysis of the water from combustion of deutero-styrene showed 9.2 mole-% of the theoretical value of 100% according to the equation:

$$C_8H_7D + O_2 \rightarrow 8CO_2 + {}^7/_2H_2O + {}^1/_2D_2O$$

If only a single hydrogen of styrene were replaced by deuterium, 12.5 mole-% of deuterium would have resulted.

A deuterium content of 9.2 mole-% of 6.78 g. of styrene indicates 0.048 equiv. of deuterium from 26.7 g. of catalyst (dry basis) or 1.8 mequiv./g. of a possible 3.09 mequiv./g. of total exchangeable D; i.e. 58.2% of D^+ exchanged by actual analysis. The deuterium content of the polymer (3 g.) was neglected since the molecular weight was 1300 (0.002 mole) and infrared spectra showed only low intensity absorption of C-D. This introduces an error of 4% in the calculation.

* Combustion analysis was done by J. C. Mayfield on National Science Foundation Summer Institute Program.

Infrared Spectra of Polymer

An infrared spectrum of polymer prepared from deutero catalyst was taken on a solid film of polymer on a Perkin-Elmer Infra-Cord spectrophotometer. The spectra showed prominent but low intensity absorption maxima at 2230 cm.$^{-1}$, showing definitely that deuterium was present in the polymer. The C-D band should occur at 2180 cm.$^{-1}$,[23] but the 50 cm.$^{-1}$ shift is attributable to instrument error. Another polymer sample from deutero catalyst showed absorption at 2180 cm.$^{-1}$.

DISCUSSION

The reaction of olefins with acid clays was found to be a heterogeneous sorption–desorption process and to involve olefin polymerization. Surface absorption occurred at an acid site with classical carbonium ion formation and subsequent polymerization.

The reaction of olefins with acid clays was ionic, rapid, and rates of polymerization were influenced by the solvent as was also the molecular weight. It can be shown that solvents of higher dielectric constant produce faster rates and higher molecular weights. Polarization of the reactive species occurs more readily in the polar media.

The activity of clay was found to be indigenous and not due to adsorbed sulfuric acid nor to homogeneous catalysis by sulfuric acid in the liquid phase.* This was shown by the experiments with solvent- and water-extracted catalyst and by the experiments with repeated acidic activity of catalyst in polymerization. The polymerization rates, monomer conversions, and molecular weights were independent of sulfuric acid content, and independent of the system employed in the extraction process, e.g., water, benzene, or styrene.

The sorption–desorption nature of the reaction was reasonably certain, particularly in view of the fact of deuterium exchange; however, heterogeneity and reaction at an acid site was more speculative. The heterogeneity of the polymerization (this applies to other reactions of olefins with acid catalysts) was indicated by the fact that polymerization ceased when catalyst was allowed to settle, by the fact that catalyst activity was independent of sulfuric acid content and by the fact that catalyst acidity was not due to some readily extractable acid.

Inhibition of polymerization was observed with water, dimethylamine, and α-methylstyrene and in trace amounts. Relative inhibition effect was in the order dimethylamine > water > α-methylstyrene. This effect was due to poisoning of the catalyst by competition for a proton, and was indicated by slower rates of reaction or complete stoppage of reaction. The quantity of inhibitor was sufficient to neutralize only a part of the acid sites of the catalyst showing a strong dependence on acid site concentration. (Catalyst poison might be a better term to use than inhibitor,

* Sulfuric acid in organic solvents has been used to study the polymerization of styrene and α-methylstyrene.

since inhibition implies reaction by chain stoppers and this is definitely not the case with these basic substances.) The dimethylamine data show that complete inhibition occurred when the catalyst was 59% neutralized, indicating that something less than 41% of the acid sites or approximately 0.11 mmole/g. was available and necessary to produce an observable rate. The remainder of the acid sites are probably of insufficient activity to combine directly with monomer. Other data certainly indicate that the rate is dependent on acid site concentration and catalyst quantity; however, apparently nonlinearly.

Exchangeable Hydrogen and Acidity

Our experimental work with clay catalysts show acid–base reactions, exchange of hydrogen for deuterium and hydrogen exchange with olefins. Total exchangeable hydrogen was present to the extent of 20 times the strong acid site concentration or about 3.1 mmoles/g. Only the strongly acid sites ($\simeq$0.15 mmole/g.) take part directly in polymerization and/or condensation. Internal exchange within the catalyst structure between H^+ and D^+ can account for the large difference in acidic H^+ and total exchangeable H.

Deuterated catalyst exchanged 58.2% of the total deuterium with styrene monomer by actual analysis, or 1.8 mmole/g. of catalyst. If the assumption is made that polymer also contains deuterostyrene in the ratio 9.2/12.5 then 2.75 mmole of D^+ exchanges per gram of catalyst. (This appears to be reasonable in view of the presence of C-D stretching bands in the infrared spectra of the polymer.) The monomer exchange ratio is 73.5%, and the catalyst exchange ratio is 89.5%. The equilibrium constant for the reaction

$$\text{D—CaT} + \text{H—StY.} \rightleftharpoons \text{H—CaT} + \text{D—StY.}$$

is then approximately 23 and this favors formation D-styrene.

The presence of low intensity carbon-deuterium stretching vibrations may be interpreted as indicating almost complete exchange of a single hydrogen in monomer; therefore, equilibration must be complete before polymerization commences. Participation of the deutero species in the polymerization is certain and if the exchange is complete prior to polymerization, homopolymerization of deutero species is indicated. Other possibilities for participation are in the initiation step which most certainly occurs or as a comonomer with H-styrene.

The following reversible reactions probably occur with styrene:

$$H^+[AlSiO_4]^-(H_2O)_x + C_6H_5CH{=}CH_2 \rightleftharpoons C_6H_5\overset{+}{C}H(CH_3)[AlSiO_4]^-(H_2O)_x \quad (1)$$

$$H^+[AlSiO_4]^-(H_2O)_x + (x + 1/2)D_2O \rightleftharpoons D^+[AlSiO_4]^-(D_2O)_x + (x + 1/2)H_2O \quad (2)$$

$$D^+[AlSiO_4]^-(D_2O)_x + C_6H_5CH{=}CH_2 \rightleftharpoons C_6H_5\overset{+}{C}H(CH_2D)[AlSiO_4]^-(D_2O)_x \quad (3)$$

$$D^+[AlSiO_4]^-(D_2O)_x + (x+1)C_6H_5CH{=}CH_2 \rightleftharpoons H^+[AlSiO_4]^-(H_2O)_x + (x+1)C_6H_5CH{=}CHD \quad (4)$$

$$C_6H_5\overset{+}{C}H(CH_2D)[AlSiO_4]^-(D_2O)_x \rightleftharpoons H^+[AlSiO_4]^-(D_2O)_x + C_6H_5CH{=}CHD \quad (5)$$

$$C_6H_5\overset{+}{C}H(CH_2D)[AlSiO_4]^-(D_2O)_x + C_6H_5CH{=}CH_2 \rightleftharpoons C_6H_5\overset{+}{C}H(CH_2D)[AlSiO_4]^-(D_2O)_{x-1} + C_6H_5CH{=}CHD \quad (6)$$

Silica–Alumina Catalyst Structure and Acidity

Silica–alumina catalysts are strong acids comparable with strong mineral acids. The evidence for their acidity is well documented. Our work with Filtrol clays has shown this acidic behavior in the polymerization of styrene and reactions with other olefins, in deuterium exchange, and in the absorption of amines from the gas phase.

Clay catalysts are inactive in polymerization and condensation reactions unless exchangeable metal ions are replaced by H^+ or D^+. Our work has also shown this; and conversely, that catalyst activity is destroyed by proton replacement with alkali or alkaline earth metals.

In general acid hydrogen is thought of as being associated with aluminum. This conclusion is based on the stoichiometry of clays and the fact that catalyst acidity increases with content of alumina.[6] Benson and Richardson[10] show an acid content of 0.14 mequiv./g. of catalyst and the data reported herein show an effective acid content of about 0.15 mequiv./g. Assuming an acidity value of 0.15 mequiv./g. and a single proton per aluminum atom, the Al_2O_3 content should be 19.3%; this is compared to the analytical value of 16.5%. The discrepancy could be due to a slightly high acidity measurement caused by incomplete desorption of base or to a small number of weakly acid sites associated with silicon.

Several views to account for the acidity and catalytic activity have been proposed, but it is generally conceded that a four coordinated aluminum ion is involved.[4,6,13] Milliken, Mills, and Oblad[13] support the formation of a Brønsted acid by coordination of a Lewis acid aluminum ion with a molecule of water in the manner of aluminum chloride. Polymerization by a Lewis acid site or 3-coordinated aluminum without water of coordination is unlikely because of the general facts of cationic polymerization.[18,24] (Boron trifluoride, which is a much stronger electrophilic agent, requires coordinated water for polymerization of isobutene.) Structures (I–IV) are possible sources of an acidic hydrogen in silica–alumina catalysts.

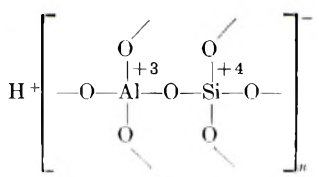

I

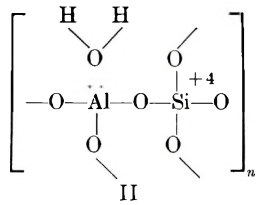

Brønsted acid from Lewis acid

II

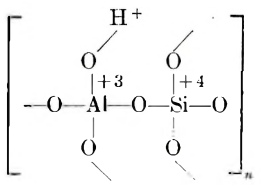

Acidity of aluminum hydroxide

III

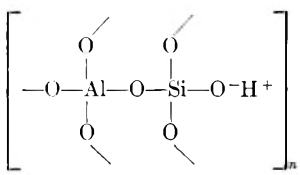

Acidity of silicic acid

IV

Structure (I) has been postulated by several workers[25] and is considered to be most likely by Pauling from a consideration of the crystallite structure of clays;[26] Oblad et al. discuss idealized silica alumina acids in olefin polymerization to liquid polymers.[15]

Tetrahedral aluminum joined with tetrahedral silicon in an infinite network is probably the active center and hydrogen may be attached directly to oxygen–aluminum or loosely associated with the negative center. Many types of structures are possible, but the essential proposition is that aluminum replaces silicon in the $(SiO_2)_n$ crystal, leaving a net deficiency of positive charge in the vicinity of the aluminum atom. This deficiency is in many types of clays made up by association with a singly charged alkali metal ion or two charges may be neutralized by association with a doubly charged alkaline earth ion. Many clays have structures[26] in which the positive ions are replaceable by protons, deuterons, and heavy metal ions. This simple ionic crystal structure and mechanism is believed to account for the acidity rather than coordination complex formation.

Tamele has reported[6] that freshly precipitated alumina and freshly precipitated silica are very weak acids with ionization constants of 10^{-13} and have little cracking activity. The aluminum hydroxide structure (III) and silicic acid structure (IV) are not responsible for polymerization as experiments in this laboratory have shown. This argument holds even though fresh aluminum oxide is reported to have an acidity of 0.12 mmole/g.[27]

In contrast to the weak acidities of the two individual oxides, a definite strong acidity develops when the alumina–silica are simultaneously

precipitated.[6] Maximum acidity and cracking activity develop at about 30% Al_2O_3 which is less than 1:1 alumina–silica (42.7% Al_2O_3). Cracking activity does not develop in freshly precipitated silica–aluminas until the polids have been calcined and adsorbed water removed. This fact corresponds with our observations on polymerization and condensation activity. An excessively high calcining temperature, however, destroys cracking activity resulting in an inactive clay. This fact has not been checked in polymerization work, but it would appear to favor formation of an uncoordinated Lewis acid site, particularly if water were excluded in a subsequent experiment. What is more likely is that the overheating rearranges tetrahedral aluminum to octahedral aluminum with six coordinations. This would result in an inactive structure.

Absorption, Initiation, and Condensation Intermediates

The existence of classical carbonium ions has been postulated for a number of years[28] and phenylcarbonium ions are discussed by Hammett.[29] The existence of the triphenyl and diphenylmethyl species was demonstrated by cryoscopic methods initially[30,31] and more recently by ultraviolet-visible spectroscopy.[32–34] Evans has discussed carbonium ion formation from aryl olefins in concentrated sulfuric acid and from 1,1-diphenylethylene in benzene containing boron trifluoride (not dried). Absorption peaks occurred consistently at 430 mμ which were attributed to diphenylethylcarbonium ion. The formation of a classical carbonium ion from phenyl olefins by proton addition is well documented in homogeneous solution chemistry.

The presence of a stable carbonium ion on a solid acid surface was recently indicated by the work of Leftin,[35] who measured the absorption spectra of 1,1-diphenylethylene on silica–alumina catalyst. The absorption spectra were consistent with other workers' results and show catalyst acidity and carbonium ion formation.

The conventional interpretation of a cationic polymerization was not applicable since clay reactions occur heterogeneously and cationic reactions occur homogeneously in solution. Initiation of styrene polymerization with clays takes place by proton addition to monomer; chain propagation, transfer, and termination occur through several modes of attack involving carbonium ion. Termination of polymer chains may occur by monomer transfer, internal cyclization (which also involves monomer), and attack on solvent. Polymerization rates, temperature dependence, and molecular weights support this mechanism. The results of a study of the kinetics of this system will be reported shortly.

The deuterium exchange measurement with monomer indicates ready formation of a carbonium ion species. Polymer structure and termination products suggest that only aliphatic hydrogen is being replaced* but do not eliminate possibilities such as aromatic H. It further suggests the for-

* The infrared spectra of polymer and endgroup structure show a distinct lack of phenyl-substituted products.

mation of a *p*-methylphenylcarbonium ion on the catalyst surface such as the following species:

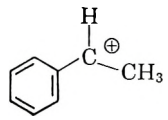

Other evidence indicating a preferred local attack on aliphatic carbon by both acid catalyst and carbonium ion has been obtained.

The absorption of styrene and other olefins on acid clay surfaces gives deeply colored complexes from gas phase, liquid phase, and solution. Absorption spectra of these complexes have not been measured, but the rapid rate of polymerization, the internal cyclization, the condensation with solvent and the solvent effect are characteristic of carbonium ion reactions.

The authors wish to acknowledge the advice and assistance of Professor C. S. Copeland in the procurement of critcal equipment and in the design and interpretation of certain experiments.

References

1. Emmett, P. H., *Catalysis*, **6**, 341 (1958).
2. Danforth, J. D., *Advan. Catalysis*, **9**, 201 (1957).
3. Salt, F. E., *Clay Minerals Bull.*, No. 2, 55 (Aug. 1948); H. M. Stanley and F. Salt (to Distillers Co., Ltd.), Brit. Pat. 524,156 (1940).
4. Jurinak, J. J., and D. H. Volman, *J. Phys. Chem.*, **63**, 1373 (1959).
5. Johnson, O., *J. Phys. Chem.*, **59**, 827 (1955).
6. Tamele, M. W., *Discussions Faraday Soc.*, **8**, 270 (1950).
7. Walling, C. W., *J. Am. Chem. Soc.*, **72**, 1164 (1950).
8. Mapes, J. E., and R. P. Eischens, *J. Phys. Chem.*, **58**, 1059 (1954).
9. Mills, G. A., E. R. Boedecker, and A. G. Oblad, *J. Am. Chem. Soc.*, **72**, 1559 (1950).
10. Richardson, R. L., and S. W. Benson, *J. Phys. Chem.*, **61**, 404 (1957).
11. Emmett, P. H., *Catalysis*, **6**, 341 (1958).
12. Bittles, J. A., A. K. Chaudhuri, and S. W. Benson, *J. Polymer Sci.*, **A2**, 1221 (1964).
13. Milliken, T. H., Jr., G. A. Mills, and A. G. Oblad, *Discussions Faraday Soc.*, **8**, 279 (1950).
14. Emmett, P. H., *Catalysis*, **7**, 17 (1960).
15. Danforth, J. D., *Advan. Catalysis*, **9**, 201 (1957).
16. Hayes, M. J., and D. C. Pepper, *Proc. Chem. Soc.*, **1958**, 228.
17. Hayes, M. J., and D. C. Pepper, *Trans. Faraday Soc.*, **57**, 432 (1961).
18. Dainton, F. S., and R. H. Tomlinson, *J. Chem. Soc.*, **1953**, p. 151; P. H. Plesch, *Cationic Polymerization and Related Complexes*, Academic Press, New York, 1953.
19. Bittles, J. A., unpublished results.
20. Bittles, J. A., A. K. Chaudhuri, and A. W. Benson, *J. Polymer Sci.*, in press.
21. Emmett, P. H., *Catalysis*, **7**, 72 (1960).
22. Kirschbaum, I., *Physical Properties and Analysis of Heavy Water*, National Nuclear Energy Series, McGraw-Hill, New York, 1951, Div. III, Vol. 4A, pp. 321–343.
23. Bellamy, L. J., *Infrared Spectra of Complex Molecules*, Methuen, London, 1954, pp. 8, 55, 67.
24. Evans, A. G., and G. W. Meadows, *Trans. Faraday Soc.*, **46**, 327 (1950).

25. Thomas, C. L., *Ind. Eng. Chem.*, **41**, 2564 (1949).
26. Pauling, L., *Nature of the Chemical Bond*, Cornell Univ. Press, Ithaca, N. Y., 1944, pp. 549–553; Bragg, W. L., *Atomic Structure of Minerals*, Cornell Univ. Press, Ithaca, N. Y., 1937.
27. Haag, W. O., and H. Pines, *J. Am. Chem. Soc.*, **82**, 2478 (1960).
28. Whitmore, F. C., *Ind. Eng. Chem.*, **26**, 94 (1934).
29. Hammett, L. P., *Physical Organic Chemistry*, McGraw-Hill, New York, 1940, pp. 292, 307–308.
30. Hammett, L. P., and A. Deyrup, *J. Am. Chem. Soc.*, **55**, 1900 (1933).
31. Gold, V., B. W. V. Hawes, and F. L. Tye, *J. Chem. Soc.*, **1952**, 2167.
32. Branch, G., and H. Walba, *J. Am. Chem. Soc.*, **76**, 1564 (1954).
33. Leftin, H. P., and W. K. Hall, *J. Phys. Chem.*, **64**, 382 (1960).
34. Evans, A. G., *Discussions Faraday Soc.*, **8**, 302 (1950).
35. Leftin, H. P., *J. Phys. Chem.*, **64**, 1714 (1960).

Résumé

On présente la preuve de l'hétérogénéité de réaction d'oléfines sur des surfaces argileuses acides et de l'acidité inhérente du catalyseur. On montre que l'activité catalytique est due à un proton actif probablement associé avec l'aluminium tétraédrique. On observe la désactivation du catalyseur par des contaminants accepteurs de proton tels que l'eau, les amines et les oléfines basiques. On a déterminé les acidités des surfaces et l'hydrazine échangeable total dans le catalyseur par absorption en phase gazeuse et par analyse de deutérium respectivement. Les mesures sont en accord avec les mesures d'acidité préalables, les vitesses de polymérisation du styrène, et le mécanisme de polymérisation. On a mesuré les vitesses de polymérisation par observation temps-température et par analyse de monomères. On a déterminé l'hydrogène échangeable par échange de deutérium et des mesures de sensité. L'échange est complet à 90% avant le début de la polymérisation.

Zusammenfassung

Die Heterogenität von Olefinreaktionen an sauren Tonerdeoberflächen und die saure Natur des Katalysators wird nachgewiesen. Die Aktivität des Katalysators geht auf ein wahrscheinlich mit tetraedrischem Aluminium verknüpftes aktives Proton zurück. Verunreingungen mit Protonenacceptorcharakter wie Wasser, Amine und basische Olefine desaktivieren den Katalysator. Overflächenacidität und gesamter austauschbarer Wasserstoff im Katalysator wurden durch Gasphasenabsorption bzw. Deuterium analyse bestimmt. Die Messungen wurden zu früheren Aciditätsmessungen, und zu Geschwindigkeit und Mechanismus der Styrolpolymerisation in Beziehung gebracht. Die Polymerisationsgeschwindigkeit wurde durch Zeit–Temperatur-Messungen und durch Bestimmung des noch vorhandenen Monomeren ermittelt. Austauschbarer Wasserstoff wurde durch Deuterium-austausch und Dichtemessungen bestimmt. 90% des Austausches trat vor Beginn der Polymerisation ein.

Received March 15, 1963

JOURNAL OF POLYMER SCIENCE: PART A VOL. 2, PP. 1863–1872 (1964)

Emulsion Copolymerization of Some Halogenated Olefins. I. Vinyl Chloride in Ternary Copolymerizations

DEAN E. LEY* and W. FRANK FOWLER, JR., *Research Laboratories, Eastman Kodak Company, Rochester, New York*

Synopsis

In the emulsion polymerization of vinyl chloride with various monomers, the rate and completeness of polymerization of this monomer depended upon the copolymerizing monomer. Vinyl chloride homopolymerized rapidly at first but did not go to completion; addition of a small percentage of acrylic acid reduced the initial rate of polymerization of vinyl chloride but complete conversion occurred. Copolymerization of vinyl chloride with alkyl acrylates having various side-chain lengths proceeded at different rates, depending inversely on the alkyl acrylate side-chain length. Effects on rate and completeness of polymerization of vinyl chloride with various alkyl acrylates and methacrylates (alkyl chain = 1–8 carbon atoms) and of the addition thereto of small percentages of acrylic acid are also described. In the ternary systems, an ideal acrylate ester side-chain length of 4 carbon atoms was apparent in the presence of which most rapid and possibly most homogeneous copolymerization occurred. The phenomenon is discussed with respect to currently accepted emulsion polymerization theory.

INTRODUCTION

It is widely accepted that the copolymerization of vinyl chloride with the lower alkyl esters of acrylic and methacrylic acids leads ordinarily to polymers which are heterogeneous.[1] Indeed, the tendency of a lower acrylate or methacrylate ester to polymerize with itself in the presence of vinyl chloride is so pronounced, that reasonably homogeneous copolymers can only be obtained by special procedures. For example, even in the preparation of copolymers of ethyl acrylate and vinyl chloride in which the ratio of acrylate to halide is to be low in the final product, recourse to stepwise addition of the acrylate to the polymerization mixture over the course of the polymerization is taken. In this manner, more homogeneous polymers are obtained.

The most intensive study of vinyl chloride copolymerization with the alkyl acrylates and methacrylates has been in copolymers with methyl acrylate, ethyl acrylate, and methyl methacrylate, respectively—work which has been reviewed by Riddle.[1] We have found that the rate of disappearance of vinyl chloride (as shown by pressure measurements) in

* Present address: B. F. Goodrich Co., Brecksville, Ohio.

emulsion copolymerizations with various acrylates and methacrylates depends not only on the monomer ratio of the initial charge, but also upon the length of the alkyl ester side chain. This paper, furthermore, describes the effect on copolymerization characteristics of such binary systems of the addition thereto of small percentages of a hydrophilic, highly reactive third monomer, acrylic acid. As will be seen, the relatively simple technique employed in this work may readily be employed to yield data of both practical and theoretical interest when one of the monomers in the system is a very volatile one.

EXPERIMENTAL

Since vinyl chloride possesses such a high vapor pressure (b.p. = −13.9°C.) and it homopolymerizes and copolymerizes only under rather carefully regulated conditions, a special technique was required. Actual polymerizations were conducted in Duraglas bottles by tumbling them at 15 rpm in an air-filled chamber which was maintained at 36.5°C. A redox catalyst system (ammonium persulfate–sodium bisulfite) was employed. All polymerizations were conducted in an inert atmosphere (nitrogen). The hydrogen ion concentration initially prevailing had to be high for polymerizations to proceed at reasonable rates. The surfactant solution selected was Triton 770 concentrated initially containing 30% sodium alkyl aryl polyethoxy sulfate, 23% isopropanol, and the balance water. It was found necessary to remove a portion of the isopropanol from the solution by evaporation in a rotating flask at room temperature using a water aspirator until the surfactant concentration was raised to 40%; otherwise latex coagulation occurred.

A. Homopolymerization of Vinyl Chloride

The following reagents were added to a Duraglas pressure vessel (380 ml. total volume): 80 ml. of distilled water (pH = 2.7, with acetic acid); 1 ml. of evacuated Triton 770.

Reaction vessel and contents were cooled to −20°C.; the following rea-

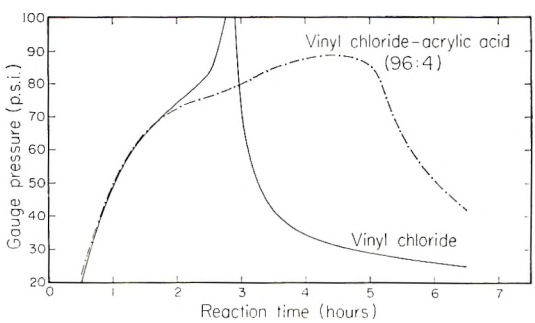

Fig. 1. Pressure–time curves for vinyl chloride homopolymerization and for vinyl chloride polymerized in presence of 4 wt.-% acrylic acid.

gents were then added: 20.0 g. of vinyl chloride (Matheson Co.); 0.082 g. of ammonium persulfate (Baker and Adamson); 0.027 g. of sodium bisulfite (Eastman P760). The free space in the reaction vessel was swept with nitrogen and then the vessel was sealed with a cap containing a puncturable, self-sealing gasket and placed on a tumbler rotating at 15 rpm in an air bath maintained at 36.5°C. In 2.75 hr., the gauge pressure (transmitted from the reaction vessel to the gauge through a hypodermic needle[2]) rose to a value in excess of 100 psi. In 2 hr. more, it had dropped to 30.0 psi, and in a total reaction time of 24 hr., the pressure had declined to 16.5 psi, as shown in Figure 1. The polyvinyl chloride had precipitated during the reaction period and the reaction did not go to completion.

B. Copolymerization of Vinyl Chloride with Various Acrylates

The following chemicals were added to a glass pressure reaction vessel (380 ml. total volume): 160.0 ml. of distilled water (pH = 2.7); 2.0 ml. of evacuated Triton 770; 20.0 g. of *n*-butyl acrylate (Rohm and Haas). The reaction vessel and contents were cooled to −20°C. and the following

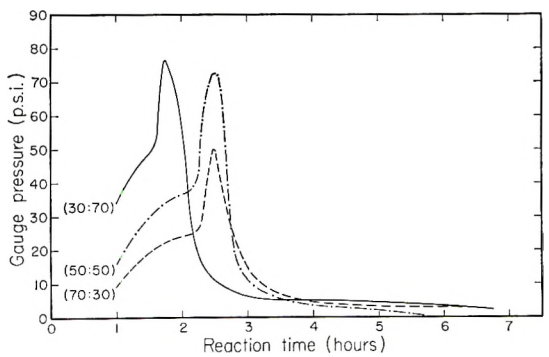

Fig. 2. Pressure–time curves for *n*-butyl acrylate–vinyl chloride copolymerizations. Ratios shown are ester:halide by weight.

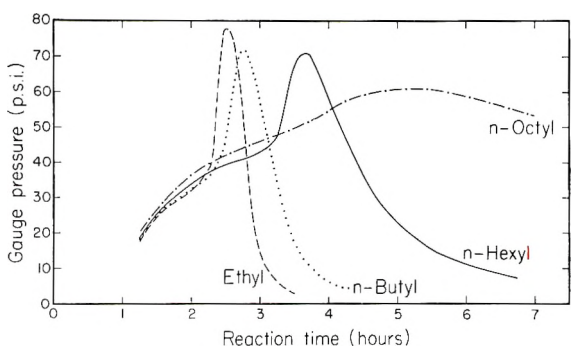

Fig. 3. Pressure–time curves for *n*-alkyl acrylate–vinyl chloride copolymerizations using acrylate esters of varying side-chain lengths. All are 1:1 by weight.

reagents added: 20.0 g. of vinyl chloride; 0.164 g. of ammonium persulfate; 0.053 g. of sodium bisulfite.

The reaction was then run as in the homopolymerization of vinyl chloride described above. Copolymerization of this 50:50 weight mixture was complete in 5.50 hr., as many be seen in Figure 2 and from the fact that the yield of subsequently coagulated, washed, and dried polymer was practically quantitative. Monomer ratios of 70:30 and 30:70 by weight of these two monomers were also copolymerized with pressure records, as shown in Figure 2; yields of isolated polymers were quantitative in these cases also. With a monomer ratio of 50 wt.-% acrylate ester and 50 wt.-% vinyl chloride, ethyl acrylate, *n*-hexyl acrylate, and *n*-octyl acrylate were substituted for the *n*-butyl ester. Pressure data for these runs are shown in Figure 3. In all these cases, hydrosols of reasonable stability were obtained, although the yield of *n*-octyl acrylate–vinyl chloride polymer was not quantitative.

C. Copolymerization of Vinyl Chloride with Acrylic Acid

The following reagents were added to the usual reaction vessel: 80 ml. of distilled water (pH = 2.7 with acetic acid); 1.0 ml. of evacuated Triton 770; 0.8 g. of acrylic acid (Rohm and Haas). The reaction vessel and contents were cooled as just described and the following were added: 19.2 g. of vinyl chloride; 0.082 g. of ammonium persulfate; 0.027 g. of sodium bisulfite. Polymerization was conducted as just stated, the pressure record being shown in Figure 1. Yield of isolated polymer in this instance was quantitative.

D. Ternary Compositions

By using the general method outlined, a wide variety of esters was copolymerized with vinyl chloride and acrylic acid. Each ester, except the *n*-octyl acrylate, was copolymerized with halide and acid in three different weight ratios; as shown in Table I.

TABLE I

Ester, wt.-%	Vinyl chloride, wt.-%	Acrylic acid, wt.-%
67.2	28.8	4.0
48.0	48.0	4.0
28.8	67.2	4.0

A record of pressure change was kept of each reaction mixture, including the "residual" gauge pressure at the end of 24 hr. of reaction time. The esters included the following: methyl acrylate, ethyl acrylate, *n*-propyl acrylate, *n*-butyl acrylate, *n*-amyl acrylate, *n*-hexyl acrylate, 2-ethylhexyl acrylate, *n*-octyl acrylate, 2-methoxyethyl acrylate, 2-butoxyethyl acrylate, ethyl methacrylate, *n*-butyl methacrylate, and *n*-hexyl methacrylate.

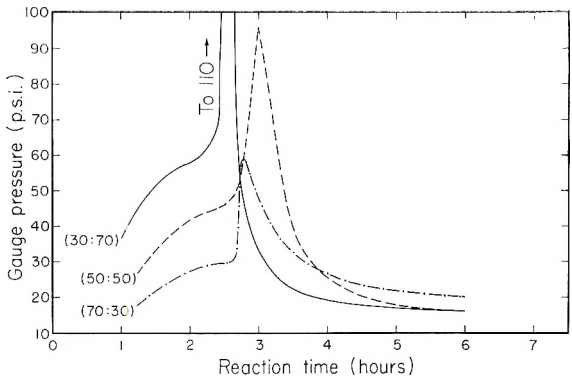

Fig. 4. Pressure–time curves for ethyl acrylate–vinyl chloride–acrylic acid copolymerizations. Ratios shown are ester:halide by weight, polymerized in presence of 4 wt.-% acrylic acid.

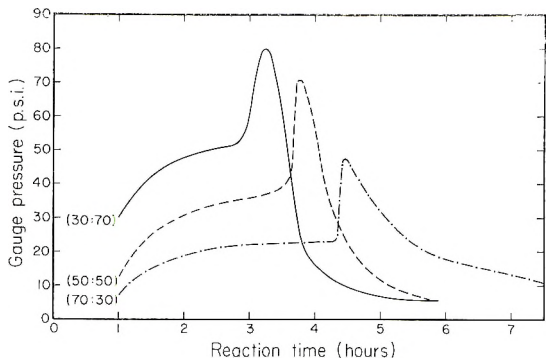

Fig. 5. Pressure–time curves for *n*-butyl acrylate–vinyl chloride–acrylic acid copolymerizations. Ratios shown are ester:halide by weight, polymerized in presence of 4 wt.-% acrylic acid.

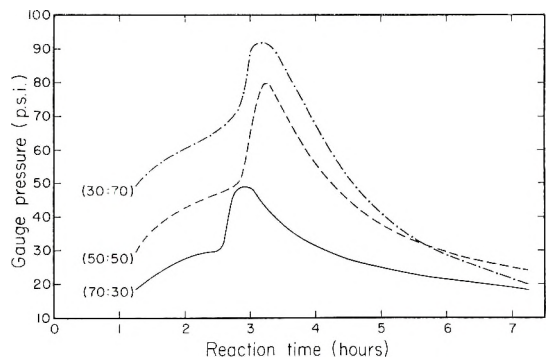

Fig. 6. Pressure–time curves for *n*-hexyl acrylate–vinyl chloride–acrylic acid copolymerizations. Ratios shown are ester:halide by weight, polymerized in presence of 4 wt.-% acrylic acid.

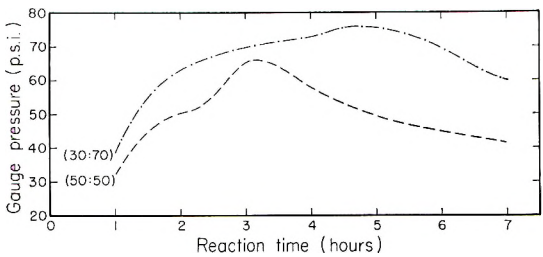

Fig. 7. Pressure–time curves for *n*-octyl acrylate–vinyl chloride–acrylic acid copolymerizations. Ratios shown are ester:halide by weight, polymerized in presence of 4 wt.-% acrylic acid.

The data for the ethyl acrylate, *n*-butyl acrylate, *n*-hexyl acrylate, and *n*-octyl acrylate copolymerizations, respectively, may be found in Figures 4–7. Residual pressures in the bottles at the end of 24 hr. may be found in Table II. Only the *n*-butyl acrylate–vinyl chloride–acrylic acid copolymerizations yielded polymeric products in nearly quantitative amounts.

TABLE II
Unpolymerized Vinyl Chloride Pressure after 24 Hr. in Ternary Copolymerizations

	Residual pressure (gauge) after 24 hr. at various ester/halide/acid monomer ratios, psi		
Acrylate ester	67.2/28.8/4	48/48/4	28.8/67.2/4
Ethyl	7.0	5.0	8.0
n-Butyl	0.0	0.0	0.0
n-Hexyl	11.5	7.0	3.5
n-Octyl	—	37.5	24.0

The pressure–time curves for the ethyl methacrylate, *n*-butyl methacrylate, and *n*-hexyl methacrylate ternary copolymerizations, respectively, show exactly the same trends as are apparent in acrylate ester series of Figures 4–7. Further, residual gauge pressures at the end of 24 hr. show exactly the same trend as that shown by the acrylate ester series in Table II.

RESULTS

The data for the gauge pressure versus reaction time curve for the homopolymerization and copolymerization of vinyl chloride, presented here, provide a relatively simple means of studying the effects of various monomers upon the rates of copolymerization of vinyl chloride with them. Under the conditions selected for this study it may be seen that vinyl chloride polymerized alone in aqueous emulsion does so with an initial surge, followed by a slower rate toward completion (Fig. 1).

The effects produced by the addition of alkyl esters of acrylic acid to the vinyl chloride on polymerization ratio may be seen in Figures 2 and 3.

While the presence of ethyl and *n*-butyl acrylates, respectively, resulted in a rapid decrease in pressure of the vinyl chloride, as has been observed by others,[3,4] a longer induction period was observed with the *n*-hexyl acrylate–vinyl chloride system. With the *n*-octyl acrylate–vinyl chloride system, a still longer induction period was noted and the subsequent decrease in pressure was very slow.

Acrylic acid in small percentage considerably tempers the initial surge observed with vinyl chloride homopolymerizations and increases the rate of disappearance of vinyl chloride in the later stages of reaction, as shown in Figure 1.

The pressure data obtained for the several acrylate ester–vinyl chloride–acrylic acid copolymerizations (see Figs. 4–7) indicate a number of significant facts. (*1*) With ethyl acrylate, there was an extremely rapid polymerization reaction at the start which quickly subsided to leave a residuum of pressure which, even in 24 hr. (see Table II), was still appreciable. (*2*) With *n*-butyl acrylate, the initial exothermic surge was not as great and residual pressure after this surge disappeared more promptly, so that, in 24 hr., gauge pressures were all zero. (*3*) With *n*-hexyl acrylate, the initial rises in pressures and the subsequent declines were both more gradual than with the *n*-butyl ester-containing monomer mixtures, so that, after 24 hr., gauge pressures were still appreciable. (*4*) With *n*-octyl acrylate, both the initial rises and the subsequent declines in pressure were still more gradual than in the presence of *n*-hexyl acrylate, so that, after 24 hr., gauge pressures in the presence of the *n*-octyl acrylate were higher than those in the presence of the *n*-hexyl ester.

DISCUSSION

In interpreting the data presented above, it should be borne in mind that the selection of a simple pressure measurement made upon a reaction mixture rotating in an air bath precludes possibility of obtaining exact kinetic data. As reaction temperatures vary over the course of polymerizations done in this simple system, monomer concentrations, solubilities and reactivities likewise vary. However, general shapes of pressure curves, presence or absence of final pressures, and relative magnitude of residual pressures (when found) offer a simple semiquantitative way of classifying relative reactivities of monomer combinations herein discussed. Qualitative substantiation of conclusions drawn must take cognizance also of whether or not yield of polymer was quantitative.

Under the particular set of reaction conditions selected for these series of experiments, the emulsion homopolymerization of vinyl chloride was found to be, though initially rapid, incomplete in 24 hr. (Fig. 1).

The addition of various proportions of *n*-butyl acrylate to the vinyl chloride markedly enhanced the rate of vinyl chloride polymerization, as shown in Figure 2. This is also true of other lower alkyl acrylate esters, as illustrated by the pressure curve for a typical ethyl acrylate–vinyl

chloride polymerization, as may be seen in Figure 3. Since with longer, side-chain alkyl acrylates, such as the *n*-hexyl and *n*-octyl acrylates, respectively, longer induction periods were noted, plus a very slow subsequent decrease in pressure in the presence of the *n*-octyl acrylate, there appears to be an ideal acrylate ester side-chain length for complete polymerization of the vinyl chloride. These results indicate further that the alkyl acrylate esters of short, side-chain length initiate free radicals, involving monomer, partly polymerized monomer, or both, more readily than vinyl chloride can generate either. Once a growing chain has been initiated in such a system via a free radical, vinyl chloride monomer appears to add to it with speed.

The addition of a small percentage of acrylic acid to the vinyl halide-containing system somewhat decreased the initial rate of polymerization of the latter, while finally resulting in a larger overall conversion (see the Experimental section and Fig. 1). These observations led to the examination of ternary monomer systems containing acrylate ester, vinyl chloride, together with a relatively small percentage of acrylic acid. It was hoped that the inclusion of the acrylic acid would so alter the rates of copolymerization that an even sharper delineation could be made with respect to the effect of the acrylate ester. Thus, an "ideal" alkyl ester side-chain length might be more easily discerned. Such proved to be the case.

In the polymerization of the various ternary monomer combinations, involving vinyl chloride, an alkyl acrylate, and a small percentage of acrylic acid, a systematic change in the shape of the pressure–time curves may be observed (Figs. 4–7), depending once again upon the length of the acrylate ester side chain. These data show that for these monomer combinations an ideal acrylate ester side-chain length exists to ensure complete polymerization of the vinyl chloride and that this is 4 carbon atoms. This is true over a rather wide range of acrylate ester:vinyl halide monomer ratios.

When the number of carbon atoms in the alkyl group of the acrylate was less than 4, a small amount of vinyl chloride remained unpolymerized even after 24 hr. (Table II). This was true even though the initial increase in pressure, owing to the heat of polymerization (or copolymerization) of the acrylate, was large and the decline in pressure from the peak attained was, at first, quite rapid. It is suggested that this observation is due to the extremely rapid rate of homopolymerization of the ester (when M_1 = vinyl chloride and M_2 = methyl acrylate, then at 50°C., $r_1 = 0.083$ and $r_2 = 9.0$[5]), combined with its high rate of diffusion from monomer droplet to soap micelle because of greater solubility in water than the vinyl chloride. The net result of these two effects, both operating to favor rapid polymerization of the acrylate ester when the alkyl group attached to the latter is small, is to produce the curves obtained in Figure 4.

When the number of carbon atoms in the alkyl group of the acrylate ester was 4, the rate of diffusion of acrylate ester from droplet to micelle and the inherent reactivity of this particular monomer are such as to result

in virtually complete polymerization of the vinyl chloride and the ester in about 8 hr. (Fig. 5). It should be noted that the order of monomer reactivities rises in the same order whether these be calculated on a molar or weight basis.

When the number of carbon atoms in the alkyl group of the acrylate was greater than 4, rate of diffusion of ester and reactivity of the ester are both sufficiently low so as to preclude rapid disappearance of vinyl chloride. Such is, indeed, observed to be the case for both *n*-hexyl acrylate copolymerization (Fig. 6) and *n*-octyl acrylate (Fig. 7), respectively.

The same relationships just observed apply, in similar fashion, to a parallel study made upon the attempted copolymerization of various lower alkyl methacrylate esters with vinyl chloride in the presence of a small percentage of acrylic acid.

Two effects, solubility in water and inherent reactivity of the various esters in copolymerization, operating together, could account for the observed results. In Table III are presented data showing the solubilities in water of the monomers involved.

TABLE III
Monomer Solubility in Water

Monomer	Solubility, g./l.
Vinyl chloride	0.9 (20°C.)[a]
Ethyl acrylate	15.1 (25°C.)
n-Butyl acrylate	1.34 (20–25°C.)
n-Hexyl acrylate	0.18 (20–25°C.)
n-Octyl acrylate	0.063(20–25°C.)

[a] Data of Schildknecht.[6]

Tkachenko and associates[7] have studied the mass copolymerization of vinyl chloride with methyl, butyl, and octyl acrylates in glass ampules under nitrogen at 45°C. using α,α'-azobisisobutyronitrile as initiator to ascertain effects of higher acrylate esters on the elastic properties of the copolymers. Rates of copolymerization and molecular weights are raised by higher proportions of acrylates. The rate constants of copolymerization, $\alpha = K_{AA}/K_{BB}$ and $\beta = K_{BB}/K_{BA}$, where A is the molar proportion of vinyl chloride and B that of the acrylates, were: for methyl acrylate, $\alpha = 0.06$ and $\beta = 4.0$; for butyl acrylate, $\alpha = 0.07$ and $\beta = 4.4$; and for octyl acrylate, $\alpha = 0.12$ and $\beta = 4.8$. From these data it appears that if the presence of water (as in the emulsion polymerizations) were not influencing copolymerization rates profoundly, the pressure–time curves of the figures shown herein would not vary as widely as observed.

Thus, *n*-butyl acrylate shows approximately the same tendency toward alteration in copolymerizing with vinyl chloride as does methyl acrylate. It is, therefore, concluded that solubility of acrylate ester in water is the predominant factor causing the observed results with a qualifying limita-

tion imposed by the fact that the reactivity ratios cited are for mass and not emulsion polymerizations of these monomers.

The authors wish to thank Dr. C. W. Zuehlke and Mrs. E. M. Gordon, of these Laboratories, for determining the solubilities of the various alkyl acrylates listed in Table III.

References

1. Riddle, E. H., *Monomeric Acrylic Esters*, Reinhold, New York, 1954, pp. 106–119.
2. Harrison, S. A., and E. R. Meincke, *Anal. Chem.*, **20**, 47 (1948).
3. Rohm and Haas Co., unpublished data.
4. Sans, M., *Inds. Plastiques*, **3**, 281 (1947).
5. Chapin, E. C., G. E. Ham, and G. R. Fordyce, *J. Am. Chem. Soc.*, **70**, 538 (1948).
6. Schildknecht, C. E., *Vinyl and Related Polymers*, Wiley, New York, 1952, p. 395.
7. Tkachenko, G. V., *Zh. Fiz. Khim.*, **31**, 2676 (1957).

Résumé

Dans la polymérisation du chlorure de vinyle avec différents monomères, la vitesse et le rendement final de la polymérisation de ce monomère dépendent du monomère copolymérisant. Le chlorure de vinyle homopolymérise d'abord rapidement mais il ne va pas jusqu'au bout, l'addition d un petit pourcentage d'acide acrylique réduit la vitesse initiale de polymérisation du chlorure de vinyle, par contre il y a conversion complète. La copolymérisation du chlorure de vinyle avec des acrylates d'alcoyle, ayant des longueurs de chaînes latérales différentes, procède à des vitesses différentes dépendant de la longueur de chaîne latérale de l'acrylate d'alcoyle. Les effets sur la vitesse et le rendement final de la polymérisation du chlorure de vinyle avec des acrylates et méthacrylates d'alcoyle différents (chaîne alcoyle de 1 à 8 atomes de carbone) et de l'addition à cela de faibles pourcentages d'acide acrylique sont aussi décrits. Dans les systèmes ternaires, il semble qu'un ester acrylique de longueur de chaîne de quatre atomes de carbone est idéal, et assure une copolymérisation à la fois plus rapide et plus homogène. Le phénomène est discuté en regard de la théorie.

Zusammenfassung

Bei der Emulsionspolymerisation von Vinylchlorid unter Zusatz verschiedener Monomerer hängen Geschwindigkeit und Vollständigkeit der Polymerisation von Vinylchlorid von copolymerisierenden Monomeren ab. Vinylchlorid homopolymerisiert anfangs rasch, doch wird keine vollständige Umsetzung erreicht. Durch Zusatz von wenigen Prozenten Acrylsäure wird zwar die Anfangsgeschwindigkeit der Vinylchloridpolymerisation erniedrigt, es tritt aber vollständiger Umsatz ein. Die Copolymerisation von Vinyl chlorid mit Alkylacrylaten verschiedener Seitenkettenlänge verlief mit unterschiedlicher Geschwindigkeit; diese ist der Länge der Alkylacrylat-Seitenkette ungekehrt proportional. Ausserdem werden die Einflüsse von verschiedenen Alkylacrylaten und -methacrylaten (Alkylketten mit 1 bis 8 C-Atomen) und von Zusätzen kleiner Mengen Acrylsäure zu diesen Gemischen auf Geschwindigkeit und Vollständigkeit der Polymerisation von Vinylchlorid beschrieben. Bei den ternären Systemen erwies sich eine Acrylester-Seitenkettenlänge von 4 C-Atomen als ideal, da bei ihrem Vorliegen die schnellste und möglicherweise die am meisten homogene Copolymerisation auftrat. Die Erscheinung wird auf der Grundlage der konventionellen Theorie der Emulsionspolymerisation diskutiert.

Received November 14, 1962
Revised March 12, 1963

JOURNAL OF POLYMER SCIENCE: PART A VOL. 2, PP. 1873–1878 (1964)

Solubility of Nonpolar Gases in Polymers: Some New Considerations

T. K. KWEI and W. M. ARNHEIM, *Central Research Laboratories, Interchemical Corporation, Clifton, New Jersey*

Synopsis

A model is proposed for the solution of gases in polymers. Gas molecules are assumed to reside in the "free" volume without net disruption of polymer–polymer contacts. A number of conclusions result from this model, which are in excellent agreement with experimental results.

I. INTRODUCTION

In a recent study of the solubility of gases in polyethylene[1] it was shown that the heat of solution $\Delta\bar{H}_1$ could be expressed as:

$$\Delta\bar{H}_1 = H_p - H^v \tag{1}$$

In eq. (1) $-H^v$ is the molal heat of condensation of the gas at its normal boiling point, T_b, and H_p is a constant for a given polymer. The heat of solution, $\Delta\bar{H}_1$, is calculated from the solubility by eq. (2):

$$S = S_0 \exp\{-\Delta\bar{H}_1/RT\} \tag{2}$$

where $S/22400$ is the solubility, usually expressed in moles of gas per milliliter of polymer at 25°C. and 1 atm. pressure. Nonpolar gases (He, N_2, CO, O_2, A, CH_4, CO_2, C_2H_6, SF_6, C_3H_6, C_3H_8, and C_3H_4) were used in the above investigation.[1] The heats of solution of a limited number of gases in rubbers also appear to obey eq. (1) approximately.[2]

If we now consider a gas at pressure P and temperature T in equilibrium with a solution in which its concentration is S, thermodynamically we obtain[3]

$$\Delta\bar{H}_1 = -H^v + \Delta\bar{H}_1^{\,m} - \int_{t_b}^{t} (\bar{C}_p - C_p^{\,g})dT \tag{3}$$

where $\Delta\bar{H}_1^{\,m}$ is the partial molar heat of mixing at the boiling point, $\bar{C}_p$ is the partial molar heat capacity of the gas in solution at 25°C. and $C_p^{\,g}$ is the corresponding heat capacity of the gas. The last term in eq. (3) is often small with respect to the others and may be neglected. Comparison of eq. (1) with eq. (3) then identifies H_p with $\bar{H}_1^{\,m}$. The heat of mixing, which originates from the replacement of contacts between like species with

contacts between unlike species, may be represented by the following stoichiometric equation according to the quasichemical method:

$$^1/_2[1,1] + {}^1/_2[2,2] = [1,2] \tag{4}$$

these symbols ([1,1], [2,2], [1,2]) representing contacts broken and contacts formed.[4] For spherical, nonpolar molecules, the pair contact energy between unlike species, W_{12}, may be approximated by:

$$W_{12}^2 = W_{11} \times W_{22} \tag{5}$$

or

$$W_{12} = {}^1/_2(W_{11} + W_{22}) \tag{5a}$$

If the gas–polymer interaction obeys eq. (5), $\Delta\bar{H}_1^m$ has a characteristic value for a given gas–polymer pair and is not a constant. If W_{12} is best expressed by the arithmetic mean of W_{11} and W_{22}, $\Delta\bar{H}_1^m$ is zero. The experimental H_p value of about 2 kcal./mole for high density polyethylene is, therefore, not easily understood.

II. A SIMPLE MODEL

Heat of Solution

We would like to propose the following model for the solution of nonpolar gases in polymers. In the theory of liquids, the concept of "free volume" has proved to be of great utility, especially in the understanding of transport phenomena.[5] For example, molecular transport may be considered to occur by the movement of molecules into "voids," not as a result of an activation in the ordinary sense, but rather as a result of the redistribution of free volume within the liquid.[5] If it is now assumed that the dissolved gas molecules reside in the "free" volume of the polymer so that the solution process is not accompanied by a net breakage of polymer–polymer contacts, the energy change for the formation of gas–polymer pair contact is simply:

$$\Delta W = W_{12} - {}^1/_2W_{11} \tag{6}$$

By introducing the arithmetic mean approximation for W_{12}, eq. (6) becomes:

$$\Delta W = {}^1/_2(W_{11} + W_{22}) - {}^1/_2W_{11} = {}^1/_2W_{22} \tag{7}$$

We now arrive at a formula where the heat of mixing of the dissolved gas molecule with the polymer is dependent on the nature of the polymer alone, in agreement with the experimental observation.

The concept described above is not entirely new and has been proposed by Lundberg and co-workers from a consideration of the positive temperature coefficients of gas solubilities[5] in polyethylene. The free volume of a polymer, although ill-defined, has been estimated by various authors to be in the range of 2.5 to about 15% of the actual volume of the amorphous

polymer at the glass transition temperature (T_g) of the polymer.[6] At temperatures above T_g, the fraction of free volume in the polymer, (V_{fp}), is presumably much larger. The solubility S of many common nonpolar gases in polymers is usually in the range of 5×10^{-7}–3×10^{-4} mole/ml. polymer. The available free space in the polymer is probably 10^1 to 10^3 times greater than the volume of the dissolved gas molecules. The above model is therefore physically possible.

Entropy of Mixing

The entropy of random mixing of n_1 gas molecules with a polymer containing n_2 molecules per milliliter can be calculated most conveniently by the free volume method.[7]

$$S^R = n_1 k \ln \left[\frac{V_{fp} - n_1 V_g}{n_1 V_{fg}} \right] + nk \ln \left[\frac{V_{fp} - n_1 V_g}{V_{fp}} \right] \tag{8}$$

where V_g is the geometrically excluded volume associated with each dissolved gas molecule and V_{fg} is the free volume per gas molecule in the gaseous state (1 atm., 25°C.) and is approximately equal to $22400T/N_{av}273$. In the limiting case where $n_1 V_g << V_{fp}$, S^R may be approximated as:

$$S^R = n_1 k \ln (V_{fp}/n_1 V_{fg}) \tag{9}$$

$$\bar{S}_1^R = \partial S^R / \partial n_1 = k \ln (V_{fp}/n_1 V_{fg}) - k = k \ln V_{fp} - k \ln S - k \ln (T/273) - k \tag{9a}$$

If the entropy of mixing is represented by $\bar{S}_1^R$, we obtain, at solution equilibrium:

$$\Delta \bar{H}_1 = T \bar{S}_1^R$$

and

$$-RT \ln S = -\Delta \bar{H}_1 + RT \ln V_{fp} - RT \ln (T/273) - RT$$
$$= -H_p + H^v + RT \ln V_{fp} - RT \ln (T/273) - RT \tag{10}$$

III. DISCUSSION

Several interesting consequences may be drawn from eq. (10).

(*1*) The dependence of ln S on the property of the gas is solely due to the $-H^v$ term. No other parameter relating to the property of the gas appears in eq. (10). The well known correlation between ln S and T_b, or Lennard-Jones constant, strongly supports our conclusion.[1,8] (In a previous study based on Flory-Huggins' lattice model,[1] the equation contains the partial molar volume of the gas and the gas–polymer interaction parameter.)

(*2*) The dependence of ln S on the properties of the polymer is due to V_{fp} and H_p, the latter term being related to the internal pressure of the polymer.

(3) Equation (10) can be rewritten as:

$$S = (273/eI)\ [V_{fp} \exp\{-H_p/RT\}]\ [\exp\{H^v/RT\}] = LW \qquad (11)$$

where W ($= \exp\{H^v/RT\}$) is a characteristic parameter of the gas and L is a characteristic parameter of the polymer. The ratio of the solubilities of two gases i and j in polymer m is simply,

$$S_{im}/S_{jm} = W_i/W_j \qquad (12)$$

and is dependent only in the nature of the two gases. Similarly the ratio of the solubilities of gas i in two polymers m and n is,

$$S_{im}/S_{in} = L_m/L_n$$

and is dependent only on the nature of the two polymers.

In a previous paper,[9] it has been shown that the ratio of the diffusion coefficients D of any gas pair in the series A, Ne, N_2, O_2, CO, CO_2, and possibly several other gases through a given polymer seems to lie within a very limited range. The quantity D_{im}/D_{jm} is approximately constant, regardless of m, with an uncertainty factor probably less than 50%. The ratio D_{im}/D_{in} for any of these gases through two polymers m and n is primary a function of m and n, regardless of i, with an uncertainty factory probably less than 100%. We can now derive two interesting relationships for the permeability constant P, which is the product of D and S:

$$\frac{P_{im}}{P_{jm}} = \frac{D_{im}}{D_{jm}} \frac{S_{im}}{S_{jm}} = F(i, j) \qquad (14)$$

and

$$\frac{P_{im}}{P_{in}} = \frac{D_{im}}{D_{in}} \frac{S_{im}}{S_{in}} = F(\mathrm{m}, \mathrm{n}) \qquad (15)$$

Experimental permeability data in support of these deductions have been reported in the literature.[8,10]

(4) According to eq. (10), a proportionality constant of unity between $-RT \ln S$ and $\Delta\bar{H}_1$ would be expected. A plot of solubility data for eleven gases in high density polyethylene[1] gives eq. (16) with a correlation coefficient of 0.986,

$$-RT \ln S = 0.76\ \Delta\bar{H}_1 + 2.35 \qquad (16)$$

and

$$RT \ln S_0 = 0.24\ \Delta\bar{H}_1 + 2.35 \qquad (16a)$$

The solubility data for ten other rubbers[2] indicate proportionality constants between $-RT \ln S$ and $\Delta\bar{H}_1$ in the range of 0.58 and 0.78, the majority being around 0.70. The correlation coefficients of these plots range from 0.933 to 0.977, the majority being greater than 0.96. It appears possible that the experimentally determined proportionality between $-RT \ln$

S and $\Delta\bar{H}_1$ is significantly less than unity. It may be recalled that it is customary to equate the entropy of random mixing S^R to the total entropy of mixing which is actually the sum of S^R and the excess function S^E.[3] The excess function S^E is usually neglected in the formulation of the theory of polymer solution. The experimentally observed proportionality constant $-RT \ln S$ and $\Delta\bar{H}_1$, however, may be construed as evidence suggesting the importance of the S^E contribution to the solubility data. If the S^E contribution is added to eq. (10) a comparison of the amended equation with eq. (16) tends to suggest a linear dependence of $\bar{S}_1^E$ on $\bar{H}_1$, which is itself an excess function in Prigogine's terminology.[3] The theoretical implication of these tentative deductions is admittedly not completely clear at present, but an example of the interrelation between the excess functions can be found in the theory of conformal solutions.[4]

(5) In a previous paper[9,12] on the diffusion of gases through polymers, a general correlation between $\log D_0$ and ΔE_D was discussed:

$$\Delta E_D/T = 6.75 \log D_0 + 23.80 \tag{17}$$

where D_0 and ΔE_D are defined by eq. (18),

$$D = D_0 \exp \{-\Delta E_D/RT\} \tag{18}$$

Combination of eqs. (16a) and (17) results in a linear dependence of $\log D_0 S_0$ on $-(\Delta E_D + \Delta\bar{H}_1)$, the former term being identical to $\log P_0$ and the latter, to $-\Delta E_p$. The quantities $\log P_0$ and $-\Delta E_p$ are defined by:

$$P = P_0 \exp \Delta - \{E_p/RT\} \tag{19}$$

The linear dependence of $\log P_0$ on $-\Delta E_p$ was first discovered experimentally by Doty.[13]

Finally it may be remarked that our model is a general one and is applicable to the solution of nonpolar, spherical gases in liquids in general. The usefulness of eq. (10) is reflected in the excellent correlation between $\log S$ and Lennard-Jones constant for the solution of gases in liquids like benzene and heptane.[1,11] Our model is not expected to be applicable to the solution of organic vapors in polymers where extensive swelling results.

References

1. Michaels, A. S., and H. J. Bixler, *J. Polymer Sci.*, **50**, 393 (1961).

2. For example, G. J. Van Amerogen, *J. Polymer Sci.*, **2**, 381 (1947); *ibid.*, **5**, 307 (1950); *J. Appl. Phys.*, **17**, 972 (1946).

3. Hildebrand, J. H., and R. L. Scott, *Solubility of Non-electrolytes*, Reinhold, New York, 1950, Chap. 15.

4. Prigogine, I., *The Molecular Theory of Solutions*, Interscience, New York, 1957, Chaps. 1, 3, and 4.

5. For example M. H. Cohen and D. Turnbull, *J. Chem. Phys.*, **31**, 1164 (1959); J. Frenkel, *Kinetic Theory of Liquids*, Clarendon Press, Oxford, 1946; J. L. Lundberg, M. B. Wilk, and M. J. Huyett, *J. Polymer Sci.*, **57**, 275 (1962).

6. Fox, T. G, S. Gratch, and S. Loshaek, in *Rheology*, Vol. I, F. R. Eirich, Ed., Academic Press, New York, 1956, Chap. 12.

7. Hildebrand, J. H., *J. Chem. Phys.*, **15**, 225 (1947).
8. Rogers, C. E., J. A. Meyer, V. Stannett, and M. Szwarc, in *Permeability of Plastic Films and Coated Paper to Gases and Vapors*, Tappi Monograph Series, No. 23, Technical Association of the Pulp and Paper Industry, New York, 1962, Chap. 2.
9. Kwei, T. K., and W. M. Arnheim, *J. Polymer Sci.*, **A2**, 957 (1964).
10. Ito, Y., *Kobunshi Kagaku*, **18**, 1 (1961); *Chem. Abstr.*, **55**, 27947i (1961).
11. Jolley, J. E., and J. H. Hildebrand, *J. Am. Chem. Soc.*, **80**, 1050 (1958).
12. Kwei, T. K., and W. M. Arnheim, *J. Chem. Phys.*, **37**, 1900 (1962).
13. Doty, P., *J. Chem. Phys.*, **14**, 244 (1946).

Résumé

On propose un modèle pour la dissolution des gaz dans des polymères. Les molécules de gaz sont situées dans le volume "libre" sans rupture nette des contacts polymère–polymère. Aux dépens de ce modèle, on peut formuler plusieurs conclusions qui sont en excellent accord avec les résultats expérimentaux.

Zusammenfassung

Es wird ein Modell für den Lösungszustand von Gasen in Polymeren vorgeschlagen. Dabei wird angenommen, dass sich die Gasmoleküle im "freien" Volumen aufhalten, ohne dass eine wesentliche Trennung von Polymer–Polymer-Kontakten auftritt. Eine Anzahl der aus diesem Modell gezogenen Folgerungen steht in ausgezeichneter Übereinstimmung mit experimentellen Befunden.

Received March 18, 1963

JOURNAL OF POLYMER SCIENCE: PART A VOL. 2, PP. 1879–1891 (1964)

Potentiometric Behavior of Polymethacrylic Acid

J. C. LEYTE and M. MANDEL, *Laboratorium voor Fysische Chemie der Rijksuniversiteit te Leiden, Leiden, Netherlands*

Synopsis

The potentiometric behavior of polymethacrylic acid is discussed in terms of a conformational transition. A thermodynamic treatment of this transition is presented. The titration curve of polymethacrylic acid is analyzed in a detailed way and quantitative information regarding the transition is obtained.

1. INTRODUCTION

It appears from published experimental evidence that the properties of polymethacrylic acid (PMA) in aqueous solution are somewhat peculiar.

From their viscosimetric investigations on PMA, Katchalsky and Eisenberg[1] concluded that the undissociated acid must be a highly coiled molecule, impermeable to the flow of the solvent. On ionization of the carboxylic acid groups the molecule unfolds, to assume highly extended conformations at large degrees of dissociation.

Arnold and Overbeek[2] and Katchalsky[3] observed the peculiar shape of the plots of the viscosity and the apparent pK [$\equiv$ pH + log $(1 - \alpha)/\alpha$, where α is the degree of dissociation] versus α. Similarly, this was found by Arnold[4] in his plots of pK versus $\alpha^{1/3}$. He observed, however, that the peculiarity is absent in the plots for polyacrylic acid (PAA) which was confirmed by the present authors.[5] The sigmoid shape of the viscosity curve was also observed by Gregor, Gold, and Frederick.[6]

From the work of Arnold and Overbeek it may be seen that the specific viscosity of 10^{-2} eq./l. PMA in the presence of $10^{-3}M$ KCl increases moderately during the first 10% of dissociation, then increases greatly and levels off at about 30% dissociation. The apparent pK, as derived from potentiometric titrations, exhibits a dependence on α that may be correlated with the observed viscosity changes. In the first region, of slow viscosity increase, the apparent pK is seen to increase greatly. The region of large viscosity increase coincides with a nearly constant pK. In the last region, both viscosity and pK increase moderately.

Katchalsky[3] and Arnold[4] relate these phenomena, qualitatively, to conformational changes of the polymer chain as a result of the repulsion of the identical charges that are fixed to the chain.

These conclusions are confirmed by the results of the investigation of the diffusion properties of PMA by Kedem and Katchalsky.[7] During the

first part of the titration of PMA, the electrostatic repulsion exerted on the chain segments of the molecule are counteracted by contractive forces, resulting on the one hand from the conformational free enthalpy of the chain and on the other hand from the intramolecular attractive forces (e.g., hydrogen bonds and van der Waals interactions). Consequently, the dimensions of the molecule will change slowly and the charge density in the polymeric regions (and as a consequence pK) increases steeply. When a certain expansion of the coil is achieved by the repulsive forces, the short-range interactions between elements situated far apart along the chain cease to influence the coil dimensions. As a result, a remarkable expansion of the polymer chain will occur during the second part of the titration. As in this region, an increase of the charge is immediately followed by an expansion of the polymer coil, no appreciable change in the charge density and in the electrostatic potential will occur.

When large expansions are reached—which for a noncharged polymer would correspond to highly improbable conformations—the influence of the conformational free enthalpy will level off the further increase of the dimensions with increasing charge and the electrostatic potential will start to rise again.

It is interesting to note that for PAA the intramolecular interaction does not seem to play a similar important role in potentiometric and viscosity behavior. This indicates that in the region where PMA changes from a dense coil to an expanded molecule the van der Waals forces due to the methyl groups are important. This region may be interpreted as an interval where a conformational transition between two different molecular forms of PMA occurs.

In the following sections of this paper this transition will be discussed from a theoretical point of view and from a detailed analysis of titration curves some quantitative information related to this transition will be obtained.

2. THEORETICAL

Zimm and Rice[8] have already given a statistical mechanical treatment for a related problem starting from a detailed model which, however, is not applicable in general. Here a more general thermodynamic treatment is used to derive some results also found by these authors.

We will consider only dilute aqueous solutions of PMA, leaving intermolecular interactions out of account. The transition will be described as occurring between two forms, a and b, in which the system (the PMA molecule) or a portion of it may exist. At low α values the a form, PMA^a, dominates and, after passing the transition region, at higher values of α, the b form, PMA^b, will occur predominantly. At all α values thermodynamic equilibrium, as specified below, is supposed to exist between the two forms.

It should be noted that, on a molecular scale, both a and b may dispose of a large number of conformations. The experimental evidence by no

means allows the conclusion that a and b should be distinguished as ordered and random conformations. Intramolecular interaction has to be admitted for both forms, leaving the magnitudes of the contributions of the different types of interactions unspecified. In fact, the system has to be described as being composed of two thermodynamically distinguishable forms of PMA without any exact picture of the physical details underlying the difference between a and b. The only statement that may be safely made, concerning the distinguishing characteristics of a and b, is that a is a more densely coiled form than b. Consequently, short-range forces between elements situated far apart along the chain will be more important in form a than in form b. Still, it might be useful to obtain information about the transition free enthalpy per monomeric unit. As this free enthalpy difference depends on the degree of ionization of the polymer molecule, the only quantity reflecting the difference between a and b in a straightforward way, will be the transition free enthalpy at $\alpha = 0$.

The thermodynamic properties of the polyacid will be formally expressed as a function of the equivalent quantities for the monomeric units. Units bearing dissociated or undissociated acid groups, will be designated by A^- and HA respectively.*

These monomeric units may take part in different simultaneous equilibria (as, for example, hydrogen bonding). These equilibria will be accounted for by assigning different thermodynamic potentials μ_A^i and μ_{HA}^j to the

* We will represent the polyelectrolyte in solution as a collection of monomeric units with a limited individual mobility. These monomeric units may have different properties and will be characterized by their chemical potential μ which may be expressed in two different ways:

$$\mu_k = \mu_k^{\circ} + RT \ln a_k = \mu_k^{\circ} + RT \ln f_k c_k$$

$$\mu_k = \mu_k^{\circ\prime} + RT \ln a_k' = u_k^{\circ\prime} + RT \ln f_k' c_k'$$

In the first equation the standard state is chosen with respect to a solution containing only monomers, c_k expressing the overall concentration of the monomeric units in the total solution. The activity coefficient f_k then takes into account all possible interactions, including intramolecular binding along the polymeric chain, etc. In the second equation, the standard state is chosen with respect to the solution inside the polymeric region so that $\mu_k^{\circ\prime}$ already contains the intramolecular binding. (As the standard state may be chosen arbitrarily another choice may be useful, as will be shown later.) The concentration c_k' expresses only the concentration of the monomeric units inside this polymeric region, which is proportional to the degree of polymerization Z and inversely proportional to the volume V_p occupied by this region.

We thus have

$$c_k' = n_k'/V_p = c_k(V/V_p)(n_k'/n_k)$$

where n_k' is the number of monomeric units of type k inside a polymeric region, n_k the total number of these monomers in the solution. Thus we may also write

$$\mu_k = \mu_k^{\circ\prime} + RT \ln f_k'' + RT \ln c_k$$

$$f_k'' = f_k'(V/V_p)(n_k'/n_k)$$

Note that n_k'/n_k is a constant for a given polymer concentration, whereas V/V_p may change if V_p is dependent upon the physical conditions of the solution.

units bearing dissociated or undissociated acid groups engaged in equilibria of type i or j.

The question, whether the a $\rightleftharpoons$ b equilibrium may be introduced as just one of all the simultaneous equilibria in which the monomeric groups engage, needs some consideration. The a $\rightarrow$ b transition is expected to have a cooperative character, as a transition to conformations consistent with a less dense coil can only affect a given monomeric unit if a number of its neighbors participate.

It will be assumed that the smallest unit capable of the a $\rightarrow$ b transition consists of q monomeric units. Part of these units may bear dissociated carboxylic acid groups and the rest bears undissociated acid groups. The introduction of the equilibrium conditions for the transition of the q units, together with the condition of the dissociation equilibrium, results in the equality of the thermodynamic potentials of the monomeric groups of the same sort (A^- or HA) in the states a and b. Consider the q units of a. Of these r will be in the A^- form. At equilibrium we must have that

$$\mu_{HA}{}^{i} = \mu_{HA}{}^{i'} = \mu_{HA}{}^{a}$$
$$\mu_{A^-}{}^{j} = \mu_{A^-}{}^{j'} = \mu_{A^-}{}^{a}$$
$$\mu_{HA}{}^{a} = \mu_{A^-}{}^{a} + \mu_{H^+}$$

where μ_{H^+} is the thermodynamic potential of the hydrogen ions. Analogous expressions hold for the units of conformation b, of which s will be in the A^- form. Therefore if one represents the transition by the formal equation

$$a \rightleftharpoons b + (s - r)\ H^+$$

then the equilibrium condition will be given by

$$(q - r)\ \mu_{HA}{}^{a} + r\mu_{A^-}{}^{a} = (q - s)\ \mu_{HA}{}^{b} + s\mu_{A^-}{}^{b} + (s - r)\ \mu_{H^+} \quad (1)$$

On the other hand, the condition of dissociation equilibrium necessitates that

$$\mu_{HA}{}^{a} - \mu_{A^-}{}^{a} = \mu_{HA}{}^{b} - \mu_{A^-}{}^{b} = \mu_{H^+} \quad (2)$$

Combining eqs. (1) and (2) yields

$$\mu_{HA}{}^{a} = \mu_{HA}{}^{b} = \mu_{HA}$$
$$\mu_{A^-}{}^{a} = \mu_{A^-}{}^{b} = \mu_{A^-}$$

Thus, at least formally the a $\rightleftharpoons$ b equilibrium may be described in the same way as the other equilibria in which the monomeric units engage.

After equilibrium has been established all $\mu_{A^-}{}^{i}$ are equal and the same holds for all $\mu_{HA}{}^{j}$. Furthermore the dissociation equilibrium demands the equality of $\mu_{HA}{}^{j}$ and $(\mu_{A^-}{}^{i} + \mu_{H^+})$, irrespective if the value of i and j.

Now, at constant pressure and temperature, a change in the free enthalpy per polyacid molecule may be written:

$$dG = \sum_i \mu_{A^-}{}^{i}\, dn_{A^-} + \sum \mu_{HA}{}^{j}\, dn_{HA} \quad (3)$$

After establishment of thermodynamic equilibrium between all i:

$$\mu_{A^-}{}^{i} = \mu_{A^-} \tag{4}$$

Also

$$\sum_{i} dn_{A^-}{}^{i} = dn_{A^-} \tag{5}$$

Together with the analogous relation for the HA groups these expressions may be substituted in eq. (3):

$$dG = \mu_{A^-}\, dn_{A^-} + \mu_{HA}\, dn_{HA} \tag{6}$$

As $n_{A^-} + n_{HA} = Z$, where Z is the total number of monomeric units in the polymer chain, and because of the dissociation equilibrium, dG becomes:

$$dG = -\mu_{H^+}\, dn_{A^-} \tag{7}$$

G may also be written as the sum of the free enthalpy contributed by the a form and the b form and as a consequence:

$$dG = dG^{a} + dG^{b} \tag{8}$$

At $\alpha = 0$ and at $\alpha = \alpha_x$, the polyacid is assumed to be completely in state a and state b respectively. Thus dG may be integrated between $\alpha = 0$ and $\alpha = \alpha_x$, giving $G^{b} - G_0{}^{a}$, which is the free enthalpy difference between PMA^{b} at a degree of dissociation α_x, and PMA^{a} at $\alpha = 0$. From eq. (7) it may be seen that the mentioned free enthalpy difference might actually be evaluated by integration of a titration curve. A quantity which is more directly related to the difference between a and b because of the elimination of charge effects, is $G_0{}^{b} - G_0{}^{a}$. This quantity may also be obtained.

Extrapolation from the titration curve of PMA^{b} to values of a below α_x produces estimated values of pH for PMA^{b} in this region. These pH values will be called pH^{b}. They refer to a virtual solution in which only PMA^{b} would exist at all values of α. Then $G_0{}^{b} - G_0{}^{a}$ may be obtained from eq. (7) by the following integration:

$$\int_0^{\alpha_x} (\mathrm{pH} - \mathrm{pH}^{b})\, d\alpha = \frac{1}{2.3ZkT} (G_0{}^{b} - G_0{}^{a}) \tag{9}$$

Here $\alpha = n_{A^-}/Z$. As will be seen later, it is useful to transform eq. (9) into a relation which is a function of the respective pK's

$$\int_0^{\alpha_x} (pK - pK^{b})\, d\alpha = \frac{1}{2.3\, ZkT} (G_0{}^{b} - G_0{}^{a}) \tag{10}$$

Thus it is seen that the transition free enthalpy at $\alpha = 0$ may be determined experimentally if pK^{b} is known in the region of α values below $\alpha = \alpha_x$ This was also established by Zimm and Rice[8] for helix–random coil transitions It is seen from the present derivation that eq. (10) has a general validity for any transition equilibrium.

Regarding the extrapolation procedure to obtain pH^b values the following observations may be made.

It has been observed experimentally (for example, Katchalsky and Spitnik,[9] Strobel and Gable,[10] Fischer and Kunin,[11]) that the titration behavior of many polyelectrolytes over a large range of α values conforms to the extended Henderson-Hasselbach equation:

$$pH = pK_a - n \log (1 - \alpha)/\alpha \tag{11}$$

Here pK_a and n are constants at constant polymer and neutral salt concentrations. The nature of pK_a may be seen by introducing the apparent pK, as defined previously, into eq (9):

$$pK = pK_a - (n - 1) \log (1 - \alpha)/\alpha \tag{12}$$

Integration of both sides of eq. (10) with respect to α between the boundaries α_1, and $1 - \alpha_1$, shows pK_a to be equal to the average of the apparent pK in a range symmetrical around $\alpha = 0.5$.

Thus, eq. (10) gives the dependence of pK on α with $pK_a = pK_{\alpha = 0.5}$ as a point of reference. The large dependence of pK on α is generally attributed to the increase of the electrostatic free enthalpy of the ionized polymer duirng the titration. It should be emphasized that the extended Henderson-Hasselbach equation gives an experimentally well tested relation between the degree of dissociation of the polyacid and the pH of the solution. Although $(n\text{-}1) \log (1\text{-}\alpha)/\alpha$ may be considered to be the term depending on the activity coefficients of the dissociated and undissociated carboxylic acid groups (pH is here supposed to equal the negative logarithm of the activity of the hydrogen ions) this is of no consequence for the way this equation is used here. Still it should be noted that both parameters pK_a and n depend strongly on the physical properties of the polyelectrolyte and its environment.

Therefore it should be expected that two regions in which an extended Henderson-Hasselbach equation is valid will be observed if PMA exists for an appreciable range of α values predominantly as PMA^a before a transition to PMA^b occurs. By extrapolation of these plots into the transition region it would then be possible to obtain, for example, pH^b values which may be transformed into pK^b values needed to evaluate eq. (10).

If $pK - pK^b$ is integrated between α_y, at which values PMA still exists as PMA^a, and α_z as defined previously, the result will evidently be $(G^b - G^a)/2.3\ ZkT$ at α_y. This free enthalpy difference, of course, contains a term related to the different intramolecular electrostatic interaction in a and b. If this term is eliminated by extrapolating $(G^b - G^a)/2.3\ ZkT$ to infinite ionic strength, the result will be $(G^b - G^a)_{\infty,\, \alpha y}/2.3\ ZkT$. Now, G may be divided in different portions:

$$G = G^* + G_{mix} + G_{el} + G_c$$

where G_{mix} is the ideal entropy of mixing for the monomeric units, G_{el} refers to the electrostatic interactions, while G_c contains the conformational en-

tropy of the chain. G^* summarizes all other contributions to the free enthalpy of the polyelectrolyte molecule. Thus defining G in terms of the chemical potentials of monomeric units, it follows that

$$(G^{b} - G^{a})_{\sim,\,\alpha_y} = Z\alpha_y(\mu_{A^-}{}^{*,b} - \mu_{A^-}{}^{*,a}) + Z\,(1 - \alpha_y)(\mu_{HA}{}^{*,b} - \mu_{HA}{}^{*,a}) - T\,(\Delta S_c)_{\infty,\,\alpha_y} \quad (13)$$

when μ^* corresponds to G^*.

At $\alpha = 0$ we have

$$G_0{}^{b} - G_0{}^{a} = Z\,(\mu_{HA}{}^{*,b} - \mu_{HA}{}^{*,a}) - T\,(\Delta S_c)_{\alpha = 0} \quad (14)$$

Now, it is reasonable to assume that the conformational entropy difference between a and b at α_y and at infinite ionic strength, where electrostatic repulsion between the fixed charges is assumed to be negligible, will be of the same order of magnitude as at $\alpha = 0$. Thus using the approximation $(\Delta S_c)_{\infty,\,\alpha_y} = (\Delta S_c)_{\alpha = 0}$, it is possible to calculate $pK_0{}^{a} - pK_0{}^{b}$, the ratio of the dissociation constants of both forms expressed in terms of the standard chemical potential μ^*. If μ^* is used as the standard chemical potential, K_0 should not depend on the charge and the conformational entropy of the chain. As K_0 is the limiting value of the apparent pK for $\alpha = 0$ it may be used as a characterizing constant for the polyacid.

3. EXPERIMENTAL

A. Materials

Polymethacrylic acid was prepared by polymerization of methacrylic acid with hydrogen peroxide as initiator. The methacrylic acid was distilled under reduced pressure immediately before the polymerization. The fraction used in the polymerization, distilled at 72°C. and about 20 mm. Hg (Merck Index: 81°C., 30 mm. Hg; 63°C., 12 mm. Hg). The polymerization was carried out in a 20% aqueous solution of the monomer under nitrogen atmosphere. It was started by introducing 5.4 g. of a 30% H_2O_2 solution into the reaction vessel which contained 180 g. methacrylic acid and 900 ml. distilled water. During the polymerization the temperature was kept between 80 and 90°C. After 5 hr. the gelled polymer system was allowed to cool. Next, the polymer was dissolved in distilled methyl alcohol and precipitated with ethyl ether. After drying, powdering, and drying under reduced pressure, 178 g. PMA was obtained.

From a 2% PMA solution in methyl alcohol, the polymer was fractionated with ethyl ether.[1] To ensure a good separation each polymer fraction that was precipitated was dissolved again by lowering the temperature and then reprecipitated by slowly increasing the temperature (1°C. in about 15 min.). The fractions were separated, dried, powdered, and dried again under reduced pressure.

During preparation and fractionation of the polymer, contact of PMA solutions with metallic objects (stirrers, etc.) was avoided.

The molecular weights of the fractions were estimated viscometrically by the method used by Arnold and Overbeek.[2] The extreme molecular weights determined were 1.7×10^6 and 0.84×10^6. All experiments were conducted with a PMA fraction of estimated molecular weight 8.7×10^5.

All PMA solutions used were prepared with conductance water having a specific resistance exceding 10^6 ohm.cm. The conductance water was prepared with a mixed bed ion exchange column. The specific resistance of the water was checked with a Philiscope (Philips PR 9500) resistance bridge.

The PMA solutions were always prepared by dilution from a more concentrated stock which was stored frozen in a polyethylene flask. The concentrations of the polymer solutions used were always determined by potentiometric titration.

Sodium hydroxide solutions of 0.1 equiv./l. were obtained with the help of Fixanal ampullae. The usual precautions were taken to avoid contamination by carbonate.

B. Potentiometric Titrations

All potentiometric titrations were conducted with a Radiometer automatic titration apparatus (TTT 1 Titrator in conjunction with a SBR 2 Titrigraph and a SBU 1 syringe buret). The change in the potential difference between the electrodes due to each successive addition of reagent is compensated automatically by a variable potentiometer. The electrodes used were a G 202 A glass electrode and a K 4312 calomel electrode (both by Radiometer).

The titrations were performed in a titration vessel in which the temperature was kept at 20 ± 0.1°C. All titrations were performed in a nitrogen atmosphere. A difference of 0.03 pH between duplicate titrations was admitted. Titrations were always performed with 0.1*N* sodium hydroxide.

4. DISCUSSION OF EXPERIMENTAL RESULTS

The titration curves in Figure 1 relate to titrations of PMA with NaOH at several $NaNO_3$ concentrations. The transition region may be observed very clearly in curve 1 between $\alpha' \approx 0.1$ and $\alpha' \approx 0.3$ (where α' represents the degree of neutralization, while α is used to express the degree of ionization). This curve corresponds to the lowest salt concentration. When this concentration increases, the transition seems to be spread over a larger titration interval. This is in accordance with the assumption that the transition is brought about by the repulsion between the fixed charges along the polymer chain. The sodium nitrate is expected to have a screening effect on this interaction.

The reversibility of the phenomenon was checked by back-titration with acid. Also, the shape of the curve did not change appreciably in the investigated region of PMA concentrations (1.73×10^{-3}–1.02×10^{-2} equiv./l.).

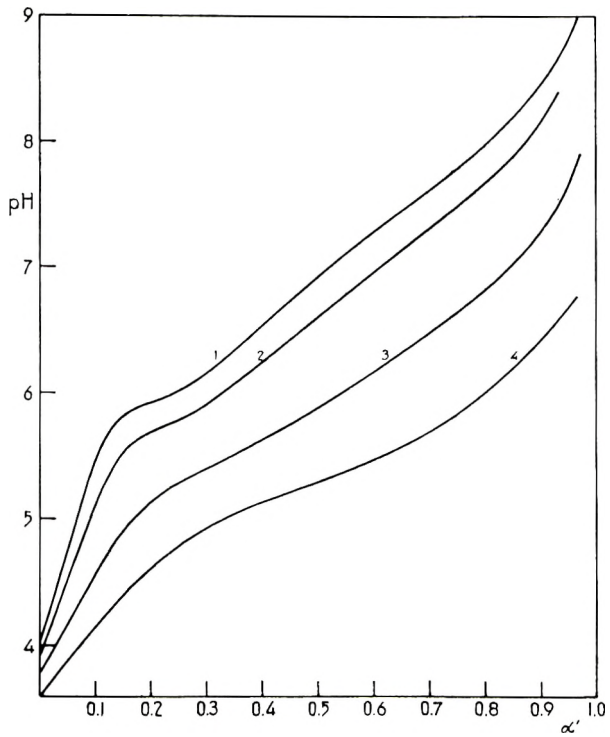

Fig. 1. Titration curves of PMA (4.81×10^{-3} equiv./l.) at several ionic strengths: (*1*) $3.33 \times 10^{-3}M$ $NaNO_3$; (*2*) $0.01M$ $NaNO_3$; (*3*) $0.1M$ $NaNO_3$; (*4*) $1M$ $NaNO_3$.

In Figure 2 some titration curves are presented as Henderson-Hasselbach plots. Clearly, for each titration two regions conform to the extended Henderson-Hasselbach equation. Extrapolation from each linear part of a Henderson-Hasselbach plot allows a calculation of pK values for PMA^a and PMA^b in the transition region. A result of this procedure, may be seen in Figure 3.

To calculate the transition free enthalpy at $\alpha = 0$, it is necessary to obtain the value of the surface between the experimental pK versus α curve and the extrapolated one for PMA^b. However, as pK values at $\alpha = 0$ may not be calculated safely, an extrapolation from the last points of these curves that may be obtained must be made to $\alpha = 0$. This is the reason why eq. (10) is used instead of eq. (9) for the determination of $G_0^b - G_0^a$ as the extrapolation of pH to $\alpha = 0$ is more difficult. For the experimental curve, $pK_0 = pK$ ($\alpha = 0$) is estimated by the extrapolation method that was proposed by Arnold,[4] who observed that pK versus $\alpha^{1/3}$ plots for PMA are linear (except in the transition region) down to low α values. It should be mentioned, however, that graphs with $\alpha^{1/2}$ and $\alpha^{1/4}$ as variables are also linear. If these are used for an estimation of pK_0 the difference between the values obtained is about one pK unit for PMA in the absence of neutral salt. For our purpose, however,

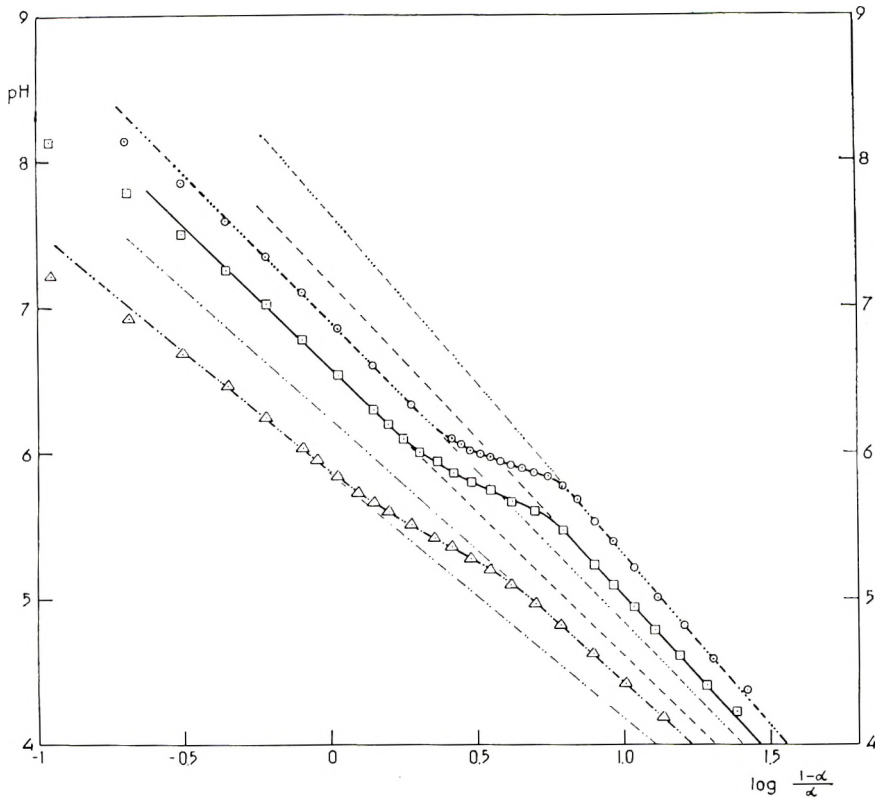

Fig. 2. Henderson-Hasselbach plots for PMA (4.81×10^{-3} equiv./l.) at different ionic strengths: (O) $3.33 \times 10^{-3}M$ $NaNO_3$; (□) $0.01M$ $NaNO_3$; (△) $0.1M$ $NaNO_3$

this does not matter. In fact it is not very important to locate the exact position of pK_0 in order to evaluate the surface enclosed between the curves because at the last points that may be obtained the two curves run very close. For the same reason, although it would be reasonable to estimate $pK_0{}^b$ some tenth's of pK units lower, pK_0 for PMA^b is as a first approximation assumed to have the same value as pK_0 for PMA^a.

In Table I some values for $(1/ZkT)(G_0{}^b - G_0{}^a)$ at 20°C. which were estimated by the foregoing procedure are presented. It is seen that no significant dependence on ionic strength is found, as is to be expected for this process at zero charge density. With regard to the accuracy of the

TABLE I

PMA $\times 10^{+3}$, equiv./l.	$NaNO_3$, M	$(1/ZkT)(G_0{}^b - G_0{}^a)$
4.81	0.003	0.20
4.81	0.01	0.20
4.81	0.1	0.18
10.21	0.003	0.24
10.21	0.01	0.22

extrapolation method used, it would be hazardous to conclude the existence of a concentration dependence. In view of the intermolecular interactions which were neglected and which may play a role here, such an effect would not, however, be surprising.

The numerical values of the transition free enthalpies in Table I relate to the monomeric units of the polymer chain. If these units could take part in the a $\rightleftharpoons$ b equilibrium independently of each other, the values in Table I would predict a smooth transition from $\alpha = 0$ upward. Thus these values indicate that the transition is of a cooperative nature, as was expected.

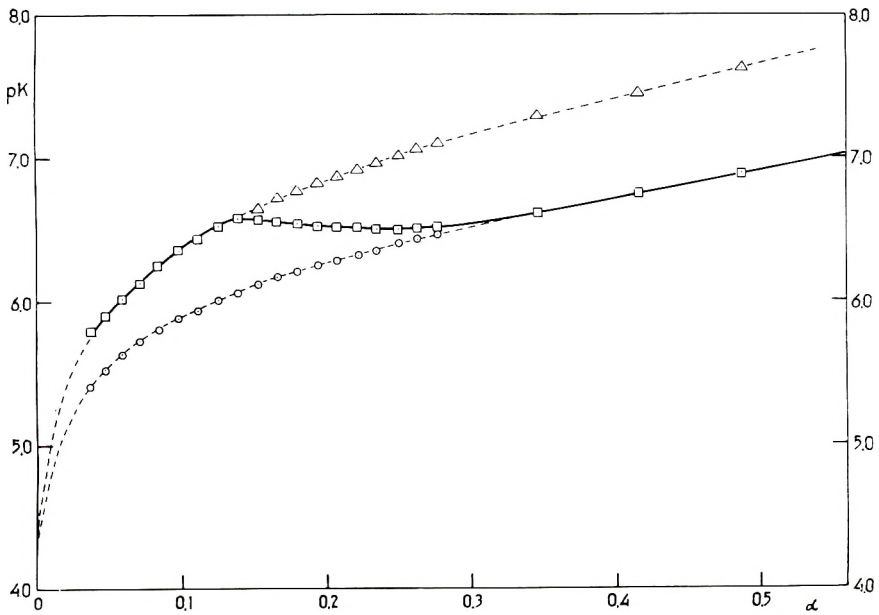

Fig. 3. Apparent pK as a function of α for PMA (4.81×10^{-3} equiv./l.) in the presence of $3.33 \times 10^{-3}M$ $NaNO_3$ solution: (□) calculated from experimental titration curve (Fig. 1); (△) points for PMA^a as extrapolated from Henderson-Hasselbach plot (Fig. 2); (○) points for PMA^a as extrapolated from Henderson-Hasselbach plot (Fig. 2).

Now, the values of $G_0^b - G_0^a$, which may be calculated if Z is known, are estimations of the free enthalpy that has to be added to a molecule PMA^a to transform it to a PMA^b molecule at $\alpha = 0$. This value may be used to test a molecular model from which $G_0^b - G_0^a$ can be calculated. As too little is known yet about the exact nature of the interactions involved, it is not felt to be profitable to perform such calculations here.

As values for pK^a and pK^b in the transition region may be obtained from plots like Figure 3, it is possible to analyze the titration curves as a function of the concentrations of forms a and b in their dissociated and undissociated states.

Assuming the existence of a mixture of acids in the transition region

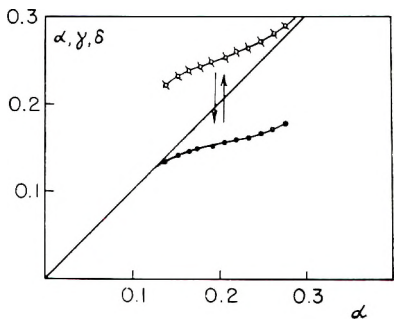

Fig. 4. Degrees of dissociation of PMA[a] γ and PMA[b] δ as a function of the overall degree of dissociation α at PMA = 4.81×10^{-3} equiv./l.; $NaNO_3 = 3.33 \times 10^{-3} M$: (●) γ; (◉) δ.

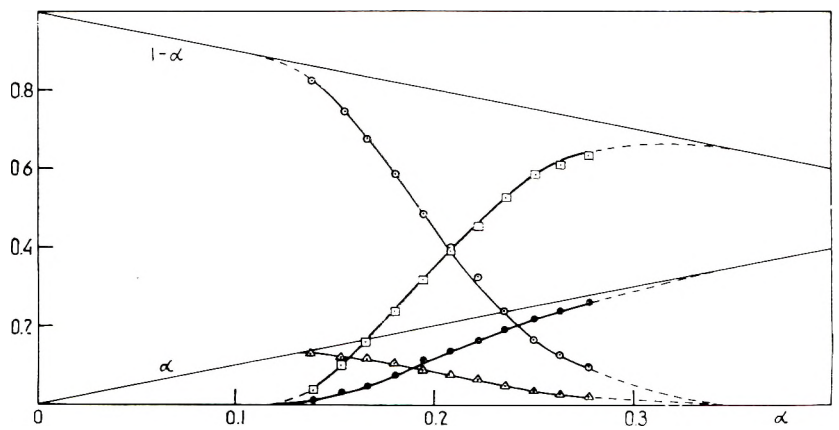

Fig. 5. Analysis of the titration curve of PMA (4.81×10^{-3} equiv./l.) in the presence of $3.33 \times 10^{-3} M$ $NaNO_3$: (○) $(1 - \gamma)\, c^a/c_t$; (△) $\gamma c^a/c_t$; (□) $(1 - \gamma)\, c_b/c_t$; (●) $\delta c_b/c_t$.

with apparent dissociation constants K^a and K^b, concentrations c_a and c_b, and degrees of dissociation γ and δ, the following relations evidently hold:

$$\gamma = K^a/(H^+ + K^a) \tag{15}$$

and

$$\delta = K^b/\ H^+ + K^b$$

If c_t is the total acid concentration, c_a may be calculated as shown below:

$$\alpha c_t = \gamma c_a + \delta c_b = \gamma c_a + \delta(c_t - c_a) \tag{16}$$

consequently:

$$c_a = [(\alpha - \delta)/(\gamma - \delta)]c_t \tag{17}$$

Finally, c_b is obtained from $c_t = c_a + c_b$.

If γ and δ are calculated from the pK values as given in Figure 3, both γ and δ are nearly constant in the transition region, as may be seen in Figure 4. Thus at a certain value for γ, PMA^a becomes unstable and transforms to PMA^b. This is also illustrated in Figure 5, in which the dissociated and undissociated fractions of a and b are given. Here it is seen that, after a relatively small concentration of dissociated PMA^a is reached, a rapid overall conversion is started, in accordance with a cooperative character of the transition.

By integrating pK − pK^b between α_y and α_x, the difference between the pK_0 values for both forms may be calculated as shown previously. This calculation was performed for 4.81×10^{-3} equiv./l. PMA. As only the three ionic strengths given in Table I were used, the calculated pK_0 difference is to be regarded as a rough estimate. Thus, with due reservations concerning the extrapolation and the approximation mentioned, a value of 0.3 for pK_0^a − pK_0^b was obtained. This may be regarded as a surprisingly reasonable value in view of the difference in apparent pK between both forms in the transition region.

To conclude it is noted, that the peculiar titration curve of PMA may be described as resulting from a transition of the PMA molecules between two states, without arriving at any obvious inconsistencies.

References

1. Katchalsky, A., and H. Eisenberg, *J. Polymer Sci.*, **6**, 145 (1951).
2. Arnold, R., and J. Th. G. Overbeek, *Rec. Trav. Chim.*, **69**, 192 (1950).
3. Katchalsky, A., *J. Polymer Sci.*, **7**, 393 (1951).
4. Arnold, R., *J. Colloid Sci.*, **12**, 549 (1957).
5. Mandel, M., and J. C. Leyte, *J. Polymer Sci.*, **56**, S25 (1962).
6. Gregor, H. P., D. H. Gold, and M. Frederick, *J. Polymer Sci.*, **23**, 467 (1957).
7. Kedem, O., and A. Katchalsky, *J. Polymer Sci.*, **15**, 321 (1955).
8. Zimm, B. H., and S. A. Rice, *Mol. Phys.*, **3**, 391 (1960).
9. Katchalsky, A., and P. Spitnik, *J. Polymer Sci.*, **2**, 432 (1947).
10. Strobel, H. A., and R. W. Gable, *J. Am. Chem. Soc.*, **76**, 5911 (1954).
11. Fischer, S., and R. Kunin, *J. Phys. Chem.*, **60**, 1030 (1956).

Résumé

Le comportement potentiométrique de l'acide polyméthacrylique est discuté en termes de transition conformationnelle. On présente un traitement thermodynamique de cette transition. La courbe de titration de l'acide polyméthacrylique est analysée de façon détaillée et des informations quantitatives sont obtenues quant à la transition.

Zusammenfassung

Das potentiometrische Verhalten von Polymethacrylsäure wird auf der Grundlage einer Konformationsumwandlung diskutiert. Es wird eine thermodynamische Behandlung dieser Umwandlung gegeben. Eine eingehende Analyse der Titrationskurve von Polymethacrylsäure liefert quantitative Informationen über die Umwandlung.

Received March 19, 1963

JOURNAL OF POLYMER SCIENCE: PART A VOL. 2, PP. 1893–1900 (1964)

Reactivities of Esters of Methacrylic Acid. Part I. Relative Reactivities of Esters toward the Benzoyloxy Radical

J. C. BEVINGTON and B. W. MALPASS, *Department of Chemistry, The University, Birmingham, England*

Synopsis

Tracer methods have been used to compare the reactivities of methyl, ethyl, phenyl, benzyl, and cyclohexyl methacrylates toward the benzoyloxy radical at 60°C. Certain of the characteristics of the polymerizations of these monomers are recorded.

This paper is the first of a series concerned with the reactivities of esters of methacrylic acid toward reagents of various types. An account is given here of studies of the reactivities of the ethyl, phenyl, benzyl, and cyclohexyl esters toward the benzoyloxy radical at 60°C. The work involved the use of tracer techniques and the general procedure has been described already in connection with similar studies involving styrene[1] and methyl methacrylate.[2]

Two types of ^{14}C-benzoyl peroxide were used to initiate the polymerizations of the monomers. Comparisons of the specific activities of the peroxides and the recovered polymers led to determination of the relative numbers of benzoyloxy and phenyl endgroups in the polymers. This information was then used to determine the ratio k_1/k_2, where k_1 and k_2 are the velocity constants for the competing reactions.

$$C_6H_5COO\cdot \rightarrow C_6H_5\cdot + CO_2 \quad (1)$$

$$C_6H_5COO + CH_2{=}C(CH_3)(COOR) \rightarrow C_6H_5COOCH_2C(CH_3)(COOR) \quad (2)$$

The value of k_1 cannot be affected appreciably by the nature of the monomer, and so the values of k_2 for the various monomers can be compared. Derivation of the expression for k_1/k_2 requires that every phenyl radical formed in eq. (1) is subsequently incorporated in polymer. This assumption has been tested and found to be valid for each of the systems considered here.

For each monomer, there were two sets of polymerizations with various concentrations of monomer in benzene and benzoyl peroxide at 1 g./l. In one set, the peroxide was labeled in its benzene rings with carbon-14, and, in the other, the peroxide was labeled at its carboxylic carbon atoms; the two types of labeled peroxide are referred to as R-peroxide and C-perox-

ide, respectively. The experiments with R-peroxide lead to the total rate R_i at which initiator fragments, both benzoyloxy and phenyl, enter polymer; this quantity is given by the expression

$$R_i = nS_{pr}R_p/7\,S_{ir} \tag{3}$$

where R_p is the rate of polymerization, n is the number of carbon atoms in the molecule of the monomer, and S_{ir} and S_{pr} are specific activities of the R-peroxide and the derived polymer, respectively (in units such as microcuries per gram of carbon). In the expression quoted previously,[1,2] the denominator was written as $6S_{ir}$; in calculations, however, the specific activity of the peroxide was taken as 7 (observed value)/6 so that the two expressions are identical.

If all the phenyl radicals produced in reaction (1) later enter polymer, the value of R_i is unaffected by the existence of a competition between reactions (1) and (2); for a given concentration of peroxide, the value of R_i should therefore be constant over a range of concentrations of monomer and should vary only slightly from one monomer to another.

If C-peroxide is used as initiator, it is possible to calculate the rate (R_{ic}) at which benzoyloxy radicals enter polymer by means of the equation

$$R_{ic} = nS_{pc}R_p/7\,S_{ic} \tag{4}$$

where S_{ic} and S_{pc} are specific activities, in the units specified above, of the C-peroxide and the derived polymer.

For a pair of polymerizations performed with the same concentration of a monomer, the one with R-peroxide and the other with the same concentration of C-peroxide

$$\frac{\text{(No. of benzoyloxy endgroups in polymer)}}{\text{(No. of benzoyloxy endgroups)} + \text{(No. of phenyl endgroups)}} = x = \frac{S_{pc}S_{ir}}{S_{pr}S_{ic}} \tag{5}$$

It has been shown[1] that

$$1/x = 1 + k_1/k_2[\mathrm{M}] \tag{6}$$

where [M] is the concentration of monomer during the polymerization.

Values of k_t/k_p^2 can be calculated by using the equation

$$k_t/k_p^2 = nS_{pr}[\mathrm{M}]^2/14S_{ir}R_p \tag{7}$$

Derivation of this equation is based on a simple kinetic scheme in which termination is supposed to occur only by the interaction of pairs of polymer radicals, and in which the rate of termination is expressed as $2\,k_t$[active centers]^2.

Experimental

Polymerizations were performed in the complete absence of air in sealed dilatometers of about 7 cc. capacity; reactions were allowed to proceed to

about 5% conversion. Polymers of ethyl methacrylate were recovered by precipitation in hexane; polymers of the other esters of methacrylic acid were precipitated in methanol. Polymers were purified by reprecipitation and dried in vacuum. Labeled materials were assayed by gas counting.

Two methods were used to determine the factors for converting rates of contraction into rates of polymerization. The first method depended upon gravimetric determination of the polymers formed in certain polymerizations; the second method involved measurements of the densities of the monomers and the polymers in benzene solution at 60°C. For each monomer, there were not less than 10 determinations of the conversion factor; there was good agreement between the results obtained by both methods.

Benzene was dried over sodium and fractionated. Ethyl methacrylate (Messrs. L. Light and Co. Ltd.) was washed several times with aqueous caustic soda and then repeatedly with water. Phenyl methacrylate was prepared by reacting methacrylyl chloride with phenol. Benzyl and cyclohexyl methacrylates were prepared by ester exchanges involving methyl methacrylate, the appropriate alcohol, and sulfuric acid as catalyst; hydroquinone was added to inhibit polymerization. Monomers were dried and then fractionated under nitrogen at reduced pressure; they were redistilled in high vacuum immediately before being charged into dilatometers.

Samples of benzoyl peroxide were prepared from suitably labeled samples of ^{14}C-benzoic acid. The specific activities of both the R-peroxide and C-peroxide were close to 14 μg./g. of peroxide. There were no detectable differences between the rates of polymerizations initiated by the two types of peroxide, for the same concentrations of reactants.

Results

Table I shows the densities of the monomers and their polymers and also conversion factors for the polymerizations.

TABLE I
Properties of Monomers and Polymers

	Ester of methacrylic acid			
	Ethyl	Phenyl	Benzyl	Cyclohexyl
Density of monomer in benzene at 60°C., g./cc.	0.868	1.020	1.000	0.925
Density of polymer in benzene at 60°C., g./cc.	1.120	1.210	1.173	1.092
Contraction for 100% polymerization at 60°C. (from densities), %	22.50	15.70	14.74	15.30
Contraction for 100% polymerization at 60°C. (gravimetrically), %	22.55	15.44	14.68	15.50

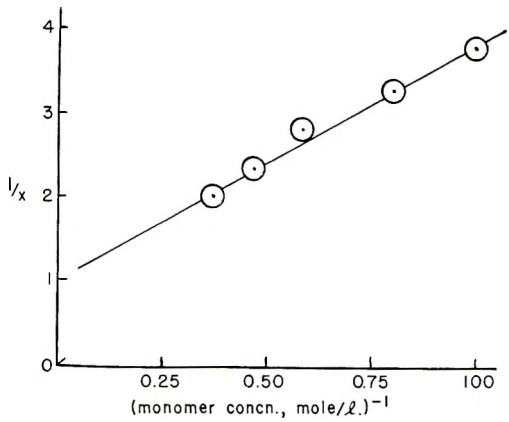

Fig. 1. Variation in the proportions of benzoyloxy and phenyl endgroups in polymers with the concentration of monomer during polymerization of ethyl methacrylate at 60°C. with benzoyl peroxide as initiator.

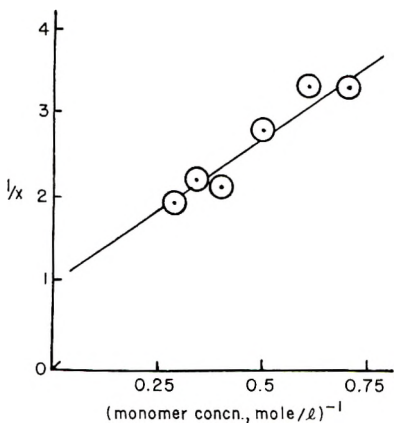

Fig. 2. Variation in the proportions of benzoyloxy and phenyl endgroups in polymers with the concentration of monomer during polymerization of phenyl methacrylate at 60°C. with benzoyl peroxide as initiator.

TABLE II

Kinetic Characteristics of the Polymerizations for Various Esters of Methacrylic Acid

Methyl		Ethyl		Phenyl		Benzyl		Cyclohexyl	
[M], mole/l.	k_t/k_p^2, mole/l./sec.	[M], mole/l.	k_t/k_p^2, mole/l./sec.	[M], mole/l.	k_t/k_p^2, mole/l./sec.	[M], mole/l.	k_t/k_p^2, mole/l./sec.	[M], mole/l.	k_t/k_p^2, mole/l./sec.
1.56	33.6	1.00	49.7	0.76	16.1	0.71	19.2	0.71	10.4
2.83	29.4	1.25	49.3	0.83	11.5	0.83	21.2	0.83	10.8
3.94	32.6	1.72	47.0	1.00	11.4	1.00	19.9	1.00	9.94
8.96	33.5	2.13	47.4	1.27	9.8	1.27	15.0	1.27	9.06
—		2.70	45.5	1.47	9.5	1.47	19.3	1.47	8.66
—		—		1.72	10.4	1.72	17.5	—	

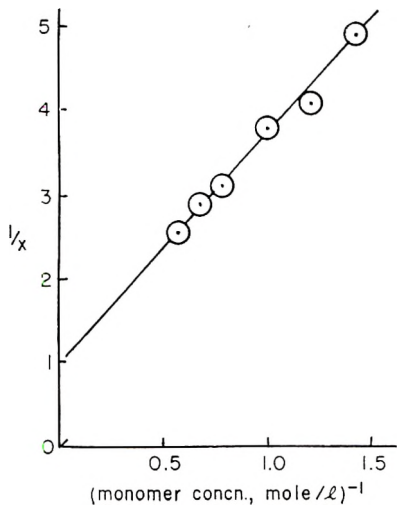

Fig. 3. Variation in the proportions of benzoyloxy and phenyl endgroups in polymers with the concentration of monomer during polymerization of benzyl methacrylate at 60°C. with benzoyl peroxide as initiator.

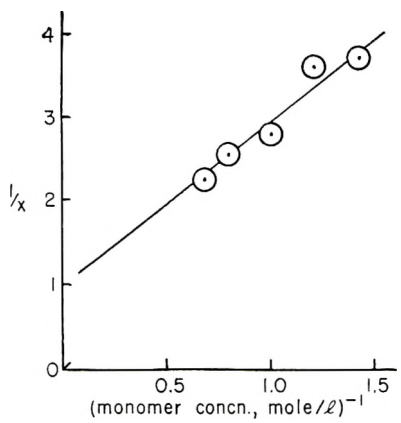

Fig. 4. Variation in the proportions of benzoyloxy and phenyl endgroups in polymers with the concentration of monomer during polymerization of cyclohexyl methacrylate at 60°C. with benzoyl peroxide as initiator.

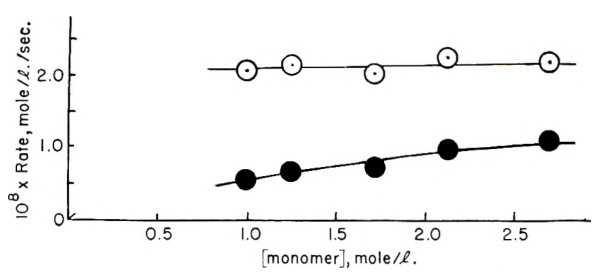

Fig. 5. Variation in (O) R_i and (●) R_{ic} for polymerization of ethyl methacrylate at 60°C. with benzoyl peroxide at 1 g./l. with concentration of monomer.

The polymerizations at 60°C. were first order with respect to monomer. For the polymers prepared with the two types of labeled benzoyl peroxide (at 1 g./l.) and with the monomers at various concentrations in benzene, values of x were calculated by eq. (5). The results are shown in Figures

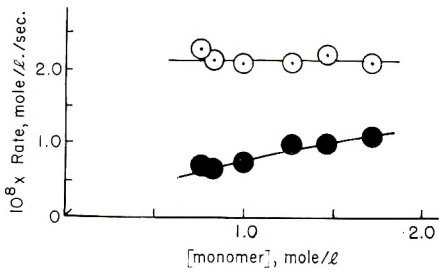

Fig. 6. Variation in (O) R_i and (●) R_{ic} for polymerization of phenyl methacrylate at 60°C. with benzoyl peroxide at 1 g./l. with concentration of monomer.

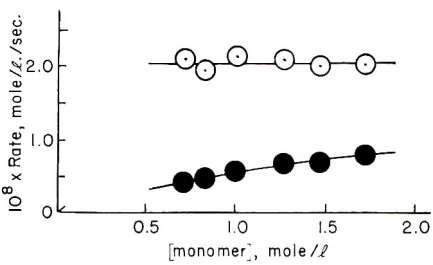

Fig. 7. Variation in (O) R_i and (●) R_{ic} for polymerization of benzyl methacrylate at 60°C. with benzoyl peroxide at 1 g./l. with concentration of monomer.

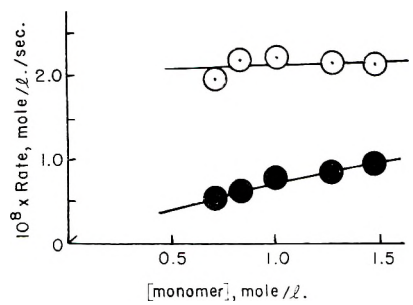

Fig. 8. Variation in (O) R_i and (●) R_{ic} for polymerization of cyclohexyl methacrylate at 60°C. with benzoyl peroxide at 1 g./l. with concentration of monomer.

1-4. The values of k_1/k_2 for ethyl, phenyl, benzyl, and cyclohexyl methacrylates are, respectively, 2.93, 1.72, 2.70, and 1.95 mole/l.; the corresponding quantity for methyl methacrylate[2] is 3.30 mole/l.

From eqs. (3) and (4), values of R_i and R_{ic} were calculated for the various polymerizations; they are shown in Figures 5-8.

From the results of experiments involving R-peroxide, values of k_t/k_p^2 were calculated by eq. (7) and are shown in Table II. This Table includes also results obtained for methyl methacrylate.[2]

Discussion

It has been shown[3] that the comparatively small structural difference between *n*-propyl and *n*-butyl methacrylates causes an appreciable difference between the kinetic characteristics of the polymerizations of the two monomers. There are significant differences also between the values of k_t/k_p^2 for the polymerizations of the esters studied in this work. The values of k_t/k_p^2 show little systematic variation with the concentration of monomer; in this respect, the polymerizations differ markedly from those of certain other monomers, e.g., vinyl acetate, methyl acrylate, and styrene. It is likely, therefore, that termination during the polymerizations of these esters of methacrylic acid is almost exclusively by interaction of pairs of polymer radicals, as assumed in the kinetic analysis.

Figures 5–8 show clearly that R_i does not depend upon the concentration of monomer or upon its nature. The value of R_{ic} falls as the concentration of monomer is reduced; this is accounted for by the shift in the balance in the competition between reactions (1) and (2) as the concentration of monomer is changed.

The values of k_1/k_2 at 60°C. are significantly different for the five esters of methacrylic acid. The relative values of k_2 for the methyl, ethyl, phenyl, benzyl, and cyclohexyl esters are, respectively, 1.00, 1.14, 1.94, 1.22, and 1.74. The reactivities of these monomers toward the benzoyloxy radical are all considerably less than that of styrene,[1] for which the relative value of k_2 is 8.25 on this scale. The relative reactivities of the monomers toward certain other reference radicals, deduced from studies of copolymerization, will be reported in a later paper; this will contain also a comparison of the results obtained for the various reference radicals.

B. W. M. thanks the University of Birmingham for the award of the A. E. Hills Memorial Scholarship.

References

1. Bevington, J. C., *Proc. Royal Soc. (London)*, **A239**, 420 (1957).
2. Bevington, J. C., *Trans. Faraday Soc.*, **53**, 997 (1957).
3. Burnett, G. M., P. Evans, and H. W. Melville, *Trans. Faraday Soc.*, **49**, 1096, 1105 (1953).

Résumé

On a utilisé la méthode des traceurs pour comparer les réactivités des méthacrylates de méthyle, d'éthyle, de phényle, de benzyle, et de cyclohexyle vis-à-vis du radical benzoyloxy à 60°C. On a retenu certaines caractéristiques de polymérisation de ces monomères.

Zusammenfassung

Unter Verwendung von Tracermethoden wurden die Reaktivitäten von Methyl-, Äthyl-, Phenyl-, Benzyl- und Cyclohexylmethacrylaten gegen das Benzoyloxyradikal bei 60°C. verglichen. Bestimmte Charakteristika der Polymerisation dieser Monomeren werden angegeben.

Received March 19, 1963

JOURNAL OF POLYMER SCIENCE: PART A VOL. 2, PP. 1901–1907 (1964)

Proton Resonance Spectra and Tacticities of Some Poly(methyl Vinyl Ethers)*

S. BROWNSTEIN and D. M. WILES, *Division of Applied Chemistry, National Research Council, Ottawa, Canada*

Synopsis

Methyl vinyl ether has been polymerized by BF_3 etherate catalyst under a variety of conditions to obtain polymers of different molecular weights and tacticities. Some properties of these polymers have been compared with those of a sample prepared with a special stereoregulating catalyst at the Hercules Powder Company. The proton magnetic resonance spectra of poly(methyl vinyl ether) in several solvents have been investigated and it has been possible to assign the absorptions by the methoxyl protons to particular steric configurations of the polymer chain. These data have been used to compare the tacticities of the different polymer samples and to establish that good steric control in the propagation reaction is possible with a soluble BF_3 etherate catalyst.

Introduction

Some years ago Schildknecht and co-workers[1,2] described the preparation of two types of poly(methyl vinyl ether) having differences in solubility, stability, and crystallinity. The crystalline type was obtained by boron trifluoride etherate catalysis at low temperature in a mixed hydrocarbon–chloroform solvent, a so-called activated polymerization. The other type, a noncrystalline, tacky product, resulted from bulk polymerizations with various Friedel-Crafts catalysts. More recent work[3] indicates that the crystalline polymer can be obtained in a homogeneous medium and that a halogenated alkane solvent is not necessary.

The formation of crystalline poly(methyl vinyl ether) has also been reported by Breslow et al.,[4] who used "highly stereospecific catalysts, including special Ziegler-types," with which a low polymerization temperature is not required. These special catalysts produce high molecular weight polymers which are more highly crystalline and less soluble than those described originally by Schildknecht. The reasonable assumption has been made, on the basis of x-ray diffraction patterns, that the crystalline methyl vinyl ether polymers, prepared both with Friedel-Crafts catalysts[3] and with the special catalysts,[4] are isotactic.

The differences in solubility between samples of poly(methyl vinyl ether) are often regarded as a criterion for differences in stereoregularity,

* Issued as N.R.C. No. 7602.

and there is some justification in this if the molecular weights are comparable. On the other hand the crystallinity of a polymer and its degree of stereoregularity may not be directly related. For example, there need be no connection in the case of isotactic poly(methyl methacrylate); the length of stereoregular sequences is important in determining whether this polymer can be crystallized by ordinary means.

The proton magnetic resonance spectrum of a polymer dissolved in a suitable solvent provides, in certain instances, an unambiguous indication of the steric structure of the molecules. Bovey and Tiers[5] first showed how the numbers of isotactic, syndiotactic, and heterotactic sequences in poly(methyl methacrylate) samples could be evaluated, and the method is now routinely applicable for this polymer. More recently, corresponding methods have been applied to determining the tacticities of poly-α-methylstyrenes[6] and polystyrenes.[7] Clearly it would be useful to be able to assess in a similar manner the tacticities of other polymers with a view to describing the stereoregulating powers of polymerization reactions as well as for the characterization of the polymers themselves.

In this paper the proton magnetic resonance spectrum of poly(methyl vinyl ether) is considered. It is shown that the tacticity of this polymer can be evaluated from such measurements and that the method can be used to compare the steric arrangements of samples having widely different molecular weights and solubilities.

Experimental

The methyl vinyl ether used in this work (The Matheson Co. Inc.) was distilled once, but no additional effort was made to remove water or to exclude it from the polymerization apparatus. The nitromethane for the proton resonance measurements and the viscosity determinations was fractionally distilled, and other organic liquids, reagent grade whenever possible, were used without further purification. The boron trifluoride etherate catalyst was made in a conventional way by mixing BF_3 and $(C_2H_5)_2O$ vapor in a stream of dry, purified nitrogen; any HF that might have formed and excess reagent were pumped off under vacuum.

The monomer was polymerized by the BF_3 etherate under a variety of conditions, modifications of the methods described by Schildknecht[2] being used. Polymerizations were terminated by adding a small amount of methanol to the reaction mixture at the polymerization temperature. Catalyst residues were removed by treatment of the polymers with water, and measurements of the polymer properties were made within a few days so that the addition of a stabilizing agent was not required.

No attempt was made to explore fully the stereoregulating potentialities of the BF_3 etherate catalyst system but rather it was intended that polymers which might be expected to have different tacticities should be produced. The polymerization conditions used to obtain the samples (see Table I) are as follows.

Sample 1. The catalyst in dilute toluene solution at -78°C. was added

dropwise over a period of 1 hr. to a toluene solution of monomer at −78°C. The monomer:catalyst ratio was 45, and the product was recovered by precipitation in heptane.

Sample 3. This sample was prepared in toluene–chloroform solvent (50/50, v/v) at −78°C., with a monomer:catalyst ratio of 50, by mixing the reagents under more concentrated conditions than was the case for sample 1.

Sample 5. Undiluted catalyst was added dropwise to a solution of monomer in toluene–hexane (40/60, v/v) at −78°C., the monomer:catalyst ratio being 4000. The product was recovered by evaporation of the polymerization mixture and was then separated in cold water into insoluble and soluble parts. The latter has been designated sample 5S.

Sample 6. This sample was the result of a bulk polymerization at −40° C., with a monomer:catalyst ratio of approximately 25, which yielded the expected balsamlike product.

Sample 8. This was made at −78°C. in toluene–hexane solvent (50/50, v/v) under very dilute conditions with a monomer:catalyst ratio of 370. The polymer was insoluble in the mixed diluent and was recovered by precipitation in heptane, the heptane-soluble material being discarded at this stage.

Sample HW was supplied by Dr. D. S. Breslow of the Central Research Division, Hercules Powder Company. The preparation and some properties of this polymer have been described previously.[4] It had a crystallinity (measured by infrared) of 26% as received and this value could be raised by extraction with hot methanol.[8] In this paper the portion of HW soluble in hot methanol has been designated sample HS, and the insoluble residue sample HI.

Viscosity measurements were made at 30°C. on samples 8I, HW, HS, and HI in nitromethane solution and on sample 6 in benzene and nitromethane solutions with a Cannon-Ubbelohde dilution viscometer. The weight-average molecular weight of sample 6 was calculated from its intrinsic viscosity in benzene solution by the equation, $[\eta] = 7.6 \times 10^{-4} M^{0.60}$, derived by Manson and Arquette.[9] From this value an estimate was made of the molecular weights of the other polymers from their intrinsic viscosities in nitromethane, compared to that for polymer 6 in the same solvent.

The proton resonance spectra were obtained at 56.4 Mcycles/sec. and temperatures around 113°C. in a manner previously described.[6] Since a variety of solvents and temperatures was used, only relative positions of the methoxyl peaks are presented.

Results and Discussion

In Figure 1 are shown the proton resonance spectra of the methoxyl protons of some poly(methyl vinyl ethers) in nitromethane solution. The peaks arising from syndiotactic, heterotactic, and isotactic species are clearly distinguishable in samples 6, HW, and HS, but only a single peak

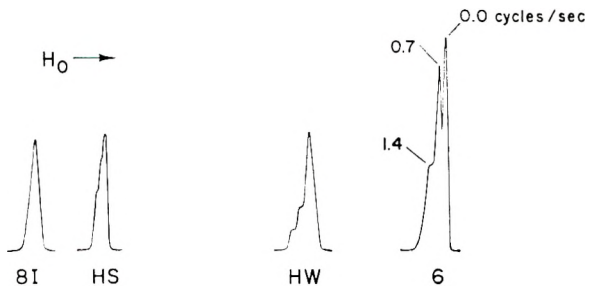

Fig. 1. Proton resonance spectra of the methoxyl region of some poly(methyl vinyl ethers).

is observed for sample 8I. For a purely syndiotactic species the CH_2 group in the polymer chain would be expected to yield a triplet. Each of these lines would be further split into four in the isotactic species.[10] Sample 8I gave a complex, incompletely resolved multiplet for the CH_2 group, strongly suggesting that this polymer is primarily isotactic.

The x-ray diffraction diagram of sample 8I consisted of many relatively sharp lines, indicative of a highly ordered polymer. Analysis of the pattern showed lattice spacings which correspond to those reported by Okamura et al.[3] for poly(methyl vinyl ether), and are consistent with those published by Natta and co-workers[11] for isotactic poly(isobutyl vinyl ether). As might be expected, the diffraction pattern for sample HS was typical of a much less ordered polymer; some of the lines in the pattern for 8I were faint but discernible in the HS diagram. Thus the implications of the x-ray data are confirmed by the proton resonance results.

If it is assumed that the growing polymer chain has a given probability σ that it will add a monomer unit to give the same configuration as that of the last unit, then the fractions P of the three possible triads are given by

$$P_i = \sigma^2$$

$$P_h = 2(\sigma - \sigma^2)$$

$$P_s = (1 - \sigma)^2$$

where the subscripts i, h, and s refer to isotactic, heterotactic, and syndiotactic, respectively.[5] It is then necessary to assign the methoxyl peak at lowest field, in nitromethane solution, to the syndiotactic species. The experimental results, along with calculated values based on a single σ value, are given in Table I. The agreement is reasonable considering that the peaks were insufficiently resolved to measure areas, and relative peak heights were used. The difference between calculated and observed values for P_h and P_s is always in the direction which would be expected if the shoulder, which is the syndiotactic peak, were actually less than measured. Partial overlap of the peaks will cause such an error. It there-

TABLE I

Properties of Some Poly(methyl Vinyl Ethers)

Sample	Nature	Measured				Calculated		$[\eta]_{30°C.}$ in nitromethane, dl./g.	Molecular weight $\times 10^{-4}$[a]
		P_i	P_h	P_s	σ	P_h	P_s		
1	Slightly tacky and rubbery, form stable	0.54[b]	0.34	0.12	0.74	0.40	0.06	—	—
3	Tacky, translucent, not form stable	0.41	0.37	0.22	0.64	0.46	0.13	—	—
5S	Tacky, semiliquid	0.43[b]	0.35	0.22	0.66	0.44	0.13	—	—
6	Tacky, very viscous liquid	0.44	0.38	0.18	0.66	0.44	0.12	0.144	0.84
8I	White, crystalline solid	1	—	—	1	—	—	0.085	0.63
HW	Rubbery solid	0.66	0.25	0.09	0.81	0.30	0.04	3.95	23
HI	Rubbery solid	—	—	—	—	—	—	3.37	20
HS	Rubbery, noncrystalline	0.47	0.35	0.18	0.68	0.42	0.11	2.51	15

[a] An estimate based on the value found for sample 6 in benzene solution where $[\eta]_{30°C.} = 0.172$ and hence MW = 0.84×10^{-4}.

[b] Determined in carbon tetrachloride solution; the others were measured in nitromethane solution.

fore seems likely that the peak assignments are correct and that a single σ can be used to describe the polymerization.

Changing the solvent has been observed to alter the peak separations in poly-(α-methylstyrene),[6] polystyrene,[7] poly(methyl methacrylate),[12] and polyisoprene.[13] In Figure 2 the effect of various solvents on the methoxyl resonance of poly(methyl vinyl ether) is shown. Only in an appropriate solvent is it possible to distinguish the three peaks. Unfortunately peak separations are so small that a significantly higher magnetic field would be required to study this phenomenon.

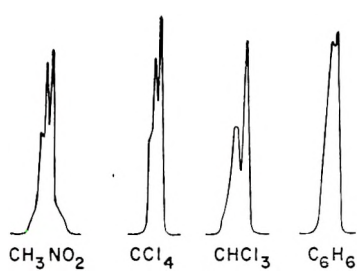

Fig. 2. Solvent effects on the methoxyl resonance.

Table I shows the large differences in the form and in the molecular weight of the polymers that were studied. They range from the balsam-like product, presumed to be amorphous, to the higher molecular weight, crystalline Hercules sample resulting from a highly stereospecific catalyst. Treatment of the latter polymer with hot methanol resulted in some degradation as well as in a separation on the basis of differences in stereoregularity, and hence in solubility. The degradation of the Hercules sample was apparent in the lowering of molecular weight and in the very broad proton resonance spectrum of the insoluble residue, HI. The original polymer, by comparison, gave moderately sharp lines. In the less highly regular samples degradation with time in the resonance cavity at 113°C. was visually obvious, by the appearance of a yellow to brown color, and in the proton resonance spectra by the disappearance of the syndiotactic methoxyl peak and a slight broadening of the remaining peaks. These results suggest that the polymer chain is more susceptible to degradation at a syndiotactic unit.

The solubilities in nitromethane (or other common solvents) of the polymer described above decreases in the order of increasing isotacticity which, as it happens, is not related to any particular trend in molecular weight. Evidently stereoregularity is far more important in determining solubility than is a nearby fortyfold difference in molecular weight. It is interesting that sample 8I, which has the lowest molecular weight exhibits the highest isotacticity even though it was prepared with a soluble Friedel-Crafts catalyst.

The authors are grateful to Dr. D. S. Breslow of the Hercules Powder Company for the gift of a poly(methyl vinyl ether) sample, to Dr. L. D. Calvert for measuring the x-ray diagrams, and to Mr. P. E. Black for technical assistance.

References

1. Schildknecht, C. E., S. T. Gross, and A. O. Zoss, *Ind. Eng. Chem.*, **41**, 1998 (1949).
2. Schildknecht, C. E., A. O. Zoss, and F. Grosser, *Ind. Eng. Chem.*, **41**, 2891 (1949).
3. Okamura, S., T. Higashimura, and H. Yamamoto, *J. Polymer Sci.*, **33**, 510 (1958).
4. Vandenberg, E. J., R. F. Heck, and D. S. Breslow, *J. Polymer Sci.*, **41**, 519 (1959).
5. Bovey, F. A., and G. V. D. Tiers, *J. Polymer Sci.*, **44**, 173 (1960).
6. Brownstein, S., S. Bywater, and D. J. Worsfold, *Makromol. Chem.*, **48**, 127 (1961).
7. Brownstein, S., S. Bywater, and D. J. Worsfold, *J. Phys. Chem.*, **66**, 2067 (1962).
8. Breslow, D. S., Hercules Powder Company, private communication.
9. Manson, J. A., and G. J. Arquette, *Makromol. Chem.*, **37**, 187 (1960).
10. Tincher, W. C., American Chemical Society Polymer Symposium, Atlantic City, September, 1962.
11. Natta, G., I. Bassi, and P. Corradini, *Makromol. Chem.*, **18/19**, 455 (1956).
12. Brownstein, S., and D. M. Wiles, unpublished results.
13. Chen, H. Y., *Anal. Chem.*, **34**, 1793 (1962).

Résumé

On a polymérisé l'éther méthyl vinylique au moyen du catalyseur BF_3-éther dans differentes conditions afin d'obtenir des polymères de poids moléculaires et de tacticités différentes. On compare quelques propriétés de ces polymères avec celles d'un échantillon préparé avec un catalyseur spécial stéréorégulier de la Hercules Powder Company. On a étudié le spectre de résonance magnétique du proton du poly(méthyl vinyl éther) dans plusieurs solvants et on a attribué les absorptions des protons méthoxyliques aux configurations stériques particuliéres de la chaîne polymérique. On a employé ces résultats pour comparer les tacticités des différentes échantillons de polymères et pour établir qu'un bon contrôle stérique dans la réaction de propagation est possible avec un catalyseur soluble BF_3-éther.

Zusammenfassung

Methylvinyläther wurde mit BF_3-Ätherat als Katalysator unter verschiedenen Bedingungen zu Polymeren mit unterschiedlichem Molekulargewicht und Taktizität polymerisiert. Gewisse Eigenschaften dieser Polymeren wurden mit denjenigen einer Probe verglichen, die bei der Hercules Powder Company mit einem speziellen stereoregulierenden Katalysator hergestellt wurde. Die magnetischen Protonenresonanzspektren von Poly(methylvinyläther) in verschiedenen Lösungsmitteln wurden untersucht und es gelang, die Absorption durch die Methoxyl-Protonen besonderen sterischen Konfigurationen der Polymerkette zuzuordnen. Diese Daten wurden zum Vergleich der Taktizität der verschiedenen Polymerproben herangezogen. Dabei wurde gefunden, dass mit einem löslichen BF_3-Ätherat als Katalysator gute sterische Kontrolle der Wachstumsreaktion möglich ist.

Received March 20, 1963

JOURNAL OF POLYMER SCIENCE: PART A VOL. 2, PP. 1909–1924 (1964)

Viscoelastic Behavior of Plasticized Polyvinyl Chloride at Large Deformations. III. The Effect of Filler*

RAFFAELE SABIA† and F. R. EIRICH, *Department of Chemistry, Polytechnic Institute of Brooklyn, Brooklyn, New York*

Synopsis

The behavior of filled and plasticized samples is similar in many ways (such as creep, critical strain for the onset of a permanent deformation, etc.) to plasticized polyvinyl chloride. The presence of small amounts of $CaCO_3$ as filler was found to result in improved mechanical response, while high amounts produced stiffening effects of the nature of an inert filler. At larger deformations, the polymer ceases to wet the filler and the volume of the filled resin increases with strain by crazing, the more so the more highly filled. Filler wetting by the resin is influenced by plasticizer content. In stress relaxation, the dewetting time, very short for the highly filled samples, increases appreciably with decreasing filler content while depending at the same time on plasticizer content. Because of this, equilibrium and delayed moduli increase with filler content at low strain and decrease variously at higher strain.

INTRODUCTION

Conventionally, plasticizers are used to lower the glass transition temperature of organic rubbers. Fillers, on the other hand, are employed[1] to raise the modulus, tear strength, and abrasive strength. A theory capable to account for all aspects of filler action is not yet available.[2,3] A partially satisfactory account of the increase in modulus has been secured through the adaptation of the theory of flow of disperse systems, especially one consisting of rigid spherical inclusions, to an elastic medium[4]

$$M = M_0 (1 + 2.5 \phi + 14.1 \phi^2) \quad (1)$$

where ϕ is the volume fraction of filler and M_0 is the modulus at zero concentration.

The stress relaxation of reinforced rubber consists[5] of (*a*) orientation of chain units (10^{-3}–10^{-6} sec.), (*b*) regrouping and slippage of segments (minutes), (*c*) regrouping of crosslinks and chain scission (months), and (*d*) separation of filler particles from rubber chains. At 100% deformation

* This work comprises a portion of a thesis presented by Raffaele Sabia in partial fulfillment of the requirements for the degree of Doctor of Philosophy at the Graduate School of the Polytechnic Institute of Brooklyn.

† Present address: Bell Telephone Laboratories, Murray Hill, New Jersey.

and zero time the modulus increases with chalk content X; the modulus after 1500 min. of relaxation depends irregularly on X; the modulus obtained by extrapolation of the linear part of the relaxation curve (ranges from 100 to 1500 hr.) back to zero time is independent of X. The "relaxation time" for mechanism d, which might better be called a separation time, is about as large as the relaxation time of b but shorter than that of c. Hence chalk is termed an inert filler. In the case of active fillers (channel black), all three moduli increase with filler content, and the separation time for mechanism d is of the same order as the relaxation time for c and much greater than for b.

Turning to filler adherence, at small strains the resin wets the filler and reinforces the system. As the strain increases, adhesives bonds begin to break (dewetting) and vacuoles form around the filler particles. After all the adhesive bonds are broken, the vacuoles enlarge and the resin stretches further.

Smith[6] has studied the dewetting of glass beads in the system polyvinyl chloride–dioctyl sebacate (PVC–DOS). If an elastic parallelopiped is deformed at constant volume V,

$$\lambda_1 \lambda_2 \lambda_3 = V/V_0 = 1 \tag{2}$$

where the subscripts correspond to the dimensions of length, width, and thickness, respectively; λ is the ratio of the strained to the unstrained dimension. Since in tension $\lambda_2 = \lambda_3$

$$\log \lambda_2/\log \lambda_1 = -1/2 \tag{3}$$

which represents Poisson's ratio in terms of the Hencky strain and is applicable to large deformations. It becomes the conventional Poisson ratio for small values of λ. Any change in slope from one-half is taken as an increase in volume and a new constant slope is taken to indicate completion of the dewetting process. Smith reports that the critical strain for the start of the dewetting process increases with temperatures. The ratio of $\log \lambda_2/\log \lambda_1$, after dewetting is completed, is independent of temperature. This latter behavior is explained by postulating that, after dewetting is completed, further stretching enlarges only the size of the vacuoles around the filler particles. As the filler content increases, the critical strain for dewetting decreases.

EXPERIMENTAL

Sample preparation of unfilled plasticized PVC was discussed in detail in a previous paper.[7] The formulations used are listed in Table I. The lot of Bakelite QYSQ resin is the same as the one used before. The plasticizers are tricresyl phosphate (TCP) and dioctyl adipate (DOA). Calcium carbonate is the filler. Unfilled samples used for comparison were made up of the same composition. Thus, TCP-20 corresponds to compositions A–C with 20 parts of plasticizer used for every 100 of resin and the same

TABLE I

Formulation of Filled Samples

		Parts by weight														
	gravity	A	B	C	D	E	F	G	H	I	J	K	L	M	N	O
QYSQ	1.40	100	100	100	100	100	100	100	100	100	100	100	100	100	100	100
TCP	1.16	20	20	20	40	40	40							60	60	60
DOA								20	20	20	40	40	40			
Mark-XI	1.22	3	3	3	3	3	3	3	3	3	3	3	3	3	3	3
Mark-XX	1.5	1.5	1.5	1.5	1.5	1.5	1.5	1.5	1.5	1.5	1.5	1.5	1.5	1.5	1.5	1.5
Atomite[a]	2.70	27.7	62.3	166.3	32.9	74.1	196.7	29.0	65.3	174.1	35.5	79.9	211.5	38.1	85.6	228.4
Filler volume, %		10	20	40	10	20	40	10	20	40	10	20	40	10	20	40
Filler weight, %		18.3	33.3	57.2	18.5	33.8	57.7	18.9	34.4	58.3	19.7	35.6	59.4	18.8	34.2	58.2

[a] Atomite is pure calcium carbonate supplied by Thompson Weinman, 0.5–10μ in size with a mean diameter of 2.5 μ.

applies to TCP-40, TCP-60, DOA-20, and DOA-40. In the text, any references to the series A–O are accompanied by the filler content such as A-10, B-20, and C–40.

RESULTS

A. Stress Relaxation

All experimental work was done at 50°C. employing the TCP samples. The data were analyzed in exactly the same manner as those for the unfilled samples discussed in our previous paper.[7] In review, the relaxation of PVC was represented by a model consisting of three Maxwell elements and one spring.

$$G(t) = Ge + G_1e^{-t/\tau_1} + G_2e^{-t/\tau_2} + G_3e^{-t/\tau_3} \tag{3}$$

where G_i and τ_i represent the shear modulus and relaxation time, respectively, and t is the time. After 90 min., the third element has relaxed only a small percentage and was assumed not to have deformed at all. The stress values of $(S_e + S_3)$, the elastic stress S_1 and S_2, the delayed stresses, are reported in Table II. The relaxation time τ_2 (independent of strain) is also reported. τ_1, in case of unfilled samples,[7] appeared independent of the variables listed and averaged about 110 sec.; the data on filled samples indicated the same relaxation time.

The values of $(S_2 + S_3)$, S_2, and S_1 were plotted versus the strain according to the theory of rubber elasticity. It is to be expected that, as long as the stress is proportional to the strain, no dewetting occurs while any curvature toward a lower modulus indicates dewetting.

Analyzing all of the $(S_e + S_3)$ curves, we found that in the range of the deformations employed, and within our experimental times, A-10 is the only formulation which shows no dewetting; the corresponding formulations (10% filler) at higher plasticizer content, D-10 and M-10, show dewetting at the higher strains. When dewetting occurs, in analogy to the work of Bartenev and Vishnitskaya[5] discussed in the introduction, we see that the separation times for dewetting are equal to, or less, than τ_2 but much smaller than τ_3.

Looking at the S_2 plots we see that the separation times for dewetting of the B-20 formulation is of the same order as τ_2 and greater than τ_1. From the S_1 plots the separation time for dewetting of the D-10 and E-20, M-10, and N-20 compositions is seen to be of the same order as τ_1.

The samples C-40, F-40, and O-40 with the highest filler content are of great interest. In these cases, the data show that the separation time for dewetting is shorter than τ_1, i.e., for all practical purposes, instantaneous. This is most revealing in view of the fact that the same samples show an S-shaped behavior in the strain–log time creep curves, to be discussed below.

B. Creep

Reviewing briefly, plasticized polyvinyl chloride has been found to undergo a permanent deformation when strained over 100%.[8] At comparable strains, it was also found that the internal energy, as reflected in the stress–strain curves, begins to rise. Plasticizer efficiency has been evaluated in several respects, namely rubberlike behavior, recovery, glass

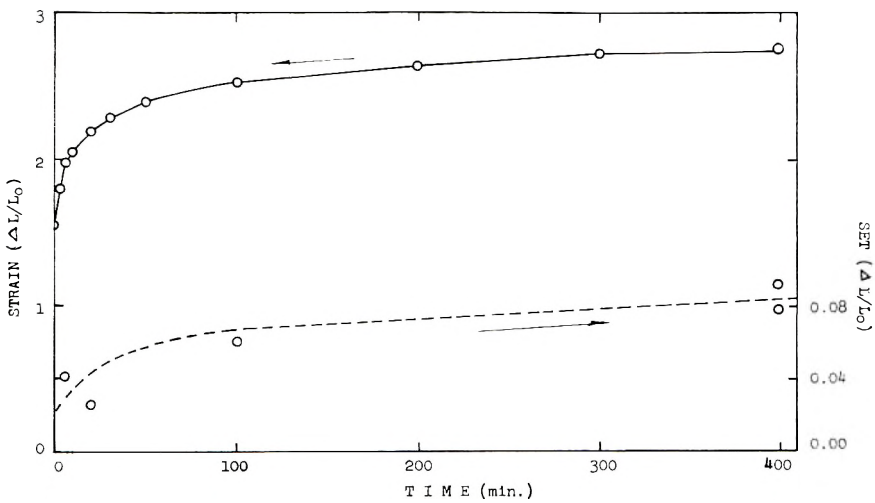

Fig. 1. Creep and set under constant load of E-20, 50°C.

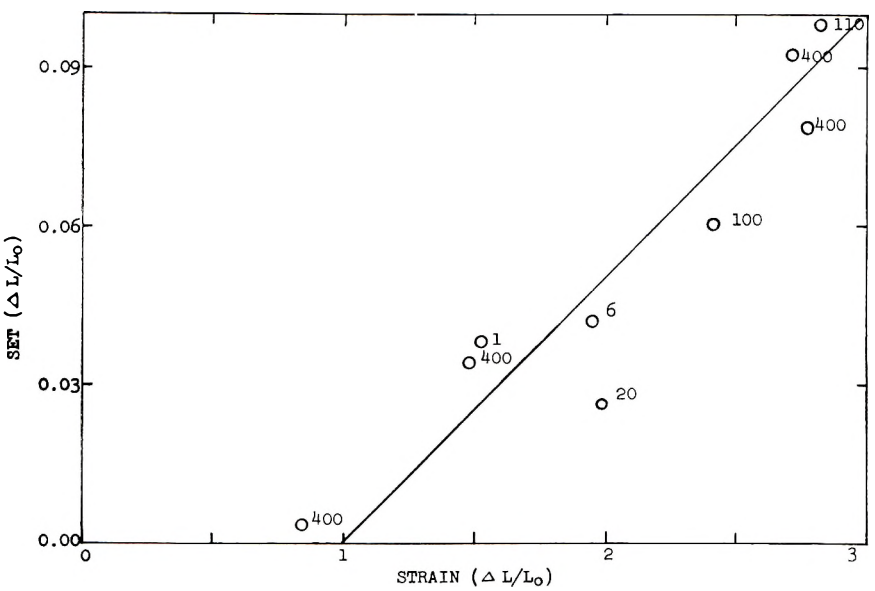

Fig. 2. Set vs. strain of E-20, 50°C., under different loads and different times (in minutes) as shown by numbers. Smaller times at the same strain represent higher loads.

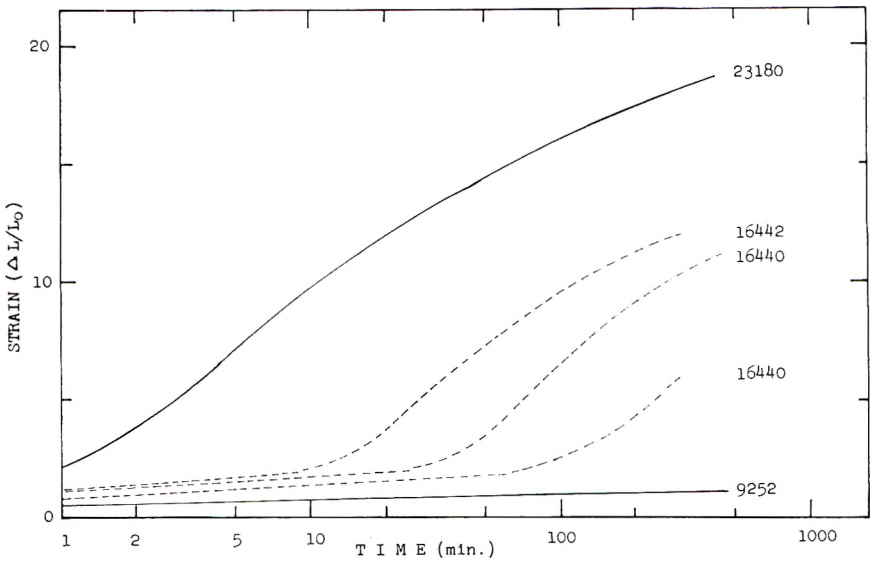

Fig. 3. Creep of highly filled samples F-40 under varying loads (in grams per square centimeter) as indicated.

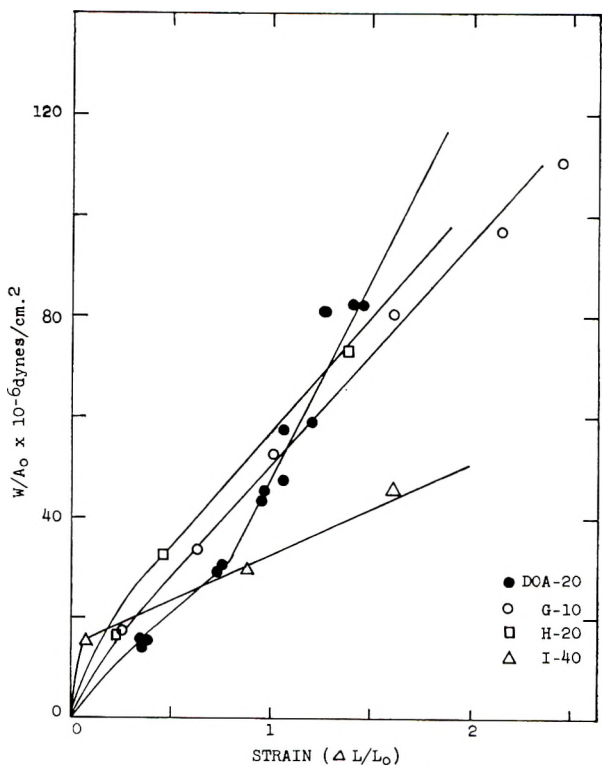

Fig. 4. Stress–strain at 400 min., 50°C.

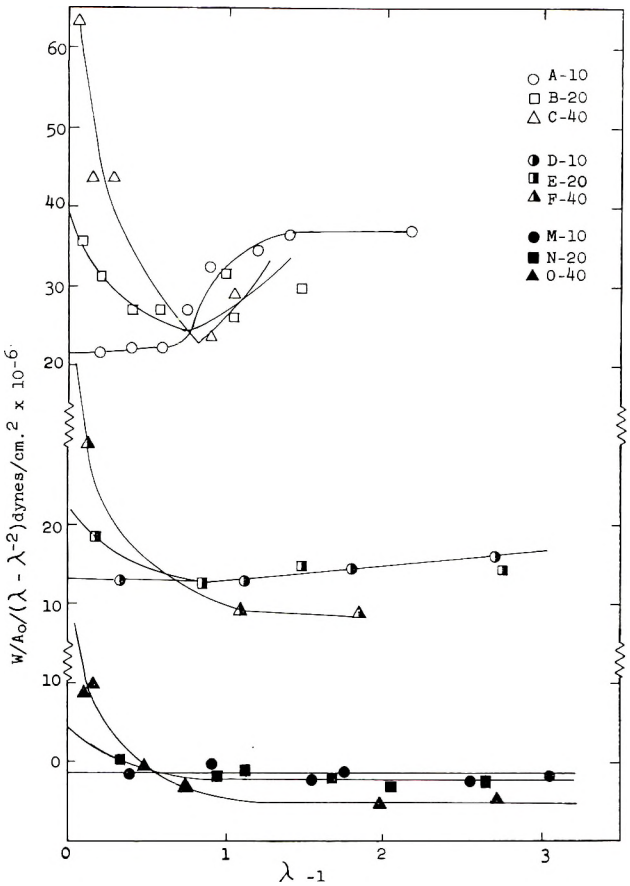

Fig. 5. Modulus at 400 min. vs. deformation of TCP-plasticized resins, 50°C.

transition, set, and stress–strain at break. No single plasticizer was outstanding. Of the plasticizers employed, DOA was found to be better than TCP with respect to the first four aspects listed above.

Filled samples behave in a similar manner. In view of our results with unfilled samples,[8] the creep time was limited to 400 min. As in the case of unfilled samples, the creep curves of the filled samples, before dewetting occurs, were not greatly differentiated (except for some cases to be discussed below) indicating that the relaxation times are independent of filler content and similar to the ones of the unfilled specimens. A typical plot is shown in Figure 1 in which we have also indicated set (permanent deformation) as a function of time.

A plot of set versus final deformation under condition of (*a*) constant load and varying time, and (*b*) constant time and varying load is shown in Figure 2 where the time of load removal is indicated to the right of each point. The data show that the set increases with the time but at an ever decreasing rate. All data fall on the same set curve indicating that the set is a func-

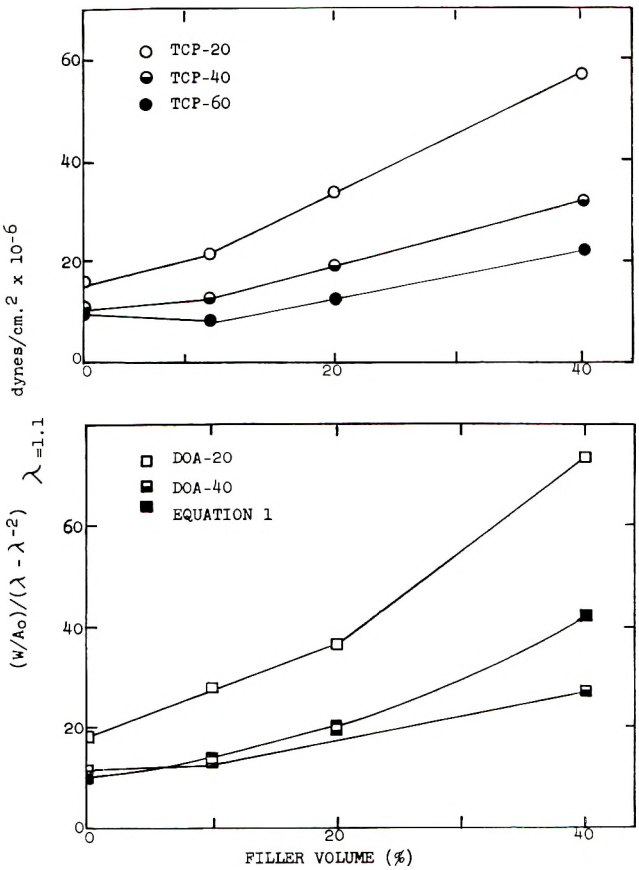

Fig. 6. Modulus at very small strains vs. filler content, 50°C.

tion of the strain. The set of filled samples approaches zero for strain values of 1.0 or less, as in the case of unfilled samples.

The influence of the amount of filler on the extent of set is not very clear. For DOA, the set drops for 10% filler and then rises toward that of the unfilled samples. For TCP, the set of the filled samples is larger with little dependence on the filler concentration.

Plotting the strain versus log time, our creep curves approximate straight lines except for the samples with the highest filler content. For these, Figure 3, accelerations of strain rates occurred at times which decreased with the stress level. Smith and Landel[9] made similar observations but did not report maxima of the strain rate (inflection of our curves) possibly because they encountered early breaks. The sharp increase in the strain rate was visually accompanied by a whitening of the samples which in turn signified the beginning of set. Similar results are obtained for compositions C-40, F-40, I-40, L-40, and O-40. In as much as whitening, rise of strain rate and set are increasing functions of the plasticizer percentage at con-

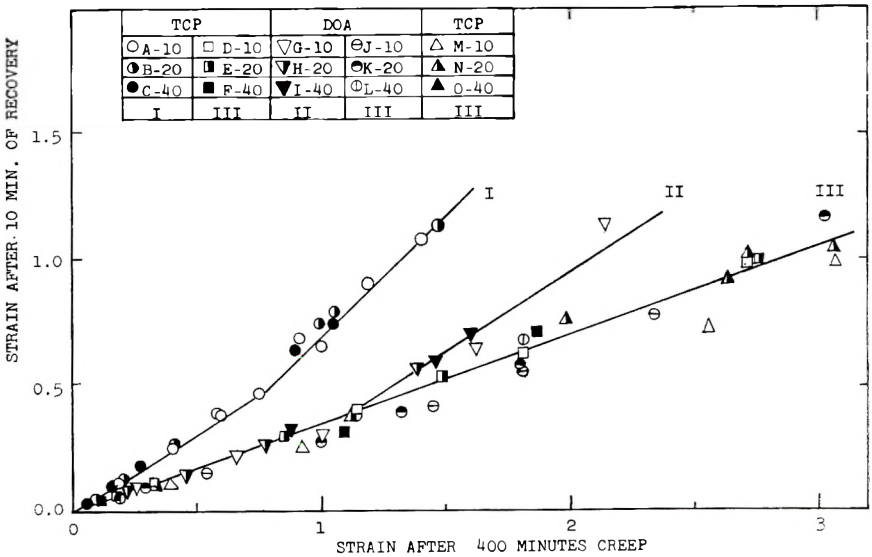

Fig. 7. Per cent creep recovery after 10 min., 50°C.

stant filler content, it follows that the filler is not only wetted by the polymer but also by the plasticizer. The fewer the bonds between polymer and filler, the earlier will dewetting be completed.

Figure 4 shows the strain–stress curves at 400 min. for some filled samples and an unfilled one for comparison. The addition of filler gives initially an increase in modulus for the lower strains but the curves cross at high strains due to the onset of dewetting.

An interesting light on the mechanism of deformation is cast by plotting the data according to the theory of rubber elasticity. For some filled samples, the data at 400 min. are shown in Figure 5. The initial moduli increase with filler content. At small strain, the moduli of the least filled samples remain constant while those of the others drop rapidly.

In Figure 6, we see the moduli at a strain of 0.15 plotted against filler content. This lowest measured strain was employed rather than values at zero strain in order to avoid uncertainties of extrapolation. The shape obtained is that attributed to inert fillers.[1] The drop of moduli for the highly filled samples as the strain increases, as seen from Figure 6, is taken as a sign of dewetting.

In Figure 7, we have plotted the remaining strain (following 400 min. of creep) after 10 min. of strain recovery against the final strain before unloading. It is seen that the filled resins containing 20 parts of TCP show the slowest recovery, while DOA is much better in this respect. DOA with 20 parts of filler actually shows an improvement over the unfilled case reported previously. In this instance, as with unfilled samples, there is hardly any difference between compositions containing 40 and 60 parts of plasticizer.

We have held TCP-20, A-10, B-20, and C-40 also under constant load while slowly increasing the temperature from 20°C. Plotting the cathetometer reading versus the temperature, the resulting strain remained constant at first and then started to increase at an ever increasing rate. The temperature at which this occurred was 37°C. for all samples; i.e., the glass temperature was independent of filler content.

C. Volume Changes

At room temperature, DOA-20 with 20 and 40% filler, respectively, shattered as the samples were deformed even by small amounts, DOA with 10% filler underwent considerable deformation before breaking and generally behaved like an unfilled sample, even up to the critical strain where the increase in volume begins. On the other hand, the TCP samples showed dewetting even at 10% filler, as shown in Figure 8. As found by Smith,[6] the critical strain for dewetting goes up with temperature. Similar agreement

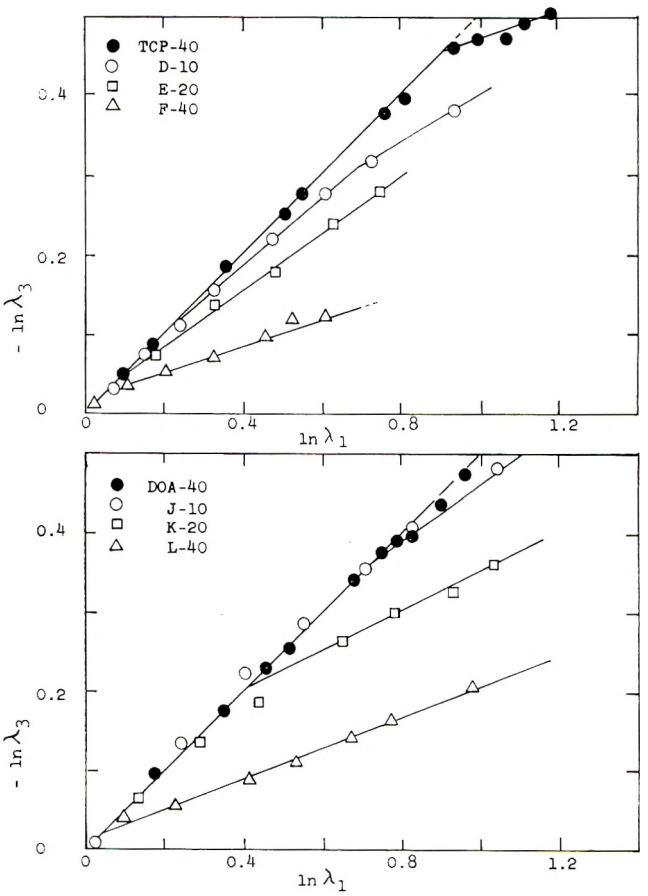

Fig. 8. Variation with thickness and length during extension.

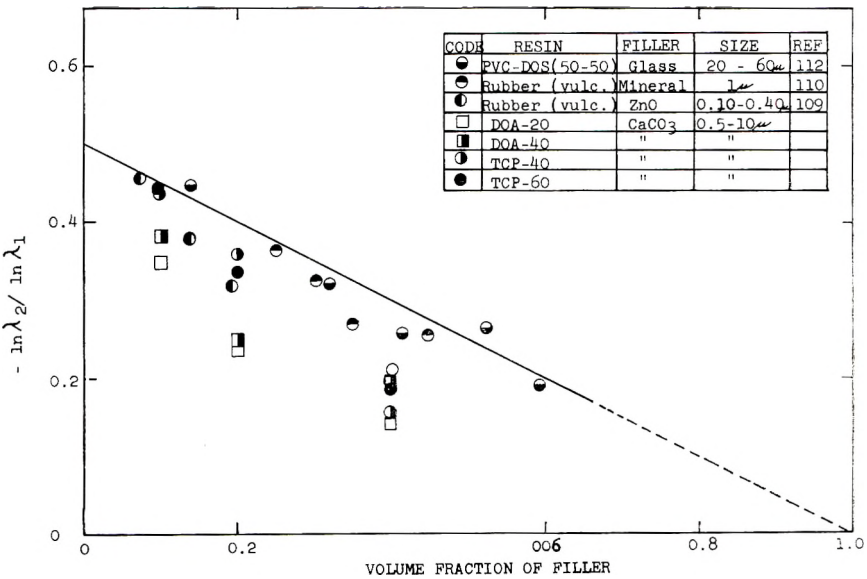

Fig. 9. Variation of $\ln \lambda_2 / \ln \lambda_1$ for several filled systems after dewetting.

is obtained if the ratios $\log \lambda_2 / \log \lambda_1$ from the slopes after dewetting are plotted versus the volume fraction (Fig. 9), showing increasing volume expansion.

DISCUSSION

In stress relaxation, the first effect of the filler to be noted is the expected stiffening of the modulus with plasticizer content. Next, also the delayed modulus is increased as long as dewetting does not occur. We have shown that the separation time for dewetting at a critical strain in highly filled samples is very short. This result may be better understood in the light of creep curves of highly filled samples, below, which showed an increase in strain rate at the onset of dewetting (Fig. 3).

The relaxation data in Table II can be plotted as stress–strain curves to show the process of dewetting as a function of filler and plasticizer content. Apart from the expected intensification of dewetting with filler concentration, it is of interest that dewetting increases also with plasticizer concentration. In other words, the plasticizer reduces the resin-filler adherence. It should be noted that the crossover of the relaxation curves at high deformation, when the apparent moduli of samples which dewet fall below those where little or no dewetting occurs, finds its counterpart in creep tests.

In creep, the curves of the 10% filled samples are similar in all aspects to those of the unfilled ones. In the cases of more highly filled samples, anomalous behavior was obtained in the form of S-shaped curves (elongation versus log time). The linear viscoelastic behavior, as represented by the

TABLE II

Stress Relaxation Data[a]

Formulation	$S_1 \times 10^{-6}$, dynes/cm.^{2}				$S_2 \times 10^{-6}$, dynes/cm.^{2}				$(S_e - S_3) \times 10^{-6}$, dynes/cm.^{2}				τ_2, sec.
	λ_1	λ_2	λ_3	λ_4	λ_1	λ_2	λ_3	λ_4	λ_1	λ_2	λ_3	λ_4	
A		7.40	10.00	12.15		2.40	3.55	4.50		6.28	8.85	10.97	1678
B	5.60	7.90	11.30	12.75	1.90	2.70	4.00	4.50	5.48	7.62	9.34	10.38	1680
C	6.70	8.90	10.00	13.00	2.15	2.90	3.90	5.40	6.40	7.85	9.66	11.10	1800
D	2.15	3.00	4.20	5.15	1.45	1.95	2.30	2.60	4.03	5.61	7.45	8.03	1758
E	3.30	4.15	5.50		1.70	2.10	2.80		5.12	6.70	7.82		1735
F	3.70	5.05	6.30		2.00	2.35	2.20		5.65	6.97	7.42		1800
M	1.43	2.05	2.93	3.25	0.85	1.25	1.58	1.75	2.44	3.71	4.78	5.33	1800
N	1.83	2.70	3.65	4.90	1.13	1.30	1.75	2.10	3.17	3.99	4.73	5.90	1800
O	2.73	4.23	3.65	3.75	1.25	1.30	1.60	1.55	4.04	5.16	4.54	5.16	1800

[a] Values for $\lambda_1 = 1.105$, $\lambda_2 = 1.201$, $\lambda_3 = 1.295$, $\lambda_4 = 1.383$.

stress independence of the 400 min. modulus of Figure 5, is limited to a very small strain and is followed by more complex behavior due to dewetting, as mentioned already above in the case of stress relaxation.

The stiffening effect shown in Figure 6 is that of an inactive filler,[1] and the curves even stay below the values given by eq. (1). In Figure 4, the moduli of filled samples as a function of the strain are seen at large deformations to drop below those of the unfilled samples, decreasing with increasing filler content, again in agreement with the relaxation behavior. Oddly, after the completion of the dewetting, the "rubber-elastic" behavior, i.e., independence of modulus on strain (Fig. 5), is improved and the modulus constancy better than in the case of the unfilled samples.[8]

The volume measurements of unfilled samples at room temperature[8] had shown pronounced increases in volume in the cases of the less plasticized samples and we attributed this to plasticizer–polymer demixing on account of the whitening of the samples which may be taken as a phase separation phenomenon. This becomes less and less pronounced when the samples are repeatedly annealed before stressing. Eventually, the volume increase all but disappears. Therefore, we attribute these phenomenon to an initially incomplete plasticizer–polymer dispersion which, in the process of sample stretching, allows local swelling pressures to vary with respect to areas of different degrees of orientation, densities, and local deficiencies of plasticizer and thus to enhance polymer crazing. It fits into this picture that at 50 °C. the phenomenon was not observed except immediately before break of the samples at very high elongation, while at 75 °C. the whitening was not observed at all. The phenomenon disappears also at high plasticizer contents.

In the case of filled resins, the critical strain for initiation of dewetting is found to increase with temperature, to decrease with filler content, and to be dependent on the nature and concentration of the plasticizer. We have plotted, in Figure 9, the slope of the lines, such as in Figure 8, after dewetting, i.e., extent of volume change with degree of extension, versus filler content. Assuming that in the case of complete wetting the dewetting behavior should be given by the solid line, it is seen that most cases fall below the line, the more so as the resins become stiffer either due to less plasticization or to a higher degree of vulcanization. We conclude that the values of these deviations occur because the resins are too stiff to wet the filler completely even in the unstressed case, i.e., vacuoles exist in the absence of any strain history. On deforming even a small amount, these vacuoles begin to increase in size and are accompanied by actual dewetting.

As dewetting occurs, the strain rates at constant load increase and go through a maximum in the case of highly filled samples (Fig. 3). Annealing did not immediately restore the polymer–filler bonds, since repeat runs exhibited dewetting sooner. On the other hand, the degree of dewetting as reflected by an increase in the compliance is again dependent on the amount of plasticizer and, in addition, seem to be independent of plasticizer type.

It is generally reported in the literature that the deformation at break decreases with filler content. We found this to be true for 20 and 40% of filler, but for the samples containing 10% filler the deformation at break is equal to, if not greater than, that of the unfilled specimen. Furthermore, formulation A-10 did not break during deformation at room temperature, while TCP-20 and formulations B-20 and C-40, all with the same plasticizer–resin ratio, shatter. This is surprising. One would expect the modulus and the internal viscosity to increase smoothly with filler content and the composite to become more brittle. The 10% filled resin does not fulfill this expectation. Similarly, the modulus-filler curve does not rise immediately with concentration (Fig. 6). Corresponding observations of an actual dip of modulus with small amounts of filler have been reported in the literature.[10] Data by Ghersa[11] show that presence of filler can counteract the modulus rise by low plasticizer additions. We interpret this as plasticizer adsorption.

In addition to modulus changes, we find that low filler content leads to effects opposite those at high content even at high plasticizer percentages and also with respect to deformation, and thus exhibits a general plasticizing action. To understand this, one has to remember that in plasticized, filled systems the resin, as well as the plasticizer, tends to wet the filler. Plasticizer–filler bonds are not expected to break on deformation. This may be deduced also from the creep curves of the highly filled samples. The nature and concentration of the plasticizer therefore will affect the nature and extent of resin–filler wetting including the critical strain for initiation of resin-filler dewetting.

It may be assumed that plasticizers act in two ways, at first assisting resin recrystallization, raising the modulus beyond the dilution effect, and later lowering the modulus by dilution. Fillers act in three ways: by replacing low modulus with high modulus domains, by deranging the resin microstructure and thus counteracting the first effect, and by hindering segment rotation raising the modulus again. With increasing filler, these effects will become important in the mentioned order. In the simultaneous presence of filler and plasticizer, and in view of the adsorption triangle just mentioned, one should expect that the two plasticizer and the three filler effects will counteract each other in all phases, and this is indicated by the data just described as well as by the apparent independence of the glass transition temperature on filler content mentioned earlier.

CONCLUSION

The presence of filler does not change the nature of the mechanical behavior of plasticized PVC basically but adds two interesting features. Small amounts of filler (10% by volume) act almost like additional plasticizer in that the moduli are lowered and the extensions at break are increased which is opposite to the effect of higher amounts of filler. This phenomenon may be attributed best to competition between plasticizer and

filler effects on the resin, and to adsorptive competition between resin and plasticizer for the filler.

At higher filler concentrations, the stiffening effects outweigh all others. Further volume increases are found at all but small deformations. These increases must be attributed partly to filler-resin dewetting and the concomitant formation of vacuoles, but also to crazing in the resin itself starting from plasticizer or resin density inhomogeneities which persist on account of the difficulty to achieve perfect equilibrium blending. For the one filler studied here ($CaCO_3$), its presence in more than about 10% concentration reduces the range of response to mechanical straining as a homogeneous material and leads to rapid modulus, volume, and elongation changes at critical stresses. This might be avoided for fillers which exhibit stronger bonds to the resin.

We wish to express our gratitude to Congoleum Nairn Co. for financial support and for the preparation of samples.

References

1. Parkinson, D., in *Advances in Colloid Science*, Vol. II, H. Mark and G. S. Whitby Eds., Interscience Publishers, New York, 1946.
2. Bueche, F., *J. Polymer Sci.*, **24**, 189 (1957).
3. Bueche, F., *J. Polymer Sci.*, **33**, 259 (1958).
4. Guth, E., *J. Applied Phys.*, **16**, 20 (1945).
5. Bartenev, G. M., and L. A. Vishnitskaya, *Kolloid. Zh.*, **18**, 135 (1956).
6. Smith, T. L., *Trans. Soc. Rheology*, **3**, 113 (1959).
7. Sabia, R., and F. R. Eirich, *J. Polymer Sci.*, **A1**, 2497 (1963).
8. Sabia, R., and F. R. Eirich, *J. Polymer Sci.*, **A1**, 2511 (1963).
9. Landel, R. F., and T. L. Smith, paper presented at the 136th Meeting of the American Chemical Society, Atlantic City, N. J., September 1959.
10. Buchdahl, R., in *Proceedings of the Second International Congress on Rheology*, W. G. W. Harrison, Ed., Butterworths, London, 1953.
11. Ghersa, P., *Modern Plastics*, **36**, No. 2, 135 (1958).

Résumé

Le comportement d'échantillons contenant des charges est trouvé semblable en maints aspects (tels que le fluage, le tension critique pour l'apparition d'une déformation permanente) au chlorure de polyvinyle plastifié. On a trouvé que la présence de faibles quantités de $CaCO_3$ comme charge amenait une réponse mécanique améliorée tandis que de grandes quantités produisent des effets de rigidité dus à la nature d'une charge inerte. Lors de déformations plus grandes, le polymère cesse de mouiller la charge et le volume de la résine chargée augmente avec la tension lors de la rupture, d'autant plus que la charge qu'elle porte sera plus importante. La trempe des charges par le résine est influencée par le contenu en plastifiant. Lorsque la tension diminue, le temps de détrempage, très court pour des échantillons hautement cargés, augmente de manière appréciable avec la décroissance du contenu en charge car il dépend en même temps du contenu en plastifiant. De ce fait, le module à l'équilibre et le module retardé augmentent avec le contenu en charge à faible tension et décroissent à des tensions plus fortes.

Zusammenfassung

Das Verhalten von Füllstoffe enthaltenden Proben ähnelt in vielen Beziehungen (wie Kriechen, kritische Dehnung für das Einsetzen einer permanenten Deformation usw.) weichgemachtem Polyvinylchlorid. Die Anwesenheit kleiner Mengen $CaCO_3$ als Füllstoff führt zu verbessertem mechanischen Verhalten, während grosse Mengen ähnlich einem inerten Füllstoff zu grösserer Starrheit führt. Bei grösseren Deformationen benetzt das Polymere den Füllstoff nicht mehr und das Volumen des Füllstoff enthaltenden Harzes nimmt beim Dehnen auf Grund von Rissbildung zu, u.zw. um so mehr, je mehr Füllstoff es enthält. Der Weichmachergehalt beeinflusst die Benetzung des Füllstoffes durch das Harz. Bei der Spannungsrelaxation nimmt der Zeitbedarf zum Aufhören der Benetzung, der für Proben hoher Füllstoffgehaltes sehr klein ist, mit abnehmendem Füllstoffgehalt merklich zu, während er gleichzeitig vom Weichmachergehalt abhängt. Daher steigen Gleichgewichts- und Nicht-Gleichgewichts-Moduln bei geringer Dehnung mit dem Füllstoffgehalt an und sinken bei stärkerer Dehnung in verschiedener Weise ab.

Received March 21, 1963

JOURNAL OF POLYMER SCIENCE: PART A VOL. 2, PP. 1925–1940 (1964)

Polymer Formation through Diazonium Coupling*

A. RAVVE and C. FITKO, *Metal R & D Laboratories, Continental Can Company, Chicago, Illinois*

Synopsis

Polymers were prepared through coupling of bisdiazonium salts to polyphenols. Three different polyphenols were employed for this condensation with four aromatic diamines. Products were obtained with molecular weights ranging from below 2,000 to over 20,000. In three of the four condensations carried out, no loss of nitrogen was detected through the coupling reactions, but some nitrogen appeared to have been lost in the fourth case. All polymers obtained were dark in color. The polymers possessing *p*-hydroxy azo groups in their makeup occluded water which was held strongly.

INTRODUCTION

Polymers with azo groups are not new. The preparation of aliphatic polyazo compounds was reported by Hill in the formation of polyazines, polyhydrazonitriles, and polyazonitriles.[1] This was accomplished through the reaction of diketones with hydrazones to form polymeric azones, then further with HCN and oxidation to obtain polymeric azonitriles:

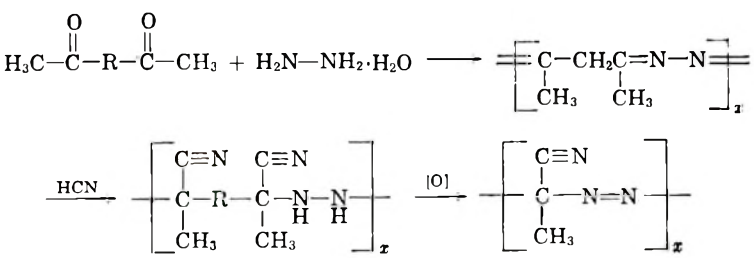

Berlin and co-workers[2] attempted the synthesis of polyaryls through the decomposition of bisdiazo salts by univalent copper. Elemental analysis of their products disclosed nitrogen, indicating that the hydrocarbon radicals tended to combine with diazo radicals with resultant partial inclusion of azo groups.

Work presented here describes, what appears to be the first attempt at polymer formation through use of diazonium coupling. Bisdiazonium salts were coupled to polyphenols:

* Presented in part at the 142nd National Meeting of the American Chemical Society, Atlantic City, N. J., September 1962.

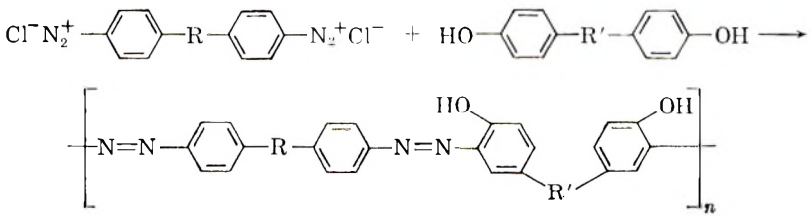

where R = CH_2, C_2H_4, SO_2, or none; R′ = CH_2, $(CH_3)_2C$, or none.

RESULTS AND DISCUSSION

It has been established that the diazonium coupling reaction with phenols involves an attack by the electrophilic substituting agent, ArN_2^+, upon the phenoxide ion.[4,5] This bimolecular reaction is one of condensation between the undissociated, polarized diazo group and the aromatic body in an activated state in which a hydrogen atom has acquired an induced positive charge.[6–9] Furthermore, the diazo group usually attached itself in the *para* position, though small amounts of *ortho* compounds are also known to form.[10] If, however, the *para* position is occupied, then the *ortho* position becomes the preferred point of attack. pH of the reaction medium is the single most important factor affecting the reaction. Coupling will occur most readily and completely in essentially neutral solutions. The diazonium ion becomes, however, quite unstable at neutrality. Such instability can be expected to have a chain terminating effect in a polymer growth. The nature of the phenolic material itself might also influence the extent of the chain growth. Three different polyphenols were used in this work to carry out condensations with four different amines. These condensations can be summarized as follows: (1) bisdiazonium salt of *p*-aminodiphenyl sulfone was coupled to a phenol–formaldehyde novolac, yielding polymer I; (2) bisdiazonium salt of *p*-aminodiphenylmethane was coupled to a phenol–formaldehyde novolac, yielding polymer II; (3) bisdiazonium salt of 1,2-di-*p*-aminophenylethane was coupled to 2,2′-di-*p*-hydroxyphenylpropane, yielding polymers III, IV, V, and VI; (4) bisdiazonium salt of *p,p*′-diaminobiphenyl was coupled to 3,3′-dihydroxybiphenyl, yielding polymers VII, VIII, and IX.

In the phenol–formaldehyde novolac, which is known to be a mixture of position isomers in polymer homologs, the unreacted phenol, probably present, could cause chain termination if it couples in one position only. This difficulty was not expected with the other phenols which were pure compounds. The *para* position in 2,2′-di-*p*-hydroxyphenyl propane is blocked, so we can expect *ortho* coupling only. In the 3,3′-dihydroxybiphenyl, on the other hand, both *para* and *ortho* positions are available, but, whereby the *para* position is preferred, steric hindrance could force greater *ortho* substitutions than should otherwise be expected.

The properties of the resulting polymers are summarized in Table I.

TABLE I

Condensation	Polymer	Elemental analysis					Softening point, °C.	Solubility	$\bar{M}_n$[a]	Appearance
		C, %	H, %	N, %	S, %	OH, %				
1	I			5.55	4.67		117–118	Ketones Aromatics	1700	Very dark red
2	II	74.22	5.22	8.23			Blackens above 280	Dimethylformamide, dimethyl sulfoxide	Unknown	Brown
3	III	76.38	6.85	5.15			45–47	Butanol, aromatics	450	Very dark red
3	IV	74.54	6.23	8.08			127–128	Hot butanol, aromatics, ketones	861	Very dark red
3	V	75.05	6.04	10.27			145–151	Aromatics, ketones, dioxane	1891	Very dark red
3	VI	74.60	5.90	10.59			190–195	Dimethylformamide	>20,000	Very dark red
4	VII	72.86	5.11	11.73		8.05	>300	Alcohols, dioxane	2885	Blue-black
4	VIII	72.71	4.91	11.38		7.00	>300	Dioxane, insol. alc.	9840	Blue-black
4	IX	72.60	4.85	11.70		7.40	>300	Insoluble in common solvent	Unknown	Blue-black

[a] The molecular weight determinations are accurate within ±10%.

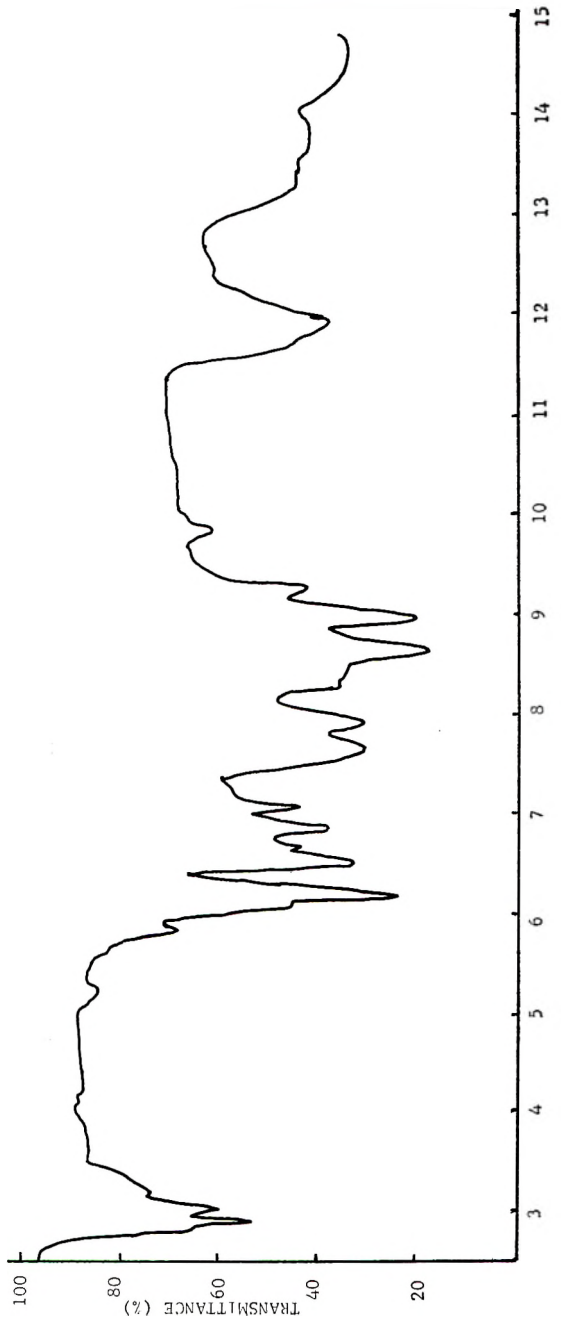

Fig. 1. Infrared spectrum of polymer I.

The products from the condensations were dark, ranging from red to brown to black. Their dilute solutions were orange.

Polymer I by combustion analysis was found to have a nitrogen:sulfur ratio of 1.18. This suggests that the structure might be:

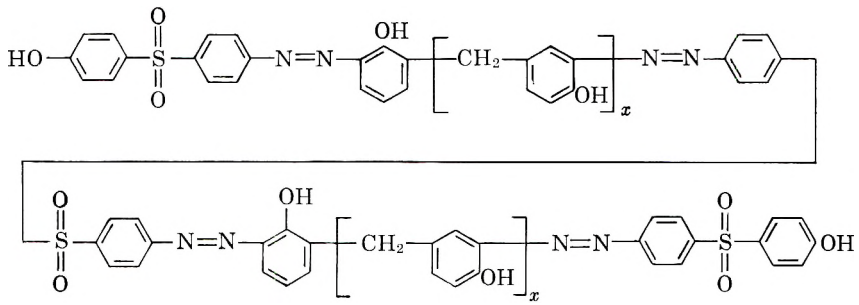

where x is an average of 5, assuming that the chain termination occurred through the hydrolysis of the diazonium salt. For the structure presented, the molecular weight should be approximately 2000, nitrogen 5.47% calculated and sulfur 4.69% calculated. This fits closely to the found quantities.

The infrared spectrum of this polymer is shown in Figure 1. The typical associated OH absorption at 2.89 μ is strong, indicating large proportions of the *para* isomer. The fact that the peak is broad, however, extending to 4.2 μ, can suggest the presence of the *ortho*-substituted phenols as well. The bonds most associated with the azo and hydrazone groups in the neighborhood of 7 μ are in the region of ring and aromatic C-H vibrations.[12] Thus, it is difficult to decide which band in this spectra should be attributed to the azo vibration. The characteristic sulfone absorption[12] at 8.62–8.93 μ is present, as should be expected.

Polymer II was not soluble in common solvents and, therefore, molecular weight was not determined. This poor solubility, on the other hand leads us to suspect that the molecular weight may be high. The infrared spectrum of this material is presented in Figure 2. Here the weak and broad absorption at 3–4.2 μ suggests a large predominance of the ortho isomer. The other bands can be assigned mainly to the high aromatic character of this molecule.

Polymers III, IV, V, and VI should be similar, the differences being mainly in molecular weights. The similarity in their structures can be readily observed from the infrared spectra shown in Figure 3. Combustion analysis, does indicate, however, that some differences do exist. Thus, polymer III might be only

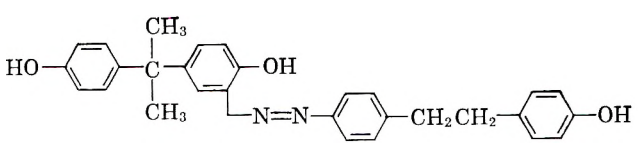

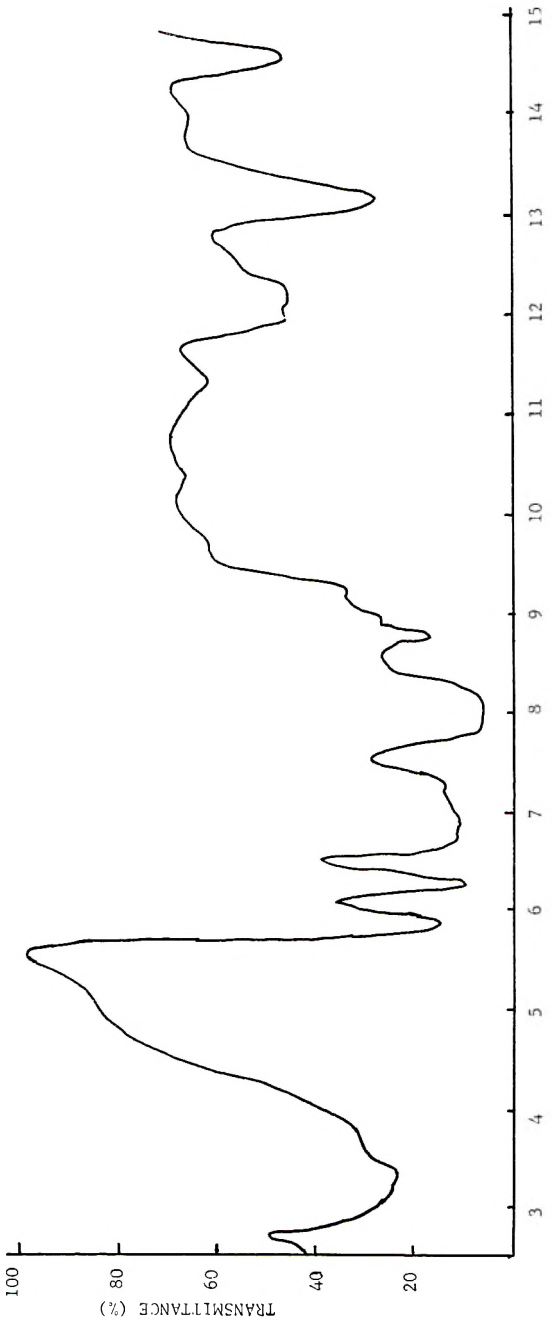

Fig. 2. Infrared spectrum of polymer II.

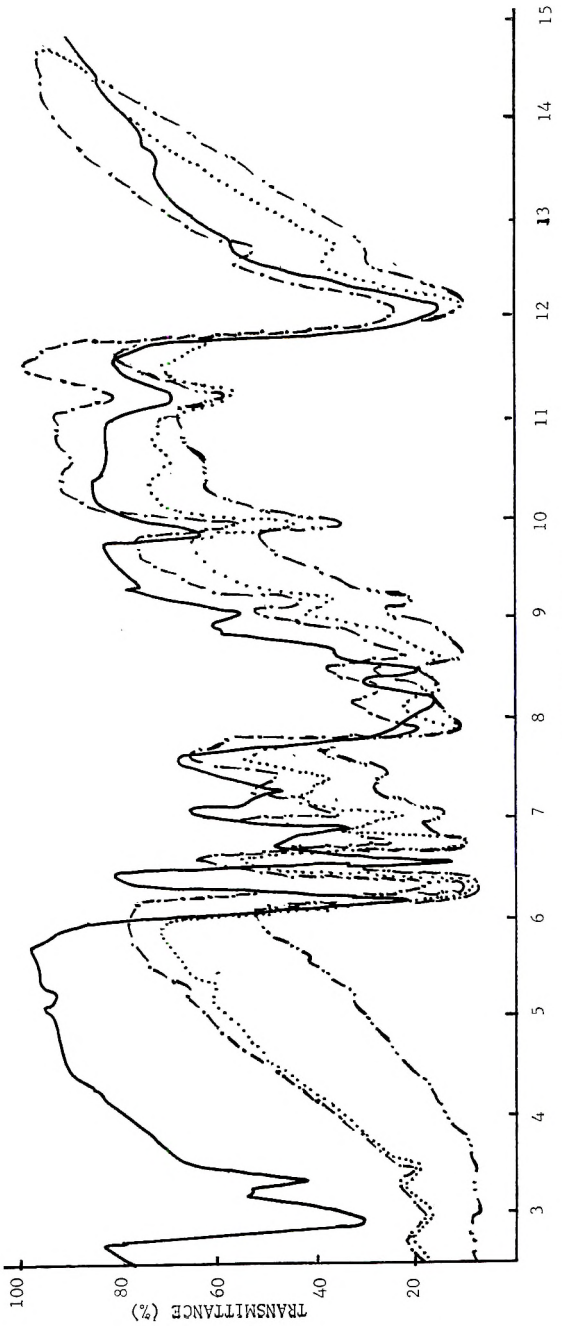

Fig. 3. Infrared spectra of: (——) polymer III; (- -) polymer IV; (-·-) polymer V; (-··-) polymer VI.

and would be a dimer with perhaps some unreacted phenol present as an impurity, which would manifest itself in a low nitrogen. For the above structure carbon is 76.99%, hydrogen 6.19%, and nitrogen 6.19%.

Polymer IV appears to be a mixture of a trimer and a tetramer. Such a mixture would place it within the range of molecular weight found experimentally. The low carbon content, however, found by combustion analysis leaves us uncertain. Polymers V and VI we believe to have the following structure:

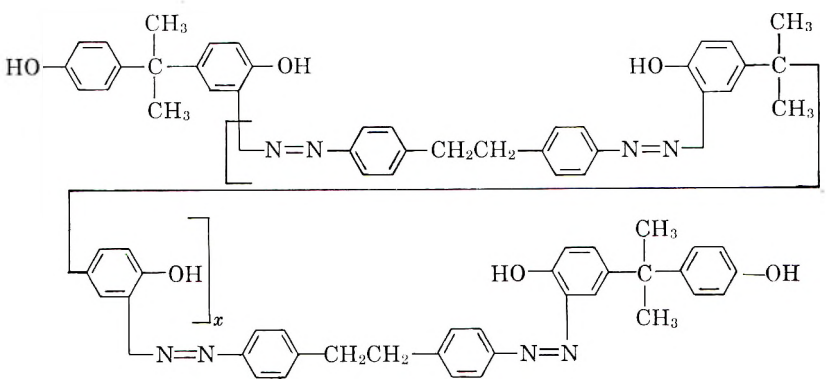

Here x can be 2 for polymer V and over 24 for Polymer VI. The above structure would have the values for carbon 75.88% calculated, hydrogen 5.77% calculated, and nitrogen 10.42% calculated. These values fit closely to the determined ones as shown in Table I. With x equal to 2 for polymer V, the calculated molecular weight is 1613. The determined molecular weight, however, was 1890, which indicates the presence of some higher molecular weight fractions. Infrared spectra can only be expected to show weak and broad absorptions in the 2.98 μ region, due to the association of the phenolic OH Group with the azo structure. The other peaks of Figure 3 again confirm the aromatic character of the molecule.

Polymers VII, VIII, and IX were separated on the basis of their solubility. Here, as in the case of Polymers III, IV, V, and VI, we expected the differences to be present mainly in molecular weights. Infrared spectra and combustion analysis tend to support this expectation.

The combustion analysis, of the three polymers, however, shows all of them to be lower in carbon and nitrogen and higher in oxygen and hydrogen than would be expected from a product of such a condensation. In fact, the structure which fits closer to these analyses would be one showing some azo groups associated with water, one out of every three or four links. This water would have to be held so tightly that repeated drying *in vacuo* would not remove it. The drying conditions were 8 hr. at 56°C. over anhydrous silica gel at 1 mm. Hg.

Brode and co-workers noticed that *p*-hydroxyphenyl azo compounds did associate strongly with water, to a point that a corresponding shift of

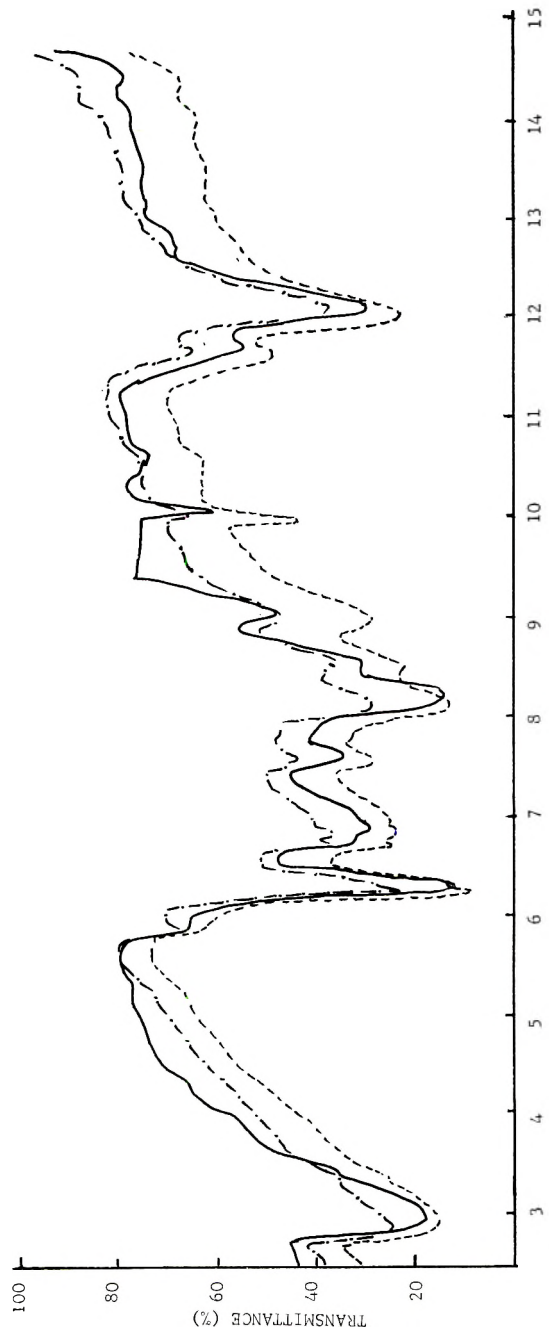

Fig. 4. Infrared spectra of: (---) polymer VII; (——) polymer VIII; (-·-) polymer IX.

the azo peak could be shown in the ultraviolet.[13] They did not indicate, however, that the water was difficult to remove by drying *in vacuo*.

Karl Fischer determinations for presence of water were then conducted on these polymers. It was determined that the polymers possessed, on the

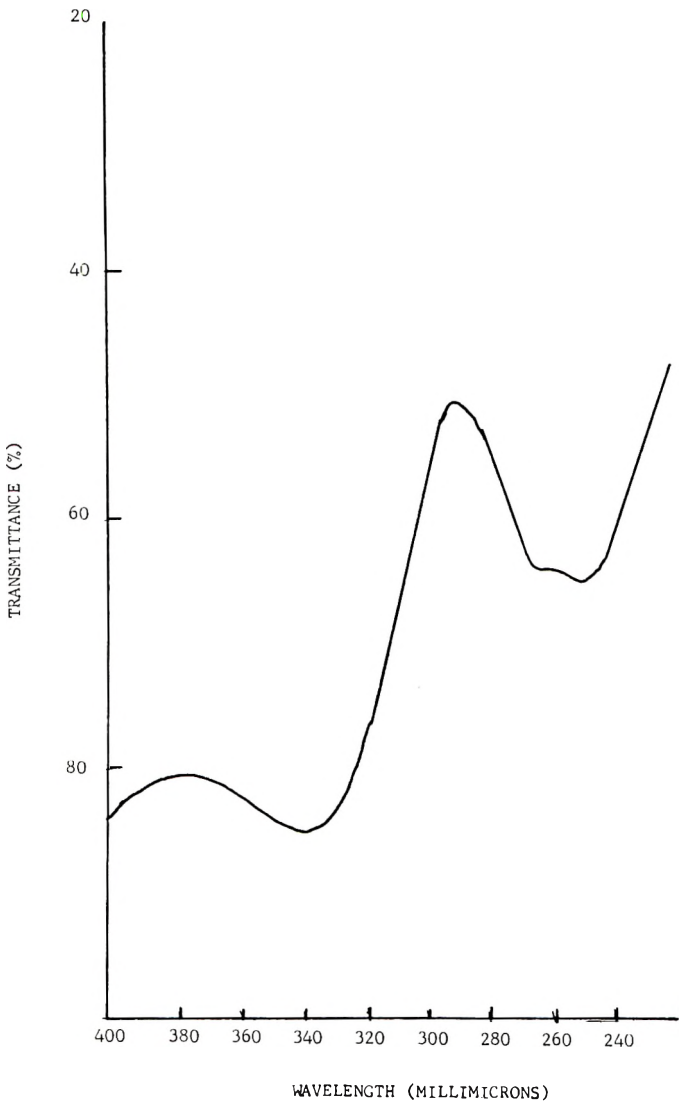

Fig. 5. Ultraviolet spectrum of polymer I.

average, 2.35% water. One molecule of water for every four azo links would amount to 2.24% water. The structure could then perhaps be represented as follows:

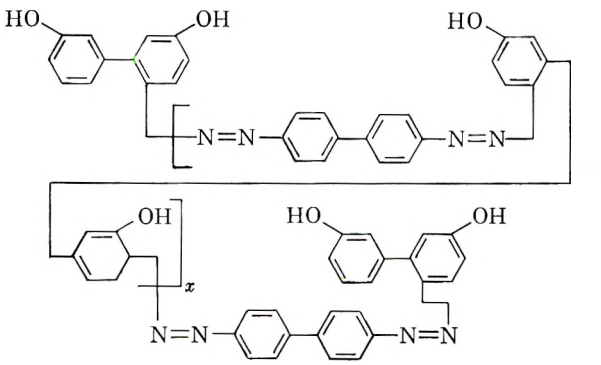

with x equal to 6 for polymer VII and 23 for polymer VIII.

Another factor, which should not be overlooked in these reactions, is the possibility of the loss of nitrogen through decomposition of the diazonium salt and the resultant free radical recombination of two aryl groups. The lower nitrogen found in these polymers would indicate that some of this indeed may have happened.

Thus, if we assume the loss of 12–14% nitrogen per mole of polymer in addition to the presence of water, then carbon becomes 73.29% calculated, hydrogen 4.41% calculated, and nitrogen 11.44% calculated for polymer VII and carbon 73.12% calculated, hydrogen 4.37% calculated, and nitrogen 11.90% calculated for polymer VIII. These quantities are close to those found experimentally.

Because these polymers are also polyphenols, another means of analysis would be the determination of their hydroxyl group content through acetylation. This was carried out on polymers VII, VIII, and IX. The values obtained fit the above shown structure if water is present and would be low for a dry material. Hydroxyl value determination conducted on a model compound, *o*-hydroxy, *p*-methylazobenzene was also low, 8.02% calculated, 7.80% found. Infrared absorption of polymers VII, VIII, and IX shown in Figure 4 indicate great similarities in structure. There appear to be no contradictions in these spectra to the molecules shown.

As already mentioned, the infrared spectrum is not a satisfactory means for establishing the presence of azo groups. The azo bond, however, does show up well in the ultraviolet region.[14,15] Thus, the ultraviolet spectrum of polymer I, presented in Figure 5 shows an azo peak between 375 and 385 mμ. The azo absorption of polymers III, IV, V, and VI appears at 330–360 mμ, as seen in Figure 6. The shift in azo absorption of polymer I could perhaps be attributed to the influence of the sulfone groups. Polymers VII, VIII, and IX also show the azo peak shifted (Fig. 7) to almost 390 mμ. The highly conjugated nature of the polymers might contribute to this shift, though azo absorption of *p*-hydroxyazobenzene was also reported in this region by Brode and co-workers.[13]

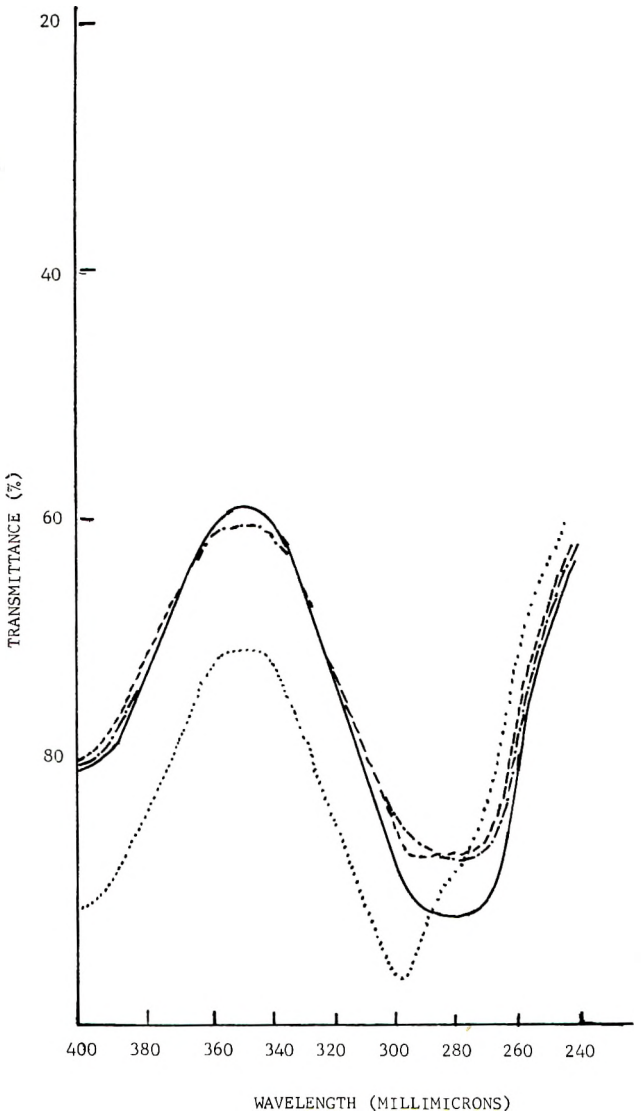

Fig. 6. Ultraviolet spectra of: (···) polymer III; (--) polymer IV; (——) polymer V; (–·–) polymer VI.

EXPERIMENTAL

Preparation of Novolac

The novolac was synthesized from reagent grade phenol (1 mole), formaldehyde solution, 37% (0.65 moles), and 0.4% hydrochloric acid (specific gravity 1.18) as catalyst. The components were reacted initially at 45°C. to remove the exotherm and then at 95°C. for 3 hr. The resin was

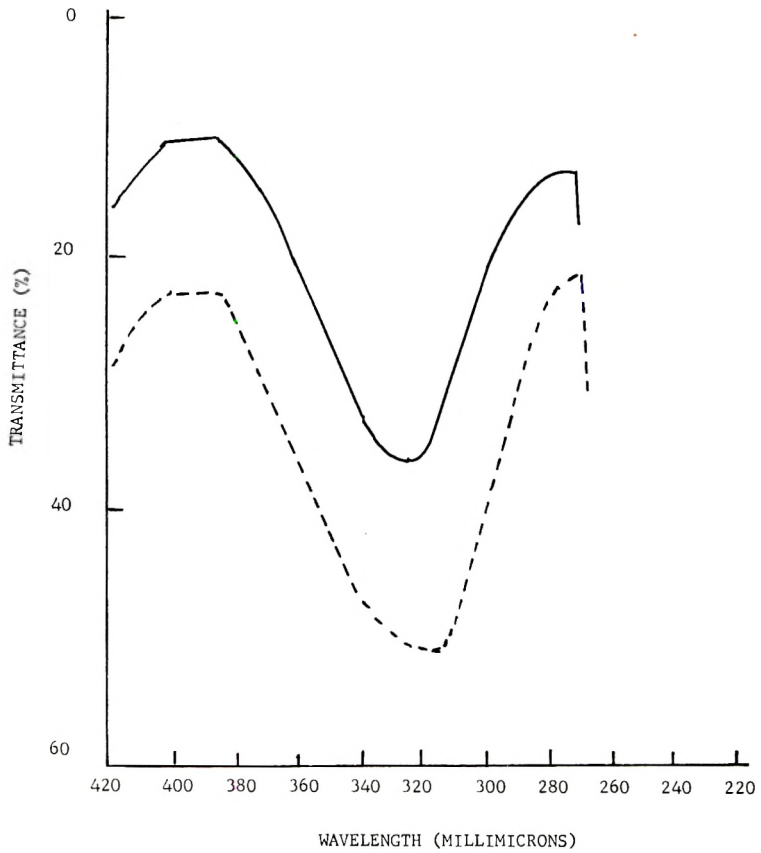

Fig. 7. Ultraviolet spectra of: (——) polymer VIII in dioxane; (---) polymer VII in dioxane.

washed repeatedly with hot water to remove the acid catalyst and the unreacted components. The finished resin was vacuum-dried.

The average molecule weight of the finished resin was found to be 400, indicating a high ratio of tetramers in this product (found: C 78.33%, H 5.73%).

Diazotization Reaction and Coupling

All diazotization and coupling reactions[3] were conducted in three-necked flasks equipped with mechanical stirrers and dropping funnels. During the reaction, the flasks were immersed to their necks in a constant temperature bath maintained at −4°C.

Condensation 1: Diazonium Salt of *p,p'*-Diaminodiphenyl Sulfone and Coupling to Novolac. Diaminodiphenyl sulfone (24.8 g.) was converted to the dihydrochloride salt. The salt was diazotized and then coupled to 92 g. of the sodium salt of the novolac[3] at −4°C. The reaction mixture was allowed to stand overnight and then gradually warmed to room tempera-

ture. The precipitate which formed was filtered off and discarded as unreacted novolac. When the filtrate was acidified with acetic acid, 59 g. of a dark red material precipitated (polymer I).

Polymer I was purified by dissolving it in amyl alcohol, filtering, and subsequently precipitating the polymer in the filtrate with petroleum ether. The procedure was repeated again with the use of hot acetone instead of amyl alcohol.

Condensation 2: Bisdiazonium Salt of Diaminodiphenylmethane and Coupling to Novolac. One mole of *p,p'*-diaminodiphenylmethane (196 g.) was diazotized and then coupled to 0.75 mole of sodium salt of the novolac. Some gas evolved during the reaction. After the reaction, the dark brown solid (polymer II) was filtered off and dispersed in glacial acetic acid for 24 hr. Following the acid treatment, it was collected on a Buchner funnel, washed repeatedly with water, and dried. The yield was 288.8 g. (found: C 74.22%, H 5.22%, N 8.23%).

Condensation 3: Diazonium Salt of 1,2-Di-*p*-aminophenylethane and Coupling to 2,2'-Di-*p*-hydroxyphenylpropane. 1,2-Di-*p*-aminophenylethane (0.2 mole) was diazotized, and the diazonium salt was coupled to 0.2 mole of the sodium salt of 2,2'-di-*p*-hydroxyphenylpropane. A very dark red, solid precipitate separated from the mixture. It was washed thoroughly with dilute acetic acid, then with water and finally dried.

The polymer was separated into four fractions by means of solvent solubilities. The polymer was extracted with room temperature butanol. Petroleum ether was added to the butanol and the very small amount of precipitate, was filtered off. The filtrate was evaporated to dryness to yield polymer III. It was then dissolved in toluene and the solution was filtered. Polymer III was precipitated from the filtrate with petroleum ether.

The residue from the cold butanol extraction was then extracted with hot butanol. Polymer IV precipitated out on cooling this extract.

The residue from the successive cold and hot butanol extractions was extracted with toluene. Polymer V precipitated when petroleum ether was added to this extract. It was then dissolved in methyl ethyl ketone, filtered, and the filtrate was evaporated to dryness.

The remaining residue from the three previous extractions was dispersed in dimethylformamide and filtered. Polymer VI was precipitated by adding water to the dimethylformamide solution. Polymer VI was further purified by titurating with hot acetone.

The separation of products from condensation 3 can be summarized in scheme 1.

Condensation 4: Bisdiazonium Salt of *p,p'*-Diaminobiphenyl and Coupling to 3,3'-Dihydroxybiphenyl. *p,p'*-Diaminobiphenyl (20.6 g.) was diazotized and then coupled to 15 g. of 3,3'-dihydroxybiphenyl as the sodium salt. A dark brown precipitate started to form almost immediately. The product was filtered and washed with dilute acetic acid and then with water. The product was separated according to scheme 2.

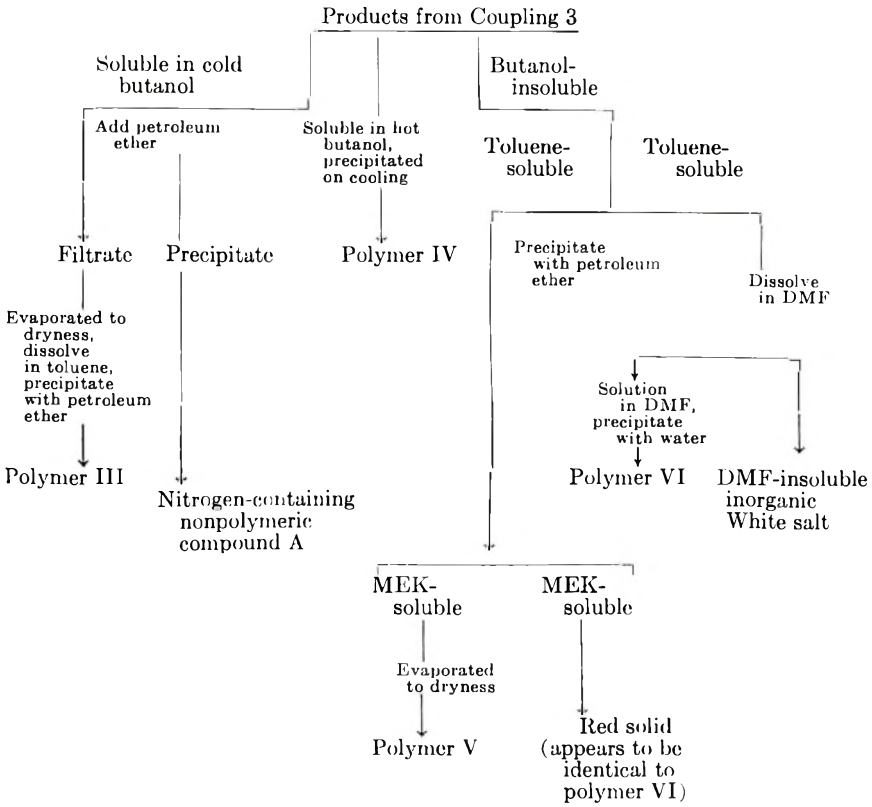

Scheme 1.

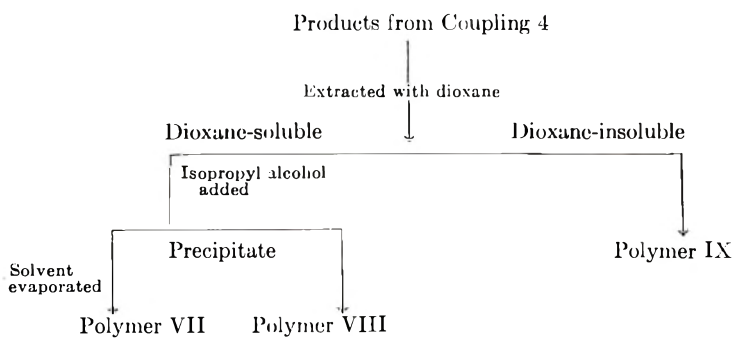

Scheme 2.

The products from coupling 4 were placed into a large Soxhlet extractor and extracted with dioxane. A dark, almost black solution of dioxane formed leaving a black residue (polymer IX). The dioxane solution was added to five times its volume of isopropyl alcohol to yield a black precipitate (polymer VIII). The alcohol–dioxane solution was allowed to evaporate to dryness, leaving a black precipitate (polymer VII).

Molecular Weight Determinations

The molecular weights of these polymers were determined in dioxane solution in a thermoelectric osmometer (Mechrolab Model 301-A).

References

1. Hill, J. W., U. S. Pat. 2,556,876 (June 12, 1951).
2. Berlin, A. A., V. I. Liogonskiĭ, and V. P. Parini, *J. Polymer Sci.*, **55**, 675 (1961).
3. Gilman, H., and A. H. Blatt, *Organic Syntheses*, Coll. Vol. I, Wiley, New York, 1948, p. 49.
4. Wistat, R., and P. D. Bartlett, *J. Am. Chem. Soc.*, **63**, 413 (1941); C. R. Hauser and D. S. Breslow, *J. Am. Chem. Soc.*, **63**, 418 (1941).
5. Goldschmidt, S., *Ber.*, **30**, 670, 2075 (1897).
6. Goldschmidt, S., *Ber.*, **32**, 355 (1899).
7. Goldschmidt, S., *Ber.*, **33**, 893 (1900).
8. Goldschmidt, S., *Ber.*, **35**, 3534 (1902).
9. Conant, J. B., and W. D. Peterson, *J. Am. Chem. Soc.*, **52**, 1220 (1930).
10. Frankland, E., *J. Am. Chem. Soc.*, **37**, 746 (1880).
11. Hadzi, D., *J. Chem. Soc.*, **1956**, 2143.
12. Bellamy, L. J., *Infrared Spectra of Complex Molecules*, Wiley, New York, 1959, pp. 272, 360.
13. Brode, W. R., I. L. Seldin, P. E. Spoerri, and G. M. Wyman, *J. Am. Chem. Soc.*, **77**, 2762 (1955).
14. Gore, P. H., and O. H. Wheeter, *J. Org. Chem.*, **26**, 3295 (1960).
15. Wheeler, O. H., and P. H. Gore, *J. Am. Chem. Soc.*, **78**, 3363 (1956); *ibid.*, **78**, 2160 (1956).

Résumé

On prépare des polymères par couplage de sels de diazonium et de polyphénols. On emploie trois différents polyphénols pour cette condensation avec quatre diamines aromatiques. On obtient des produits de poids moléculaires de l'ordre de moins de 2.000 à plus de 20.000. Dans trois des quatre condensations effectuées, on ne détecte pas de perte d'N_2 par réaction de couplage, mais dans le quatrième cas, on détecte une faible perte d'N_2. Tous les polymères obtenus sont de couler foncée. Les polymères possédant des groupes *p*-hydroxy-azo lors de leur formation, occluent de l'eau qui y est attachiée fortement.

Zusammenfassung

Durch Kupplung der Bis-diazoniumsalze von vier aromatischen Diaminen mit drei verschiedenen Polyphenolen wurden Polymere hergestellt, deren Molekulargewicht in einem Bereich von weniger als 2000 bis über 20000 lag. Bei dreien der vier Kondensationen war während der Kupplungsreaktion kein Stickstoffverlust festzustellen, während im vierten Falle anscheinend etwas Stickstoff abgespalten wurde. Alle Polymeren waren dunkel gefärbt. Diejenigen Polymeren, die *p*-Hydroxyazogruppen enthalten, okklúdieren Wasser und halten es sehr fest gebunden.

Received October 18, 1962
Revised March 22, 1963

JOURNAL OF POLYMER SCIENCE: PART A VOL. 2, PP. 1941–1953 (1964)

ω-Cyanothiaalkyl Polyacrylates: A New Class of Synthetic Rubbers

JULIANNE H. PRAGER, RICHARD M. McCURDY, and GEORGE B. RATHMANN, *Central Research Laboratories, Minnesota Mining and Manufacturing Company, St. Paul, Minnesota*

Synopsis

The synthesis and polymerization of a series of ω-cyanothiaalkyl acrylates, $CH_2{=}CHCO_2(CH_2)_mS(CH_2)_nCN$, are described. The length of the side chain and the position of the sulfur atom are varied. Microgelation is found to occur during polymerization, as indicated by viscosity and molecular weight measurements (for 5-cyano-3-thiapentyl polyacrylate at 90% conversion: $[\eta]$, 0.37 in acetone; $\bar{M}_w$, 600 million). Possible mechanisms of gelation are considered. Glass transition temperatures and solvent swellings are reported as follows: 4-cyano-3-thiabutyl polyacrylate, T_g −24°C., 14% volume swell in benzene; 5-cyano-3-thiapentyl polyacrylate, −50°C., 20%; 6-cyano-3-thiahexyl polyacrylate, −58°C., 38%; 6-cyano-4-thiahexyl polyacrylate, −58°C., 42%; 8-cyano-7-thiaoctyl polyacrylate, −59°C., 120%. The relation between these properties and the structure of the polymers is discussed. The swelling of 5-cyano-3-thiapentyl polyacrylate in eighteen other fluids is given; an estimate (between 10 and 12.5) is made of the solubility parameter of this polymer. Bulk properties are reported for the vulcanizate of 5-cyano-3-thiapentyl polyacrylate.

INTRODUCTION

It is widely recognized that the affinity of hydrocarbon polymers for solvents of a similar nature is reduced by the incorporation of polar groups into the polymer structure. Such groups also increase interactions between polymer chains, however, and give rise to systems which exhibit a sluggish response to an applied stress. Thus, the very polar groups which enhance solvent resistance tend to reduce elasticity, particularly at low temperatures.

There has long been interest in obtaining solvent-resistant rubbers with a broad useful temperature range. In consequence, numerous studies have been made of elastomers containing various polar groups in order to observe the effect of different types of substituents on the properties of the polymer. Perhaps the best known systems of this type are the copolymers of butadiene and acrylonitrile.[1] Butadiene has also been copolymerized with acrylic acid[2] and, in addition, many polyacrylates have been prepared containing polar substituents in their alcohol side chains, including the chloro[3,4], bromo,[4] fluoro,[5] cyano,[4] nitro,[4,6] nitrato,[7] and alkoxy groups,[8] as well as combinations thereof.[9,10]

In this investigation we have examined the effect of the incorporation in an elastomer of both the cyano and the thio ether groups. The cyano group was included for its high dipole moment (the dipole moments[11] of aliphatic nitriles are in the range 3.5–4.0D) and relatively compact size, the thio ether linkage for its low energy of rotation and not insignificant polar character (aliphatic sulfides have moments[11] in the range 1.55–1.60D). A study of the thiaalkyl polyacrylates is reported in another paper.[12] Of course, a great variety of elastomeric structures could be proposed which would include these two groups, structures of both the condensation and addition polymer types. We chose to incorporate both groups into a single vinyl monomer and selected for the polymerizing unit the acrylic ester structure.

This paper describes the preparation and polymerization of several acrylic esters and discusses the properties of the resulting ω-cyanothiaalkyl polyacrylates.

$$\left[\mathrm{CH_2{-}\underset{\displaystyle \mathrm{CO_2(CH_2)_mS(CH_2)_nCN}}{\overset{|}{C}}H}\right]_x$$

in which the position of the sulfur atom and the length of the side chain have been varied. In all cases the nitrile group has been placed in the terminal position to permit its maximum exposure with consequent enhancement of solvent resistance. Branched structures have not been investigated extensively, because it has been shown for numerous polymer systems, including the unsubstituted polyacrylates[13] and the polyvinyl ethers,[14] that branching in the side chain decreases flexibility.

EXPERIMENTAL METHODS

A. Monomer Preparation

The preparation of a series of acrylic esters of the general formula, $CH_2 = CHCO_2(CH_2)_mS(CH_2)_nCN$, was carried out. The following members were synthesized: $m = 2$, $n = 1$ (4-cyano-3-thiabutyl acrylate); $m = 2$, $n = 2$ (5-cyano-3-thiapentyl acrylate); $m = 2$, $n = 3$ (6-cyano-3-thiahexyl acrylate); $m = 3$, $n = 2$ (6-cyano-4-thiahexyl acrylate); $m = 6$, $n = 1$ (8-cyano-7-thiaoctyl acrylate). These esters have not been reported previously, nor have the alcohols from which they were prepared, with the exception of 5-cyano-3-thiapentanol-1, which was synthesized by Gribbins and co-workers[15] by the cyanoethylation of 2-mercapto-1-ethanol. This procedure was used by us, with the modifications of Hurd and Gershbein,[16] for the alcohols in which n is equal to 2 (method A):

$$HO(CH_2)_mSH + CH_2{=}CHCN \rightarrow HO(CH_2)_mS(CH_2)_2CN$$

The other alcohols were obtained by reacting the sodium mercaptide of a mercaptoalcohol with the appropriate chloronitrile (method B):

$$HO(CH_2)_mSNa + Cl(CH_2)_nCN \rightarrow HO(CH_2)_mS(CH_2)_nCN$$

The acrylates were prepared by treating the alcohol with acrylyl chloride (method C) or by ester interchange with ethyl acrylate (method D):

$$HO(CH_2)_mS(CH_2)_nCN \xrightarrow[\text{or } CH_2{=}CHCO_2Et]{CH_2{=}CHCOCl} CH_2{=}CHCO_2(CH_2)_mS(CH_2)_nCN$$

Direct esterification with acrylic acid was found to produce only negligible quantities of the desired esters.

Starting Materials

3-Mercapto-1-propanol. This material was synthesized from 3-bromo-1-propanol by the method of Clinton and co-workers.[17]

6-Mercapto-1-hexanol. A mixture of 1.2 moles of 6-chloro-1-hexanol (prepared in 46% yield from 1,6-hexanediol and hydrochloric acid by the method of Campbell and Sommers[18]), 1.3 moles of thiourea, and 800 cc. of 95% ethanol was refluxed for 24 hr. After the addition of 200 cc. of water, the solution was distilled until 800 cc. of liquid was collected. In an atmosphere of nitrogen, 600 g. of 10% sodium hydroxide solution was added, and the mixture was refluxed for 2 hr. The aqueous layer was acidified with dilute sulfuric acid; the oily layer was taken up in benzene, water-washed, dried, and distilled. A 74% yield of colorless, somewhat viscous 6-mercapto-1-hexanol, b.p. 78–80°C./0.5 mm., n_D^{22}1.4845, was obtained.

ANAL Calcd. for $C_6H_{14}OS$: S, 23.9%. Found: S, 23.6%.

ω-Cyanothiaalkanols

The physical properties and method of preparation of these alcohols are listed in Table I. They are colorless, somewhat viscous liquids with a pronounced mercaptanlike odor.

Method A. Acrylonitrile was added to the appropriate mercaptoalcohol in the manner described by Gershbein and Hurd[16] for 5-cyano-3-thiapentanol-1.

Method B. The sodium mercaptide of the appropriate mercaptoalcohol was prepared by adding cautiously 1 mole of sodium metal and then 1 mole of mercaptoalcohol to 400 cc. of absolute ethanol. To this solution at 10–15°C. was added dropwise 1 mole of the appropriate chloronitrile. After the addition was complete, the mixture was heated at reflux until neutral; it was then filtered, and the product was separated by distillation under vacuum.

ω-Cyanothiaalkyl Acrylates

The physical properties and method of preparation of the acrylates are shown in Table II. They are colorless, mobile liquids with a slight odor.

Method C. To a stirred solution at 10–15°C. of 1 mole of ω-cyanothiaalkanol and 1.10 moles of triethylamine (dried over potassium hydroxide, refluxed with α-naphthyl isocyanate, distilled, and stored over

TABLE I
Physical Properties and Analyses of ω-Cyanothiaalkanols

Alcohol $HO(CH_2)_m$-$S(CH_2)_nCN$	m	n	Prep.	Yield, %	B.P., °C./mm. Hg	n_D (at T, °C.)	Carbon, %		Hydrogen, %		Nitrogen, %		Sulfur, %	
							Calcd.	Found	Calcd.	Found	Calcd.	Found	Calcd.	Found
4-Cyano-3-thia-butanol-1	2	1	B	68	112–118/3.5	1.5174 (24)	41.0	41.3	6.0	5.9	12.0	11.4	27.4	27.0
5-Cyano-3-thia-pentanol-1	2	2	A	88	119–121/0.7	1.5103 (24)	45.8	45.8	6.9	7.1	10.7	10.5	24.4	24.4
5-Cyano-4-thia-pentanol-1	3	1	B	37	109–110/1	1.5033 (22)	45.8	44.8	6.9	7.2	10.7	9.4		
6-Cyano-3-thia-hexanol-1	2	3	B	76	138–140/2	1.5067 (21)	49.6	49.4	7.6	7.4	9.7	9.3	22.1	22.2
6-Cyano-4-thia-hexanol-1	3	2	A	76	115–118/0.25	1.5027 (22)	49.6	49.7	7.6	7.4	9.7	9.5	22.1	21.9
8-Cyano-7-thia-octanol-1	6	1	B[a]											

[a] Not characterized; converted directly to the acrylate.

TABLE II
Physical Properties and Analyses of ω-Cyanothiaalkyl Acrylates

Acrylate $CH_2{=}CHCO_2$-$(CH_2)_mS$-$(CH_2)_nCN$	m	n	Prep.	Yield, %	B.P., °C./mm. Hg	n_D (at T, °C.)	Carbon, %		Hydrogen, %		Nitrogen, %		Sulfur, %	
							Calcd.	Found	Calcd.	Found	Calcd.	Found	Calcd.	Found
4-Cyano-3-thiabutyl-1-acrylate	2	1	C	45	101–105/0.5	1.5017 (23)	49.7	49.5	5.2	5.0	8.09	7.99	18.5	18.4
5-Cyano-3-thiapentyl-1-acrylate	2	2	C D	77 60	115–117/0.4	1.4999 (23)	51.9	51.8	6.0	5.8	7.56	7.52	17.3	17.3
5-Cyano-4-thiapentyl-1-acrylate	3	1	C	45	Percolated	1.4946 (22)	51.9	52.3	6.0	6.4	7.56	6.93		
6-Cyano-3-thiahexyl-1-acrylate	2	3	C	77	125–126/0.5	1.4964 (23)	54.2	54.4	6.6	6.6	7.03	7.06	16.1	16.3
6-Cyano-4-thiahexyl-1-acrylate	3	2	C	58	Percolated	1.4955 (25)	54.2	54.5	6.6	6.5	7.03	6.92	16.1	16.4
8-Cyano-7-thiaoctyl-1-acrylate	6	1	C	65	Percolated	1.4889 (22)	58.1	58.7	7.5	7.5	6.16	6.09	14.1	14.1

sodium) in 200 cc. of dry benzene was added dropwise 1.05 moles of freshly distilled acrylyl chloride. The mixture was allowed to stand for 2 hr., filtered, washed with dilute acid and limited amounts of water, and dried. The acrylates were purified by distillation under vacuum from copper powder or by percolation through activated alumina.

Method D. A mixture of 3.5 moles of ω-cyanothiaalkanol, 10.5 moles of ethyl acrylate, 0.035 moles of tetraisopropyl titanate (E. I. du Pont de Nemours and Company) and 10 g. of copper powder was heated to boiling and the azeotrope of ethyl acrylate was removed slowly by distillation through a 30-cm. Vigreux column. The remaining ethyl acrylate was taken off under vacuum, and the residue was diluted with benzene, washed with saturated sodium sulfate solution, dried, and purified as in method C.

B. Polymerization

The ω-cyanothiaalkyl acrylates can be polymerized in solution or in emulsion. Screening polymerizations were carried out on a 1-g. scale in sealed, evacuated ampules, while large laboratory runs were made in bottles or flasks. Solvents used in solution polymerization included acetone and dioxane; azobisisobutyronitrile was used as initiator. A variety of emulsion systems was evaluated; in general, "activated" recipes[19a] were found to produce the best latexes. The polymers reported in this paper were prepared by recipe IIIa in Table III; it has since been found that recipe IIIb produces a latex of superior shear stability.

TABLE III

	Parts (by weight)
IIIa. Standard polymerization recipe	
Monomer	100
Water	180
Dodecylamine hydrochloride	5
Cumene hydroperoxide (72.5%)	0.5
Triethylenetetramine	0.5
IIIb. Improved polymerization recipe	
Monomer	100
Water	180
Emcol K-8300[a]	5
Potassium persulfate	0.5
Sodium bisulfite	0.3

[a] Complex aliphatic sulfonate (Witco Chemical Co., Inc., New York, N. Y.).

In general, the polymerizations were carried out at 25°C. Reaction was essentially complete in 3 hr. The raw polymers were isolated by coagulation of the latex in methanol and were then water-washed and dried under vacuum at 50°C.

C. Vulcanization

For evaluation of bulk properties, the raw polymers were subjected to a peroxide cure. The recipe given in Table IV was found to be satisfactory.

TABLE IV
Vulcanization Recipe

	Parts (by weight)
Polymer	100
HAF Black[a]	35
Magnesium oxide	10
Di-Cup 40C[b]	3
Press cure 30 min. at 310°F.	

[a] Philblack O (Phillips Chemical Co., Akron, Ohio).

[b] 40% dicumyl peroxide supported on precipitated calcium carbonate (Hercules Powder Co., Wilmington, Delaware).

PROPERTIES OF POLYMERS

A. Viscosity and Molecular Weight

ω-Cyanothiaalkyl acrylates have a tendency to crosslink during solution polymerization and to form microgel in emulsion systems. The term microgel will be used to describe highly crosslinked latex particles which are dispersible because of their microscopic dimensions.[19b] In general, crosslinking during polymerization takes place only with difunctional monomers, e.g., with butadiene or divinylbenzene. It has been studied extensively in connection with butadiene–styrene copolymerization; an analytical survey of this subject has been published.[20] Under certain conditions network formation may also occur through chain transfer of growing radicals with polymer formed previously; such a phenomenon has been proposed to explain the formation of crosslinked polymer in the polymerization of methyl acrylate.[21]

It is known that microgel formation is greatest at high conversions. Furthermore, the greater the extent of crosslinking at a given molecular weight, the more compact is the molecule and hence the lower the dilute solution viscosity of the species. Repeatedly we have found that in the emulsion polymerization of an ω-cyanothiaalkyl acrylate the dilute solution viscosity decreases as the conversion increases. Light-scattering molecular weight measurements made on samples of 5-cyano-3-thiapentyl polyacrylate with a Debye-type light-scattering instrument[22] provide further confirmation of the occurrence of crosslinking during polymerization. Thus, a sample withdrawn at 70% conversion, which had an intrinsic viscosity of 0.42 in acetone, was found to have a light-scattering molecular weight of 500 million. A sample which was polymerized to 90% conversion

had an intrinsic viscosity of 0.37 in acetone and a molecular weight of 600 million.

The mechanism of gelation during polymerization of these ω-cyanothiaalkyl acrylates is not known, although we believe that crosslinking occurs because of chain transfer of growing radicals with polymer already formed. However, the possibility cannot be completely eliminated that crosslinking takes place because of copolymerization of trace quantities of a difunctional impurity. In view of the fact that the viscosity of polymer specimens prepared from very pure monomer was only slightly increased over that obtained from monomer of lesser purity, it is difficult to believe that an impurity is responsible for the extensive microgelation observed.

B. Low Temperature Properties

The glass transition temperature T_g of the raw polymers was measured with a modified Abbé refractometer by the method of Wiley and Brauer.[23] The data are listed in Table V. A plot of glass temperature against the number of methylene groups in the alcohol side chain is shown in Figure 1. As the length of the side chain increases, the glass temperature decreases, apparently leveling off at about five methylene groups. Transition temperatures have been reported for a few of the unsubstituted *n*-alkyl polyacrylates; it is apparent from the results of Wiley and Brauer[24] that in this series also, the glass transition temperature reaches a minimum at some temperature below the value found for the *n*-butyl member, −70°C.

TABLE V
Glass Transition Temperatures and Swelling Volumes of ω-Cyanothiaalkyl Polyacrylates

Acrylate side chain	T_g, °C.	Swelling volume in benzene (cured, filled polymer), %
4-Cyano-3-thiabutyl	−24	14
5-Cyano-3-thiapentyl	−50	20
6-Cyano-3-thiahexyl	−58	38
6-Cyano-4-thiahexyl	−58	42
8-Cyano-7-thiaoctyl	−59	120

C. Swelling

The swelling in benzene of the cured, filled polymers was investigated; the data obtained for the various members of the series are given in Table V Figure 2 shows a plot of swelling volume in benzene against the number of methylene groups in the side chain. If the regular solution theory of Hildebrand[25] is applied, it may be said that the cohesive energy density (C.E.D.) of the polymer decreases as the polar centers in the side chains become diluted with hydrocarbon units. Thus, as can be seen from Figure

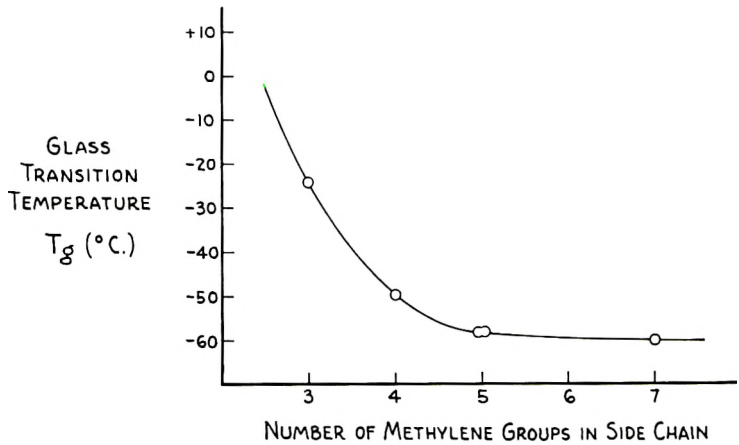

Fig. 1. Glass transition temperature as a function of the number of methylene groups in the side chain of ω-cyanothiaalkyl polyacrylates.

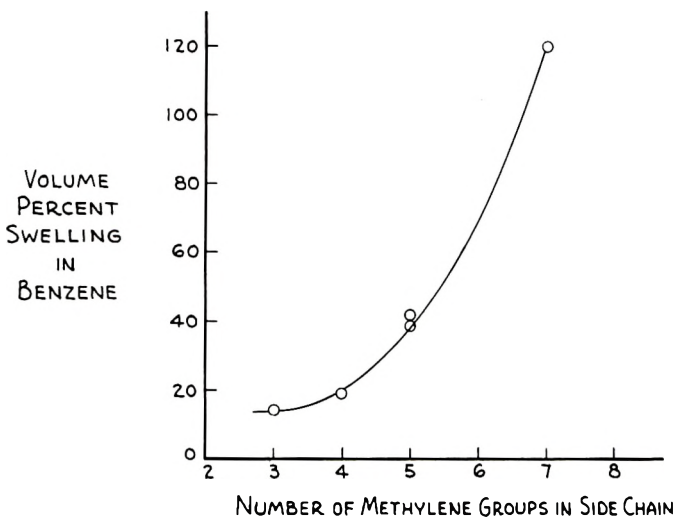

Fig. 2. Swelling volume in benzene as a function of the number of methylene groups in the side chain of ω-cyanothiaalkyl polyacrylates; cured by standard recipe (Table IV).

2, the lower members of the series have little affinity for benzene, while the higher members are swollen to an increasing degree by this solvent.

An estimate of the solubility parameter $\delta[\delta = (\text{C.E.D.})^{1/2}]$ of one member of the series, viz., 5-cyano-3-thiapentyl polyacrylate, has been made by measuring its swelling in a variety of fluids. For this study, we did not use standard vulcanizates; instead a very lightly crosslinked, unfilled sample was used, permitting greater accuracy in measuring swelling, particularly in poor solvents. The swelling data are given in Table VI, along with the δ values of the solvents, and are shown graphically in Figure 3. From the graph one can estimate a δ value between 10 and 12.5 for this polymer.

TABLE VI
Swelling of 5-Cyano-3-thiapentyl Polyacrylate in Various Liquids (unfilled, cured with 1.5 parts Di-Cup 40C)

No.	Solvent	Hildebrand solubility parameter	Swelling, volume, %
1	Ethyl ether	7.4	0
2	Methyl isobutyl ketone	7.9	20
3	Carbon tetrachloride	8.6	0
4	Toluene	8.9	13
5	Ethyl acetate	8.95	36
6	Benzene	9.15	31
7	Methyl ethyl ketone	9.3	53
8	Chlorobenzene	9.5	21
9	Acetone	9.9	665
10	Carbon disulfide	10	10
11	Nitrobenzene	10	676
12	Dioxane	10	138
13	Pyridine	10.7	1070
14	Dimethyl sulfoxide	11.7	1800
15	Acetonitrile	11.9	710
16	Propyl alcohol	11.9	2
17	Nitromethane	12.6	1100
18	Dimethyl formamide	14.0	2400
19	Methyl alcohol	14.4	10

Thus, the polymer is soluble in dioxane, acetone, pyridine, and acetonitrile but insoluble in solvents of low δ value. As might be expected for a highly polar system, the solubility characteristics are not adequately described in terms of simplified regular solution theory (compare swelling values for

TABLE VII
Properties of 5-Cyano-3-thiapentyl Polyacrylate Vulcanizate

Tensile strength, psi	1200–1500
Ultimate elongation, %	200–300
Set at break, %	3–6
Modulus at 100% elongation, psi	300–600
Hardness, Shore A_2	40–70
Resilience, %	5
Compression set B	
(70 hr. at 212°F.), %	60
Tempered 24 hours at 250°F., %	50
Useful temperature range, °F.	0–250
Ozone resistance	Excellent
Dielectric constant (23°C.)[a]	
100 cycles/sec.	26.9
100 kcycles/sec.	17.1
Dissipation factor (23°C.)[a]	
100 cycles/sec.	0.46
100 kcycles/sec.	0.054

[a] Measured on unvulcanized gum stock.

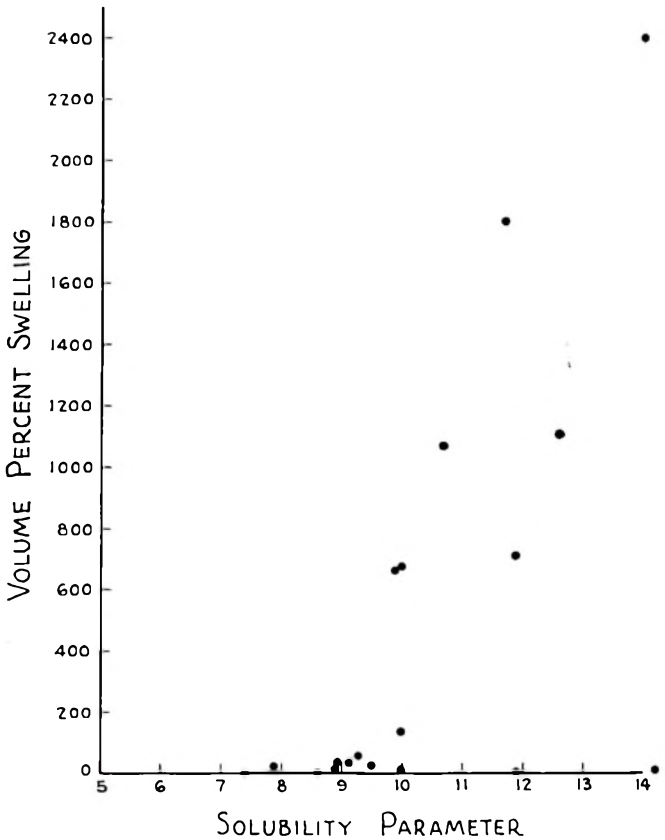

Fig. 3. Swelling volume of 5-cyano-3-thiapentyl polyacrylate vs. solubility parameter of solvent.

acetonitrile and propyl alcohol), which is based on a molecular model of additive, spherically symmetrical force fields. Although refinements of theory to take into account dipolar contributions to the C.E.D. may be possible, it is unlikely that such an approach would offer significant improvement unless some estimate could be made of molecular asymmetry.

D. Mechanical and Electrical Properties

The data obtained for 5-cyano-3-thiapentyl polyacrylate compounded according to the recipe given in Table IV are given in Table VII.

The excellent technical assistance of Ivan M. Maw is gratefully acknowledged. We also wish to thank the Analytical Section of the Central Research Laboratories for the microanalyses and Dr. Frank A. Bovey for many helpful and stimulating discussions.

The authors wish to express appreciation to Samuel Smith and Mrs. Patsy O. Sherman for developing the improved emulsion system and to Robert L. Keech for compounding and evaluation studies on 5-cyano-3-thiapentyl polyacrylate.

We are grateful to Paul I. Roth for light-scattering measurements and transition temperature determinations.

References

1. Schildknecht, C. E., *Vinyl and Related Polymers*, Wiley, New York, 1952, pp. 286–292.

2. Marvel, C. S., T. R. Fukuto, J. W. Berry, W. K. Taft, and B. G. Labbe, *J. Polymer Sci.*, **8**, 599 (1952).

3. Mast, W. C., C. E. Rehberg, T. J. Dietz, and C. H. Fisher, *Ind. Eng. Chem.*, **36**, 1022 (1944).

4. Rehberg, C. E., M. B. Dixon, and W. A. Faucette, *J. Am. Chem. Soc.*, **72**, 5199 (1950).

5. Bovey, F. A., J. F. Abere, G. B. Rathmann, and C. L. Sandberg, *J. Polymer Sci.*, **15**, 520 (1955).

6. Marans, N. S., and R. P. Zelinski, *J. Am. Chem Soc.*, **72**, 2125 (1950).

7. Marans, N. S., and R. P. Zelinski, *J. Am. Chem. Soc.*, **72**, 5330 (1950).

8. Fein, M. L., W. P. Ratchford, and C. H. Fisher, *J. Am. Chem. Soc.*, **66**, 1201 (1944).

9. Bovey, F. A., and J. F. Abere, *J. Polymer Sci.*, **15**, 537 (1955).

10. Butler, J. M., U. S. Pat. 2,720,512 (Oct. 11, 1955).

11. Wesson, L. G., *Tables of Electric Dipole Moments*, Technology Press, Cambridge, Mass.

12. McCurdy, R. M., and J. H. Prager, *J. Polymer Sci.*, **A2**, 1185 (1964).

13. Rehberg, C. E., W. A. Faucette, and C. H. Fisher, *J. Am. Chem. Soc*, **66**, 1723 (1944).

14. Schildknecht, C. E., S. T. Gross, H. R. Davidson, J. M. Lambert, and A. O. Zoss, *Ind. Eng. Chem.*, **40**, 2104 (1948).

15. Gribbins, M. F., F. W. Miller, and D. K. O'Leary, U. S. Pat. 2,397,960 (April 9, 1946).

16. Hurd, C. D., and L. L. Gershbein, *J. Am. Chem. Soc.*, **69**, 2331 (1947); L. L. Gershbein and C. D. Hurd, *Organic Syntheses*, Coll. Vol. III, Wiley, New York, 1955, pp. 458–459.

17. Clinton, R. O., C. M. Suter, S. C. Laskowski, M. Jackman, and W. Huber, *J. Am. Chem. Soc.*, **67**, 592 (1945).

18. Campbell, K. N., and A. H. Sommers, *Organic Syntheses*, Coll. Vol. III, Wiley, New York, 1955, pp. 446–448.

19. Bovey, F. A., I. M. Kolthoff, A. I. Medalia, and E. J. Meehan, *Emulsion Polymerization* (High Polymers, Vol. IX), Interscience, New York, (a) Chapter XI; (b) pp. 318–322.

20. Baker, W. O., *Ind. Eng. Chem.*, **41**, 511 (1949).

21. Fox, T. G, and S. Gratch, *Ann. N. Y. Acad. Sci.*, **57**, 367 (1953).

22. Debye, P. P., *J. Appl. Phys.*, **17**, 392 (1946).

23. Wiley, R. H., and G. M. Brauer, *J. Polymer Sci.*, **3**, 445 (1948).

24. Wiley, R. H., and G. M. Brauer, *J. Polymer Sci.*, **3**, 647 (1948); *ibid.*, **4**, 351 (1949).

25. Hildebrand, J. H., and R. L. Scott, *Solubility of Nonelectrolytes*, 3rd Ed., Reinhold, New York, 1950.

Résumé

On décrit la synthèse et la polymérisation d'une série d'acrylates ω-cyanothiaalkyles, $CH_2{=}CHCO_2(CH_2)_mS(CH_2)_nCN$ La longueur de la chaîne latérale et la position de l'atome de soufre ont varié. On trouve qu'il y a formation de microgels au cours de la polymérisation, ainsi que le montrent les mesures de viscosité et de poids moléculaire (pour le 5-cyano-3-thiapentyl-polyacrylate à 90 % de conversion: $(\eta) = 0.37$ dans l'acétone; $\bar{M}_w = 600$ millions). On considère des mécanismes possibles de formation de gels. Les températures de transition vitreuse et les gonflements dans le solvant s'élèvent à:

polyacrylate de 4-cyano-3-thiabutyle, T_g − 24°C; 14 % comme gonflement (de volume) dans le benzène; polyacrylate de 5-cyano-3-thiapentyle, −50°C, 20%; polyacrylate de 6-cyano-3-thiahexyle, −58°C, 38%; polyacrylate de 6-cyano-4-thiahexyle, −58°C, 42%; polyacrylate de 8-cyano-7-thiaoctyle, −59°C, 120%. On discute la relation entre ces propriétés et la structure des polymères. On donne le gonflement du polyacrylate de 5-cyano-3-thiapentyle dans 18 autres liquides; on fait une estimation du paramètre de solubilité de ce polymère (entre 10 et 12.5). On donne les propriétés de masse pour la vulcanisation du polyacrylate de 5-cyano-3-thiapentyle.

Zusammenfassung

Es werden Synthese und Polymerisation einer Reihe von ω-Cyan-Thiaalkylacrylaten $CH_2{=}CHCO_2(CH_2)_mS(CH_2)_nCN$ beschrieben. Länge der Seitenkette und Lage des Schwefelatoms wurden variiert. Wie aus Viskositäts- und Molekulargewichtsmessungen hervorgeht (für 5-Cyan-3-thiapentylpolyacrylat bei 90% Umsatz fand man: $[\eta]$ = 0,37 in Aceton; $\bar{M}_w$ = 600 Millionen), findet während der Polymerisation Mikrogelbildung statt. Mögliche Mechanismen für die Gelbildung werden in Erwägung gezogen. Es werden folgende Glasumwandlungs-temperaturen und Lösungsmittelquellungen angegeben: 4-Cyan-3-thiabutylpolyacrylat: T_g −24°C, 14% Volumsquellung in Benzol; 5-Cyan-3-thiapentylpolyacrylat: −50°C, 20%; 6-Cyan-3-thiahexylpolyacrylat: −58°C, 38%; 6-Cyan-4-thiahexylpolyacrylat: −58°C, 42%; 8-Cyan-7-thiaoctylpolyacrylat: −59°C, 120%. Die Beziehung zwischen diesen Eigenschaften und der Struktur des Polymeren wird diskutiert. Ferner wird die Quellung von 5-Cyan-3-thiapentylpolyacrylat in achtzehn weiteren Flüssigkeiten angegeben und die Löslichkeitsparameter dieses Polymeren bestimmt (zwischen 10 und 12,5). Für das Vulkanisat von 5-Cyan-3-thiapentylpolyacrylat werden Eigenschaften der festen Substanz beschrieben.

Received January 22, 1963
Revised March 25, 1963

JOURNAL OF POLYMER SCIENCE: PART A VOL. 2, PP. 1955–1976 (1964)

Fine Texture in Necking Portions of Cold-Drawn Polyethylene

NOBUTAMI KASAI, *Department of Applied Chemistry, Faculty of Engineering, Osaka University, Higashinoda, Miyakojima-ku, Osaka, Japan,* and MASAO KAKUDO, *Institute for Protein Research, Osaka University, Joancho, Kita-ku, Osaka, Japan*

Synopsis

Continuous structure change in the necking part of the cold-drawn polyethylene has been examined by the wide- small-angle x-ray diffractions. A specially designed microbeam x-ray camera which permits both wide- and small-angle diagrams to be obtained at the same position at the same time was used. With increasing draw ratio, along the center axis of the specimen, first the crystallites are aligned with the *a* axes perpendicular to the draw direction; this is followed by a gradual orientation of the c axis to the draw direction. On the other hand, an isotropic ring-shaped small-angle halo continuously changes to an elliptical halo with its minor axis on the meridian. After this stage, a meridional scattering in layer streaks appears superposed on the flat elliptical halo, then the elliptical halo disappears and the layer streaks on the meridian remain, and finally the quadrant meridional scattering appears as diffuse layer streaks with intensity maxima on both sides of the meridian. On the stream line, nearly the same variations of the wide- and small-angle diagrams as those on the center axis are observed; however, the meridian of each diagram is not parallel to the draw direction but coincides with the tangent of the stream line at each irradiated position. The stream line was conventionally defined so as to divide the *y* coordinates from the center axis to the surface at every point on the line into the same ratio. One characteristic diagram along the stream line is a small-angle oblique two-point pattern, appearing as off-meridian layer streaks. From each wide-angle diagram, the average orientation angle between the *c* axis and the meridian, degree of crystallite parallelity, and the apparent crystallite size were estimated. The Bragg distance, identity period along the meridian, and the azimuthal angle on the film between the meridian and the direction from center to the diffraction peak were determined by the small-angle scattering. In considering these results, a series of plausible models for continuous structure change in necking is presented.

I. INTRODUCTION

It is well known that cold drawing is one of the most important operations in synthetic fiber production, and during drawing, necking down deformation of fiber occurs under comparatively low temperature.

In structural studies on drawn polyethylene, some models[1–3] have been presented to explain the x-ray small angle diagrams. Fischer and Schmidt[4] examined the variations in the long period of the drawn polyethylene. Very recently, Hosemann[5] reviewed the structure studies of polyethylene, and he presented a model based on his paracrystal theory.

In a study of the mechanism of cold drawing, Fankuchen and Mark[6] first showed changes of the crystallite orientations in the necking part of nylon filament by an x-ray microtechnique. Aggarwal and his co-workers[7] also investigated the changes in orientation during stretching and relaxation of polyethylene films.

In the present study, the continuous structure change in the necking portions of the cold drawn polyethylene has been more precisely examined by the wide- and small-angle x-ray diffractions by using a specially designed micro-beam camera which permits both wide- and small-angle x-ray diagrams to be obtained at the same position at the same time.

II. EXPERIMENTAL

A. Polyethylene Sample

I.C.I. Alkathene 511D polyethylene with a density of 0.928 g./cc. was used. An extruded rod sample about 3 mm. in diameter with no preferred orientation of crystallite was heated at 100°C. for 3 hrs. in order to reduce strain in the original sample before cold drawing, and cooled at a cooling rate of 10°C./hr.

The sample rod was drawn at 10°C. Then a thin plate specimen, about 0.3 mm. in thickness, which includes both a diameter and the center axis of the rod, was cut out at the necking part of the drawn sample as sketched in Figure 1.

In order to ascertain with accuracy the location of the irradiated positions of the x-ray beam on the specimen, the cross point as the origin of coordinates of the positions was marked with a sharp knife edge on the

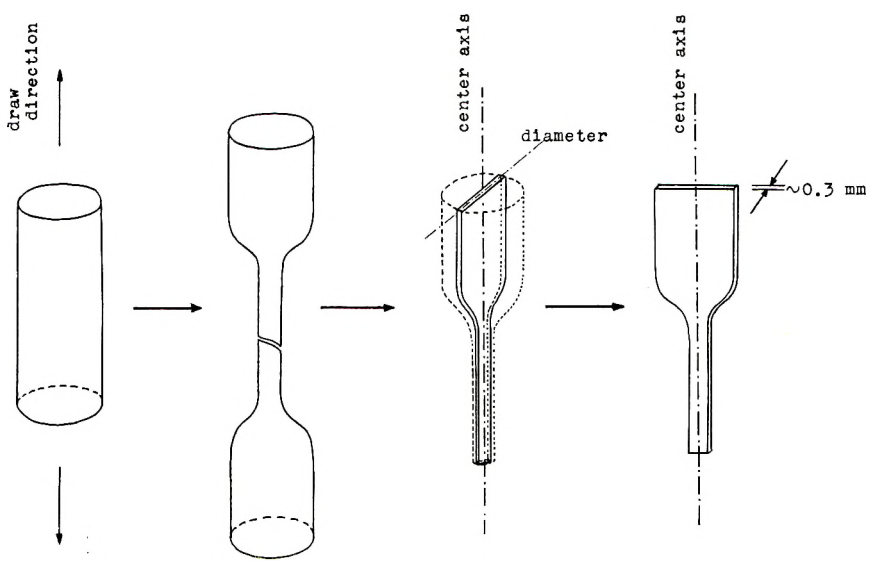

Fig. 1. Diagram of specimen preparation.

center axis in the undrawn part as shown in Figure 2. Thus, the irradiated positions of the specimen were easily defined in terms of the x and y coordinates (in millimeters), which could be accurately measured under microscope.

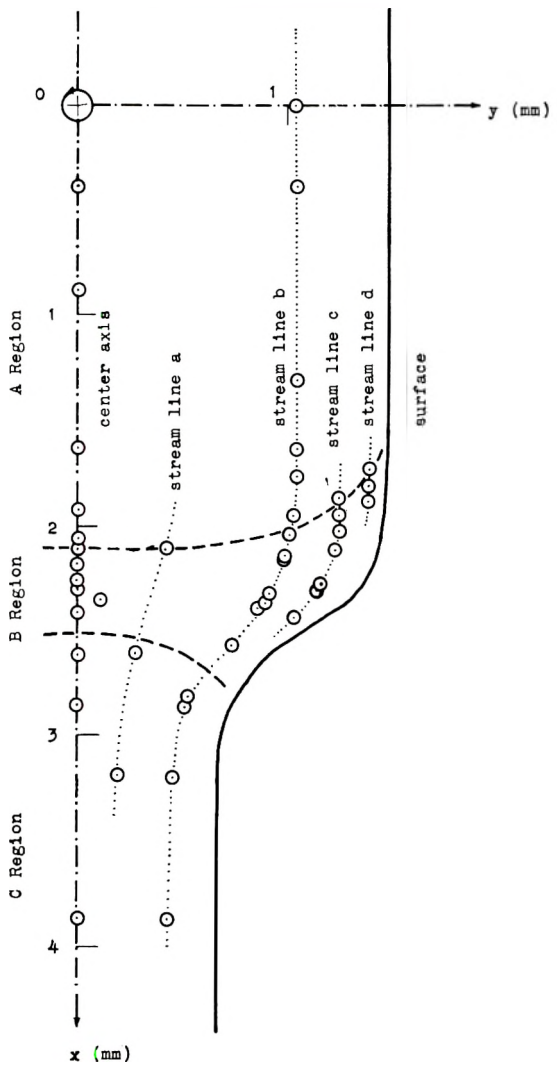

Fig. 2. Specimen. Right half is shown. A large circle represents the origin of the coordinates which define the irradiated position of x-ray. Small circles indicate the irradiated positions.

The partial draw ratio of the specimen around the necking part continuously increases with increase of the x coordinates along each stream line thus defined, and the draw ratio at the fully drawn part of the specimen is about 750%.

The x-ray diffraction diagrams were first made on the positions along the center axis of the specimen, and then measurements were repeated in the same way along the outer stream lines. In this study, the stream line was so defined as to divide the y coordinates from the center axis to the surface at every point on the line into the same ratio. In Figure 2, four stream lines are shown in the right half of the specimen.

B. X-Ray Measurements

X-ray diffraction diagrams were made with nickel-filtered CuKα radiation.

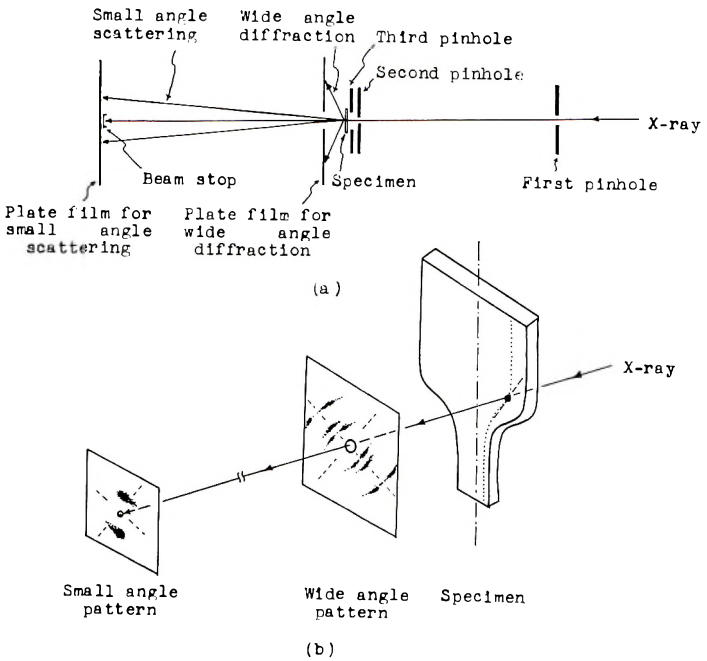

Fig. 3. Schematic illustration of the specially designed microbeam x-ray camera: (*a*) camera geometry; (*b*) diffraction diagrams and specimen.

For taking x-ray diagrams, a specially designed small-angle camera, schematically shown in Figure 3*a*, was used in this experiment. Two pin-hole collimators, 150 μ in diameter, 20 cm. apart, were aligned on an optical bench. The specimen was directly attached to the back side of the third pin-hole. Films were set for both the wide- and small-angle x-ray diffractions on the same part of the specimen at the same time, and the specimen–film distances were 1.5 and 13 cm. for the wide- and small-angle diagrams, respectively. The small-angle diffraction passes through a small window at the center of the film placed for the wide-angle diffraction. The arrangement is schematically illustrated in Figure 3*b*.

III. RESULTS

Some of the characteristic diagrams are selected from many diffraction diagrams taken at various points on the center axis, along the intermediate

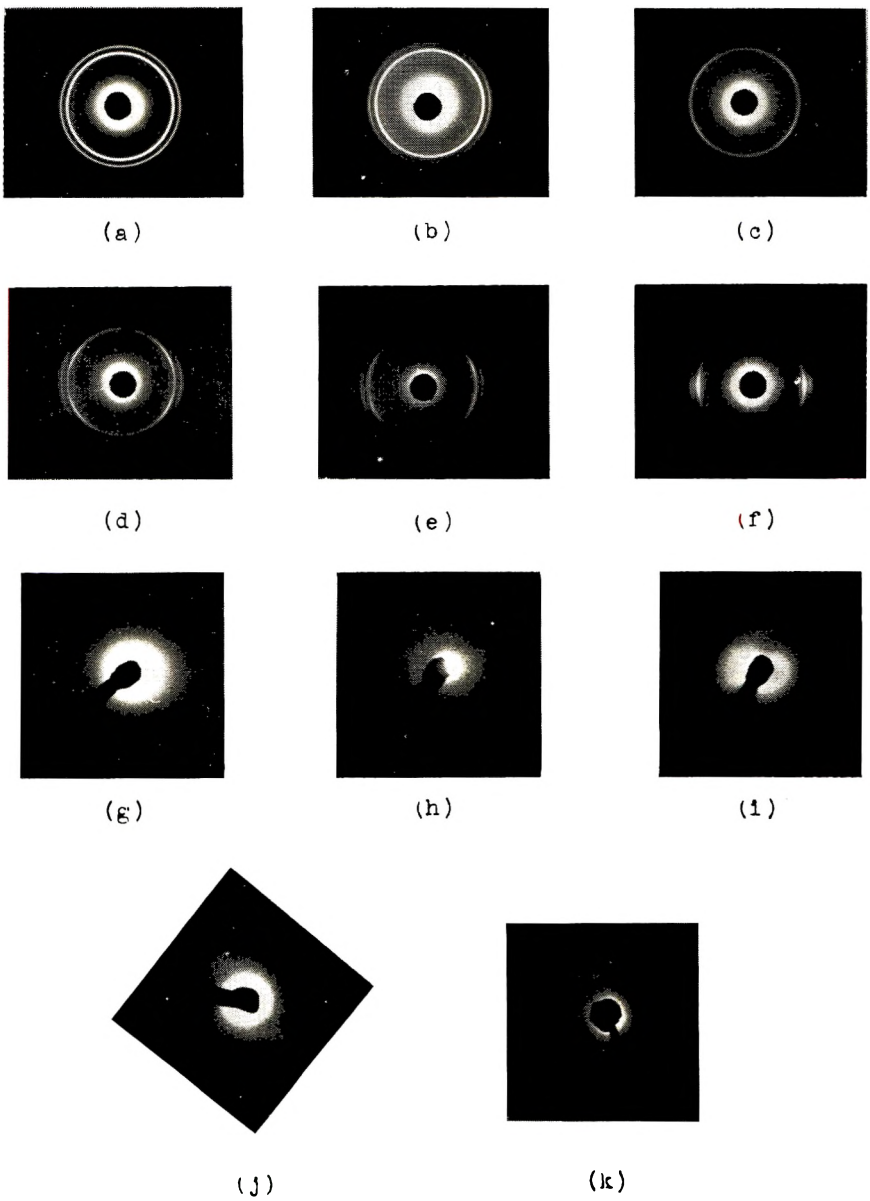

Fig. 4. Some characteristic wide- and small-angle x-ray diffraction photographs. (*a*)-(*f*) Wide-angle patterns taken at the positions in Fig. 2: (*a*) (1.66, 0), (*b*) (2.19, 0), (*c*) (2.27, 0), (*d*) (2.47, 0), (*e*) (2.61, 0), and (*f*) (2.85, 0). (*g*)-(*k*) Small-angle patterns taken at the positions: (*g*) (1.66, 0), (*h*) (2.19, 0), (*i*) (2.27, 0), (*j*) (2.35, 0.90), and (*k*) (2.85, 0).

stream lines, and also along the surface of the specimen, and they are reproduced in Figure 4.

For convenience, variations in the x-ray diagrams are separately described in the three regions, the A, B, and C regions (see Fig. 2).

Wide-Angle Diffraction

A Region. No change on wide-angle diffraction diagrams was observed all over this region. The diagrams all consist of well defined rings of uniform intensity.

B Region. Crystallite orientation occurred in this region. The (200) reflection appeared as a well defined single arc on the equator. On the other hand, the (110) reflection was split into two arcs on both sides of the equator. The (020) and (310) reflections were also split in the same way. In Figures 4*b*–4*e*, the progressive concentration of the (200) reflection at the equator was observed. Each splitting angle between a pair of arcs on both sides of the equator for the (110), (020), (310), and other reflections decreased gradually with increase of the draw ratio.

On the stream lines, similar changes as along the center axis were observed; however, beside the center axis, the meridian of each x-ray diagram was not parallel to the draw direction of the specimen, but coincided with the tangent of the stream line at each irradiated position.

C Region. Through this fully drawn region, all the (*hk*0) reflections were very well concentrated on the equator (Fig. 4*f*). The (110) and (200) reflections were accompanied by diffuse scattering. In addition, some of the so-called amorphous halo was also concentrated at the equator.

The average orientation angle φ between the c axis of the crystallite and the stream line running through each irradiated position was calculated from the angular position of the (110) reflection by use of Polanyi's equation.[8] The degree of the crystallite parallelity π (in per cent) was conventionally determined from the angular half width μ of diffraction arc in the fiber pattern by the relation:[9]

$$\pi = [(180° - \mu)/180°] \times 100$$

The apparent crystallite size L was estimated by using Warren's approximation for Scherrer's formula[10] from the line broadening of the wide-angle diagram. As the line broadening due to crystallite lattice distortion and other imperfections could not be separated from that due to crystallite size, these contributions on the broadening were not taken into account in the estimation. The results of these determinations are summarized in Tables I and II.

Small-Angle Scattering

A Region. An isotropic ring-shaped halo (Fig. 5*a*) was observed through this region.

TABLE I
Results of the Wide- and Small-Angle Diffractions (Along the Center Axis)

	Wide-angle diffraction			Small-angle scattering			
x, mm.	φ	π, %	L, A.	D, A.[a]	J, A.	δ[b]	Remarks
1.66	Random orientation	0	245	130			A region
1.93	Random orientation	0	230	130			—
—							
2.19	42.5°	80	200	170(m) 130(eq)			
2.27	35°	80	165	170(m) 130(eq)	(110)		B region
2.47	18.5°	85	150		(140)		
—							—
2.61	<15°	86	110		125	±42°	
2.85	Very small	90	110		125	±40°	C region
3.87	Very small	93	90		125	±40°	

[a] m: meridian, eq: equator.
[b] ± denotes existence of maxima on the layer streaks on both sides of the meridian.

TABLE II
Results of Wide- and Small-Angle Diffractions (Along the Stream Line b)

	Wide-angle diffraction			Small-angle scattering			
x, mm.	φ	π, %	L, A.	D, A.[a]	J, A.	δ[b]	Remarks
1.66	Random orientation	0	245	130			A region
—							—
1.98	25.5°	45	120	167(m) 125)eq)			
2.15	23.5°	47		167(m) 140(eq)	(120)	(−40°)	
2.31	18.7°	69	75		115	−40°	B region
2.35	13.5°	83			125	−37°	
2.38	<10°	88			120	−40°	
—							—
2.41	Very small	89	70		125	±40°	
2.85	Very small	91	75		123	±38°	C region
3.87	Very small	93	70		125	±38°	

[a] m: meridian, eq: equator.

[b] ± denotes existence of maxima on the layer streaks on both sides of the meridian; − means that the oblique pattern has maxima in the second and fourth quadrant.

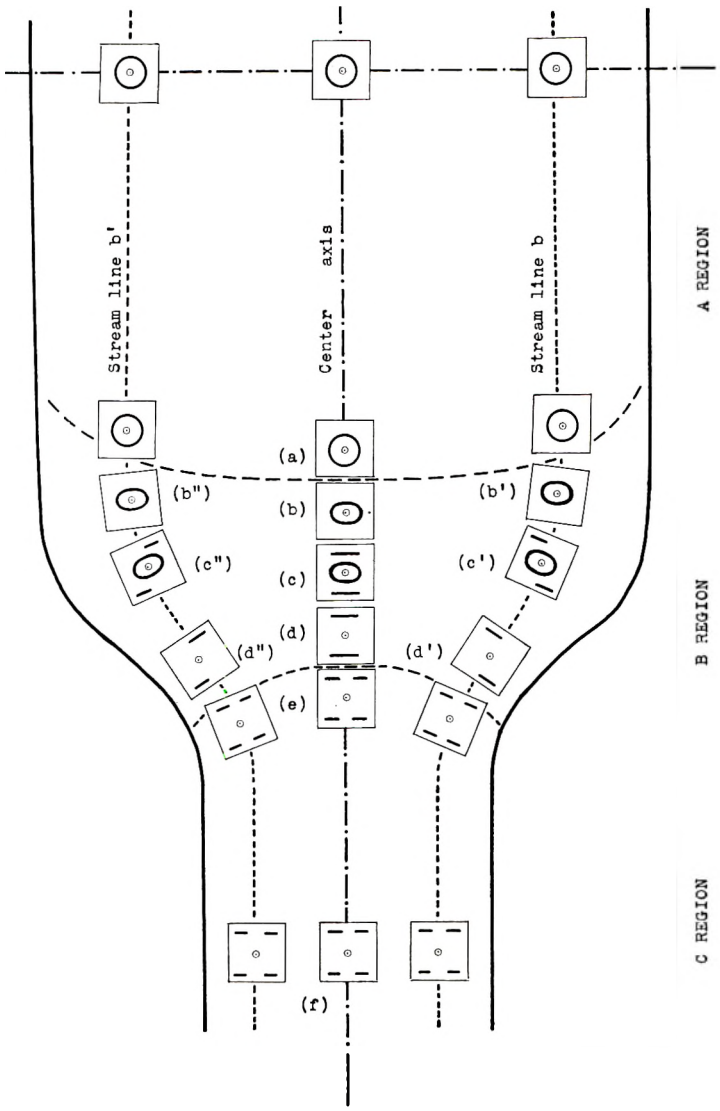

Fig. 5. Characteristic figures of the small-angle x-ray patterns along the stream lines.

B Region. The small-angle scattering diagrams in this region show interesting variations along each stream line. These are shown schematically in Figure 5.

Along the center axis of the specimen, with increase of the draw ratio, an elliptical halo with its minor axis on the meridian (Fig. 5*b*) first appeared in this region. After this stage, a diffuse meridional scattering in layer like streaks appeared superposed on the flat elliptical halo (Fig. 5*c*). Then the elliptical halo disappeared, and the diffuse layer streaks on the meridian (Fig. 5*d*) remained at the lower part of this region.

Along the intermediate stream lines, rather similar changes (Fig. 5*a'*–*c'*) and 5*a''*–*c''*) were observed, however, the meridians of these x-ray diagrams were parallel to the tangents of the stream lines at the position where the diagrams were taken. One characteristic diagram obtained along the stream line shows asymmetrical off-meridian streaks as seen in Figure 5*d'*, which corresponds to Figure 5*d* on the center axis. This is a new kind of small-angle scattering diagram.[15] A detailed discussion of this will be given later.

C Region. Through this region, the quadrant meridional scattering appeared as diffuse layer streaks with intensity maxima on both sides of the meridian (Figs. 5*e* and 5*f*).

The values of D, J, and δ determined from the small-angle scattering diagrams are also listed in Tables I and II, where D is the Bragg distance, J is the identity period along the meridian (so-called long period), and δ is the azimuthal angle on the film between the meridian and direction from center to the diffraction peak.

IV. DISCUSSION

For convenience, structure changes in the specimen are also discussed separately into the A, B, and C regions.

A Region

Both the wide-angle diffraction and the small-angle scattering of this region show ring-shaped diagrams without any anisotropy. This means that no preferred orientation of the crystallites exists in this region, and that at the same time distribution of density inhomogeneities in the specimen is isotropic. The crystallite size estimated from the (200) diffraction width is about 200–240 A., and this is comparable to that obtained

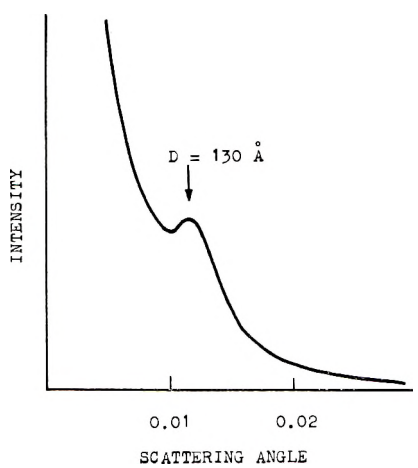

Fig. 6. Radial intensity distribution curve of the ring-shaped small-angle halo.

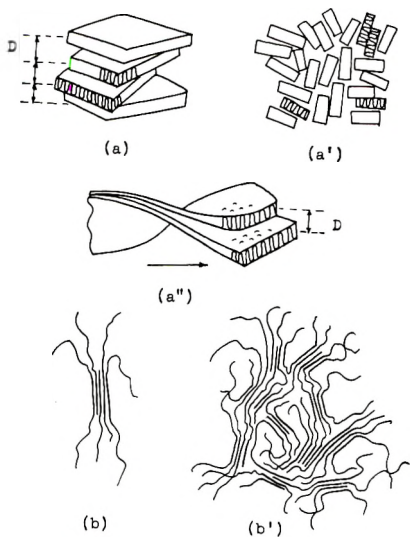

Fig. 7. Models for the fine texture in the A region: (*a*) nearly parallel stacking of lamellar crystallites with mean repeat distance *D*; (*a'*) random assembly of the partially parallel lamellar stackings (each block represents a lamellar crystallite); (*a"*) spherulitic assembly of the lamellar crystallites due to Keller's scheme; (*b*) fringed micelle type crystallites; (*b'*) random assembly of the fringed micelle.

from the single crystal aggregate.[17] Thus, estimated crystallite size may be interpreted as concerning the extent of lattice perfection in the paracrystalline state. The radial intensity distribution curve of the small-angle scattering is shown in Figure 6. The value of Bragg distance *D* corresponding to the maximum of the curve was found to be 130 A. This value is nearly half the crystallite size, and also is comparable to the thickness of lamellar single crystals obtained from xylene solution.

TABLE III
Results of the Wide- and Small-Angle Diffractions in the A Region

Crystallite orientation	Random
Crystallite size L_{200}, A.	~240
Distribution of density inhomogeneities	Isotropic
D, A.	~130

The results summarized in Table III lead to the schematic pictures of the fine texture in this region of the specimen as shown in Figure 7. Figure 7*a* indicates a stacking of lamellar crystallites. Every crystallite is about 100 A. or more in thickness; they are stacked up approximately parallel to each other, their repeat distances being about 130 A. The texture of this region is composed of disordered assembly of these stacked lamellar crystallites (Figs. 7*a'* and 7*a''*). It is still not certain whether the fine tex-

ture of crystalline polymer can be always described as lamellar packing composed of leaflet crystallites with folded molecules as shown in Figures 7*a'* and 7*a''*, even in this sample crystallized from molten state. So, there may also exist ordered or disordered entanglements of molecules (Fig. 7*b'*) in some parts of the texture.

B Region

1. Upper Part

The wide-angle x-ray diagram shows the crystallite orientation. The orientation of the *c* axis is still imperfect, while the *a* axis of the crystallite is almost perpendicular to the stream line. It seems that the orientation occurs rather on the *a* plane at first, and then the *c* axis is oriented gradually to the draw direction. The apparent crystallite size on the center axis in this part remains almost unchanged with increasing draw ratio. On the other hand, a striking fact was found on the stream lines other than the center axis: crystallites increased in size with increasing draw ratio and the increase of the size was considerably greater on the outer stream line (Fig. 8). This slight increase of crystallite size is interpreted as that some strain initially existing in the (110) and (200) planes of lamellar crystallites

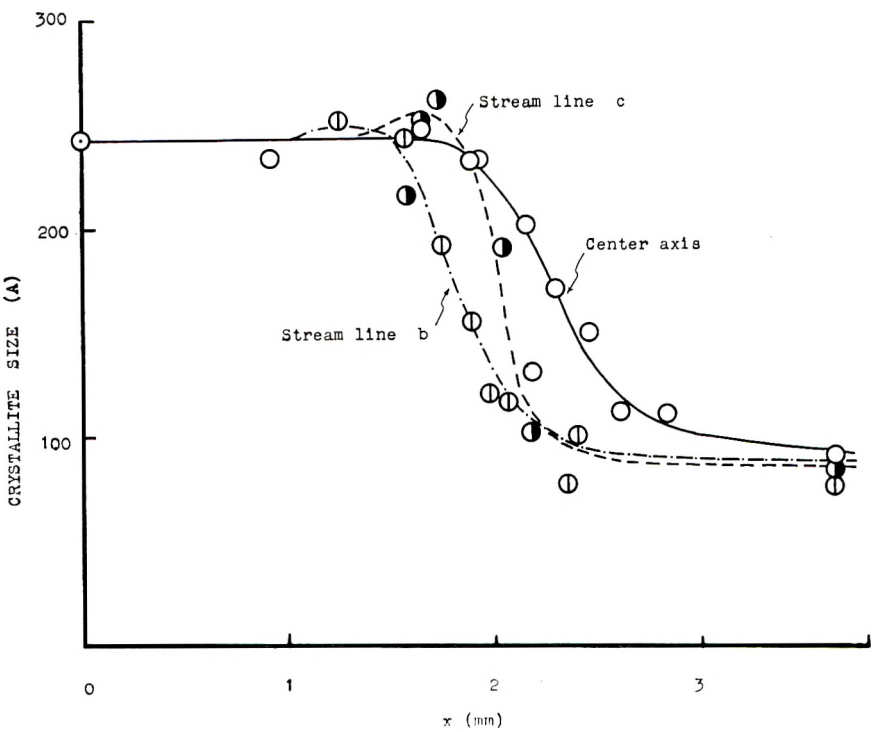

Fig. 8. Variations in crystallite size along the center axis and the stream lines of the specimen.

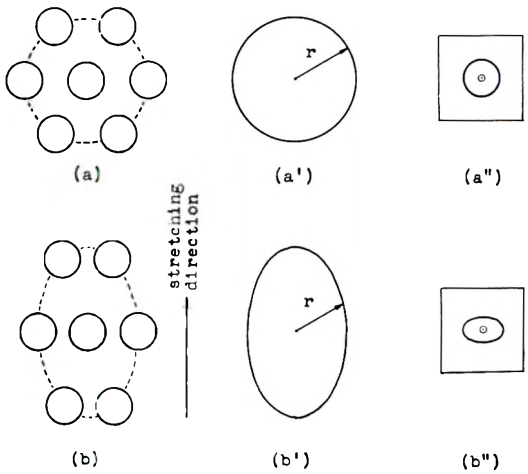

Fig. 9. A schematic view of crystallite assembly: (*a*) statistically isotropic distribution of crystallites represented by circles (before stretching). (*a'*) spherically symmetrical density distribution of crystallites corresponding to (a), where the first maximum of the distribution due to the nearest neighbors is on a sphere surface; (*a"*) small-angle x-ray pattern expected from the (*a'*) system; (*b*) statistically cylindrical symmetric assembly of crystallites (after stretching) (Mean interparticle distance elongated in the stretching direction); (*b'*) radial density distribution shows first maximum on an ellipsoidal surface; (*b"*) small-angle x-ray pattern expected from the (*b'*) system.

is released by slight drawing, and consequently the effective coherent region of lattice diffraction may be extended by the structure deformation.

In this part, the ring-shaped small-angle halo becomes elliptical in shape, with its minor axis parallel to the meridian. The major axis is equal in length to the diameter of the ring-shaped halo appearing in the A region. From the maximum points of the radial intensity distribution curves on the meridian and equator, the Bragg distances D_m and D_{eq} were found to be 170 and 130 A., respectively. With increase of the draw ratio, the intensity of the elliptical halo gradually concentrates on the off-meridian part of the halo. A similar change has already been observed by the present authors on stretched polyvinyl alcohol (PVA) film.[11]

The elliptical halo of the small-angle scattering was first observed on the cold-working of age-hardened Al–Ag alloy by Jan.[12] On the cold-worked single crystal of the Al–Ag alloy, Sato and Kelly[13] also observed the elliptical halo, and explained it as due to deformation in the Guinier-Preston zone. The oval small-angle halo was also found on the stretched polyethylene by Hendus[14] and on the stretched PVA film by the present authors.[11] In the stretched PVA film, the present authors obtained the elliptical halo at a draw ratio of 20 and 50%, and they suggested that the elliptical halo might indicate a change in the density distributions of crystallites dispersion in the specimen, as shown in Figure 9.

Figure 7*a'* shows a random assembly of stacked lamellar crystallites. In Figure 10a_1 and 10a_2 are represented one of these stacking groups in

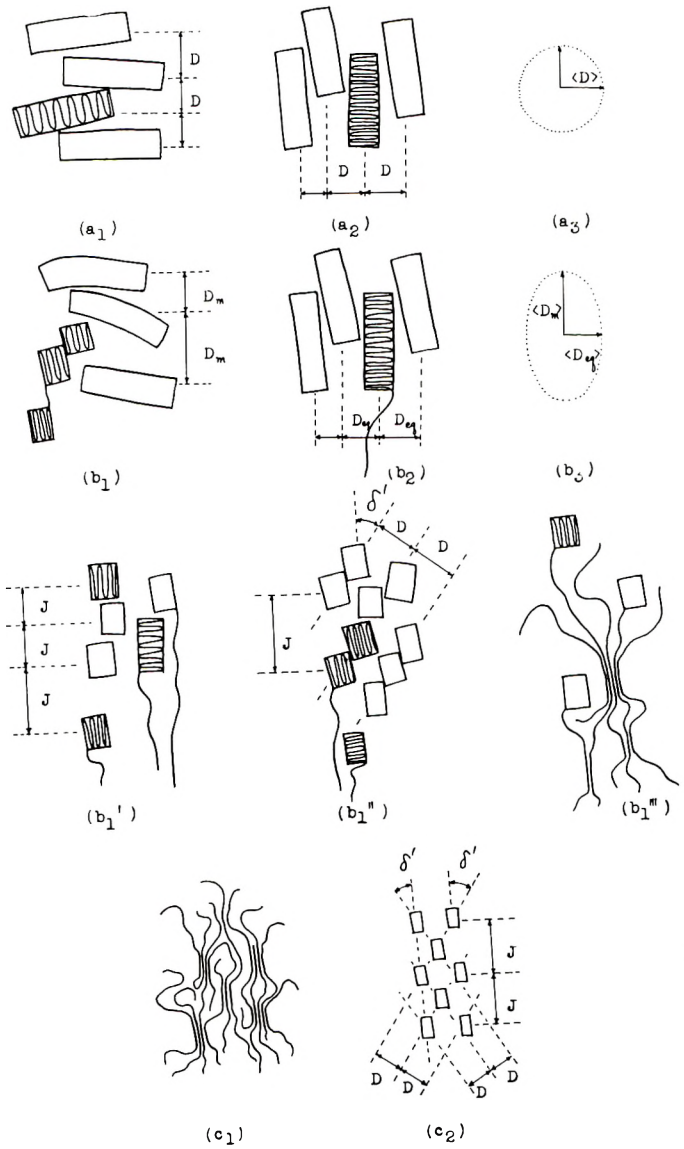

Fig. 10. Demonstration of the structure change in the necking part, based on the lamellar crystallite model. Draw direction is vertical. Each block represents a lamellar crystallite with folded chain molecules. It is generally considered that there may exist some amount of fringed micelle type crystallites also in the undrawn region. On the other hand, in the fully drawn region, most of the crystallites are unfolded in the fringed micelle type. (a_1) and (a_2) represent the lamellar stacking blocks, in which the surfaces are perpendicular and parallel to the draw direction respectively. In the A region, these stacking blocks are distributed in all directions, so the average lamellar spacings derived from small-angle scattering is equal in all directions as shown by (a_3). In the B region, crystallite deformation and cleaving at the (100) plane may occur by drawing, as shown

(caption continued on next page

which the surfaces are perpendicular and parallel to the draw direction of the specimen respectively. In the upper part of the B region, the structure changes such as a_1 to b_1 and a_2 to b_2 of Figure 10 may result from drawing, at least in a short range. In the change from structures of the type shown in Figure $10a_1$ to $10b_1$, deformation and cleavage of the lamellar crystallites and widening of the spacing between lamellar crystallites may occur at the same time. If the lamellar surface is nearly parallel to the draw direction, such a change as that of structure $10a_2$ to $10b_2$ may not be accompanied by so much widening of the lamellar spacing. Including these local structure changes, as a whole, it results that the structure in this part deforms in such a way that the azimuthal distribution of lamellar spacings (Fig. $10b_2$) gives an elliptical small-angle scattering halo.

On the other hand, the structure change in this part is also explained by another picture as the change from the form shown in Figure 11*a* to that shown in Figure 11*b*. By cold drawing, spherically symmetrical distribution of the nearest neighbor distance of crystallites in the draw direction may be elongated to change into an oblong elliptical distribution.

Hendus[14] observed the appearance of the flat elliptical small-angle halo with polyethylene specimens when the specimen was stretched about 20–50%. On the PVA film,[11] the oval halo was found at the same magnitude of stretching as with the stretched polyethylene. From these results it may be considered that the partial draw ratio in this part increased about 20–50% or more.

2. Middle Part

Diffraction diagrams showed better orientation than those in the upper part. The small-angle pattern was observed as a superposition of the flat elliptical halo found in the upper part and the diffuse layer streaks on the meridian in the lower part.

These observations lead to a conclusion that the texture in this part takes a mixed and intermediate structure of the upper and lower part.

3. Lower Part

a. On the Center Axis. Orientation of the crystallite along the center axis is better than that in the upper two parts and is progressively improved with increase of the draw ratio. Almost all the *c* axis is parallel in the azimuthal angle. Crystallite size estimated from the (200) reflection is nearly halved from the original size. This suggests that cleavage of crystallites occurred in this part.

---

by (b_1). Unfolding of the molecules in the lamellar crystallite may also begin. On the other hand, the average spacings in (b_2) remains almost unchanged, though in this direction the unfolding may more easily occur. As a result, in the upper part of the B region, the average spacings of every direction should be expected as shown in (b_3). In the lower part of the B region, more marked deformation, cleaving, and unfolding occur, as shown in (b_1'), (b_1''), and (b_1'''), and there may exist some regularity of arrangement of crystallites in short-range as in (b_1''). (c_1) and (c_2) show the short-range regularity in the fringed micelle assembly in the C region.

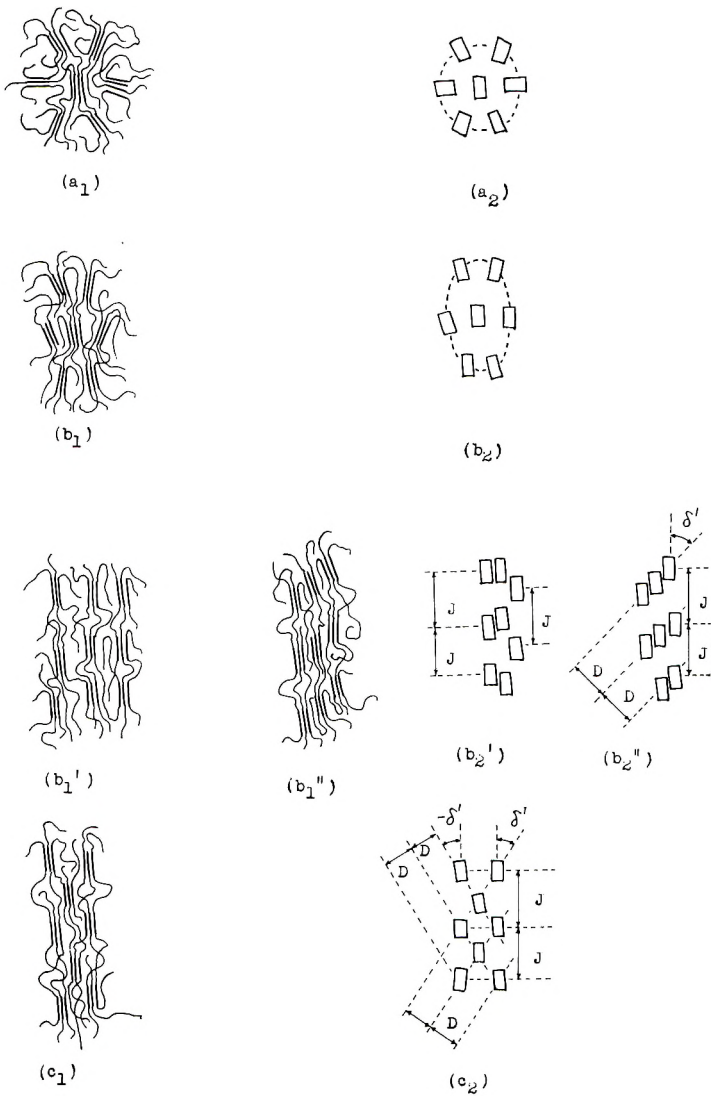

Fig. 11. Demonstrations of the structure change in the necking part, based on the fringed micelle model. The fringed micelle type crystallites may also exist in the undrawn region. The right half row of the figure represents the corresponding model for the scattering system of x-ray small-angle scattering. (a_1) shows a random assembly of crystallites (A region). The nearest neighbor distance is elongated in the draw direction (upper part of B region). (a_1), (a_2), and (b_1), (b_2) are similar to Fig. 9. In the lower part of this region (b_1') is ordinary long period regularity along the center axis. Two-dimensional regularity also may occur in short-range like (b_1'') along the stream line on the right side of the necking shoulder. (b_2') and (b_2'') show corresponding model of scattering system. (c_1) and (c_2) show two-dimensional regularity in short-range at the fully drawn region C.

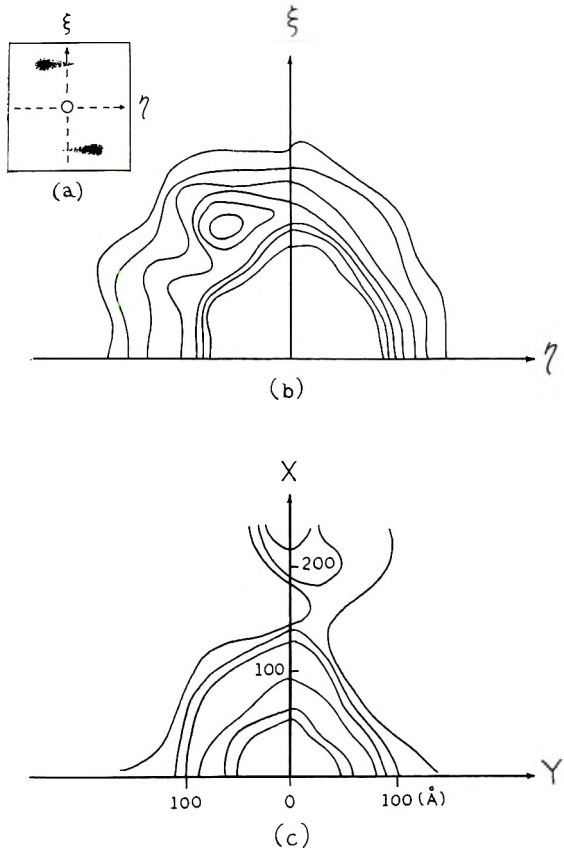

Fig. 12. Oblique long-period x-ray pattern: (*a*) schematic representation of the pattern at the position of (2.35, 0.90) in Fig. 2 (fiber axis vertical); (*b*) contour map of two-dimensional intensity distribution on the film (Contours in arbitrary scale); (*c*) is Fourier transform of (*b*).

The small-angle pattern contains a rather diffuse meridional layer streak with the Bragg distance of the order of 120 A. and is very weak in its intensity. This kind of small-angle scattering has been interpreted first as a regular arrangement of crystalline and amorphous regions along the microfibril axis (Fig. 11b_2).[1,2] Guinier and Belbéoch[3] determined a density distribution function by means of a Fourier transform of this kind of pattern. According to the paracrystal theory, Hosemann[5] proposed a model, and gave its optical transform quite similar to the pattern.

In this experiment, it is concluded that most of the lamellar crystallites in this part may be divided by drawing, as stated before, and progressive unfolding of the folded molecules in the lamellar crystallite may also occur. Accompanying these changes there may also be formation of some amount of microvoids along the extended microfibrils in the structure. The divided crystallites may take similar arrangement as Hosemann[5] proposed. At the same time, in some parts having good lateral order between the

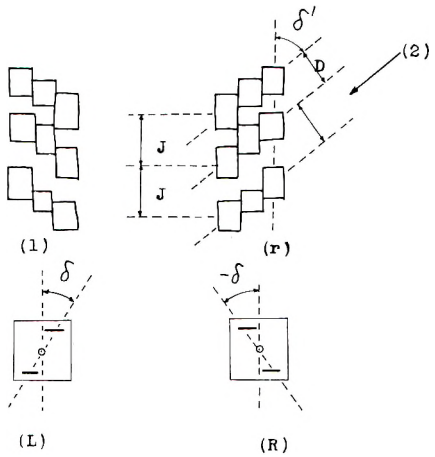

Fig. 13. A plausible model of the fine texture corresponding to the oblique two points pattern. (l) and (r) are the structures on the left and right side of the specimen. Each block represents crystallites. δ' was derived from the azimuthal angle δ on the film. The vertical lines in these figures represent the tangential direction of the stream line at each observed position. (L) and (R) are respective oblique x-ray patterns corresponding to the structure (l) and (r).

adjacent stretched chains, the regularity of the chains extends over neighboring chains, and fibrillar crystallites arise. These are shown in Figure $11b_2$.

b. On the Outer Stream Line. As seen in Figure $4j$, the small-angle pattern contains two rather diffuse off-meridian layer streaks perpendicular to the fiber axis. This oblique two-point small-angle pattern has somewhat different character from the ordinary small-angle scattering pattern of fiber as mentioned before, and gives some clue to the fine texture in this part. The result of analysis of this pattern is listed in Table IV.

Figure $5d'$ shows the pattern which was taken at the position of (2.35, 0.90) in Figure 2, on the right side of the specimen. On the left side, a similar but inversely inclined oblique pattern was obtained at the position of (2.35, −0.90). The relationship between these patterns is shown in Figures $5d'$ and $5d''$.

TABLE IV

Results of the Wide- and Small-Angle X-Ray Diffractions on the Position (2.35, 0.90) of the Specimen

Crystallite orientation	Inclination of the c axis from the tangent of the stream line, 13.5°; (a axis is vertical to the tangent)
Crystallite parallelity, %	80%
Crystallite size L_{200}, A.	ca. 70∼80
D, A.	∼100
J, A.	∼125
δ	—37°.

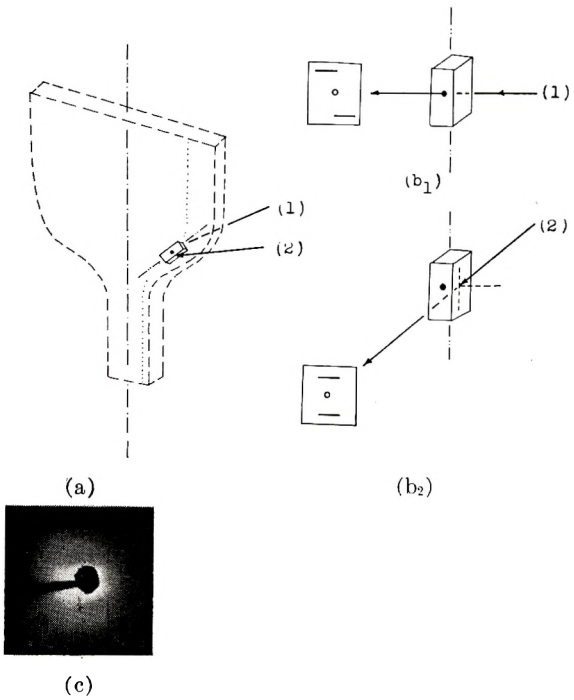

Fig. 14. Schematic view on the relationships of the specimen, incident beam and diffraction patterns at the oblique structure. (*a*) shows the position of the small specimen cut out from the oblique structure part. Direction (1) is the incident beam of the oblique pattern system (b_1) which is similar to Fig. 13. The (b_2) system shows the diffraction due to the incident beam (2) in (*a*) and Fig. 13. (*c*) is the small angle pattern obtained by the (b_2) system. The pattern is reasonably interpreted by the structure model and incident direction (2) drawn in Fig. 13.

In order to obtain more precise information on the structure corresponding to the small-angle patterns like Figure 5*d'*, the scattering intensity of the pattern was carefully observed by microphotometer. The contour map of two-dimensional intensity distribution on the film is shown in Figure 12*b*. Figure 12*c* is the Fourier transform of Figure 12*b*. A detailed report on this Fourier transform will be published later.

As seen in Figure 12*c*, the transformed map is very simple, and the density inhomogeneity of the scattering matter does not so distinctly show up in the contour map. However, some modulation of the contour along the meridian indicates the existence of a periodicity of crystallite alignment.

A plausible model of the structure[15] derived from the x-ray diffraction in this part is illustrated in Figure 13. In Fig. 13 (*l*) and (*r*) correspond to structures in the left side and right side of the specimen, respectively. The diffraction patterns like (*L*) and (*R*) in Figure 13 can be reasonab'y interpreted with these structure models.

Since the two diffuse off-meridian streaks of this pattern are not orthogonal to the draw direction of the specimen, Hosemann[5] called this kind

of pattern a "non-orthogonal pattern," and he also explained the occurrence of this pattern as due to the change in paracrystalline macrolattice cell resulting from the shearing.

If the fine texture in this part of the specimen corresponds to a model such as that shown in Figure 13, and if the specimen is irradiated from the direction (2) in Figure 14b_1, it should be expected that a small-angle scattering with long spacing about 100 A. will appear exactly on the meridian. Actually Figure 14*c* shows the above-mentioned meridional scattering. This pattern was obtained by using a small specimen cut out from the position predicted in Figure 14b_1 from the necking part.

C Region

In this region, the wide angle diffraction diagrams indicate the best orientation of crystallites. All the (*hk*0) reflections are very well concentrated on the equator, and it is concluded that the alignment of the *c* axis of the crystallites is nearly perfect. It is interesting that some amount of amorphous halo was also concentrated on the equator, though most of that remained unoriented. The (110) and (200) reflections were accompanied by diffuse scattering. This diffuse scattering may be caused by the paracrystalline state at the fringed part of the crystallites.

Through this region, the quadrant meridional small-angle pattern is obtained as diffused layer streaks with intensity maxima on both sides of the meridian. The intensity of the pattern becomes a little stronger with increase of x coordinates.

A schematic model[11,16] of the structure in this region is illustrated in Figures 10*c* and 11*c*. These two figures show the same structures. Such a periodic arrangement of crystallites, at least in two-dimensional and in short-range order, reasonably explains the appearance of the quadrant small-angle pattern. The direction of stacking of crystallites in the illustration was assumed from the angle δ in the small-angle pattern.

In relation with this study, secondary changes in the structure resulting from heat treatment, γ-ray irradiation, and aging in air were examined by the wide- and small-angle x-ray diffraction. Results of these studies will be published soon.

References

1. Hess, K., and H. Kiessig, *Naturwiss.*, **31**, 171 (1943).
2. Statton, W. O., *J. Polymer Sci.*, **41**, 143 (1959).
3. Belbéoch, B., and A. Guinier, *Makromol. Chem.*, **31**, 1 (1960).
4. Fischer, E. W., and G. F. Schmidt, *Angew. Chem.*, **74**, 551 (1962).
5. Hosemann, R., *Polymer*, **3**, 349 (1962).
6. Fankuchen, I., and H. Mark, *J. Appl. Phys.*, **15**, 368 (1944).
7. Aggarwal, S. L., G. P. Tilley, and O. J. Sweeting, *J. Polymer Sci.*, **51**, 551 (1961).
8. Polanyi, M., *Z. Physik*, **7**, 149 (1921).
9. Go, Y., and T. Kubo, *J. Soc. Chem. Ind. Japan*, **39**, 929 (1936).
10. Klug, H. P., and L. E. Alexander, *X-Ray Diffraction Procedures*, Wiley, New York, 1954.

11. Kasai, N., M. Kakudo, and T. Watase, *Kogyo Kagaku Zasshi*, **59**, 786 (1956).
12. Jan, J. P., *J. Appl. Phys.*, **26**, 1291 (1955).
13. Sato, S., and A. Kelly, *Acta Met.*, **9**, 59 (1961).
14. Hendus, H., *Kolloid-Z.*, **165**, 32 (1959).
15. Kasai, N., S. Fujiwara, S. Morioka, H. Kurose, M. Kakudo, and T. Watase, *Kogyo Kagaku Zasshi*, **64**, 55 (1961).
16. Kasai, N., Thesis, Osaka University, 1961.
17. Statton, W. O., and P. H. Geil, *J. Appl. Polymer Sci.*, **3**, 356 (1960).

Résumé

On a examiné, au moyen de la diffraction à grand et petit angle des rayons-X, la partie rétrécie du polyéthylène étiré à froid. On a utilisé une caméra, à microfaisceau de rayons-X spécialement construite avec laquelle il est possible d'obtenir à la fois des diagrammes à grand et petit angle à la même position au même moment. Avec une augmentation du rapport d'étirement le long de l'axe central de l'échantillon, les cristallites prennent d'abord l'alignement des axes a perpendiculairement à la direction d'étirement suivi par une orientation graduelle de l'axe x en direction de l'étirement. D'autre part un halo à petit angle en forme d'anneau isotropique se transforme progressivement en un halo elliptique dont le petit axe est sur le méridien. A ce stade apparaît une diffusion méridionale, semblable à des couches de stries, superposée au halo elliptique plat; ensuite le halo elliptique disparaît et les couches striées restent sur le méridien, finalement la diffusion du quadrant méridional apparaît sous forme de stries en couche diffuse avec des intensités maxima des deux cotés du méridien. Sur la ligne d'écoulement, on observe presque les mêmes variations des diagrammes à grand et petit angle que celles observées sur l'axe central, cependant le méridien de chaque axe n'est pas parallèle à la direction d'étirement mais coincide avec la tangente à la ligne d'écoulement en chaque position irradiée. La ligne de flux est conventionnellement fixée pour diviser les coordonnées y depuis l'axe central jusqu'à la surface dans le même rapport pour chaque point sur la ligne. Un diagramme caractéristique au long de la ligne de flux est un "modèle oblique à deux points" à petit angle, il apparaît sous la forme de couches striées en dehors du méridien. À partir de chaque diagramme, on a estimé l angle moyen d'orientation entre l'axe c et le méridien, le degré de parallélisme des cristallites et les dimensions apparentes des cristallites. Par diffusion à petit angle on a déterminé la distance de Bragg, l'élement périodique au long du méridien et l'angle azimuthal sur le film entre le méridien et la direction du centre au pic de diffration. Après examen de ces résultats, on présente une série de modèles plausibles pour un changement continu de structure dans la partie retrécie.

Zusammenfassung

Die kontinuierliche Strukturänderung in der Einschnürungsstelle von kalt verstrecktem Polyäthylen wurde mittels Röntgenweit- und -kleinwinkelstreuung unter Verwendung einer speziellen Mikrostrahl-Röntgenkamera intersucht, die die gleichzeitige Aufnahme von Weit- und Kleiwinkeldiagrammen an derselben Stelle gestattet. Längs der Mittelachse der Probe richten sich die Kristallite mit steigendem Streckungsverhältnis zuerst mit ihrer a-Achse senkrecht zur Streckrichtung aus, worauf eine schrittweise Orientierung der c-Achsen in die Streckrichtung folgt. Andererseits geht ein isotroper ringförmiger Kleinwinkelhalo kontinuierlich in einen elliptischen Halo mit der kleinen Achse im Meridian über. Hierauf überlagern Meridianreflexe in Form von Schichtlinienstreifen den flachen elliptischen Halo, der dann verschwindet. Es bleiben die Schichtlinienstreifen am Meridian zurück und schliesslich treten die Quadranten-Meridianreflexe in Form diffuser Schichtlinienstreifen mit Intensitätsmaxima beiderseits des Meridians auf. An der Strömungslinie wurden fast dieselben Veränderungen der Weit- und Kleinwinkeldiagramme beobachtet, wie an der Mittelachse, doch war der Meridian eines jeden dieser Diagramme nicht der Streckungsrichtung parallel, sondern

fiel mit der Tangente der Strömungslinie an der jeweils bestrahlten Stelle zusammen. Die Strömungslinie war wie üblich so definiert, dass sie die y-Koordinate von der Mittelachse bis zur Oberfläche an jedem Punkt der Linie im gleichen Verhältnis teilt. Ein charakteristisches Diagramm längs der Strömungslinie, ein "schiefes Zweipunkt"-Kleinwinkeldiagramm, trat als off-Meridian-Schichtlinienstreifen auf. Aus jedem Weitwinkeldiagramm wurden mittlerer Orientierungswinkel zwischen c-Achse und Meridian, Grad der Kristallitparallelität und scheinbare Kristallitgrösse bestimmt. Mittels der Kleinwinkelstreuung wurden der Bragg-Abstand, die Identitätsperiode längs des Meridians und der vom Meridian und der Verbindungsline Mittelpunkt-Reflex auf dem Film gebildete Azimutalwinkel bestimmt. Auf der Grundlage dieser Ergebnisse wird eine Reihe plausibler Modelle für die kontinuierliche Strukturänderung in der Einschnürungsstelle angegeben.

Received March 22, 1963

JOURNAL OF POLYMER SCIENCE: PART A VOL. 2, PP. 1977–1986 (1964)

Copolymerization of Tetrafluoroethylene with Ethylene Induced by Ionizing Radiation*

YONEHO TABATA, HIROSHI SHIBANO, and HIROSHI SOBUE,
Faculty of Engineering, University of Tokyo, Tokyo, Japan

Synopsis

Radiation-induced copolymerization of tetrafluoroethylene with ethylene was carried out. It was found from this investigation that the composition of copolymers varied continuously in a wide range of molar concentrations of one component. The melting point of the copolymers obtained varied continuously with the molar concentration of one component in monomer mixture between the melting points of both homopolymers. The x-ray diffraction measurements showed that the copolymer obtained was crystalline. The copolymerization proceeds by a radical mechanism. It was concluded that both the energy transfer to ethylene from tetrafluoroethylene during irradiation and great affinity of hydrogen atom for fluorine atom would play an important role in the copolymerization.

Introduction

Radiation-induced polymerization of tetrafluoroethylene was reported in a previous paper.[2] There has been no investigation on the copolymerization of tetrafluoroethylene by ionizing radiation. In this paper, the copolymerization of tetrafluoroethylene with ethylene by ionizing radiation is reported.

It was found from this investigation that the copolymerization could take place to yield copolymers with a statistical distribution of the monomer units.

Experimental

The tetrafluoroethylene used was a Nitto Kagaku product. The melting point was −145.5°C. Ethylene monomer was purified by treatment with 30% aqueous NaOH and 87% aqueous H_2SO_4 and was dried by passage through a trap (methanol–solid CO_2) at −78°C. Tetrafluoroethylene was condensed into an ampule containing solid ethylene monomer at liquid nitrogen temperature. The ampule containing solid monomers was evacuated to 10^{-2}–10^{-3} mm. Hg. Irradiation was carried out by γ-rays from a Co^{44} source at −78°C.

* A part of this paper was published previously.[1] Most of this paper was presented at the Fourth Radioisotopes Conference in Kyoto, October 1961.[2]

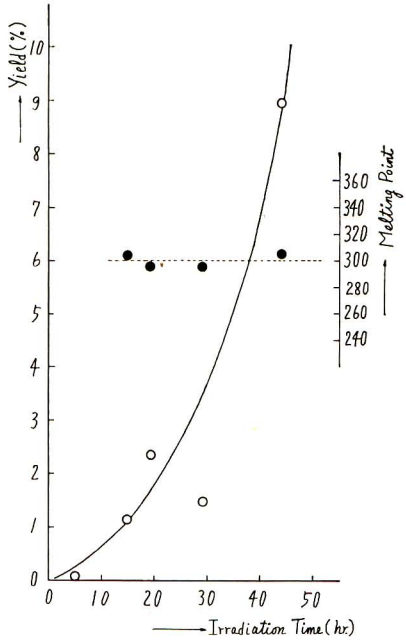

Fig. 1. Copolymerization of tetrafluoroethylene with ethylene. The relation between the copolymerization yield (weight per cent for total monomer mixture) and irradiation time at dose rate of 2×10^5 r/hr. at $-78°C$. Content of ethylene in monomer mixture was 44.7 mole-%. The points (●) show the effect of conversion on the melting point of the copolymer

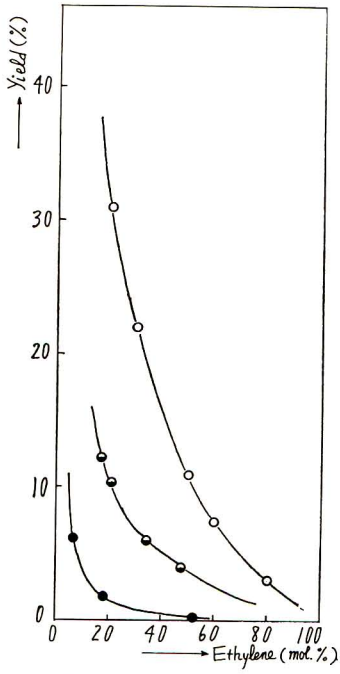

Fig. 2. The relations between the copolymerization yield and mole per cent of ethylene in monomer mixture in total dose of (○) 8.9×10^6 r (2×10^5 r/hr.), (◒) 4×10^6 r (6.4×10^4 r/hr.), and (●) 1.5×10^6 r (6.4×10^4 r/hr.).

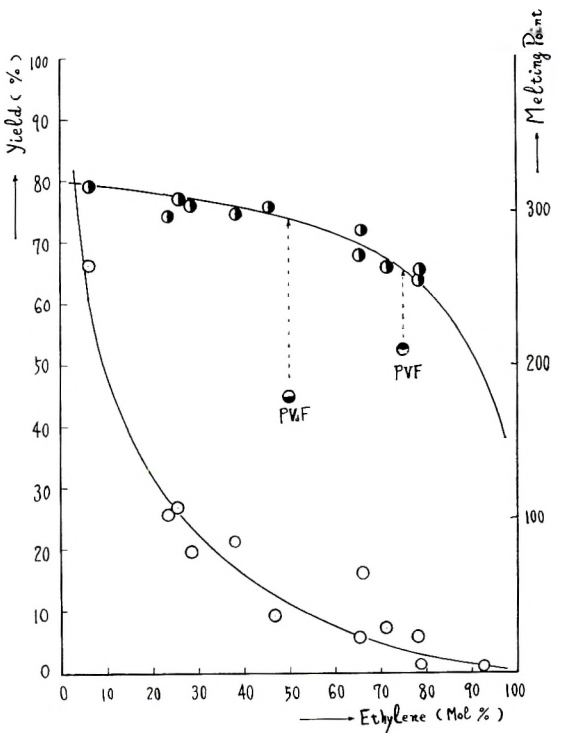

Fig. 3. The relations between (◑) melting point or (○) copolymerization yield and the molar concentration of ethylene in monomer mixture. The melting points of polyvinyl fluoride (◓) and polyvinylidene fluoride (◒) are also shown for comparison with that of copolymers.

Melting points, infrared spectra, and x-ray diffraction of the copolymers were determined.

Results and Discussion

The data on conversion versus irradiation time and data showing the effect of conversion on the melting point of the copolymer are given in Figure 1. It is obvious from the results that the melting point of the copolymer (probably depending on the degree of polymerization) does not depend on conversion.

The relations between the conversion and the mole fraction of ethylene in the monomer mixture are shown in Figure 2. It is apparent from the figure that the rate of copolymerization decreased rapidly with the molar concentration of ethylene in the monomer mixture. The data showing the effect of molar concentration of ethylene in the monomer mixture on the melting point of the copolymer is plotted graphically in Figure 3. It is evident from the figure that the melting point of the copolymer decreased gradually with the molar concentration of ethylene from about 320°C. to 240°C.

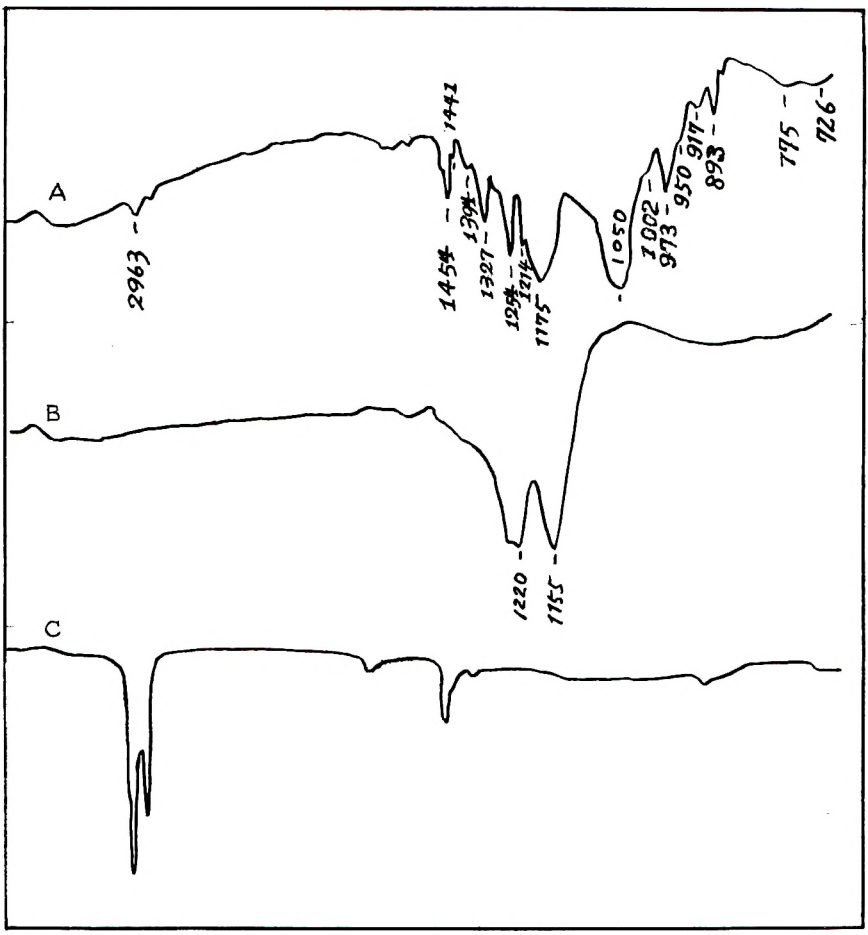

Fig. 4. Infrared spectra of (*A*) copolymer (molar ratio of monomer mixture: $C_2H_4/C_2F_4 = 2.60$); (*B*) polytetrafluoroethylene and (*C*) polyethylene in the region of wavelength of 2–16 μ.

TABLE I
Effect of DPPH on the Copolymerization

Monomers and added compounds, mmoles	Polymerization temperature, °C.	Dose rate $\times 10^4$, r/hr.	Dose, Mrad	Conversion, %
C_2F_4, 15.1 C_2H_4, 20.5 DPPH, 0.2 CH_2Cl_2, 11.7	−78	6.4	0.96	0
C_2F_4 15.1 C_2H_4 20.5 CH_2Cl_2 11.7	−78	6.4	0.96	1.36

It is interesting that the melting points of the copolymers with the same fluorine content are appreciably higher than those of polyvinyl fluoride and polyvinylidene fluoride, respectively.

These copolymerizations were completely inhibited by several radical scavengers. For example, the effects of 1,1′-diphenylpicrylhydrazyl (DPPH) on the copolymerization are summarized in Table I. The infrared spectrum of one of the copolymers is shown in Figure 4*A*.

In order to compare the spectrum with those of both homopolymers, the spectra of polyethylene (Fig. 4*C*) and polytetrafluoroethylene (Fig. 4*B*)

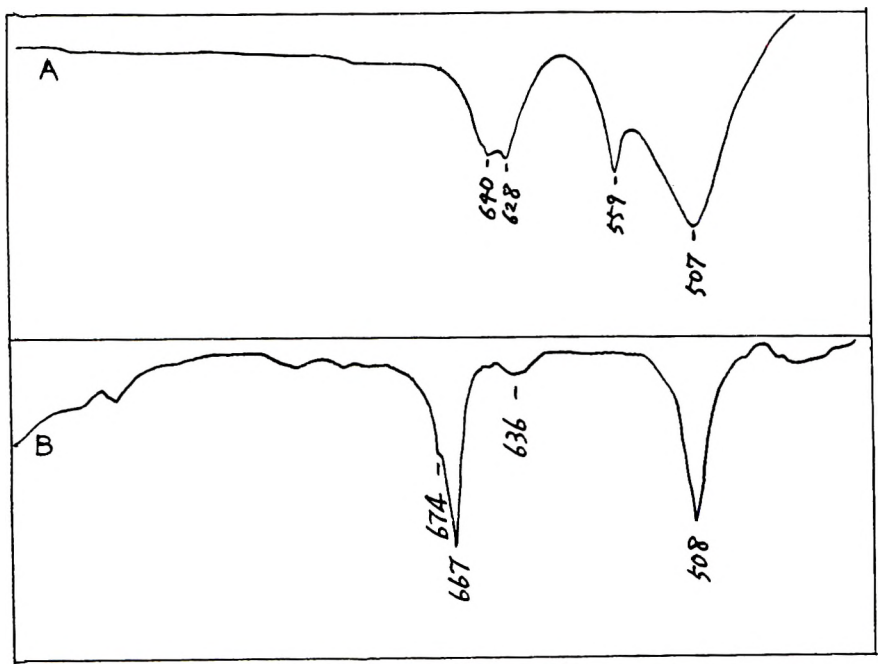

Fig. 5. Infrared spectra of (*A*) polytetrafluoroethylene and (*B*) the copolymer (molar ratio of monomer mixture: C_2H_4/C_2F_4 = 2.60) in the region of wavelength of 10–25 μ.

are shown in the same figure. The spectra in the KBr prism region are shown in Figure 5. It is evident from the figure that the spectrum of the copolymer is quite different from those of the two homopolymers, and the spectrum is not obtained by superposition of the spectra of the two homopolymers.

The spectra of polyvinyl fluoride, the copolymer, and polyvinylidene fluoride are shown in Figures 6*A*, 6*B*, and 6*C*, respectively. It is obvious from the figure that the spectra are also quite different from each other, in spite of the similar contents of fluorine and hydrogen in the copolymer.

The alternative possibilities of the production of a mixture of homopolymer or a block copolymer can be definitely excluded.

It is well known that the interaction between hydrogen and fluorine atoms is very strong. Therefore it is easily understood that the stretching vibration of ν(C-F) would be influenced profoundly by a nearest hydrogen atom in the same polymer.

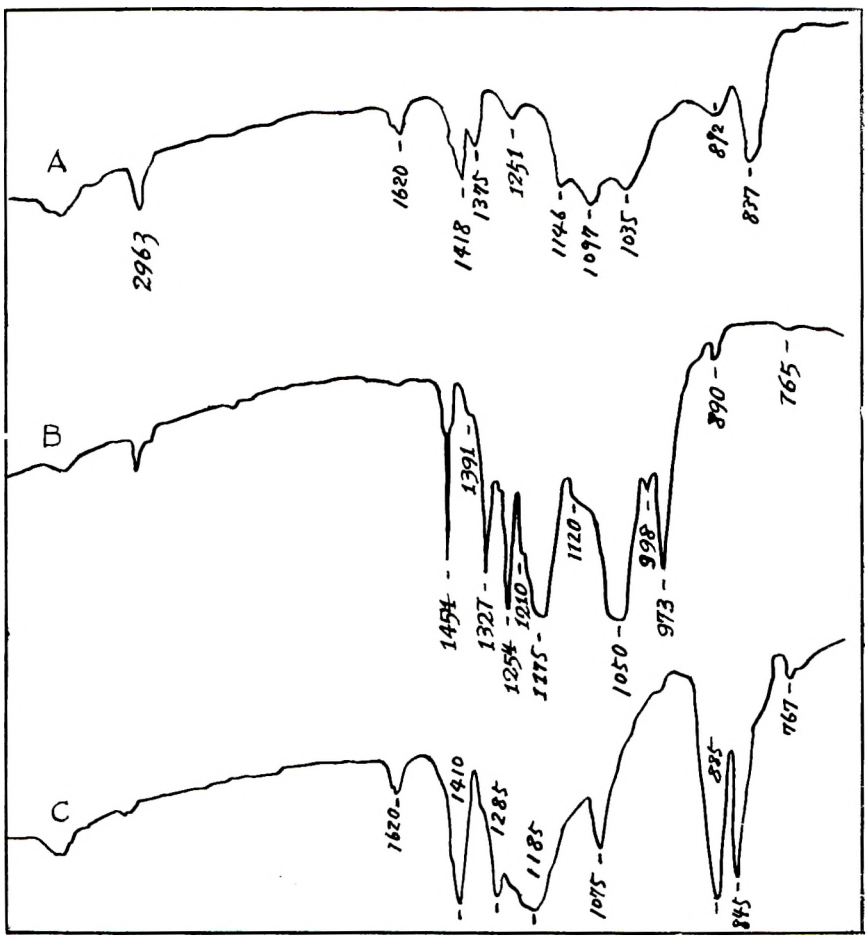

Fig. 6. Infrared spectra of (*A*) polyvinyl fluoride, (*B*) copolymer (molar ratio C_2H_4/C_2F_4 = 1.30 in monomer mixture), and (*C*) polyvinylidene fluoride.

Many characteristic absorption bands were observed in the copolymers. The influence of the molar ratio (C_2H_4/C_2F_4) in the monomer mixture on the infrared spectra are shown in Figure 7. Tentative assignments of the absorption bands of the copolymer are shown in Table II. As is obvious from the table, almost all the absorption bands increase or decrease continuously with the molar concentration of one component in the monomer mixture. These experimental facts suggest that the copolymerization leads to copolymer with a statistical distribution in a wide range of molar ratios.

The determination of fluorine contents in the copolymer are now progressing in our laboratory by an elemental analysis and by measurements of nuclear magnetic resonance of proton and fluorine.

The X-ray diffraction curves of polyethylene, a copolymer, and poly-

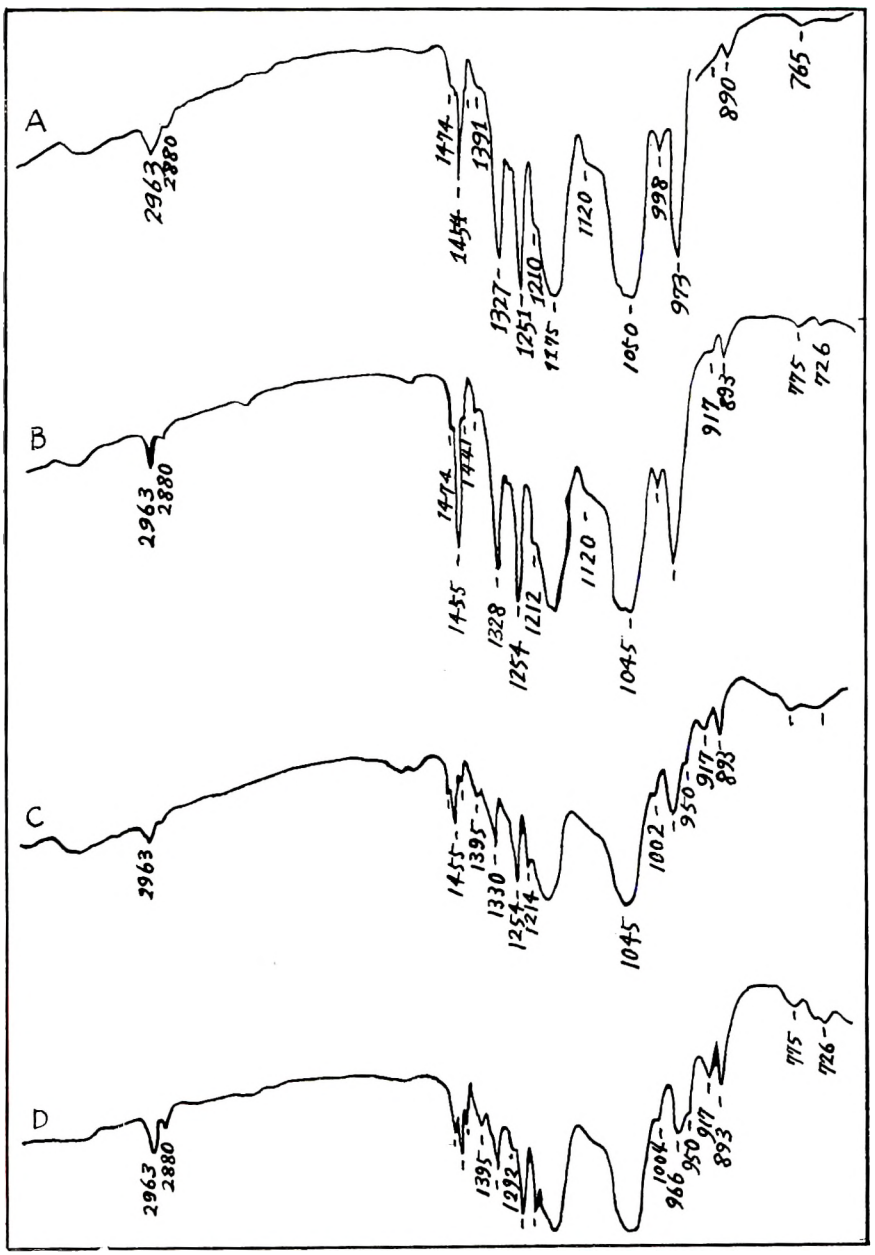

Fig. 7. Infrared spectra of copolymers having various molar ratios of C_2H_4/C_2F_4 in monomer mixture: (*A*) 1.08, (*B*) 1.30, (*C*) 2.60, and (*D*) 4.16.

tetrafluoroethylene are given in Figures 8*A*, 8*B*, and 8*C*, respectively. The peaks at $2\theta = 18.4$ and $2\theta = 21.5$ were observed in the diffraction intensity curve of the copolymer.

TABLE II
Tentative Assignments for Ethylene–Tetrafluoroethylene Copolymer

Wavelength, cm.$^{-1}$	Intensity	Component		Assignment
		C_2H_4	C_2F_4	
2963	m	Inc.	Dec.	$\nu a(CH_2)$
2880	w	Inc.	Dec.	$\nu s(CH_2)$
1474	w	Inc. sharp	Dec. shoulder	$\delta(CH_2)$
1456	s. sharp			$\delta(CH_2)$
1441	m	Inc. sharp	Dec. shoulder	
1395	w	Inc.	Dec.	
1352	v, w, shoulder	Slightly inc.		$\omega(CH_2)$
1330	s. sharp			
1292	v, w, shoulder	Slightly inc.		$\omega(CH_2)$
1254	s. sharp			
1214	w	Inc. sharp	Dec. shoulder	
1175	v, s, broad			$\nu a(CF_2)$
1120	v, w	Shoulder	Slightly inc. sharp	
1045	v, s, broad			$\nu s(CF_2)$
1004	w	Dec. shoulder	Inc. sharp	
975 966	m	m gradually shift m		
950	w	w	v.v.w.	
917	w	Inc.		
893	m	Inc.		
775	w	Inc.	Dec.	$\gamma(CH_2)—(C_2H_4)_l—$
726	w	Inc.	Dec.	$\gamma(CH_2)—(C_2H_4)_n—$
690	m, shoulder			
674	m	Inc.		
667	s		Inc.	
647	w, shoulder		Inc.	$\omega(CF_2)$
628				
600	w, broad	Inc.		
591	w, broad	Inc.		
571	w		Inc.	$\delta(CF_2)$
531	w, shoulder			
520	w, shoulder			
508	s		Inc.	$\gamma(CF_2)$

The spacing of the strongest diffraction peak ($2\theta = 18.4$) of the copolymer is an intermediate value between that of ethylene ($2\theta = 21.1$) and tetrafluoroethylene ($2\theta = 17.3$). The spacing of the copolymer varies continuously, depending on the molar ratio in monomer mixture. This seems

to be the first case in which a vinyl copolymer is crystalline over the entire monomer composition range.

Polymerization Mechanism

As reported in previous papers,[2,3] the polymerization of tetrafluoroethylene proceeds by a radical mechanism in the liquid state of the monomer at −78°C., while the polymerization of ethylene proceeds under the

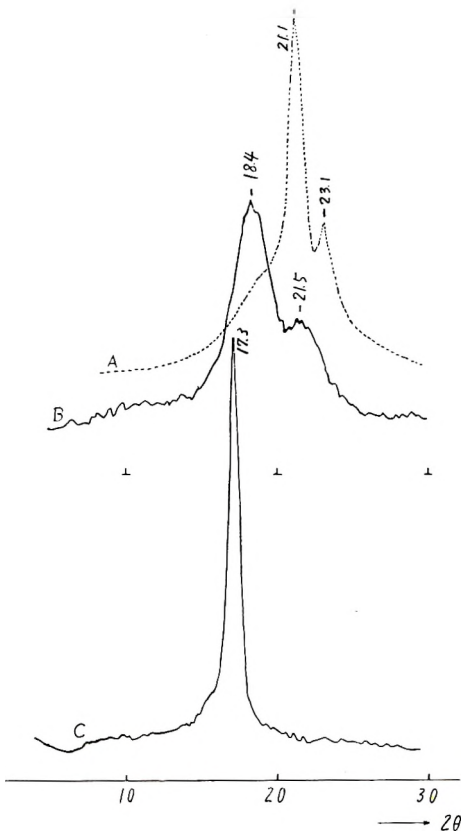

Fig. 8. X-ray diffraction intensity curves of (*A*) polyethylene A, (*B*) copolymer (ethylene was 24 mole-% in monomer mixture) and (*C*) polytetrafluoroethylene.

same conditions by a cationic mechanism. Since the copolymerization of both monomers was inhibited by radical scavengers, as described above, the copolymerization proceeds by a radical mechanism. In this copolymerization, it seems that the energy transfer to ethylene from tetrafluoroethylene during irradiation plays an important role. On the other hand, the great affinity of hydrogen for fluorine atoms would also play an important role in the copolymerization.

The copolymerization process appears to follow the scheme:

$$C_2H_4 \rightsquigarrow C_2H_4^*$$

$$C_2F_4 \rightsquigarrow C_2F_4^*$$

$$C_2H_4 + C_2F_4^* \rightarrow C_2F_4 + C_2H_4^*$$

The authors wish to express their thanks to Prof. Morawetz for his helpful discussion.

References

1. Tabata, Y., H. Shibano, and H. Sobue, *Ann. Rept. Japan Assoc. Radiation Res. Polymers*, **2**, 333 (1960).

2. Tabata, Y., H. Shibano, and H. Sobue, paper presented at 4th Japanese Conference of Radioisotopes, Kyoto, Japan, October 1961.

3. Tabata, Y., A. Hara, H. Shibano, and H. Sobue, *J. Polymer Sci.*, **A1**, 1049 (1963).

Résumé

On a effectué la copolymérisation, induite par radiation, du tétrafluoroéthylène avec l'éthylène. A partir de cette étude, on a trouvé que la composition des copolymères varie continuellement dans un large domaine de concentrations molaires d'un composant. Le point de fusion des copolymères obtenus varie continuellement avec la concentration molaire d'un composant dans le mélange des monomères entre les points de fusion des deux homopolymères. Les mesures de diffraction aux rayons-X montrent que le copolymère obtenu est cristallin. La copolymérisation a lieu par un mécanisme radicalaire. On peut conclure que le transfert d'énergie du tétrafluoroéthylène à l'éthylène pendant l'irradiation ainsi que la grande affinité de l'atome d'hydrogène pour l'atome de fluor pourrait jouer un rôle important dans la copolymérisation.

Zusammenfassung

Es wurde die Strahlungscopolymerisation von Tetrafluoräthylen und Äthylen untersucht. Die Zusammensetzung der Copolymeren ändert sich kontinuierlich über einen weiten Bereich der molaren Konzentration der einen Komponente. Der Schmelzpunkt der hergestellten Copolymeren variiert kontinuierlich mit der molaren Konzentration der einen Komponente im Monomergemisch zwischen den Schmelzpunkten der beiden Homopolymeren. Wie Röntgenbeugungsuntersuchungen ergaben, ist das gebildete Copolymere kristallin. Die Copolymerisation verläuft über einen radikalischen Mechanismus. Man nimmt an, dass sowohl die Energieübertragung von Tetrafluoräthylen auf Äthylen als auch die hohe Affinität des Wasserstoffatoms zum Fluoratom bei der Copolymerisation eine entscheidende Rolle spielen.

Received March 26, 1963

JOURNAL OF POLYMER SCIENCE: PART A VOL. 2, PP. 1987–1999 (1964)

Elemental Sulfur as a Plasticizer for Polysulfide Polymers and Other Polymers

A. V. TOBOLSKY and N. TAKAHASHI, *Department of Chemistry, Princeton University, Princeton, New Jersey*

Synopsis

In a recent publication from this laboratory it has been shown that the so-called elastic sulfur obtained by quick quenching molten sulfur from a temperature of 250°C. to a temperature of about −10°C. is really a mixture of polymeric sulfur and monomeric S_8 sulfur, the latter in a metastable condition. The reason why quick quenched sulfur is elastic is because of the plasticizing effect of the liquid S_8 sulfur on the polymeric sulfur. In this publication we show that large concentrations of S_8 can exist dissolved in a liquid condition in other polymers where it also acts as a plasticizer. In many cases these compositions appear completely stable, i.e., there is no tendency for the dissolved sulfur to crystallize out. The best example is crosslinked polyethylene tetrasulfide polymers. We show that these polymers can retain 40% of dissolved sulfur in the form of liquid S_8 over indefinitely long periods of time. We prove that the sulfur is in its elemental form by quantitative extraction with CS_2. The specific volume of the dissolved sulfur shows it is in a liquid condition. The mechanical properties of the sulfur plasticized crosslinked polymers are just what would be expected from this type of structure. Preliminary information concerning sulfur in other polymers is presented.

INTRODUCTION

In a recent publication from this laboratory[1] it has been shown that so-called elastic sulfur obtained by quick quenching molten sulfur from a temperature of 250°C. to a temperature of about −10°C. is really a mixture of polymeric sulfur and monomeric S_8 sulfur, the latter in a metastable liquid condition. The reason why this quick quenched sulfur is elastic is because of the plasticizing effect of the liquid S_8 sulfur on the polymeric sulfur. The unplasticized polymeric sulfur has a glass transition temperature of about 75°C. and is not rubbery at room temperature.

Quick-quenched elastic sulfur rather rapidly reverts to a nonelastic form because the liquid S_8 crystallizes out very rapidly at room temperature.

In this paper we show that large concentrations of S_8 can exist dissolved in a liquid condition in other polymers, where it also acts as a plasticizer. In many cases these compositions appear completely stable, i.e., there is no tendency for the dissolved sulfur to crystallize out.

The best example is crosslinked polyethylene tetrasulfide polymers. We show that these polymers can retain 40% of dissolved sulfur in the form of liquid S_8 over indefinitely long periods of time. We prove that the sulfur

is in its elemental S_8 form by extracting it quantitatively from the polymers by CS_2. We show that the specific volume of the dissolved sulfur plotted against temperature fits smoothly with the data of specific volume of molten sulfur versus temperature. Finally we show that the mechanical properties of the crosslinked polymers containing dissolved sulfur are just what would be expected from plasticized, crosslinked, amorphous polymers.

EXPERIMENTAL

Crosslinked polyethylene tetrasulfide polymers were prepared by reacting mixtures of ethylene dichloride and 1,2,3-trichloropropane with sodium tetrasulfide in a manner that has been described previously.[2] For simplicity the following notation has been adopted: C_0 represents noncrosslinked polyethylene tetrasulfide obtained when no trichloropropane was used; C_{10} represents the polymer obtained when 10 mole-% of trichloropropane was used in the above recipe, etc.

These samples were recovered from the polymerization bath in the form of crumb or powder. All these polymers, crosslinked or not, could be readily compression-molded to transparent sheets at 130–150°C. because of the very rapid interchange reaction of the tetrasulfide linkage.

These same polymers could also be mixed with elemental sulfur in the following manner. The required quantities of polymer in powder or crumb form and highly purified sulfur were mixed, placed in Pyrex glass tubes, and thoroughly degassed under high vacuum. The glass tubes were then sealed and the mixtures were heated for approximately 1 hr. at 155°C., after which the mixtures were homogeneous. The samples were molded into sheets on a hydraulic press at approximately 40,000 psi at temperatures between 125–155°C. (below the "floor" temperature of sulfur which is 160°C.) and for the minimum length of time necessary to obtain transparent homogeneous samples free from air bubbles and voids (generally less than 1 min.). After molding, the samples were quick quenched between two blocks of Dry Ice and kept in Dry Ice to prevent possible crystallization until measurements were started.

The following notation was used as exemplified below. C_{10} 60/S 40 means a sample made from 60 wt.-% of C_{10} polymer and 40 wt.-% of sulfur. Sometimes for even greater brevity the above composition is denoted as C_{10} 60.

Polybutyl acrylate film containing 1 mole-% of glycol dimethacrylate as crosslinking agent was prepared by photopolymerization between two glass plates in front of an RS sunlamp for 48 hr. with the use of benzoin as a photosensitizer. The films were extracted with CS_2 and vacuum-dried for two days. Other polymers used in the swelling experiments were provided by some industrial firms.

The densities of the samples were determined in distilled water at 23°C. by the displacement method of Wiley,[4] and the specific volume–temperature

curves were determined by the same method with the use of silicone oil whose specific volume as a function of temperature was known.

The 10-sec. shear moduli $G(10)$ were measured over a wide range of temperature with a Gehman torsion testing apparatus.[5] Stress relaxation experiments were carried out with the use of a stress relaxation balance described previously.[6]

The swelling experiments were carried out by keeping polymer films in liquid sulfur under a CO_2 atmosphere at 140°C. for 10 hr. and weighing the samples.

RESULTS AND DISCUSSION

Evidence for the Existence of Sulfur as a Supercooled Liquid in the Mixtures

It is reasonable to assume that the sulfur in the mixtures exists as liquid S_8 immediately after molding, since the temperature used for molding was above the melting point of monomeric sulfur but below the "floor" temperature of sulfur. Support for the hypothesis that the sulfur in the quick-quenched samples remains in a supercooled liquid state is provided by the following facts.

1. All the samples were transparent immediately after molding and showed no tendency to grow cloudy or otherwise indicate crystallization of the sulfur in the mixtures.

2. As indicated in Table I, all the sulfur in the mixtures was extractable by CS_2, showing that only monomeric sulfur was present. (However, this would not in itself distinguish between rhombic crystalline sulfur and supercooled liquid sulfur.)

TABLE I
Extraction of Sulfur by CS_2

Composition	Heating temp., °C.	Extractable, %
C_{50}20/S 80	126	79
	155	78
	179	80
	191	81
C_{50}40/S 60	155	60

3. In Figure 1, a plot of specific volumes measured at 23°C. immediately after molding against weight fraction of sulfur is given for six systems of various crosslink density. It can be seen that for each of the systems the experimental data fall on straight lines which extrapolate to the same point: 0.528 at weight fraction of sulfur = 1. This shows that the relationship:

$$v = w_p v_p + (1 - w_p) v_s \quad (1)$$

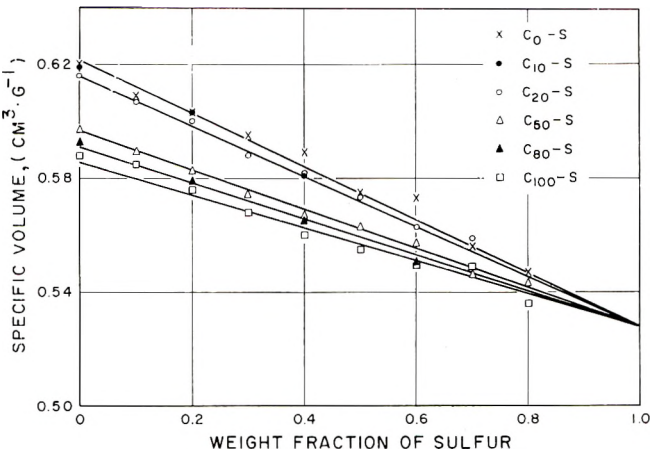

Fig. 1. Specific volume vs. weight fraction of sulfur for some poly(ethylene tetrasulfide)—sulfur mixtures of varying crosslink density.

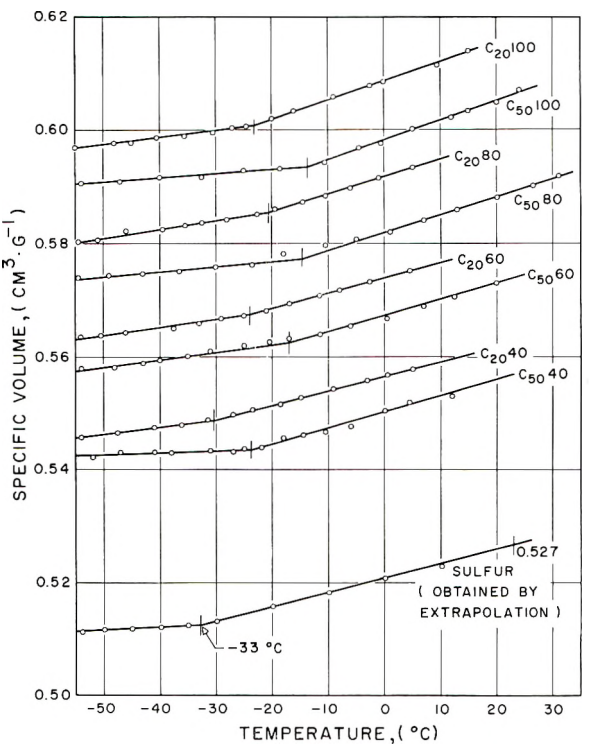

Fig. 2. Specific volume vs. temperature curves of some poly(ethylene tetrasulfide)—sulfur mixtures of various crosslink densities and sulfur contents showing the T_g of the mixtures.

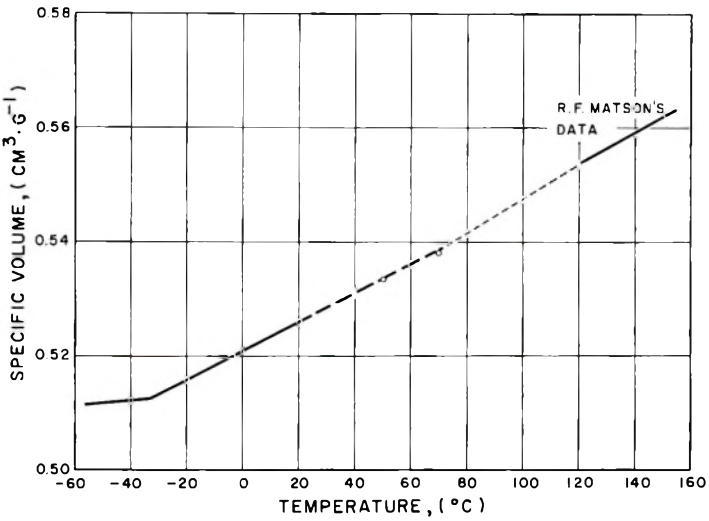

Fig. 3. Specific volume vs. temperature for supercooled liquid monomeric sulfur obtained by extrapolation. The dotted portion of the curve is extrapolated from the data of Matson on the density of liquid sulfur above its melting point.

(where v, v_p, and v_s are the specific volumes of mixture, polymer, and sulfur, respectively, and w_p is the weight fraction of polymer in the mixture) is obeyed by the mixtures; (i.e. the specific volumes are additive) with v_s = 0.528. The value of 0.528 for the specific volume of pure sulfur is quite close to the value predicted by extrapolating specific volume data on liquid sulfur above its melting point down to 23°C. and is far different from the specific volume of rhombic sulfur at 23°C.

4. The extrapolation technique for obtaining the specific volume of pure sulfur in the mixtures described above may be used to obtain the specific volume of the sulfur in the mixtures as a function of temperature, and this curve is shown in Figure 2 along with that of some mixtures of C_{50}-S and C_{20}-S which were used for the extrapolation. It is seen that in all cases there is a point of inflection in the curve corresponding to the glass transition temperature of the substance. Such behavior is common to polymers and many supercooled organic mixtures but is not manifested by simple crystalline substances. Thus we conclude that the sulfur in the mixtures exists as a supercooled liquid with a glass transition temperature of approximately −33°C. (This value is sufficiently different from the value of 75°C. obtained for the glass transition temperature of pure polymeric sulfur[1] to confirm the existence of the sulfur in the liquids in a monomeric S_8 state.) The specific volume–temperature curve for the sulfur in the mixtures is replotted in Figure 3 with two additional points at 50 and 70°C. obtained by the same extrapolation technique. Matson's data for the specific volume of liquid sulfur are plotted on the same graph, and it is seen that the extrapolated data of Matson lie very nearly on the same straight

line as the part of the curve above the glass transition temperature. This tends to further confirm that the sulfur in the mixtures exists in a supercooled liquid state.

Modulus–Temperature Curves, some Characteristic Parameters, and Front Factors of the Mixtures

Some typical plots of log $3G(10)$ as a function of temperature for C_{50}-S mixtures are shown in Figure 4. These curves show the various regions of viscoelastic behavior characteristic of amorphous polymers.[6] The curves for mixtures of high sulfur content such as C_{50} 10/S 90 and C_{50} 20/S 80 show a sharp increase in modulus at the beginning of the rubbery plateau region due to the onset of crystallization of the sulfur.

From the curves, we can obtain characteristic parameters[7] which describe the viscoelastic properties of the mixtures and with which we can discuss the effect of composition and crosslink density on these properties. Values for the four characteristic parameters: glassy state modulus $3G_1$, rubbery modulus $3G_2$, inflection temperature T_i (defined as the T where $3G(10) = 10^9$) and the negative slope of the curve, s, in the neighborhood of T_i are given in Table II for the various mixtures. Table II also shows T_g values for these polymers obtained by specific volume-temperature measurements.

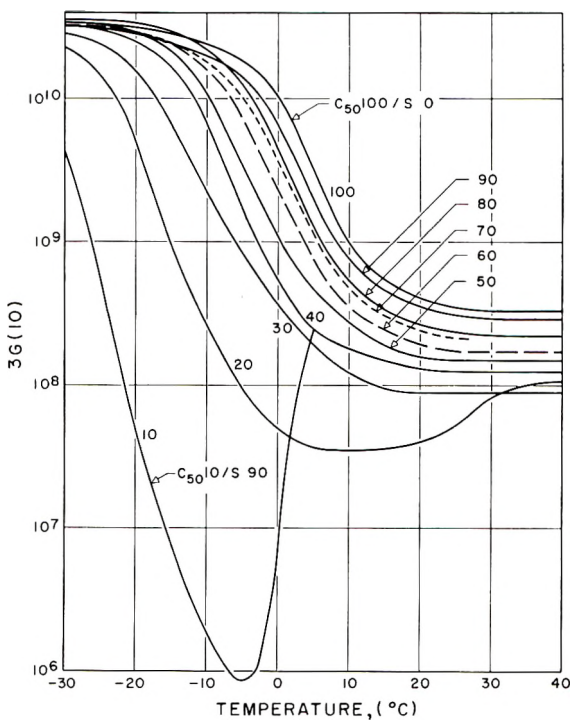

Fig. 4. Modulus temperature curves for various mixtures of polyethylene tetrasulfide of 50% crosslink density with sulfur.

TABLE II

Some Characteristic Parameters of the C_i–S Systems

Sample	$3G_1 \times 10^{10}$, dyne/cm.^{2}	T_i, °C.	T_g, °C.	s, °C.$^{-1}$	$3G_2 \times 10^7$, dyne/cm.^{2}	$\epsilon\Phi$
$C_0$100/S 0	2.5	−24		0.16	2.5	
90 10	2.0	−24		0.14	2.4	
80 20	2.3	−22		0.13	2.0	
70 30	2.5	−23		0.16	2.0	
60 40	2.9	−22		0.14	1.5	
50 50	2.2	−23		0.14	1.4	
40 60	3.1	−20		0.13	1.4	
30 70	2.3	−24		0.24	0.24	
20 80	—	−29		0.22	0.087	
C_{10}100/S 0	2.8	−20		0.14	8.5	0.73
80 20	2.8	−20		0.15	7.6	0.78
60 40	3.0	−20		0.14	5.4	0.69
C_{20}100/S 0	3.0	−17	−23	0.15	15.1	0.68
90 10	2.5	−16		0.15	9.4	0.46
80 20	2.7	−16	−21	0.15	11.0	0.59
70 30	2.6	−16		0.14	10.2	0.60
60 40	3.0	−16	−24	0.13	9.4	0.63
50 50	2.9	−18		0.14	6.8	0.53
40 60	2.5	−18	−30	0.18	5.2	0.50
30 70	2.7	−20		0.18	2.8	0.35
C_{50}100/S 0	3.4	10	−14	0.07	33	0.65
90 10	3.2	8		0.07	29	0.62
80 20	3.6	6	−15	0.08	22	0.52
70 30	3.5	6		0.08	21	0.54
60 40	3.5	4	−17	0.10	17.2	0.51
50 50	3.5	1		0.10	15.0	0.53
40 60	3.3	− 3	−23	0.11	12.5	0.54
30 70	—	− 6		0.09	8.9	0.49
20 80	—	−15		0.13	3.5	0.29
10 90	—	−26		0.21	0.09	
C_{80}100/S 0	3.6	25		0.13	27	0.37
80 20	3.5	20		0.11	23	0.37
60 40	3.5	14		0.10	22	0.44
40 60	3.3	2		0.08	13.4	0.40
C_{100}100/S 0	3.2	42		0.14	38	0.42
90 10	3.5	32		0.11	29	0.34
80 20	3.4	36		0.07	32	0.42
70 30	3.8	33		0.08	29	0.43
60 40	3.5	20		0.08	16.7	0.28
50 50	3.7	13		0.08	14.6	0.29
40 60	3.5	7		0.07	14.6	0.35
30 70	3.6	− 1		0.10	8.6	0.27
20 80	3.5	−14		0.12	1.9	0.09

$3G_1$ appears to remain almost constant for all compositions of mixtures of a given crosslink density but it shows a slight increase with increasing crosslink density. Table II shows the dependence of T_i and T_g on weight fraction of sulfur. In the mixtures of lower crosslink density (<50%) it can be seen that the T_g values remain fairly constant from pure polymer up to about 60 wt.-% sulfur content. In the mixtures of higher crosslink density (>50%) increasing the sulfur content depresses T_i almost linearly at first. This behavior is usual in the case of plasticized polymers in which the T_g of the plasticizer is far below that of the polymer as in these cases obtained by specific volume–temperature measurements. It is seen that the T_g values of the C_{20}-S mixtures are considerably lower than their T_i values. These results may be interpreted by assuming that within the experimental range of crosslink density, increasing crosslink density is not very effective in preventing the short range segmental motions of the molecules which occur at T_g but is quite effective in preventing the longer-range segmental motions of the molecules which occur at T_i.

s varies from 0.07 to 0.24 and is slightly dependent on the crosslink density. s remains approximately constant with increasing sulfur content in a mixture of given crosslink density up to very high sulfur contents where it increases.

$3G_2$ is dependent on both crosslink density and sulfur content, and Table II and Figure 4 show that $3G_2$ decreases with increasing sulfur content.

From the kinetic theory of rubber elasticity it can be shown that:

$$G = \Phi\epsilon cRT \tag{2}$$

where G is the rubbery shear modulus, Φ is the "front factor" ($\Phi = 1$ for an ideal rubber network), c is the theoretical number of moles of network chains per cubic centimeter obtained from the relative amount of ethylene dichloride and trichloropropane, ϵ is the efficiency of the crosslinking reaction, ($\epsilon = 1$ if the polymerization reaction involving dihalide and trihalide goes to completing), R is the gas constant, and T is the absolute temperature.

The values of $\epsilon\Phi$ were calculated from eq. (2) and are presented in Table II. All the $\epsilon\Phi$ values are less than unity and remain fairly constant over the range of crosslink densities and sulfur content of the mixtures although there is a tendency for $\epsilon\Phi$ to decrease at higher crosslink densities and sulfur content. This is probably due to a decrease in ϵ rather than in Φ as the efficiency of the crosslinking reaction is believed to decrease with increasing crosslink densities. Support is lent to the hypothesis that Φ should be independent of sulfur content by the fact that the tetrasulfide linkages in the polymer undergo interchange reactions at the temperature of molding and the network chains of all the samples should therefore be in an equilibrium (unstrained) state regardless of their sulfur contents. Thus, to a first approximation the configurations of the chains of all mixtures of a given crosslink density should be the same. From Table II it is seen that the $\epsilon\Phi$

values do indeed remain fairly constant for mixtures of a given crosslink density in the range from 0 to 0.6 weight fraction sulfur.

Stability of the Mixtures

The stability of the mixtures was determined over a period of about 100–150 days by measuring their moduli and densities from time to time by the methods previously discussed. In the case of the stable mixtures, their appearance did not change nor did their moduli or densities over the

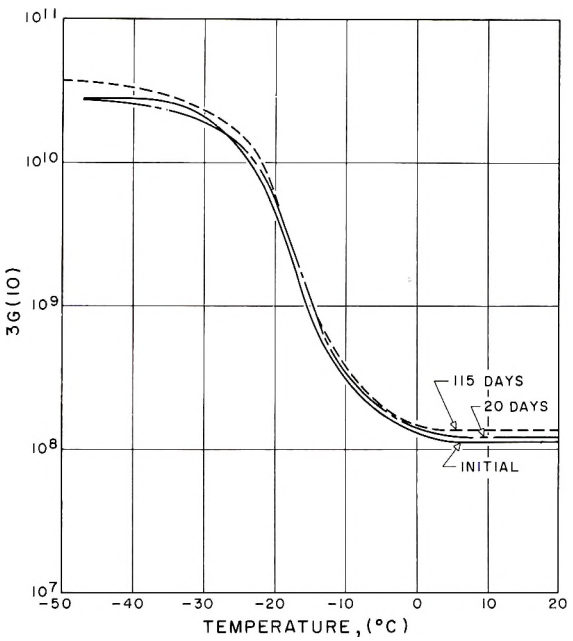

Fig. 5. Modulus temperature curves of the system C_{20} 80/S 20 measured at various times over a period of 115 days.

period of observation. Figure 5 shows the modulus temperature curve of a stable mixture (C_{20} 80/S 20) measured at various times over a period of 115 days and it is clear from the figure that the properties of the mixture remained unaltered during this time. In the case of the unstable mixtures, they became opaque as the sulfur in the mixtures crystallized and their moduli and densities showed corresponding changes.

Figure 6 summarizes these results, illustrating the relationship among the stability, the composition and the crosslink density of the polymer component of the mixtures. From this it can be seen that the limiting quantity of sulfur in the mixtures for stability increases with increasing crosslink density.

Stress Relaxation at Higher Temperatures

Stress relaxation studies on several crosslinked polyethylene tetrasulfides have been reported in a previous publication from our laboratory.[3] In this section we shall present the results of stress relaxation experiments on a few mixtures such as C_{50} 60/S 40, C_{20} 70/S 30, and C_{20} 40/S 60, both to determine the flow properties of sulfur containing systems close to the usual extrusion temperatures and to compare the behavior of polyethylene tetrasulfide plasticized with elemental sulfur to that of unplasticized polyethylene tetrasulfide.

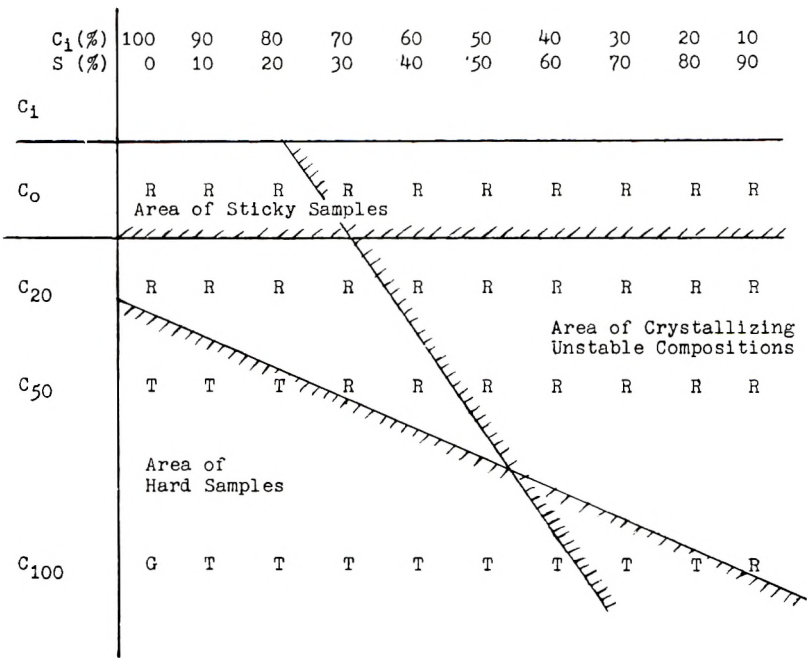

Fig. 6. R = rubbery state at room temperature; T = transition state at room temperature; G = glassy state at room temperature.

In the case of the crosslinked polysulfide rubbers, the mechanism of stress decay is a bond interchange reaction.[3] We assume that stress decay in the mixtures is due to the bond interchange reaction of the tetrasulfide linkage in the polymer. Then the stress-relaxation curve can be expressed mathematically in the same way as the stress-relaxation curve for unplasticized polyethylene tetrasulfide.[3]

$$f(t) = f(0) \exp\{-t/\tau_{ch}\} \tag{3}$$

$$\tau_{ch} = 1/km \tag{4}$$

where $f(t)$ and $f(0)$ are the stress at time t and the initial stress, respectively, τ_{ch} is the chemical relaxation time defined as the value of t when $f(t)/f(0) =$

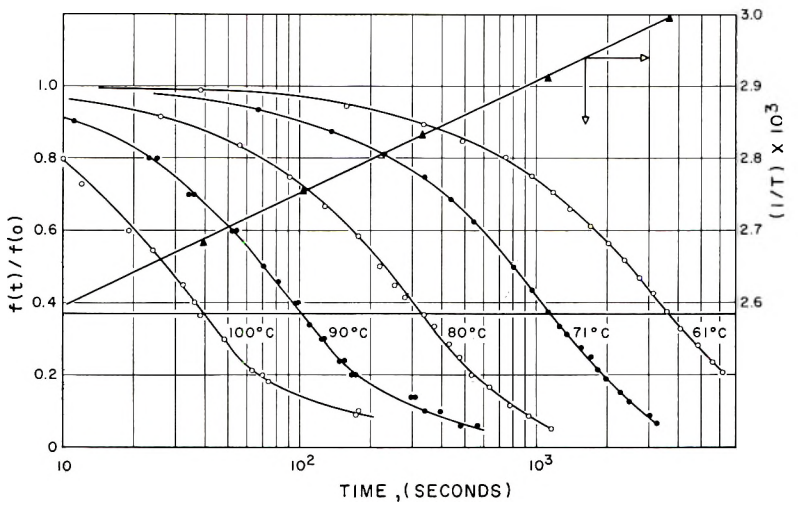

Fig. 7. Stress relaxation curves at various temperatures for the system C_{50} 60/S 40.

$1/e$, k is the specific rate constant for the bond interchange reaction, and m is the number of tetrasulfide linkages per network chain.

Figure 7 shows the stress relaxation curves of the C_{50} 60/S 40 system at several temperatures. The curves are very nearly Maxwellian in shape and therefore obey eq. (3) quite closely. Values of τ_{ch} were obtained at different temperatures from these curves and Figure 7 also shows a plot of log τ_{ch} versus $1/T$ which is seen to give a straight line obeying the Arrhenius rate law.

The activation energies obtained from the plot in Figure 7 and similar ones for three other systems are given in Table III. The values are slightly higher than those obtained for unplasticized polyethylene tetrasulfides having the same crosslink densities as these samples.[3]

TABLE III

Activation Energies E_{act}, Chemical Relaxation Times τ_{ch}, and Flow Viscosity in Shear η of C_{50} 60/S 40, C_{20} 70/S 30, and C_{20} 40/S 60

Sample	E_{act}, kcal./mole	A, sec.	T, °C.	τ_{ch}, sec.	$\eta = G_2\tau_{ch}$
C_{50} 60/S 40	29.3	2.4×10^{16}	150	3.3×10^{-1}	1.90×10^{7}
			190	1.62×10^{-2}	9.4×10^{5}
			210	4.3×10^{-3}	2.5×10^{5}
C_{20} 70/S 30	25.6	2.4×10^{14}	150	3.9×10^{-1}	1.33×10^{7}
			190	2.8×10^{-2}	9.6×10^{5}
			210	8.9×10^{-3}	3.0×10^{5}
C_{20} 40/S 60	26.6	4.2×10^{15}	150	2.14×10^{-1}	3.7×10^{6}
			190	1.41×10^{-2}	2.4×10^{5}
			210	4.17×10^{-3}	7.2×10^{4}

The flow viscosity in shear η in the region of bond interchange can be approximately estimated from:

$$\eta = G_2\tau_{ch} \tag{5}$$

The calculated values of η at elevated temperatures are collected in Table III. It is interesting to note that some of the values are almost small enough for practical applications, such as injection molding and extrusion.

Plasticizing Action of Sulfur on Other Polymers

This paper has demonstrated that monomeric sulfur exists in the liquid state when mixed with polyethylene tetrasulfide and acts as a plasticizer in such mixtures. A previous paper from this laboratory has shown that liquid monomeric sulfur also acts as a plasticizer for polymeric sulfur.[1] We are beginning to investigate the plasticizing properties of liquid sulfur when mixed with other polymers.

The results of preliminary experiments on the swelling of hydrocarbon polymers are given in Table IV. Many of these swollen polymers show

TABLE IV
Swelling of Various Polymers in Liquid Sulfur

Polymer	Weight gain at 140°C., 10 hr., %
Polyethylene	9.7
Ethylene–propylene rubber	8.1
Polypropylene	7.7
Polyisobutylene	5.8
Butyl rubber	6.6
Poly(butyl acrylate)	5.4

extremely interesting properties which will be reported in future publications from our laboratory. At 140°C. the sulfur in these polymers must be dissolved in the polymer in a liquid state. When these polymers are quick-quenched to room temperature, the sulfur remains in this dissolved liquid state for some time, and then, depending on the polymer, begins to crystallize out to different extents and at different rates.

We are pleased to acknowledge the kind assistance of Mr. W. J. MacKnight and we are also grateful to the Sulphur Institute for partial support of this work.

References

1. Tobolsky, A. V., W. J. MacKnight, R. B. Beevers, and V. D. Gupta, *Polymer*, in press.
2. Tobolsky, A. V., R. B. Beevers, and G. D. T. Owen, *J. Colloid Sci.*, **18**, 353 (1963).
3. Tobolsky, A. V., R. B. Beevers, and G. D. T. Owen, *J. Colloid Sci.*, **18**, 359 (1963).
4. Wiley, F. E., *Ind. Eng. Chem.*, **34**, 1052 (1942).
5. *A.S.T.M. Standards* (**1958**), Am. Soc. Testing Materials, Philadelphia, Pa., 1958, D1043-51.
6. Tobolsky, A. V., *Properties and Structure of Polymers*, Wiley, New York, 1960.
7. Tobolsky, A. V., and M. Takahashi, *J. Appl. Polymer Sci.*, **7**, 1341 (1963).

Résumé

Dans une récente publication provenant de ce laboratoire, on a montré que le soufre appelé "élastique" obtenu par un rapide refroidissement du soufre fondu d'une température de 250°C à une température d'environ −10°C est réellement un mélange de soufre polymérique et monomérique S_8, ce dernier étant dans un état métastable. La raison pour laquelle le soufre rapidement refroidi est élastique est que le soufre liquide S_8 joue le rôle de plastifiant sur le soufre polymérique. Dans cette publication, nous montrons que de grandes concentrations de S_8 peuvent exister dissous à l'état liquide dans d'autres polymères où il joue le rôle de plastifiant. Dans plusieurs cas ces compositions semblent complètement stables, par exemple, le soufre dissous m'a pas tendance à cristalliser. Le meilleur exemple est fourni par les polysulfures d'éthylène pontés (thiokol). Nous montrons que ces polymères peuvent retenir 40% de soufre dissous sous forme de liquide S_8 pendant des périodes indéfinies de temps. Nous prouvons que le soufre est sous sa forme élémentaire par extraction quantitative au CS_2. Le volume spécifique du soufre dissous montre qu'il est sous forme liquide. Les propriétés mécaniques des polymères ramifiés par le soufre comme plastifiant sont exactement celles que l'on peut attendre de ce type de structure. On présente des informations préliminaires concernant le soufre dans d'autres polymères.

Zusammenfassung

Wie aus einer neueren Arbeit aus diesem Laboratorium hervorgeht, ist der durch rasches Abkühlen von geschmolzenem Schwefel von 250°C. auf −10°C. hergestellte sogenannte elastische Schwefel eine Mischung von polymerem Schwefel und monomerem S_8-Schwefel, wobei letzterer in einer metastabilen Form vorliegt. Die Elastizität rasch abgekühlten Schwefels wird durch die Weichmacherwirkung des flüssigen S_8-Schwefels auf den polymeren Schwefel hervorgerufen. In der vorliegenden Arbeit wird gezeigt, dass S_8 auch in anderen Polymeren in hoher Konzentration in flüssiger Form gelöst und als Weichmacher wirksam sein kann. Diese Mischungen scheinen häufig vollkommen stabil zu sein, d.h. der gelöste Schwefel neigt nicht zur Kristallisation. Das beste Beispiel für dieses Verhalten sind vernetzte Polyäthylentetrasulfidpolymere. Diese Polymeren können 40% gelösten Schwefel in Form von flüssigem S_8 über unbegrenzt lange Zeit zurückhalten. Durch quantitative Extraktion mit CS_2 wurde nachgewiesen, dass der Schwefel in elementarer Form vorliegt, u.zw., wie aus dem spezifischen Volumen des gelösten Schwefels ersichtlich ist, in flüssiger Form. Die mechanischen Eigenschaften der mit Schwefel weichgemachten vernetzten Polymeren stimmen mit den für diesen Strukturtyp erwarteten überein. Ausserdem wird eine vorläufige Mitteilung über das Verhalten von Schwefel in anderen Polymeren gemacht.

Received March 27, 1963

JOURNAL OF POLYMER SCIENCE: PART A VOL. 2, PP. 2001–2009 (1964)

Transformation of Mechanical Model Representations of Viscoelasticity to Operator Equations

R. A. WESSLING, *Polymer Research Laboratory, The Dow Chemical Company, Midland, Michigan*

Synopsis

A general method has been developed with which mechanical model representations of viscoelasticity can be transformed into the corresponding operator equation. The method is restricted to linear systems but is equally applicable to any type of model within these limits.

Mechanical models composed of springs and dashpots are often employed to represent viscoelastic behavior in polymers.[1] These models are generally constructed from series arrays of Voigt elements (a spring and dashpot in parallel) or parallel arrays of Maxwell elements (a spring and dashpot in series). The former are useful when the stress is a known function of time, the latter when strain is a known function of time. It is possible to construct more complicated arrays. The various ladder models[2] which arise in some molecular theories of viscoelasticity fall into this category.

A more general method of describing viscoelastic behavior is the operator equation.[3] No particular form of stress or strain is favored by this approach; this makes it more useful in mechanical analysis. Since mechanical analysis is one principal aim in the study of material properties it is desirable to be able to transform a model into the equivalent operator equation.

A method of transformation has been described by Alfrey and Gurnee.[3] This involves the successive addition of one new element to the known operator equation for a set of similar elements. It becomes unwieldy, however, when applied to models of more than a few elements. A new technique is proposed here which is suitable for transforming models with any number of elements even in complicated arrays.

The behavior of a linear viscoelastic body in shear is governed by the operator equation

$$Ps_{ij} = 2\,Q\,e_{ij} \tag{1}$$

where

$$P = \frac{\partial^m}{\partial t^m} + p_{m-1}\frac{\partial^{m-1}}{\partial t^{m-1}} + \ldots + p_0 \tag{1a}$$

$$Q = q_n \frac{\partial^n}{\partial t^n} + q_{n-1} \frac{\partial^{n-1}}{\partial t^{n-1}} + \ldots + q_0 \tag{1b}$$

and s_{ij} = component of the deviatoric stress tensor, e_{ij} = corresponding component of the deviatoric strain tensor.

The coefficients in P and Q are parameters characterizing the material properties. They can be related to the model parameters η and G.

The springs and dashpots represent stress–strain equations, while the mechanical models represent sets of simultaneous differential equations obtained by combining these fundamental equations according to the structure of the model. A model of N Voigt elements in series leads to the set

$$s_{ij}(t) = 2G_n e_{ij,n}(t) + 2\eta_n \dot{e}_{ij,n}(t)$$
$$n = 1,2 \ldots, N \tag{2}$$

where $e_{ij,n}$ refers to the strain in the nth element of the model. A Maxwell model represents a similar set.

$$\frac{s_{ij,m}(t)}{\eta_m} + \frac{\dot{s}_{ij,m}(t)}{G_m} = 2\dot{e}_{ij}(t)$$
$$m = 1,2, \ldots, M \tag{3}$$

The various ladder models give more complicated sets. However, ladder models represent sets of equations which can be written in a form similar to one of the above types, i.e., the equations have the forms

$$f(s_{ij,m}, \dot{s}_{ij,m}) = \dot{e}_{ij}$$

or

$$f(e_{ij,n}, \dot{e}_{ij,n}) = s_{ij}$$

The sets of simultaneous differential equations can be expressed in operator notation. The operators are linear, nonzero, and commute and can be treated as ordinary polynomials in D, the differential operator.[4] The problem is not to solve the differential equations; it is to manipulate them to obtain a single Nth-order differential equation from N first-order equations. This can be done by suitable operations described in the following sections. The system of equations is transformed to a new set whose sum is the viscoelastic operator eq. (1). Use is made of the requirement that the total stress on a set of parallel elements is the sum of the stresses on the individual elements

$$s_{ij}(t) = \sum_{m=1}^{M} s_{ij,m}(t) \tag{4}$$

and that the total strain on a set of elements in series is the sum of the strains in the individual elements

$$e_{ij}(t) = \sum_{n=1}^{N} e_{ij,n}(t) \tag{5}$$

In the following sections a method for simple models is shown first and then a more general matrix method is developed. Simple transformations are carried out to illustrate each case.

1. Voigt Model to Operator Equation

The set of differential equations in operator notation is (ij subscripts are omitted for convenience):

$$2\,Q_n\,e_n(t) = s\,(t) \qquad n = 1,2,\ldots,N \tag{6}$$

where the operators are defined as

$$Q_n = \eta_n D + G_n \tag{7}$$

Operating on the nth equation of this set with Q_n^{-1} gives a new set

$$2e_n(t) = Q_n^{-1}\,s(t) \qquad n = 1,2,\ldots,N \tag{8}$$

The sum of this set is

$$2\sum_{n=1}^{N} e_n(t) = 2\,e(t) = \sum_{n=1}^{N} Q_n^{-1}\,s(t) \tag{9}$$

This equation can be put in standard form* by operating on it with the quantity

$$\frac{\prod_{n=1}^{N} Q_n}{\sum_{n=1}^{N} \frac{\prod_{n=1}^{N} \eta_n}{\eta_n}} \tag{10}$$

$$2\left[\frac{\prod_{n=1}^{N} Q_n}{\sum_{n=1}^{N} \frac{\prod_{n=1}^{N} \eta_n}{\eta_n}}\right] e(t) = \left[\frac{\sum_{n=1}^{N} \frac{\prod_{n=1}^{N} Q_n}{Q_n}}{\sum_{n=1}^{N} \frac{\prod_{n=1}^{N} \eta_n}{\eta_n}}\right] s(t) \tag{11}$$

The operators P and Q can now be identified by comparing eqs. (1) and (11). Each coefficient is evaluated by expanding terms. An example is shown below.

* In standard form, the coefficient of the highest derivative in P is unity.

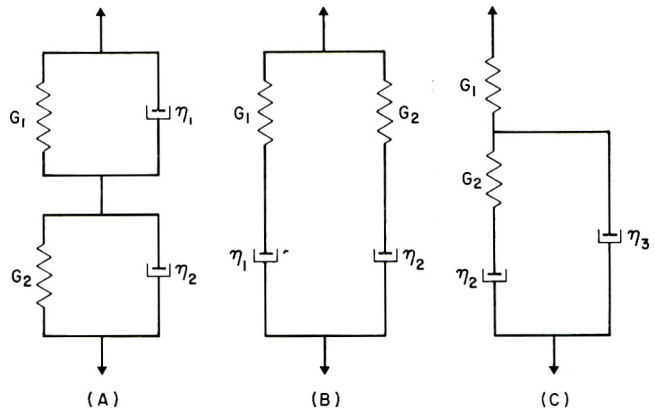

Fig. 1. Four-parameter mechanical models: (*A*) Voigt model; (*B*) Maxwell model; (*C*) a ladder model.

Example (See Fig. 1*A*): Two Voigt elements in series; for $N = 2$ in this case and by using eq. (11), the operator equation is

$$2\left[\frac{(\eta_1 D + G_1)(\eta_2 D + G_2)}{\eta_1 + \eta_2}\right] e(t) = \left[D + \frac{G_1 + G_2}{\eta_1 + \eta_2}\right] s(t)$$

Expanding, the coefficients are

$$p_0 = \frac{G_1 + G_2}{\eta_1 + \eta_2}$$

$$p_1 = 1$$

$$q_0 = \frac{G_1 G_2}{\eta_1 + \eta_2}$$

$$q_1 = \frac{\eta_1 G_2 + \eta_2 G_1}{\eta_1 + \eta_2}$$

$$q_2 = \frac{\eta_1 \eta_2}{\eta_1 + \eta_2}$$

2. Maxwell Model to Operator Equation

The set of equations in operator notation is

$$P_m s_m(t) = 2\, e(t)$$

$$m = 1,2, \ldots, M \qquad (12)$$

The operator

$$P_m = \frac{D}{G_m} + \frac{1}{\eta_m} \qquad (13)$$

operating on the mth equation of this set with P_m^{-1} yields a new set

$$s_m(t) = 2 P_m^{-1} e(t) \qquad m = 1,2, \ldots, M \tag{14}$$

The sum of these equations is

$$\sum_{m=1}^{M} s_m(t) = s(t) = 2 \sum_{m=1}^{M} P_m^{-1} e(t) \tag{15}$$

The viscoelastic operator equation is obtained from eq. (15) by operating with $\prod_{m=1}^{M} G_m P_m$

$$\prod_{m=1}^{M} G_m P_m \, s(t) = 2 \left[\sum_{m=1}^{M} \frac{\prod_{m=1}^{M} G_m P_m}{P_m} \right] e(t) \tag{16}$$

Again the operators P and Q can be identified by comparing eqs. (1) and (16).

Example (See Fig. 1*B*): Two Maxwell elements in parallel; for $M = 2$ the operator equation is:

$$\left[\left(D + \frac{1}{\tau_1}\right)\left(D + \frac{1}{\tau_2}\right)\right] s(t) = 2\left[G_1 D\left(D + \frac{1}{\tau_2}\right) + G_2 D\left(D + \frac{1}{\tau_1}\right)\right] e(t)$$

where $\tau_m = \frac{\eta_m}{G_m}$ the relaxation time.

The coefficients are

$$p_0 = 1/\tau_1\tau_2$$

$$p_1 = 1/\tau_1 + 1/\tau_2$$

$$p_2 = 1$$

$$q_0 = 0$$

$$q_1 = \frac{G_1}{\tau_2} + \frac{G_2}{\tau_1}$$

$$q_2 = G_1 + G_2$$

3. The General Transformation Method

The algebraic method used in sections 1 and 2 owes its success to the fact that each equation in a set contains only one element variable, e.g., $e_n(t)$ in the Voigt model. When this is not true as in a ladder model, the algebraic method becomes more difficult and matrix formalism can be advantageously employed.

The mechanical models under consideration can be represented by either of two matrix equations, described by eqs. (17) and (18).

Type a:

$$2[Q][E] = [\mathrm{s}] \tag{17}$$

where

$$[E] = \begin{bmatrix} e_1(\mathrm{t}) \\ e_2(\mathrm{t}) \\ \cdot \\ \cdot \\ \cdot \\ e_N(t) \end{bmatrix}$$

$$[s] = \begin{bmatrix} s(t) \\ s(t) \\ \cdot \\ \cdot \\ \cdot \\ s(t) \end{bmatrix}$$

and

$$[Q] = \begin{bmatrix} Q_{11}\ Q_{12} \cdots \\ Q_{21}\ Q_{22} \cdots \\ \cdot \\ \cdot \quad \cdots \quad Q_{NN} \end{bmatrix}$$

In a series of Voigt elements, the operator matrix $[Q]$ is a diagonal matrix. The simplicity of operations in section 1 is thus explained!

Type b:

$$[P]\ [S] = 2[\dot{e}] \tag{18}$$

where

$$[S] = \begin{bmatrix} s_1(t) \\ s_2(t) \\ \cdot \\ \cdot \\ \cdot \\ s_M(t) \end{bmatrix}$$

$$[\dot{e}] = \begin{bmatrix} \dot{e}(t) \\ \dot{e}(t) \\ \cdot \\ \cdot \\ \cdot \\ \dot{e}(t) \end{bmatrix}$$

and

$$[P] = \begin{bmatrix} P_{11} & P_{12} & \cdots \\ P_{21} & P_{22} & \cdots \\ \cdot & & \\ \cdot & & \\ \cdots & & P_{MM} \end{bmatrix}$$

The matrix $[P]$ is a diagonal matrix in the case of a Maxwell model.

Once the matrix equation is written, the transformation to an operator equation can be carried out in a very straightforward manner. This is illustrated below for models of type a.

The solution of eq. (17) for $[E]$ is well known.[5]

$$2[E] = \frac{\text{Adj}\,[Q][s]}{|Q|} \tag{19}$$

where the adjoint matrix is the transpose of the cofactor matrix

$$\text{Adj}\,[Q] = [(-1)^{r+n} M_{rn}]'$$

M_{rn} is the minor of $|Q|$ obtained by deleting the rth row and the nth column.

The set of equations represented by eq. (19) are now in a form which can be summed to obtain a single Nth-order operator equation. Note that the matrix is

$$\text{Adj}\,[Q][s] = \begin{bmatrix} \sum_{r=1}^{N} (-1)^{r+1} M_{r1}\, s(t) \\ \sum_{r=1}^{N} (-1)^{r+2} M_{r2}\, s(t) \\ \cdot \\ \cdot \\ \cdot \\ \sum_{r=1}^{N} (-1)^{r+N} M_{rN}\, s(t) \end{bmatrix}$$

The equations in the new set are therefore

$$2|Q|e_n(t) = \sum_{r=1}^{N} (-1)^{r+n} M_{rn} s(t) \qquad n = 1,2,\ldots,N \tag{20}$$

The sum is

$$2|Q| \sum_{n=1}^{N} e_n(t) = 2|Q|e(t) = \sum_{r=1}^{N} \sum_{n=1}^{N} (-1)^{r+n} M_{rn}\, s(t) \tag{21}$$

This can be written in standard form by proper manipulation.

The general method is used in section 4 to transform a four-parameter ladder model.

4. Ladder Model to Operator Equation

One type of ladder model is shown in Figure 1*C*. The set of two simultaneous differential equations representing this model can be obtained by combining the equations of the various elements in a manner consistent with the way they are connected. The strains associated with each element are related to the total strain as

$$e(t) = e_1(t) + e_3(t) = e_1(t) + e_2(t) + e_4(t)$$

and the stresses

$$s(t) = s_2(t) + s_3(t)$$

The elemental strains and stresses are identified in the elemental eqs. (22)–(25) given below:

$$2G_1e_1(t) = s(t) \tag{22}$$

$$2G_2e_2(t) = s_2(t) \tag{23}$$

$$2\eta_2\dot{e}_4(t) = s_2(t) \tag{24}$$

$$2\eta_3\dot{e}_3(t) = s_3(t) \tag{25}$$

Since three elemental strains must be specified but only two stresses, the former are eliminated. This can be done only by combining the derivatives, $\dot{e}$. (Therefore this model is of type b.) One way is to add the derivative of eq. (23), eq. (24), and the derivative of eq. (22) to obtain an equation in $e(t)$:

$$\left(\frac{D}{G_1} + \frac{D}{G_2} + \frac{1}{\eta_2}\right)s_2 + \frac{D}{G_1}\,s_3 = 2(\dot{e}_1 + \dot{e}_2 + \dot{e}_4)$$
$$= 2\ \dot{e}(t)$$

The second equation is obtained by adding the derivative of eq. (22) to eq. (25):

$$\frac{D}{G_1}\,s_2 + \left(\frac{D}{G_1} + \frac{1}{\eta_3}\right)s_3 = 2(\dot{e}_1 + \dot{e}_3)$$
$$= 2\ \dot{e}(t)$$

The matrix operator $[P]$ can now be constructed

$$[P] = \begin{bmatrix} \left(\dfrac{D}{G_1} + \dfrac{D}{G_2} + \dfrac{1}{\eta_2}\right) & \dfrac{D}{G_1} \\ \dfrac{D}{G_1} & \left(\dfrac{D}{G_1} + \dfrac{1}{\eta_3}\right) \end{bmatrix}$$

The solution by the general method is

$$[S] = \frac{2\ \mathrm{Adj}\,[P][\dot{e}]}{|P|}$$

where

$$|P| = \frac{D_2}{G_1 G_2} + D\left(\frac{1}{G_1\eta_2} + \frac{1}{G_1\eta_3} + \frac{1}{G_2\eta_3}\right) + \frac{1}{\eta_2\eta_3}$$

and

$$\mathrm{Adj}\,|P| = \begin{bmatrix} \left(\frac{D}{G_1} + \frac{1}{\eta_3}\right) & -\frac{D}{G_1} \\ -\frac{D}{G_1} & \left(\frac{D}{G_1} + \frac{D}{G_2} + \frac{1}{\eta_2}\right) \end{bmatrix}$$

The sum of the new set is (in standard form)

$$\left(D^2 + \left[\frac{1}{\tau_2} + \frac{G_2}{\eta_3} + \frac{G_1}{\eta_3}\right]D + \frac{G_1}{\tau_2\,\eta_3}\right) s(t) = 2\left(G_1 D^2 + \left[\frac{G_1}{\tau_2} + \frac{G_1 G_2}{\eta_3}\right]\mathrm{D}\right) \mathrm{e}\ (\mathrm{t})$$

The author gratefully acknowledges the many valuable discussions with Dr. T. Alfrey, Jr. during the course of this work.

References

1. Alfrey, T., Jr., *Mechanical Behavior of High Polymers*, Interscience, New York, 1948.
2. Marvin, R. S., in *Viscoelasticity*, J. T. Bergen, Ed., Academic Press, New York, 1960.
3. Alfrey, T., Jr., and E. F. Gurnee in *Rheology*, Vol. I, F. R. Eirich, Ed., Academic Press, New York, 1951.
4. Kaplan, W., *Operational Methods for Linear Systems*, Addison-Wesley, Reading, Mass., 1962.
5. Perlis, S., *Theory of Matrices*, Addison-Wesley, Reading, Mass., 1958.

Résumé

On a développé une méthode générale qui permet de transformer la représentation de la viscoélasticité sous forme de modèle mécanique en son équation correspondante. La méthode est limitée aux systèmes linéaires, mais avec cette restriction, elle est applicable à n'importe quel genre de modèlel.

Zusammenfassung

Es wurde eine allgemeine Methode zur Transformation von mechanischen Modelldarstellungen der Viskoelastizität in die entsprechenden Operatorgleichungen entwickelt. Die Methode ist zwar auf lineare Systeme beschränkt, lässt sich aber innerhalb dieser Grenzen auf jeden Modelltyp in gleicher Weise anwenden.

Received April 1, 1963

BOOK REVIEWS

N. G. GAYLORD, Editor

Orbitals in Atoms and Molecules. CHR. K. JØRGENSEN, Academic Press, London–New York, 1962. v + 162 pp., $6.00 (35 s.).

C. K. Jørgensen's "Orbitals in Atoms and Molecules" appears to possess two nonconflicting aims: The first of these is a unified review, predominantly from the author's viewpoint on orbital theory, of the many similarities in the treatment of gaseous atoms, spherically symmetric monoatomic ions, ligand field transitions, and electron transfer spectra of simpler polyatomic complexes of high (e.g., octahedral) symmetry and energy levels of crystals. In the 162 pages of this book, the author covers a great diversity of systems, ranging from atoms to crystals. The reader, though, will not find here a discussion of the molecular quantum mechanics of hydrocarbons or big organic molecules. The second aim of the book appears to be a systematic comparison of the opposing valence bond and molecular orbital theories of various properties of inorganic compounds, particularly electronegativities and bond strengths, the assignment of absorption spectra, and energy levels in crystals. The author brings together a considerable amount of evidence from these areas in support of his preference of molecular orbital theory to the valence bond approach.

Specifically, the first three chapters, on well-defined electron configurations, degenerate orbitals in high symmetry, and correlation effects deal with the application of orbital theory to atoms. The next two chapters are devoted to the application of molecular orbital theory to systems with octahedral symmetry and to pointing out the difficulties encountered with molecular orbital theory at large internuclear distances. Chapter 6 is devoted to a survey of the pros and cons of equivalent orbitals. Then follow three survey chapters on electronegativity and chemical bonding, the identification of absorption spectra, and energy levels in crystals. The next chapter deals with electrodynamic (relativistic) effects and is followed by an account of the lanthanides and 5*f* elements. X-ray spectra are discussed in the short concluding chapter.

For the sake of brevity in reviewing these interdisciplinary topics, the explanations of the underlying physics are kept very terse. This book is not self-contained in the sense that a reader desiring a more fundamental understanding, particularly of certain necessary mathematical details underlying the subjects, will have to refer to original papers. This book should prove useful to suitably prepared inorganic chemists and certain spectroscopists, but will fall short in satisfying the needs of solid-state physicists. Some acquaintance with quantum mechanics of atoms and molecules is prerequisite to following the author's discussions.

H. L. Frisch

Bell Telephone Laboratories
Murray Hill, New Jersey

Crystallography and Crystal Perfection, G. N. RAMACHANDRAN, ed., Academic Press, London-New York, 1963, x + 374 pp., 75 s. ($12.00).

This volume covers the proceedings of a Symposium held in Madras (India) last year. It is composed of 30 papers mostly dedicated to present problems of x-ray diffraction—phase angle determination, crystal perfections and disorder, and anomalous dispersion. There are also some papers concerned with other techniques (including infrared, Raman, neutron, and electron diffraction), theoretical approaches to symmetry, and improvement of x-ray diffraction instruments. Only about half of these papers are generalizations or can be extended to other structures than the ones shown. The others are particular cases of limited application.

The interest of the contributions depends directly on the field of research of the reader. X-ray crystallographers working on structural problems of single crystals can find many of the papers valuable. The general scientist will find them of little application to his work.

In the case of polymer research, this difference in value is still greater, in spite of the potential usefulness of the solutions to the problems analyzed.

Attempts to attack polymer structures in the light of this volume will need much more "bridge" work to join both directions of research and to make them mutually applicable.

It is not the first time, and will not be the last, that Proceedings of Meetings are presented as a book. The clarity and neat presentation is laudable but it is a fact that a group of papers cannot form a book in spite of how good each one may be. The presentation of this volume with a different name other than "Proceedings of, etc." is misleading. A reader looking for detailed information on crystal perfection will only find a limited aspect of it in the book's 374 pages. As might be expected from papers in a large symposium, unity among them is difficult to achieve. They provide more of a scattered view of some new approaches to crystal structure solution and crystal perfection than might be expected from the title.

In summary, this is a collection of papers generally concerned with crystal structure which may be of interest to the serious crystallographer but which probably will not be suitable for nonspecialist scientists.

L. G. Roldan

Central Research Laboratory
Allied Chemical Corporation
Morristown, New Jersey

Organic Reactions, Vol. XIII, A. C. COPE, ed., Wiley, New York, 1963. 382 pp. $12.50.

Volume XIII of Organic Reactions follows the well-known pattern of this renowned series which concerns the synthetic applications to organic chemistry. Every chapter in this volume has been contributed by a very active worker and authority in the area, and generally deals with reactions involving additions to olefins. It should be of general interest to polymer chemists.

Professors George Zweifel of the University of California and Henry Brown of Purdue University are largely responsible for our present knowledge of the reactions of diborane and organoboranes with unsaturated compounds. Their chapter, "Hydration of Olefins, Dienes, and Acetylenes via Hydroboration," includes the very useful synthetic application of this technique to the preparation of alcohols by oxidation of organoboranes

They have obviated the hazards of handling diboranes and organoboranes by developing procedures which do not necessitate isolation of these intermediates, and thus makes the procedure of convenient and general use. Selective and stereospecific addition of boranes to unsaturated compounds and subsequent oxidation is shown to generate alcohols uniquely. This chapter is a very useful companion to Professor Brown's book which deals more generally with the hydroboration reaction.

The impetus that Hine and Doering and Hoffman lent to the chemistry of divalent carbon is dealt with in the chapter by Professors William Parham of the University of Minnesota and Edward Schweizer of the University of Delaware on the formation and reaction of "Halocyclopropanes from Halocarbenes." α-Elimination from a polyhalocarbon in basic media in the presence of olefins yields cyclopropanes, presumably via carbene intermediates. Halocyclopropanes undergo some interesting rearrangements.

Chapters 3 and 4 concern the application for synthetic purposes of free radical additions to the double bond by chain processes. Professors Cheves Walling of Columbia University and Earl Huyser of the University of Kansas discuss carbon addends in the chapter on "Free Radical Addition to Olefins to Form Carbon-Carbon Bonds." Except with polyhalogenated compounds, the chain transfer reaction competes significantly with addition to cause telomer formation to be a serious problem. Nonetheless, this method offers a one-step synthesis of compounds generally difficult to obtain by other routes.

The last chapter, by Drs. F. Stacey and J. Harris, Jr. of the Central Research Department of Du Pont Company, is an extensive compilation of hetero-atom addends in the "Formation of Carbon-Hetero Atom Bonds by Free Radical Chain Additions to Carbon-Carbon Multiple Bonds." The choice is limitless; it starts from hydrogen bromide and encompasses thiols, and other sulfur compounds, silanes, germanes, phosphorus and nitrogen compounds—withal quite exotic!

Jay K. Kochi

Department of Chemistry
Case Institute of Technology
Cleveland, Ohio

The Chemistry of Wood. B. L. BROWNING, ed., Interscience, New York, 1963. x + 689 pp. Illus. $25.00.

Sometime in the last twenty years or so, it has become accepted in the book writing business that technical subjects are becoming too complex for a single author. As in research then, the team approach is now in vogue for covering so complex a subject as wood chemistry. It does not seem to be true that a narrower subject area would allow a return to the one author system since a recent monograph on wood extractives has no less than ten contributors. To achieve uniformity of coverage and scholarship under this system is a task which would be a major challenge to the most gifted and experienced editor. Most scientists who put together one or two books in a lifetime measure up to the task by selecting a sufficiently wide subject area whereby the various contributions dovetail but seldom overlap to a serious degree.

The present book is of this kind, i.e., a series of twelve related contributions. Each one is rather well done in its own right and fulfills the editor's aim "of providing the outstanding features of the chemistry of wood and its components in a critical if not exhaustive survey." The only common thread is the title itself for there is little difficulty in reading a given chapter separately. Each one is self-contained and needs very little reference to the others for comprehension. For the chemist who is seeking a general

introduction to the complex facets of wood anatomy, information on the extraneous components of wood, or ideas on how wood might be used or has been used as a chemical raw material there is a most readable presentation.

Chapters on "The Chemistry of Bark" and "The Chemistry of Developing Wood" are very worthwhile innovations for a book of this type. In fact, one is disappointed not to find more coverage on the biogenesis of wood and wood components in relation to morphology and fine structure. The excellent work of Colvin and Hestrin on the development of cellulose microfibrils is ignored. Some discussion on the evolution of trees would also be in order.

Although lacking critical evaluation in places, the presentation on the chemistry and physics of cellulose is indeed, as one reviewer has said, the best available single chapter survey on the subject. The hemicellulose review, written at a time when rapid developments were occurring in this field, nevertheless, is up to date. The rest of the book is to be recommended as a convenient first reference for most technical libraries on any conceivable chemical or morphological aspect of wood chemistry. It should be of particular help in orienting the research chemist who is having to work with wood or one of its components for the first time. By reading two or three chapters, both the chemical and anatomical aspects are brought into focus. The chapter on "The Structure of Wood" provides an excellent orientation in an area where most "cellulose and polymer chemists" are deficient. The high quality plates of wood sections are particularly effective in this chapter. Dr. Browning's greatest service may well be in introducing many chemists to the idea of how some polymer molecules grow on trees.

R. H. Marchessault

Cellulose Research Institute
State University College of Forestry
Syracuse University
Syracuse, New York

Progress in Physical Organic Chemistry, Vol. 1, S. G. COHEN, A. STREITWIESER, JR., and R. W. TAFT, eds., Interscience, New York, 1963. ix + 411 pp., $15.00.

Three-quarters of this volume is taken up by two chapters, "Secondary Isotope Effects" by E. A. Halevi and "Quantitative Comparison of Weak Organic Bases" by E. A. Arnett. The rest comprises shorter discussions of "Ionization Potentials in Organic Chemistry" by A. Streitwieser, Jr., "Nucleophilic Aromatic Substitution Reactions" by S. D. Ross, and "Ionization and Dissociation Equilibria in Solution in Liquid Sulfur Dioxide" by N. A. Lichtin.

It is generally recognized that the increasing volume of the scientific literature has increased the importance of review articles, particularly if they are written by prominent investigators in a given field. By this token it is to be welcomed that the present series is to be added to the various other "Progress" series and the first volume gives all assurance of its high quality. For research workers in the polymer field some of the chapters will be of particular interest. The discussion of ionization potentials gives an insight into the relative thermodynamic stability of various carbonium ions, which is of fundamental importance in cationic polymerization and copolymerization. Determinations of secondary isotope effects have found a wide variety of applications and it is somewhat disconcerting to find that nobody seems to have thought of determining the copolymerization behavior of vinyl monomers with their deuterated analogs. Arnett's

extensive discussion of the measurement of the strength of weak bases is pertinent to numerous problems in polymer chemistry. The author is extremely careful in pointing out the ambiguity in the concept of a "base strength" which will frequently make the order of basicities in a series of compounds dependent on the method employed for their characterization. The review contains 68 pages of valuable tabulations of experimental data.

Herbert Morawetz

Polytechnic Institute of Brooklyn
Brooklyn, New York

Polymer Single Crystals (Polymer Reviews, Vol. 5), P. H. GEIL, Interscience, New York, 1963. xii + 560 pp., $16.00.

Since the recognition (in 1957) that polymers could be obtained regularly from dilute solution in single crystal form, a wealth of information has become available on what might be considered as the emergence of a field of "solid state polymer physics." Indeed, the terms "defect," "dislocation," and "slip" are now widely used in discussions of the properties of crystalline polymers. It was inevitable, therefore, that someone would attempt to assemble the information available in a coherent form. This book, written by one of the leading experimentalists in this field, has two main objectives: (*1*) to review critically the present state of the field and (*2*) to stimulate additional research in the area of morphology leading, thereby, to the development of the foundations of the solid-state physics of polymers. The author has particularly limited himself mainly to a presentation and review of the work on single-crystal morphology and structure and of its relevance to the polymer structure field as a whole.

Of the two objectives, the latter one should certainly be attained. The reviewer found much to speculate about as he studied this volume—indeed, this book may well be as important for what the author was unable to say as for the material actually included. Even for those familiar with the material covered, this book should serve as a frequent reminder of our limited knowledge of the details of the crystalline structure of polymers and of the interplay between structure and properties.

The author has not met his first objective as well. However, barring a critical review, he has presented us with an acceptable substitute—an attempt (on the whole, quite successful) to present an exhaustive compilation of available information, even to the extent of persuading many laboratories to allow him to present heretofore unpublished results. In this respect, the book is particularly valuable as a collection of electron microscopic and diffraction studies from 1957 through the first half of 1963. As relevant, the author has included discussion of the results of x-ray diffraction (including small angle scattering), of optical microscopy, and of the relationship of properties to morphology in order to relate the single crystals obtained from dilute solutions to the crystals in bulk samples. The presentation (Chap. VI) of the theoretical aspects of chain-folding was found to be particularly interesting and stimulating. Similarly, the discussion on the annealing of crystalline polymers (Chap. V) should stimulate much thought and study. On the other hand, the section on "*As*-Polymerized and Amorphous Polymers," (Chap. VIII) might well have been eliminated.

The book has three drawbacks whose relative importance will depend upon the state of sophistication of the reader: (*1*) organization, (*2*) coverage, and (*3*) editing. The author recognizes (Preface) the mutually incompatible desires of presenting a book which is both well-organized *and* current. One example will suffice to alert the reader: the index lists thirteen different sections of the book in which to find information on "small-

angle x-ray diffraction." However, the text at any one of these places gives little indication that the discussion is incomplete. Indeed, one has to read all of the sections to ascertain the present status of this important technique and, even then, the reader will be uncertain of the meaning one may give to the results of small-angle studies.

The unevenness of coverage reflects the author's own interests. For example, the reviewer feels that too much space has been devoted to a discussion (Chap. II) of the indices appropriate to various fold domains and surfaces in the absence of an existence theorem demonstrating the importance of this information. On the other hand, in the section on transitions (Chap. IX), the author has presented the viewpoint essentially of only one author, without giving cognizance to the existence of divergent viewpoints.

The third drawback is perhaps the most serious. Errors and inconsistencies are frequent, words are misspelled, reference citations are incorrect, mathematical equations and symbols are incorrect, etc. Many of these mistakes are simply irritating and will be discerned by the astute reader. These include: (*1*) the reference in the legend of Fig. III-26 to III-21 rather than III-25, (*2*) the fact that Fig. III-24 is printed in reverse, (*3*) the incorrect placement of arrows in Fig. II-66, (*4*) the mislabeling of parts (*b*) and (*c*) of Fig. VII-5 and the incorrect reference for it, (*5*) the lack of consistency between the crystal structure data for polybutene-1 given in Chapter I and the data presented in Appendix I, and (*6*) the use of the phrase "isotactic polyethylene" on p. 506. Some of the errors, though, are quite serious. For example, (*1*) in the discussion of the possible slip systems for polyethylene (pp. 458ff.), the order of importance of the two main slip systems has been reversed, (*2*) on p. 463 the slip direction in nylon 66 should be ⟨001⟩ rather than ⟨010⟩ (*3*) on p. 400, a proofreading error in the expression for the average fluctuation in fold period, and (*4*) a number of proofreading errors in equations and in symbols scattered throughout the text, particularly in the chapter on chain-folding (Chap. VI). Indeed, the serious reader would be advised to refer to the original references cited for the mathematical details, while following the organization of the subject in the chapter.

The author has undertaken a momentous task in attempting to assemble this compilation of the information in this rapidly expanding field. Indeed, the past six months have seen the publication of work clarifying (or, in some instances, refuting) some of the statements in the book. To a certain extent, the contents of this book would have been less subject to the results of further studies had the author been able to supply a critical review, particularly if his considered opinion were more in evidence. In lieu of this, the book should still serve as an excellent introduction for the novice and as a valuable guide to most of the current literature for the initiated. Its price will tend to limit its purchase only to those actively working (or intending to work) in the field.

Robert L. Miller

Chemstrand Research Center, Inc.
Research Triangle Park
Durham, North Carolina